EFFECTS OF FEED COMPOSITION AND GASIFICATION PARAMETERS ON PRODUCT GAS FROM A PILOT SCALE FLUIDIZED BED GASIFIER

By

BRUNO GHISLAIN CATENI

Bachelor of Science in Food Engineering
E.N.S.I.A.
Massy, France
1996

Master of Science in Industrial Food Process Engineering
E.N.S.I.A.
Massy, France
1997

Submitted to the Faculty of the
Graduate College of the
Oklahoma State University
in partial fulfillment of
the requirements for
the Degree of
DOCTOR OF PHILOSOPHY
July, 2007

EFFECTS OF FEED COMPOSITION AND

GASIFICATION PARAMETERS ON PRODUCT GAS

FROM A PILOT SCALE FLUIDIZED BED GASIFIER

Dissertation Approved:

Raymond. L. Huhnke

Dissertation Adviser

Danielle Bellmer

Timothy Bowser

Arland Johannes

Lloyd Caldwell

A. Gordon Emslie

Dean of the Graduate College

ACKNOWLEDGEMENTS

This research project was an enriching experience as much from the theoretical and technical point of view as from the human relations point of view. This is why it is important for me to express my recognition to many people who helped, and advised me in a pleasant work environment, relaxed but serious.

I first would like to thank my committee advisor, Dr. Raymond L. Huhnke, for supporting me and allowing me to carry out my doctorial research as an active part of the GRASSohol project.

It has been a blessing to be surrounded by my two families, in France and in the USA, whose prayers, love and support were at the core of the strength that carried me to the completion of this endeavor. Thanks to my wife, Tamara, for her patience, love and support through years of challenges.

So many individuals are vital for the completion of an undertaking such as this. My heartfelt gratitude goes to the entire Biosystems and Agricultural Engineering Department for their generosity, sympathetic help, and the administrative/technical assistance they provided to me throughout this venture.

The list is too long to cite them all here, but for those directly involved in this effort, my thanks go to the following indivividuals:

- Committee:
  - Dr. T. Bowser
  - Dr. D. Bellmer
  - Dr. L. Caldwell
  - Dr. R. Huhnke
  - Dr. A. Johannes
- Administration:
  - J. Hicks
  - J. Hite
  - G. Lacy
  - R. Ladd
  - N. Rogers
  - B. Tessmann
- Electrical & Electronical:
  - M. Veldman
  - Dr. M. Stone
- Analytical:
  - R. Ingraham
- Technical:
  - B. Flores
  - R. Harrington
  - R. Harshman
  - W. Kiner
  - J. Walker
  - S. Gilstrap
- Computer technology:
  - C. Trible
- Engineering advise:
  - Dr. G. Brown
  - Dr. G. Brusewitz
  - Dr. G. Kranzler
  - Dr. D. Sanders
- Experimental:
  - Dr. K. Patil
  - Dr. A. Ahmed
- Students:
  - P. Bele
  - A. Birjie
  - P. Chaudhari
  - K. Jones
  - M. Lemmon
  - L. Marine
  - S. Nabar
  - R. Patil
  - V. Sharma
- Modeling:
  - Dr. H. Burchard
  - Dr. R. Ghisleni
  - R & D National Instrument
- Personal support:
  - Lifechurch.tv
- Overall most important support:
  - YHWH, God is Good

I dedicate this dissertation to the two I miss the most. From the generation before me, my father, Robert Cateni, who passed away before his time. Bright man who taught me that learning is a life long interest accessible to all people. From the generation after me, my son Enzo Ralphaël Cateni, who came and went too fast through my life during this undertaking. Through his short life and his fight, he taught me never to let go, no matter the circumstances or the pain. He helped redirect me towards the path of the ONE that matters the most.

Finally, I also dedicate this dissertation to my mother, Colette Cateni, the strongest, most resourceful person I know. She raised two sons on her own and gave them the means to attain their goals to a great career, despite disadvantaged conditions and life's rollercoaster ride. She opened another door, after my attempt to mix career and passion, when the system had already given up on me. This is my gift to you mom, a Dr. in front of the name.

TABLE OF CONTENTS

LIST OF TABLES

LIST OF FIGURES

NOMENCLATURE

ΔCp_i	Change in specific heat of i
ΔG	Change in Gibbs energy
ΔHf_i	Change in enthalpy of formation of i
ΔH_i	Change in enthalpy of i
ΔH_R	enthalpy of reaction, kJ/mol or kJ/kg
ΔS_i	Variation of entropy of i
A	amperes
a_i	Activity of i
AI	Analog input
a_{ik}	Number of element k in i
AO	Analog output
atm	Atmosphere (pressure unit)
bar	Bar (pressure unit)
Btu	British Thermal Unit (energy unit)
C	Atom of carbon
C_2H_2	Acetylene molecule
C_2H_4	Ethylene molecule
C_2H_6	Ethane molecule

cc	cubic centimeter (volume unit)
CH_4	methane molecule
cm	Centimeter
CO	Carbon monoxide molecule
CO_2	Carbon dioxide molecule
Cp_i	Specific heat of specie i (kJ/kg/K)
C_s	Carbon solid
db	Dry basis
DH_R	enthalpy of reaction, kJ/mol or kJ/kg
DI	Digital input
dm^3	Cubic decimeter (volume unit)
DO	Digital output
Eff_i	Efficiency of i, %
ER	Equivalence ratio
FBG	Fluidized bed gasifier
F_i	Mole flow rate of i, (mol/h)
ft.	Foot
g	Gram
gal.	Gallon
G_i	Gibbs energy of i
GC-MS	Gas chromatograph with mass spectrometer detector
GC-TCD	Gas chromatograph with thermal conductance detector
gpm	Gallons per minute

H	Atom of hydrogen
h	Hour
H_2	Hydrogen molecule
H_2O	Water molecule
He	Atom of helium
Hf_i	Enthalpy of formation of i, kJ/mol or kJ/kg
HHV	High heating value
hp	Horse power (power unit)
IC	Ions chromatography
in.	Inch
J	Joule (energy unit)
K	Equilibrium constant
K	Kelvin (temperature unit)
kg	Kilogramm
kJ	KiloJoules (energy unit)
kPa	kilopascal (pressure unit)
kW	KiloWatt (power unit)
l	Liter (volume unit)
LHV	Low heating value
$\dot{m}_i$	Mass flow rate of i, m^3/h
m	Meter (length unit)
m^3	Cubic meter (volume unit)
mg	Milligram (mass unit)

M_i	Molecular mass of i, g/mol
ml	Milliliter
mm	Millimeter(length unit)
mol	Mole
ms	millisecond
MW	Molecular weight, g/mol
m_x	Mass of x, kg
M_x	Molecular weight of x, g/mol
N	Atom of nitrogen
N_2	Nitrogen molecule
NI	National instrument
n_i	Number of mole of i
O	Atom of oxygen
O_2	Oxygen molecule
^oC	Degrees Celsius
P	pressure (kPa, Pa, atm, psi or bar)
$P7^T$	Strain of *C. carboxidivorans*
Pa	Pascal (pressure unit)
PAH	Polycyclic aromatic hydrocarbon
P_i	Pressure of i
PID	Proportional integrator derivator controller
PM	Particulate matter
ppm	Parts per million

psi	Pounds per square inch (pressure unit)
$\dot{Q}_i$	Heat flow of i, kW
Q_x	Sensitive heat of x, kW
ρ_i	Density of i, kg/m^3
R	Ideal gas constant
rpm	Rotations per minute
s	Second (time unit)
S/B	Steam to biomass ratio
scfm	Gas flow rate standard cubic feet per minute
SR	Stoichiometric ratio
ton	Cooling unit used in refrigeration (energy unit)
$\dot{V}_{Gas}$	Gas volume flow rate, m^3/s, l/min
V	Volt
V_i	Liquid volume in reactor of i
vi	Virtual instrument
V_i	Volume of i, m^3
VOC	Volatile organic compounds
V_v	Revolving valve volume, m^3
wb	Wet basis
y_i	Molar fraction of the i
λ_k	Lagrange coefficient for the element k
μm	Micron or micrometer(length unit)

1 INTRODUCTION

1.1 A NEED FOR RENEWABLE ENERGY

Energy is economically crucial for every industrialized country's economy. For a large majority, the dependence on foreign oil has been an important concern, particularly since the 1970s when an oil shortage generated a near crisis situation for all countries in the entire developed world. Today more than ever and despite all the protections taken to prevent a highly fluctuating market, international politics are affected by this aspect of foreign dependence.

The present effects of terrorism and instability of the large world oil reserve countries of the Middle East raise further concerns about the supply stability. Chaotic markets lead to high prices and slowing the economy in developed countries.

In the rural United States, like here in Oklahoma, the effect of the production decline has already impacted the economy. Major oil companies are leaving the state, relocating to bigger cities to manage economic difficulties.

The recent discovery of an increase in greenhouse gases levels, especially CO_2, in the earth's atmosphere since the industrial revolution, raises concerns regarding the quality of life for future generations. In order to stabilize the concentration of these gases in the atmosphere and prevent potential interferences with climate change, 169 nations ratified the Kyoto protocol and committed to reduce their emission of CO_2 from fossil fuel combustion.

History shows that when absence of readily available oil becomes a problem, countries begin investigating alternatives to fossil fuel. During World War II the Fischer-Tropsch process was used to convert synthesis gas to liquid fuel. This process is being re-examined.

Renewable energy sources could be one solution to many of the problems discussed above. One such energy source is ethanol. The availability of developing technologies producing ethanol, with low environmental impact, makes it an increasingly attractive fuel option.

Ethanol has been produced for thousands of years dating from the time of the Pharaohs. Today, fuel-grade ethanol is industrially produced from simple sugars and yeast fermentation. This process generates large quantities of byproducts once considered as a waste, most being of cellulosic nature.

These agricultural wastes are called biomass. The use of biomass to produce fuel-grade ethanol through enzymatic preparation and fermentation is currently being studied, but preparation processes of the biomass are expensive and technologically challenging.

The solution could be in the implementing of an innovative process that can bypass these technological challenges, and produce ethanol from a different type of fermentation by transforming the biomass feedstock through a simple, low cost process, i.e. using gasification to produce a gas that can then be fermented.

1.2 AN INNOVATIVE NEW PROCESS AND ITS CHALLENGES

In the gasification-fermentation process low cost biomass is gasified producing a producer gas, a mix of elemental gases that includes hydrogen and carbon monoxide, which is the primary focus of this study. These are fed through an anaerobic fermentor, containing a unique Clostridial bacterium currently named C. Carboxidivorans ($P7^T$), first obtained from an agricultural lagoon, and provided by Dr. Tanner at University of Oklahoma (Lewis et al., 2002). Hydrogen and carbon monoxide are then converted to ethanol and other valuable products, including acetic acid, butanol and butyric acid. The presence of oxygen, nitrous oxides, ammonia or tars in the gas is inhibitive and possibly toxic to the microorganisms depending on concentration levels.

Previous research shows the feasibility of this process from mixed clean bottled gases (Ghady, 1992, Klasson et al., 1992, Lewis et al., 2002). No research has been published evaluating the impact of the gas quality from a gasifier on an anaerobic fermentor. At present, there is no single source of technical information that provides effective guidance concerning the specialized requirements of such a process.

The tremendous advantages of this process over all other ethanol producing technologies is not only the low cost of the biomass utilized as the feedstock but also the process simplicity, resulting in low production costs. Previous research indicates that this process is technically feasible, its overall environmental impact on greenhouse gas CO_2 would be positive, and it is economically competitive (Lewis et al., 2002). Such a process would reduce dependency on foreign oil. This process would not increase greenhouse gases emissions since the biomass does not have a fossil fuel origin. This process would

improve rural economies by offering a new revenue source, and help rural oil producers on the decline to stay in the energy production market by switching from fossil energy oil to energy crop production and conversion. It would enhance economic development, as poorly utilized land would be given economic value by becoming productive.

1.3 OBJECTIVES

The overall objective of this study is to measure the quality and quantity of producer gas generated from the gasification of various kinds of biomass (low-cost biomass, agricultural, and industrial waste) in a 25-cm diameter, fluidized bed, pilot-scale atmospheric gasifier. Results of this study are important to the overall gasification-fermentation project in that the gas generated is fed into a bioreactor for conversion into ethanol. The bioconversion process, i.e. converting gas to ethanol, is highly dependent on gas composition.

It is important to understand what parameters influence the quality of the gas used in this fermentation. In this study, a number of gasification parameters will be varied, including biomass compositions, gasifying agents, biomass-to-agent ratios, and operating temperatures to determine the quality and quantity of a representative range of gas and tar compounds. This study will also provide information on the removal of possible contaminants by separating these compounds from the gas stream.

The decision to use a fluidized bed gasifier was made prior to this study. Fluidized bed gasifiers have a high heat and mass transfer rates and an efficient mixing. They are easily scalable and are well suited for lignocellulosic feedstocks. The pilot-scale fluidized bed air gasifier at Oklahoma State University was constructed utilizing an initial design

developed by Carbon Energy Technology, Inc. and the Center for Coal and the Environment at Iowa State University. It is important to note that the gasifier, as originally designed, did not operate efficiently with the biomass used in this study and lacked several systems necessary to measure gasification parameters.

Specific objectives of the gasification study are:

1. Design and develop the modifications of an existing fluidized bed gasifier, including a cleaning, cooling and storage system, to improve generated gas quantity and quality.
2. Develop an analytical procedure to identify major tar compounds using various feedstocks and process modes.
3. Evaluate the products of gasification from selected scenarios:
    A. Evaluate the effect of feed moisture content during air gasification of switchgrass.
    B. Air gasification of switchgrass, corn gluten, and bermudagrass.
    C. Low equivalence ratio (ER) flaming pyrolytic gasification of switchgrass, corn gluten, and bermudagrass.
    D. Steam gasification of switchgrass, corn gluten, and bermudagrass at different steam to carbon ratios (S/C).
4. Model the gasification equilibrium with the different gasifying agents and operating temperatures.

1.4 REVIEW OF LITERATURE

1.4.1 Fluidized Bed Gasification

There are several existing technologies available for atmospheric gasification. These technologies can be classified in four major groups: fixed bed updraft, fixed bed downdraft, bubbling fluidized bed and circulating fluidized bed.

An updraft gasifier is a counter flow unit where the air is introduced at the bottom and the feed at the top. The incoming air at the bottom of the unit first totally combusts the outgoing char. Resulting hot gases then pass through the above feed bed where reduction takes place and reduces the moisture content of the entering biomass. The major disadvantage of an updraft gasifier is that it produces large quantities of tar in gas. (Klass, 1998; and Reed, 1981)

Downdraft gasifiers use co-current flows, where air and low moisture feed are both introduced at the top of the reactor where ignition occurs. The hot pyrolysis gas flows downward and reacts through the char bed. This process produces virtually no tar but often with far more unconverted char than other gasifier types. (Klass, 1998; and Reed, 1981)

A bubbling fluidized bed gasifier consists of a cylinder of fine inert particulates of silica sand or alumina, selected for size, density and thermal properties, resting on a perforated plate. The agent (air, steam or oxygen) is forced below the plate and through the bed. At a certain velocity (often minimum fluidization velocity), all bed particulates become suspended in the agent stream, resulting in the bed behaving like a fluid. Bubbling fluidization will occur depending on the nature of the particulate and stream

velocity. The feed is forced through the preheated fluidized bed where friction reduces the biomass ensuring good heat transfer. The advantages of this type of gasifier are numerous, it accepts a wide range of fuel size, has a uniform temperature distribution, provides high rate of heat transfer, and performs at a high conversion rate with low levels of tar and unconverted char. (Klass, 1998; and Reed, 1981)

Circulating fluidized beds use higher gas velocities than bubbling bed resulting in elutriation of the bed particles and char that are separated from the gas stream outlet with a cyclone and recirculated into the bed. It has many of the advantages of the bubbling fluidized bed and is suitable for rapid reactions though with a less efficient heat exchange. Their major disadvantage is the complexity of operation and the internal erosion at high recirculation rates. (Klass, 1998; and Reed, 1981)

The gasifier currently used for this project is a bubbling fluidized bed reactor, which has been used in numerous applications (Narvaez et al., 1996). Fluidized bed reactors provide excellent mixing characteristics, high mass transfer reaction rates between gas and solid mixtures, and are one of the most reliable methods available for feedstocks that are prone to agglomeration in other types of gasifiers. Fluidized bed reactors are also unique in that biomass fuel of any particle size or moisture content can be gasified, thus accommodating a large variety of fuel types (Reed, 1981). In addition, fluidized bed reactors can be scaled up with considerable confidence (Natarajan et al., 1998). Because of better mixing properties and better temperature homogenization, fluidized bed gasifiers are less prone to generate high levels of tar than other gasifier types. This wide range of accommodations makes it a great candidate for this bioconversion project.

1.4.2 Gasification Parameters

1.4.2.1 Agents

Typical gasifying agents include air, steam, and steam plus oxygen mixtures. The composition of the raw gas produced depends on the gasifying agent used and the gasifier operating conditions. In this study, oxygen will not be considered. The cost of oxygen makes the process uneconomical (Gil et al., 1997).

Air is the most commonly used agent at demonstration and commercial scales (Gil et al., 1997). With the use of air, the reaction is exothermic and temperature-wise self-sustainable. The flue gas from the air process is called producer gas and typically contains a large fraction of N_2, along with CO, CO_2, H_2, CH_4, water, tars, and higher hydrocarbons. N_2 is an inert gas in this process, representing about 50% of the producer gas, but it could contribute to the generation of trace amounts of toxic NO_X and NH_3 (Cooper et al., 1986) . This volume of N_2 is costly in the cleaning and compressing stages of the process since it cannot be separated from the mix.

Furthermore, producer gas fermentation is mass transfer limited because at mild temperatures (bioreactor temperature of 35°C), CO and H_2 , the main constituents of producer gas have aqueous solubilities of 77% and 68% that of O_2 on a molar basis, respectively. These low solubilities result in low concentration driving forces, and, hence low volumetric mass transfer rates to the bioreactor media (Bredwell et al., 1998; Worden et al., 1997; Bredwell et al., 1995). The presence of N_2 greatly reduces the partial pressures of CO and H_2 in the gas, which reduces even further the mass transfer driving forces from the gas to the bioreactor media. Klasson et al. (1992) conducted a study which involved CO uptake rate with time using various initial CO partial pressure. Their

finding shows an increase in the rate of the reaction with an increase in the CO partial pressures.

When steam is used as the gasifying agent, the flue gas from the steam process is called synthesis gas or syngas, and does not contain N_2, thus increasing the partial pressures of other important constituents such as H_2, CO, and CO_2 (Klasson et al., 1992). While this gas is of higher heating value, steam gasification is an endothermic process, i.e. not self-sustainable and thus requiring heat. The heat could be supplied via a separate reactor where the char produced in the steam process is burned such as the Battelle-Columbus demonstration unit in Vermont (Gil et al., 1997). Although the char could be used to provide heat to our fluidized bed reactor, electric heaters were added to the bed for experimental purposes, as demonstrated by Dr. R. Bailie (Environmental Energy Engineering, Inc.) in 1979 (Reed, 1981).

In oxygen steam gasification, exothermic partial oxidation reactions of carbon with oxygen provide the heat required by endothermic steam reactions of carbon with water, therefore maintaining thermal balance. In this study, steam gasification (without oxygen) will be examined and heat will be provided electrically. Klass (1998) discussed the steam to carbon ratio. He stated that in oxygen steam gasification the hypothetical amount of oxygen required is 0.27 mol/mol of carbon and the amount of steam is 0.45 mol/mol of carbon. Selection of the temperature, pressure, reactant and recycle product feed rates, reaction times, and oxygen-steam ratios can favor certain reactions and products. The oxygen-steam ratio to maintain zero net enthalpy depends on pressure and temperature conditions. At lower temperatures, the oxygen-steam ratio value doubles for each 100K in temperature increase, and increases much less at higher temperatures above

about 1200°C. CO and H_2 tend to be maximized at lower pressures and high temperatures, according to the following reactions:

$$C + H_2O \rightarrow CO + H_2 \quad \textbf{(1.1)}$$

$$C + 0.5\ O_2 \rightarrow CO \quad \textbf{(1.2)}$$

1.4.2.2 Equivalence Ratio

The theory of gasification process design thermally balances endothermic and exothermic reactions. Carbon, oxygen, and/or steam feed rates are controlled to balance heat requirements of the design with or without heat inputs (Reed, 1981).

According to Reed (1981), the equivalence ratio (ER) for air-blown gasification should be between 0.2 and 0.4 for maximum chemical energy conversion into producer gas. His studies found the optimum for gasification of wood to be 0.255. Equivalence ratio (ER) is defined as:

$$ER = \frac{Weight\ of\ \ oxidant\ /\ weight\ of\ \ dry\ biomass}{Stoichiometric\ oxidant\ /\ dry\ biomass\ ratio} \quad \textbf{(1.3)}$$

In his intent to establish a roadmap to biomass pyrolysis, gasification and combustion, Reed (1981) defines these three ideal processes. ER conditions are shown on an ER diagram by three points P, G, and C as shown in Figure 1.1.

For Reed (1981), pure pyrolytic gasification (P) necessitates external heat and operates at 450 to 600°C. It produces a high heating value gas plus 20 to 30% free carbon and 30% of a low temperature tar. Isothermal or conventional gasification (G) occurs at approximately 0.25 ER and produces gases like CO and H_2 with relatively small amounts of free carbon. Reed defines the FP area as flaming pyrolytic gasification a zone between pure pyrolytic gasification or pyrolysis (P) and isothermal gasification (G). It uses

smaller amounts of O_2 than conventional gasification passing through a bed of biomass at 700°C producing a flammable gas tar and free carbon. As ER increases, the temperature reaches a maximum at (C) point of stoichiometric combustion.

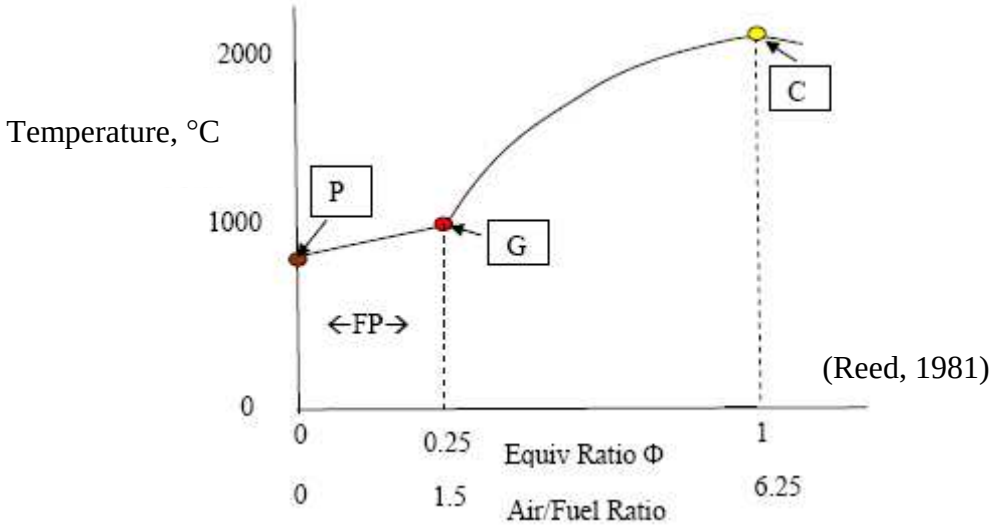

Figure 1.1 Equivalence ratio and air fuel diagram (Air/Fuel values shown for biomass)

1.4.2.3 Operating temperature

Gasification process temperatures also have a significant effect on combustion products. In fluidized bed studies using sawdust as the feedstock, researchers found that the quantities of all four major components in the producer gas, i.e. CO, CO_2, H_2, and CH_4, were affected by temperature (Wang and Kinoshita, 1992). As bed temperature was raised from 700°C to 900°C, CO and H_2 increased while levels of CO_2 and CH_4 decreased. Research involving the gasification of sugarcane bagasse indicated that as the operating temperature was increased from 600 to 900°C, the quantity of H_2 increased, but the other three main components (CO, CO_2, and CH_4) remained fairly constant (Gomez et al., 1998). Similar studies have also shown that increasing the operating temperature increases the total gas yield during gasification (Natarajan et al., 1998; Gil et al., 1997).

1.4.2.4 Feedstock

1.4.2.4.1 Type

Gasification of biomass in fluidized beds has been studied for many years. Numerous works exist involving gasification of various feedstocks such as sawdust, woodchips, sugarcane bagasse, and solid waste (Narvaez et al., 1996; Natarajan et al., 1998; Wang and Kinoshita, 1992; Gomez et al., 1998; Klass, 1998; and Reed, 1981).

1.4.2.4.2 Moisture content

Klass (1998) and Reed (1981) mention that biomass feedstock moisture content is an important parameter to be considered. Moisture content has been shown to have a significant effect on the composition of the resulting producer or synthesis gas and the temperature of the process. A moisture content of 15%wb is generally recognized as the optimum for efficient thermochemical gasification of biomass (Klass, 1998 and Reed, 1981). A low moisture content biomass saves appreciable energy in later processing. Exceptions are made in steam gasification in which water is one of the process feed materials. According to Narvaez et al. (1996), studies with sawdust have shown that an increased moisture content in the feed increases the H_2 content of the gas, while decreasing the quantity of tar present. The added water seems to enhance both the steam reforming and the water-gas shift reactions, but may decrease the temperature of the steady state process for the same run conditions.

1.4.2.5 Tar

The presence of condensable organic compounds in the producer or synthesis gas renders the gasification technologies unsuitable for specific applications. Tars condense at reduced temperatures blocking and fouling process equipment such as engines and turbines (Klass, 1998).

In our situation, the lack of literature on the unique microorganism, P7, used in this bioconversion project forces us to consider that most organic compounds could have a toxic effect. Recent bioreactor experiments have shown that tar can have an adverse effect on the microorganism and that poor gas cleaning will inhibit biochemical pathways (Lewis et al., 2002).

There is currently no standard analytical procedure for tar measurement. However, a draft for such a standard (Energy project ERK6-CT1999-20002 (Tar protocol): www.tarweb.net) has been elaborated. The guidelines for sampling and analysis of tar and particles in biomass producer gases are available in Appendix 8.3. These guidelines have been prepared by representatives from the following organizations:

-European Commission (DGXII)

-Netherlands Agency for Energy and the Environment (NOVEM)

-Swiss Federal Office of Education and Science

-Danish Energy Agency (Energistyrelsen)

-US Department of Energy (DOE)

-National Resources Canada.

1.4.3 Gasification Chemistry and Modeling

1.4.3.1 Mechanism of gasification

Reed (1981) describes the mechanism of biomass pyrolysis and gasification. He suggests that biomass and heat alone result in char. There must be a change in composition if biomass is to be completely gasified. The heat and mass flows during biomass gasification are illustrated in Figure 1.2.

Process:	Drying	Primary pyrolysis	Secondary pyrolysis	Char gasification	Char combustion
Temp°C:	<120	200-600	300-800	800-1100	800-1500

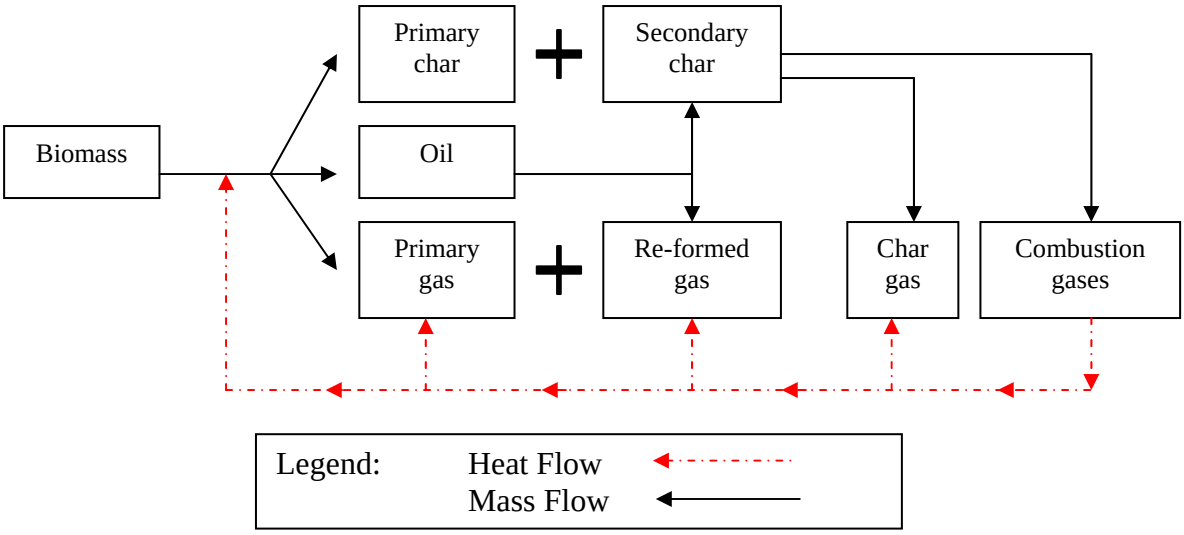

Figure 1.2 Heat and mass flow in biomass pyrolysis and gasification

Reed (1981) divides the mechanism of char gasification (principally composed of carbon) into five sequential steps:

1. Diffusion of reactants to the char external surface through the surrounding stagnant film;
2. Pore diffusion of gas inside the particle;
3. Adsorption, surface reactions, and desorption on the pore walls and/or on the external surface;
4. Diffusion of products outside the pores; and
5. Diffusion of products through the stagnant film.

1.4.3.2 Gasification chemistry

In the case of fluidized bed reactors, steps 2, 3 and 4 of char gasification are minimized because the fluidized bed, with sand as a media, has a constant mechanical grinding effect on char particles. Porosity of the char and gas diffusion have a negligible effect on the reactions.

Most gasification reactions are reversible, and not all reactants transform into products. At certain concentrations, the rates of the forward and reverse reactions reach a dynamic equilibrium, defining the kinetics of the reactions involved.

The chemistry of biomass gasification involves different chemical reactions depending on the process parameters (D.L. Klass, 1998):

Partial oxidation (air gasification)	Enthalpy	
$C_6H_{10}O_5 + 0.5\ O_2 \rightarrow 5\ H_2 + 6\ CO$	(96 kJ @ 1000K)	(1.4)
$C_6H_{10}O_5 + O_2 \rightarrow 4\ H_2 + 6\ CO + H_2O$	(-142 kJ @ 1000K)	(1.5)
$C_6H_{10}O_5 + O_2 \rightarrow 5\ H_2 + 5\ CO + CO_2$	(-180 kJ @ 1000K)	(1.6)
$C_6H_{10}O_5 + 1.5\ O_2 \rightarrow 3\ H_2 + 6\ CO + 2\ H_2O$	(-389 kJ @ 1000K)	(1.7)
$C_6H_{10}O_5 + 1.5\ O_2 \rightarrow 5\ H_2 + 4\ CO + 2\ CO_2$	(-464 kJ @ 1000K)	(1.8)
$C_6H_{10}O_5 + 2\ O_2 \rightarrow 5\ H_2 + 3\ CO + 3\ CO_2$	(-745 kJ @ 1000K)	(1.9)

Pyrolysis	Enthalpy	
$C_6H_{10}O_5 \rightarrow 5\ H_2 + 5CO + C$	(209 kJ @ 1000K)	(1.10)
$C_6H_{10}O_5 \rightarrow 3H_2 + 5CO + CH_4$	(120 kJ @ 1000K)	(1.11)
$C_6H_{10}O_5 \rightarrow 2H_2 + 4CO + CH_4 + H_2O + C$	(-16 kJ @ 1000K)	(1.12)
$C_6H_{10}O_5 \rightarrow H_2 + 3CO + 2CH_4 + CO_2$	(-140 kJ @ 1000K)	(1.13)
$C_6H_{10}O_5 \rightarrow H_2 + 3CO + CH_4 + 2H_2O + 2C$	(-152 kJ @ 1000K)	(1.14)
$C_6H_{10}O_5 \rightarrow 2CO + 2CH_4 + CO_2 + H_2O + C$	(-276 kJ @ 1000K)	(1.15)

Steam gasification	Enthalpy	
$C_6H_{10}O_5 + H_2O \rightarrow 6\ H_2 + 6\ CO$	(322 kJ @ 1000K)	(1.16)
$C_6H_{10}O_5 + 2\ H_2O \rightarrow 7\ H_2 + 5\ CO + CO_2$	(310 kJ @ 1000K)	(1.17)
$C_6H_{10}O_5 + 3\ H_2O \rightarrow 8\ H_2 + 4\ CO + 2\ CO_2$	(276 kJ @ 1000K)	(1.18)
$C_6H_{10}O_5 + 7\ H_2O \rightarrow 12\ H_2 + 6\ CO_2$	(137 kJ @ 1000K)	(1.19)
$C_6H_{10}O_5 + H_2O \rightarrow 4\ H_2 + 4\ CO + CO_2 + CH_4$	(85 kJ @ 1000K)	(1.20)
$C_6H_{10}O_5 + H_2O \rightarrow 2\ H_2 + 2\ CO + 2\ CO_2 + 2\ CH_4$	(-175 kJ @ 1000K)	(1.21)

1.4.3.3 Modeling

Ciesielczy and Gawdzik (1994) developed a two-phase model taking the non-isothermal character of coal gasification and the bubble growth into account. The bed is divided into compartments in which the bubble level is assumed to be constant.

Several models for the bubbling fluidized bed hydrodynamics have been extensively used for coal combustion. To model the description of the hydrodynamic behavior of the bubbling bed, Werther (1980) assumes the existence of a film between the bubble and the emulsion phase, i.e. buffer zone. Marias et al. (2001) assumes that the zone above the bed is divided in two perfectly stirred regions. The first zone is just above the bed where the bubbles burst out of the bed and still contain solid particles, i.e. disengagement zone. Milioli and Foster (1995) evaluated the amount of sand and fuel material in this zone. Above the disengagement zone is a second perfectly stirred zone where homogeneous gas combustion is taking place, i.e. post-combustion zone. These zones are displayed in Figure 1.3. The model assumes three sources for heat generation: homogeneous combustion of volatile, heterogeneous combustion of biomass particles, and heat transfer with sand and char.

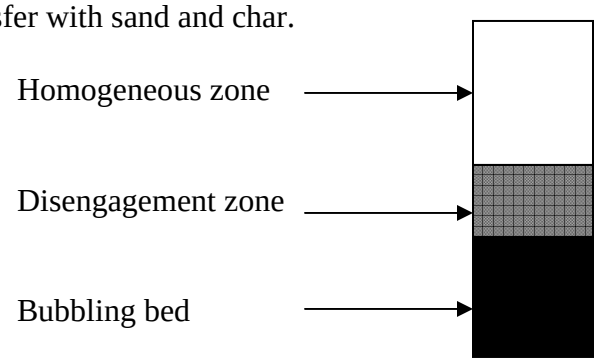

Figure 1.3 Modeling of a fluidized bed gasifier

Sadaka et al. (2002) developed a two-phase model dividing the bed into three zones: jetting, bubbling, and slugging. For each zone, hydrodynamics, transport and

thermodynamic properties were included. Researchers assumed that the devolatilization is instantaneous and considered the major compounds in his gasification model to be: H_2, CO, CO_2, H_2O, CH_4, O_2, N_2, char, and tar in two reacting systems. The first reacting system is the bubble phase with a single gas phase. The second reacting system is the emulsion phase with a solid carbon phase in addition to the gas phase. Sadaka et al. (2002) approximated the tar yield according to an empirical equation developed from four data points from the steam gasification of straw from Corella et al. (1989) as:

$$Tar_y = 3598 * e^{-0.0029*Ts} \quad \textbf{(1.22)}$$

where T_s is average temperature (K) of the particles. The model then approximates tar and C_2 compounds as CH_4. This approximation does not change the overall results.

To find a solution to the differential equations of the model, Sadaka et al. (2002) divides the bed into multiple control volumes. Solutions are calculated numerically by using the finite element method solving for heat and mass transfer and equilibrium by minimization of the Gibbs enthalpy of the system.

Because of the numerous previously mentioned approximations involved in the modeling of the gasification of biomass, this study will focus instead on modeling the equilibrium of biomass gasification at temperatures between 600°C and 900°C, where most of the primary pyrolysis reactions are minimal. The intent is to model the gasification parameters and products concentrations on a wide range of equivalence ratios between 0 and 0.4 in the most pertinent temperature range for gasification between 700°C and 900°C. The mathematical model used in this study is an equilibrium reactor; i.e. a Gibbs reactor model, taking solid carbon and tar into account.

2 RESEARCH DESIGN

The present research involves the gasification of various biomass feedstocks for which all producer gas characteristics are yet unknown. The gasification process is an integral part of the further development of a bioconversion technology. It is important to characterize, quantitatively and qualitatively the gas and byproducts generated during the gasification process.

The conversion of producer or synthesis gas from biomass gasification to ethanol has not been extensively investigated to date. Although many experiments have been made with bottled gas, few (none in the literature) have ever used actual producer or synthesis gas from a gasifier through an anaerobic fermentor. Traces of toxic compounds created during the gasification could inhibit biochemical pathways for the production of valuable products and/or harm the microorganism (Lewis et al., 2002). To further understand the overall process, experimentation on the gasification feedstocks, agents, parameters, and toxic hydrocarbons reforming and/or removal are necessary.

The first step of this study was to design and develop the modifications for an existing fluidized bed gasification system in order to conduct experiments in steady state atmospheric air gasification, flaming pyrolytic gasification and steam gasification of low cost biomass (switchgrass, bermudagrass, and corn gluten). For this purpose, the modified pilot plant includes a computerized control and data collection system, a temperature controlled gas-sampling system, and a scrubbing and storage system.

2.1 INITIAL DESIGN

The pilot-scale fluidized bed air gasifier at Oklahoma State University, from an initial design developed by Carbon Energy Technology, Inc. and the Center for Coal and the Environment at Iowa State University, consists of a fuel hopper, feed auger, injection auger, reactor, and ignition system. A schematic of the initial system is shown in Figure 2.1.

The fluidized-bed reactor is 25-cm in diameter and is constructed of mild steel with a 5-cm refractory lining. The bed is 30-cm high and consists of sand particles with a geometric mean diameter of approximately 900 μm. The air, supplied by piston compressors, is injected into the plenum underneath the distribution plate at a volumetric flow rate of 0.4 m^3/min. Air is fed through the bottom of the bed through a distribution plate which has 177 uniformly spaced 2-mm holes. A manually controlled metering auger pushes the material from the bottom of the mixed bin directly into a perpendicular injection auger, which rotates at constant high speed, and pushes the biomass into the reactor bed. During startup only, the bed is preheated with propane gas up to 800°C in temperature. The biomass material is gasified as it enters the high temperature fluidized bed.

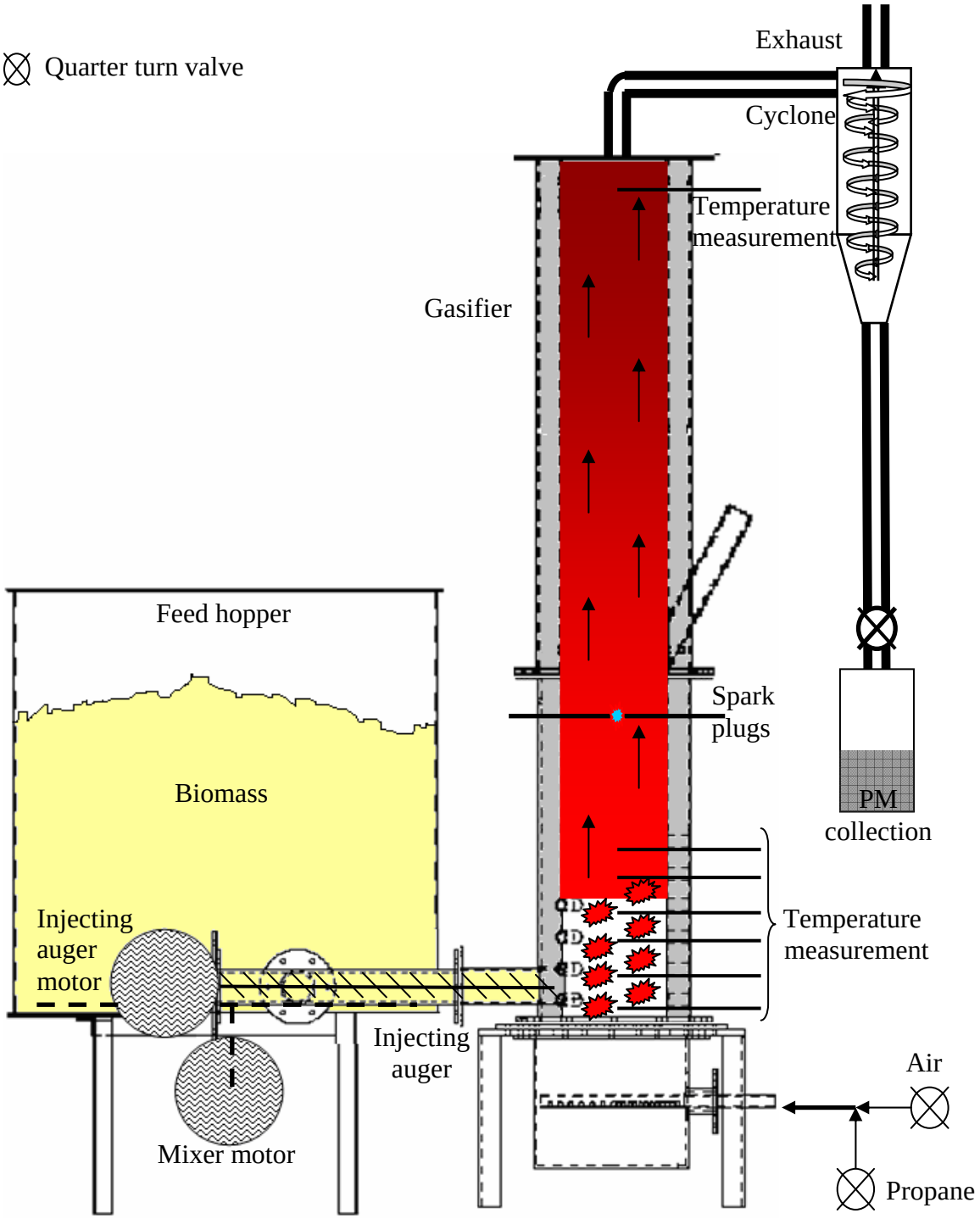

Figure 2.1 Fluidized bed air gasifier initial design schematic

The producer gas exits at the top of the gasifier where it is centrifuged through a 13-cm diameter cyclone. Ashes are collected at the bottom of the cyclone in a stainless steel container.

This design functioned correctly and provided producer gas. However several difficulties were experienced in the areas of startup, data recording, ash collection, process control and biomass feeding. Modifications were necessary to overcome these difficulties.

2.2 GASIFICATION SYSTEM MODIFICATIONS

The initial design was not functional. Therefore several changes to the gasification system were necessary in order to achieve biomass gasification with gas storage. The challenges included correcting feeding system breakdowns, providing heat to the endothermic processes, cleaning the produced gas and setting up process controls and data acquisition systems.

2.2.1 Feeding system

The initial feeding system (Figure 2.2) described in the previous paragraph was able to handle loose non-compressible solids like wood pellets, but the system was unable to function correctly with low density biomass such as chopped grasses. Because of their compressibility, chopped grasses agglomerate, forming plugs through the initial components of the feeding systems.

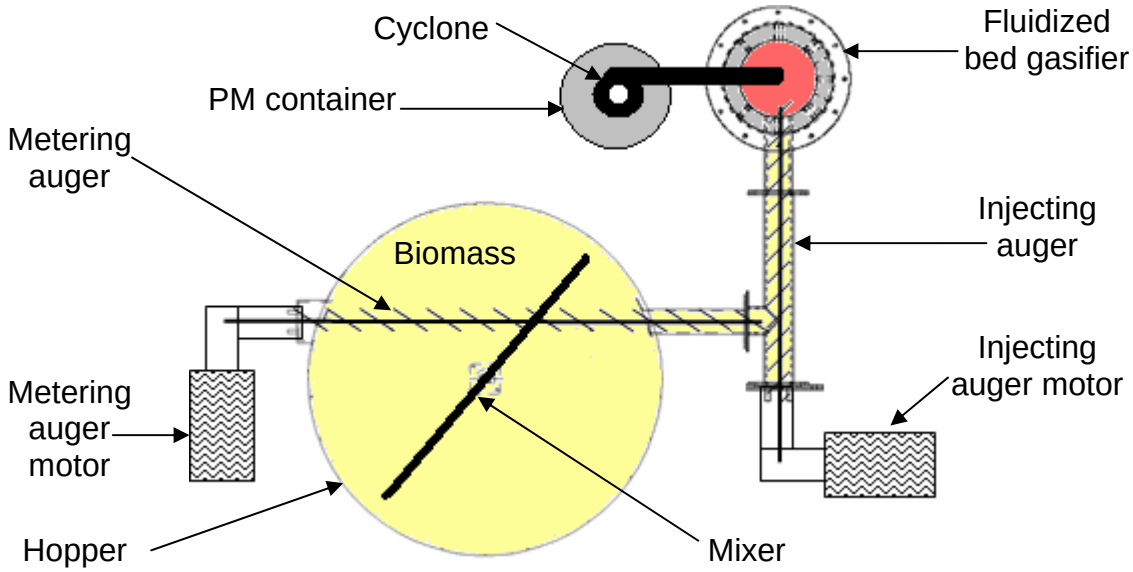

Figure 2.2 Top view of initial feeding system

2.2.2 Mixer

Chopped grasses do not flow consistently. Because of their compressibility and bridging properties, they necessitate constant mixing to loosen them up and avoid bridging around the metering auger.

The mixing system at the bottom of the tank consisted of a 2.5-cm wide square tubing placed across the tank diameter, welded on the end of a rod linked through the tank bottom plate to a worm gear reducer mounted directly under the tank. The torque necessary for the mixing of a full tank of chopped grass was too high for this setup, resulting in breakdowns: broken welds, broken worm-gear reducer and electrical motor overheating.

The square tubing was replaced with a wider 5-cm by 2.5-cm solid metal bar. This new width allows the mixer axle to go through the bar with a system consisting of two metal keys, stronger than the previously used weld. The electrical motor driving the mixer was increased from 0.5hp to 1.0hp. A heavy-duty worm-gear reducer linked to a large double sprocket system with a higher torque capability with a total ratio 875:1 replaces the directly linked worm-gear reducer.

2.2.3 Metering auger

Located at the bottom of the tank, the metering auger exits the bin 5-cm above the bottom through a 7.5-cm diameter housing pipe. This initial system faced intermittent jamming due to the agglomeration of the chopped biomass. When compressed in the metering auger housing, chopped grasses stuck to the auger and formed a hard wood-like

plug. This plug rotated in the housing with the auger, resulting in no forward motion. This plug sometimes reached the injection auger, causing a jam.

Increasing the housing cross section vertically reduced the pressure of the material around the auger, preventing plugging at this location. The 7.5-cm pipe was cut horizontally with the top half raised 2.5-cm. Two 2.5-cm wide plates were welded along each side, resulting in a sleeve with an oval cross section. The added space above the auger allows the biomass to remain loose and flows evenly.

Because the initial feeding system did not allow weight measurements, a correlation of the metering auger rotation i.e. rpm, with the mass flow rate was initially attempted. Due to the compressible nature of chopped grasses, this correlation appeared to be a function of the biomass pressure around the auger at the bottom of the tank, thus a function of the biomass level in the tank. Results did not show sufficient repeatability and were abandoned. This feeding system necessitated a different measurement of the mass flow rate than the metering auger speed. The weight of the entire bin is now measured with a load cell.

2.2.4 Injection auger

In the initial design, a rigid Tee junction existed between the metering auger and the auger that injected the biomass into the reactor bed. At this intersection of the slow moving metering auger and the fast rotating injection auger, material would often form a plug. This rigid junction also prevented an accurate measurement of the small weight variation of the low-density chopped grasses in comparison to the weight of the entire

hopper system. This design also allowed producer gas to back flow into the tank. Weather-stripping was used to prevent gas back draft into the tank was inadequate.

A 20-cm rotary feeder was designed, built and installed on top of the injection auger housing preventing hot gas from back flowing. This new design permits the feed tank to be disconnected from the injection system, allowing the tank to hang free from a load cell for precise weight measurement.

2.2.5 Rotary feeder

The sizing of the rotary feeder (Figure 2.3 and 2.4) is based on the special characteristics of the chopped grass: low density, high bridging capacity, high compressibility.

The material must remain loose all along the feeding system until the sand bed. Lack of data from the literature on the material characteristics of the chopped grass drove the choice for a volumetric flow rate capacity of the rotary valve equal or larger than the metering auger maximum volume capacity.

The capacity of the rotary feeder depends on two design parameters: rotor volume capacity, rotor speed

Increasing the rotor speed would in fact increase the volume flow rate capacity but it would also increase the gas leakage through the feeder.

Solid mass flow rate: $\dot{m}_S = \rho_S \times V_V \times RPM$ **(2.1)**

Rotary feeder gas leakage: $\dot{V}_{Gas} = P_{Ratio} \times V_V \times RPM$ **(2.2)**

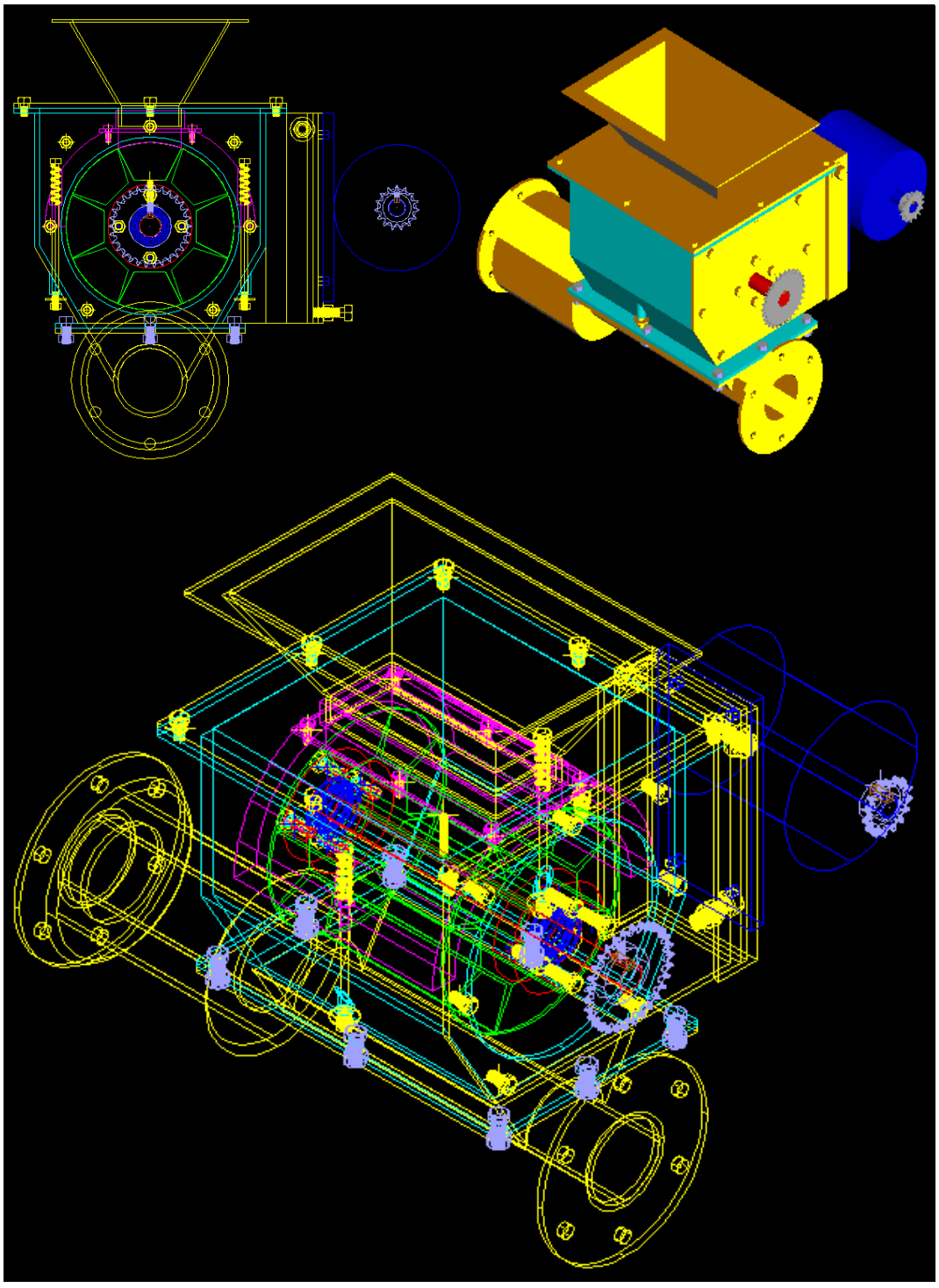

Figure 2.3 Rotary feeder CAD

Figure 2.4 Upgraded feeding system

With

$\dot{m}_S$: solid mass flow rate, m^3/h

ρ_S : solid density, kg/m^3

$\dot{V}_{Gas}$: standard volumetric gas flow rate, m^3/h

V_v : revolving valve volume, m^3

P_{ratio} : feeder inner over outer pressure ratio

RPM : Valve rotation speed, round per minutes

The volume of agent (air or steam) fed to the fluidized bed gasifier pilot is 17 m^3/h in order to sustain minimum fluidization, with an inner pressure of 0.07 atm

(gauge). The maximum mass flow rate of chopped grass achieved by the metering system is 100 kg/h.

Since the width of the inlet was planned to be approximately 1/8 of the perimeter of the valve (8 cavities rotating valve), it was necessary to size the width to a minimum in order to keep the valve diameter small. Lumps of chopped grass formed in the 7.62-cm diameter metering auger housing, which could clog the device inlet. Consequently, the inlet width was sized to 7.62 cm (3 in.), the perimeter of the rotary valve is 61 cm (24 in) and the diameter 20 cm (8 in.).

Considering a lump of chopped grass as a ball and the V shape cavity, only the first half of the lump can enter in the cavity. The depth of the cavity is then 3.8 cm (1.5 in.). Then, the final cavity volume is 502 cm^3 (30.6 in^3) for a revolving volume (V_v) of 4 l (245 in^3). Using equation 2.1, RPM is then 3.2. Using equation 2.2, the theoretical leakage of this airlock is :

$\dot{V}_{Gas}$ = 13.7 l/min = 0.82 m^3/h

To avoid accumulation of tar due to the gas back draft. The airlock is kept under agent pressure (air or steam) equal to the one in the reactor, so that the leak itself does not consist of hot gases and tar.

Because of air leakage through the rotary feeder and the difficulty to quantify this leakage using nitrogen particularly in the case of steam gasification, a different tracer other than nitrogen must be used

As a result, helium is used as the tracer because it has a good response on the GC-TCD for gas analysis and it is easily available. The precision of the flow of tracer must be of the most precise accuracy possible in order to rely on this data for cross calculation of

all gases material balance. As Nitrogen was initially used, the data for the steam gasification process are altered by the airlock leakage high variability.

2.2.6 Disengagement section

A disengagement section (Figure 2.5) built on top of the existing gasifier increases the cross section diameter from 25 to 53 cm before the 2-in. diameter exhaust pipe. This feature allows the main stream velocity to decrease by a ratio of 4.5:1 in order to prevent sand elutriation from the fluidized bed gasifier pilot.

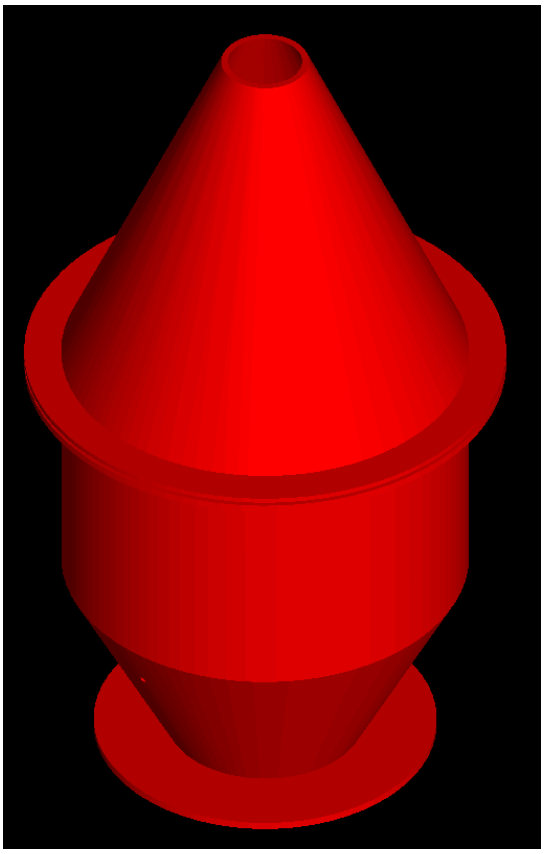

Figure 2.5 Top expansion disengagement section.

2.2.7 Electrical heating systems

Three superposed 7.5 kW electric conic spiral shaped heating elements (Figure 2.6) are installed in the reactor bed to allow the process to sustain bed temperature and act as baffles to prevent slugging. The ends of the elements exit through the gasifier wall for connecting the 3 phase, 208 V electrical circuit in a delta configuration. Each phase is actuated by a 100 A solid-state relay.

Because the minimum-bending radius of these heating elements is 3.8 cm, the baffle heaters are not present in a 7.6-cm diameter cylindrical zone in the bed center. To prevent channeling, three stainless steel grids with 1.25-cm diameter holes are installed in the center of each spiral coil to cover the opened center zone.

Figure 2.6 Baffle heaters in sand bed

2.2.8 Ash collection system

In the initial design, the ash collection system consisted of one cyclone and one stainless steel container, and performed adequately for low tar producing conditions. When the equivalence ratio was reduced, tar condensation in the pipe connecting the cyclone to the stainless steel barrel induced ash agglomeration, and obstruction of the pipe, thus preventing any ash collection.

The long pipe connecting the container to the cyclone required shortening and, the cyclone, to be maintained above tar condensing temperature using electric band heaters. For convenience, a 10-cm rotary airlock (Figure 2.7 and 2.8) was designed and installed 15 cm underneath the cyclone. A second smaller diameter cyclone with an identical airlock is installed in series following the first to collect smaller-sized particulates and enhance gas cleaning. Figures 2.9-11 show the modified fluidized bed gasification process.

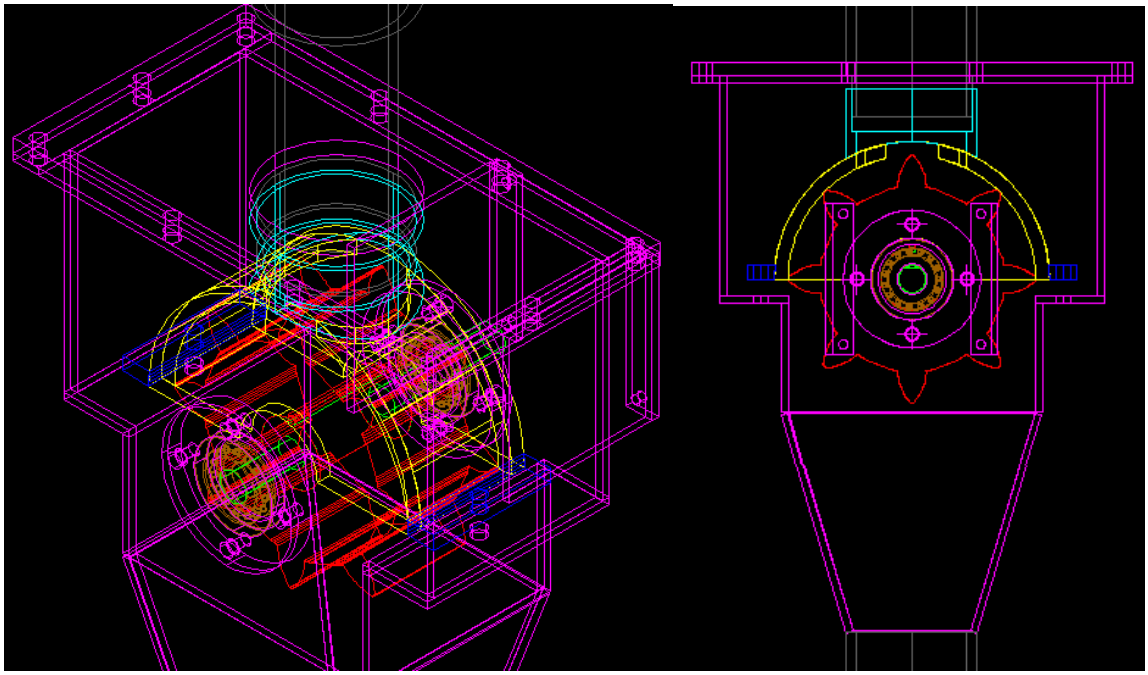

Figure 2.7 Ash collection rotary airlock design

Figure 2.8 Ash collection rotary airlock

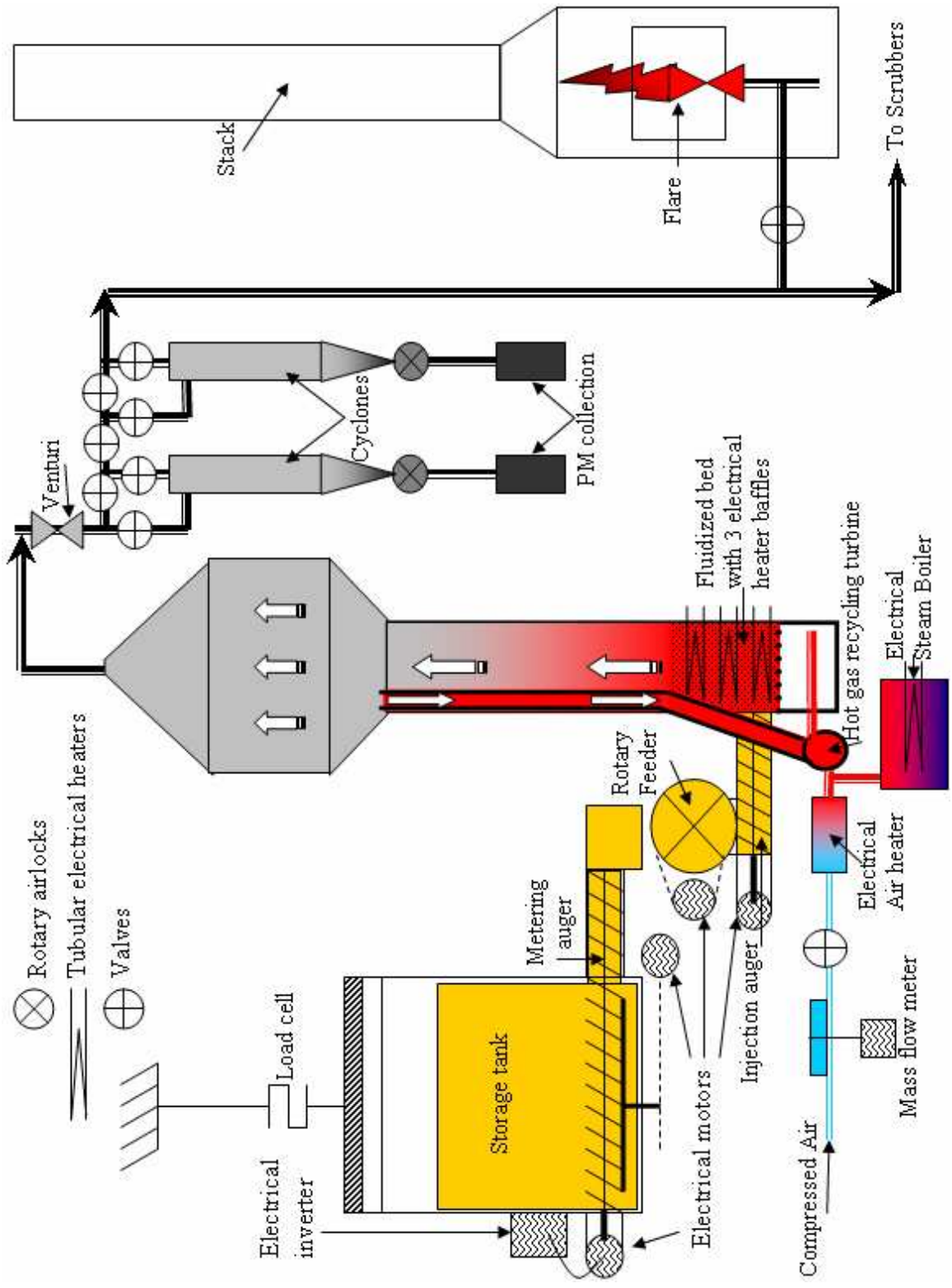

Figure 2.9 Modified fluidized bed gasification process schematic

Figure 2.10 Gasifier pilot plant

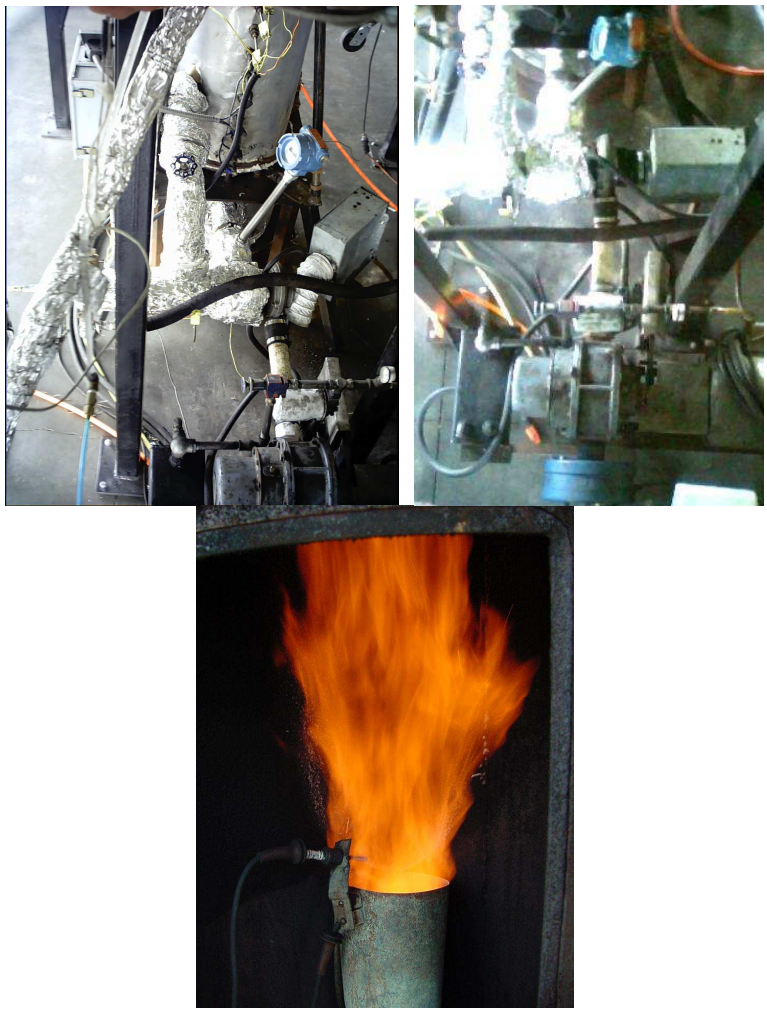

Figure 2.11 Hot gas recycling turbine and lobe blower (left and center) and flare (right)

2.2.9 Scrubbing system

After the two cyclones, the producer gas passes through an ash trap (Figure 2.12) and two vertical scrubbers (Figure 2.13) installed in series. The purpose is to remove the ash and tar from the produced gas.

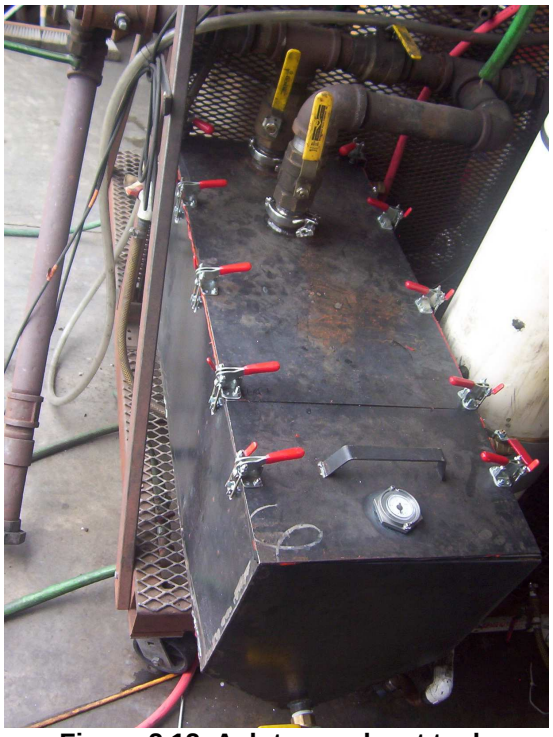

Figure 2.12 Ash trap-solvent tank

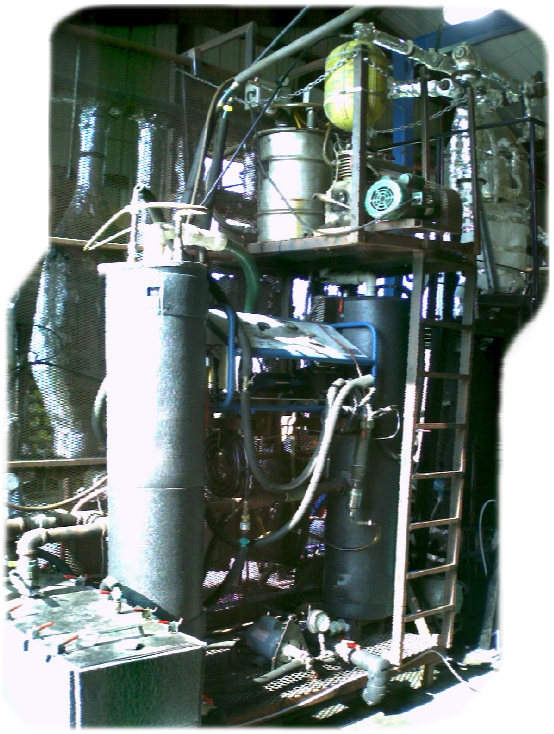

Figure 2.13 Scrubbing unit

The ash trap-solvent tank (Figure 2.12) is composed of a 38-in. L × 16-in. W × 12-in. H_{back} × 19-in. H_{front} container with a sloped bottom filled with solvent. The container is partitioned into two compartments by an open base wall at about ¾ of its length; a bubbling compartment with a copper coil heat exchanger (Figure 2.14) and a decanting compartment Figure 2.16. Gas enters from the top at the rear of the tank and bubbles in the longest partition through a bubbler, a 2-in. diameter, 24 in. long perforated pipe located horizontally at the bottom of that partition (Figure 2.15). Gas exhausts at the top back of this first compartment just in front of the gas inlet. Gas then flows out

towards the first of two scrubbing columns, which are in series. Once wet, ash remains in the solvent and decants at the bottom of the trap under the dividing wall. The solvent flows up behind the wall in the second compartment of the ash trap. Solvent is pumped from the top of the ash trap of the second compartment through a mini aluminum/stainless steel suction strainer, 100 mesh, 10 gpm capacity, 5.625 in. long, by 1.625 in. diameter, cooled through a 3-ton counter current heat exchanger and sprayed at the top of the columns at 3 gpm at 150psi (three nozzles on first column and one on second column).

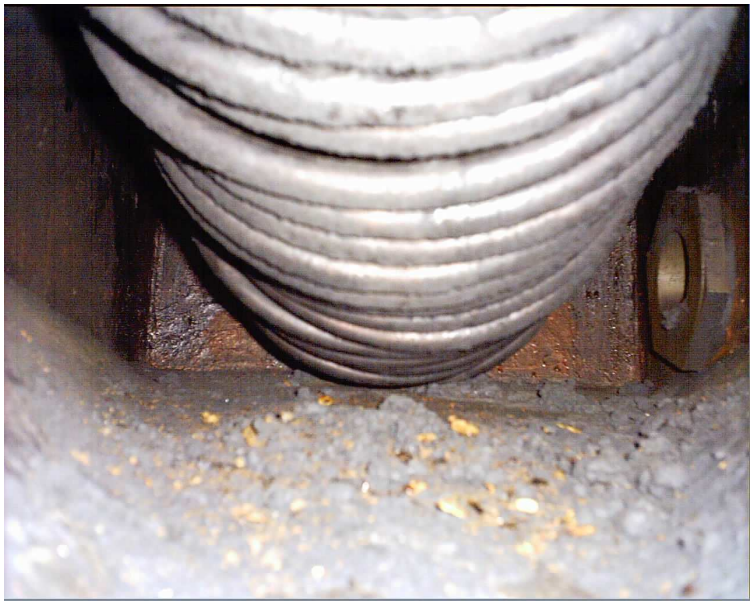

Figure 2.14 Bubbling compartment with heat exchanger

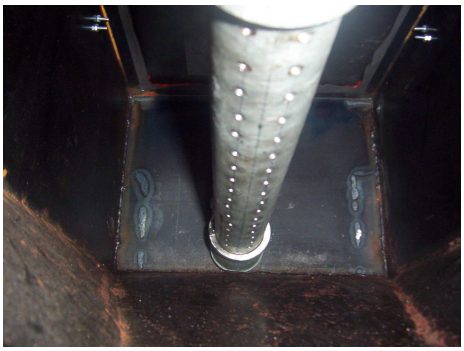

Figure 2.15 Bubbler

Figure 2.16 Strainer

The scrubbing system is composed of two 12-in. diameter columns each packed 4 feet deep with stainless steel pall rings (0.75-in. diameter by 0.75 in. long) with a total approximate exchange area of 41.6 m^2. They are showered with 0°C cold solvent from the column top down through the packed bed counter current to the gas flow. Solvent is collected at the bottom of the columns, and recycled to the ash trap.

Water alone was first used as a cooling media to condense the tar on the packing. Because tar does not dissolve in water, acetone is mixed with the water at a ratio of 20:80 allowing the tar to dissolve in the liquid phase, increasing the scrubbing efficiency. To avoid the evaporation of the acetone into the gas phase the cooling of the liquid phase is essential.

A 10-gal stainless steel drum filled with pall rings has been setup at the column exhaust to avoid droplets of liquid to be carried out downstream. Clean gas then circulates to a compressor-booster unit where it is compressed at 400 psi. The gas passes through a 0.5-ton water-cooled counter current heat exchanger to condense any excess solvent. Located at the outlet of the heat exchanger is a liquid trap with an automatic drain valve to the solvent tank.

Gas is then stored in tanks with 675 liters total capacity. This volume provides over two months of feed for the bench-top bioreactor running at 4 psi and 200 cc/min.

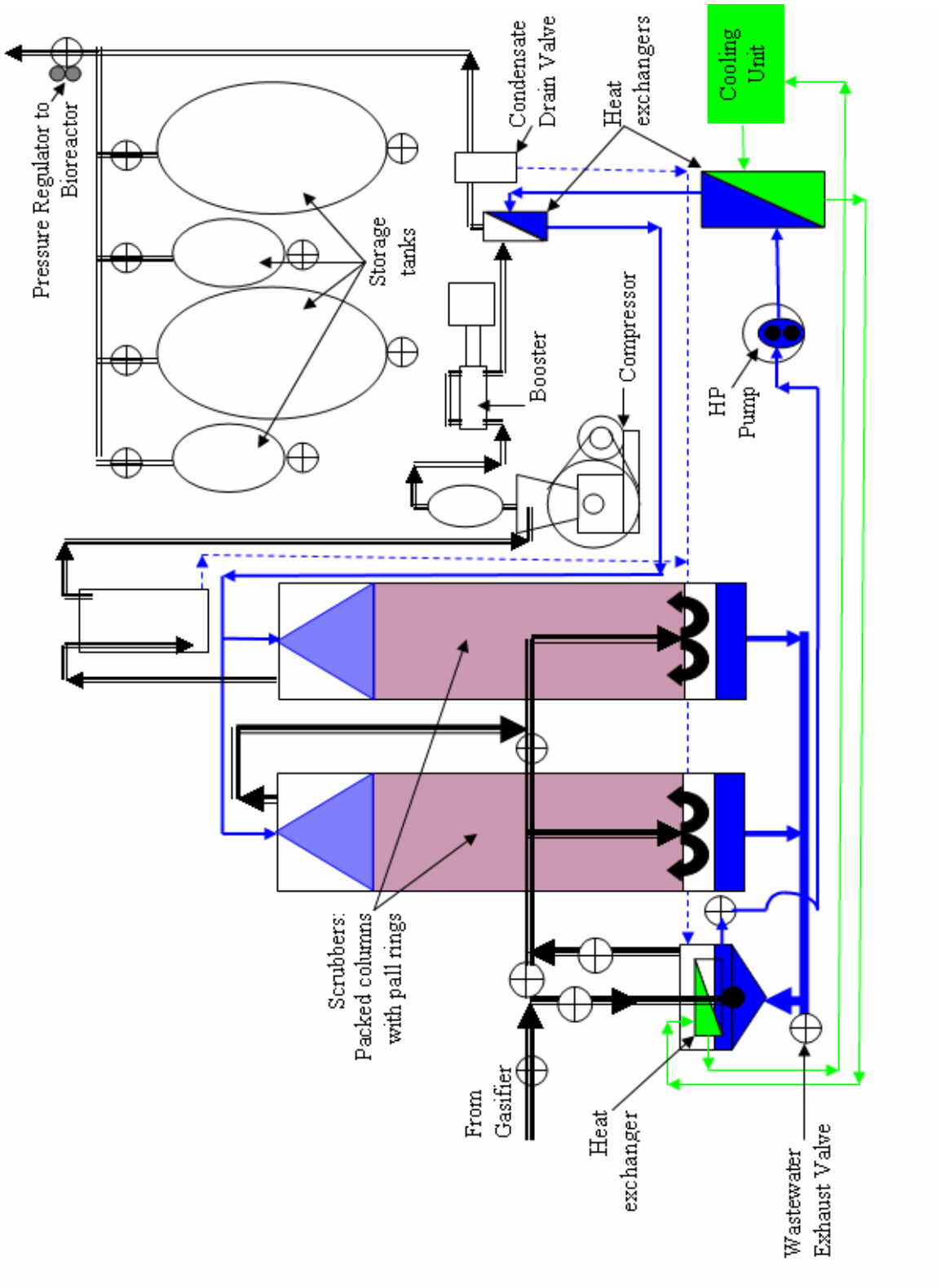

Figure 2.17 Gas scrubbing, compressing and storage system schematic

2.2.10 Data acquisition system and process monitoring

The process is monitored and controlled via numerous sensors, all of which are connected to a computer for process supervision and data acquisition. The SCXI system data interface was purchased from National Instruments, which includes:

- Computer card E-6425 with 2 analog outputs, 5 counters or digital inputs/outputs and 30 analog/thermocouple inputs
- Chassis SCXI 1000
- SCXI 1102 module for all inputs
- SCXI 1180 feed through panel for outputs

2.2.11 Computer program for process control

The programming interface used is National Instruments LabView graphic programming (LabView, 1999). The virtual instrument name is GAS11.vi (Appendix 8.6.1). Its basic principle is a continuous looping program that updates all inputs and outputs every 500 ms. It records all data to a user-chosen file every 10s. It is programmed to automatically control biomass input, air input, and process temperature. Figure 2.18 explains the various functions of the subprograms found in Gas11.vi. The program's control panel is shown on Figures 2.19 and 2.20.

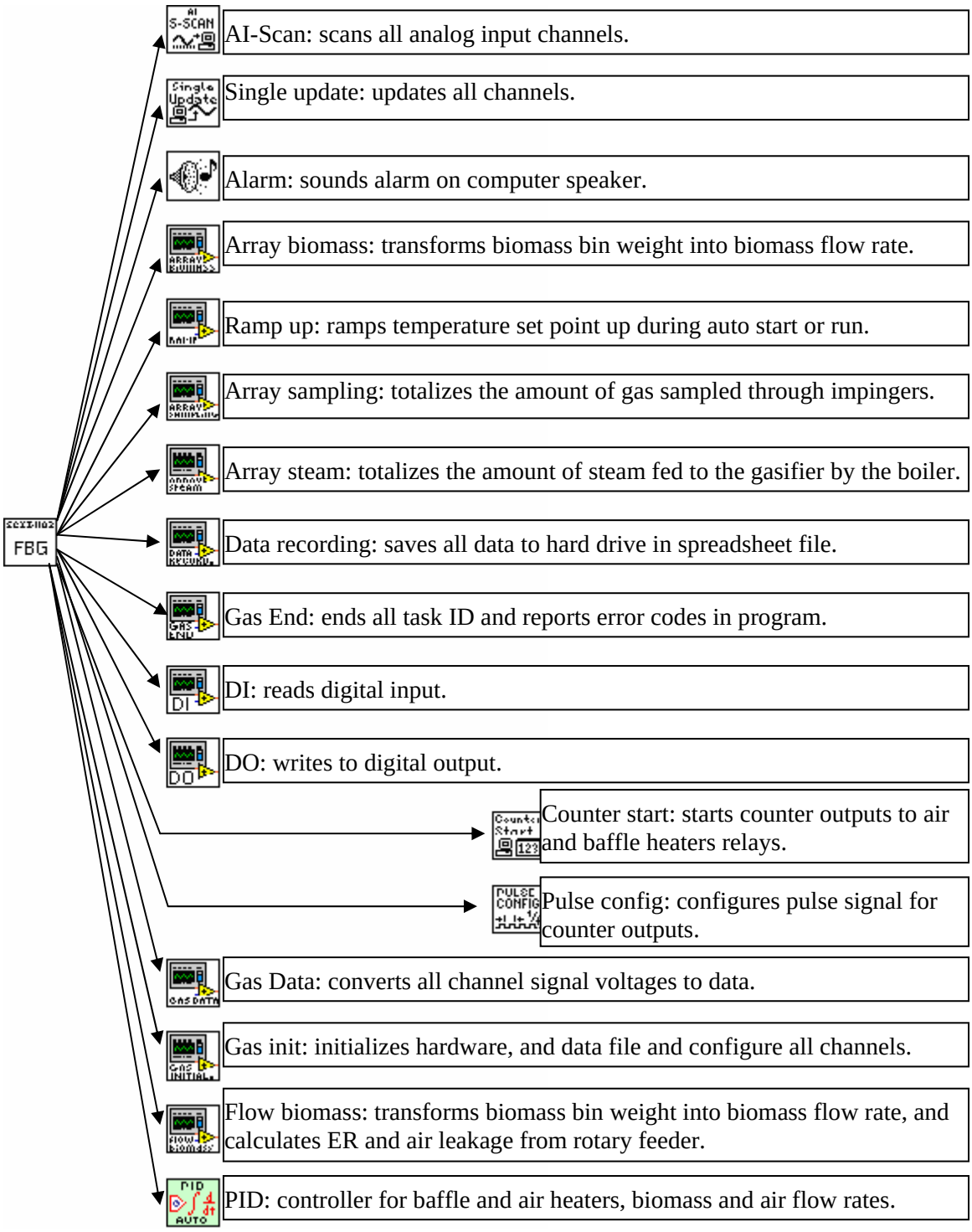

Figure 2.18 VIs hierarchy in the main program

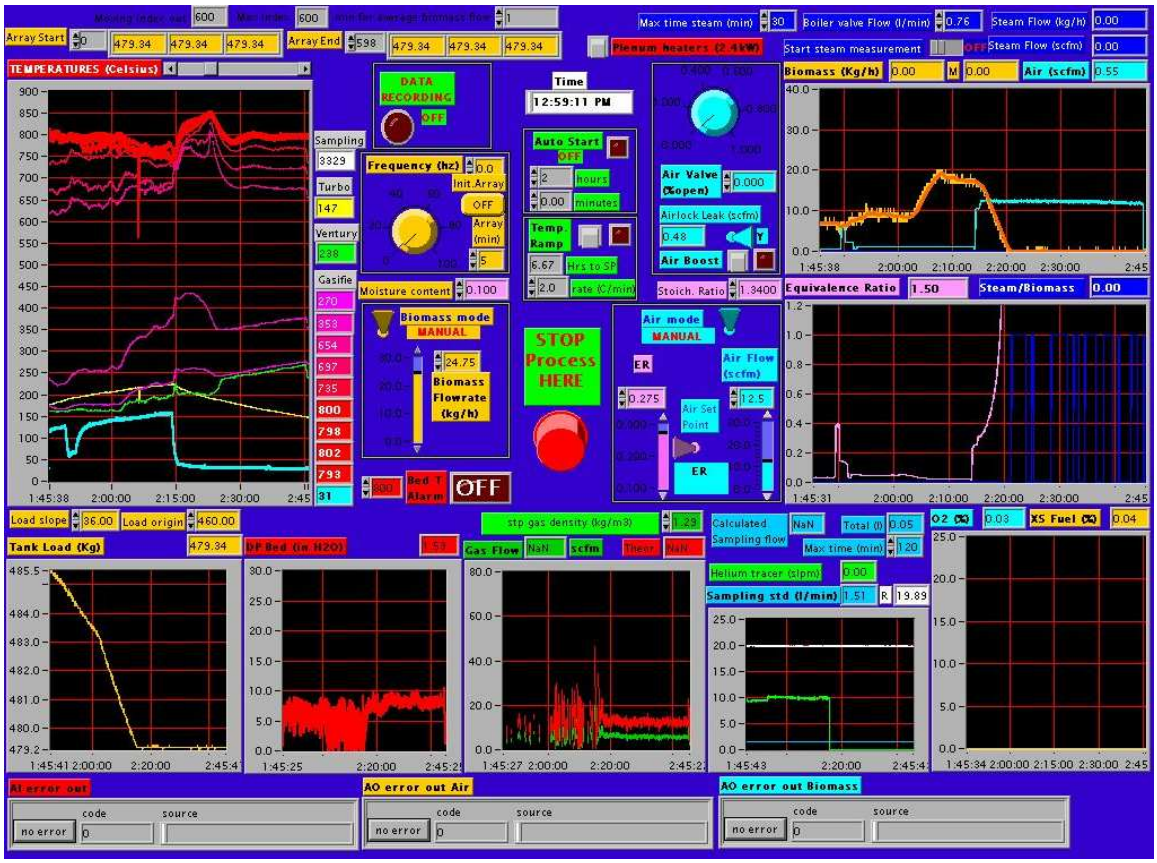

Figure 2.19 Control panel screen 1: graphs and controls

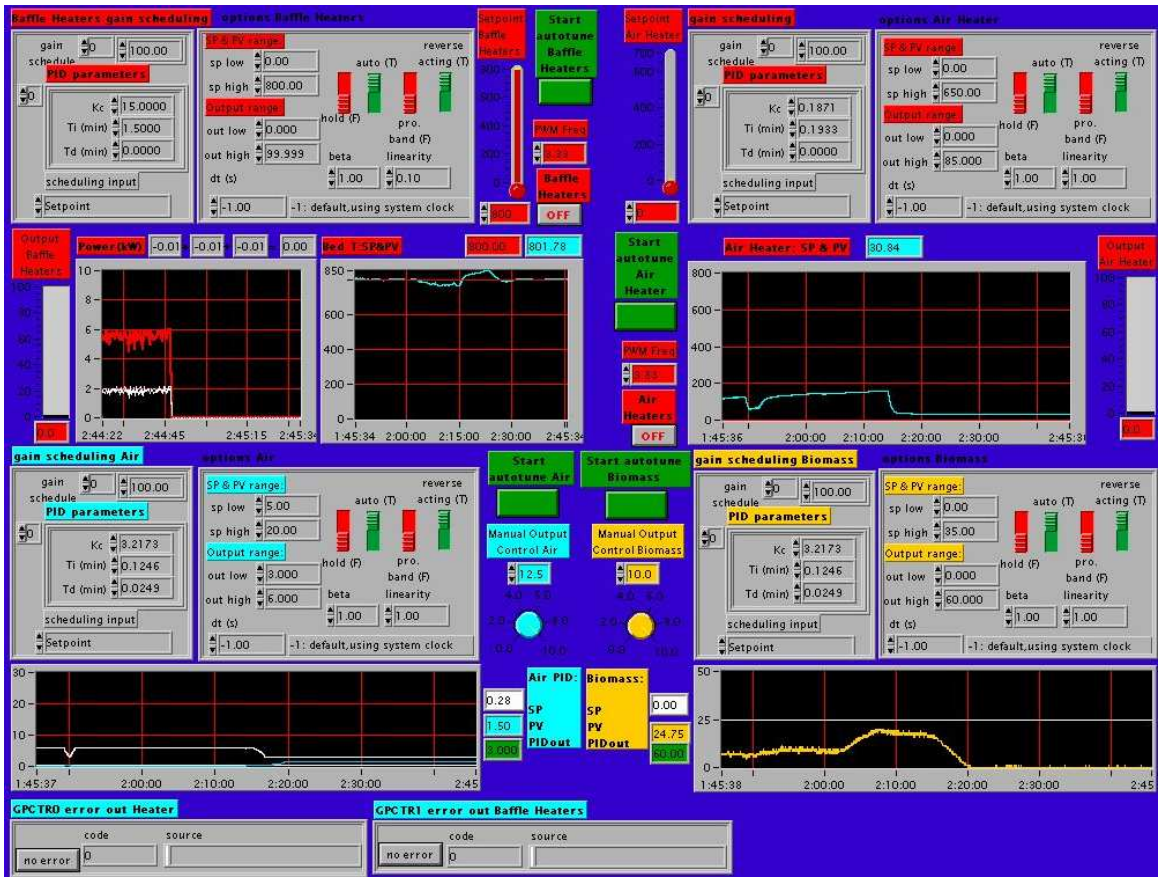

Figure 2.20 Control panel screen 2: automation proportional integrator derivator (PID) controllers (feed, air, power baffle heaters, power air heater)

Sensors

- Load cell (maximum 2268-kg capacity) is used to monitor feed hopper weight.
- 14 Type-K thermocouples used to monitor temperatures of the air heater outlet, in and above the fluidized zone of the bubbling sand bed, at the top of the gasifier, at the venturi, and at the gas sampling flow meter.
- Differential pressure gage to measure the pressure drop through the bed.
- Differential pressure gage across a venturi used to measure exhaust gas flow.
- Mass flow meter (30 scfm maximum) used to measure airflow.

Controls

- 3 phase, 220 V inverter to control the biomass flow metering auger.
- 1-cm opening, ¼ turn valve and a 12 V actuator to control the airflow.
- Three 100 A solid-state relays to control the three baffle heaters.
- 75 A solid-state relay to control the air heater.

2.3 AIR GASIFICATION PRELIMINARY ENERGY BALANCE

The thermal balance between endothermic and exothermic reactions is the base of an air gasifier design. Carbon and air feed rates are controlled to balance heat requirements of the reaction without heat inputs. In order to study the process, it is important to understand the heat requirement of the chemical reaction for this gasifier design.

The reaction is based on cellulose composition, and a moisture ash free (maf) biomass input at 20 kg/h. For the following calculation, 5%wt ash is assumed in the biomass.

$$C_6H_{10}O_5 + 2\ O_2 + 7.52\ N_2 + Ash \xrightarrow{\Delta H_R} 5\ H_2 + 3\ CO + 3\ CO_2 + 7.52 N_2 + Ash \qquad \textbf{(2.3)}$$

With ΔH_R = -745 kJ/mol @ 1000 K from equation (1.9)

Parameters a compound x:

Q_x = sensitive heat of x, kW
m_x = mass flow rate of x, kg/h
F_x = mole flow rate of x, mol/h
M_x = molecular weight of x, g/mol
Cp_x = specific heat of x, J/mol.K
$Q_{react.}$ = heat of reaction, kW
ΔH_R = enthalpy of reaction, kJ/mol
a,b,c,d,e,f,g = stoichiometric coefficients

Mass and mole flow rate calculations through the gasifier on the base of a biomass feed flow rate of: $\dot{m}_{biomass}$ = 20 kg/h

$$M_{biomass} = M_{C_6H_{10}O_5} = 6 * M_C + 10 * M_H + 5 * M_O \qquad \textbf{(2.4)}$$

$M_{biomass}$ = 6 * 12 g/mol + 10 * 1 g/mol + 5 * 16 g/mol

$M_{biomass}$ = 162 g/mol

$$F_{biomass} = \dot{m}_{biomass} * M_{biomass} \qquad \textbf{(2.5)}$$

$F_{biomass}$ = 20 kg/h * 1000 g/kg / 162 g/mol

$F_{biomass}$ = 123.5 mol/h

Calculations for all other compounds are similar:

Example of O_2:

M_{O_2} = 2 * M_O **(2.6)**

M_{O_2} = 2 * 16 g/mol

M_{O_2} = 32 g/mol

F_{O_2} = 2* $F_{biomass}$ **(2.7)**

F_{O_2} = 2 * 123.5 g/mol

F_{O_2} = 246.9 mol/h

$\dot{m}_{O_2}$ = M_{O2} * F_{O2} **(2.8)**

$\dot{m}_{O_2}$ = 32 g/mol*246.9 mol/h / 1000g/kg

$\dot{m}_{O_2}$ = 7.9 kg/h

For all reactants and products, the following results are obtained:

From equation (1.15)

$C_6H_{10}O_5 + 2\ O_2 + 7.52\ N_2 + Ash \rightarrow 5\ H_2 + 3\ CO + 3\ CO_2 + 7.52N_2 + Ash$

$\dot{m}$ (kg/h)	20.00	7.90	25.99	1	1.23	10.37	16.30	25.99	1
F (mol/h)	123.5	246.9	928.4		617.3	370.4	370.4	928.4	

The heat consumed to increase the incoming ambient air temperature (300K) to reaction temperature of the reactor (1000K) is:

$$\dot{Q}_{air} = - F_{air} * Cp_{air} * (T_2 - T_1) \quad \textbf{(2.9)}$$

$$F_{air} = F_{O_2} + F_{N_2} \quad \textbf{(2.10)}$$

F_{air} = (246.9 mol/h + 928.4 mol/h) / 3600 s/h = 0.3265 mol/s

$\dot{Q}_{air}$ = - 0.3265 mol/s * 29 J/mol*K * (1000 K – 300 K)

$\dot{Q}_{air}$ = - 6.63 kW

The heat released by the reaction is:

$$\dot{Q}_{reaction} = \Delta H_R * F_{biomass} \quad \textbf{(2.11)}$$

$F_{biomass}$ = 123.5 mol/h / 3600 mol/s = 0.0343 mol/s

$\dot{Q}_{reaction}$ = -745 kJ/mol * 0.0343 mol/s

$\dot{Q}_{reaction}$ = -25.56 kW

The heat lost by the hot exhaust gas (1000 K) leaving the reactor:

$$\dot{Q}_{gas} = \left(F_{H_2} \times Cp_{H_2} + F_{CO} \times Cp_{CO} + F_{CO_2} \times Cp_{CO_2} + F_{N_2} \times Cp_{N_2}\right) \times \left(T_3 - T_2\right) \quad \textbf{(2.12)}$$

$\dot{Q}_{gas}$ = (617.3 mol/h * 28.8J/mol * K + 370.4 mol/h * 29.1 J/mol*K + 370.4 mol/h * 37.1 J/mol*K + 928.4 * 29.1 J/mol*K) * (300 K – 1000 K) / (3600 s/h)

$\dot{Q}_{gas}$ = -13.48kW

Energy lost by the hot solids (1000 K) leaving the reactor:

$$\dot{Q}_{ash} = \dot{m}_{ash} \times Cp_{ash} \times (T_3 - T_2) \quad \textbf{(2.13)}$$

$\dot{m}_{ash}$ = 1 kg/h / 3600s/h = $2.78*10^{-4}$ kg/s

$\dot{Q}_{ash}$ = $2.78 * 10^{-4}$ kg/s * 1 kJ/kg.K * (300 K - 1000 K)

$\dot{Q}_{ash}$ = -0.19 kW

Overall energy balance:

$$\dot{Q}_{air} + \dot{Q}_{reaction} + \dot{Q}_{gas} + \dot{Q}_{ash} = \dot{Q}_{balance}$$

$\dot{Q}_{balance}$ = - 6.63 kW + 25.56 kW - 13.48 kW - 0.19 kW = -5.26 kW

$\dot{Q}_{balance}$ represents 20% of the heat generated by the gasification reaction in the fluidized bed reactor. It is a sufficient excess to account for heat loss through the insulation.

2.4 MODIFICATIONS FOR STEAM GASIFICATION

Because steam gasification is an endothermic reaction, the fluidized bed gasifier modifications for steam gasification mainly involve the installation of electric heaters and a steam generator. The steam is be fed into the fluidized bed gasifier plenum below the sand bed and used to fluidize the bed instead of air. For conditions requiring a low steam flow rate that will not satisfy minimum fluidization, a high temperature air driven turbine is used to recirculate outlet gases in order to maintain fluidization.

Steam reforming from equation 1.16:

$$C_6H_{10}O_5 + H_2O \longrightarrow 6CO + 6H_2 \quad 322kj/mole@1000K$$

According to the above equation, for a biomass feed rate of 20kg/h the steam feed rate would be:

$$\dot{m}_{steam} = \dot{m}_{biomass} * M_{H2O} / \dot{m}_{biomass} \quad \textbf{(2.14)}$$

$$\dot{m}_{steam} = 20 \text{ kg/h} * 18 \text{ g/mol} / 162 \text{ g/mol} = 2.22 \text{ kg/h}$$

With the ideal gas law (PV=nRT) and $F_{steam} = \dot{m}_{steam} * M_{steam}$, the steam flow rate is:

$$\dot{V}_{steam} = \frac{(F_{steam} \times R \times T)}{P} \quad \textbf{(2.15)}$$

$\dot{V}_{steam}$ = 2.22 kg/h *1000 g/kg * 8.2*10^{-2} dm^3*atm/mol*K *373.15 K / (60 min/h * 18 g/mol *1 atm)

$\dot{V}_{steam}$ = 62.9 dm^3/min

$\dot{V}_{steam}$ = 2.22 cfm

Heat requirement for the steam will be:

$$\dot{Q}_{steam} = \dot{m}_{steam} * (Cp_{liquid\ water} * (T_2-T_1) + \dot{Q}_{latent\ heat\ of\ evaporation} + Cp_{steam} * (T_3-T_2)) \quad \textbf{(2.16)}$$

$\dot{Q}_{steam}$ = 2.22 kg/h * (4.18 kJ/kg*K * (100-25) + 2258 kJ/kg + 1.97 kJ/kg*K * (700-100)) / 3600 s/h

$\dot{Q}_{steam}$ = 2.31 kW

And the reaction heat requirement would be:

$$\dot{Q}_{reaction} = -\Delta H_R \times F_{biomass}. \quad \textbf{(2.17)}$$

$\dot{Q}_{reaction}$ = 322 kJ/mol * 20 kg/h * 1000 g/kg / (3600 s/h * 162 g/mol)

$\dot{Q}_{reaction}$. = 11.04 kW

Considering excess of 20% to account for heat loss, the heat requirement becomes:

$$(11.04 \text{ kW} + 2.31 \text{ kW})* 1.2 = 16.02 \text{ kW}$$

Three 7.5 kW - 240V spiral conic shaped heating elements are superposed 7.62 cm apart in the sand bed and temperature controlled. When connected in parallel, these provided a total of 22.5 kW.

Because the exhaust mass flow rates will be lower than for air gasification, the second cyclone is reduced in diameter for steam gasification.

Although the biomass moisture content in steam gasification is not as important as it is in air gasification, the biomass materials tested are at the same moisture content considered in the first objective. To maintain the thermal balance in air gasification, heat necessary for the endothermic reactions is mainly provided by the double oxidation of the carbon forming CO_2 . In the steam gasification, heat is provided externally. The steam-to-carbon ratio and temperature are not as dependent on equivalence ratio and temperature as in the air gasification case.

2.5 ANALYSIS

2.5.1 Solids analysis

In order to generate mass and energy balances of the system, flow rates of the reactants and products are recorded. Biomass input flow rate is measured with the combination of a load cell and a computer program calculating the variation of weight with time. Solids outlet flow rate is measured through isokinetic sampling, filtration and solvent extraction. After extraction of the tar, the solids are dried and weighed. This calculation necessitates isokinetic conditions at the sampling probe. Proximate and

ultimate analyses of each material tested and corresponding solid output are determined through an external laboratory; Hazen Research, Inc.

2.5.2 Gas Analysis

Producer gas, synthesis gas and flame pyrolytic gas are sampled from the exhaust in syringes and then analyzed using a gas chromatograph (GC) equipped with a thermal conductivity detector (TCD). The GC uses Argon as the carrier gas. The injector is a constant volume injection loop of 1.0 ml. The column is a packed type, Hayesep DB 100/120 mesh. Producer gas analysis results show hydrogen (H_2), nitrogen (N_2), oxygen (O_2), carbon monoxide (CO), methane (CH_4), carbon dioxide (CO_2), ethylene (C_2H_2), acetylene (C_2H_4) and ethane (C_2H_6). Calibration of the GC was performed using Supelco Scotty 2 analyzed gases mix 216 and mix 234, ambient air, and a certified specialty gas mix containing 15% CO_2, 25% CO, and 60% N_2. See Appendix 8.1 for calibration curves.

Temperature changes are programmed as follows for each sample separation: 6min at 40°C, ramp up to 140°C at 100°C/min, 20 min 140°C, then ramp down to 40°C at 100°C/min.

Percentage volume results are corrected for potential air leaks during syringe sampling using the oxygen peak, and are then removed with results normalized in the analysis, using Excel based software. See Chapter 4.

2.5.3 Tar analysis

There is no standard analytical procedure for tar measurement. Though a tar protocol has been elaborated (Energy project ERK6-CT1999-20002 (Tar protocol)): Guidelines for Sampling and Analysis of Tar and Particles in Biomass Producer Gases (Appendix 8.3).

The guidelines describe the basic concept of the sampling train which consists of 4 main modules and respective submodules. The main modules are gas preconditioning, particle collection, tar collection and volume measurement (Figure 2.21).

1. In the preconditioning module (Module 1), the process gas is heated to a constant temperature of 300-350°C using a heated probe. The sampling probe is designed according to Abatzoglou et al. (2000).
2. In the particle collection module (Module 2), a heated filter, maintained at the same temperature as the probe, collects the solids from the gas.
3. The tar collection module (Module 3) consists of three submodules. In the first submodule, the gas is cooled resulting in moisture and some of the tar being collected in a condenser at a temperature of approximately 20°C. A liquid quench, which facilitates cleaning of sampling lines after the sampling, is optional. In the second submodule, tar and volatile organic compounds (VOC) are absorbed into the solvent at -20°C in a series of impinger bottles. In the third, and optional submodule, a backup VOC adsorber collects residual VOC's which may have penetrated the impinger train. The backup VOC adsorber is not necessary when enough impinger bottles, appropriate solvents and collection temperatures are used.

4. The volume-sampling module (Module 4) consists of three submodules. The purpose of these submodules is to: (a) maintain the sample flow by a pump (not needed in pressurised gasification); (b) adjust and control of flow rate; (c) measure the sample volume; and (d) vent the gas. See Appendix 8.3 for information on the sampling unit operation.

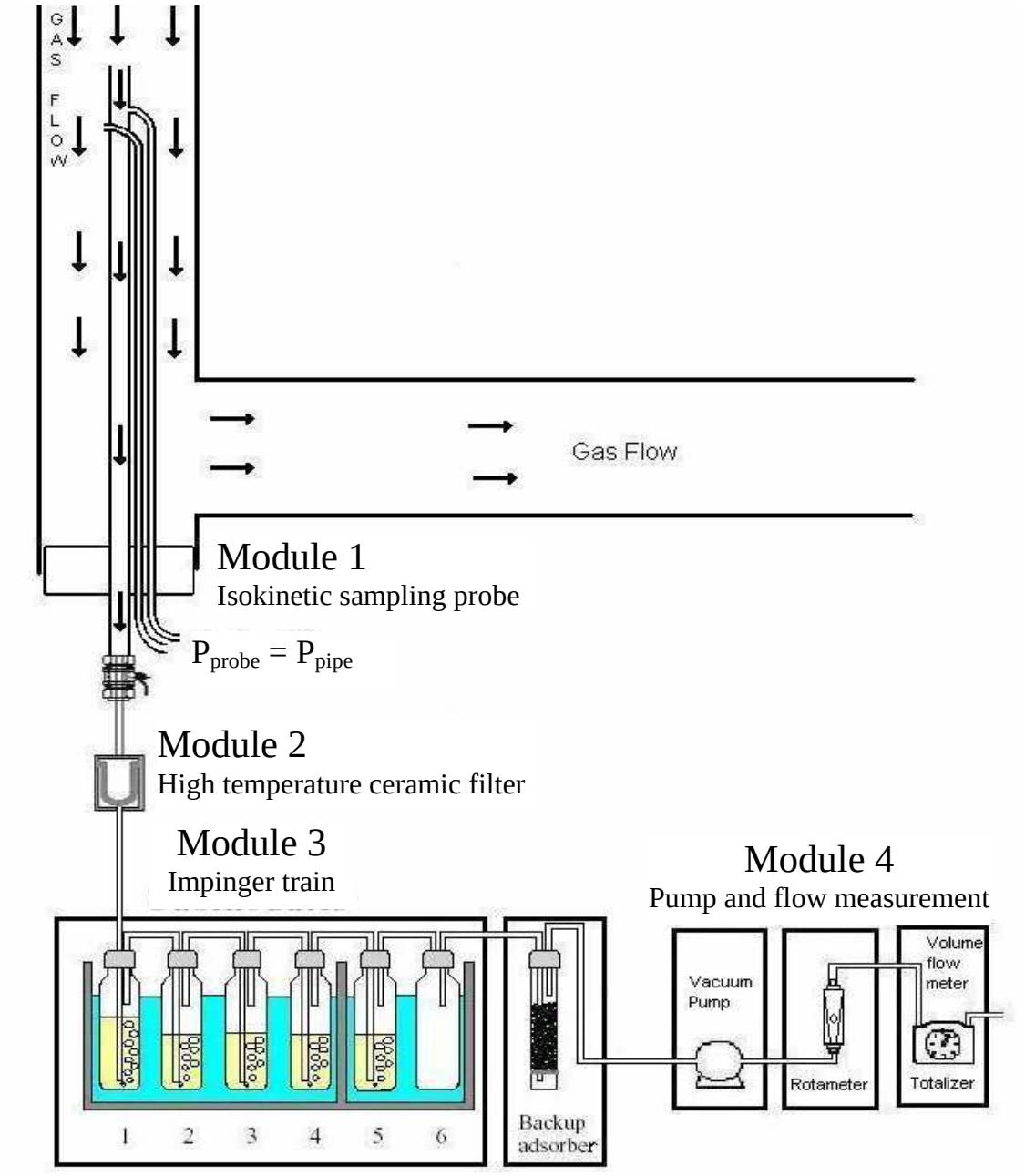

Figure 2.21: schematic of the sampling probe and impinger train connected to the pilot plant exhaust pipe

2.5.3.1 Experimental procedure

Tar sampling is performed intermittently during steady state operation of the gasifier. A stainless steel sampling probe (Figure 2.22 and 2.23) (0.683 cm in diameter designed according to 1998 tar sampling guidelines) is located inside the gasifier exhaust pipe, where the gas temperature is approximately 350^{o}C. The gas flow rate in the probe is set with the rotameter valve after the vacuum pump to maintain isokinetic sampling conditions. It is preferable to have the valve in a positive pressure environment in order to prevent eventual oxygen leakage into the system.

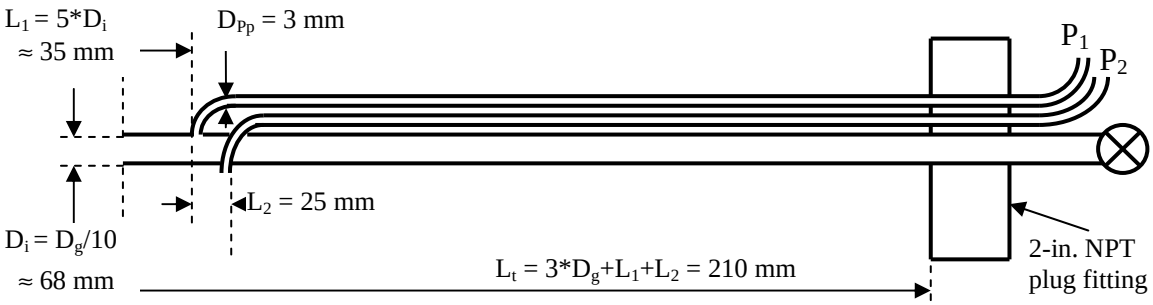

Figure 2.22 Sampling probe design

The ratio of the pipe diameter and the sampling nozzle diameter must be at least 10 so that 1% of the gas is sampled.

The sampling apparatus (Figures 2.21, 2.24 and 2.25) consists of:

- filter
- series of condensers
- series of impingers
- VOC backup with activated carbon
- vacuum pump
- rotameter
- turbine gas flow meter
- flow totalizer (in computer program).

Figure 2.23 Sampling probe

A high temperature ¼-turn valve is placed between the probe outlet and the filter. The filtration device is a stainless steel filter holder SFA-300 with ceramic or fiberglass thimble filters, maintained at approximately 150^{o}C with a band-heater. All pipes before and after the filter are heated to prevent tar condensation. At the filter outlet, four glass condensers in series are maintained in an ethylene glycol bath at a controlled temperature of –5^{o}C. Upon exiting the condensers, the gas is drawn through one acetone-filled impinger plus a dry impinger, both immersed in an ethylene glycol bath at or below –20^{o}C. Sample flow rate is maintained at around 11 l/min (depending on isokinetic conditions for the gasifier exhaust flow rate) using a vacuum pump at desired time intervals.

Upon completion of sampling, all unheated parts of the sampling system are rinsed with acetone to collect tar deposits, and mixed with the acetone collected from the impingers, and condensers. At this point, a 20-cc sample is taken for gas chromatography mass spectrometry (GC-MS) analysis. The remainder of the solution is evaporated and quantified gravimetrically.

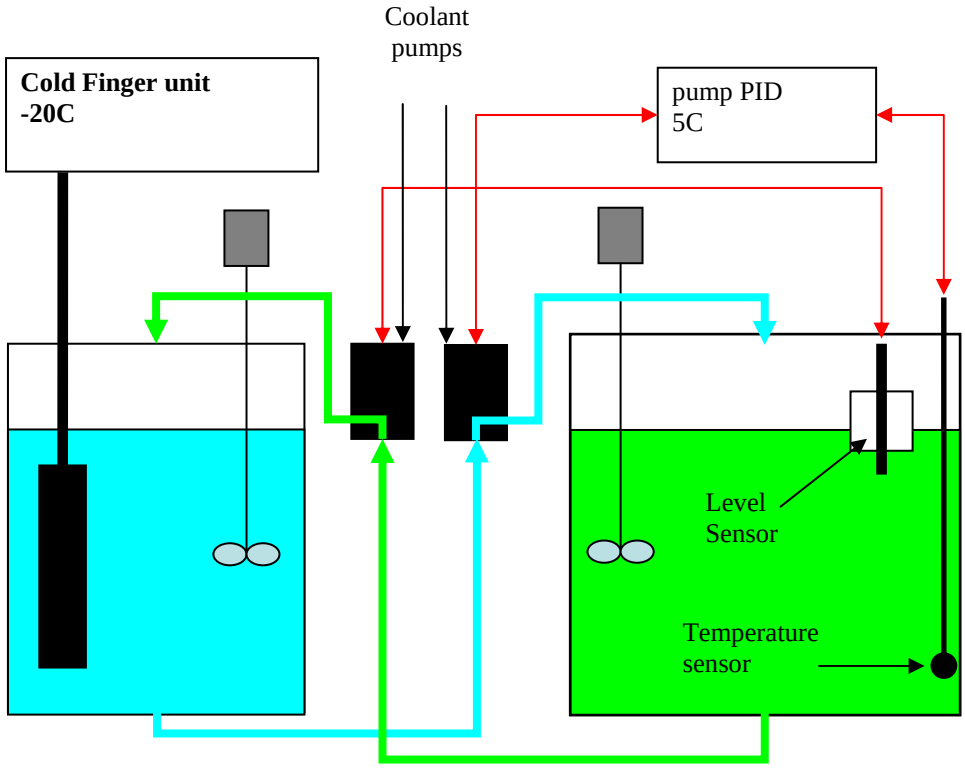

Figure 2.24 Schematic of the cold bath regulation in sampling unit

To cool the bath of this sampling system (Figure 2.24 and 2.25), a single cold finger unit is immersed into the second impinger bath, maintaining a temperature below -20°C. The temperature of the first impinger bath was regulated using a PID controlled flow of coolant from the second bath to maintain a temperature at 5°C. (For more technical information about this unit and how it runs, see Appendix 8.2)

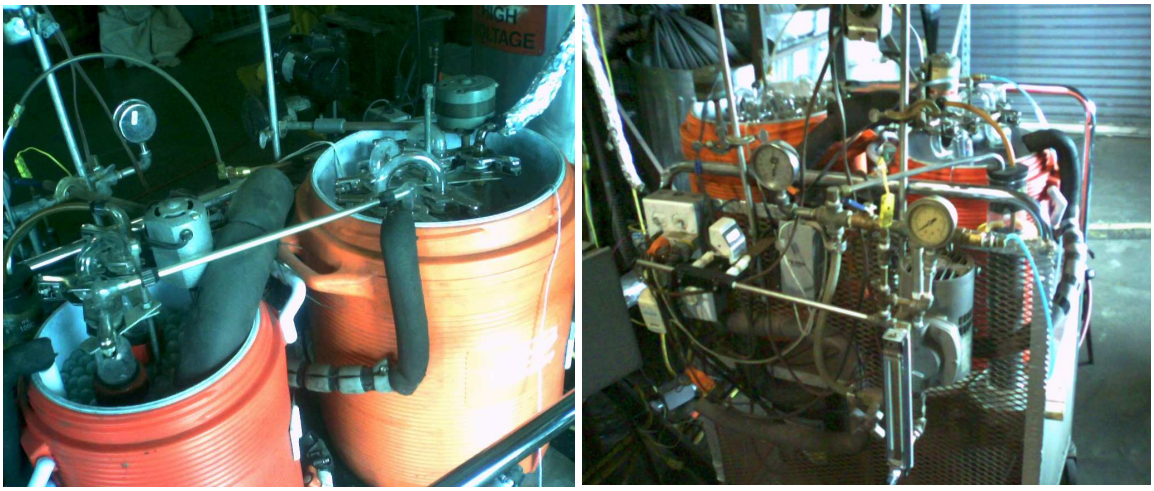

Figure 2.25 Sampling unit

2.5.3.2 Gravimetric analysis

To evaluate the tar concentration gravimetrically, 100cc of acetone-tar solution is evaporated in a buchi rotavapor according to the guidelines in Appendix 8.3.

2.5.3.3 Tar GC-MS analysis

A quality analysis of the tar is performed with a GC-MS through a 60-m long, 0.25-mm diameter capillary column with a 0.25-μm thick diphenyl dimethyl film.

Using a method (Appendix 8.4) built from three external standard mixes (referred to as BTEX, Mix 4, PAHs), and one internal standard added to each sample tested, the GC-MS provides the composition of the tar for 210 compounds for each process and biomass material gasified.

The methodology offered in the guidelines (Appendix 8.3) is applied for determination of the tar concentration in the gas.

Once the solutions from the sampling and rinsing of the impinger train and from the ash soxhlet extraction are mixed together, the total volume is recorded as $V_{solvent}$. A 1-ml sample is placed in the GC-MS with 20 µl of internal standard.

Once recognized and quantified, those compounds that could be potentially harmful to the downstream bioreaction are identified and will merit further testing this experiment.

The expected compounds in the tar are: carboxylic acids, sugars, alcohols, phenols, guaiacols, mixed oxygenates furans, aromatics, polycyclic aromatic hydrocarbons (PAH), and nitrogen containing aromatics. The present analysis concentrates on the main compounds of the tar listed in Table 8.1 in Appendix 8.4.

3 AIR GASIFICATION OF MOIST SWITCHGRASS

Knowledge of the effects of biomass moisture content on gasification process parameters and resulting producer or synthesis gas composition for selected feedstocks is essential to further develop the gasification-fermentation bioconversion process.

3.1 EXPERIMENTAL PROCEDURE

For the first series of experiments with moist switchgrass only, the water and tar sampling system was different than the procedure used in all other experiments. It consisted of a stainless steel sampling probe (1.0 cm in diameter) located inside the gasifier exhaust pipe in laminar flow conditions, where the gas temperature is approximately 600^{o}C. The sampling apparatus consisted of a filter, three vertical condensers in series, and a series of impingers. A high temperature 1.0-cm diameter valve was placed between the probe outlet and filter. The filtration device was a stainless steel wire mesh (rated at 0.4 micron), maintained at approximately 350^{o}C with a band heater. All pipes, before and after the filter, were band heated to prevent tar condensation. At the filter outlet, three glass condensers in series were maintained at –5^{o}C as a water trap. Upon exiting the condensers, the gas was drawn through a series of three acetone-filled impingers, and a dry impinger, immerged in an ethylene glycol bath at –20^{o}C. Sample flow rate was maintained at 11.2 l/min using a rotameter and a vacuum pump to maintain isokinetic conditions.

Upon completion of sampling, all unheated parts of the sampling system were rinsed with acetone to collect tar deposits, mixed with the acetone collected from the impingers, and evaporated at 60^{o}C under atmospheric pressure. Remaining water droplets were separated from the tar through a centrifugation process. Water and tar were both quantified gravimetrically.

3.2 BIOMASS PREPARATION AND PROPERTIES

Moist switchgrass was cut the morning of November 12, 2002, and allowed to field cure before round baling in late afternoon. Two bales were immediately processed in a tub grinder with a ½-inch screen for size reduction and then gasified. Six additional bales were stored under cover, with four being artificially dried until they reached successively lower levels of moisture content. After being dried to the approximate desired moisture content, the bales were processed in the tub grinder and gasified. The initial three target moisture levels were 30, 20, and 10% wet basis.

The bale drying system consisted of a compressor, an electric air heater electronically controlled to maintain a temperature of 70^{o}C, and a series of perforated galvanized pipes for distribution of the air within the bales. Each bale was equipped with a 5-cm diameter pipe, perforated every 15 cm along its length with 8 holes, each 0.8 mm in diameter. Airflow rate through the bales was maintained at 0.14 m^{3}/min.

Moisture content of the switchgrass was determined according to ASTM standard E1756-01. Switchgrass samples were sent to Hazen Research, Inc., for proximate and ultimate analysis (Table 3.1). As can be seen, the switchgrass has a relatively low hydrogen and nitrogen content.

	Composition				
Ultimate % db wt	C	H	O	N	Ash & S
	50.15	6.92	37.07	0.52	5.34
Proximate % db wt	Volatiles	Fixed Carbon		Ash	
	79.09	15.64		5.27	

Table 3.1 Proximate and ultimate switchgrass analysis

3.3 RESULTS

The artificial drying process resulted in five distinct moisture contents (wet basis): 34%, 29%, 25%, 19%, and 9%. The first observed effect of switchgrass moisture content on gasifier operating conditions was the effect on reactor bed temperature. Figure 3.1 shows the change in gasifier operating temperature for each moisture content at various equivalence ratios. It can be clearly seen that as moisture content is increased, operating temperature is decreased. For biomass moisture contents above 19%, bed temperature could not be maintained at 800°C in the range of ER chosen for the experiment. The temperature difference is as much as 100°C between the high and low moisture contents for a given equivalence ratio. This loss in temperature is the consequence of both the additional latent heat of water vaporized and the endothermic chemical reactions with the water.

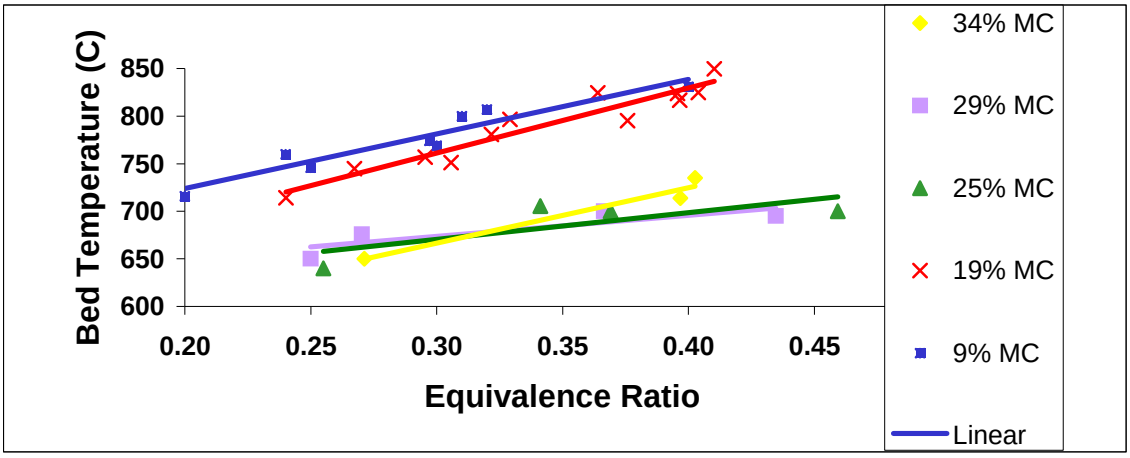

Figure 3.1 Effect of switchgrass moisture content on gasifier operating temperature at various equivalence ratios.

Figure 3.2 shows the mole percent composition of various components of the producer gas resulting from gasification of switchgrass at moisture contents (wet basis) of 9%, 19%, and 29%, respectively. Each data point represents the average of three replicate samples. As shown, CO production ranges from 15-20%, H_2 from 4-8%, CO_2 from 15-20%, while the other hydrocarbons are less than 5%.

Figure 3.3 shows a direct comparison of the production of CO, H_2, CO_2 and CH_4 at various moisture contents. As switchgrass moisture content increases, production levels of both CO and H_2 greatly decrease, CO_2 slightly increases, and CH_4 slightly decreases. A decrease in production of carbon monoxide and hydrogen are consistent with the decrease in operating temperature of the gasifier.

An additional experiment was conducted in which the fluidized bed gasifier was operated at an ER of 0.3 with switchgrass at 19% MC. An external heat source was used to increase the input air temperature to 350^{o}C, allowing the bed to be maintained at a temperature of 800^{o}C. The concentration of the components in the producer gas increased to: 5.8% H_2, 20.0% CO, 14.0% CO_2, and 5.2% CH_4.

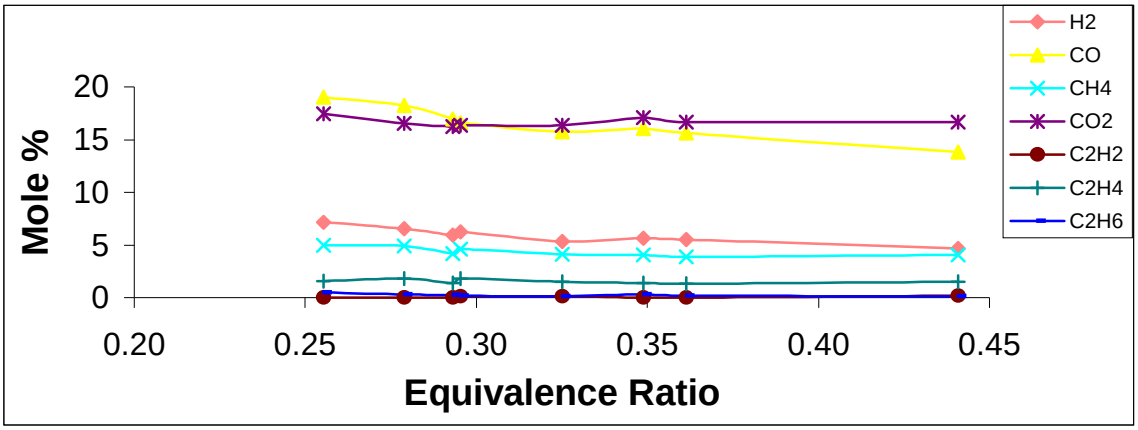

a) 9% moisture content

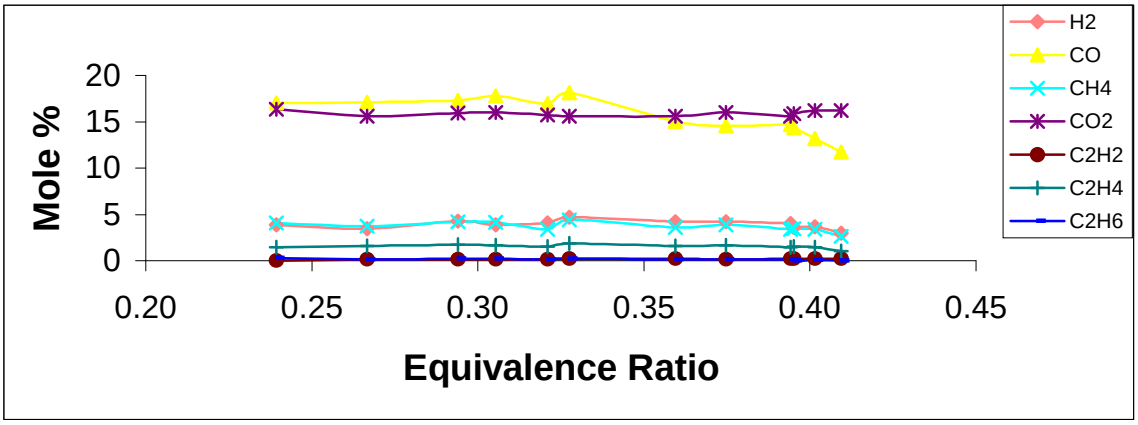

b) 19% moisture content

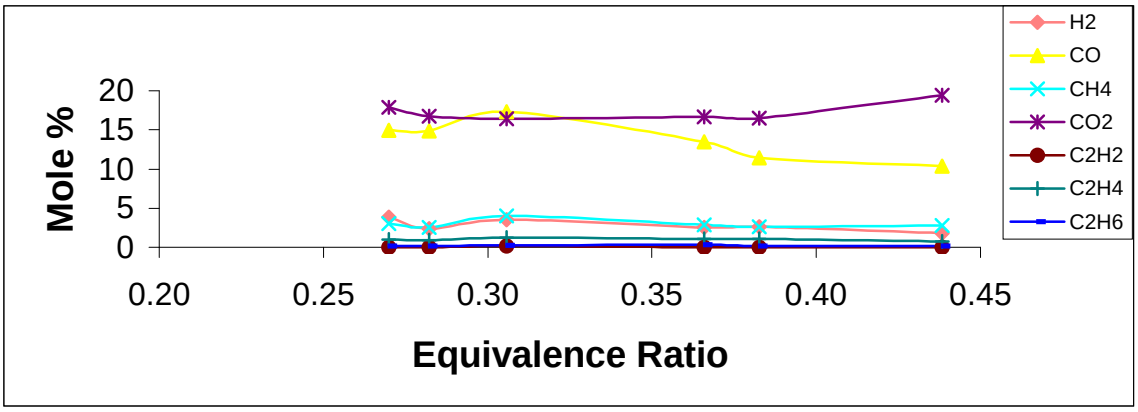

c) 29% moisture content

Figure 3.2 Producer gas composition with switchgrass at moisture contents of a) 9%, b) 19%, and c) 29%.

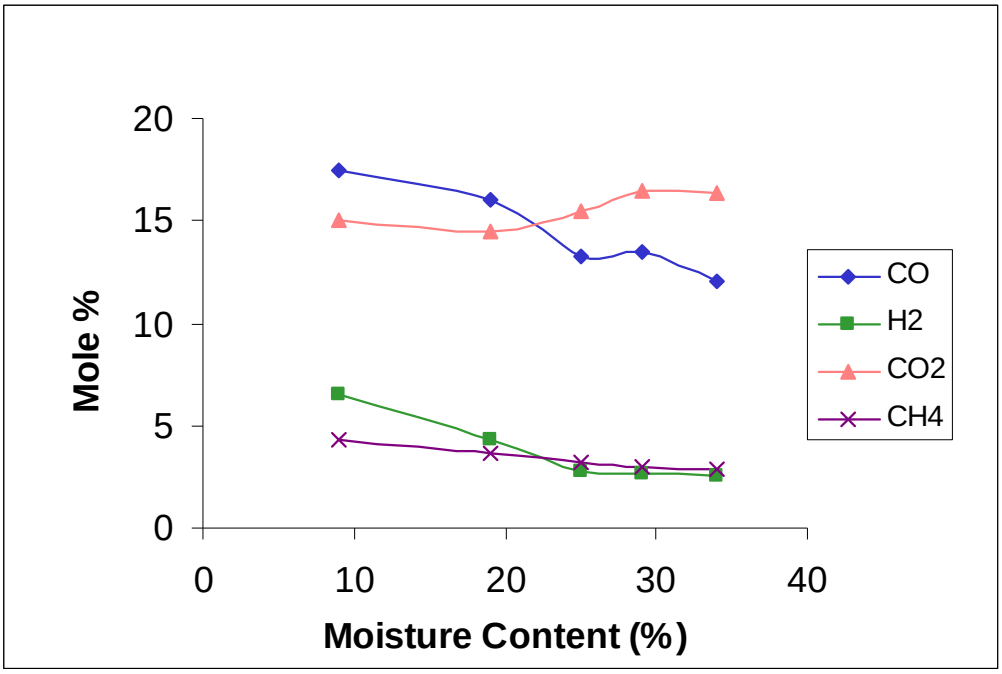

Figure 3.3 Effect of switchgrass moisture content on production of CO, H_2, CO_2, and CH_4 at an equivalence ratio of 0.27.

Table 3.2 shows all gasification products as a function of moisture content at an equivalence ratio range of 0.27-0.3. All values listed are in units of weight percent of incoming biomass feed. Products shown include all gases as well as tar, ash, and water. As shown, levels of CO, H_2, and CH_4 clearly decrease with increasing moisture content. Also, levels of tar and ash remain relatively constant at about 2% and 8% of feed flow rate, respectively. Of the ash values given, it should be noted that chemical analyses revealed that approximately 36% of the 'ash' samples collected in the cyclones was fixed carbon. Due to the difficulty of tar and water measurement and the variability of the results, values determined in this experiment do not appear to change appreciably with respect to changes in moisture content of the biomass. It is generally observed, however, that tar production increases at lower values of ER for all moisture contents.

M.C. (% w.b.)	Gasification Products (% Feed Weight)						
	H_2	CO	CH_4	CO_2	tar	H_2O	Ash
9	0.90	37.91	5.74	55.92	2.81	17.71	8.94
19	0.59	34.54	4.62	51.07	2.14	20.26	8.47
25	0.37	29.85	3.83	56.46	1.44	28.01	8.28
29	0.43	29.42	3.41	50.01	1.62	21.06	8.28

Table 3.2 Gasification products (in % wt of the feed) at various levels of switchgrass moisture content, using an equivalence ratio range of 0.27-0.3. All values shown are the average of at least three replicates.

When considering just carbon conversion, it can be deduced that approximately 90% of the carbon entering the process in the biomass is converted to producer gas, with the remainder going to tar and ash. Depending on the moisture content considered, approximately 30-40% of the carbon is converted to CO, 25-35% to CO_2, and the remainder to other hydrocarbons, tar and ash.

3.4 CONCLUSIONS

For this gasification-fermentation process, it is desirable to maximize both CO and H_2 production, to be converted into ethanol by anaerobic acetogenic microorganisms. This study showed that elevated biomass moisture contents decrease the operating temperature of the gasification system by as much as 100^{o}C for a 20% change in MC. Decreased operating temperatures alter the composition of the producer gas. Specifically, CO and H_2 concentrations were lowered by 30-40 % when increasing moisture content from 9% to 29%. Changes in the quantity of ash, tar, and water produced during gasification did not seem to show specific patterns with changes in biomass moisture content.

As in all gasification systems, waste heat is always a concern. It was also briefly shown in this situation that gasification of moist switchgrass can be performed with the same output levels of H_2, CO and CH_4 if the loss of temperature due to the water evaporation is compensated for with an external source of heat input, as was accomplished by heating the incoming air.

Other biomass (bermudagrass and corn gluten) were gasified at the most adequate moisture content obtained from the conclusion of the first series of air gasification experiments and at various equivalence ratios. All gasification experiments were run at steady state and at the same constant airflow rate to maintain the same fluidization of the bed.

4 GASIFICATION AT LOW MOISTURE CONTENT

During these series of experiments with low moisture content (approximately 10%) biomass, the tar sampling system used was the one described in chapter two. The solvent was acetone because it provided better results than isopropyl alcohol particularly at low equivalence ratio (ER).

Some of the acetone-washed particulate matter was sent to Hazen Research Laboratories, along with three types of biomass for proximate and ultimate analyses. Results are shown in red in Table 4.1.

The pilot plant is programmed to start automatically at night on a ramped-up temperature set point to allow a slow warm up and preserve the gasifier refractory from thermal shock. The start up procedure is described in Appendix 8.2. The program is described in Chapter 2. All experiments are done with the process at steady state.

All biomass were allowed to dry down to a moisture content of 9 to 10% wb. The two grasses (switchgrass and bermudagrass) were chopped with a tub grinder with a ½-in. screen. The majority of the particles were approximately ¾ in. in length.

4.1 BIOMASS PROPERTIES

Biomass properties in Table 4.1 are based on ultimate and proximate analysis (italics).

Properties	Switchgrass		Bermudagrass		Corn Gluten	
Atomic %wt db	Total biomass	PM	Total biomass	PM	Total biomass	PM
C	***49.67***	***50.08***	***45.67***	***44.13***	***47.50***	***47.57***
H	***5.27***	***0.68***	***4.76***	***0.64***	***5.49***	***0.68***
O	***40.31***	***1.97***	***34.77***	***2.15***	***37.28***	***2.21***
N	***0.57***	***1.00***	***1.83***	***1.42***	***3.88***	***3.09***
S	***0.07***	***0.15***	***0.33***	***0.65***	***0.40***	***0.20***
Ash	***4.11***	***46.12***	***12.64***	***51.01***	***5.45***	***46.25***
HHV (Btu/lb)	***8056***	***7346***	***7459***	***6509***	***8432***	***7135***
MAF Btu/lb	***8401***	***13635***	***8537***	***13287***	***8918***	***13274***
LHV (Btu/lb)	***7353***	***6991***	***6765***	***6218***	***7627***	***6858***
# of atom of C	6	6	6	6	6	6
# of atom of H	7.64	0.98	7.50	1.04	8.32	1.03
# of atom of O	3.65	0.18	3.43	0.22	3.53	0.21
# of atom of N	0.06	0.10	0.21	0.17	0.42	0.33
C6HxOy g/mol	138.07	75.81	134.32	76.55	136.83	76.37
CHO %wt db	95.25	52.73	85.20	46.92	90.27	50.46
SR	1.34	1.37	1.25	1.21	1.33	1.30
# of atom of C	1	1	1	1	1	1
# of atom of H	1.27	0.16	1.25	0.17	1.39	0.17
# of atom of O	0.61	0.03	0.57	0.04	0.59	0.03
# of atom of N	0.01	0.02	0.03	0.03	0.07	0.06
CHxOy g/mol	23.01	12.63	22.39	12.76	22.81	12.73
CHO %wt wb	86.93	50.18	77.28	44.82	81.65	48.51
Hf kJ/mol CHxOy	-126.23	-16.46	-128.14	-24.44	-119.12	-25.39
Hf kJ/kg CHxOy	-5485.4	-1302.6	-5724.1	-1915.8	-5223.6	-1994.3
%wt wb	Switchgrass	Ash S	Bermudagrass	Ash B	Corn Gluten	Ash CG
H2O	***8.73***	***4.84***	***9.30***	***4.47***	***9.55***	***3.87***
C	45.33	47.66	41.42	42.16	42.96	45.73
H	4.81	0.65	4.32	0.61	4.97	0.65
O	36.79	1.87	31.54	2.05	33.72	2.12
N	0.52	0.95	1.66	1.36	3.51	2.97
S	0.06	0.14	0.30	0.62	0.36	0.19
Ash	3.75	43.89	11.46	48.73	4.93	44.46

Table 4.1 Biomass characteristics; proximate and ultimate analysis, stoichiometric ratio, molecular formula and enthalpy of formation at 298K

4.2 AIR GASIFICATION RESULTS

4.2.1 Temperature profiles

Air gasification temperature plays an important role as it improves carbon conversion to the gas when it increases, hence the importance of the thermal insulation of the gasifier. Air gasification experiments are done at or slightly above minimum fluidization with an ambient air flow rate inlet of 17 to 20m^3/h.

Literature states (Reed, 1981) that the reactor bed temperature for air gasification depends directly on the ER. A well-defined range for air gasification is between 0.2 to 0.4 ER.

Temperature profiles in Figures 4.1, 4.2 and 4.3 represent the air gasification of switchgrass, bermudagrass and corn gluten, respectively, at 9% moisture content in the fluidized bed gasifier (FBG) pilot plant. The data confirms that in the case of air gasification temperature is clearly a function of ER. As ER values decrease so does the bed temperature. This reduction in temperature is the consequence of an increasing lack of oxygen. The reduction of the number of exothermic oxidations such as the formation of CO_2 gives way to an increase in endothermic reactions. Although the amount of oxidations of C to CO increases, it only releases 1/3 of the heat of the second oxidation from CO to CO2.

The average temperature difference between the bed and the fluidized bed gasifier outlet is around 150°C for switchgrass, bermudagrass and corn gluten. The large variation of the outlet temperature data is considered to be more of a measurement problem. The average difference decreases with ER mostly due to a decrease in residence time in the reactor.

The bed temperature influences the residence time. As it decreases, the volumetric flow rate in the constant cross section of the gasifier decreases as well. But the amount of gas produced has more influence on this variation in stream velocity than the decrease in temperature. Because the inlet air flow rate is maintained constant for all ERs, the amount of biomass fed to the fluidized bed gasifier is increased to lower the ER value. This increase in feed rate increases the amount of gas produced and influences greatly the residence time of the gas in the reactor.

While running using the same conditions all biomass materials do not gasify at the same temperature for the same ER. Corn gluten gasifies at 725°C for an ER=0.25, bermudagrass and switchgrass reach higher temperatures 750°C and 775°C, respectively.

All temperatures are maintained at or below the 800°C to avoid bed agglomeration particularly in the case of corn gluten and bermudagrass where high ash content make them prone to agglomeration. These ashes contain alkali compounds consisting of K, Na, Mg, and Ca, which have melting points that are slightly above 800°C.

Analysis using ion chromatography (IC) revealed that the proportions of K^+, Na^+, Mg^+ and Ca^+ are the same covering the sand particles that agglomerated after a corn gluten run compared to the corn gluten material itself.

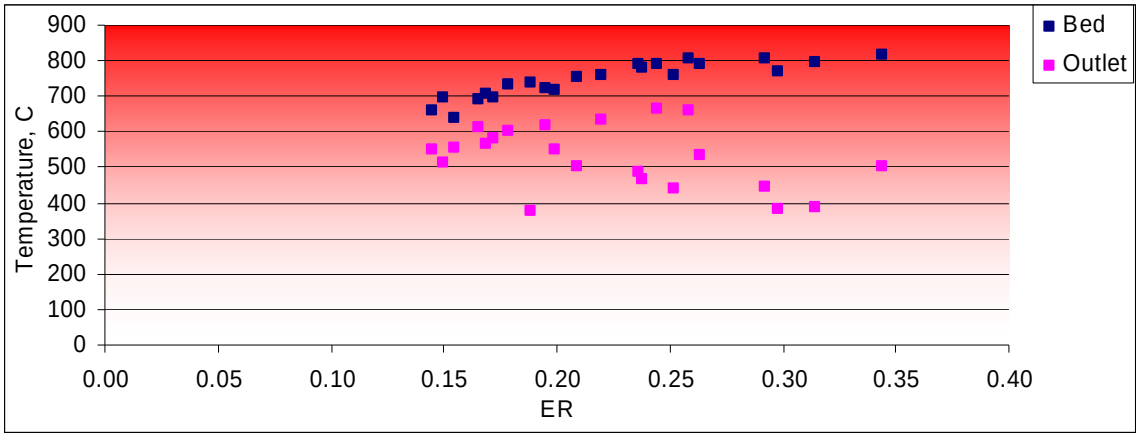

Figure 4.1 Air gasification of switchgrass temperature profile

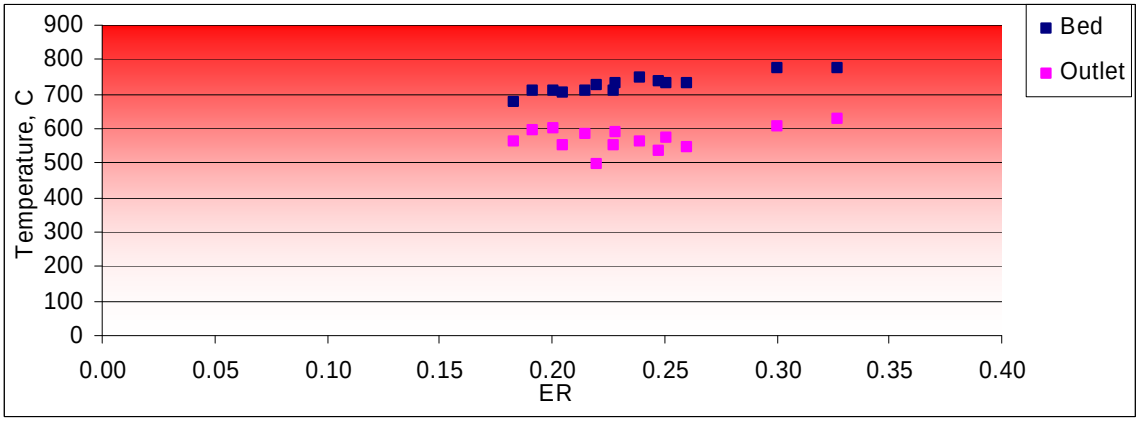

Figure 4.2 Air gasification of bermudagrass temperature profile

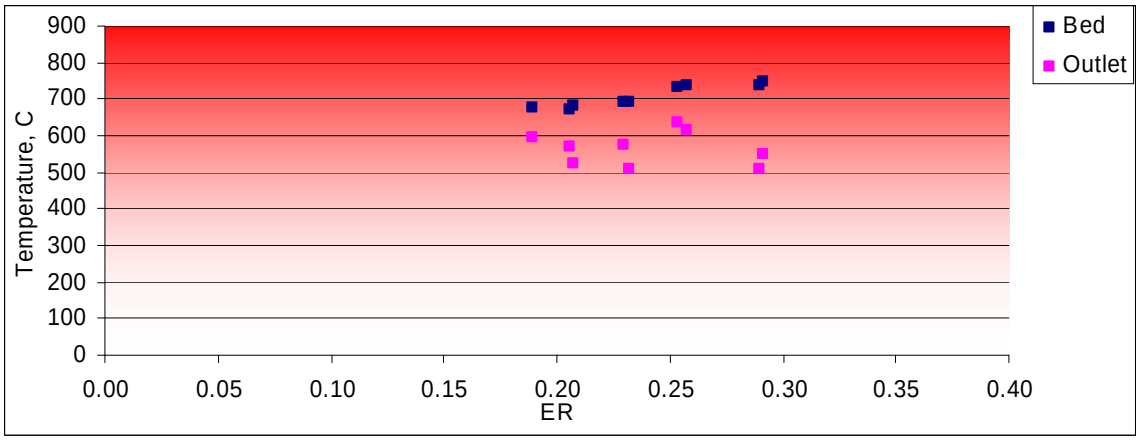

Figure 4.3 Air gasification of corn gluten temperature profile

4.2.2 Gas compositions

Gas compositions during air gasification displayed in Figures 4.4, 4.5 and 4.6 show only the four major gases: H_2, CO, CO_2, CH_4. For switchgrass, bermudagrass and corn gluten, all gas concentrations are increasing with a decrease in ER inducing a drop in temperature as endothermic reactions are taking over to form these higher concentrations. Although it is not shown, the concentration of nitrogen decreases with ER as the proportion of air supplied is decreased with lower ER values.

In the ER range experimented, switchgrass produces CO level between 15 and 20%, slightly higher than bermudagrass and corn gluten which have CO levels between 12 to 15%.

Bermudagrass gasification shows slightly higher H_2 levels 5 to 7%, compared to corn gluten and switchgrass gasification at 5%.

These concentrations were measured by GC analysis after the gas cooled to ambient temperature. It must be noted that these values are not representative of the levels at the bed or outlet temperature of the of the pilot plant. This point will be further discussed in the equilibrium modeling in Chapter 5.

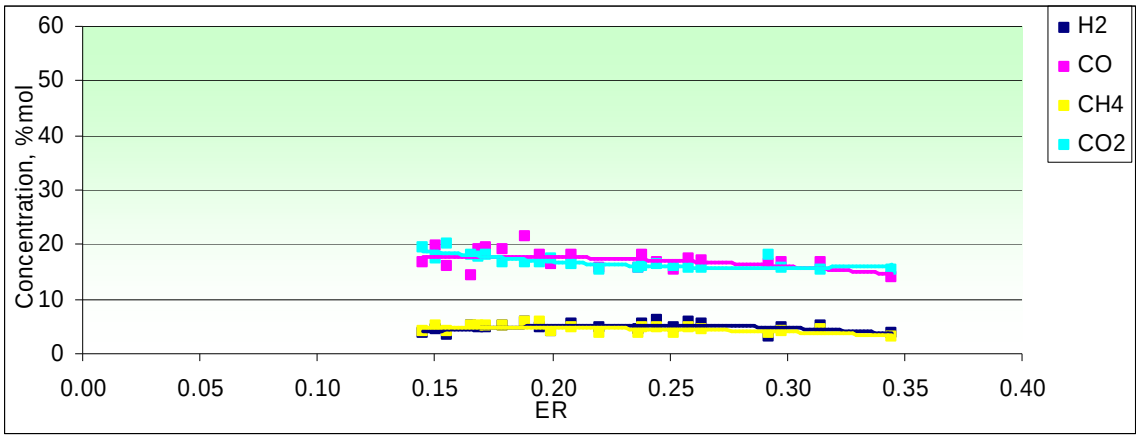

Figure 4.4 Dry gas molar composition from air gasification of switchgrass

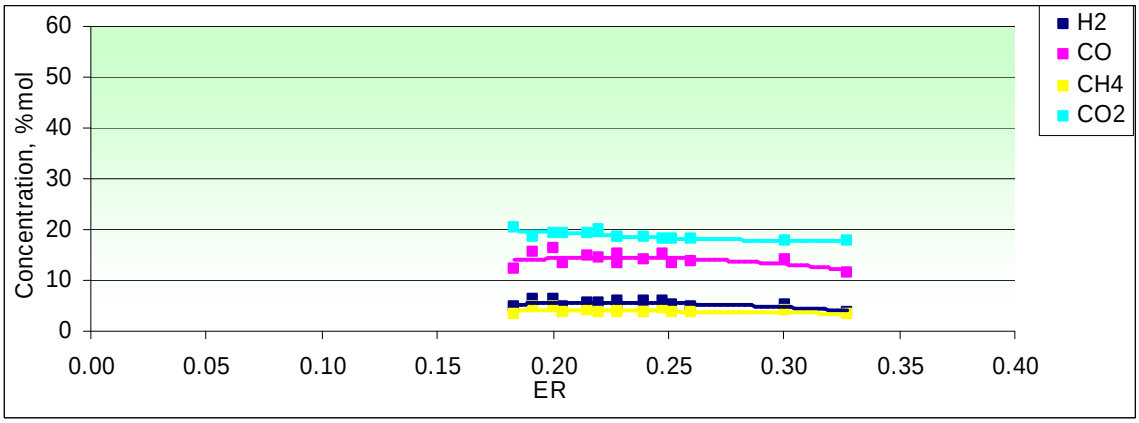

Figure 4.5 Dry gas molar composition from air gasification of bermudagrass

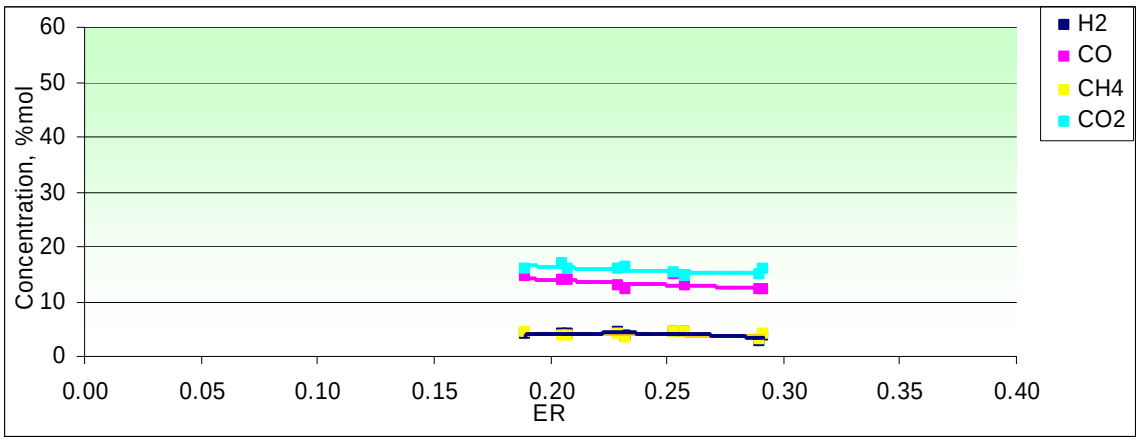

Figure 4.6 Dry gas molar composition from air gasification of corn gluten

4.2.3 Water

In all three biomass cases shown in Figures 4.7, 4.8 and 4.9, water production increases rapidly in the ER range from 0.35 to 0.2. Switchgrass, bermudagrass and corn gluten do not produce equal amounts. Corn gluten produces from 150 to 450 g/Nm^3, whereas the water for switchgrass is measured between 130 and 380 g/Nm^3. Bermudagrass generates the less water with values between 100 and 250 g/Nm^3 in the same ER range. Water concentrations shown reflect the hydrogen levels before the gas is cooled which shifts the equilibrium towards water production.

An exponential trend line could be a good match for these data. This choice of function implies a water concentration close to zero for ER = 1, which could be satisfactory, since hydrogen production reduces with increasing ER, inducing a decrease in water shift. However, a polynomial is a better choice, because it is important to consider that at ER = 1, or stoichiometric combustion, the water produced should be at its highest level. It is then possible that the last data points at the highest ER, showing what seems to be minimums on all three graphs, Figures 4.7, 4.8 and 4.9, are not data dispersions due to measurement error, but higher values of water content suggesting an increasing amount of combustion versus gasification reactions between the minimum at its respective ER and when ER = 1. These multiple hydrogen pathways to water in the gas stream, explains the presence of a minimum in the range of ER 0.25 to 0.3, which also correspond to the best air gasification range (Reed, 1981). The polynomial equations shown in Figure 4.7 and 4.9 for switchgrass and corn gluten account for 68 to 80 %, respectively of the variation in the observations. However, the polynomial equations for bermudagrass Figure 4.8 accounts for only 44% of the variation in the observations.

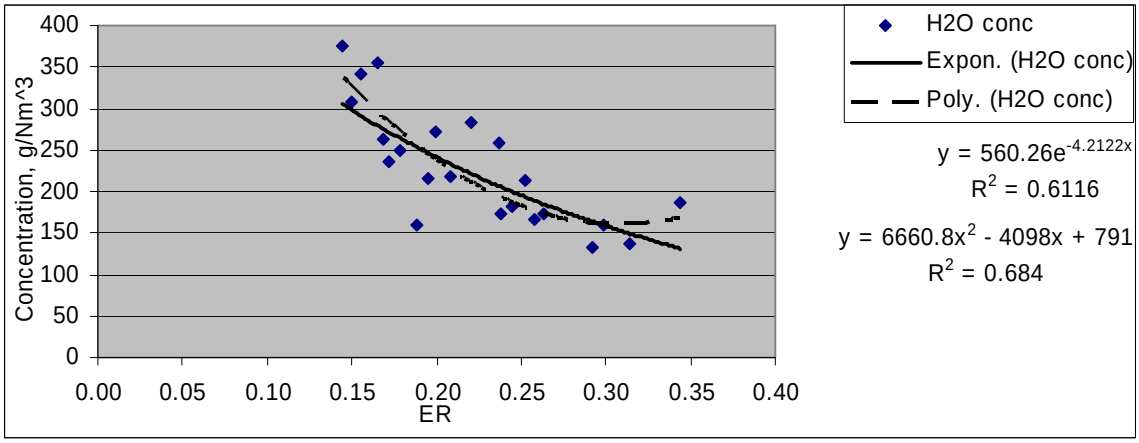

Figure 4.7 Water concentration in gas from air gasification of switchgrass

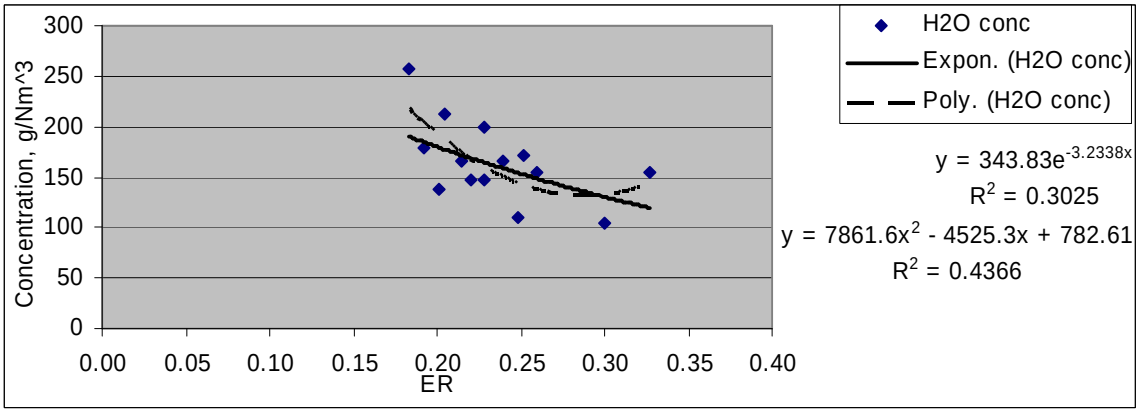

Figure 4.8 Water concentration in gas from air gasification of bermudagrass

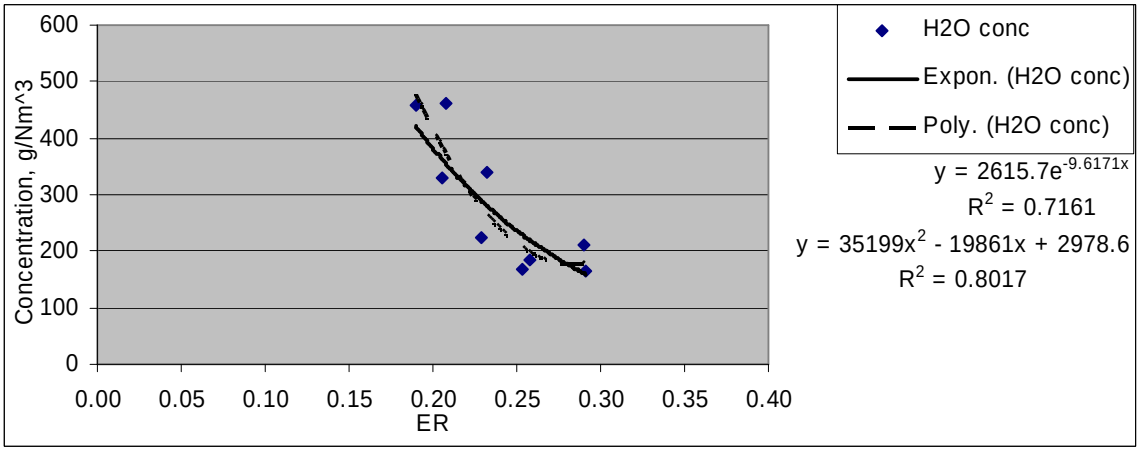

Figure 4.9 Water concentration in gas from air gasification of corn gluten

4.2.4 Tar

Figures 4.10-12 show both the results of the gravimetric and GC-MS tar analysis. The latter procedure is more precise because the gravimetric method looses some of the lighter compounds in the solvent evaporation step process. On the other hand, the GC-MS method may be a challenge for heavier polycyclic aromatic hydrocarbon (PAH) compounds as polycyclic molecules of 4 cycles and above, face challenges to enter the capillary column of the GC-MS and remain in the injection port. Both methods are highly dependent on the precision of the sampling step.

In air gasification of switchgrass and bermudagrass, tar levels increase exponentially from 10 to 20 g/Nm^3 at ER = 0.35 and up to 50 to 60 $g/Nm^3$with ER = 0.15 for switchgrass and 0.17 for bermudagrass.

The gravimetric data for corn gluten are the result of an oven drying method of the sample before the tar guidelines recommended a rotary evaporator. However, this still does not explain why the GC-MS data show a decrease in tar amounts. It appears the data for higher ERs are higher than expected because the remainder of the GC-MS data for corn gluten seems to agree with the levels found in switchgrass and bermudagrass. One hypothesis is that the high ash content of the corn gluten could have affected the catalysis of tar.

All six curves match an exponential type equation as seen in the literature (Corolla et al., 1989), resulting in tar approaching zero at combustion conditions ER=1. The equations for tar (GC-MS) shown in Figure 4.10 and 4.11 account for 80% to 90% of the variation in observations. However the equation for Tar (GC-MS) from gasification of corn gluten shown in Figure 4.12 does not explain the variation of the observations. The

exponential is not a proper match and more likely dispersion in the data measurement is too important.

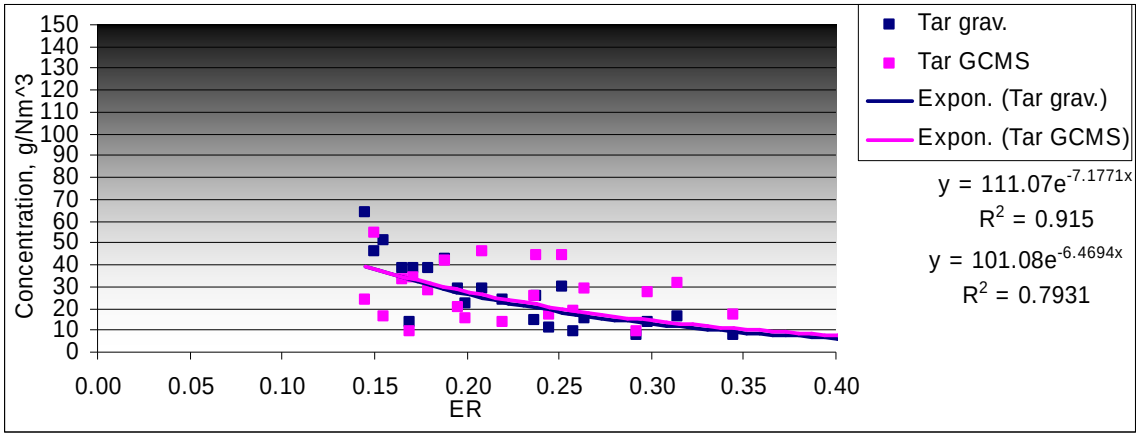

Figure 4.10 Tar concentration in gas from air gasification of switchgrass

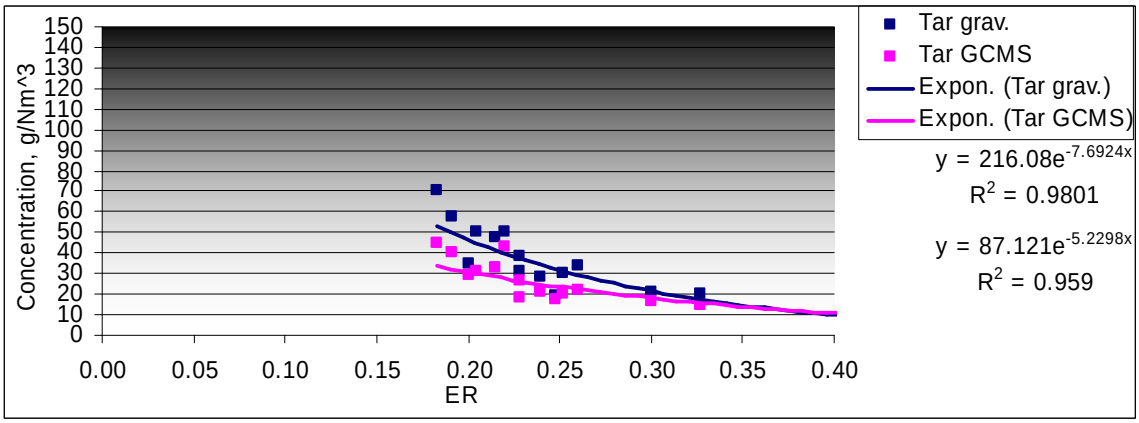

Figure 4.11 Tar concentration in gas from air gasification of bermudagrass

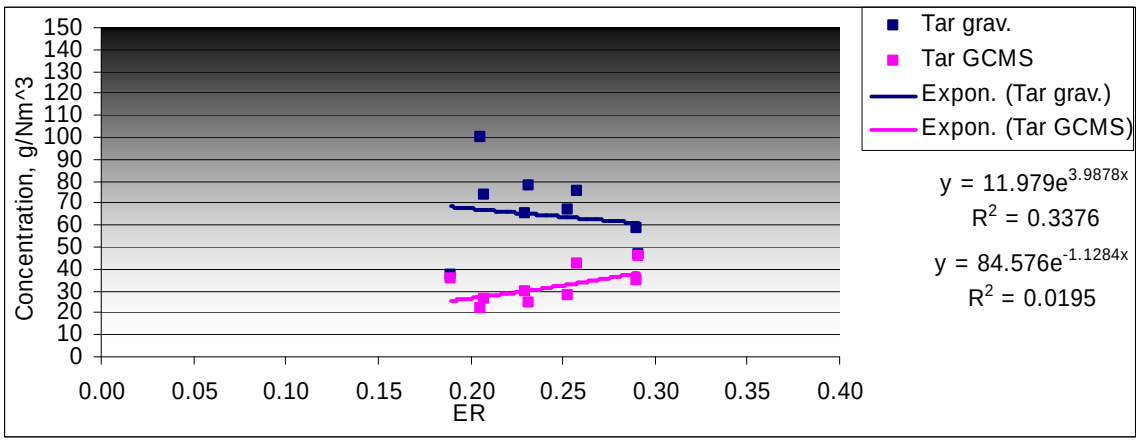

Figure 4.12 Tar concentration in gas from air gasification of corn gluten

Tar atomic compositions, shown in Figures 4.13, 4.14, and 4.15, and average molecular weight do not depend on the ER, nor do they depend on the temperature since ER and temperature are interrelated in air gasification.

Tar average atomic composition is constant regardless of the conditions of air gasification (Table 4.2).

	C	H	O	N	MW
Switchgrass	7.785	8.060	0.390	0.054	108.640
Bermudagrass	7.383	8.855	0.406	0.251	107.460
Corn gluten	7.170	8.866	0.341	0.355	105.357

Table 4.2 Tar average atomic composition and molecular weight in air gasification

Another interesting aspect of the tar is, despite an average atomic weight relatively constant at all conditions of air gasification, the enthalpy of formation (Figures 4.16, 4.17 and 4.18) varies according to a trend that is almost linear. Procedure for calculation of enthalpy of formation is in Appendix 8.5. The significance of this is although the atomic composition is not changing, the nature of the compound is changing towards compounds of lower free energy as the ER decreases. A similar trend is also found in bermudagrass and corn gluten but dispersion of the data due to technical difficulties during storage and analysis of the tar samples make the trends less apparent. The equation shown in Figure 4.16 accounts for 88% of the variation in the observations for switchgrass.

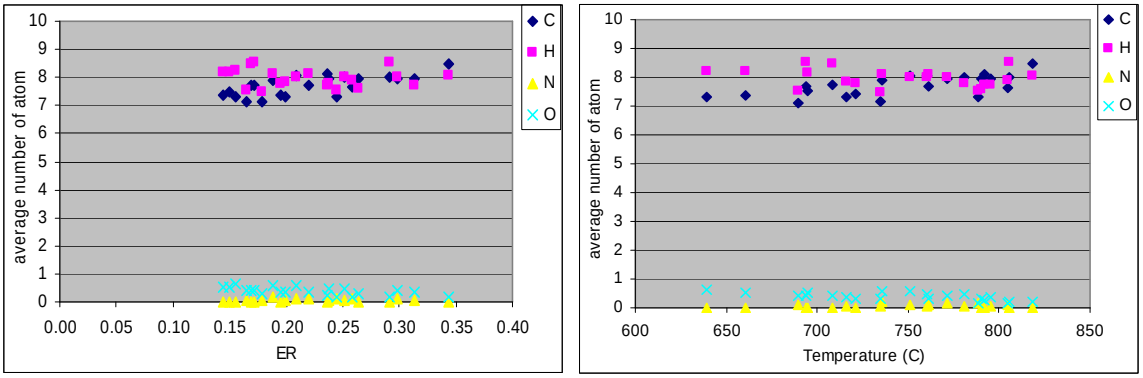

Figure 4.13 Switchgrass average tar atomic composition vs ER vs temperature in air gasification.

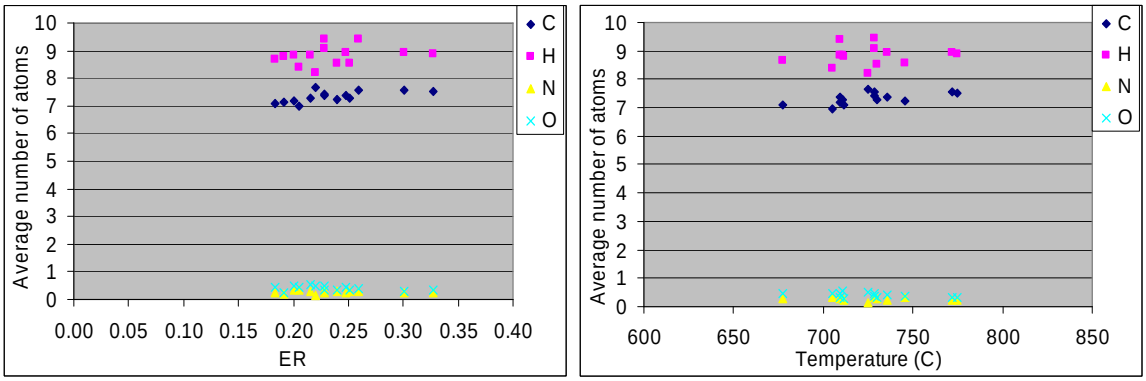

Figure 4.14 Bermudagrass average tar atomic composition vs ER vs temperature in air gasification.

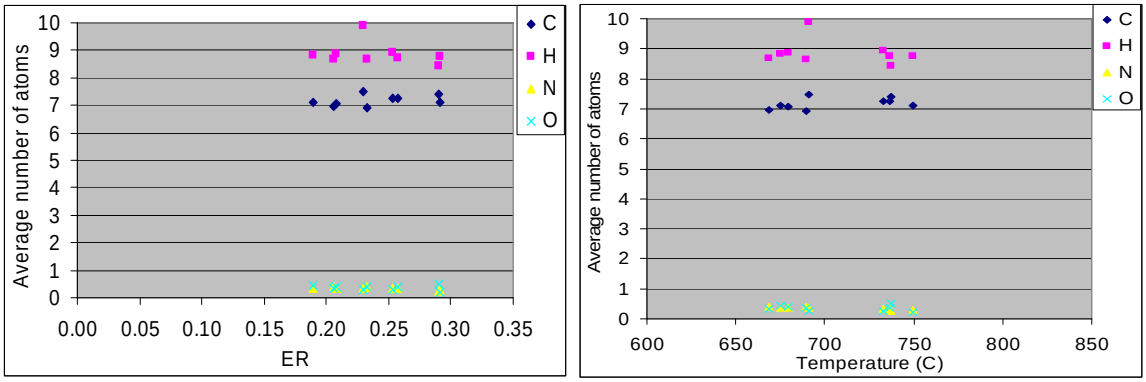

Figure 4.15 Corn gluten average tar atomic composition vs ER vs temperature in air gasification.

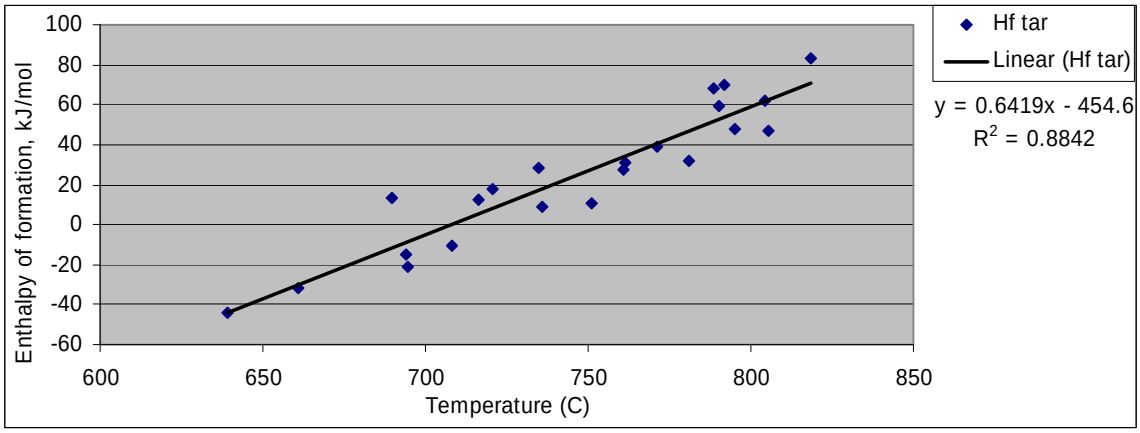

Figure 4.16 Enthalpy of formation of tar at 298K for air gasification of switchgrass.

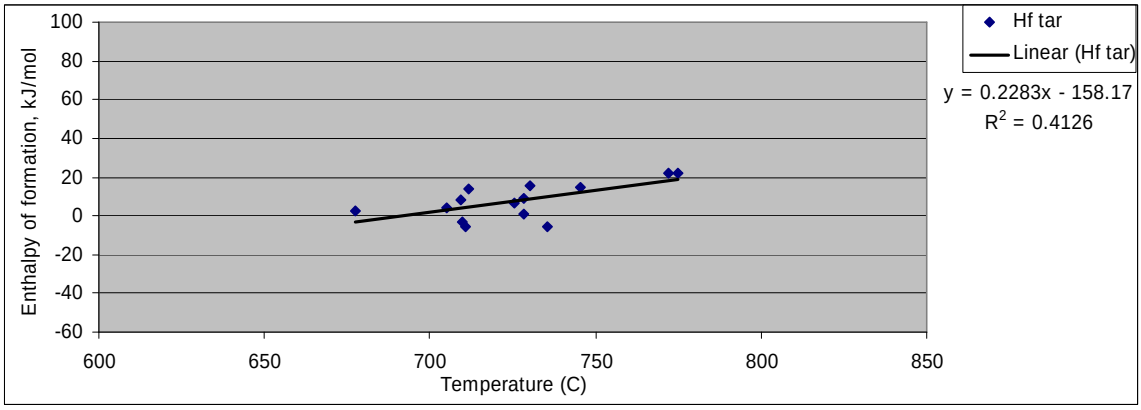

Figure 4.17 Enthalpy of formation of tar at 298K for air gasification of bermudagrass.

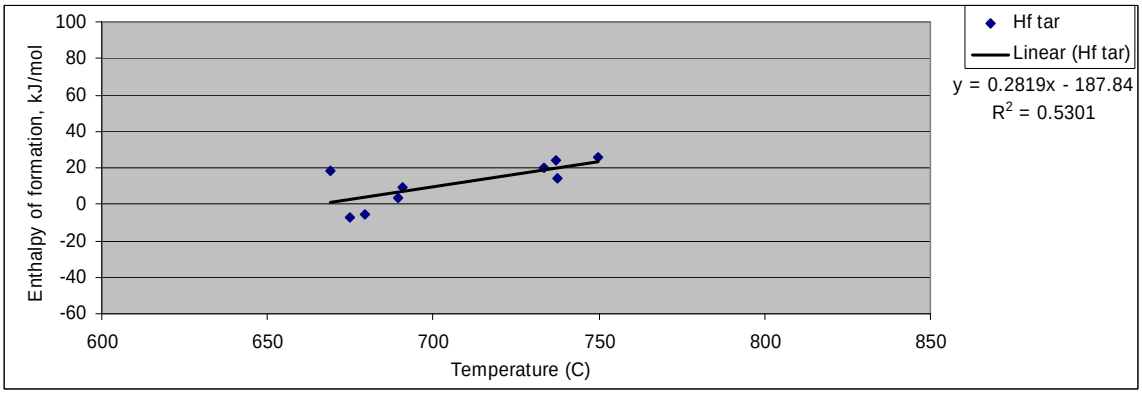

Figure 4.18 Enthalpy of formation of tar at 298K for air gasification of corn gluten

4.2.5 Carbon to gas efficiency

As ER decreases in Figures 4.19, 4.20 and 4.21, so does the conversion of the carbon from the biomass to the gas. For all three biomass types, the conversion decreases from 80-90% for an ER of about 0.3 to 50% for ER values between 0.15 and 0.2.

Switchgrass and bermudagrass conversion values are higher than corn gluten for the same ER values. As ER decreases, bermudagrass stays at 90% conversion, further in ERs than switchgrass. Bermudagrass conversion starts reducing at lower ER values than switchgrass. Bermudagrass conversions reduce rapidly to end at the same level than switchgrass for the same ER value.

Excel is unable to calculate an appropriate curve fitting for the carbon C to gas efficiency itself, but does for both C to tar efficiency and C to particulate matter (PM) efficiency as exponential forms.

Since the sum of the three efficiencies is 100%, the best curve fitting for C to gas efficiency is 100 minus the two exponential terms of the two other efficiencies:

$$Eff_{C\ to\ gas}=100 - Eff_{C\ to\ PM} - Eff_{C\ to\ tar} \quad (4.1)$$

Although tar increases as ER decreases, unreacted carbon in the char remains the primary reason for the reduction in efficiency.

The equations shown in Figure 4.19, 4.20 and 4.21 account for 56% and 86% of the variation in the observations in particulate matter and tar, respectively, for switchgrass to over 80 to 90% for bermudagrass and corn gluten.

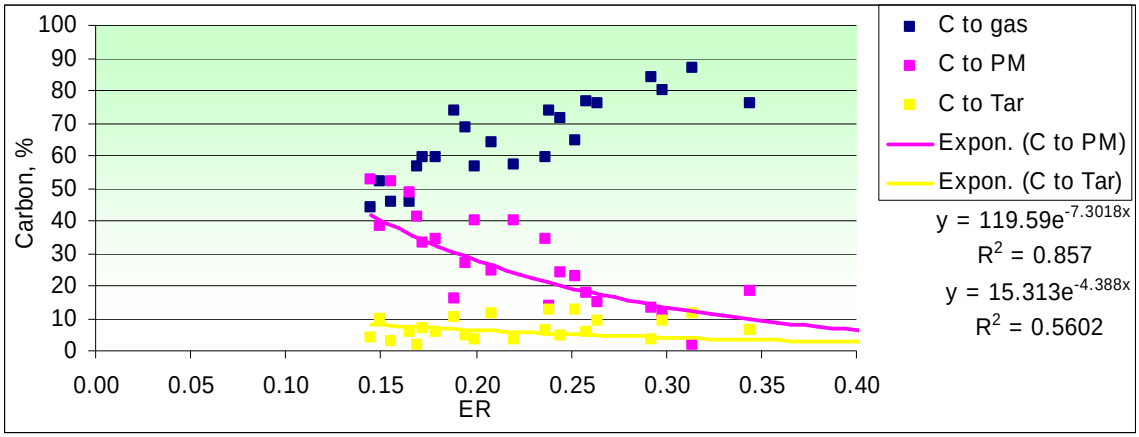

Figure 4.19 Carbon to gas efficiency from air gasification of switchgrass

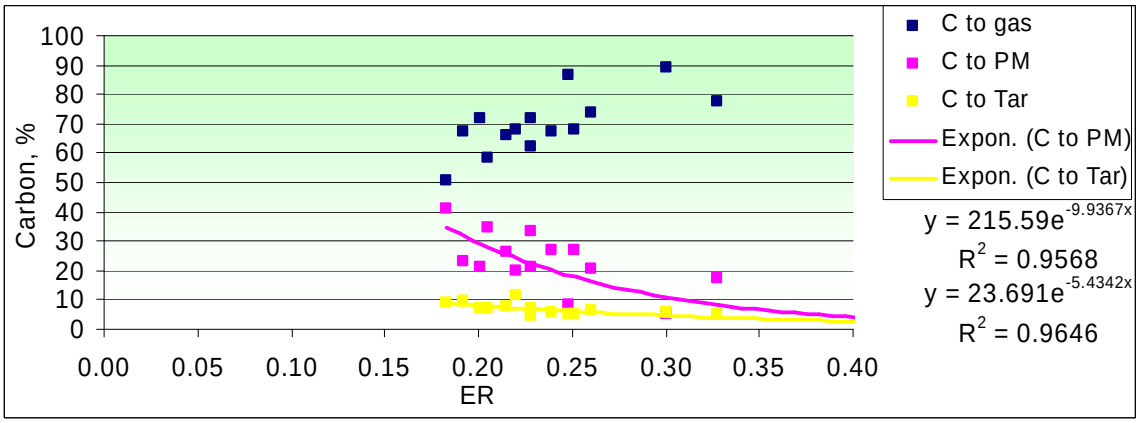

Figure 4.20 Carbon to gas efficiency from air gasification of bermudagrass

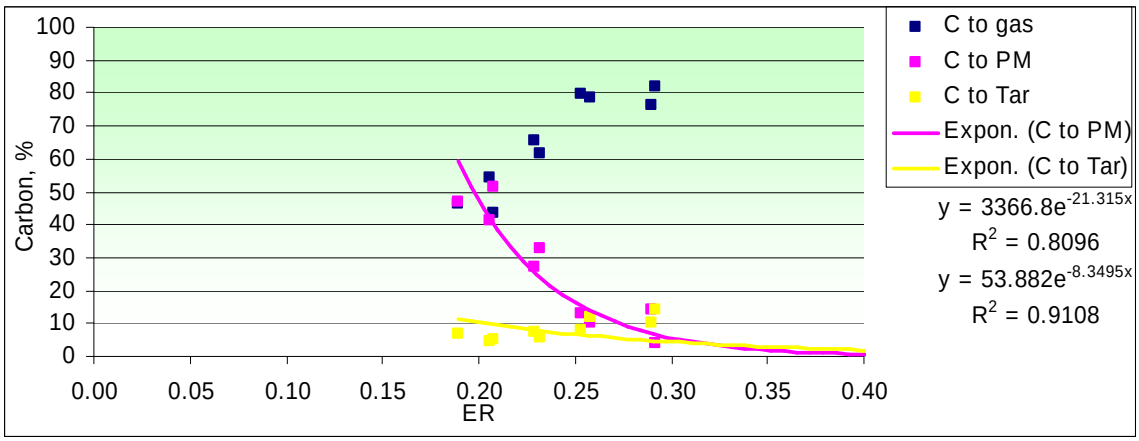

Figure 4.21 Carbon to gas efficiency from air gasification of corn gluten

4.2.6 Carbon to CO efficiency

Figures 4.22, 4.23 and 4.24 show the carbon to CO efficiencies of the air gasification for all three biomasses. All three graphs seem to show a maximum efficiency around the ER 0.25 to 0.3. The presence of a maximum is logical since no carbon goes to CO at combustion conditions ER=1, and at low ER conditions the tar and char portion increase exponentially. This value of maximum efficiency is verified in the literature (Reed, 1981) and other fluidized bed gasifier results.

The equations shown in Figure 4.22, 4.23 and 4.24 account for 45% of the variation in the observations for bermudagrass to approximately as 65% for switchgrass and corn gluten.

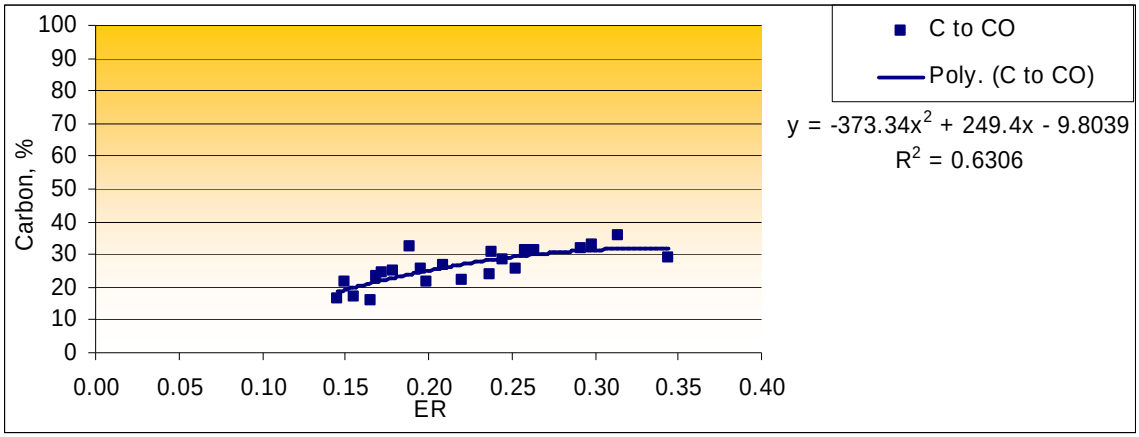

Figure 4.22 Carbon to CO efficiency from air gasification of switchgrass

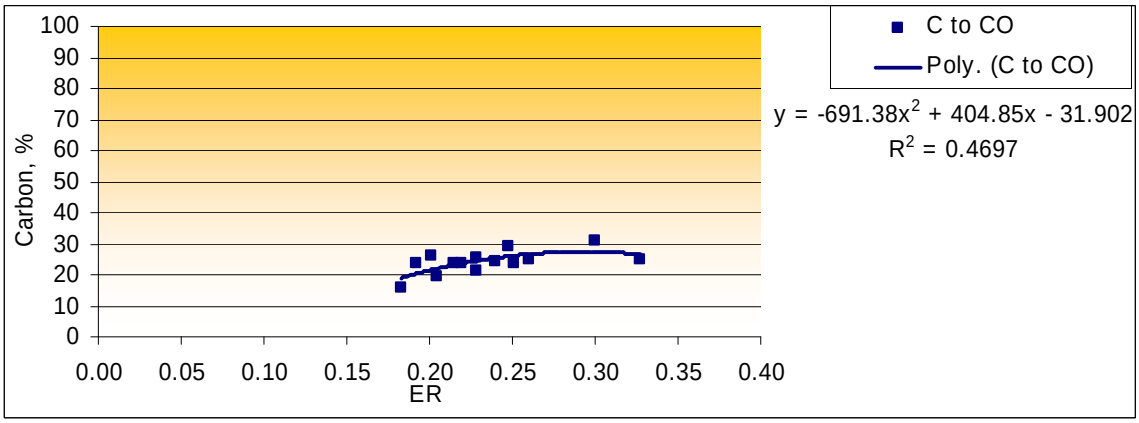

Figure 4.23 Carbon to CO efficiency from air gasification of bermudagrass

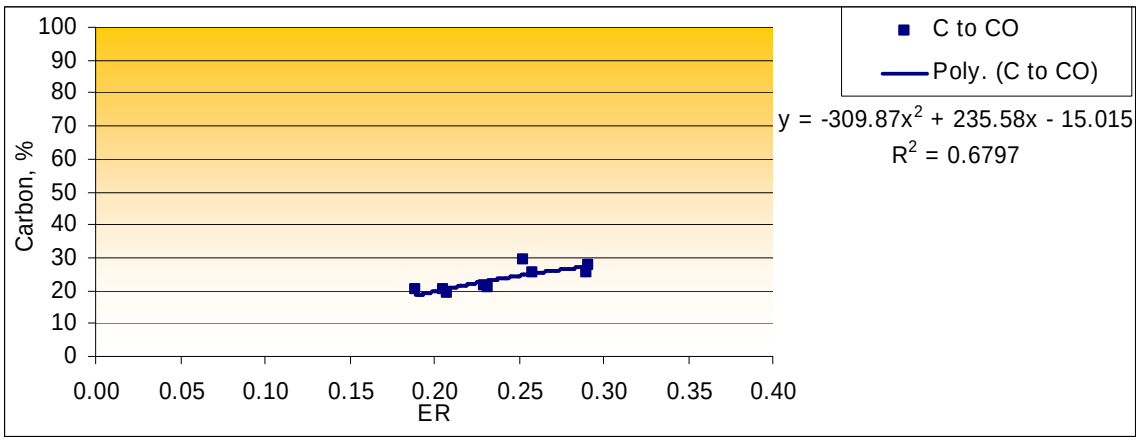

Figure 4.24 Carbon to CO efficiency from air gasification of corn gluten

4.2.7 Enthalpy of the gas

Figures 4.25, 4.26 and 4.27 show the enthalpy of the gas versus ER. The enthalpy of gas increases as ER decreases. This is due to the formation of methane a high heating value (HHV) gas and higher concentration of H_2 and CO.

Switchgrass and corn gluten show the most variation of heating value in the produced gas from 4000 to 6000 kJ/kg between ERs of 0.35 to 0.18. The HHV of the gas from bermudagrass increases and then stabilizes at a value close to 4000 kJ/kg as ER decreases in the same range as switchgrass.

The equations shown in Figures 4.25, 4.26 and 4.27 have a wide range of data points, which does not provide a meaningful trendline.

4.2.8 Enthalpy of reaction

Figures 4.28, 4.29 and 4.30 show the standard enthalpies of the air gasification reaction versus ER in the fluidized bed gasifier pilot plant. As the enthalpy of reaction increases steadily for switchgrass with lowering ER, bermudagrass and corn gluten reach a maximum at different values of enthalpy and ER, -3000 kJ/kg of CH_xO_y fed to the reactor at ER = 0.15, -4000 kJ/kg at ER = 0.225 respectively. Switchgrass shows a higher enthalpy of reaction at -2500 kJ/kg of CH_xO_y for ER=0.18. It is expected that this value for switchgrass would have reached a maximum as well if the experiments were conducted at a lower ER.

The equations shown in Figure 4.28, 4.29 and 4.30 account for only 40% of the variation in the observations for corn gluten to over 99% for switchgrass and bermudagrass.

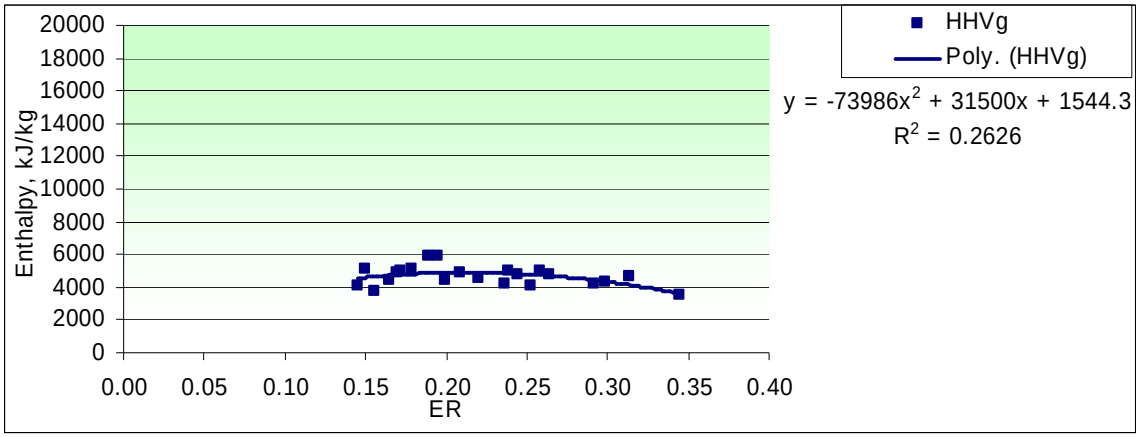

Figure 4.25 Enthalpy of gas from air gasification of switchgrass

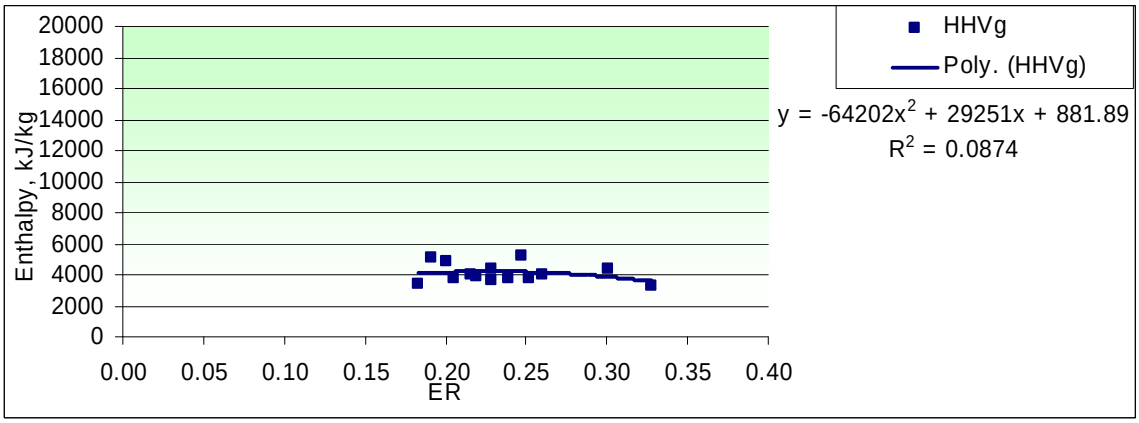

Figure 4.26 Enthalpy of gas from air gasification of bermudagrass

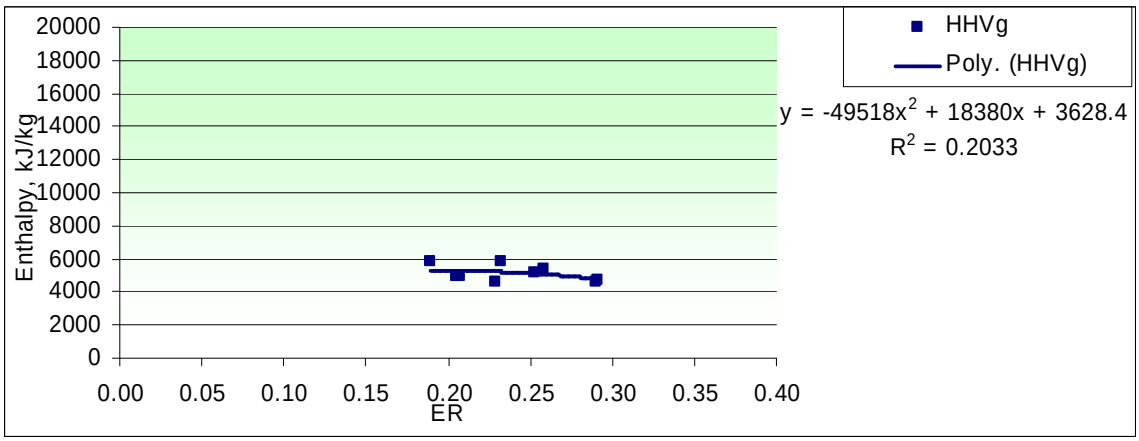

Figure 4.27 Enthalpy of gas from air gasification of corn gluten

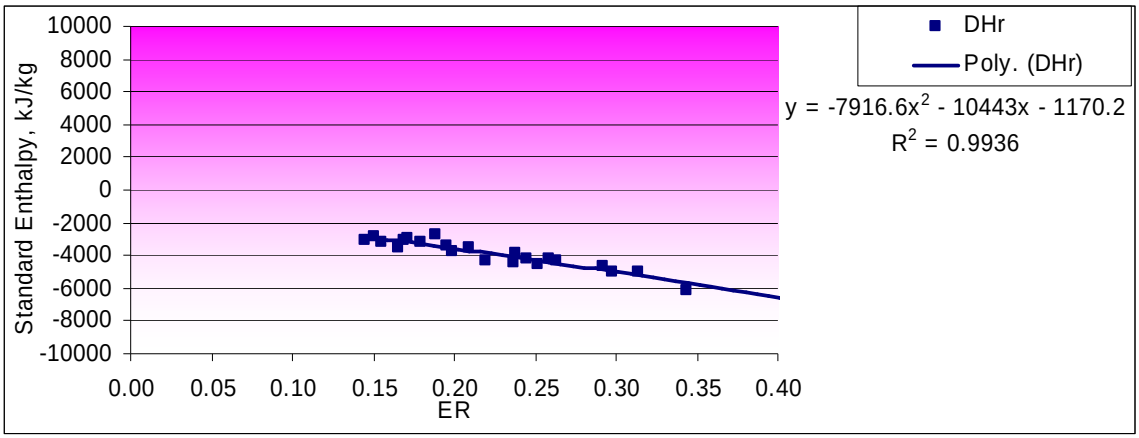

Figure 4.28 Standard enthalpy of reaction from air gasification of switchgrass

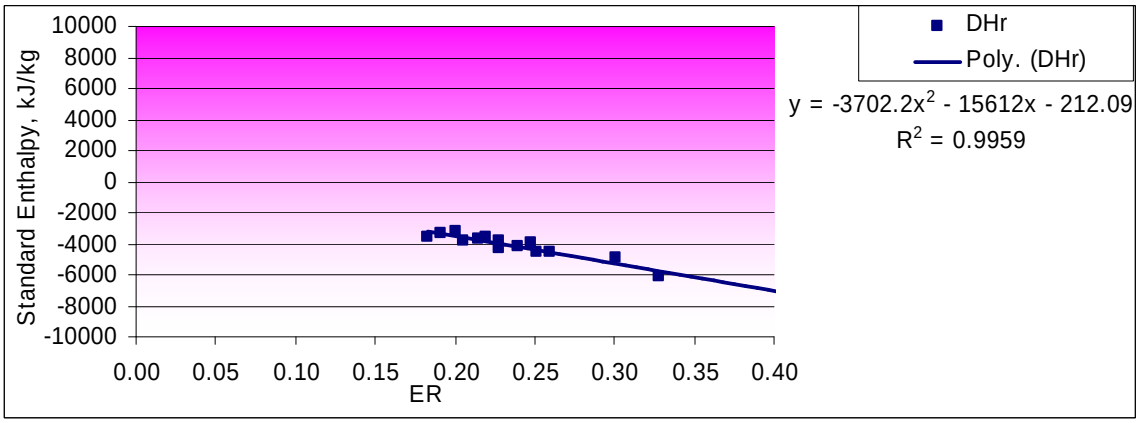

Figure 4.29 Standard enthalpy of reaction from air gasification of bermudagrass

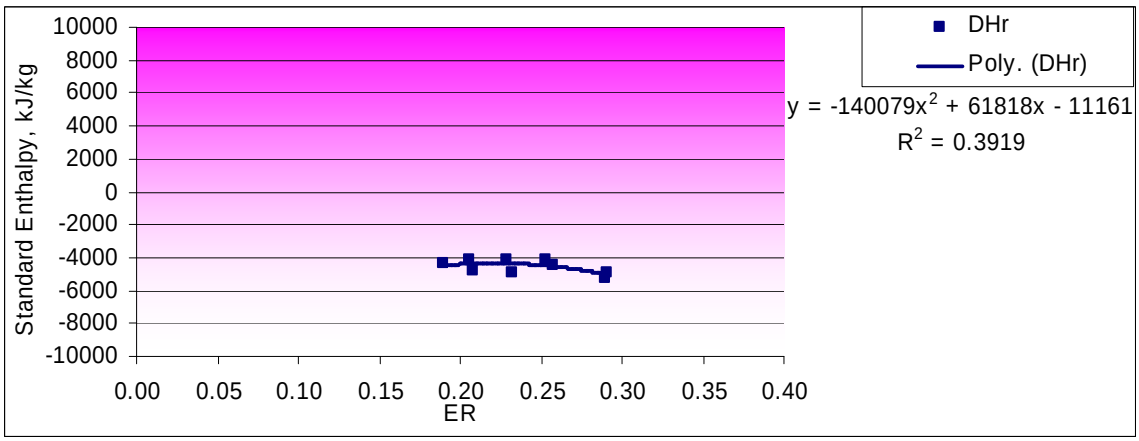

Figure 4.30 Standard enthalpy of reaction from air gasification of corn gluten

4.3 FLAMING PYROLYTIC GASIFICATION

4.3.1 Temperature profiles

In this experiment, the temperature of the reactor is maintained at 775°C. There are two reasons for this choice; 1) a limitation in heating element sheath maximum temperature of 850°C and 2) the likelihood for bermudagrass and corn gluten to agglomerate the bed at temperatures above 800°C.

Figures 4.31, 4.32 and 4.33 show steady temperatures, except in the case of pure pyrolysis of bermudagrass while using two heaters because one failed, when the system was limited in power to sustain the desired temperature of 775°C.

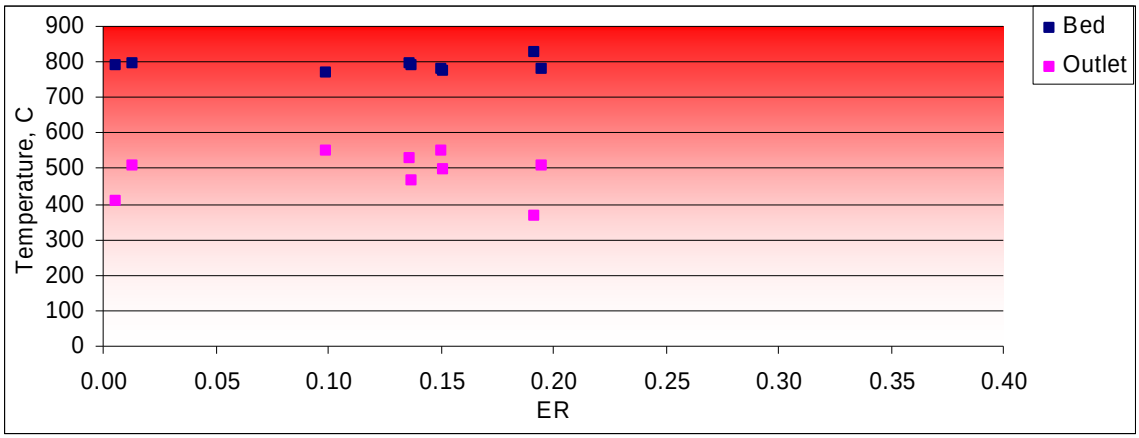

Figure 4.31 Flaming pyrolytic gasification of switchgrass temperature profile

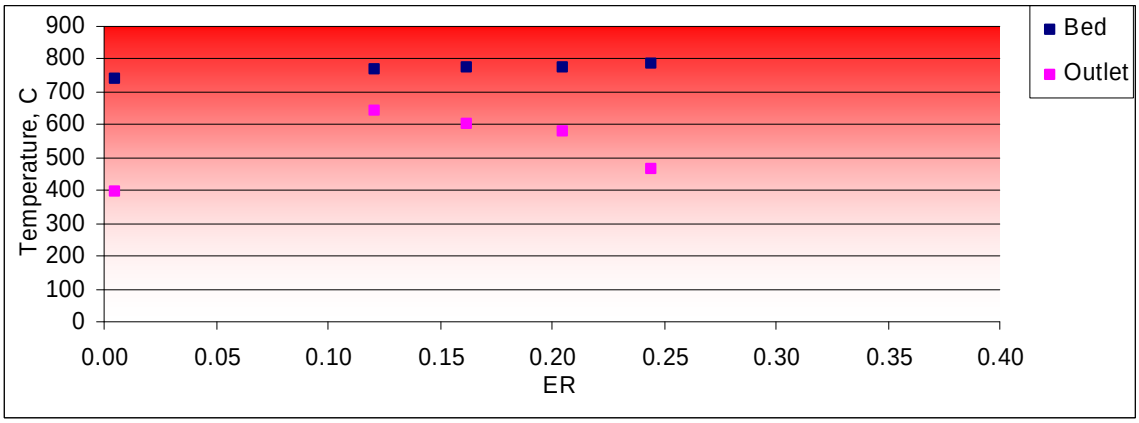

Figure 4.32 Flaming pyrolytic gasification of bermudagrass temperature profile

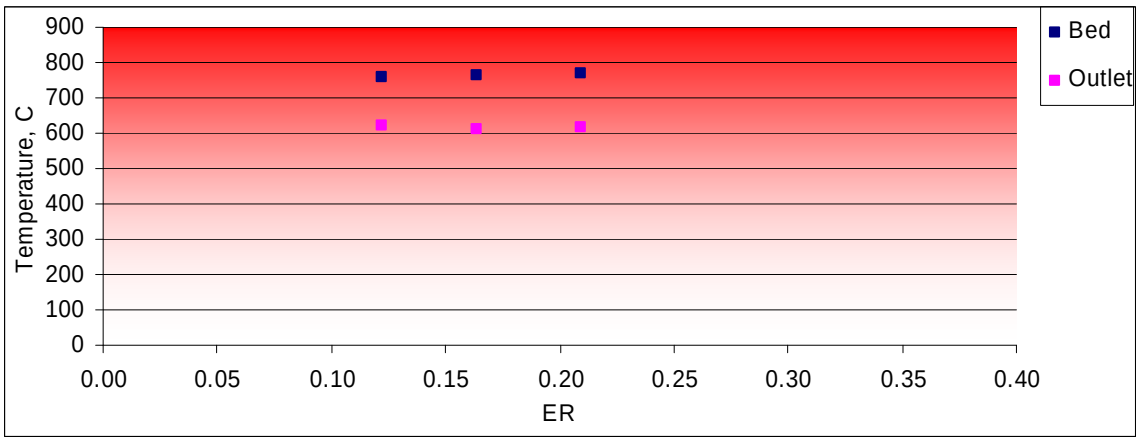

Figure 4.33 Flaming pyrolytic gasification of corn gluten temperature profile

4.3.2 Gas composition

Figures 4.34, 4.35 and 4.36 show the dry gas compositions for flaming pyrolytic gasification. Percentages of combustible gases of greatest interest, CO and H_2, are increasing exponentially for switchgrass and bermudagrass between the values of ER where air gasification experiments ended, about 0.2, down to 0.0 for pure pyrolysis. Within this ER range, CO increases from 20 to 40% for switchgrass and from 15 to 30% for bermudagrass. H_2 increases from 5 to 22% for switchgrass and from 5 to 26% for bermudagrass. CH_4 increase from 5 to 14% for switchgrass and bermudagrass. On the other hand CO_2 remains stable for switchgrass, and has a slight increase of 3% for bermudagrass.

In the case of corn gluten, CO_2 actually decreases 6% while CO, H_2, and CH_4 remain relatively constant. Experimentation of corn gluten towards pyrolysis could not verify increases in those gas concentrations at lower ERs, because of repetitive bed agglomeration at these conditions limited the study. Further experimentation could be of interest, if the bed agglomeration can be avoided while maintaining a temperature adequate for high gas conversion and low tar production.

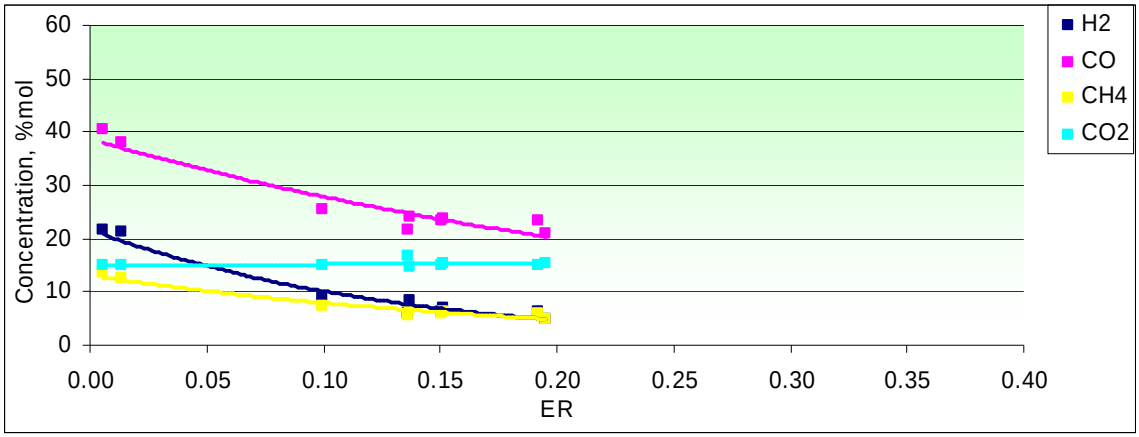

Figure 4.34 Dry gas molar composition from flaming pyrolytic gasification of switchgrass

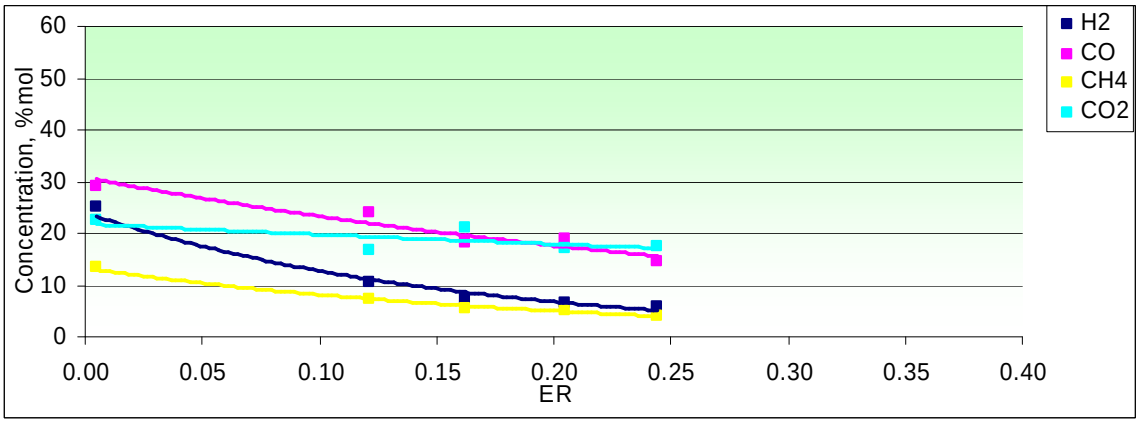

Figure 4.35 Dry gas molar composition from flaming pyrolytic gasification of bermudagrass

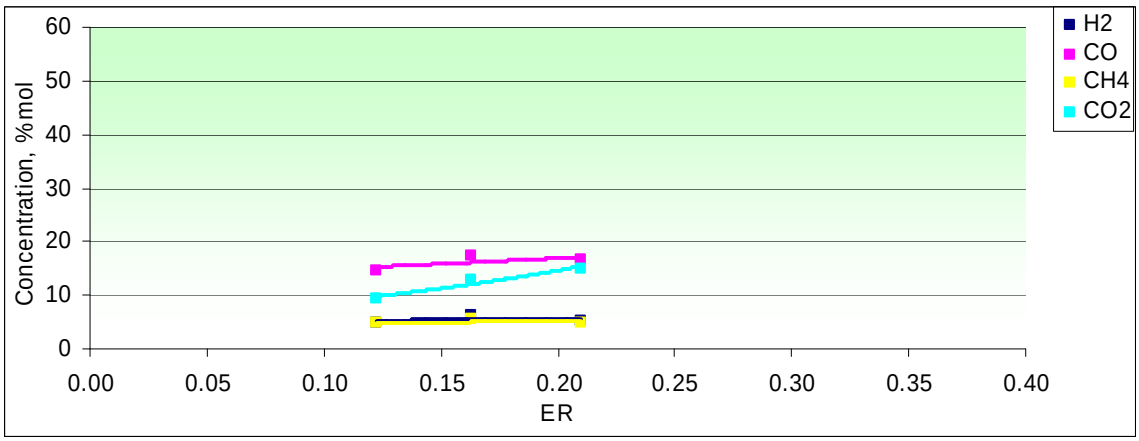

Figure 4.36 Dry gas molar composition from flaming pyrolytic gasification of corn gluten

4.3.3 Water

The water measured comes primarily from the conversion of the H_2 to water as the equilibrium changes during cool down. Figures 4.37, 4.38, and 4.39 show a large increase in water production for switchgrass and bermudagrass, in the order of 250 g/Nm^3 and 600 g/Nm^3 respectively, with a small decrease for corn gluten. These values are in the same order as air gasification. After cool down, the levels of H_2 stabilized at higher H_2 gas compositions than the ones in air gasification.

Because of limited data for bermudagrass and corn gluten, it is difficult to assess if these opposite variations are reflecting the trend of flaming pyrolytic gasification of these materials or if analytical measurement are at fault.

Technical difficulties during the storage and analysis of samples were common, resulting in significant variability, making it difficult to identify trends.

The equations shown in Figures 4.37, 4.38 and 4.39 account for 75% of the variation in the observations for switchgrass.

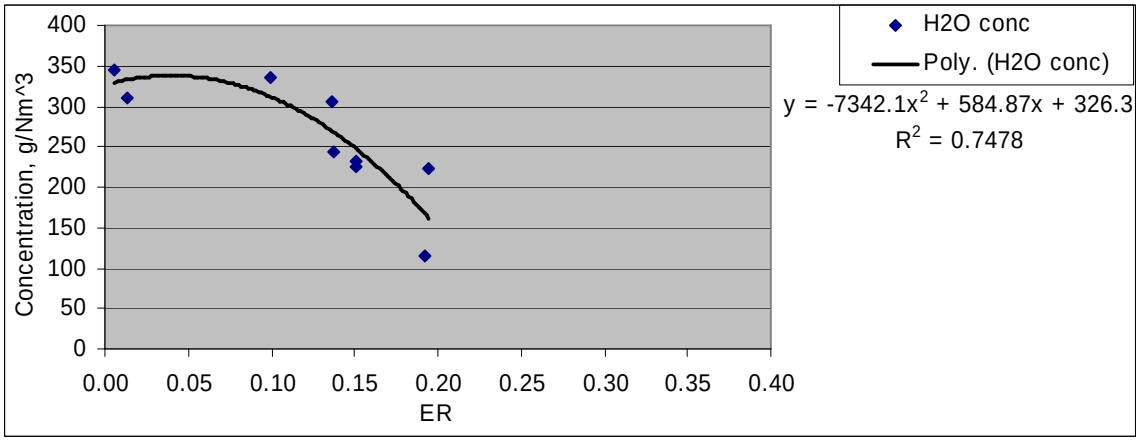

Figure 4.37 Water concentration in gas from flaming pyrolytic gasification of switchgrass

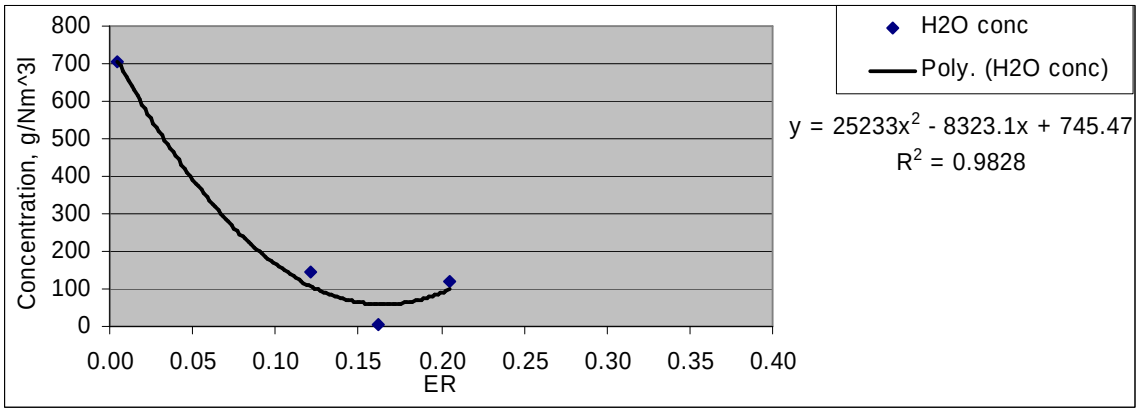

Figure 4.38 Water concentration in gas from flaming pyrolytic gasification of bermudagrass

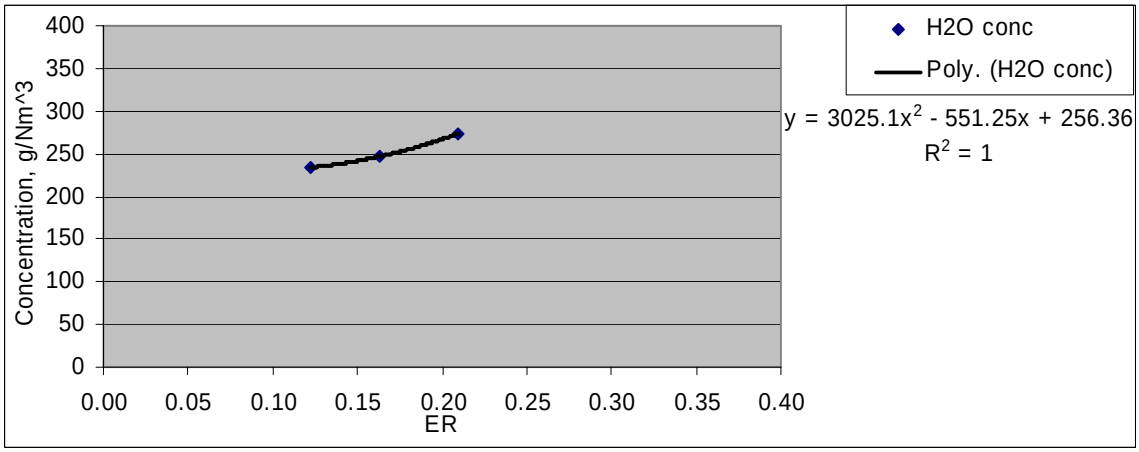

Figure 4.39 Water concentration in gas from flaming pyrolytic gasification of corn gluten

4.3.4 Tar

Similar to the previous process discussion, Figures 4.40, 4.41 and 4.42 show both the results of the gravimetric and GC-MS tar analysis.

In flaming pyrolytic gasification and pyrolysis with ER=0.2 to 0, switchgrass and bermudagrass reach tar levels between 25 to 110 g/Nm^3. Tar levels increase exponentially from 25 g/Nm^3 at ER = 0.2 up to 110 g/Nm^3 at ER = 0.

As for the previous process, the gravimetric data for corn gluten are the result of an oven drying method before the tar guidelines recommended a rotary evaporator. This explains why the gravimetric tar is so much higher than the GC-MS data.

In flaming pyrolytic gasification and pyrolysis, the corn gluten tar GC-MS data show a slight reduction in tar, not an exponential increase as expected. This confirms the hypotheses shown previously in air gasification, that corn gluten, unlike switchgrass and bermudagrass, has a reduction of tar as ER decreases when temperature is maintained around 775°C.

In flaming pyrolytic gasification and pyrolysis, all six curves match an exponential-type equation, resulting in tar approaching zero at combustion conditions ER=1 and increases as ER decreases.

The equations for tar (GC-MS) shown in Figures 4.40, 4.41 and 4.42 account for over 83% of the variation in observations.

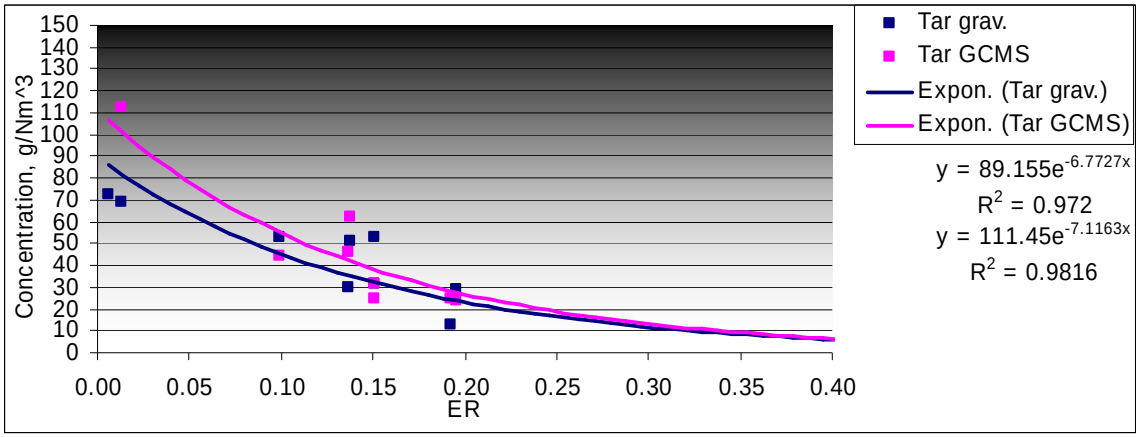

Figure 4.40 Tar concentration from flaming pyrolytic gasification of switchgrass

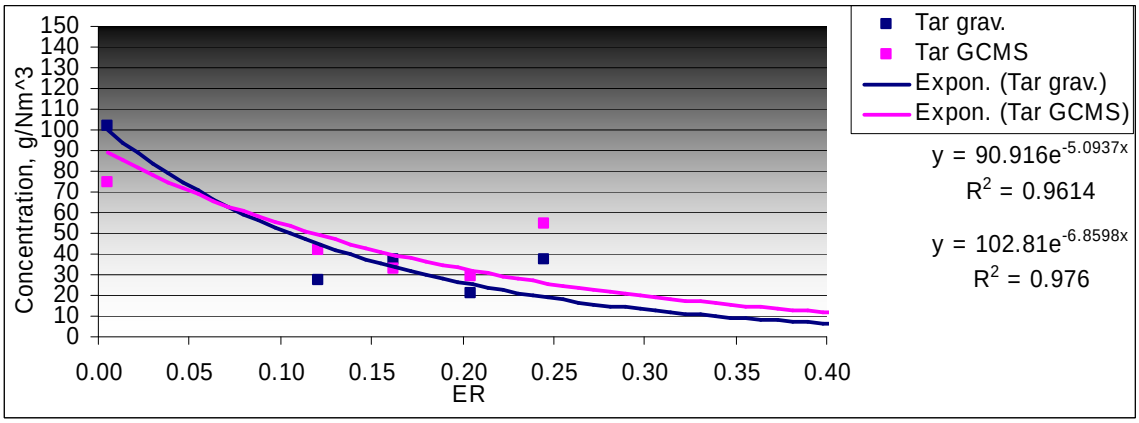

Figure 4.41 Tar concentration from flaming pyrolytic gasification of bermudagrass

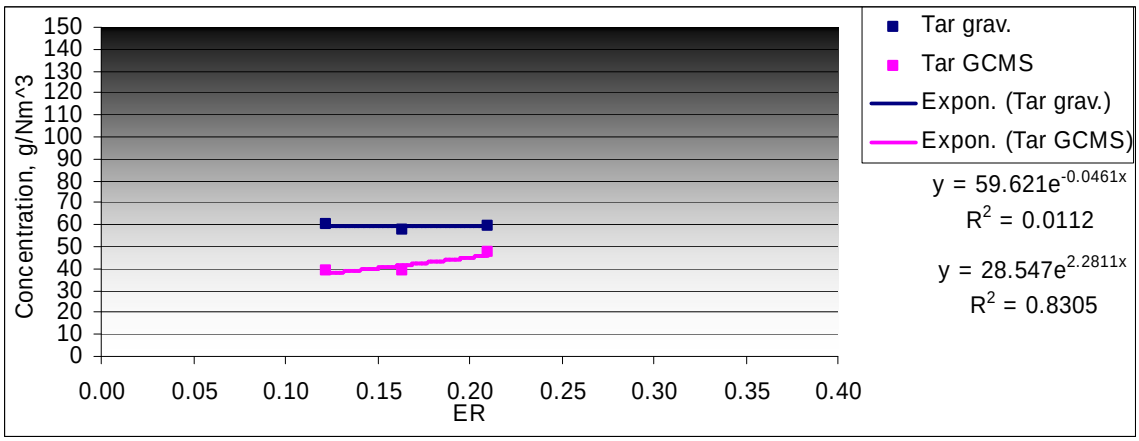

Figure 4.42 Tar concentration from flaming pyrolytic gasification of corn gluten

Flaming pyrolytic gasification tar atomic composition (Figures 4.43, 4.44 and 4.45) and average molecular weight do not depend on ER, but seem to depend on the temperatures. Although the effort is to keep bed temperature at 775°C, as temperature decreases near pyrolysis by lack of electrical heating power (one element malfunctioned) there is a slight change in tar atomic composition.

Tar average atomic composition shows little change for switchgrass, bermudagrass and corn gluten in flaming and pure pyrolytic gasification. Average results are in Table 4.3.

	C	H	O	N	MW
Switchgrass	7.818	7.903	0.279	0.043	106.773
Bermudagrass	7.662	8.955	0.332	0.219	109.279
Corn gluten	7.705	9.088	0.264	0.379	111.296

Table 4.3 Tar average atomic composition and molecular weight in flaming pyrolytic gasification and pyrolysis

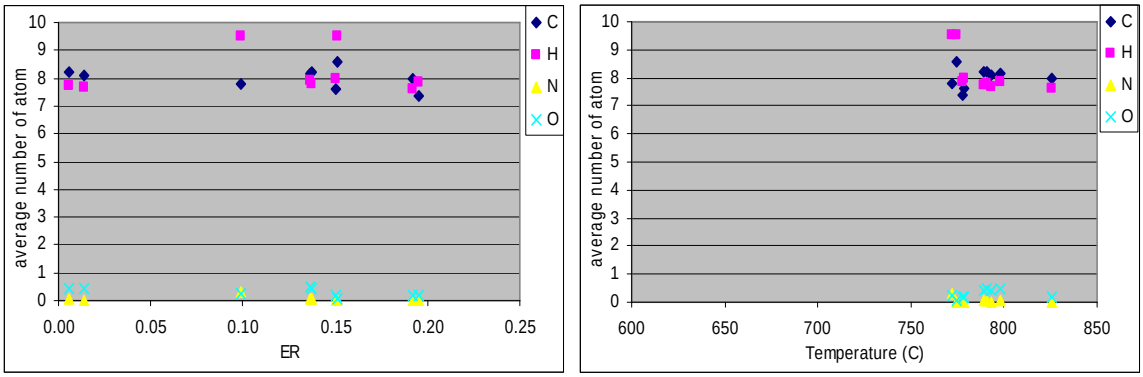

Figure 4.43 Switchgrass average tar atomic composition vs ER vs temperature in flaming pyrolytic gasification and pyrolysis.

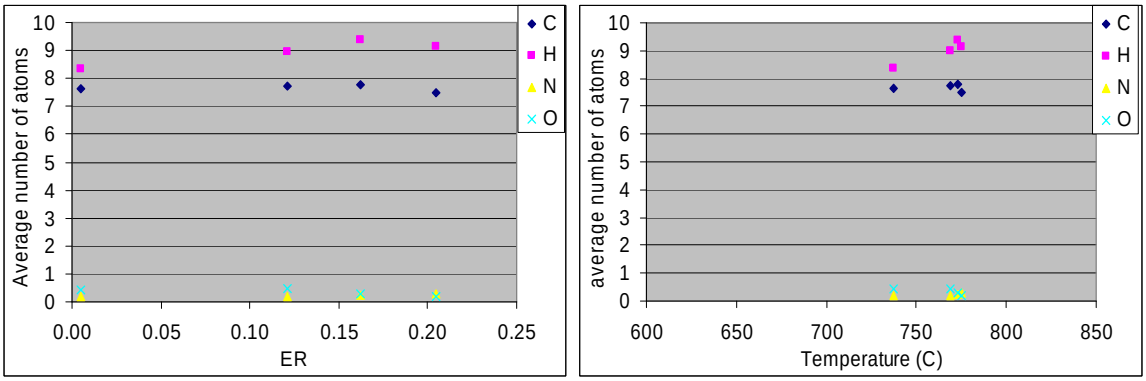

Figure 4.44 Bermudagrass average tar atomic composition vs ER vs temperature in flaming pyrolytic gasification and pyrolysis.

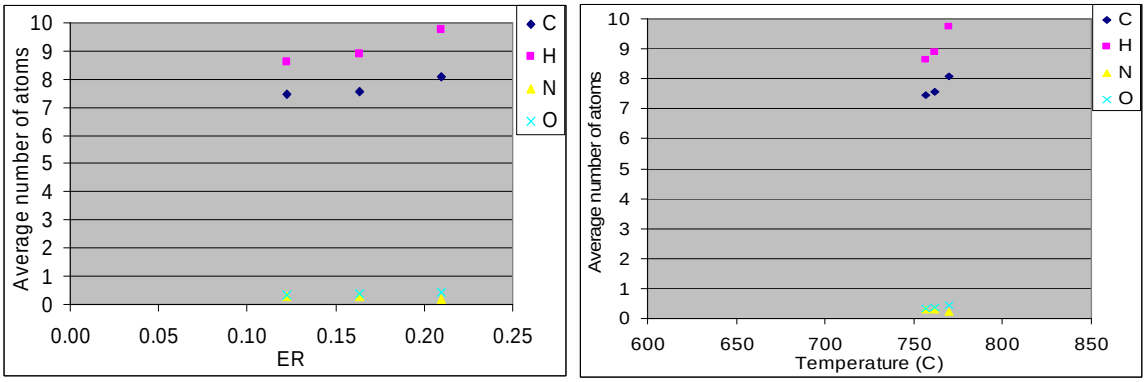

Figure 4.45 Corn gluten average tar atomic composition vs ER vs temperature in flaming pyrolytic gasification and pyrolysis.

Another interesting aspect of the tar is that despite an average atomic weight relatively constant at all conditions of flaming pyrolytic gasification and pyrolysis, the enthalpy of formation of switchgrass (Figure 4.46) does not vary since the process temperature is maintained relatively constant. This confirms that tar is mainly a function of the temperature.

On the other hand, since temperature was not perfectly maintained to the same value for bermudagrass and corn gluten, a linear variation of the enthalpy of formation can be observed as in air gasification. Dispersion of the data due to technical difficulties during storage and analysis of the tar samples significantly altered the accuracy of the result trends. The equations shown in Figure 4.46 account for 40% of the variation in observations. The equations shown in Figures 4.47 and 4.48 have only very few data points, which is insufficient for a meaningful trendline.

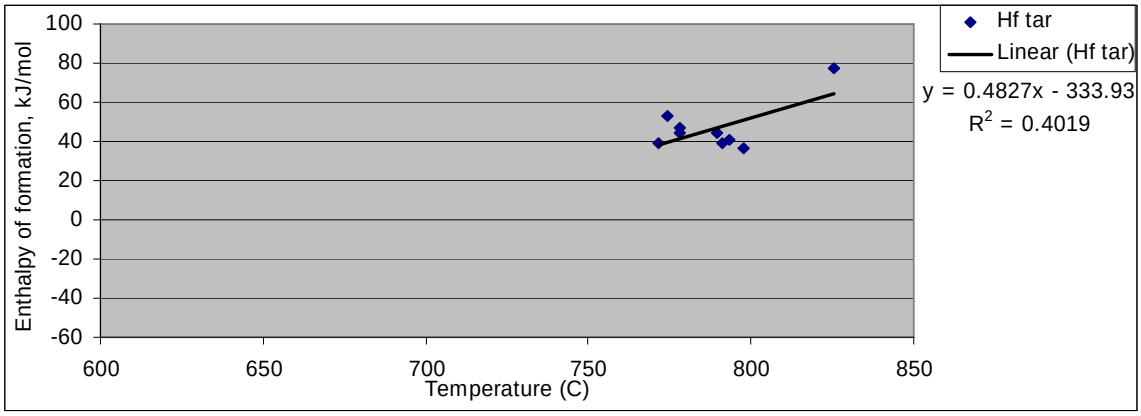

Figure 4.46 Enthalpy of formation of tar at 298K for flaming pyrolytic gasification of switchgrass.

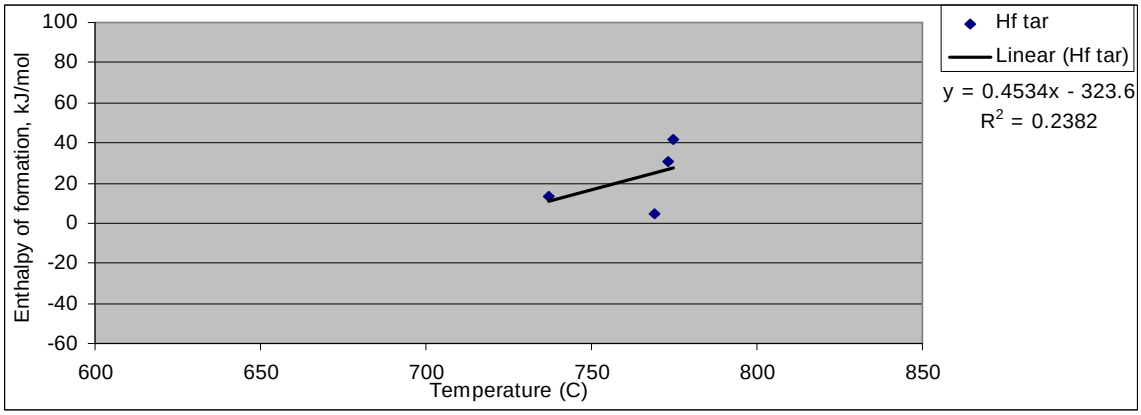

Figure 4.47 Enthalpy of formation of tar at 298K for flaming pyrolytic gasification of bermudagrass.

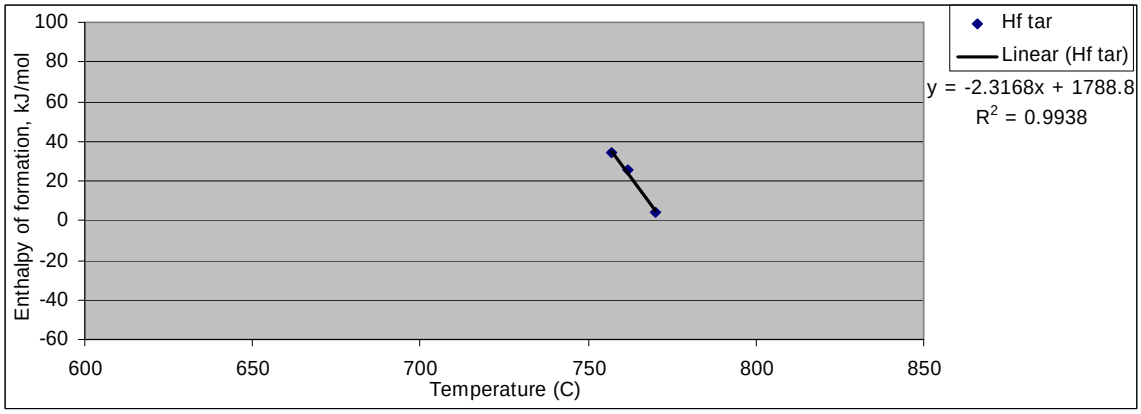

Figure 4.48 Enthalpy of formation of tar at 298K for flaming pyrolytic gasification of corn gluten

4.3.5 Carbon to gas efficiency

As ER decreases in Figures 4.49, 4.50 and 4.51, so does the conversion of the carbon from the biomass to the gas. For all three biomass types, the conversion decreases from 80% for ER around 0.3 down to 50% for pyrolysis of switchgrass, 30% for pyrolysis of bermudagrass.

When air gasification was converting around 50% to 60% of the carbon to the gas at an ER of 0.2, flaming pyrolitic gasification at the same ER is able to achieve 70% to 80% of conversion with corn gluten being the lowest and switchgrass the highest of these values. This confirms the importance of maintaining reactor temperature as high as possible, and how a small decrease of the temperature of 50°C from 775°C for FPG to 725°C for air gasification can disrupt the carbon conversion process.

Switchgrass and bermudagrass conversion values are higher than corn gluten for the same ER values. Bermudagrass stays closer to 80% conversion more than switchgrass as ER starts to lower, before reducing rapidly to a lower level of conversion than switchgrass at pyrolysis. But optimum temperature is not sustained for this particular ER for bermudagrass which explains the loss of conversion at pyrolysis.

As for air gasification, Excel is unable to calculate an appropriate curve fitting for the efficiency data, but it is able to do so for both sets per material.

Since the sum of the three efficiencies is 100%, the best curve fitting for the hard to fit efficiency is 100 minus the two other trend lines efficiency terms. For the cases of switchgrass and corn gluten:

$$Eff_{C\ to\ PM} = 100 - Eff_{C\ to\ gas} - Eff_{C\ to\ tar} \quad \textbf{(4.2)}$$

For bermudagrass:

$$Eff_{C\ to\ gas} = 100 - Eff_{C\ to\ PM} - Eff_{C\ to\ tar} \quad \textbf{(4.3)}$$

Although tar increases as ER decreases, unreacted carbon in the char remains the main reason for loss of efficiency.

The equations shown in Figure 4.49 account for 67% of the variation in observations for carbon to tar and 72% for carbon to gas. For bermudagrass, (Figure 4.50), the equations offered account for 99% of the variation in carbon to tar and 80% for the carbon to gas. The equations shown in Figure 4.51 have only very few data points, which is insufficient for a meaningful trendline.

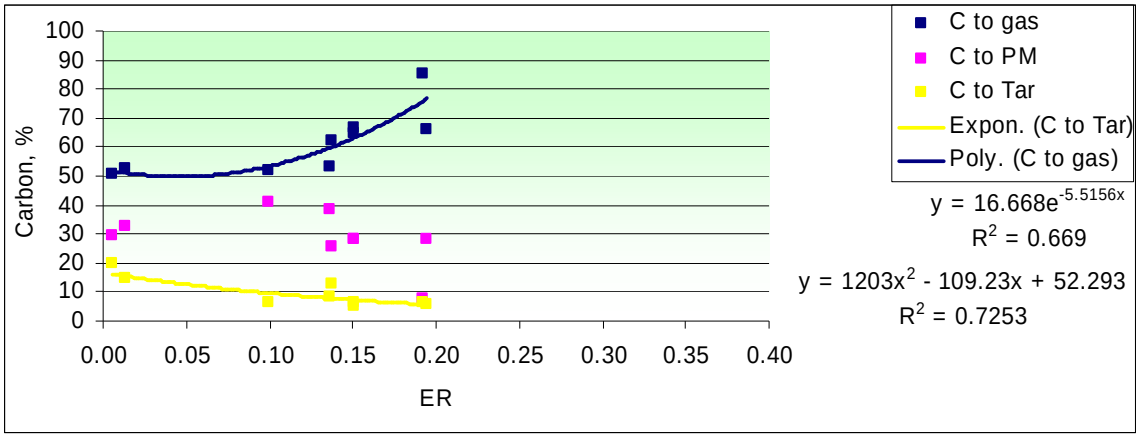

Figure 4.49 Carbon to gas efficiency from flaming pyrolytic gasification of switchgrass

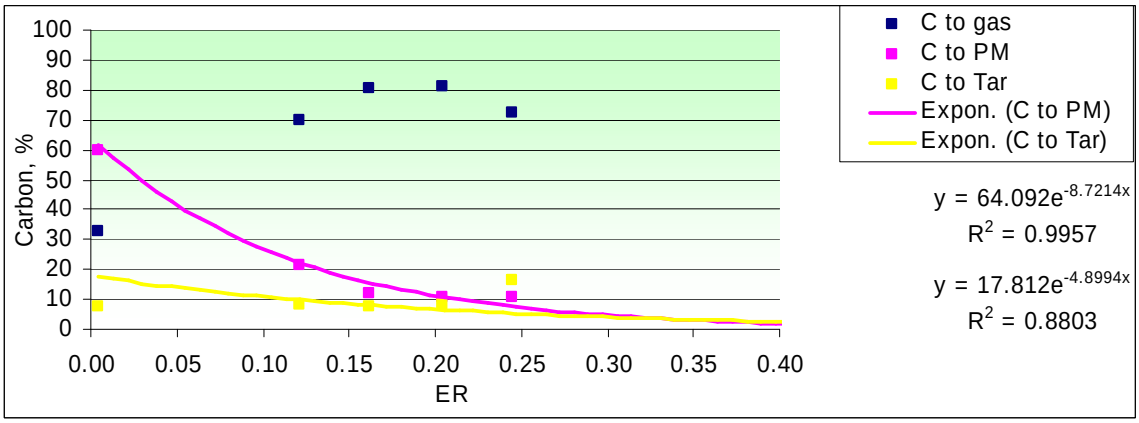

Figure 4.50 Carbon to gas efficiency from flaming pyrolytic gasification of bermudagrass

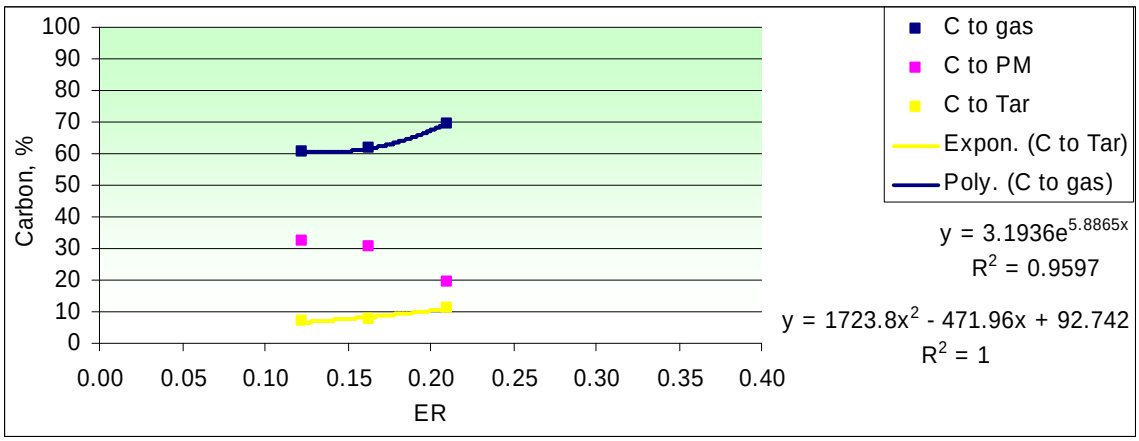

Figure 4.51 Carbon to gas efficiency from flaming pyrolytic gasification of corn gluten

4.3.6 Carbon to CO efficiency

Figures 4.52, 4.53 and 4.54 show the carbon to CO efficiencies of the flaming pyrolytic gasification for all three biomasses. At ER = 0.2, compared to air gasification, FPG reaches conversion 10% higher for all three biomasses tested.

Considering the difficulty of sustaining temperature all the way down to ER=0 for pyrolysis all three graphs show a slowly decreasing efficiency from 35 to 25% between the ER values 0.2 and 0.

It is important to note that despite a lower carbon to gas conversion than air gasification, FPG achieved levels of carbon to CO conversion equal and sometimes greater than air gasification with no inert gas in the gas stream.

The equation shown in Figure 4.52 account for 61% of the variation in observations for carbon to CO for switchgrass. For bermudagrass, (Figure 4.53), the equation offered account for 82% of the variation in carbon to CO. The equation shown in Figure 4.54 have only very few data points, which is insufficient for a meaningful trendline.

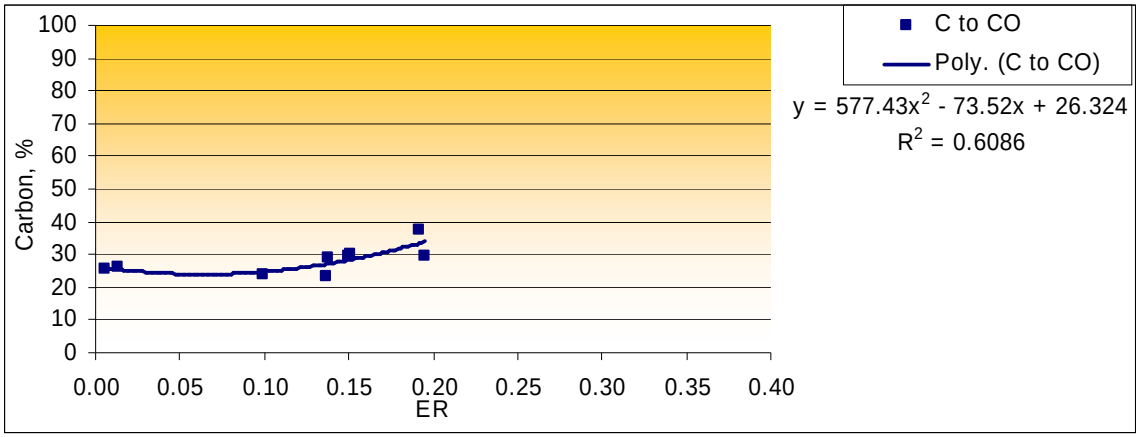

Figure 4.52 Carbon to CO efficiency from flaming pyrolytic gasification of switchgrass

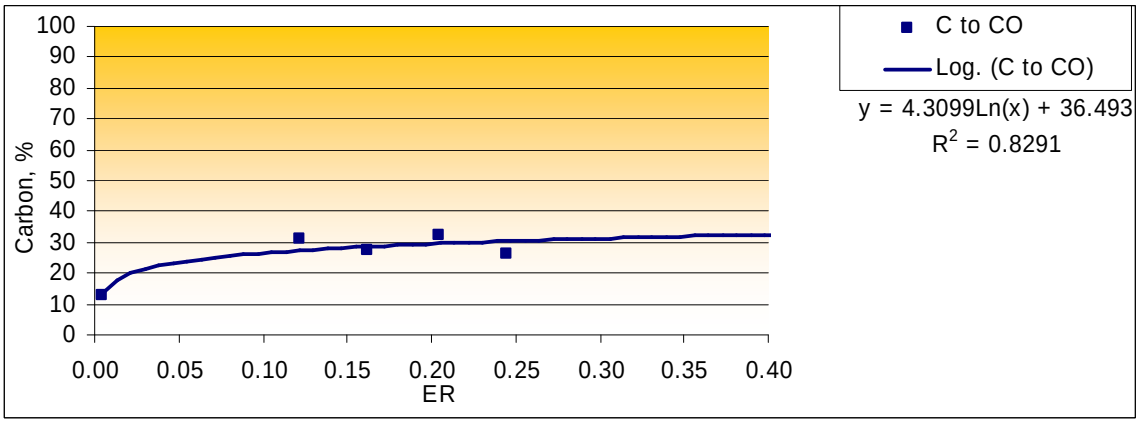

Figure 4.53 Carbon to CO efficiency from flaming pyrolytic gasification of bermudagrass

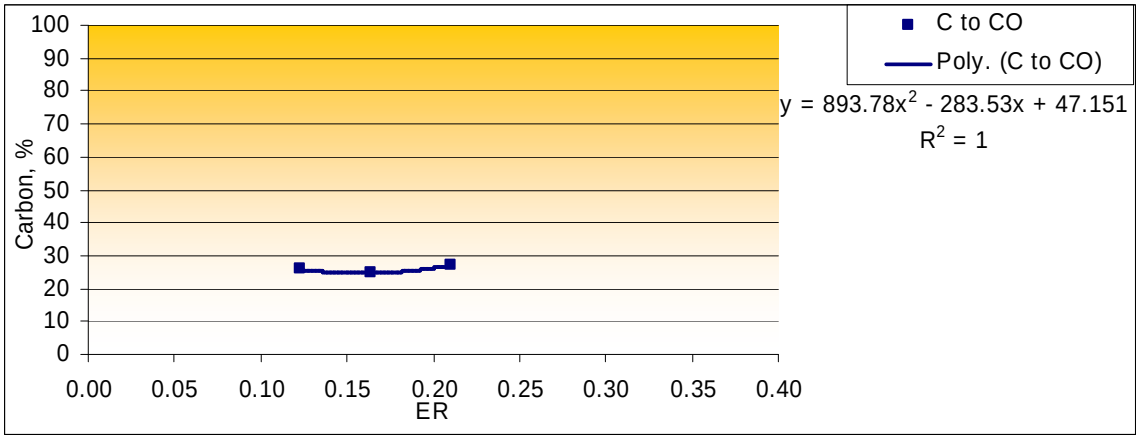

Figure 4.54 Carbon to CO efficiency from flaming pyrolytic gasification of corn gluten

4.3.7 Enthalpy of the gas

Figures 4.55, 4.56 and 4.57 show the enthalpy of the gas versus ER. The enthalpy of the gas increases as ER decreases from 0.2 to 0.15 with little variation in conversion, then past 0.15 to pyrolysis the variation in enthalpy increases greatly up to values around 16000 kJ/mol for switchgrass and bermudagrass. This is due to a large increase in the formation of methane a HHV gas H_2 and CO.

All three biomass types seem to show the same variation of heating value in the produced gas from 6000 to 8000 kj/kg between ER values of 0.2 to 0.15 and up to 16000 kJ/mol at ER = 0.

The equations shown in Figures 4.55 and 4.56 account for 98% and 99% of the variation in observations for carbon to CO for switchgrass and bermudagrass. The equation shown in Figure 4.57 have only very few data points, which is insufficient for a meaningful trendline.

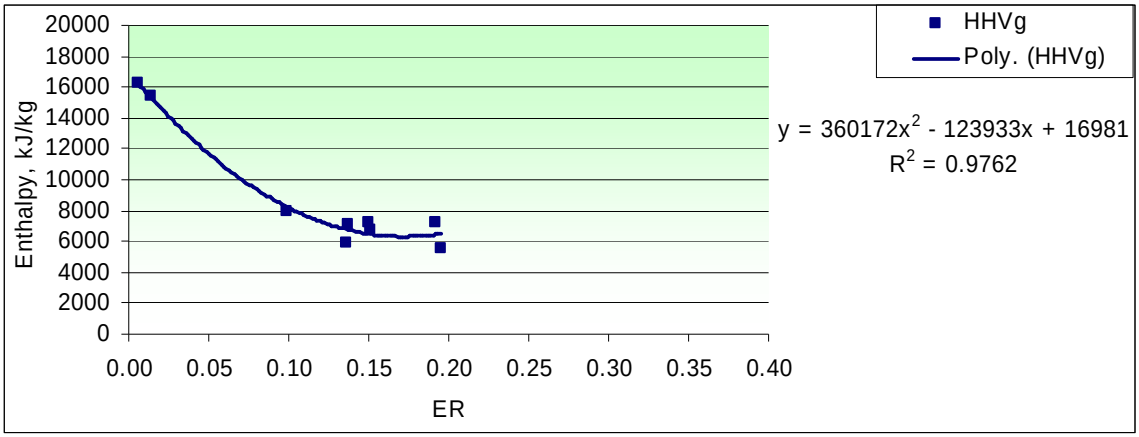

Figure 4.55 Enthalpy of gas from flaming pyrolytic gasification of switchgrass

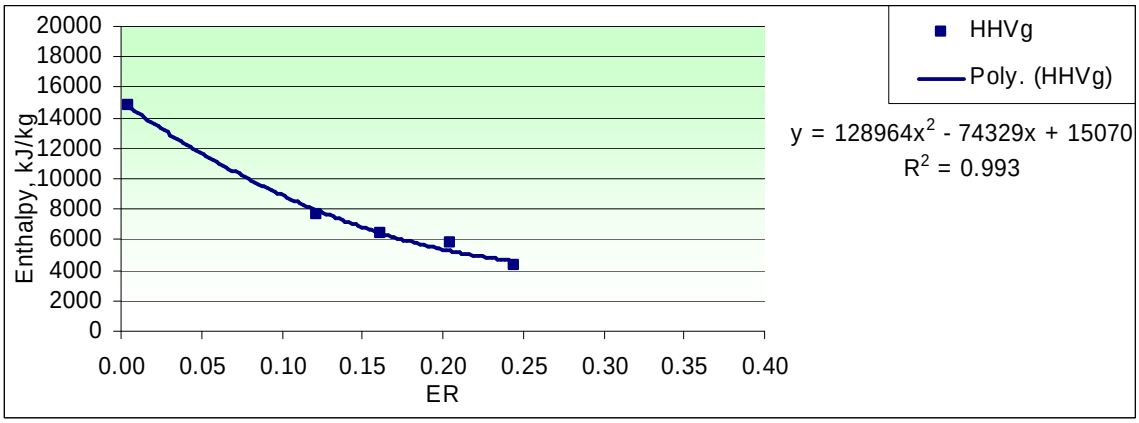

Figure 4.56 Enthalpy of gas from flaming pyrolytic gasification of bermudagrass

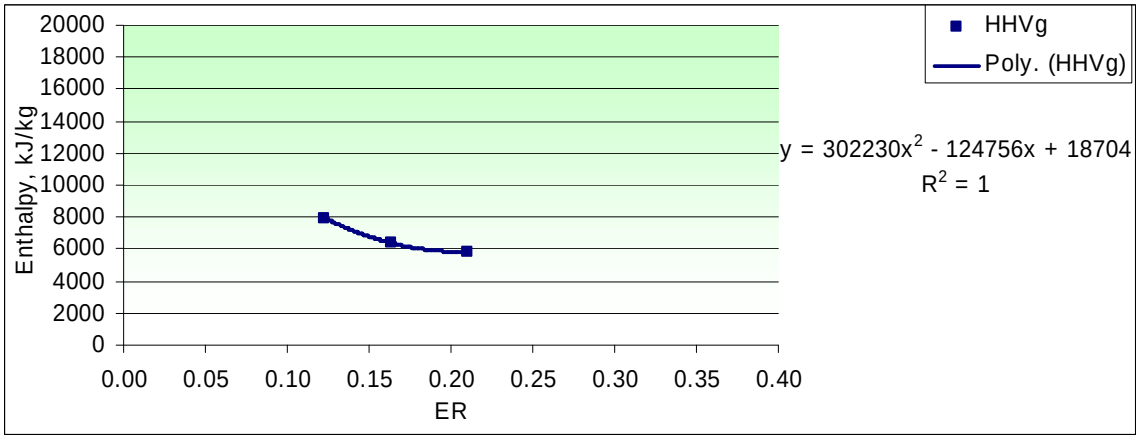

Figure 4.57 Enthalpy of gas from flaming pyrolytic gasification of corn gluten

4.3.8 Enthalpy of reaction

Figures 4.58, 4.59 and 4.60 show the standard enthalpies of the gasification reaction versus ER in the fluidized bed gasifier. As it increases steadily for switchgrass with lowering ER, bermudagrass and corn gluten come to a maximum of 0 kJ/kg of CH_xO_y fed to the reactor at ER = 0 in pyrolysis conditions. Though each biomass having different enthalpy values at ER=0.2, switchgrass: -2500 kJ/kg, bermudagrass: -4000 kJ/kg and corn gluten: -4500 kJ/kg of CH_xO_y. Corn gluten curve does not show any data at ER = 0. However it is expected from the trend that the enthalpy of reaction for corn gluten would have stabilized around 0 kJ/kg of CH_xO_y as well, if experiments were to have been conducted for pyrolysis.

The equations shown in Figures 4.58 and 4.59 account for 95% of the variation in observations for switchgrass and for 84% for bermudagrass. The equation shown in Figure 4.60 have only very few data points, which is insufficient for a meaningful trendline.

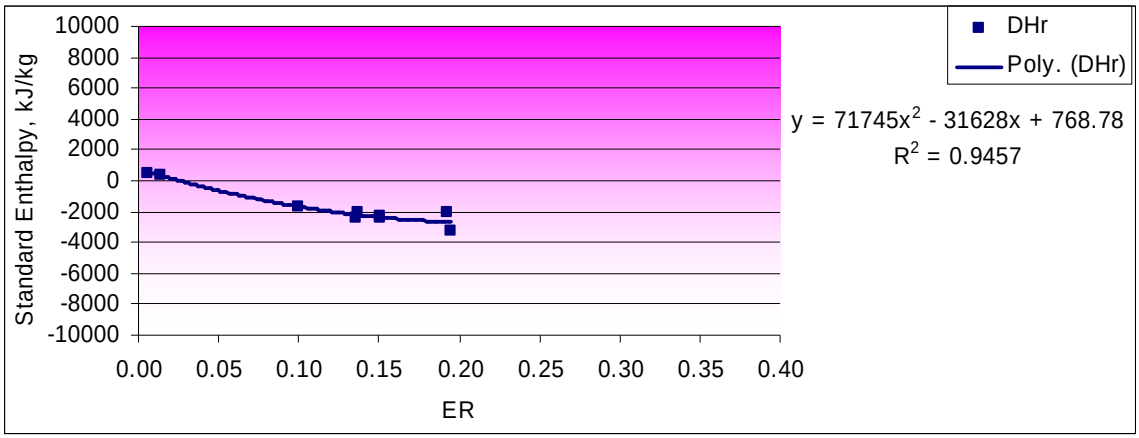

Figure 4.58 Enthalpy of reaction from flaming pyrolytic gasification of switchgrass

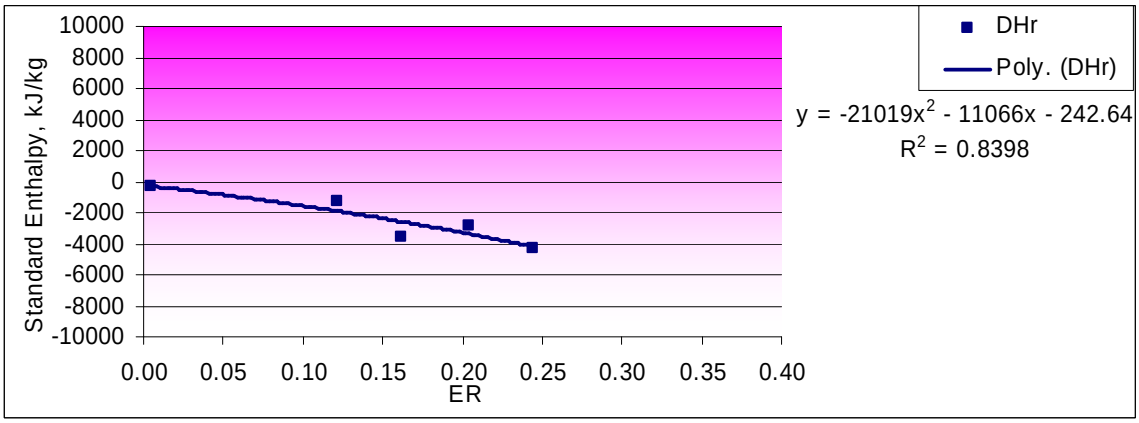

Figure 4.59 Enthalpy of reaction from flaming pyrolytic gasification of bermudagrass

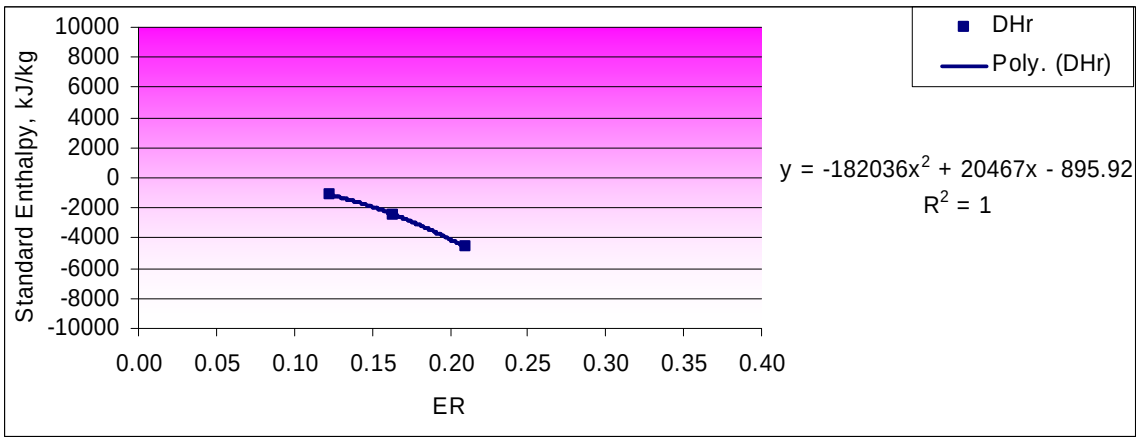

Figure 4.60 Enthalpy of reaction from flaming pyrolytic gasification of corn gluten

4.4 STEAM GASIFICATION

Steam gasification is tested with varying steam-to-carbon ratios at different temperatures for each biomass material. Results show the concentrations in CO and H_2, carbon conversion to the gas, and the tar production for each material. These experiments show differences between the steam gasification conditions of the different materials.

4.4.1 Temperature profile

In this experiment, the temperature of the reactor is set at 775°C. The reasons motivating this choice are the same limitations as those for flaming pyrolytic gasification, i.e. the heating element sheath maximum temperature of 850°C and the likelihood for bermudagrass and corn gluten to agglomerate the bed at about 800°C.

Figures 4.61, 4.62 and 4.63 show steady temperatures, except in the case of low steam to biomass ratio S/B of bermudagrass and corn gluten; running on two heaters limited to sustainable temperature to 775°C.

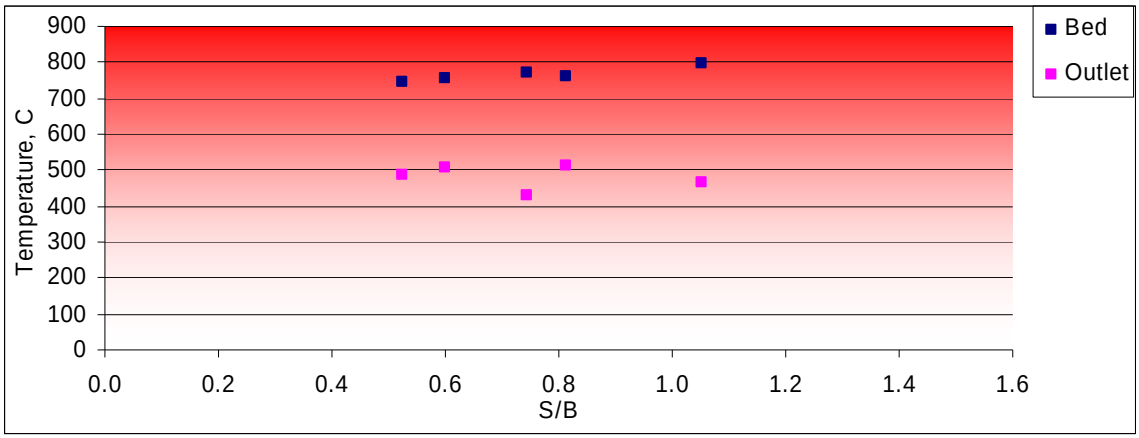

Figure 4.61 Steam gasification of switchgrass temperature profile

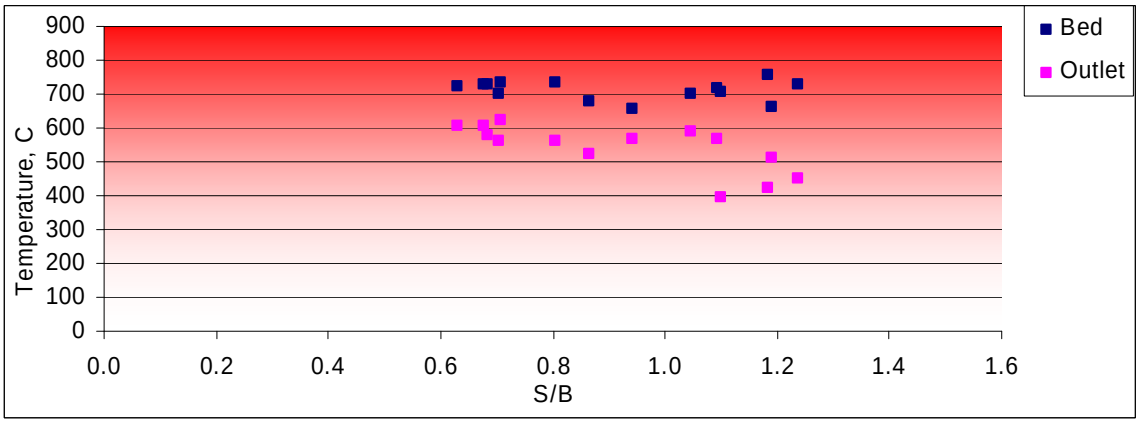

Figure 4.62 Steam gasification of bermudagrass temperature profile

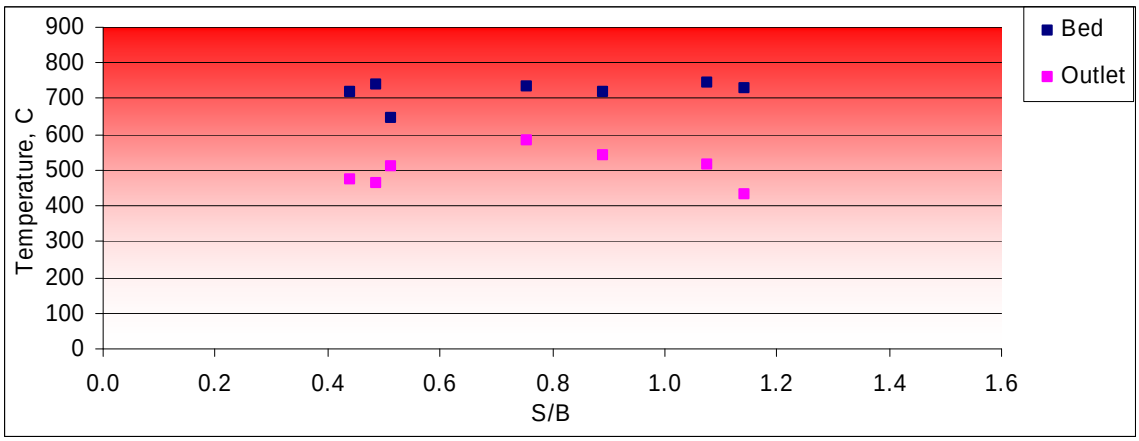

Figure 4.63 Steam gasification of corn gluten temperature profile

4.4.2 Gas composition

Figures 4.64, 4.65 and 4.66 show the dry gas compositions for steam gasification. Percentage of combustible gas of greatest interest, CO, is increasing for switchgrass from 30% up to 40% between the S/B ratios from 1.1 down to 0.5. Bermudagrass, on the other hand, shows lower or equal values of CO and H_2 with almost constant values through the same range of S/B ratios. Despite a much lower reactor bed temperature than the switchgrass runs, corn gluten shows similar concentrations of CO but with lower values in H_2. In the same range of S/B, H_2 decreases from 35% down to 23% for switchgrass and from 28% down to 15% for corn gluten.

On the other hand, CH_4 remains stable at about 10% for switchgrass, bermudagrass and corn gluten at all S/B values. CO_2 stays constant for bermudagrass but decreases with H_2 for switchgrass and corn gluten. These variations in concentration of gases from switchgrass and corn gluten correspond to the variation in reactor bed temperature discussed in the previous paragraph. It is quite noticeable that although corn gluten was a bad candidate for air and flame pyrolytic gasification because of temperature limitations due to an agglomeration potential inducing lower concentrations in gases of greatest interest, it is a potential good candidate from steam gasification with compositions matching those of the switchgrass.

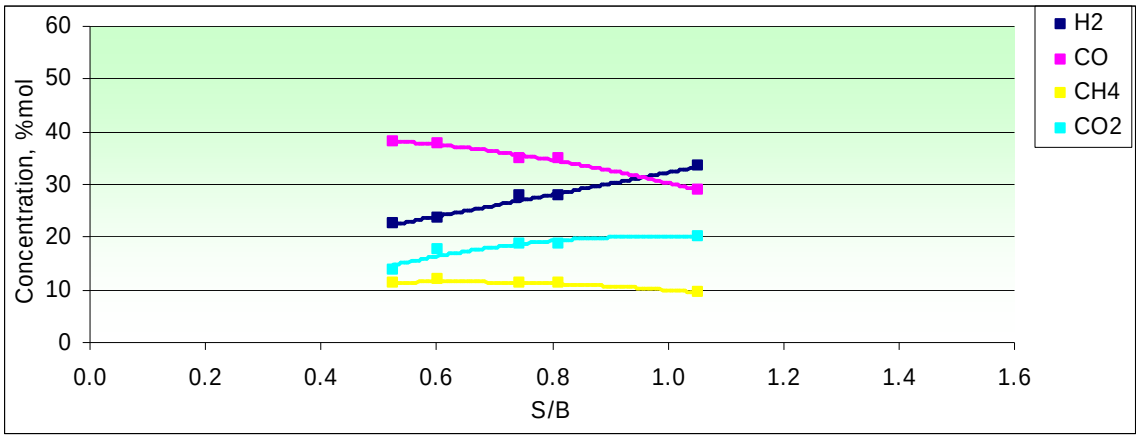

Figure 4.64 Dry gas molar composition from steam gasification of switchgrass

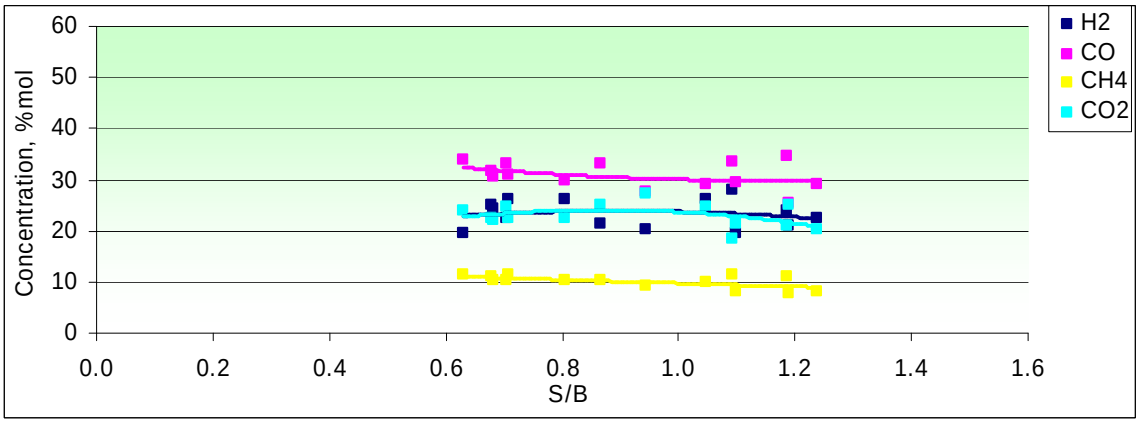

Figure 4.65 Dry gas molar composition from steam gasification of bermudagrass

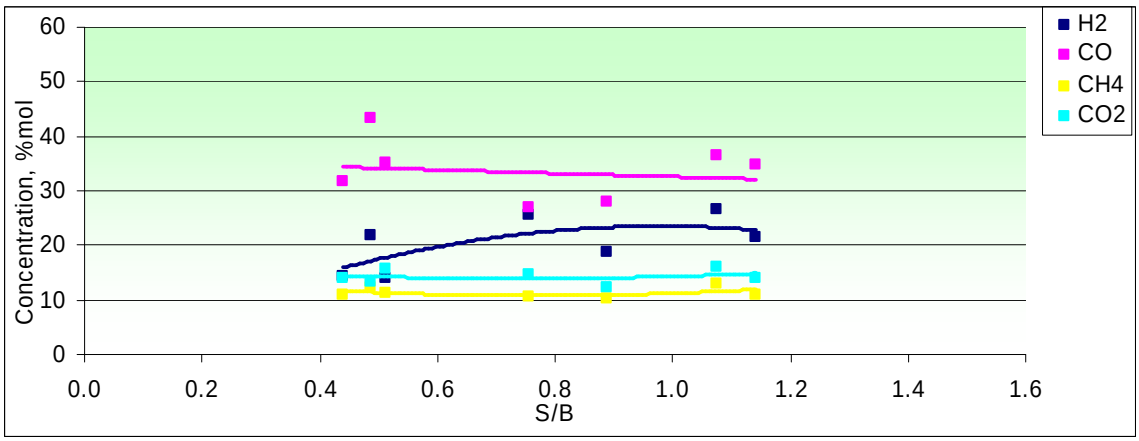

Figure 4.66 Dry gas molar composition from steam gasification of corn gluten

4.4.3 Water

In steam gasification, the level of water as shown in Figures 4.67, 4.68 and 4.69 are, as expected, well above those measured in the two previous processes. Little of this water measured comes from the conversion of the H_2 to water, as the equilibrium is less likely to shift towards water production during cool down because of the excess of water that is already present in the gas.

Figures 4.67, 4.68 and 4.69, show a large decrease in water production for switchgrass from S/B 1.1 to 0.4, for bermudagrass from S/B 1.3 to 0.6 and for corn gluten from S/B 1.2 to 0.4, in the order of 600 g/Nm^3, 1500g/Nm^3, and 600 g/Nm^3, respectively.

Switchgrass, bermudagrass and corn gluten follow a polynomial trend that reaches a minimum of 900 g/Nm^3 in the case of switchgrass and corn gluten and 2250 g/Nm^3 for bermudagrass at S/B = 0.5.

The polynomial equations shown in Figures 4.67, 4.68 and 4.69 account for 82 to 99.9 % of the variation in the observations.

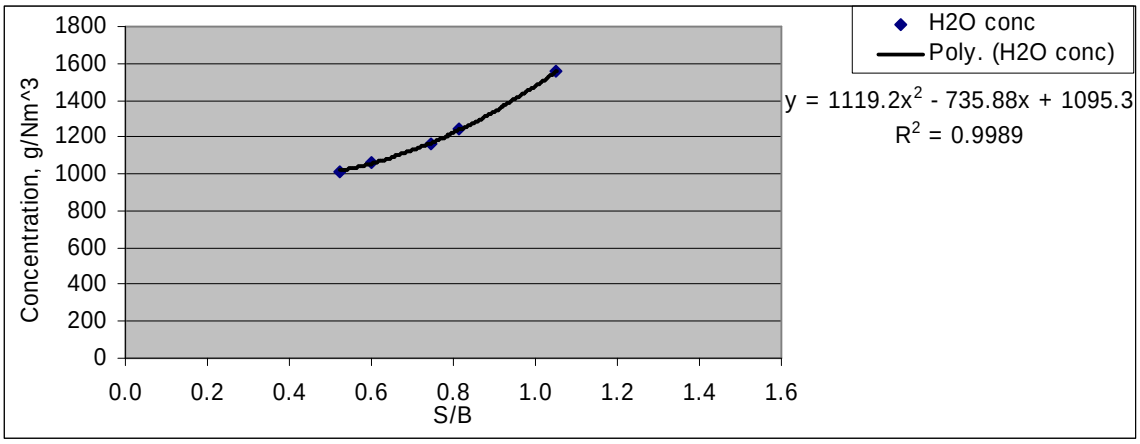

Figure 4.67 Water concentration in gas from steam gasification of switchgrass

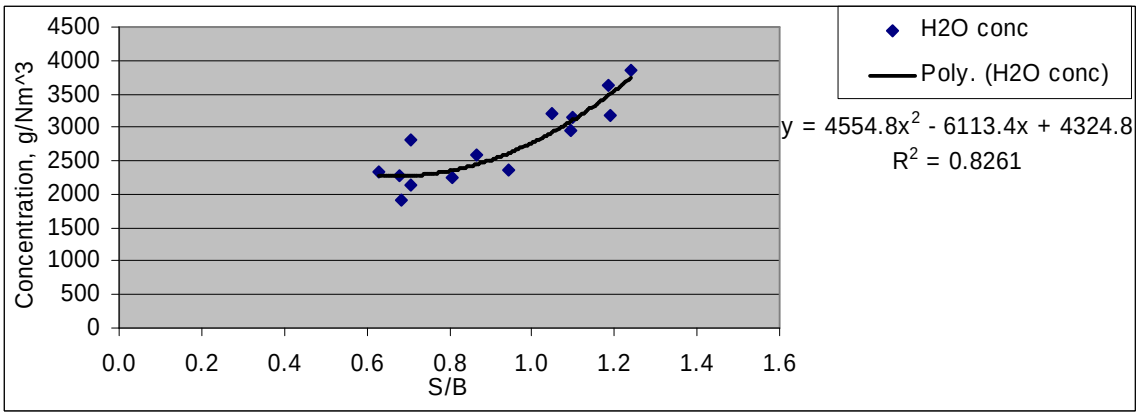

Figure 4.68 Water concentration in gas from steam gasification of bermudagrass

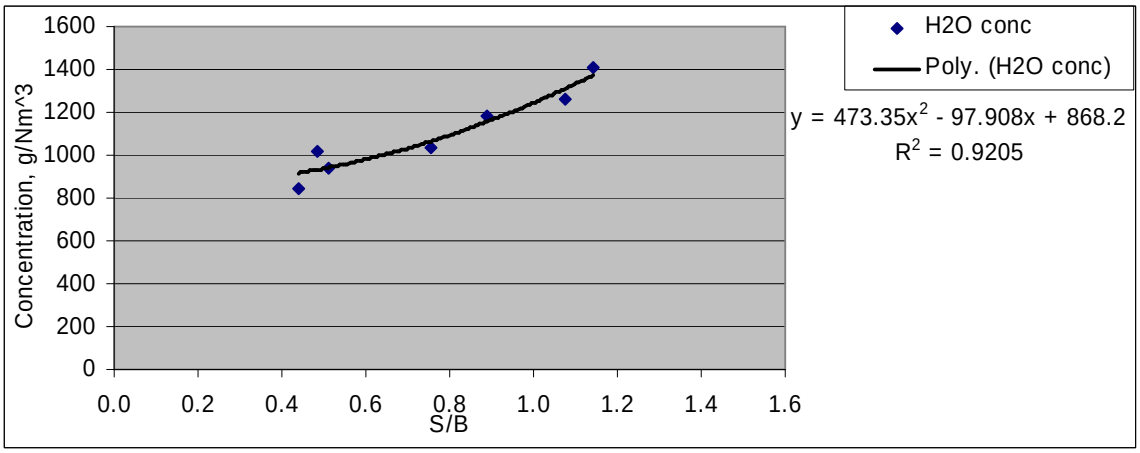

Figure 4.69 Water concentration in gas from steam gasification of switchgrass

4.4.4 Tar

Similar to the previous process, Figures 4.70, 4.71 and 4.72 show the results of both the gravimetric and GC-MS tar analyses for steam gasification runs. In steam gasification, switchgrass reaches GC-MS tar levels between 80 to 125 g/Nm^3, bermudagrass between 50 to 100 g/Nm^3, and corn gluten between 25 to 100 g/Nm^3. Tar levels follow exponential trends for switchgrass and corn gluten. The same trend would have been expected from bermudagrass but it has a minimum of 50 g/Nm^3 at S/B = 0.9 primarily due to measurement error than a representative aspect of tar production because of the dispersion of the data.

As for the previous processes, the gravimetric data for corn gluten are the result of an oven drying method of the sample, prior to the suggested tar guidelines identified which recommended a rotary evaporator. This explains why the gravimetric tar is sometimes so much higher than the GC-MS data. Despite the changes in reactor bed temperatures experienced for switchgrass and corn gluten as S/B decreases, tar is also the lowest in this range of S/B ratios for both switchgrass and corn gluten since the extrapolation of the exponential trend of corn gluten tar decreased approaching this value.

The equations for Tar (GC-MS) shown in Figures 4.70 and 4.72 account for 76% to 92% of the variation in observations for switchgrass and corn gluten, respectively.

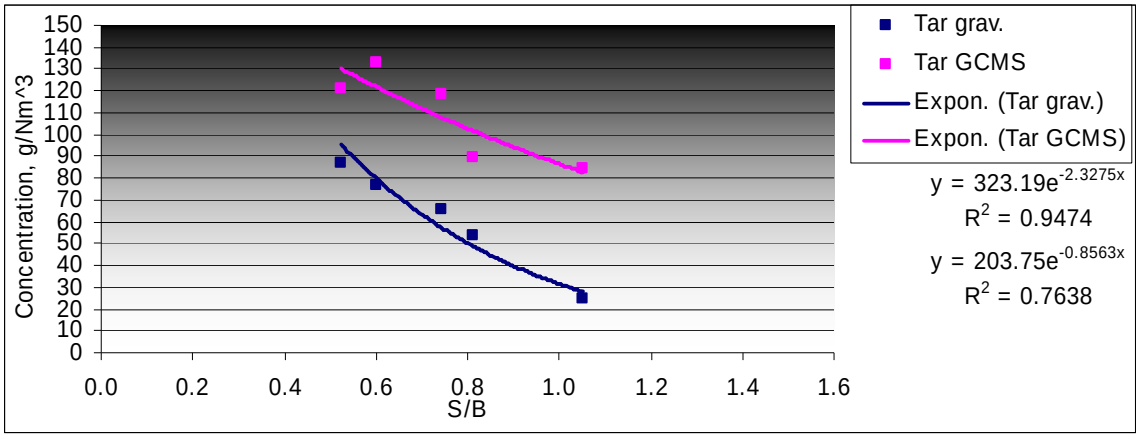

Figure 4.70 Tar concentration in gas from steam gasification of switchgrass

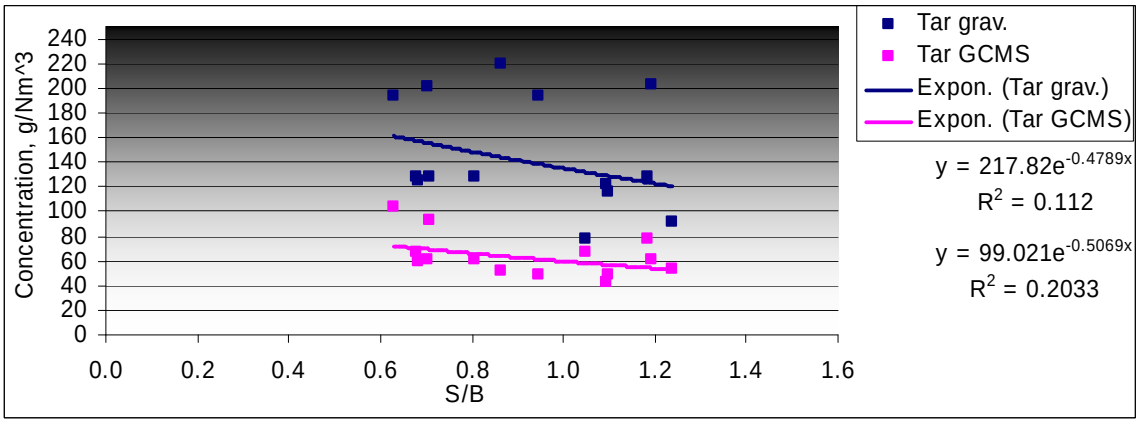

Figure 4.71 Tar concentration in gas from steam gasification of bermudagrass

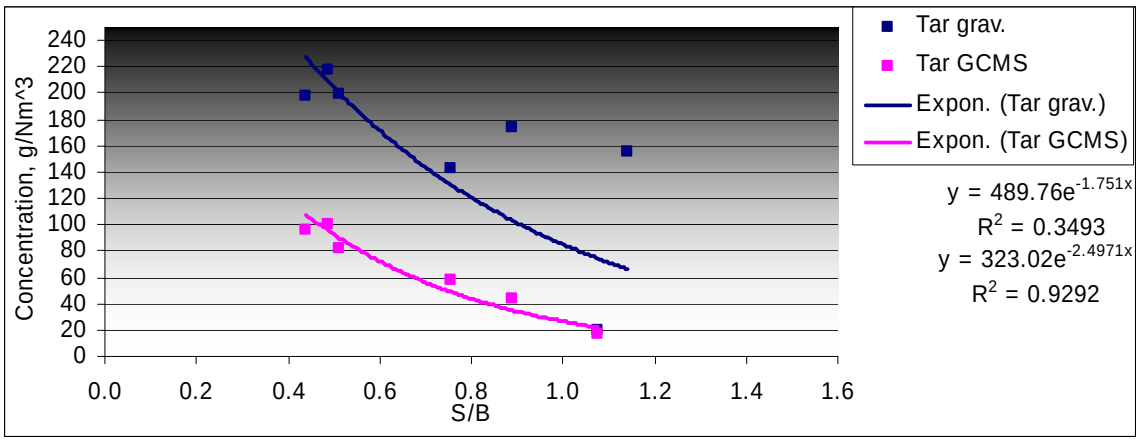

Figure 4.72 Tar concentration in gas from steam gasification of corn gluten

Flaming pyrolytic gasification, tar atomic composition (Figures 4.73, 4.74 and 4.75) and average molecular weight do not depend on ER, but seem to depend on temperature. Although the effort is to keep bed temperature at 775°C, as temperature decreases near pyrolysis by lack of electrical heating power (one element malfunctioned) there is a slight change in tar atomic composition.

Tar average atomic composition shows little change for switchgrass, bermudagrass and corn gluten in steam gasification. Average results are in Table 4.4.

	C	H	O	N	MW
Switchgrass	7.698	8.081	0.482	0.013	108.346
Bermudagrass	7.480	9.007	0.521	0.259	110.729
Corn gluten	7.272	8.795	0.299	0.263	104.524

Table 4.4 Tar average atomic composition and molecular weight in steam gasification

Another interesting aspect of the tar is, despite an average atomic weight relatively constant at all conditions of steam gasification, the enthalpy of formation of switchgrass and bermudagrass Figures 4.76 and 4.77 do not vary much since the process temperature is maintained relatively constant. This confirms that tar is primarily a function of the temperature.

On the other end, since temperature was not perfectly maintained to the same value for corn gluten, it is more difficult to observe a linear variation of the enthalpy of formation. Dispersion of the data due to technical difficulties during storage and analysis of the tar samples significantly altered the accuracy of the result trends.

The equations shown in Figures 4.76, 4.77 and 4.78 account for 60% to 80% of the variation in observations for all three biomasses.

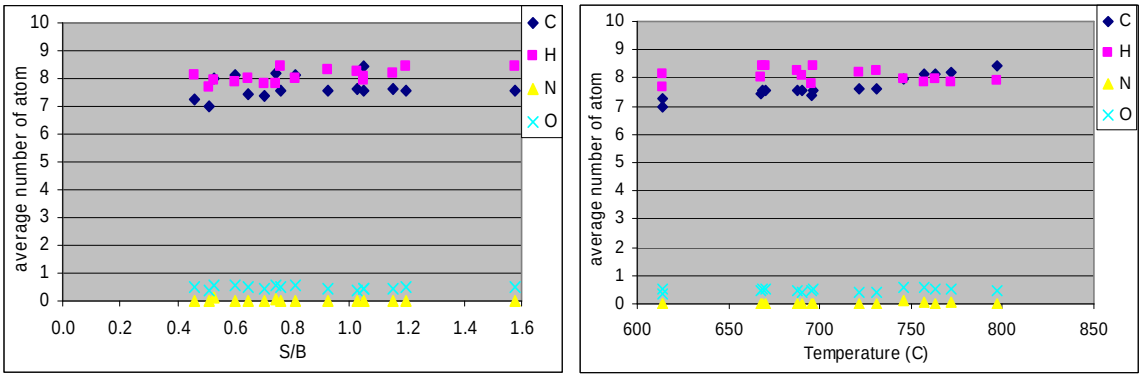

Figure 4.73 Switchgrass average tar atomic composition vs ER vs temperature in steam gasification

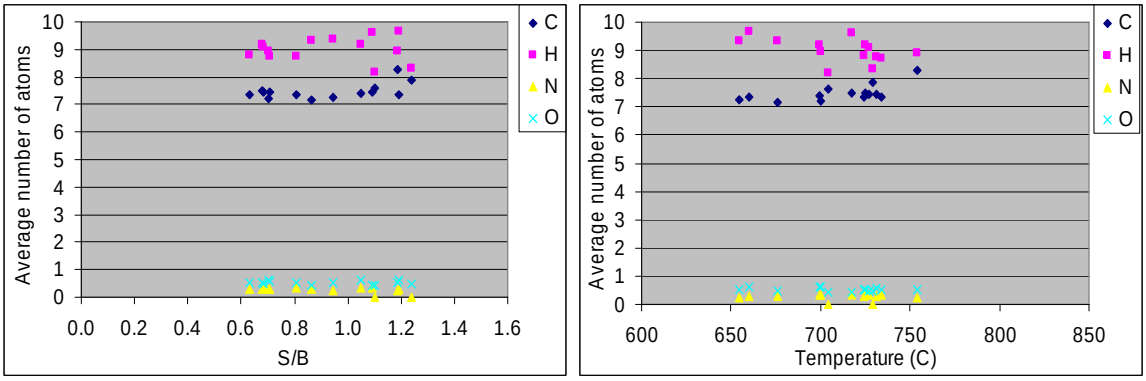

Figure 4.74 Bermudagrass average tar atomic composition vs ER vs temperature in steam gasification

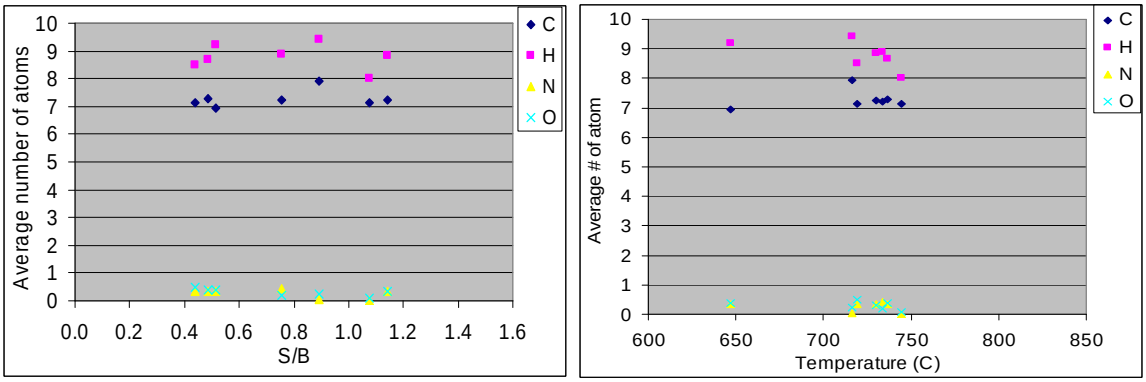

Figure 4.75 Corn gluten average tar atomic composition vs ER vs temperature in steam gasification

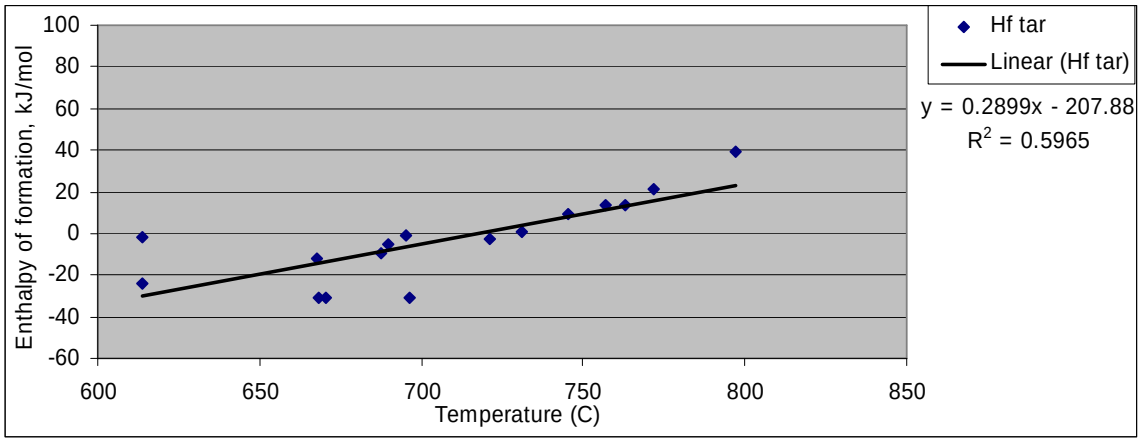

Figure 4.76 Enthalpy of formation of tar at 298K for steam gasification of switchgrass.

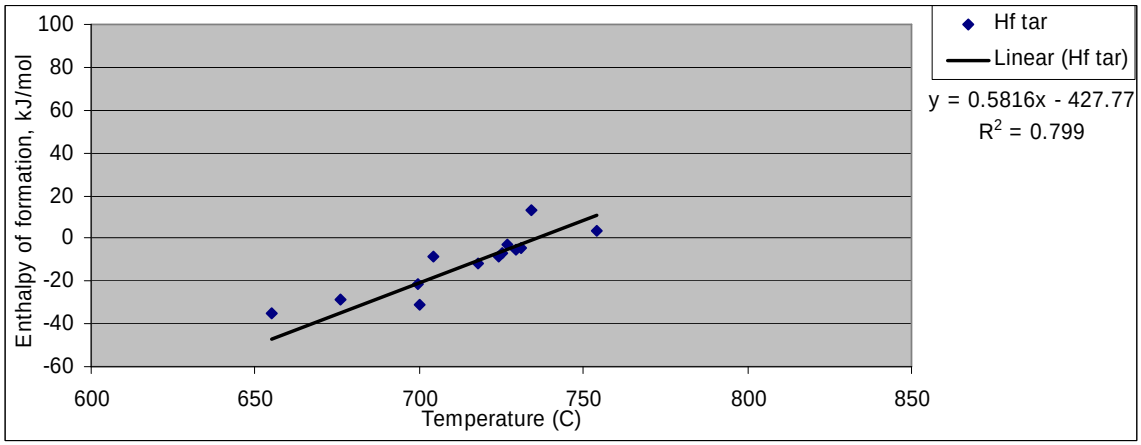

Figure 4.77 Enthalpy of formation of tar at 298K for steam gasification of bermudagrass.

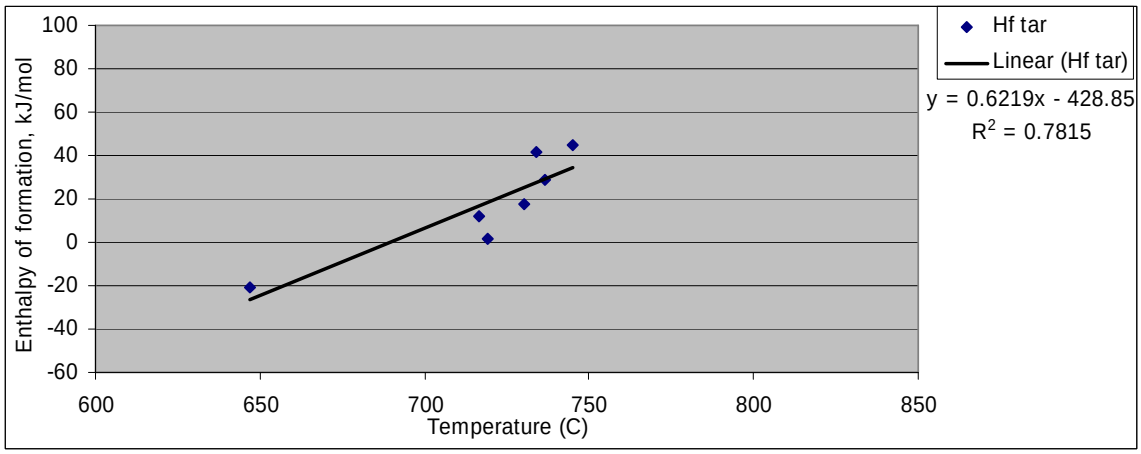

Figure 4.78 Enthalpy of formation of tar at 298K for steam gasification of corn gluten.

4.4.5 Carbon to gas efficiency

As S/B ratio decreases in Figures 4.79, 4.80 and 4.81, so does the conversion of the carbon from the biomass to the gas. The variation of C to gas conversion is very different for the three biomasses experimented. These differences are not only the consequence of the biomass type, but are primarily the result of the difference in reactor bed temperature achieved during the experiments.

For switchgrass, the conversion stays in the 50 to 60% range with a maximum at S/B of 0.8. For bermudagrass the conversion remains between 30 and 40% with a maximum at about 0.85 S/B. The temperature for that material was 75°C to 100°C lower than the one for switchgrass, which can explain this important change in C conversion. This confirms the importance of sustaining reactor bed temperature as high as possible, and how a small decrease of the temperature from 775°C to 700°C can disrupt the carbon conversion process.

Although corn gluten is experimented with a lower temperature than switchgrass but comparable to the one of bermudagrass, the conversion obtained does not reach a maximum like switchgrass and bermudagrass. The conversion for corn gluten is higher than the one of switchgrass with values of 75% at S/B of 1.1 dropping to 55% at S/B of 0.5.

In this process, tar levels depend on the biomass in a way that is opposite to how temperature usually influences the production of tar. Although switchgrass had the highest bed temperature, it produces the highest tar levels; 12 to 16% tar as S/B decreases from 1.1 to 0.5. Bermudagrass stays around 5% tar across the range of values of S/B and corn gluten climb from 5% to 10% tar in that same range. More experiments are

necessary to confirm this result. At this point, corn gluten which has such better results than the other processes is a great candidate for steam gasification. Unreacted carbon in the char still remains the main reason for loss of efficiency.

As shown in Figure 4.79, the polynomial equations account for nearly 100% of the variation in carbon to gas and 88% of the carbon to particulate matter. In Figure 4.81, the equations account for 88% of the vatiation in carbon to gas and 92% of the carbon to particulate matter.

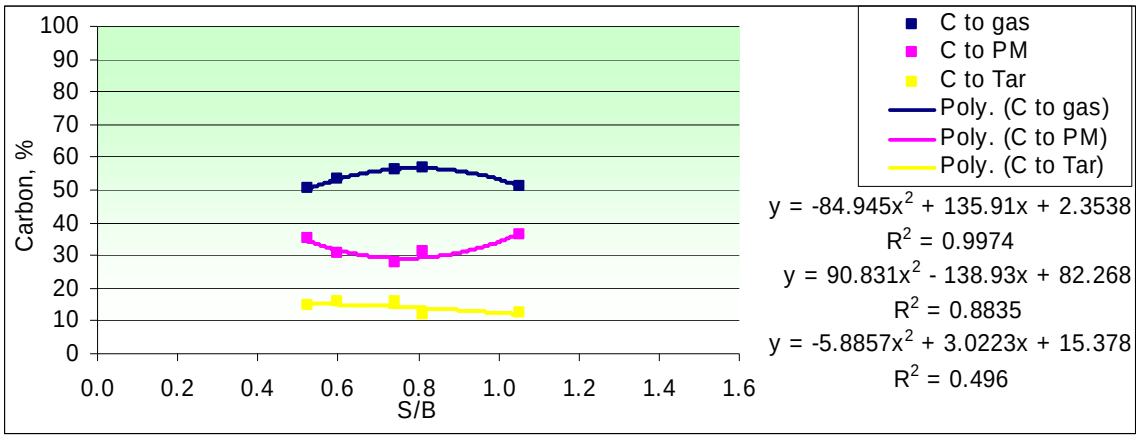

Figure 4.79 Carbon to gas efficiency from steam gasification of switchgrass

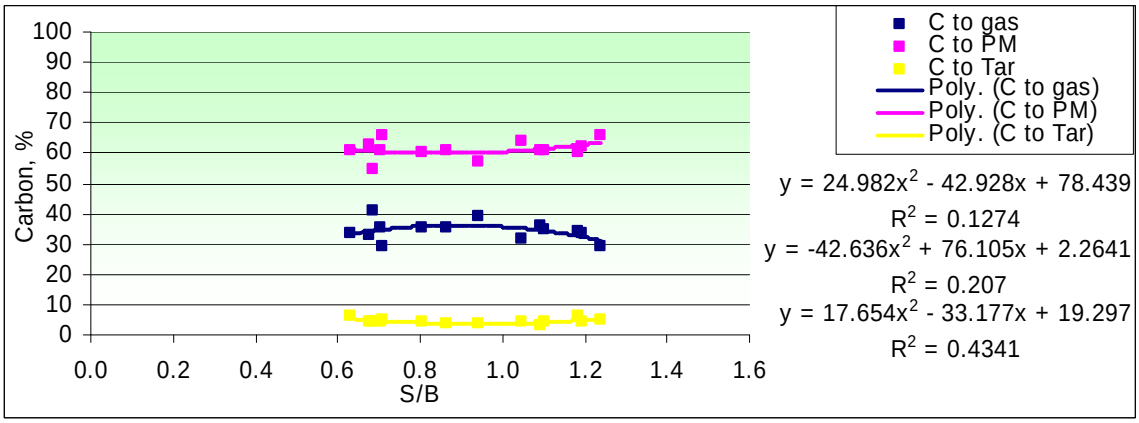

Figure 4.80 Carbon to gas efficiency from steam gasification of bermudagrass

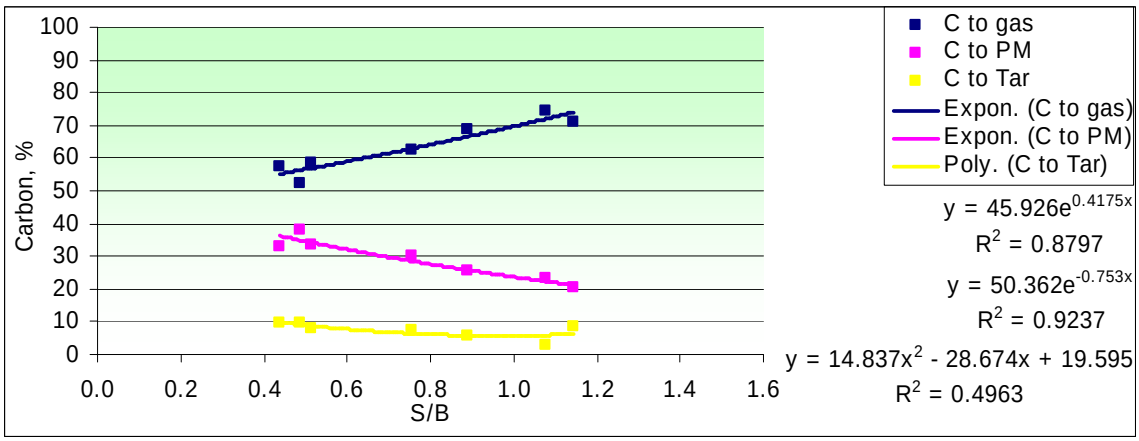

Figure 4.81 Carbon to gas efficiency from steam gasification of corn gluten

4.4.6 Carbon to CO efficiency

Figures 4.82, 4.83 and 4.84 show the carbon to CO efficiencies of the steam gasification for all three biomass materials. Compared to air and flaming pyrolytic gasification at the optimum range of 25 to 30% conversion to CO, steam gasification reaches conversion efficiencies slightly lower for switchgrass and bermudagrass around 25%, but shows a higher conversion for corn gluten at 34% of the carbon input. This last result is very interesting considering the temperature was at 700°C during these runs and not at 775°C as originally planned. Further experimentation could determine if the high ash content or particular nature of the ashes of corn gluten is responsible for this high conversion level.

It is important to note that, despite a lower carbon to gas conversion than air gasification, steam gasification, as does flaming pyrolytic gasification, achieves a level of carbon to CO conversion equal and sometimes greater than air gasification, and without inert gases present in the gas stream, which is a great advantage for gas fermentation downstream.

The equations shown in Figures 4.82 and 4.84 account for 95% and 87% of the variation in observations for switchgrass and corn gluten, respectively. The equation shown in Figure 4.83 for bermudagrass has a wide range of data points, which does not provide a meaningful trendline.

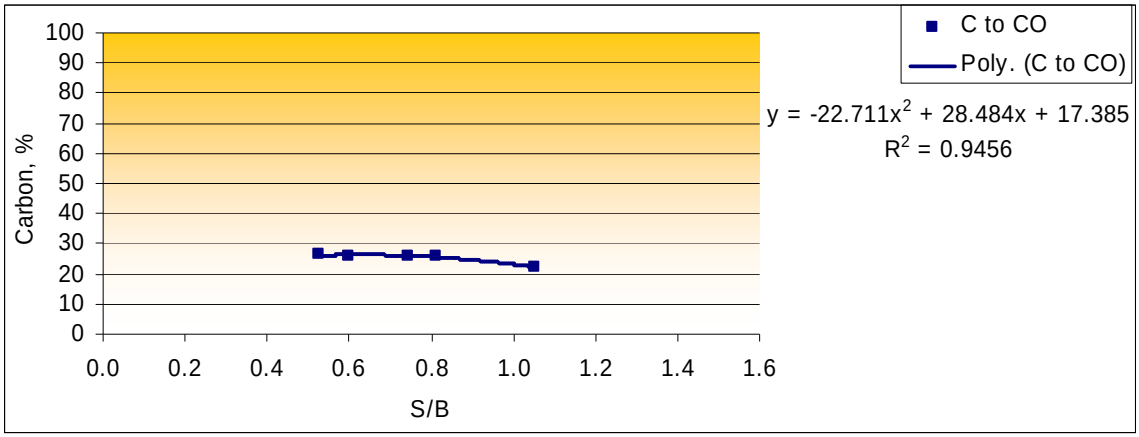

Figure 4.82 Carbon to CO efficiency from steam gasification of switchgrass

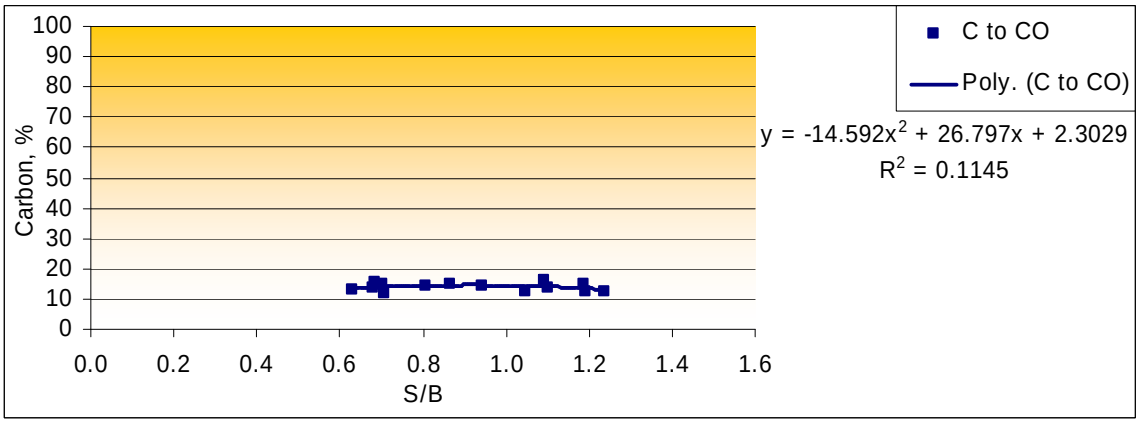

Figure 4.83 Carbon to CO efficiency from steam gasification of bermudagrass

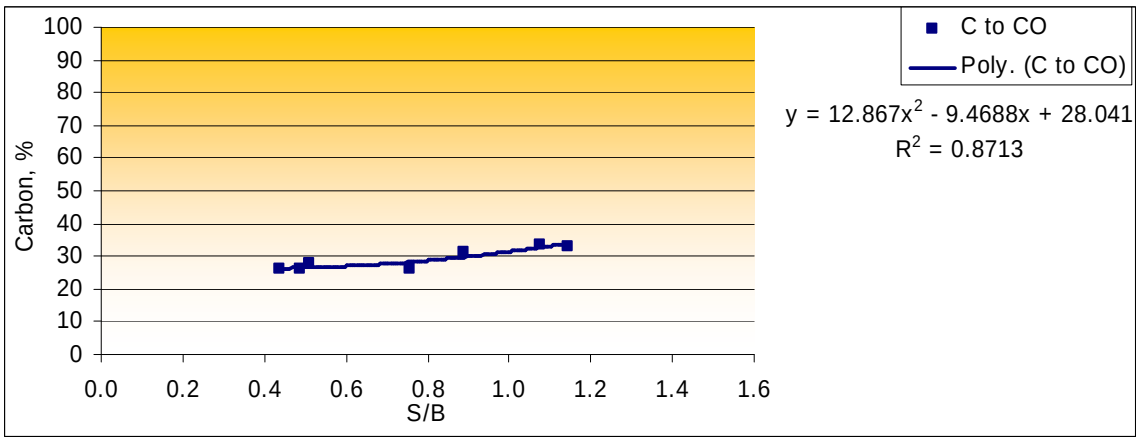

Figure 4.84 Carbon to CO efficiency from steam gasification of corn gluten

4.4.7 Enthalpy of the gas

Figures 4.85, 4.86 and 4.87 show the enthalpy of the gas versus S/B. The enthalpy of the gas increases remain in the range of 15,000 to 16,000 kJ/kg for switchgrass with a maximum at 0.85 S/B. Bermudagrass gas enthalpy values are slightly lower than switchgrass values (considering a lower reactor bed temperature for bermudagrass) with an increasing trend from 12,000 to 15,000 kJ/kg as S/B ratios decreases. Corn gluten produces the highest enthalpy of the three gases produced at 18,000 kJ/kg decreasing slightly towards 16,000 kJ/kg as S/B decreases to 0.5 with a bed temperature at 700°C.

The equations shown in Figures 4.85 and 4.87 account for 99.8% and 57% of the variation in observations for switchgrass and corn gluten, respectively. The equation shown in Figure 4.86 for bermudagrass has a wide range of data points, which does not provide a meaningful trendline.

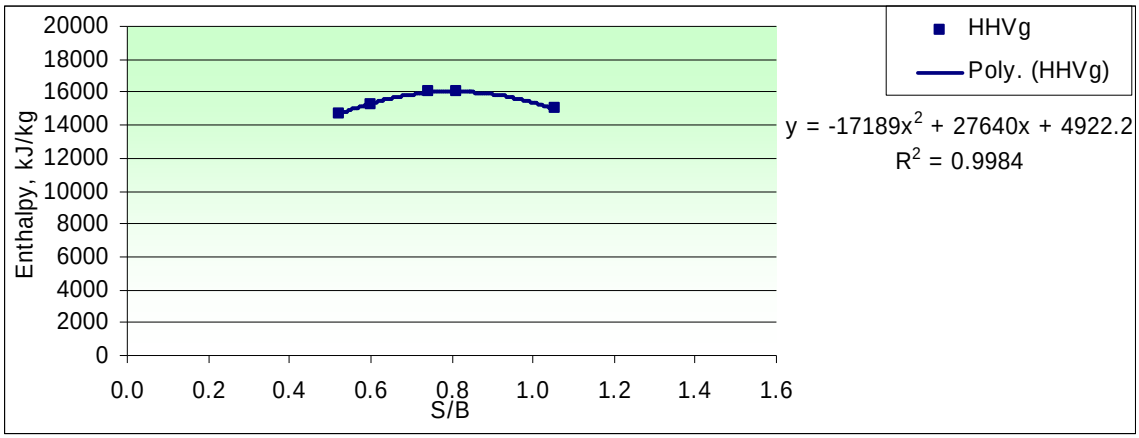

Figure 4.85 Enthalpy of gas from steam gasification of switchgrass

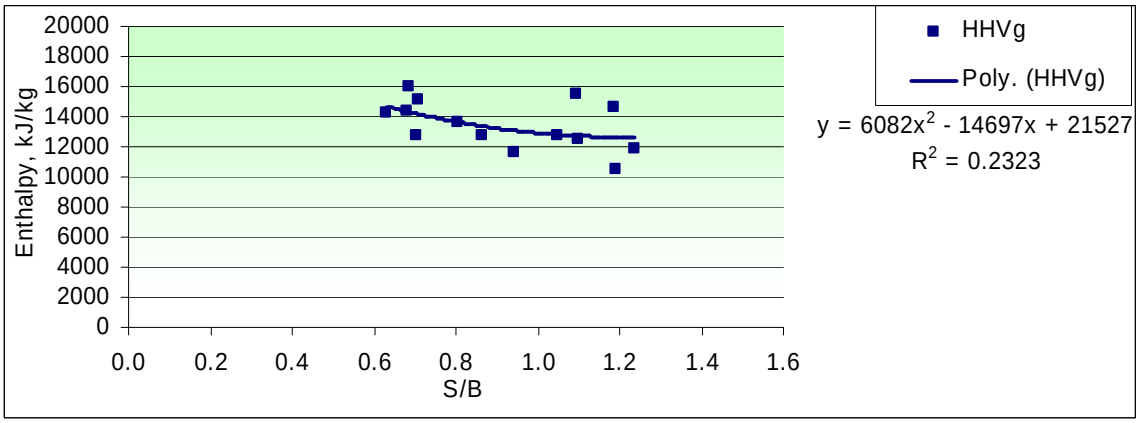

Figure 4.86 Enthalpy of gas from steam gasification of bermudagrass

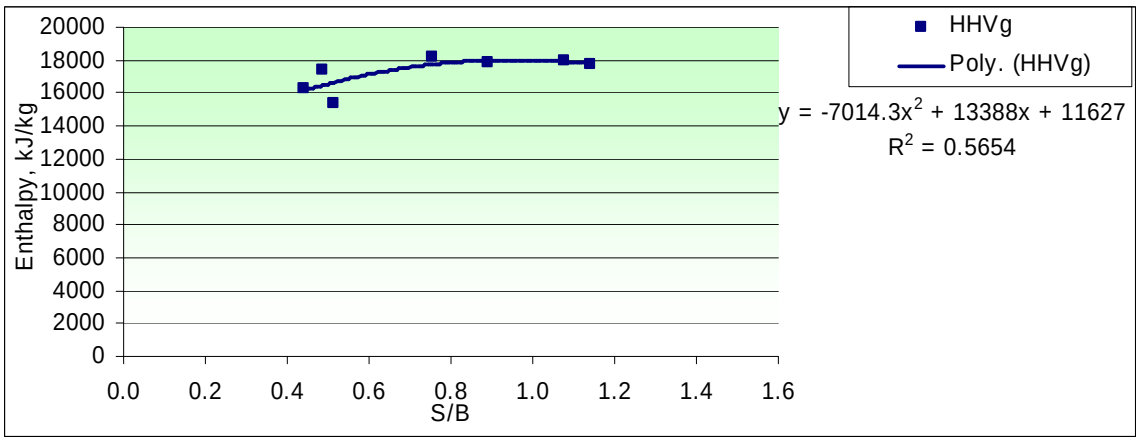

Figure 4.87 Enthalpy of gas from steam gasification of corn gluten

4.4.8 Enthalpy of reaction

Figures 4.88, 4.89 and 4.90 show the standard enthalpies of the steam gasification reaction versus S/B ratios in the fluidized bed gasifier. The enthalpies of reactions have, for most cases, positive values indicating the endothermic nature of the process. Switchgrass values are between 500 to 1000 kJ/kg of CH_xO_y fed to the reactor, while bermudagrass is lower, around 0 kJ/kg and corn gluten decreases from 1500 to 1000 kJ/kg with lowering S/B ratios.

The equations shown in Figures 4.88 and 4.90 account for 94% and 78% of the variation in observations for switchgrass and corn gluten, respectively. The equation shown in Figure 4.89 accounts for 56% of the variation in observations for bermudagrass.

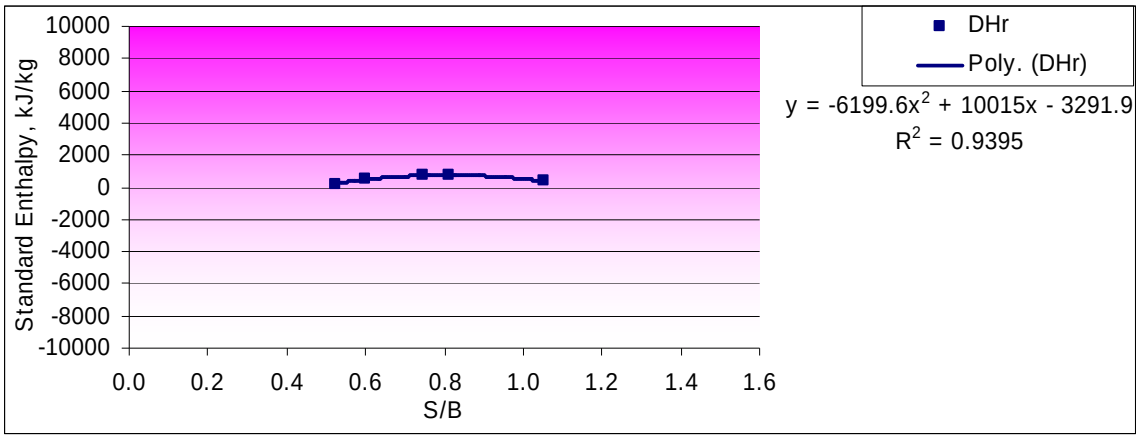

Figure 4.88 Enthalpy of reaction from steam gasification of switchgrass

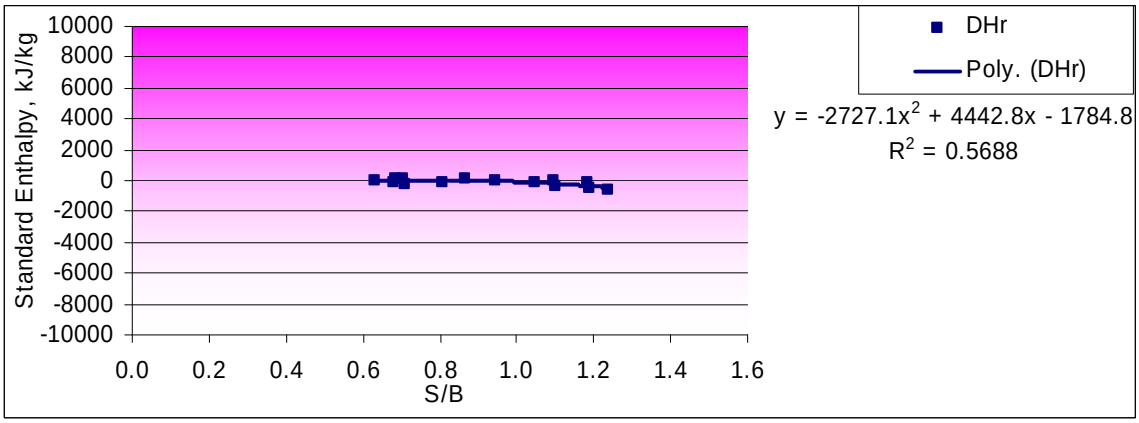

Figure 4.89 Enthalpy of reaction from steam gasification of bermudagrass

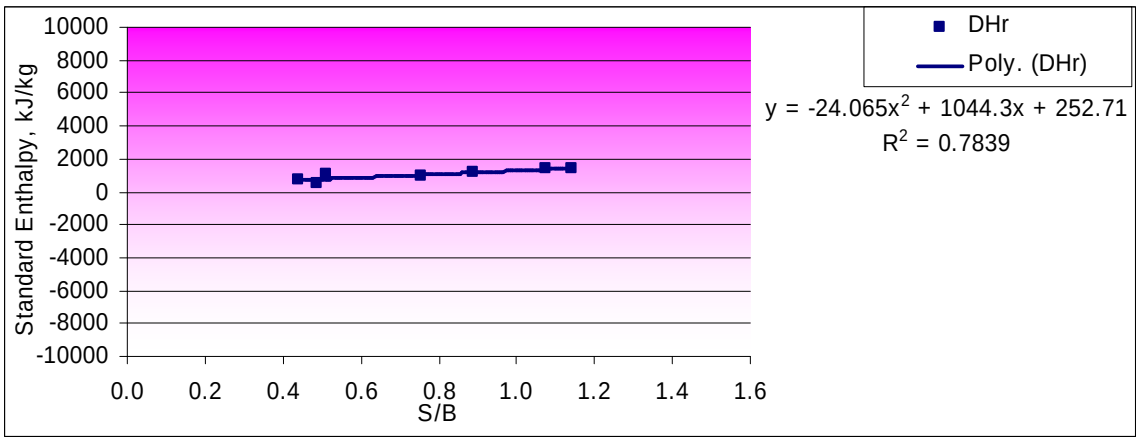

Figure 4.90 Enthalpy of reaction from steam gasification of corn gluten

4.5 OVERALL TAR CHARACTERISTICS

4.5.1 Average atomic composition

For the three gasification processes used in this study, the atomic compositions of tar for all three feedstocks gasified in the temperature range of 700 to 800°C are very similar as provided in Tables 4.2, 4.3 and 4.4. The average of those 9 results for each element, representing 100 gasification experiments with over 210,000 tar compounds tested, provides the average atomic tar composition for all biomasses and all processes experimented as:

$$C_{7.553}H_{8.623}O_{0.368}N_{0.204}$$

This result is of particular importance for the equilibrium modeling discussed in Chapter 5. It is the basis for considering the hypothesis of tar as one molecule with properties averaged from empirical data.

4.5.2 Average molecular weight

From the above average atomic tar composition, the average molecular weight for tar can also be calculated for all biomasses and all processes resulting in the following:

$$MW_{tar} = 108.045 \text{ g/mol}$$

4.5.3 Average determination of the free enthalpy ΔG(T) for tar

Because it is difficult to find free enthalpy ΔG(T) functions for all 210 tar compounds, as opposed to the enthalpy of formation, the free enthalpy for tar is the result average of the one of the major compounds. Considering the average proportion of the

first 10 main compounds of tar for switchgrass (Table 4.5), the sum represents approximately 75% of the total mass of the tar.

Substance	Mol. Formula	Mol. Weight	A	B	C	%
Benzene	C6H6	78.114	**81.078**	**0.16**	**1.76E-05**	28.89
Toluene	C7H8	92.141	**47.987**	**0.24**	**2.45E-05**	17.65
Phenol	C6H6O	94.113	**-98.451**	**0.22**	**1.34E-05**	13.72
Ethylbenzene	C8H10	106.167	**27.095**	**0.34**	**2.82E-05**	9.78
Methylphenol	C8H10O	122.167	**-130.92**	**0.32**	**1.80E-05**	8.22
Styrene	C8H8	104.152	**146.28**	**0.22**	**2.08E-05**	5.77
Xylene	C8H10	106.167	**15.327**	**0.35**	**3.11E-05**	5.01
naphthalene	C10H8	128.174	**147.69**	**0.25**	**1.91E-05**	3.97
dimethylnaphthalene	C12H12	156.227	**79.111**	**0.45**	**2.61E-05**	3.73
methylnaphthalene	C11H10	142.2	**113.27**	**0.34**	**2.27E-05**	3.26
Weighted averages			**31.978**	**0.24635**	**2.073E-05**	100

Table 4.5 Average tar composition for free enthalpy $\Delta G_{tar}(T)$ calculation

The function for free enthalpy of tar is then:

$$\Delta G_{Tar}(T) = 31.978 + 0.24635 \times T + 2.073 \times 10^{-5} \times T^2 \qquad \textbf{(4.4)}$$

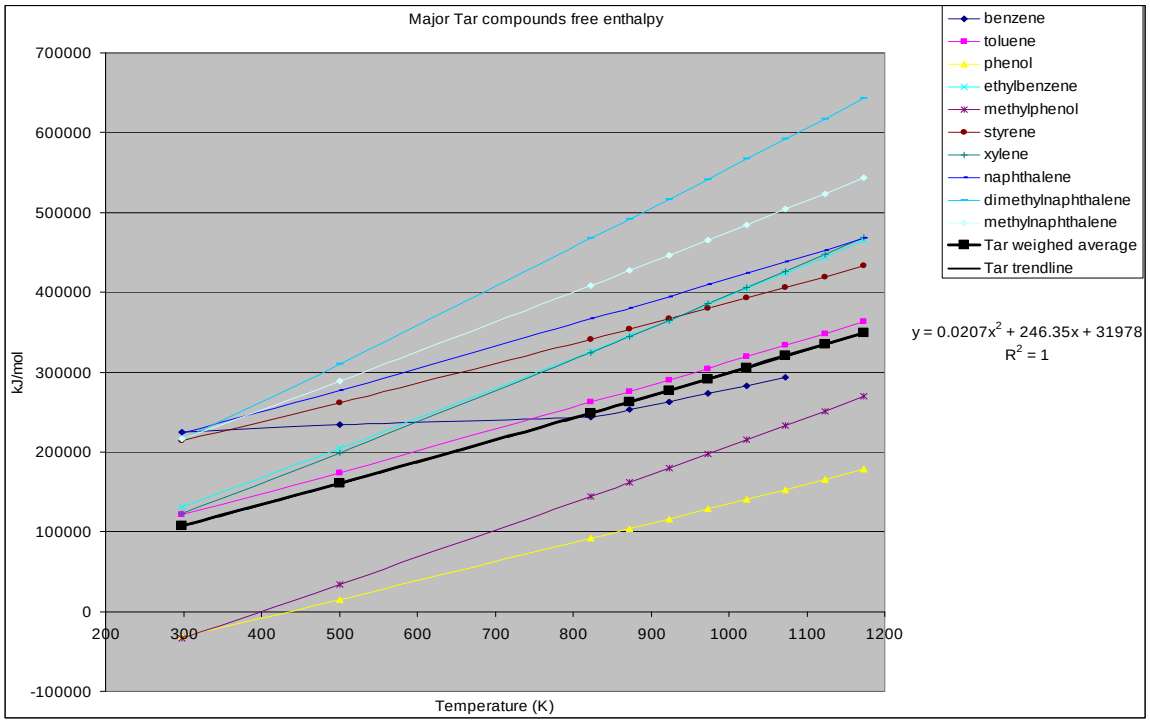

Figure 4.91 Average tar free enthalpy.

5 EQUILIBRIUM METHODOLOGY

5.1 EQUILIBRIUM MODELING

Gasification of several biomass types was modeled with a Gibbs reactor at atmospheric pressure representing equilibrium of the major compounds at different temperatures and Equivalence Ratios.

What is a Gibbs reactor? A Gibbs reactor is a form of equilibrium reactor. It minimizes the total Gibbs energy subject to a material balance. When the variation of the free enthalpy G (or Gibbs energy, or thermodynamic potential at constant pressure and constant temperature) of a thermodynamic system is minimized ($\Delta G = 0$), the system is at equilibrium. If a mixture of chemical species is not at equilibrium: $\Delta G \neq 0$, any reactions that occurs at constant pressure and temperature must minimize the total Gibbs energy G of the system until $\Delta G = 0$.

In this type of reactor, only the feed and product streams are specified, but the reactions are not. Considering a reversible chemical reaction of ideal gases A, B, C and D with respective stoichiometric coefficient a,b,c and d such as equation 5.1.

$$A + \frac{b}{a}B \Leftrightarrow \frac{c}{a}C + \frac{d}{a}D \qquad \textbf{(5.1)}$$

For each gas chemical species, the free enthalpy is:

$$G_i = \Delta G_i^o + RT\ln(P_i) \qquad \textbf{(5.2)}$$

For this reaction the free enthalpy variation is:

$$\Delta G = \left(\frac{c}{a}(G_C^o + RT\ln(P_C)) + \frac{d}{a}(G_D^o + RT\ln(P_D)) - \frac{b}{a}(G_B^o + RT\ln(P_B)) - (G_A^o + RT\ln(P_A)) \right) \quad \textbf{(5.3)}$$

$$\Delta G = \left(\frac{c}{a}G_C^o + \frac{d}{a}G_D^o - \frac{b}{a}G_B^o - G_A^o \right) + RT\left(\frac{c}{a}\ln(P_C) + \frac{d}{a}\ln(P_D) - \frac{b}{a}\ln(P_B) - \ln(P_A) \right) \quad \textbf{(5.4)}$$

$$\Delta G = \left(\Delta G^o\right) + RT\ln\left(\frac{P_C^{\frac{c}{a}}\ P_D^{\frac{d}{a}}}{P_A^1\ P_B^{\frac{b}{a}}} \right) \quad \textbf{(5.5)}$$

$$\Delta G = \Delta G^o + RT\ln M \quad \textbf{(5.6)}$$

Equation 5.6 gives the value of ΔG of the reaction whatever the conditions. If ΔG ≠ 0, products and reactants are not at the same "potential". The reaction is going to take place in such a way that ΔG is negative; the potentials of the reactants and the products tend to equalize and the total free enthalpy of the system tends toward its minimum. When equilibrium is reached, the result is:

$$\begin{gathered} \Delta G = \Delta G^o + RT\ln M = 0 \\ \Delta G^o = -RT\ln M \quad or \quad M = e^{-\frac{\Delta G^o}{RT}} \end{gathered} \quad \textbf{(5.7)}$$

The equilibrium constant (K) is this particular value of M for which equilibrium made:

$$\Delta G^o = -RT\ln K \quad or \quad K = e^{-\frac{\Delta G^o}{RT}} \quad \textbf{(5.8)}$$

For this ideal gas reaction, the equilibrium law is:

$$K = \frac{\prod_{\text{Products}} P_i^{\nu_i}}{\prod_{\text{Reactants}} P_j^{\nu_j}} = \frac{P_C^{\frac{c}{a}}\ P_D^{\frac{d}{a}}}{P_A^1\ P_B^{\frac{b}{a}}} \quad \textbf{(5.9)}$$

This previous description is for ideal gas, but the same principle applies for all single phase systems, and K becomes a function of the activity:

$$K = \frac{\prod_{\text{Products}} a_i^{\nu_i}}{\prod_{\text{Reactants}} a_j^{\nu_j}}$$ where a_i is the activity of the chemical specie i.

It is important to note that gasification is not a single phase system. Although the products of interest are gases, gasification is the transformation of a solid phase reactant to a mixed gas phase/solid phase product. In most fluidized bed modeling, the first aspect is a devolatilization step where it is assumed that most of the carbon in the biomass is instantaneously transformed into the gas phase as CO, CH_4, and CO_2. This consideration leaves the solid phase out of the equilibrium calculations. The instantaneous hypothesis of this transformation relies on the negligible aspect of the char porosity in fluidized bed reactor because char is reduced to a fine powder, thus maximizing the mass transfer between the solid phase and the gas phase.

In the equilibrium model described in this chapter, solid carbon is considered to be a powder so fine that it reacts as a gas. Although carbon boiling point is at a temperature of 5100K, for the necessity of the model, the hypothesis of elemental pure carbon interacting with the gas mixture is formulated. Furthermore, the effect of pressure on the activity of a solid is very small, so the activity of carbon solid is considered to be unity: $a_{C_S} = 1$.

Calculating the product fractions at equilibrium consists of minimizing the free enthalpy by solving a nonlinear system of equations involving:

- free enthalpy for each compound
- number of moles for each compound
- mole balance and
- atomic balance.

5.2 PROGRAM

5.2.1 Program inputs

The program for this model was created using LabView graphic programming from National Instrument (1999). The program requests the user to enter the following parameters:

Gasification agents:

- Air
- Pressure (Pa)
- Temperature (K)
- volumetric flow rate (m^3/h)
- Steam mass flow rate (kg/h)
- Biomasses and chars compositions (array of four types)
- C, H, O, N, S and ash (wt % db)
- Moisture content (wt % wb)
- biomasses flow rates (kg/h wb) (array of 11 user modifiable)
- biomasses and chars HHVs (J/kg)

5.2.2 Program flow diagram

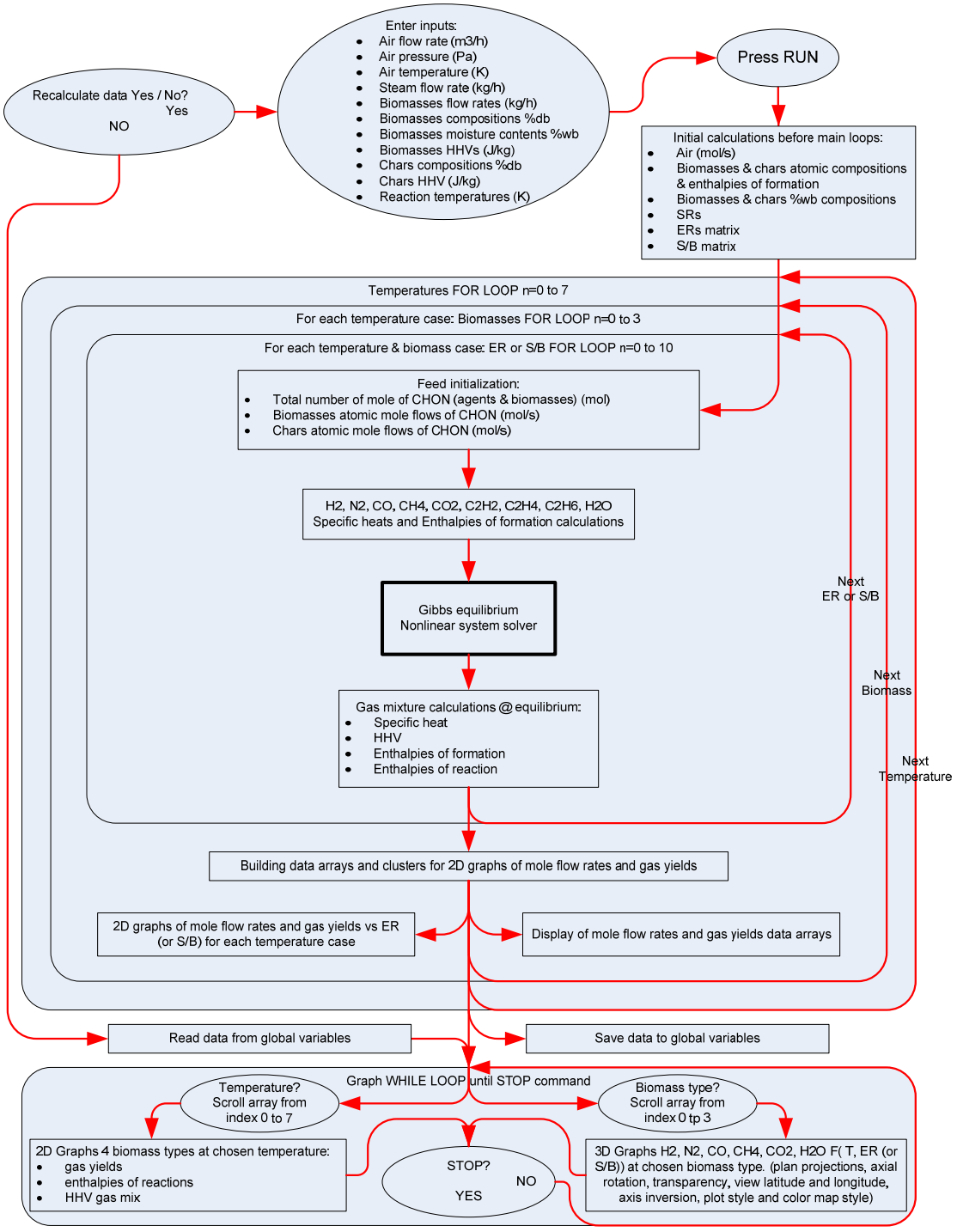

Figure 5.1 Program flow diagram

3D-graphic.vi: The results of the main program for all four biomasses may also be viewed all at once with a simple stand alone 3D-graphic.vi program that calls the same

global variables. This virtual instrument (vi) is voluntarily kept separated from the main program for facility of use, but it is also possible to add this vi to the main program.

5.2.3 Virtual instruments (VI) hierarchy

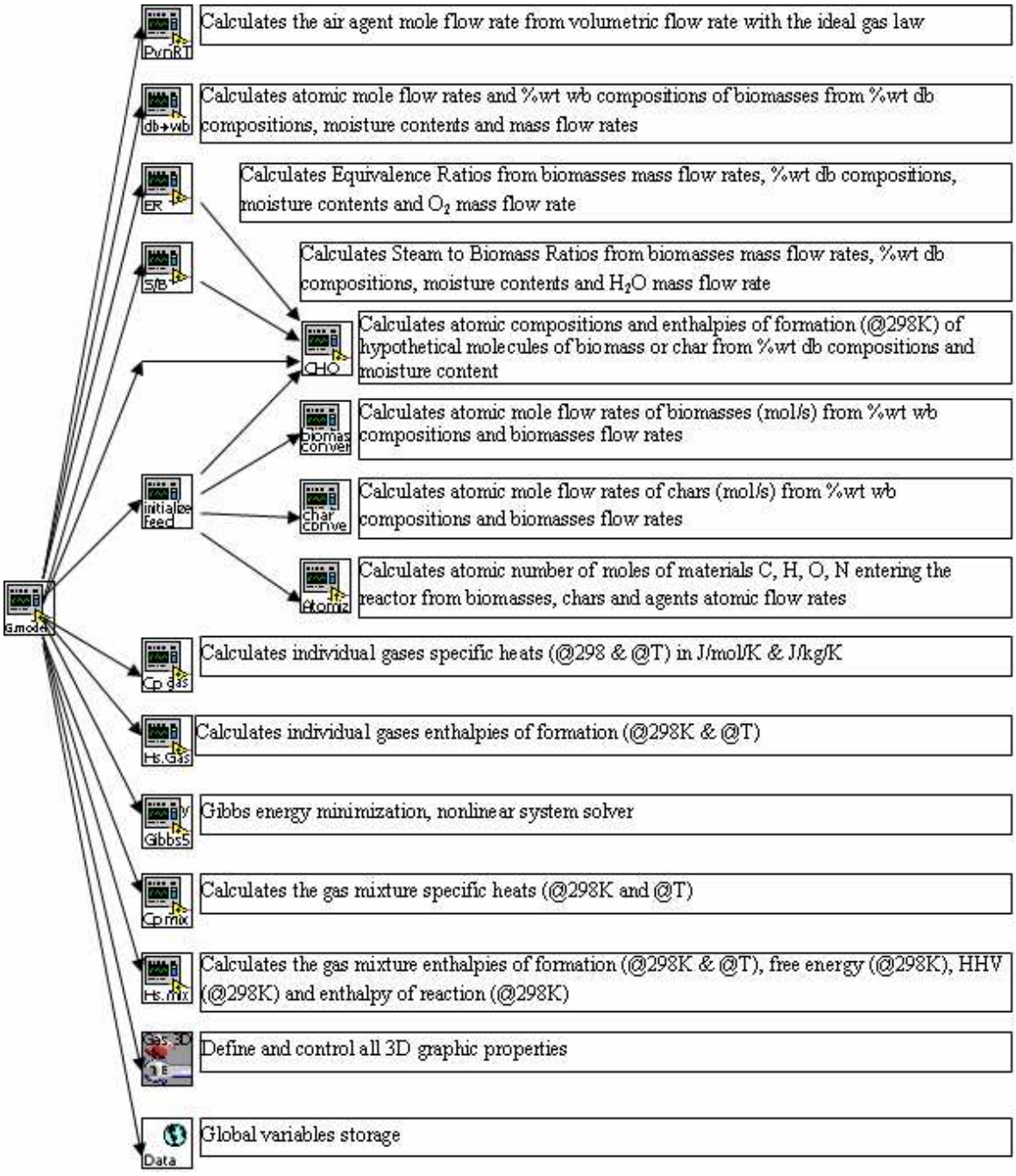

Figure 5.2 VI hierarchy

5.3 VIRTUAL INSTRUMENTS (.vi) CALCULATIONS

The following calculations are shown in vi hierarchy (Figure 5.2).

5.3.1 Dry to Wet basis.vi: % composition basis conversion

This virtual instrument calculates wet basis percentage composition of the biomass from a dry basis percentage composition input and moisture content.

$$\%\ i^{wt\,wb} = \%\ i^{wt\,db} \times \frac{100 - \%\ H_2O_{biomass}^{wt\,wb}}{100} \qquad \textbf{(5.10)}$$

5.3.2 CHO.vi: conversion to atomic composition

This virtual instrument defines the properties of the biomasses. It calculates the ratio of atoms C, H and O for each biomass on the basis of one carbon. This defines a hypothetical molecule of biomass with the form CH_xO_y

$$Atomic\#_H = x = \frac{\frac{H\%}{M_H}}{\frac{C\%}{M_C}} \quad Atomic\#_O = y = \frac{\frac{O\%}{M_O}}{\frac{C\%}{M_C}} \qquad \textbf{(5.11)}$$

This virtual instrument also calculates the enthalpie of formation of this hypothetical molecule of biomass from the measured HHV (J/kg) of a biomass sample.

Considering the stoichiometric combustion of this hypothetical molecule of biomass:

$$CHxOy + (1 + \frac{x}{4} - \frac{y}{2})O_2 \xrightarrow{HHV} CO_2 + \frac{x}{2} H_2O \qquad \textbf{(5.12)}$$

and

$$HHV = \sum \text{products} - \sum \text{reactants} \qquad \textbf{(5.13)}$$

since $\Delta H_{f\,O_2} = 0$

$$\Delta H_{CH_xO_y} = \Delta H_{f\,CO_2} + \Delta H_{f\,H_2O} - HHV \qquad \textbf{(5.14)}$$

since $\Delta H_{f\,CO_2} = -393510 J.mol^{-1}$ and $\Delta H_{f\,H_2O} = -285830 J.mol^{-1}$

$$\Delta H_{f\,CH_xO_y} = -393510 J.mol^{-1} - 285830 J.mol^{-1} \times \frac{x}{2} - HHV \qquad \textbf{(5.15)}$$

5.3.3 ER.vi: calculation of ER ratio

The ER is the abscise variable that permits the comparison of various biomasses air gasification and it is defined and calculated in this vi.

Considering the stoichiometric combustion of biomass:

$$1\ CH_xO_y + (1+x/4-y/2)\ O_2 \rightarrow 1\ CO_2 + x/2\ H_2O \qquad \textbf{(5.16)}$$

The stoichiometric ratio is:

$$\text{SR} = \frac{mass\ of\ \ oxygen\ \ for\ combustion}{mass\ of\ \ dry\ biomass} = \frac{M_{O_2} \times \left(1 + \frac{x}{4} - \frac{y}{2}\right)}{\left(M_C + x \times M_H + y \times M_O\right) \times \left(\frac{100}{\frac{}{wt\,db}\ \%\ CHO_{biomass}}\right)} \qquad \textbf{(5.17)}$$

From equation 1.3, the equivalence ratio (ER) is:

$$ER = \frac{Gasification\ ratio}{Stoichiometric\ Ratio\ (SR)} = \frac{Mass\ of\ oxidant\ /\ Mass\ of\ \ dry\ biomass \quad @\ gasification}{Mass\ of\ oxidant\ /\ Mass\ of\ dry\ biomass \quad @\ combustion}$$

$$ER = \frac{\dot{m}_{O_2}}{\dot{m}_{biomass} \times \left(1 - \overset{wt\,wb}{\%}\ H_2O_{biomass}\right)} \Bigg/ \frac{M_{O_2} \times \left(1 + \frac{x}{4} - \frac{y}{2}\right)}{\left(M_C + x \times M_H + y \times M_O\right) \times \left(\frac{100}{\overset{wt\,db}{\%}\ CHO_{biomass}}\right)} \qquad \textbf{(5.18)}$$

5.3.4 SB.vi: calculation of S/B ratio

This vi calculates the steam to biomass ratio in the case of steam gasification, that is define as follow:

$$S/B = \frac{\dot{m}_{Steam} + \dot{m}_{moisture}}{\dot{m}_{biomass} \times \left(1 - \overset{wt\,wb}{\%}\ H_2O_{biomass}\right)} \qquad \textbf{(5.19)}$$

Whether the data display would use ER or S/B for abscise, is defined in the main program by the comparison of the agents mass flow rates.

5.3.5 Biomass composition conversion and Char composition conversion VIs

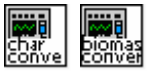

Technically the same, these two vi's calculate atomic mole flow rate of biomass and char from % dry basis composition, % wet basis moisture content and biomass mass flow rate.

$$F_{i_{biomass}} = \frac{1000 \times \dot{m}_{biomass} \times \overset{wt\,wb}{\%}\ i_{biomass}}{3600 \times M_i \times 100} \qquad \textbf{(5.20)}$$

$$\dot{m}_{char} = \dot{m}_{biomass} \times \frac{\overset{wt\,db}{\%}\ Ash_{biomass}}{\overset{wt\,db}{\%}\ Ash_{Char}} \qquad \textbf{(5.21)}$$

$$F_{i\,char} = \dot{m}_{biomass} \times \frac{\overset{wt\,db}{\%}\ Ash_{biomass}}{\overset{wt\,db}{\%}\ Ash_{Char}} \qquad \textbf{(5.22)}$$

5.4 FREE ENTHALPY CALCULATIONS

To calculate the equilibrium concentrations with the nonlinear equations system solver, it is necessary to build the set of equations with known parameters.

The known values of the nonlinear equations system solver are:

- the free enthalpy value of each individual gases at process temperature T
- the atomic elemental mole flow rates of Carbon, Hydrogen and Oxygen in the chemical system

5.4.1 DG_Knovel.vi: free enthalpy calculations from Knovel tables

This vi calculates free enthalpy of the various compounds of the gas from temperature dependant equations of the Knovel database:

$$\Delta G_i = A_i + B_i \times T + C_i \times T^2 \qquad \textbf{(5.23)}$$

	A	B	C	
0	0.0000E+0	0.0000E+0	0.0000E+0	H2
0	0.0000E+0	0.0000E+0	0.0000E+0	N2
	0.0000E+0	0.0000E+0	0.0000E+0	O2
	-1.0994E+2	-9.0000E-2	5.7289E-7	CO
	-7.4826E+1	8.0000E-2	1.7205E-5	CH4
	-3.9300E+2	0.0000E+0	5.9300E-7	CO2
	2.2846E+2	-6.0000E-2	2.2383E-6	C2H2
	5.1887E+1	5.0000E-2	1.5435E-5	C2H4
	-8.4856E+1	1.7000E-1	2.4303E-5	C2H6
	-2.4200E+2	4.3500E-2	6.1000E-6	H2O

Table 5.1 ΔGKnovel database

The temperature limitation of the Knovel database is a maximum of 1000K. Free enthalpy values calculated from specific heat (Cp) and enthalpy of formation (H_f) valid up to 1500 K of the gas compounds are compared to Knovel data:

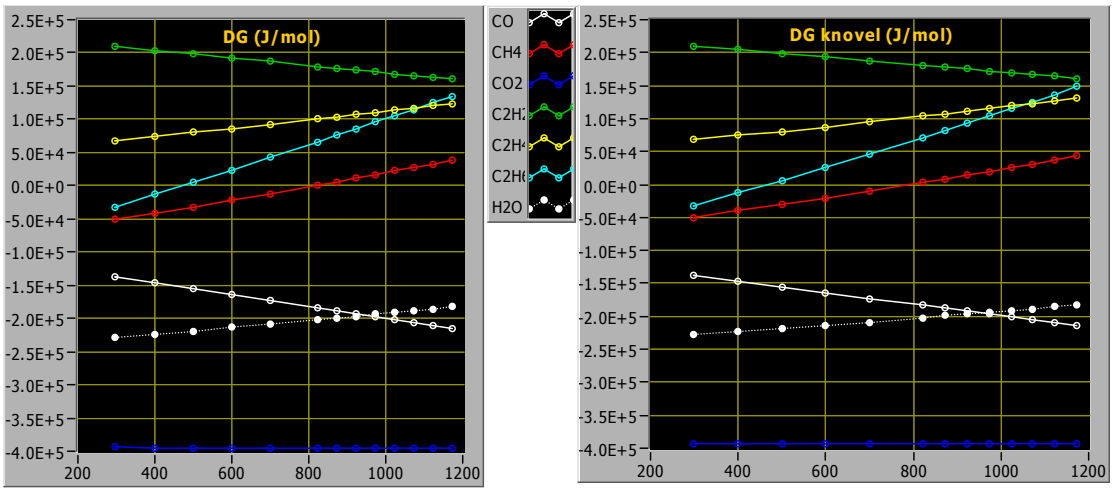

Figure 5.3 ΔG calculated and ΔG from the Knovel database

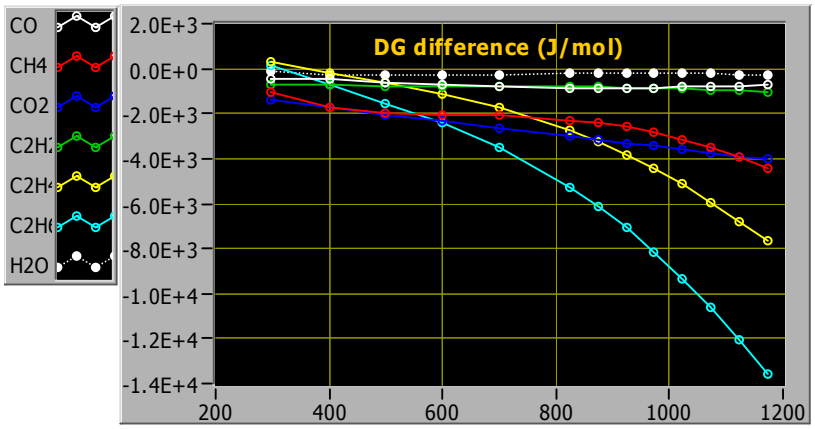

Figure 5.4 Difference ΔG calculated - ΔG from the Knovel database

Because of the limitation in temperature of the Knovel database equations, the values of free energies were calculated from specific heat and enthalpies of formation of the gas compounds (next section), but a user may insert DG Knovel.vi if preferred.

5.5 COMPOUNDS FREE ENTHALPY CALCULATIONS

Free enthalpy at standard temperature T=298K:

$$\Delta G^o = \Delta H^o - T^o \times \Delta S^o \quad \textbf{(5.24)}$$

Or

$$\Delta S^o = \frac{\Delta H^o - \Delta G^o}{T^o} \quad \textbf{(5.25)}$$

Free enthalpy at a temperature T (Kelvin):

$$\Delta G^T = \Delta H^T - T \times \Delta S^T \quad \textbf{(5.26)}$$

With

$$\begin{cases} \Delta H^T = \Delta H^o + \int_{T^o}^{T} \Delta Cp\, dT & \textbf{(5.27)} \\ \Delta S^T = \Delta S^o + \int_{T^o}^{T} \frac{\Delta Cp}{T} dT & \textbf{(5.28)} \end{cases}$$

Using equation 5.27 & 5.28 in equation 5.26, the free enthalpy becomes:

$$\Delta G^T = \Delta H^o + \int_{T^o}^{T} \Delta Cp\, dT - T\left(\Delta S^o + \int_{T^o}^{T} \frac{\Delta Cp}{T} dT \right) \quad \textbf{(5.29)}$$

Using equation 5.25 in equation 5.29, the free enthalpy becomes:

$$\Delta G^T = \Delta H^o + \int_{T^o}^{T} \Delta Cp\, dT - T\left(\frac{\Delta H^o - \Delta G^o}{T^o} + \int_{T^o}^{T} \frac{\Delta Cp}{T} dT \right) \quad \textbf{(5.30)}$$

Because the functions defining Cps (Table 5.2) are given divided by the ideal gas constant R, equation 5.30 becomes:

$$\Delta G^T = T \frac{\left(\Delta G^o - \Delta H^o\right)}{T^o} + \Delta H^o + R\int_{T^o}^{T} \frac{\Delta Cp}{R} dT - RT\int_{T^o}^{T} \frac{\Delta Cp}{RT} dT \quad \textbf{(5.31)}$$

Specific heat variation ΔCp across any reaction:

$$\Delta Cp = \sum_{\text{products}} Cp_i - \sum_{\text{reactants}} Cp_i \tag{5.32}$$

Integral from the enthalpy term in equation 5.31:

$$\int_{T^o}^{T} \frac{\Delta Cp}{R} dT = \int_{T^o}^{T} \left[\sum_{\text{products}} \left(\frac{Cp_i}{R} \right) - \sum_{\text{reactants}} \left(\frac{Cp_i}{R} \right) \right] dT \tag{5.33}$$

$$\Leftrightarrow \int_{T^o}^{T} \frac{\Delta Cp}{R} dT = \sum_{\text{products}} \left[\int_{T^o}^{T} \left(\frac{Cp_i}{R} \right) dT \right] - \sum_{\text{reactants}} \left[\int_{T^o}^{T} \left(\frac{Cp_i}{R} \right) dT \right] \tag{5.34}$$

Integral from the entropy term in equation 5.31:

$$\int_{T^o}^{T} \frac{\Delta Cp}{RT} dT = \int_{T^o}^{T} \left[\sum_{\text{products}} \left(\frac{Cp_i}{RT} \right) - \sum_{\text{reactants}} \left(\frac{Cp_i}{RT} \right) \right] dT \tag{5.35}$$

$$\Leftrightarrow \int_{T^o}^{T} \frac{\Delta Cp}{RT} dT = \sum_{\text{products}} \left[\int_{T^o}^{T} \left(\frac{Cp_i}{RT} \right) dT \right] - \sum_{\text{reactants}} \left[\int_{T^o}^{T} \left(\frac{Cp_i}{RT} \right) dT \right] \tag{5.36}$$

Using equation 5.34 & 5.36 in equation 5.31, the free enthalpy becomes:

$$\begin{aligned} \Delta G^T = T \frac{\left(\Delta G^o - \Delta H^o \right)}{T^o} + \Delta H^o + R \sum_{\text{products}} \left[\int_{T^o}^{T} \left(\frac{Cp_i}{RT} \right) dT \right] - \sum_{\text{reactants}} \left[\int_{T^o}^{T} \left(\frac{Cp_i}{RT} \right) dT \right] \\ - RT \times \sum_{\text{products}} \left[\int_{T^o}^{T} \left(\frac{Cp_i}{RT} \right) dT \right] - \sum_{\text{reactants}} \left[\int_{T^o}^{T} \left(\frac{Cp_i}{RT} \right) dT \right] \end{aligned} \tag{5.37}$$

Specific heat calculation of each gas (Smith et al.,1996):

$$\frac{Cp_i}{R} = A_i + B_i \times T + C_i * T^2 + \frac{D_i}{T^2} \qquad \textbf{(5.38)}$$

Using equation 5.38 the integral from the enthalpy term equation 5.37 becomes:

$$\int_{T^o}^{T} \frac{\Delta Cp_i}{R} dT = \sum_{\text{products}} \left[\int_{T^o}^{T} \left(\frac{Cp_i}{R} \right) dT \right] - \sum_{\text{reactants}} \left[\int_{T^o}^{T} \left(\frac{Cp_i}{R} \right) dT \right] \qquad \textbf{(5.39)}$$

$$\int_{T^o}^{T} \frac{\Delta Cp_i}{R} dT = \sum_{\text{products}} \left[\int_{T^o}^{T} \left(A_i + B_i T + C_i T^2 + \frac{D_i}{T^2} \right) dT \right] - \sum_{\text{reactants}} \left[\int_{T^o}^{T} \left(A_i + B_i T + C_i T^2 + \frac{D_i}{T^2} \right) dT \right] \qquad \textbf{(5.40)}$$

$$\int_{T^o}^{T} \frac{\Delta Cp_i}{R} dT = \sum_{\text{products}} \left[A_i T + \frac{B_i T^2}{2} + \frac{C_i T^3}{3} - \frac{D_i}{T} \right]_{T^o}^{T} - \sum_{\text{reactants}} \left[A_i T + \frac{B_i T^2}{2} + \frac{C_i T^3}{3} - \frac{D_i}{T} \right]_{T^o}^{T} \qquad \textbf{(5.41)}$$

Using equation 5.38 the integral from the entropy term equation 5.37 becomes:

$$\int_{T^o}^{T} \frac{\Delta Cp_i}{RT} dT = \sum_{\text{products}} \left[\int_{T^o}^{T} \left(\frac{Cp_i}{RT} \right) dT \right] - \sum_{\text{reactants}} \left[\int_{T^o}^{T} \left(\frac{Cp_i}{RT} \right) dT \right] \qquad \textbf{(5.42)}$$

$$\int_{T^o}^{T} \frac{\Delta Cp_i}{RT} dT = \sum_{\text{products}} \left[\int_{T^o}^{T} \left(\frac{A_i}{T} + B_i + C_i T + \frac{D_i}{T^3} \right) dT \right] - \sum_{\text{reactants}} \left[\int_{T^o}^{T} \left(\frac{A_i}{T} + B_i + C_i T + \frac{D_i}{T^3} \right) dT \right] \qquad \textbf{(5.43)}$$

$$\int_{T^o}^{T} \frac{\Delta Cp_i}{RT} dT = \sum_{\text{products}} \left[A_i \ln(T) + B_i T + \frac{C_i T^2}{2} - \frac{D_i}{2T^2} \right]_{T^o}^{T} - \sum_{\text{reactants}} \left[A_i \ln(T) + B_i T + \frac{C_i T^2}{2} - \frac{D_i}{2T^2} \right]_{T^o}^{T} \qquad \textbf{(5.44)}$$

Using equation 5.41 & 5.44 in equation 5.37, the free enthalpy equation becomes:

$$\begin{aligned} \Delta G_i^{\,T} &= T \frac{\left(\Delta G_i^{\,o} - \Delta H_i^{\,o} \right)}{T^o} + \Delta H_i^{\,o} \\ &+ R \sum_{\text{products}} \left[A_i T + \frac{B_i T^2}{2} + \frac{C_i T^3}{3} - \frac{D_i}{T} \right]_{T^o}^{T} - \sum_{\text{reactants}} \left[A_i T + \frac{B_i T^2}{2} + \frac{C_i T^3}{3} - \frac{D_i}{T} \right]_{T^o}^{T} \\ &- RT \times \sum_{\text{products}} \left[A_i \ln(T) + B_i T + \frac{C_i T^2}{2} - \frac{D_i}{2T^2} \right]_{T^o}^{T} - \sum_{\text{reactants}} \left[A_i \ln(T) + B_i T + \frac{C_i T^2}{2} - \frac{D_i}{2T^2} \right]_{T^o}^{T} \end{aligned} \qquad \textbf{(5.45)}$$

The calculation of ΔG_i for the array of gases is performed through two vi$_s$:

 Cp Equil gases.vi

 EquilEnthalpies1.vi

5.5.1 Cp Equil gases.vi: gases heat capacities calculations

This vi calculates specific heat values of each gas from []:

$$\frac{Cp_i}{R} = A_i + B_i T + C_i T^2 + \frac{D_i}{T^2} \qquad \textbf{(5.46)}$$

Cpig/R = A + BT + CT^2 + DT^-2

	A	B	C	D
H2 0	3.2490E+0	4.2200E-4	0.0000E+0	8.3000E+3
N2 0	3.2800E+0	5.9300E-4	0.0000E+0	4.0000E+3
O2	3.6390E+0	5.0600E-4	0.0000E+0	-2.2700E+4
CO	3.3760E+0	5.5700E-4	0.0000E+0	-3.1000E+3
CH4	1.7020E+0	9.0810E-3	-2.1640E-6	0.0000E+0
CO2	5.4570E+0	1.0450E-3	0.0000E+0	-1.1570E+5
C2H2	6.1320E+0	1.9520E-3	0.0000E+0	-1.2990E+5
C2H4	1.4240E+0	1.4394E-2	-4.3920E-6	0.0000E+0
C2H6	1.1310E+0	1.9225E-2	-5.5610E-6	0.0000E+0
H2O	3.4700E+0	1.4500E-3	0.0000E+0	1.2100E+4
C(s)	1.7710E+0	7.7100E-4	0.0000E+0	-8.6700E+4

Table 5.2 Cp coefficient (Smith et al.1996)

This vi also calculates the integrals terms $\int_{T^o}^{T}\left(\frac{Cp_i}{R}\right)dT$ and $\int_{T^o}^{T}\left(\frac{Cp_i}{RT}\right)dT$:

$$\int_{T^o}^{T}\left(\frac{Cp_i}{R}\right)dT = \left[A_i T + \frac{B_i T^2}{2} + \frac{C_i T^3}{3} - \frac{D_i}{T}\right]_{T^o}^{T} \qquad \textbf{(5.47)}$$

$$\int_{T^o}^{T}\left(\frac{Cp_i}{RT}\right)dT = \left[A_i \ln(T) + B_i T + \frac{C_i T^2}{2} - \frac{D_i}{2T^2}\right]_{T^o}^{T} \qquad \textbf{(5.48)}$$

Only reactions from pure elements were considered for the calculations of the integrals of ΔCp, except for the pure elements themselves, i.e. H_2 , N_2, and O_2 for which $\Delta G^T = 0$

ΔCp calculations of non elemental compounds:

- Carbon monoxide: $\begin{cases} C_s + \frac{1}{2}O_2 \rightarrow CO \\ \Delta Cp = Cp_{CO} - \frac{1}{2}Cp_{O_2} - Cp_{C_s} \end{cases}$ **(5.49)**

- Methane: $\begin{cases} C_s + 2H_2 \rightarrow CH_4 \\ \Delta Cp = Cp_{CH_4} - 2Cp_{H_2} - Cp_{C_s} \end{cases}$ **(5.50)**

- Carbon dioxide: $\begin{cases} C_s + O_2 \rightarrow CO_2 \\ \Delta Cp = Cp_{CO_2} - Cp_{O_2} - Cp_{C_s} \end{cases}$ **(5.51)**

- Acetylene: $\begin{cases} 2C_s + H_2 \rightarrow C_2H_2 \\ \Delta Cp = Cp_{C_2H_2} - Cp_{H_2} - 2Cp_{C_s} \end{cases}$ **(5.52)**

- Ethylene: $\begin{cases} 2C_s + 2H_2 \rightarrow C_2H_4 \\ \Delta Cp = Cp_{C_2H_2} - 2Cp_{H_2} - 2Cp_{C_s} \end{cases}$ **(5.53)**

- Ethane: $\begin{cases} 2C_s + 3H_2 \rightarrow C_2H_6 \\ \Delta Cp = Cp_{C_2H_2} - 3Cp_{H_2} - 2Cp_{C_s} \end{cases}$ **(5.54)**

- Water: $\begin{cases} \frac{1}{2}O_2 + H_2 \rightarrow H_2O \\ \Delta Cp = Cp_{H_2O} - Cp_{H_2} - \frac{1}{2}Cp_{O_2} \end{cases}$ **(5.55)**

To build values for $\int_{T^o}^{T} \frac{\Delta Cp}{R} dT$ and $\int_{T^o}^{T} \frac{\Delta Cp}{RT} dT$ in vector array, $\int_{T^o}^{T} \left(\frac{Cp_i}{R} \right) dT$ and $\int_{T^o}^{T} \left(\frac{Cp_i}{RT} \right) dT$ arrays are multiplied by the following matrix built from the above reactions equations 5.49-5.55:

DCp matrix

	H2	N2	O2	CO	CH4	CO2	C2H2	C2H4	C2H6	H20	Cs	
0	0.0	0.0	0.0	0.0	0.0	0.0	0.0	0.0	0.0	0.0	0.0	H2
0	0.0	0.0	0.0	0.0	0.0	0.0	0.0	0.0	0.0	0.0	0.0	N2
	0.0	0.0	0.0	0.0	0.0	0.0	0.0	0.0	0.0	0.0	0.0	O2
	0.0	0.0	-0.5	1.0	0.0	0.0	0.0	0.0	0.0	0.0	-1.0	CO
	-2.0	0.0	0.0	0.0	1.0	0.0	0.0	0.0	0.0	0.0	-1.0	CH4
	0.0	0.0	-1.0	0.0	0.0	1.0	0.0	0.0	0.0	0.0	-1.0	CO2
	-0.5	0.0	0.0	0.0	0.0	0.0	0.5	0.0	0.0	0.0	-1.0	C2H2
	-1.0	0.0	0.0	0.0	0.0	0.0	0.0	0.5	0.0	0.0	-1.0	C2H4
	-1.5	0.0	0.0	0.0	0.0	0.0	0.0	0.0	0.5	0.0	-1.0	C2H6
	-1.0	0.0	-0.5	0.0	0.0	0.0	0.0	0.0	0.0	1.0	0.0	H20

Table 5.3 ΔCp reactions matrix

5.5.2 Equil_enthalpy_w_char.vi: enthalpies of formation and free enthalpy calculation

This vi calculates enthalpies of formation and free energies values of each individual gas from equation 5.31:

$$\Delta G_i^{\ T} = T\frac{\left(\Delta G_i^{\ o} - \Delta H_i^{\ o}\right)}{T^o} + \Delta H_i^{\ o} + R\int_{T^o}^{T}\frac{\Delta Cp_i}{R}dT - RT\int_{T^o}^{T}\frac{\Delta Cp_i}{RT}dT$$

From the following values:

DGi(j/ mole)@298K	
H2	0.00
N2	0.00
O2	0.00
CO	-137169.00
CH4	-50460.00
CO2	-394359.00
C2H2	209970.00
C2H4	68460.00
C2H6	-31855.00
H2O	-228572.00
C(s)	0.00

Table 5.4 ΔGi at 298K (Smith et al.,1996)

DHfi(j/ mole)@298K	
H2	0.00
N2	0.00
O2	0.00
CO	-110525.00
CH4	-74520.00
CO2	-393509.00
C2H2	227480.00
C2H4	52510.00
C2H6	-83820.00
H2O	-241818.00
C(s)	0.00

Table 5.5 ΔHfi at 298K (Smith et al.,1996)

5.6 EQUILIBRIUM CALCULATION

This chapter discusses the culmination of the calculations for the entire system of non linear equations. At constant atmospheric pressure the gas phase system containing the species: H_2, CO, CH_4, CO_2, C_2H_2, C_2H_4, C_2H_4, H_2O, will reach equilibrium depending only on the temperature and the number of mole of C, H and O in the system.

5.6.1 Mole balance equations

Carbon balance:

$$n_{CO} + n_{CH_4} + n_{CO_2} + 2\times n_{C_2H_2} + 2\times n_{C_2H_4} + 2\times n_{C_2H_6} + 7.722\times n_{C_{Tar}} - n_{C_{in}} = 0 \quad \textbf{(5.56)}$$

Hydrogen balance:

$$2\times n_{H_2} + 4\times n_{CH_4} + 2\times n_{C_2H_2} + 4\times n_{C_2H_4} + 6\times n_{C_2H_6} + 2\times n_{H_2O} + 7.997\times n_{H_{Tar}} - n_{H_{in}} = 0 \quad \textbf{(5.57)}$$

Oxygen balance:

$$n_{CO} + 2\times n_{CO_2} + n_{H_2O} + 0.377\times n_{C_{Tar}} - n_{O_{in}} = 0 \quad \textbf{(5.58)}$$

Total mole balance:

$$n_{H_2} + n_{CO} + n_{CH_4} + n_{CO_2} + n_{C_2H_2} + n_{C_2H_4} + n_{C_2H_6} + n_{H_2O} + n_{Tar} - n_{total} = 0 \quad \textbf{(5.59)}$$

In the hypothesis of ideal gases, the 10 equilibrium equations, one for each chemical species, are of the form:

$$\frac{\Delta G_i}{RT} + \ln(y_i) + \sum_k \frac{\lambda_k}{RT} a_{ik} = 0 \quad \textbf{(5.60)}$$

Where

ΔG_i = free enthalpy of the compound i.
λ_k = Lagrange coefficient for the element k.
R = ideal gas constant.
T = temperature in Kelvin.
y_i = fraction of the compound i.
a_{ik} = number of element k in compound i.

The 10 equilibrium equations from equation 5.60, one for each chemical species are:

H_2: $$\frac{\Delta G_{H_2}}{RT} + \ln\left(y_{H_2}\right) + 2\frac{\lambda_H}{RT} = 0 \quad \textbf{(5.61)}$$

CO: $$\frac{\Delta G_{CO}}{RT} + \ln\left(y_{CO}\right) + \frac{\lambda_C}{RT} + \frac{\lambda_O}{RT} = 0 \quad \textbf{(5.62)}$$

CO_2: $$\frac{\Delta G_{CO_2}}{RT} + \ln\left(y_{CO_2}\right) + \frac{\lambda_C}{RT} + 2\frac{\lambda_O}{RT} = 0 \quad \textbf{(5.63)}$$

CH_4: $$\frac{\Delta G_{CH_4}}{RT} + \ln\left(y_{CH_4}\right) + \frac{\lambda_C}{RT} + 4\frac{\lambda_H}{RT} = 0 \quad \textbf{(5.64)}$$

C_2H_2: $$\frac{\Delta G_{C_2H_2}}{RT} + \ln\left(y_{C_2H_2}\right) + 2\frac{\lambda_C}{RT} + 2\frac{\lambda_H}{RT} = 0 \quad \textbf{(5.65)}$$

C_2H_4: $$\frac{\Delta G_{C_2H_4}}{RT} + \ln\left(y_{C_2H_4}\right) + 2\frac{\lambda_C}{RT} + 4\frac{\lambda_H}{RT} = 0 \quad \textbf{(5.66)}$$

C_2H_6: $$\frac{\Delta G_{C_2H_6}}{RT} + \ln\left(y_{C_2H_6}\right) + 2\frac{\lambda_C}{RT} + 6\frac{\lambda_H}{RT} = 0 \quad \textbf{(5.67)}$$

H_2O: $$\frac{\Delta G_{H_2O}}{RT} + \ln\left(y_{H_2O}\right) + 2\frac{\lambda_H}{RT} + \frac{\lambda_O}{RT} = 0 \quad \textbf{(5.68)}$$

Defined by empirical data from the previous chapter, the tar equation becomes:

$$\frac{\Delta G_{Tar}}{RT} + \ln\left(y_{Tar}\right) + 7.553\frac{\lambda_C}{RT} + 8.623\frac{\lambda_H}{RT} + 0.368\frac{\lambda_O}{RT} = 0 \quad \textbf{(5.69)}$$

In addition to the gas phase system, the unreacted carbon is taken into account in the model:

$$\frac{\Delta G_{C_S}}{RT} + \ln\left(y_{C_S}\right) + \frac{\lambda_C}{RT} = 0 \quad \textbf{(5.70)}$$

The resolution of this nonlinear system of equation is done with one of the following vi$_s$ depending on the type of compounds searched:

 Equil Yield.vi solves for: H_2, CO, CH_4, CO_2, H_2O

 Equil Yield All.vi solves for: H_2, CO, CH_4, CO_2, C_2H_2, C_2H_4, C_2H_4, H_2O

 Equil Yield tar.vi solves for: H_2, CO, CH_4, CO_2, H_2O, tar

 Equil Yield All n tar.vi solves for: H_2, CO, CH_4, CO_2, C_2H_2, C_2H_4, C_2H_4, H_2O, tar

Each of the vi$_s$ also calculate the mole flow rates of the compounds from the solution yield of the solver considering the inert gas (N_2) not included in the solver and readjusting for the total number of moles with N_2 after solver calculations.

5.6.2 Cp Equil mix.vi and Equil Enthalpies mix.vi: gas mix heat capacity and enthalpies calculation

 The calculation of ΔG_{mix} for the gas mixture at equilibrium is done through two vi$_s$:

Cp Equil mix.vi

- $Cp_{mix} = \sum_{products}(Cp_i y_i)$ J/mol/K **(5.71)**

- $Cp_{mix} = \sum_{products}\left(\frac{1000 Cp_i y_i}{M_i}\right)$ J/kg/K **(5.72)**

 Equil Enthalpies mix.vi

- $\Delta G_{mix} = \sum_{products}(\Delta G_i y_i)$ **(5.73)**

- $HHV_{mix} = \sum_{products}(M_i HHV_i y_i)$ **(5.74)**

- $\Delta H^{o}_{f\ mix} = \sum_{products}\left(y_i \Delta H^{o}_{f\ i}\right)$ **(5.75)**

- $\Delta H^{T}_{f\ mix} = \sum_{products}\left[y_i \left(\Delta H^{o}_{f\ i} + R\int_{T^o}^{T}\left(\frac{Cp_i}{R}\right)dT \right)\right]$ **(5.76)**

- $\Delta H^{o}_{r} = \Delta H^{o}_{f\ mix} - \Delta H^{o}_{f\ (Biomass-Char)}$ **(5.77)**

6 MODELING RESULTS

This chapter highlights the gas compositions predicted from the modeling program described previously. The compositions results are given at the chosen temperature of the model. The compositions from the fluidized bed gasifier are the results of GC-TCD analyses at ambient temperature. The gas starts cooling when exiting the gasifier. During cool down, equilibrium does change the composition of the gas. This decrease in temperature modifies the equilibrium consuming H_2 and producing water. As water condenses, the equilibrium is shifted further in the same direction consuming most of the H_2.

In equilibrium models, cooling the gas down to 298K results in H_2 being totally consumed. The pressure of saturation of water in the gas must be taken into consideration, explaining why data show low levels of H_2.

6.1 TAR AND CHAR CHARACTERIZATION

In most models, (Sadaka et al., 2002) tars are not defined as such, but assumed to be part of the CH_4 for mass balance reasons. This assumption is valid since the amount of tar is small in comparison to the other compounds.

The model developed in this research focuses on tar despite the small amounts being generated by the fluidized bed gasifier.

Tar is generated in the primary char during the pyrolysis. In this model a small variation in the definition of char greatly influences tar production.

The tar and chars are not element-defined in any database. Ultimate analysis of char for switchgrass, bermudagrass and corn gluten show similar results in the ER range for air gasification. For this model, that this composition will be the same for flaming pyrolytic gasification, pyrolysis and steam gasification. Table 6.1 shows ultimate and proximate analysis results of char sampled at various ER after soxhlet extraction.

	Atomic composition	H_f^0, kJ/mol
Switchgrass	$C_1H_{0.16}O_{0.03}N_{0.02}$	-16.46
Bermudagrass	$C_1H_{0.17}O_{0.04}N_{0.03}$	-24.44
Corn gluten	$C_1H_{0.17}O_{0.03}N_{0.06}$	-25.39

Table 6.1: Char average atomic composition and enthalpy of formation

In most models, because char is mostly carbon, it is assumed to be pure carbon element with an enthalpy and free energy of zero. However, ultimate analysis of the char shows the presence of other compounds, thus char is not a pure element with an enthalpy of formation (ΔH_f^0). Even so, with no empirical data on char from switchgrass, bermudagrass and corn gluten, the standard free enthalpy of char is assumed to be 0. The Cp(T) for char is assumed to be that of graphite.

For equilibrium modeling, it is necessary to have Cp(T) function, ΔH_f^0 and ΔG^0 for each compound present in the system. In this case both pure carbon and char are considered.

An extensive review of literature resulted in no data on tar. Therefore, the attempt is made in the model to define tar from the empirical data collected in previous experiments.

It was concluded from previous experiments that tar atomic composition was almost constant and could be averaged to:

$$C_{7.553}H_{8.623}O_{0.368}N_{0.204}$$

In these experiments, tar was analyzed for 210 compounds, with 10 of them constituting approximately 75% of the total tar mass. It is then possible to hypothesize that tar free enthalpy closely follows the weighted average of these 10 compounds. Equation (5.4) gives:

$$\Delta G_{Tar}(T) = 31.978 + 0.24635 \times T + 2.073 \times 10^{-5} \times T^2$$

For the two following cases (Figures 6.1 and 6.2), the model was run in air and flame pyrolytic gasification at a constant incoming air flow, of 17m^3/h and varying the biomass flow rate from 10 to 1000 kg/h.

Figures 6.1 and 6.2 are tables of graphs resulting from the Labview model, showing the fractions for the three biomass types (switchgrass row 1, bermudagrass row 2 and corn gluten row 3) being studied for the two different hypotheses considered, i.e. C_{Solid} and char, at a temperature of 1023K (750°C). In both tables of graphs, the first column of graphs shows the fractions of gases, Tar Moisture Ash Free (TMAF). The second and third columns of graphs show the fractions of gases, tar, water and solids at high, and low fraction scale.

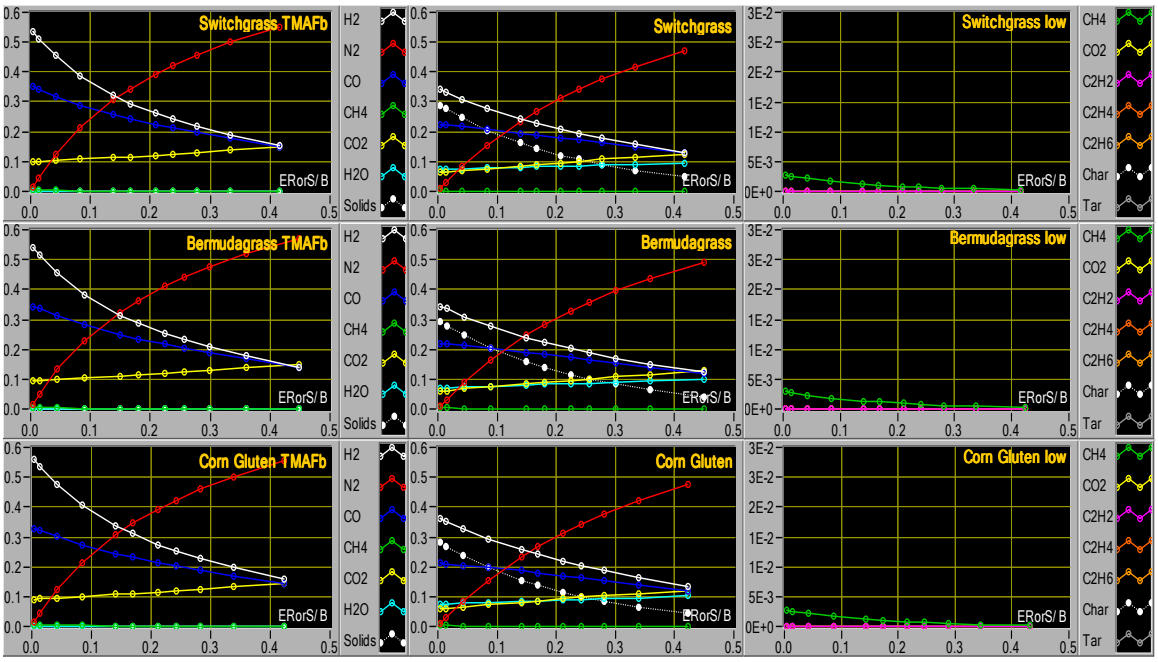

Figure 6.1 Gas and Cs fractions from Gibbs equilibrium of air gasification of switchgrass row #1, bermudagrass row #2 and corn gluten row #3 at 1023 K in raw gas column #2-3 and tar moisture ash free gas columns #1

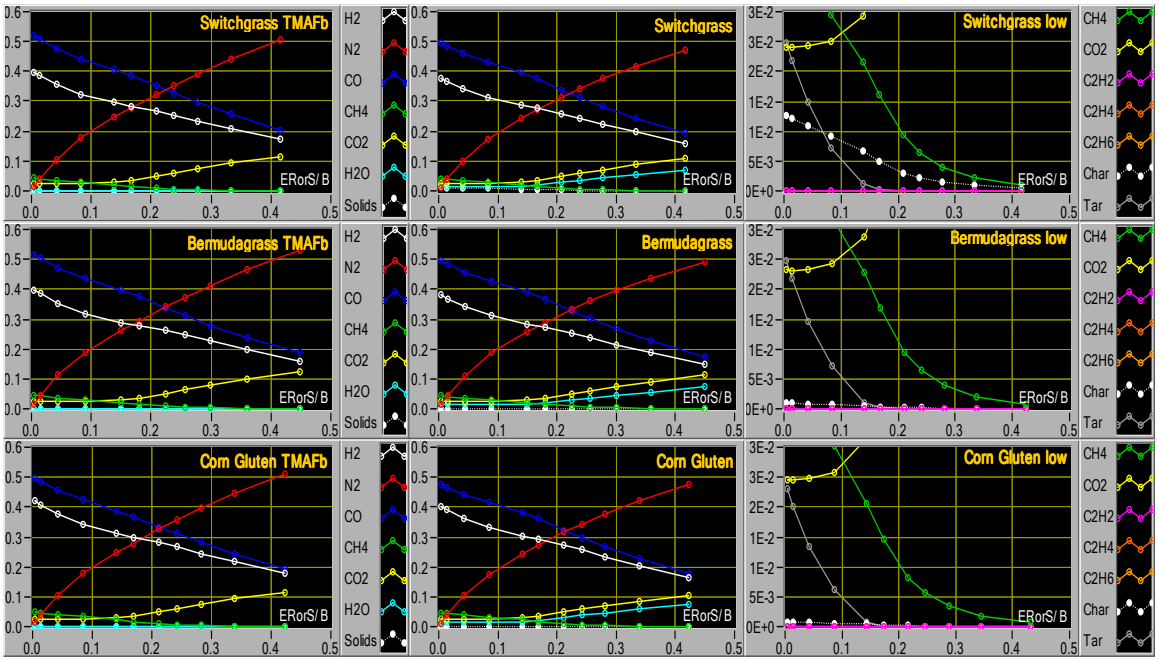

Figure 6.2 Gas and char fractions from Gibbs equilibrium of air gasification of switchgrass row #1, bermudagrass row #2 and corn gluten row #3 at 1023 K in raw gas column #2-3 and tar moisture ash free gas columns #1

Graphs (Figure 6.1 in the case of the pure carbon hypotheses) show that there is little variation in gas, tar and solids compositions between the different biomass types. Switchgrass and bermudagrass show a slightly higher fraction of CO (0.01) than corn gluten. However, corn gluten shows a slightly higher level of H_2 (0.02) with a little more water (0.01) and less CO_2 (0.01) than switchgrass and bermudagrass. For all three biomass types, CH_4 , C_2 gases and tar levels are low or do not exist at this temperature.

The differences between experimental and modeled fraction are not only due to the change in equilibrium of the various gas species considered during gas cool down, but also of other type of parameters than the thermodynamic equilibrium as the consideration of particulate matter (PM) as non-elemental carbon compound.

Graphs (Figure 6.2 in the case of the char hypotheses) show that there is little variation in gas, tar and solids compositions between the different biomass types. However, there is a large difference between these char hypotheses results and the pure carbon hypotheses results (Figure 6.1). The gas fractions of CO and H_2 are reversed and are larger in comparison to the pure carbon hypotheses results, particularly for CO. H_2 and CO are higher by a factor of 1.1, and 1.5 to 2.25 respectively, as ER varies from 0.4 to 0.

Although there are little difference between biomass types, the variations in char fraction in the stream are quite important particularly for switchgrass. This is the result of the analysis of the PM product from air gasification of switchgrass that has a HHV slightly higher than the PM resulting from bermudagrass and corn gluten air gasification. Hence, the resulting enthalpy of formation is lower for switchgrass PM than bermudagrass PM and corn gluten PM. Considering the same Cp(T) function for all three

biomass types, this HHV measurement directly influences the free energy value of the char in the model.

Because it was not possible to measure the composition of the char for each gasifier run, the hypothesis was made that PM would always have the same proportion of CHO as for air gasification.

In the char hypothesis, case methane and C_2 gases have fractions similar than in the pure carbon hypothesis case. For all three biomasses, C_2 gas levels are low or do not exist. However, tar appears at an ER of 0.17 and increases to a maximum fraction of 0.25 at ER = 0. Tar varies with an exponential trend as in the experimental data.

In the series of 12 3-dimensional Figures 6.3 to 6.14, temperature is changed from 773K (500°C) to 1123K (850°C) both for air and flaming pyrolytic gasification and for steam gasification for all three biomass types. In the case of air and flaming pyrolytic gasification, ER is changed from 0.4 to 0 and in the case of steam gasification, S/B is changed from 1.25 to 0.4. (Note: vertical fraction axis is set at a maximum of 0.6 except in the case of tar and C_2 gases that are set at 0.1)

In all PM hypothesis cases, it is interesting to see on Figures 6.3 to 6.14, the same behavior of the tar and solids model regardless of the process type.

As expected, CO and H_2 obtain maximum values at low ER and high temperature regardless of the C_{solid} or char hypothesis, as does the enthalpy of the reaction. Though it is interesting to note that in the char hypothesis case, the enthalpy of reaction maximums are shifted slightly from the ER=0 (S/B=0) and maximum temperature top left corner of the graph to a position with still the maximum possible temperature but at an ER of approximately 0.12 or S/B of approximately 0.22.

A better definition of the tar in the model with a variation of its composition taken into account when ER or S/B varies would probably change the coordinate of these maximums shifting slightly along the ER or S/B axis. These maximums are displayed in Table 6.2:

	Air gasification and flaming pyroysis gasification C_{Solid} hypothesis (MJ/mol)	Air gasification and flaming pyroysis gasification Char hypothesis (MJ/mol)	Steam gasification C_{Solid} hypothesis (MJ/mol)	Steam gasification char hypothesis (MJ/mol)
Switchgrass	54	57	53	50
Bermudagrass	49	52	48	44
Corn gluten	43	46	42	40

Table 6.2 Maximum values of ΔH_R at 298K for C_{solid} and char hypothesis

Switching between the two hypotheses, i.e. from C_{solid} to char, affect only slightly the value of the enthalpy of reaction maximum, increasing it by 3 MJ/mol in the case of air and flaming pyrolitic gasification, while decreasing by up to 4 MJ/mol in the steam gasification case.

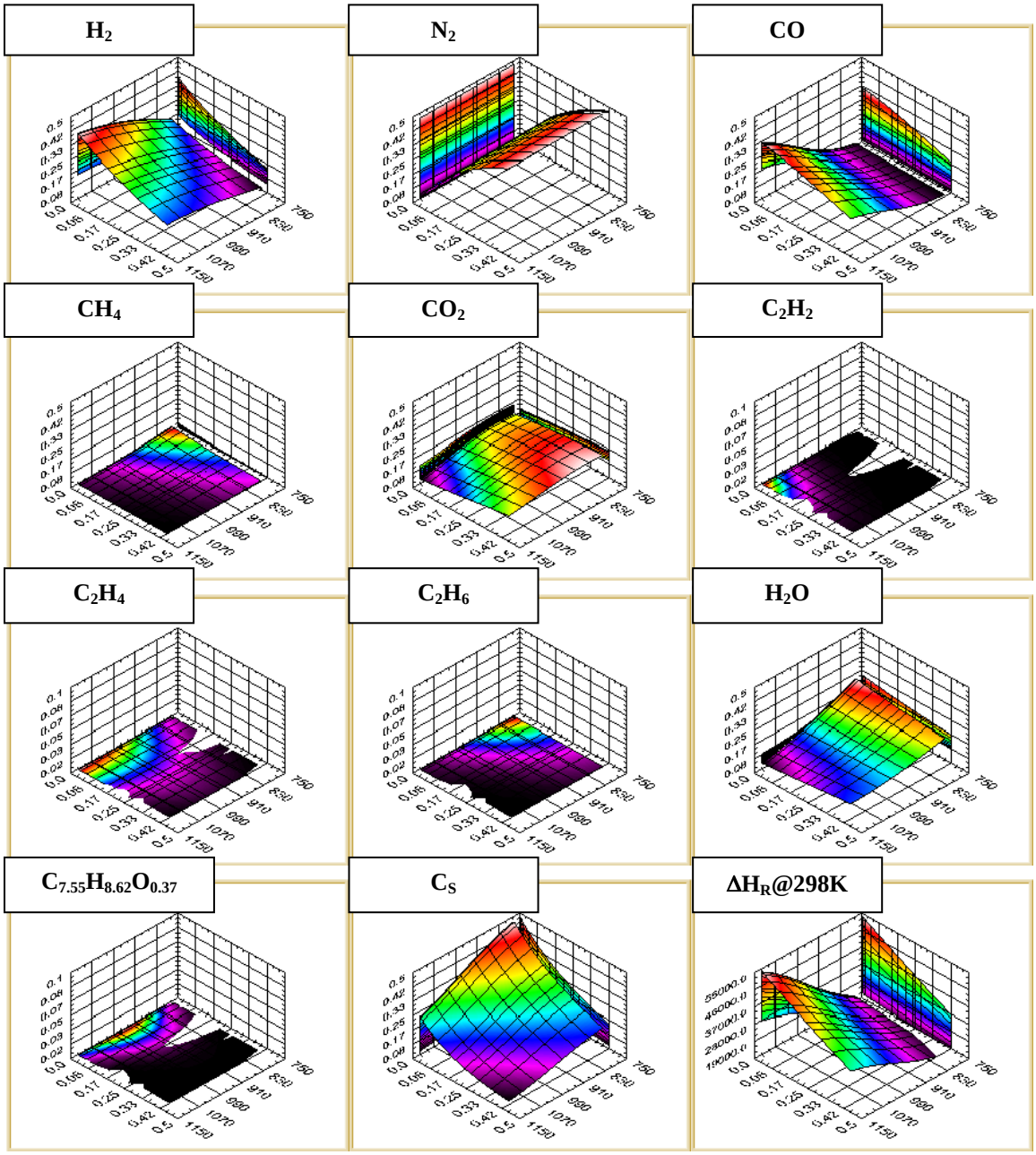

Figure 6.3 Gas, tar and solids fractions and enthalpy of reaction, in air gasification of switchgrass in the Cs hypothesis

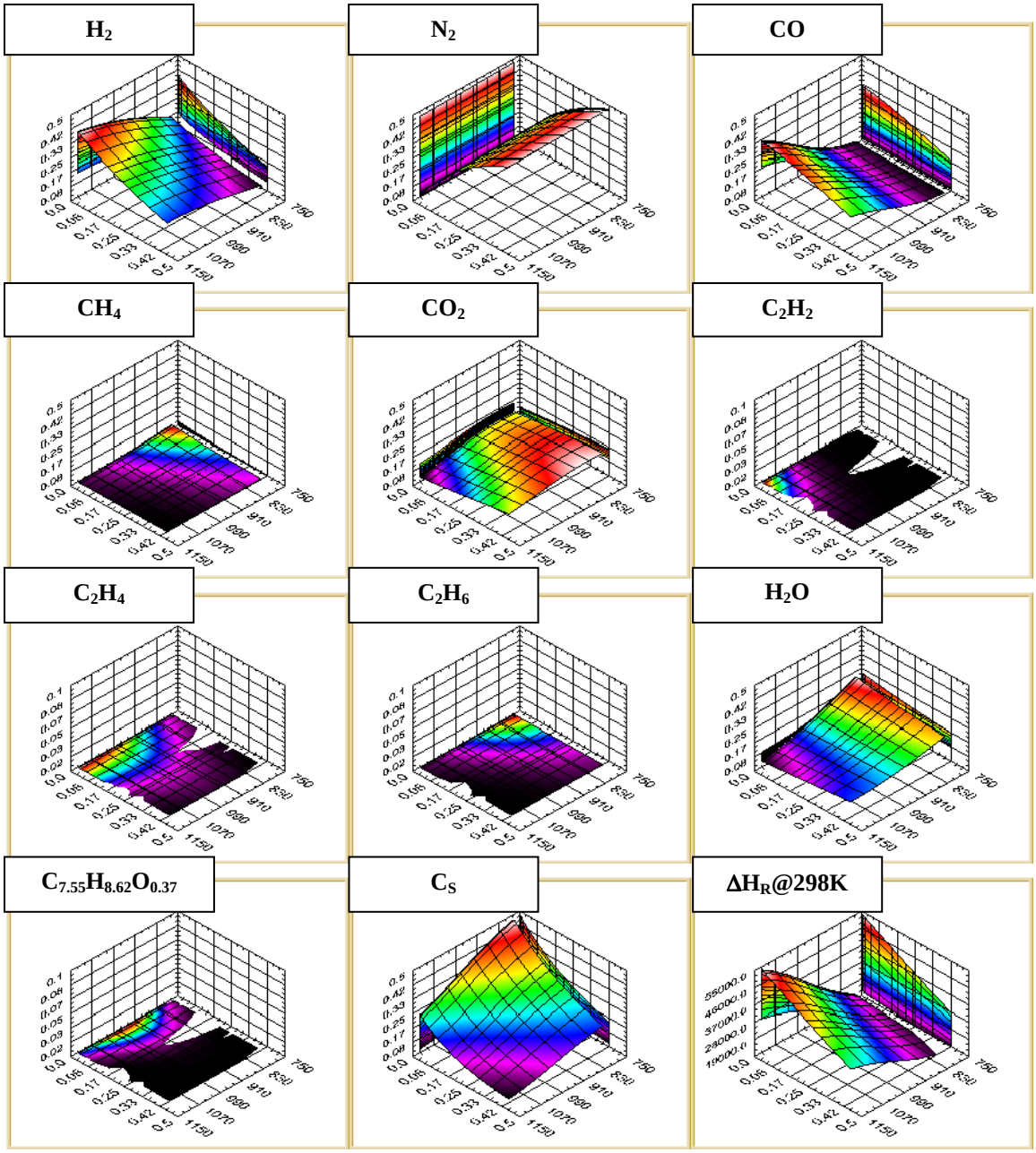

Figure 6.4 Gas, tar and solids fractions and enthalpy of reaction, in air gasification of bermudagrass in the Cs hypothesis

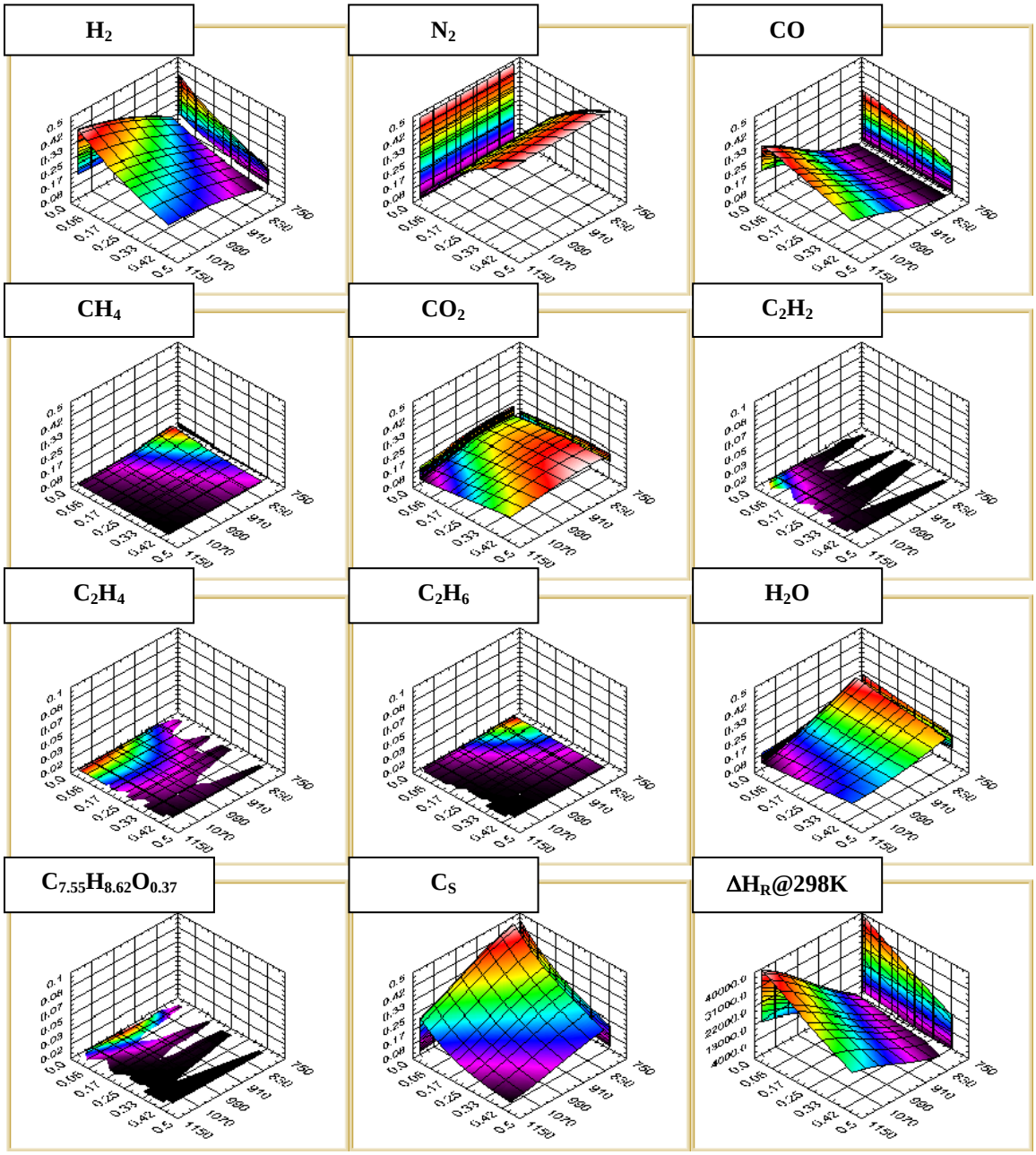

Figure 6.5 Gas, tar and solids fractions and enthalpy of reaction, in air gasification of corn gluten in the Cs hypothesis

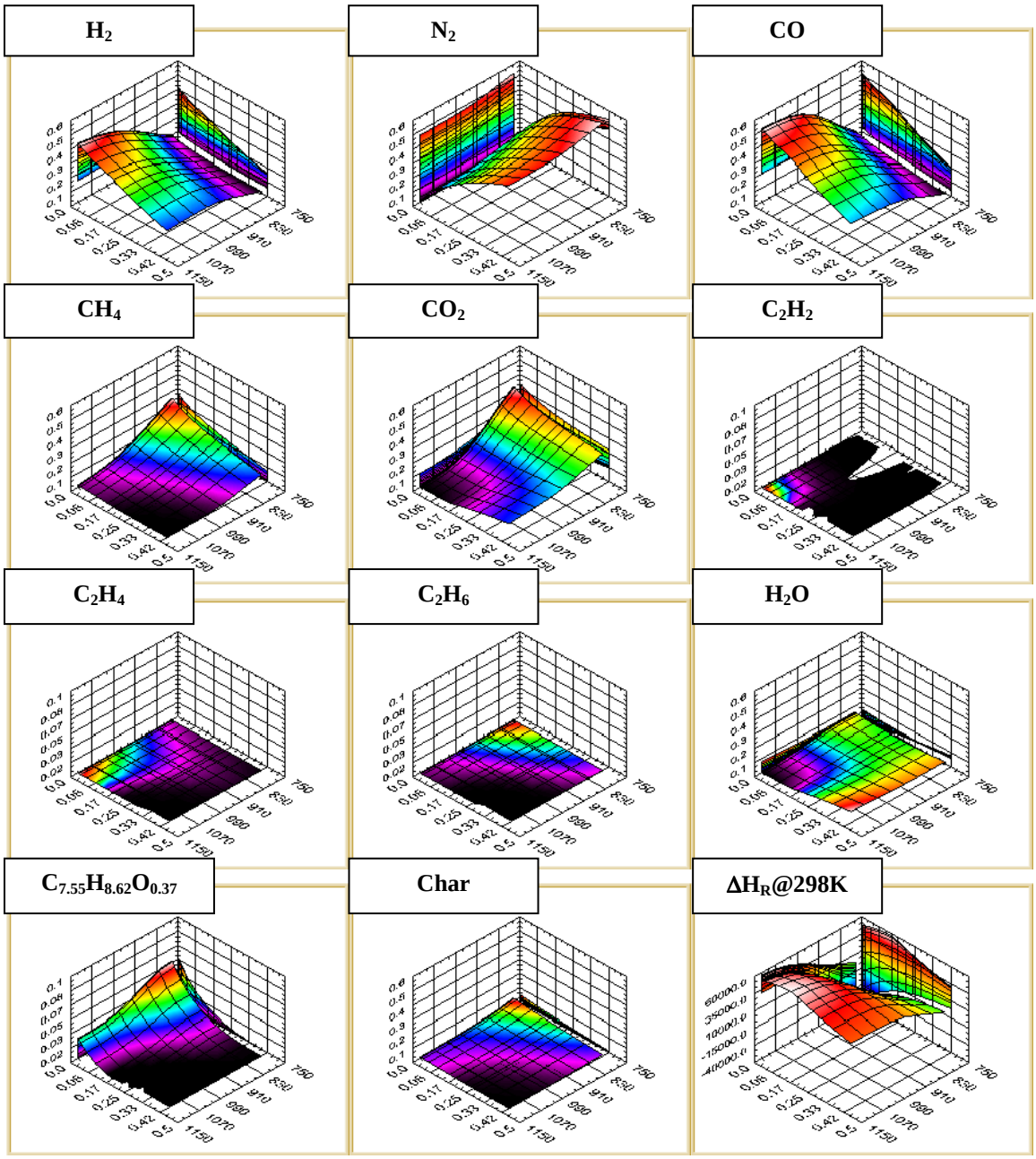

Figure 6.6 Gas, tar and solids fractions and enthalpy of reaction, in air gasification of switchgrass in the char hypothesis

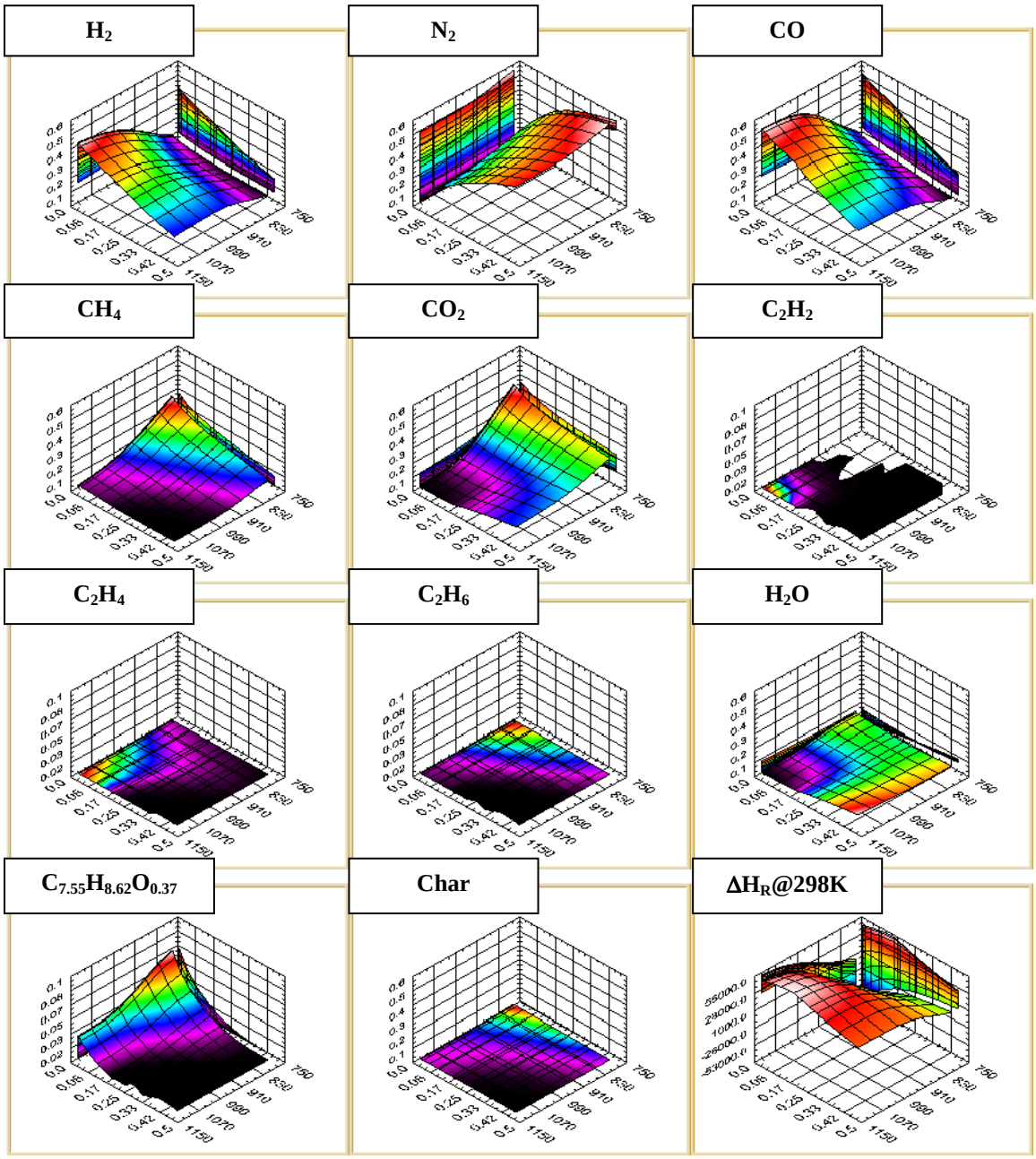

Figure 6.7 Gas, tar and solids fractions and enthalpy of reaction, in air gasification of bermudagrass in the char hypothesis

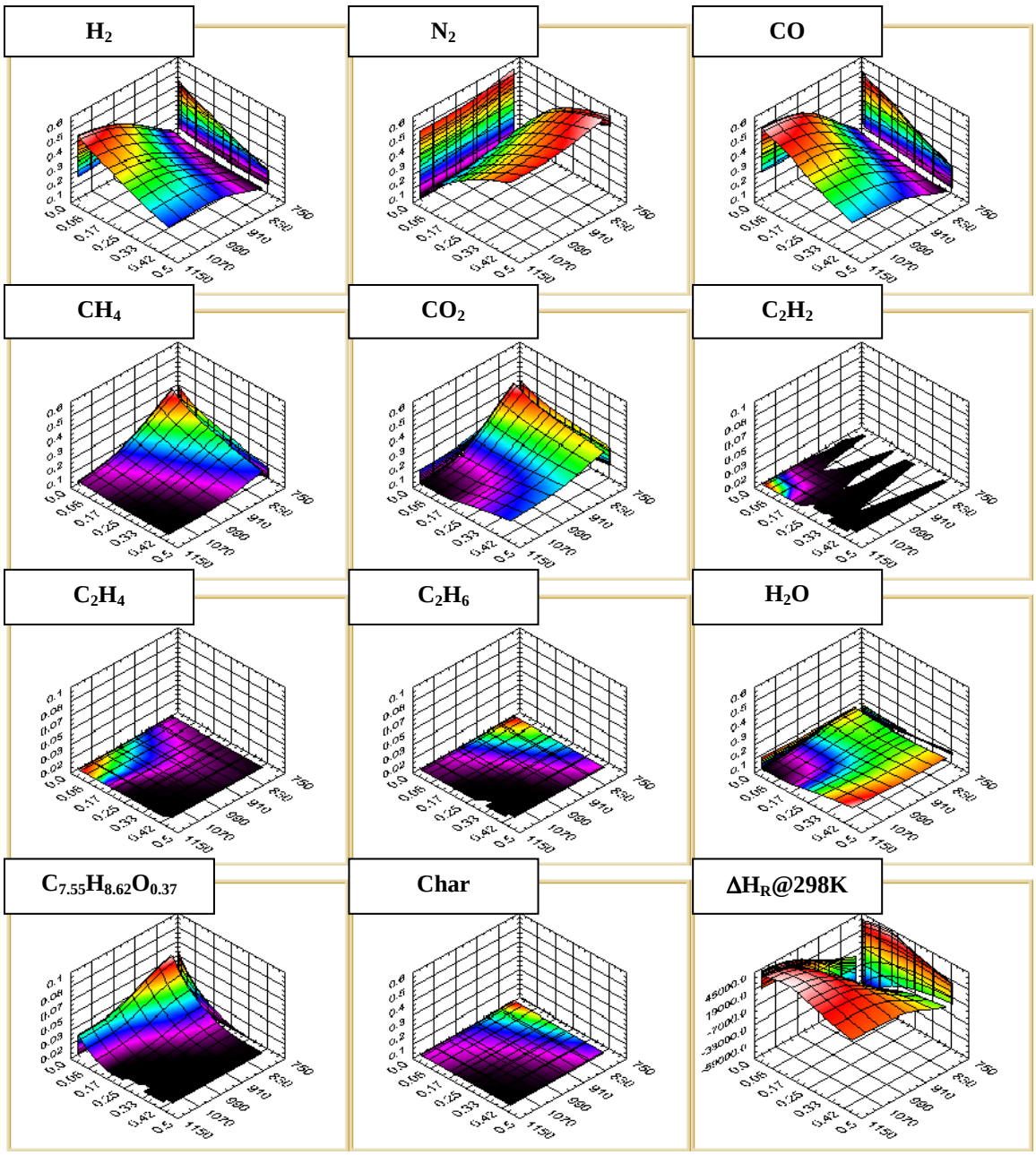

Figure 6.8 Gas, tar and solids fractions and enthalpy of reaction, in air gasification of corn gluten in the char hypothesis

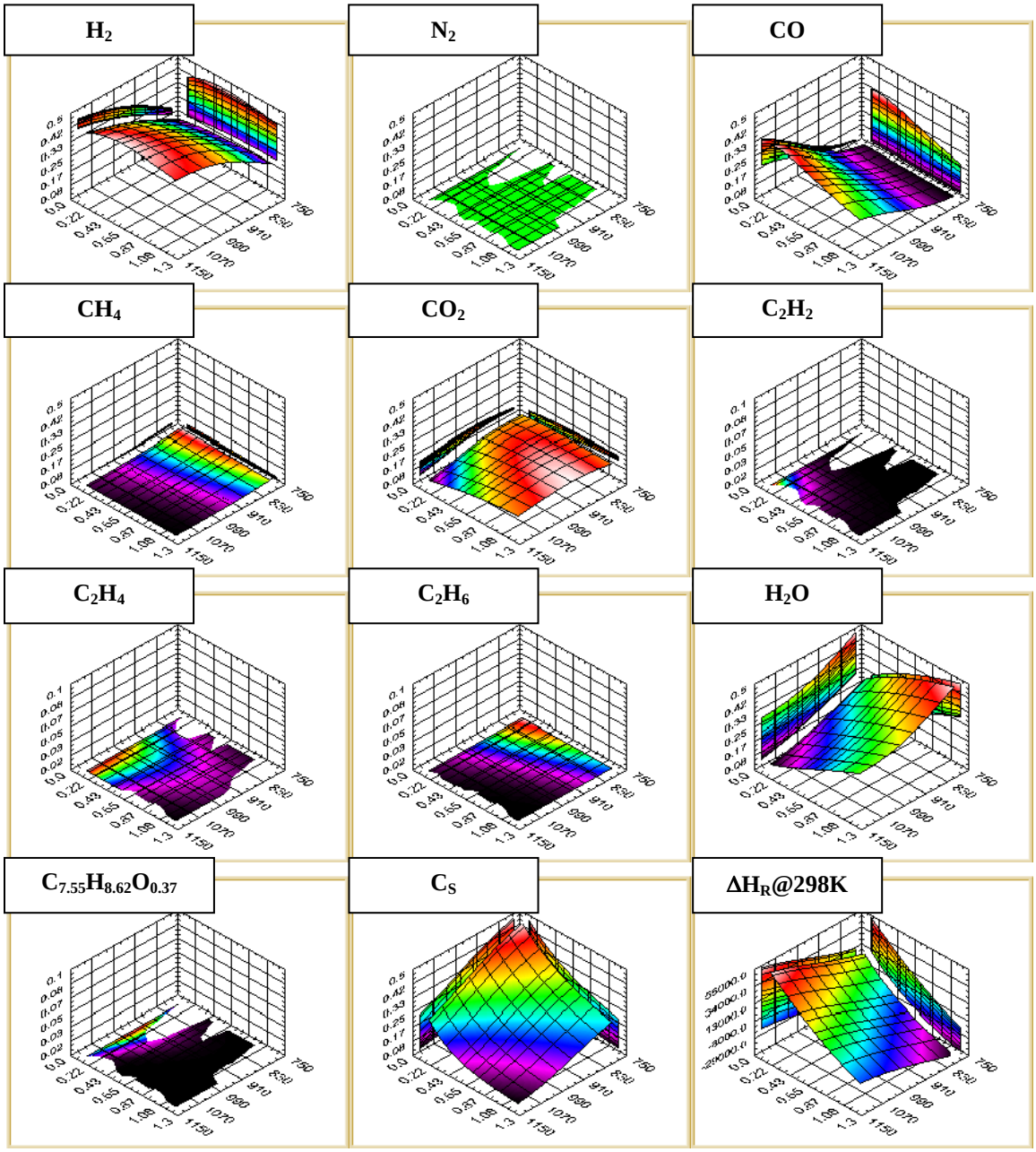

Figure 6.9 Gas, tar and solids fractions and enthalpy of reaction, in steam gasification of switchgrass in the Cs hypothesis

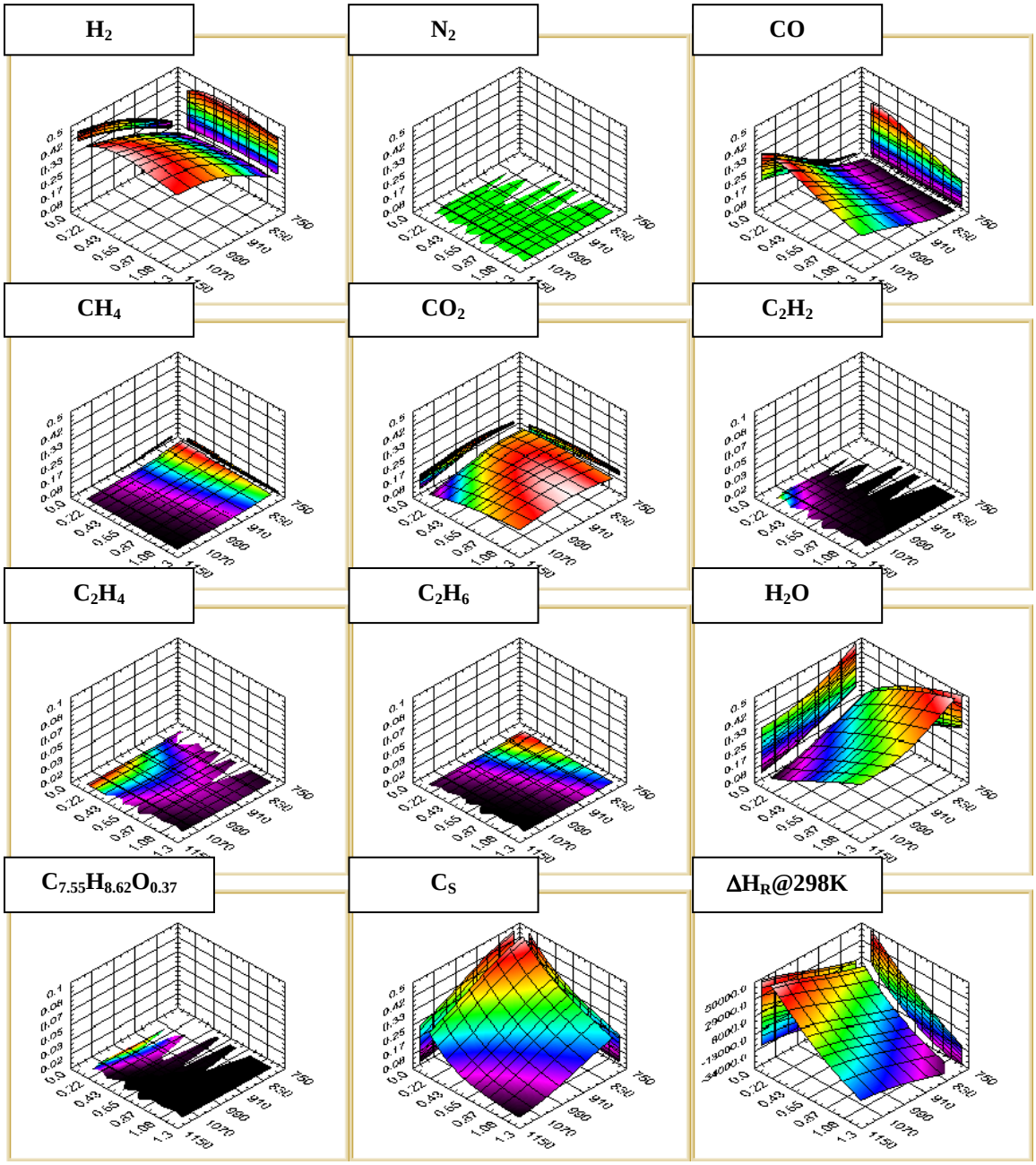

Figure 6.10 Gas, tar and solids fractions and enthalpy of reaction, in steam gasification of bermudagrass in the Cs hypothesis

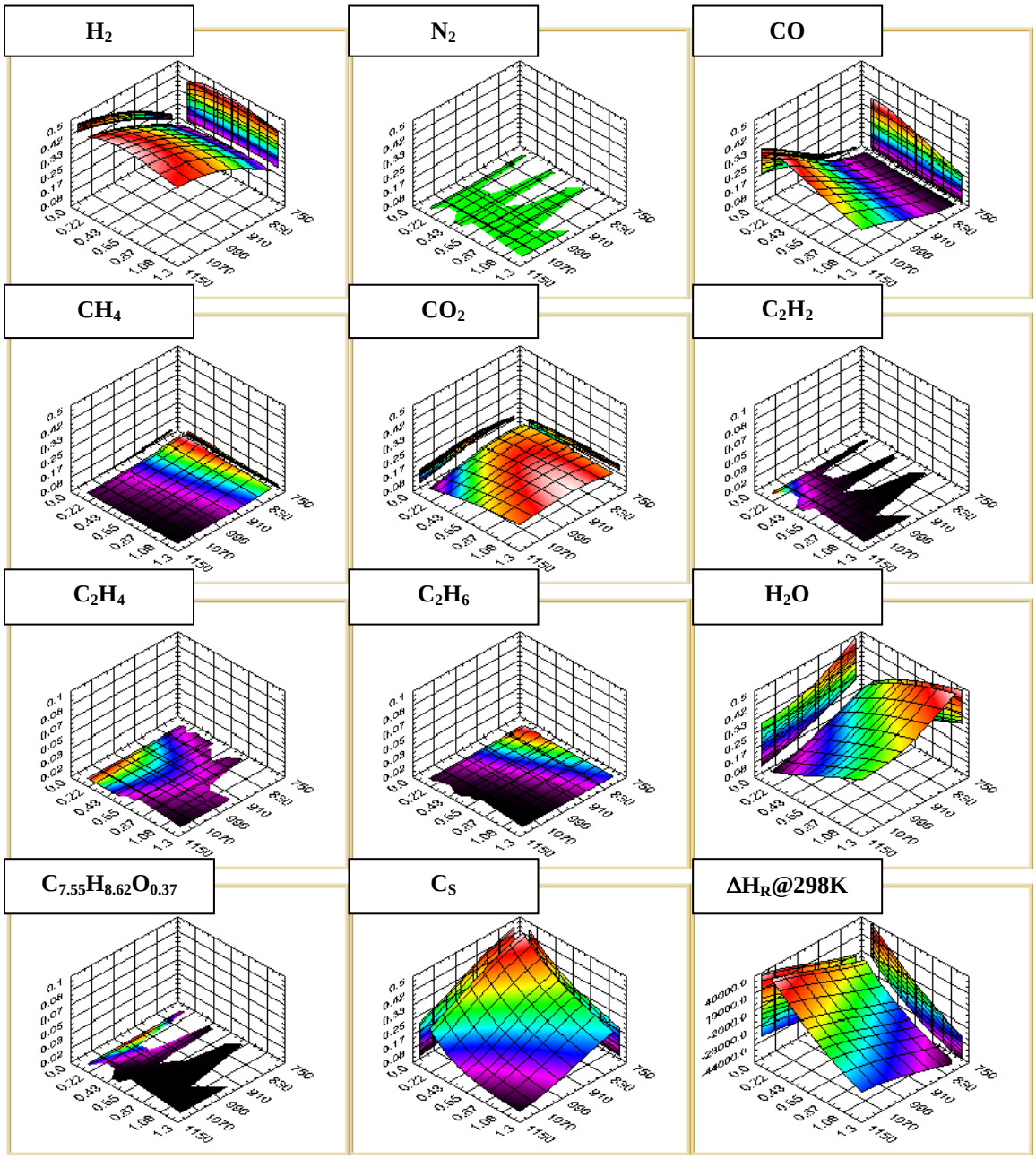

Figure 6.11 Gas, tar and solids fractions and enthalpy of reaction, in steam gasification of corn gluten in the Cs hypothesis

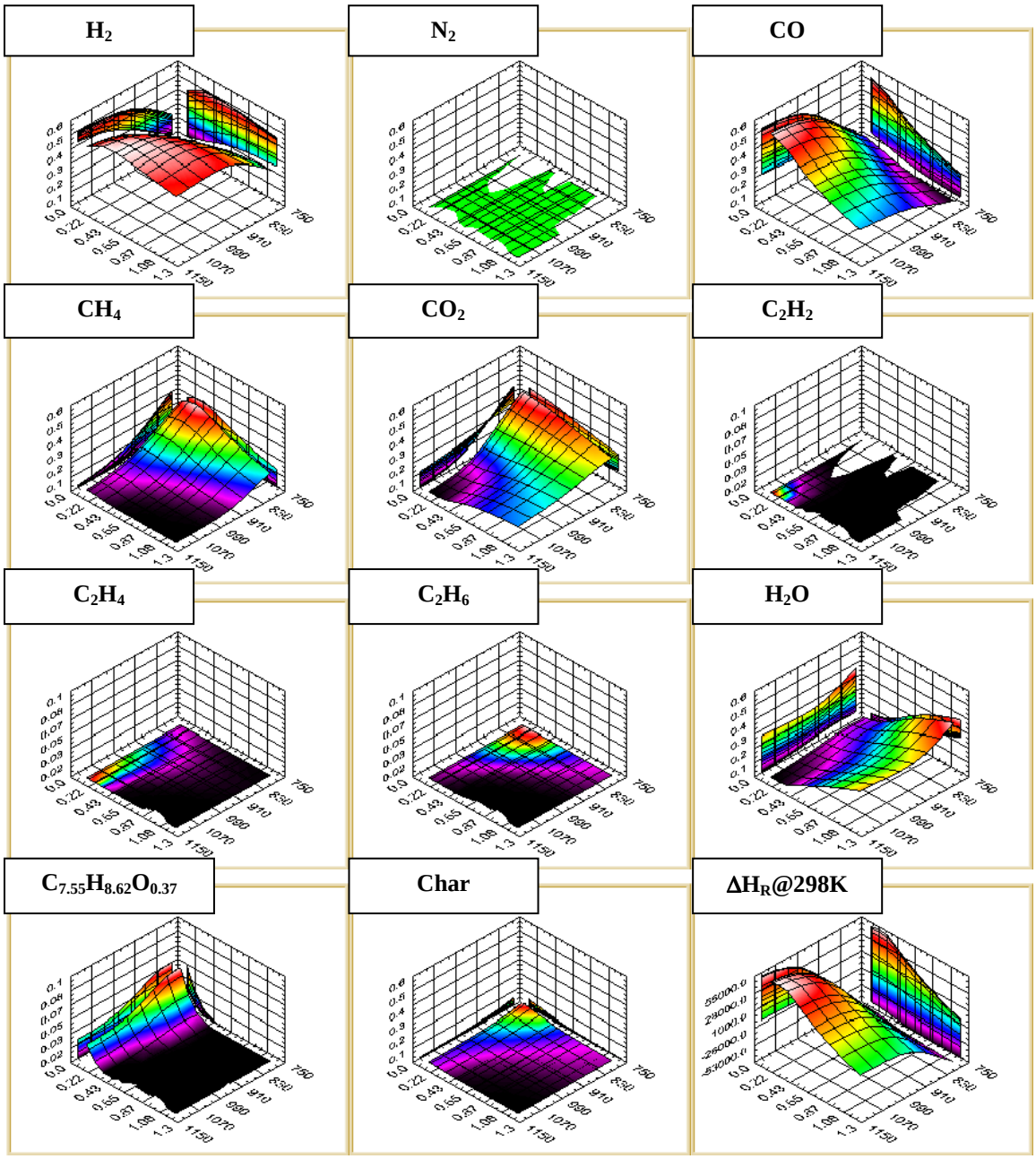

Figure 6.12 Gas, tar and solids fractions and enthalpy of reaction, in steam gasification of switchgrass in the char hypothesis

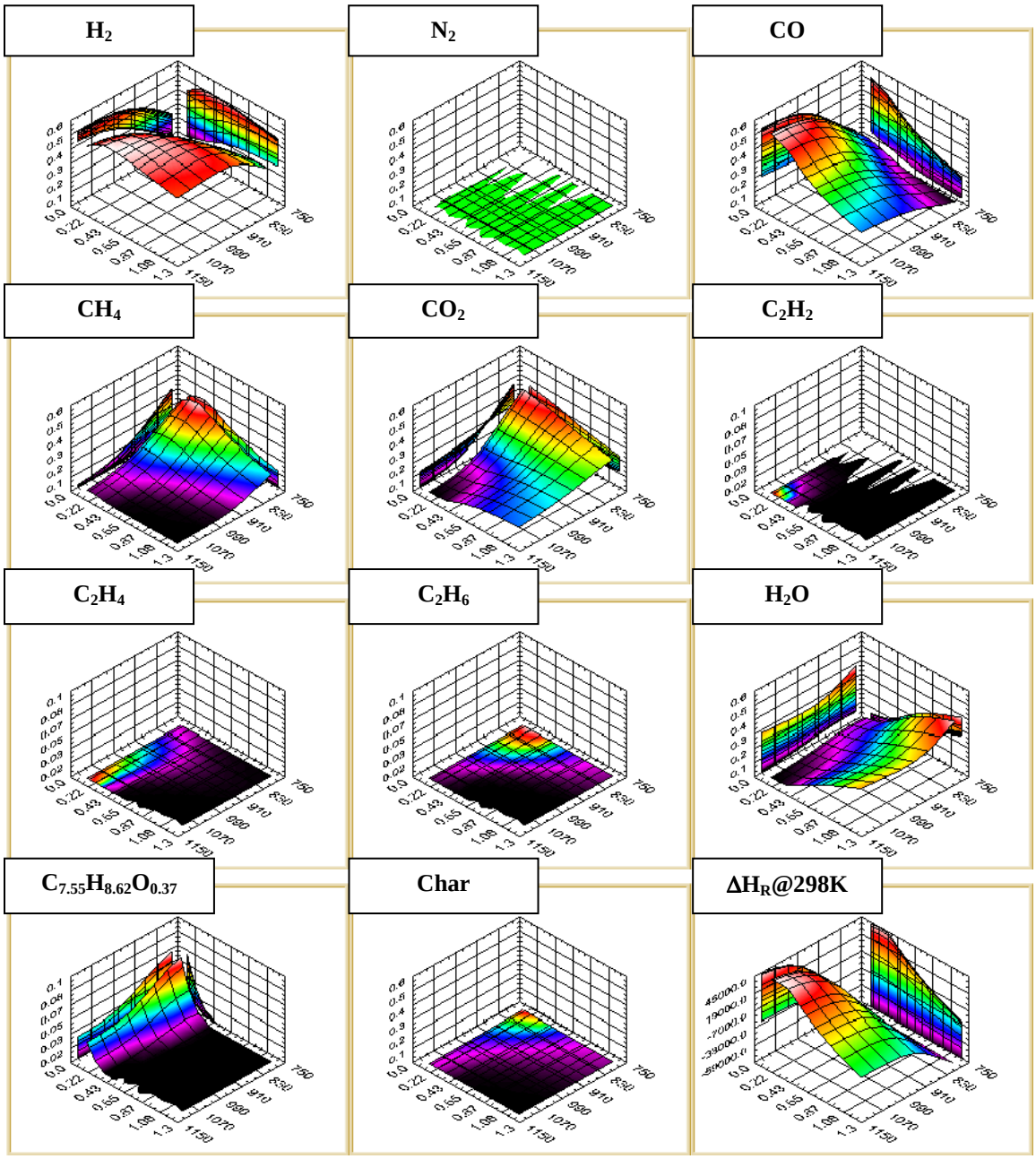

Figure 6.13 Gas, tar and solids fractions and enthalpy of reaction, in steam gasification of bermudagrass in the char hypothesis

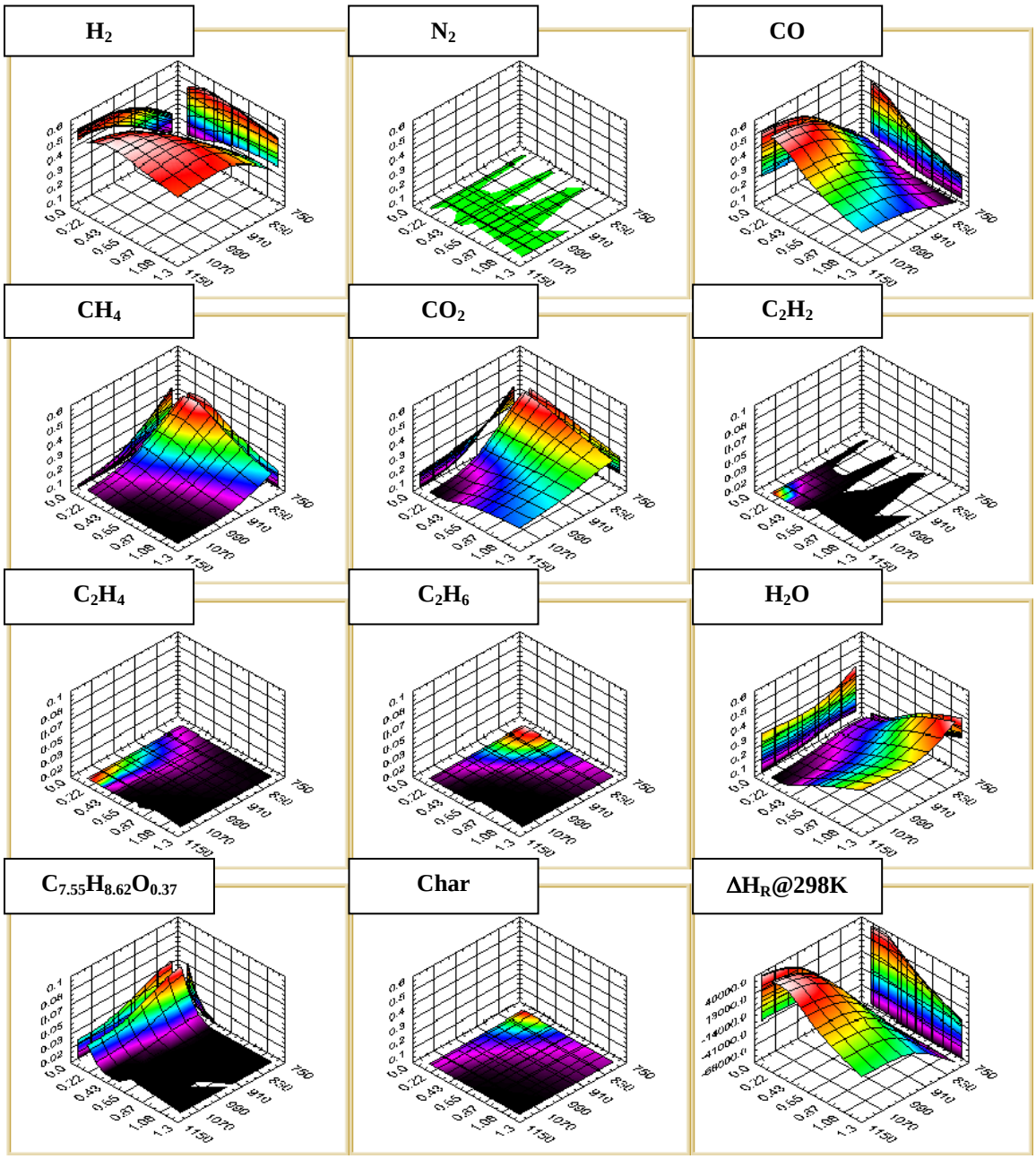

Figure 6.14 Gas, tar and solids fractions and enthalpy of reaction, in steam Gasification of corn gluten in the char hypothesis

In the next series of Figures 6.15 to 6.23, data of the experimental conditions: CHO feed rates, ER, S/B and temperatures, are loaded in the model and solved with the char hypothesis. The result is a series of 2D-graphs displaying fractions versus ER or S/B ratios where each data point is at the experimental bed temperature recorded during the fluidized bed gasifier run. From these graphs, a comparison with the real data would be possible if the non linear solver virtual instrument could have found solutions for low temperature (298K). Assistance was sought from National Instrument Research and Development responsible for Labview performance. This department recognized the problem with the nonlinear equation solver virtual instrument, but was not able to make the appropriate correction.

The model shows CO levels higher than H_2 for air gasification and flaming pyrolytic gasification similar to the experimental results at 298K measured by the GC-TCD. The model also calculates a maximum of CO between ER=0.2 and 0.25, and an increase in methane and tar with decreasing ER or S/B.

The model also confirms the experimental order of CO and H_2 for steam gasification with H_2 fractions above CO fractions and a higher methane level than air gasification.

For flaming pyrolytic gasification, the level of CO and H_2 at ER=0.2 are higher than air gasification for the same ER and continues to increase as ER decreases.

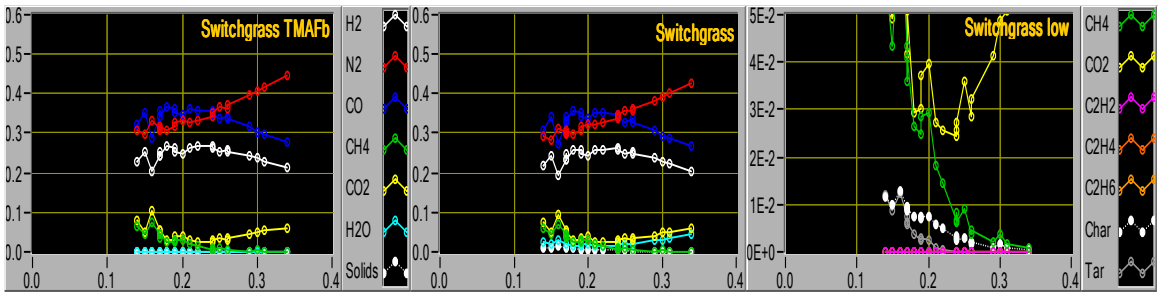

Figure 6.15 Data from air gasification of switchgrass modeled equilibrium

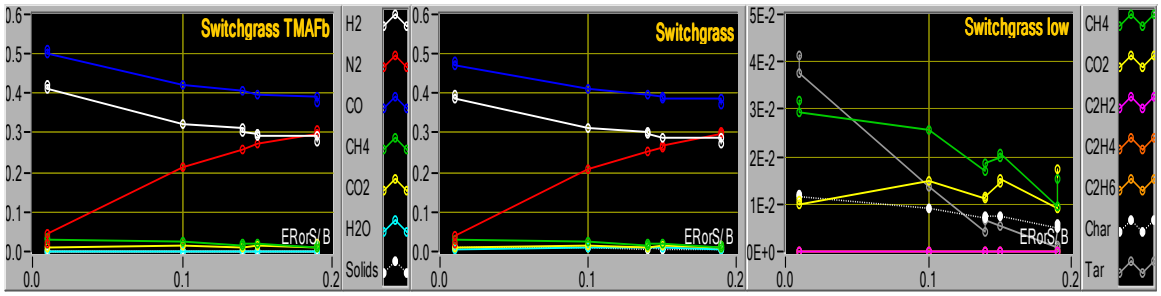

Figure 6.16 Data from flaming pyrolitic gasification of switchgrass modeled equilibrium

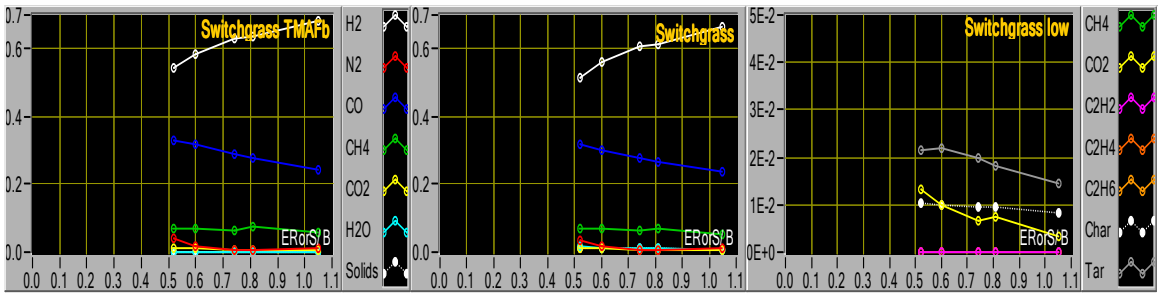

Figure 6.17 Data Steam Gasification of switchgrass modeled equilibrium

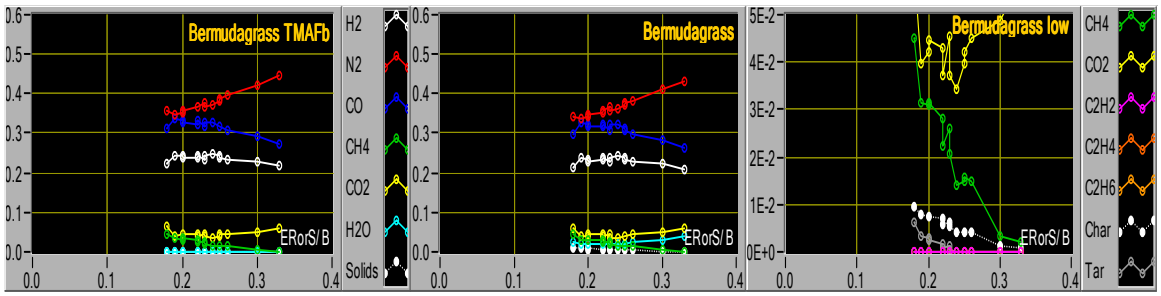

Figure 6.18 Data from air gasification of bermudagrass modeled equilibrium

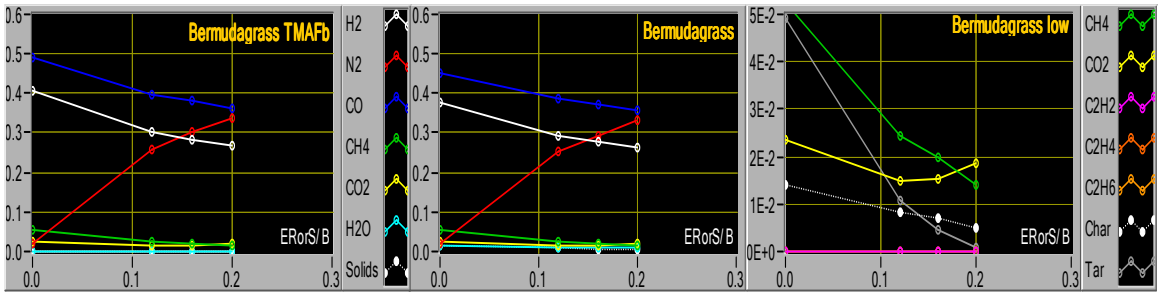

Figure 6.19 Data from flaming pyrolitic gasification of bermudagrass modeled equilibrium

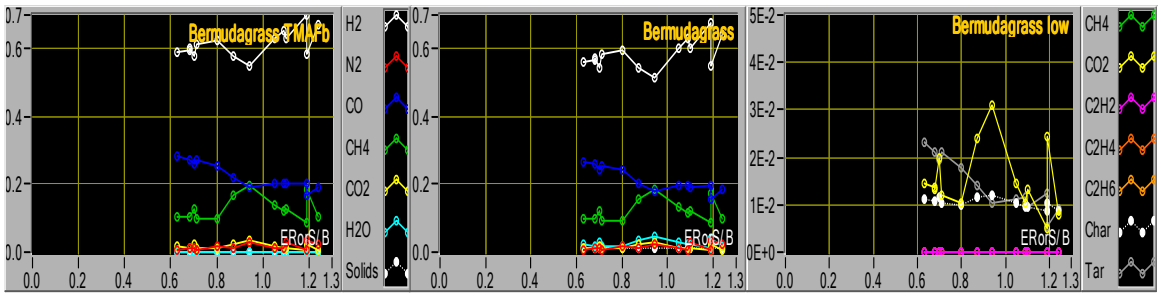

Figure 6.20 Data from steam gasification of bermudagrass modeled equilibrium

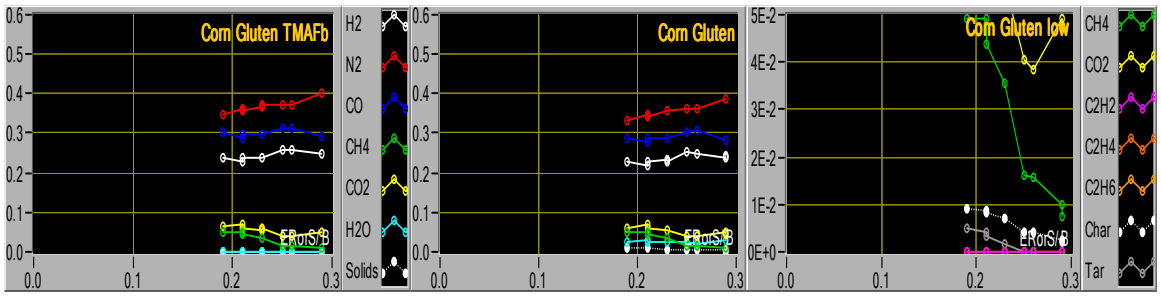

Figure 6.21 Data from air gasification of corn gluten modeled equilibrium

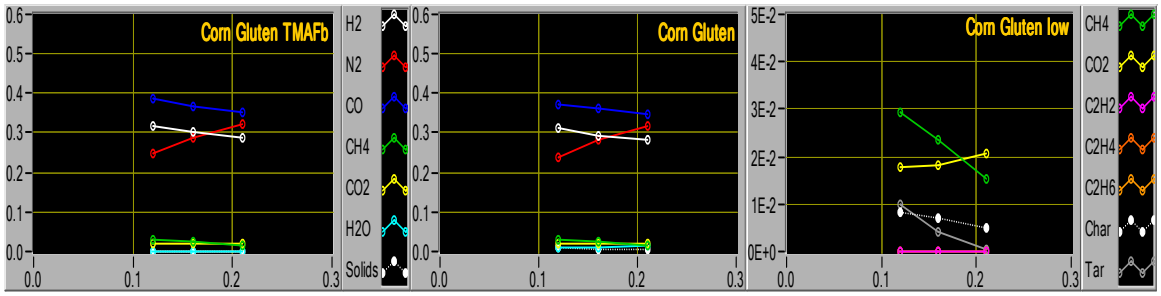

Figure 6.22 Data from flaming pyrolitic gasification of corn gluten modeled equilibrium

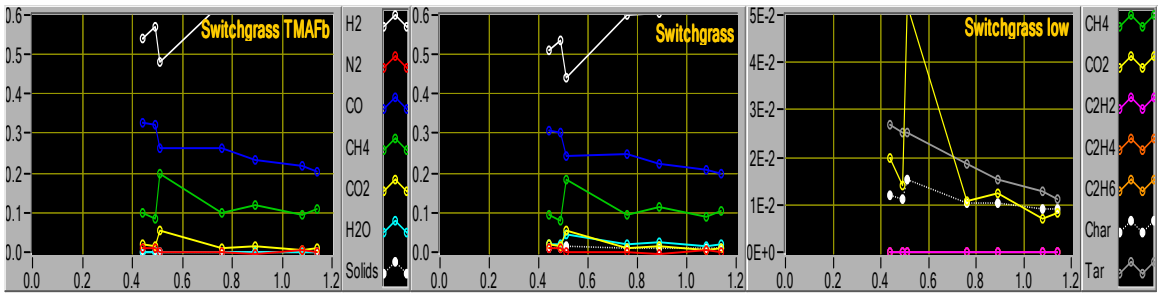

Figure 6.23 Data from steam gasification of corn gluten modeled equilibrium

6.2 EQUILIBRIUM CHANGE DURING GAS COOL DOWN

As previously discussed, gas cool down has a significant effect on the gas equilibrium. Figures 6.24 to 6.28 show the effect of such cool down for pyrolysis conditions of switchgrass in Figure 6.24 to close to combustion conditions in Figure 6.28, with HSC Gibbs reactor model (HSC5 2002).

In each figure, as temperature decreases CO and H_2 mol % decrease while CO_2 and H_2O increase. The presence of methane in gas samples indicates that the cool down equilibrium is not totally reached as methane is maximized around 350°C and almost absent at ambient temperature and at 800°C.

Gasification equilibrium results of HSC5 (HSC5 2002) Gibbs reactor modeling of 1 mol of $CH_{1.27}O_{0.03}$ (Switchgrass) from pyrolysis to near combustion.

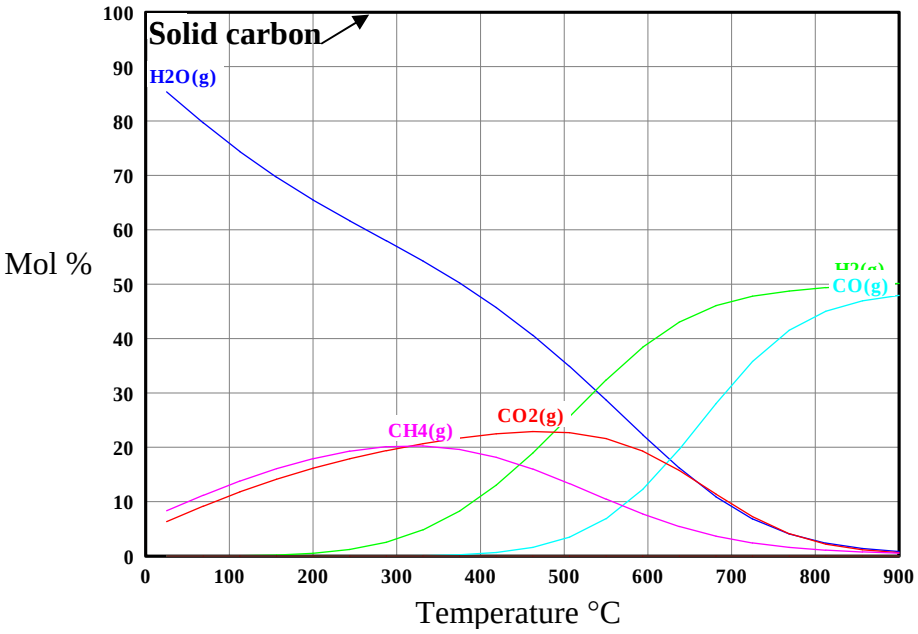

Figure 6.24 Gas cool down after pyrolysis, O_2 = 0 mol

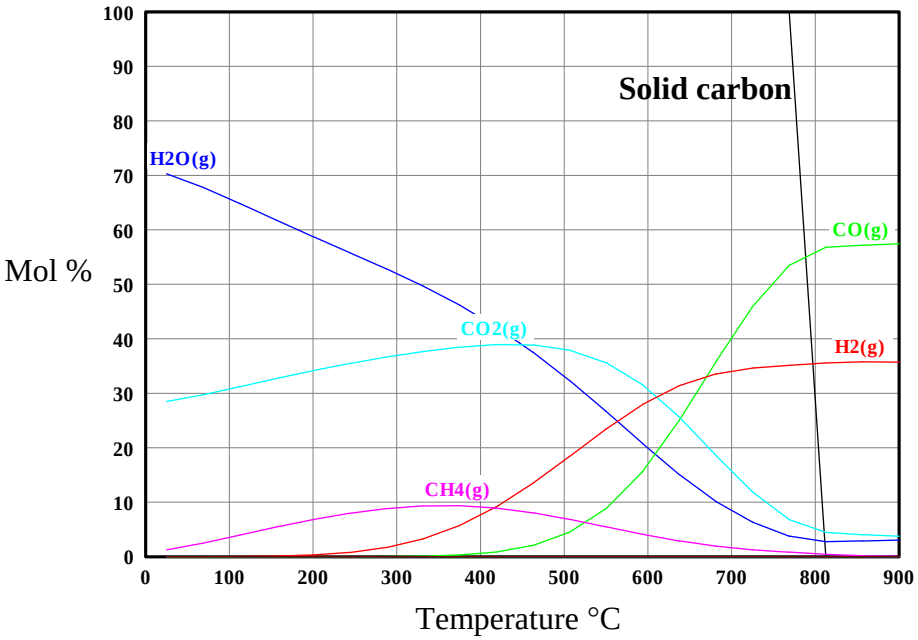

Figure 6.25 Gas cool down after gasification, O_2 = 0.25 mol

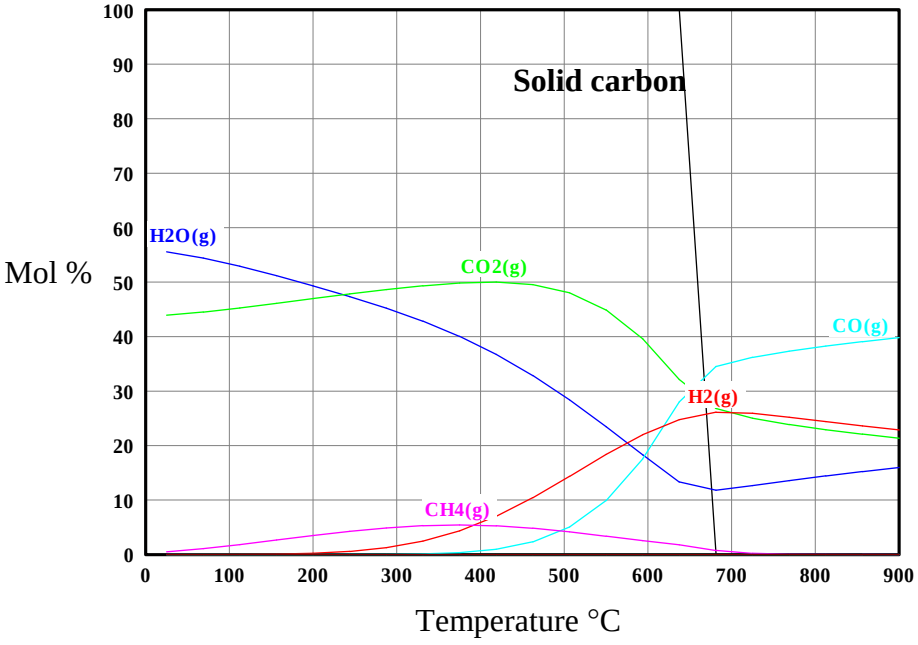

Figure 6.26 Gas cool down after gasification, O_2 = 0.5 mol

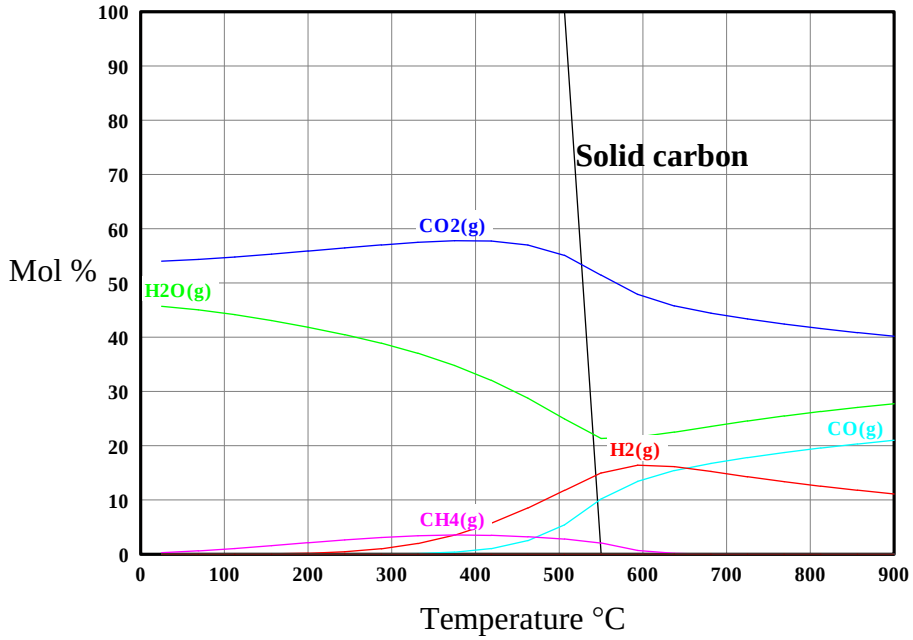

Figure 6.27 Gas cool down after gasification, O_2 = 0.75 mol

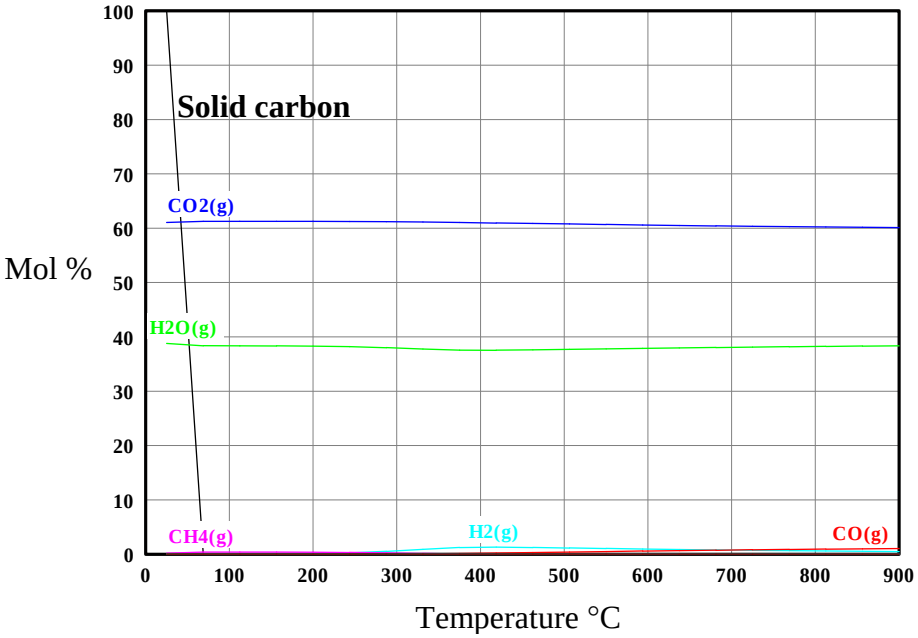

Figure 6.28 Gas cool down after near combustion, O_2 = 1 mol

7 CONCLUSION

7.1 ACHIEVEMENT OF OBJECTIVES

7.1.1 Design and develop the modifications of an existing fluidized bed gasifier.

Significant modifications were successfully incorporated in an existing fluidized bed gasifier pilot plant reactor enabling it to be operated as an air, steam and flaming pyrolytic gasifier, and pyrolyser. Three different biomass types were used to evaluate its operation efficiency. In addition, the feeding system was successfully modified for compressible chopped grass material handling and low density solid flow measurement. An isokinetic gas particulate matter sampling system with condensable products sampling were successfully designed and implemented. A hot gas recycling loop system for pyrolytic mode operation was designed, constructed and operated successfully. A computer program controls the pilot plant functions automatically and has the ability to measure and record process parameters for mass and energy balance analysis. The user managing the plant can manually activate the cleanup and compression process of producer and synthesis gas for storage for gas fermentation downstream.

7.1.2 Develop an analytical procedure to identify major tar compounds.

An analytical procedure was successfully established on the bases of the tar guidelines. The use of acetone as a solvent was preferred to the isopropyl alcohol offered by the tar measurement guidelines. A total of 210 compounds were calibrated for the GC-MS method. During the time of these experiments, there were no officially recognized standard for tar measurement.

7.1.3 Evaluate the products of gasification

7.1.3.1 A. Air gasification of switchgrass at different feed moisture contents.

Bed temperature decrease was the main consequence of an increase in biomass moisture content. This temperature reduction induced a reduction in concentration of the gases of primary interest, CO and H_2. Though gasification of high moisture content switchgrass can be performed with the same output levels or better as dry switchgrass, if the temperature in the reactor can be maintained by external means.

7.1.3.2 B. Gasification using various feedstocks

7.1.3.2.1 Air gasification of dry switchgrass, bermudagrass and corn gluten.

Air gasification was successfully achieved in the fluidized bed pilot plant using switchgrass, bermudagrass and corn gluten. Gas compositions, tar and water were measured and analyzed after gas cool down.

Air gasification temperature was found to be dependant on equivalence ratio for all three biomass types. Carbon to CO efficiency was found to be maximized at ER=0.25

to 0.3 for all three biomasses at values of 30 to 35% of the incoming carbon for switchgrass, and 25 to 30% for bermudagrass and corn gluten. At this same equivalence ratio range, tar levels are found to be 10 to 15 g/Nm^3 for switchgrass, 15 to 20 g/Nm^3 for bermudagrass and 30 to 35g/Nm^3 for corn gluten. All were relatively constant in atomic composition.

High heating value of the gas was highest for corn gluten at -5000 kJ/kg of gas compared to switchgrass and bermudagrass with both at -4000 kJ/kg. The enthalpy of the air gasification reaction stayed between -4000 to -5000 kJ/kg of feed for all three biomass types. Water was produced at a similar rate for all three biomass types at 150 to 200 g/Nm^3.

7.1.3.2.2 Flaming pyrolytic gasification of dry switchgrass, bermudagrass and corn gluten.

Flaming pyrolytic gasification and pyrolysis were successfully achieved in the fluidized bed pilot plant using switchgrass, bermudagrass and corn gluten. Gas compositions, tar and water were measured and analyzed after gas cool down.

Reactor temperature was set to 775°C and mostly maintained as close to that set point as possible throughout the experimentation. Although the temperature, which is the key parameter for gasification was fixed, the Carbon to CO efficiency was found to be maximized at ER = 0.1 to 0.2 for all three types: 30 to 38% of the incoming carbon for switchgrass, 28 to 33% for bermudagrass, and 25 to 28% for corn gluten. At this same equivalence ratio range, tar levels increased exponentially with equivalence ratio from 25

to 50g/Nm^3 for switchgrass bermudagrass and corn gluten. Tar was relatively constant in its atomic composition.

Though the high heating value of the gas is increased between the same values for all three biomass types in the same equivalence ratio range (0.1 to 0.2); -6000 to -8000 kJ/kg of gas, this increase seemed to occur towards the lower end of the equivalence ratio range, leaving the high heating value value closer to -6000 kJ/kg between 0.2 and 0.15 equivalence ratio values. The enthalpy of the air gasification reaction stayed between -3000 to -1500 kJ/kg of feed for switchgrass and bermudagrass and between -4000 to -1000 kJ/kg for corn gluten. The lower value, i.e. -4000 kJ/kg, was a sign that despite the agglomeration complications, corn gluten required less external heat than switchgrass and bermudagrass to achieve similar results within this range of equivalence ratio. However, this is arguable because water, that influences the enthalpy of reaction, showed a decreasing trend in corn gluten from 275 to 180 g/Nm^3 while it increased for bermudagrass from 100 to 150 g/Nm^3 and from at 100 to 325 g/Nm^3 for switchgrass across the same equivalence ratio range.

7.1.3.2.3 Steam gasification of dry switchgrass, bermudagrass and corn gluten.

Steam gasification was successfully achieved in the fluidized bed pilot plant using switchgrass, bermudagrass and corn gluten. Gas compositions, tar and water were measured and analyzed after gas cool down.

Reactor temperature was set to 775°C and maintained as close to set point as possible throughout the experimentation. Although the temperature was fixed, the carbon to CO efficiency was found to be maximized at S/B = 0.6 to 0.8 for switchgrass with

27%, S/B = 0.8 to 1.0 for bermudagrass with 15% and S/B = 1.0 to 1.2 for corn gluten with 35% of the incoming carbon. This value of carbon to CO efficiency for corn gluten makes this feedstock an excellent candidate for steam gasification. When carbon to gas efficiency is maximum for each biomass type, H_2 concentration is around the same value of 25%, and tar levels are the lowest for corn gluten. Tar is also relatively constant in its atomic composition.

The high heating value of the gas is maximized at the same values of S/B ratio around 0.85 with -16,000 kJ/kg for switchgrass and -18,000 kJ/kg for corn gluten. The enthalpy of the steam gasification reaction stays around 0 kJ/kg of feed for switchgrass and bermudagrass, however it is at 1000 kJ/kg for corn gluten. This higher value of 1000 kJ/kg shows that more heat was provided to achieve higher results with corn gluten than switchgrass and bermudagrass. This observation is arguable because water measurement made after cool down, which influences the enthalpy of reaction calculation, is showing a lower value for corn gluten maximum gas HHV at 1100 g/Nm^3 than the two other grasses 1250 g/Nm^3 for switchgrass and 2500 g/Nm^3 for bermudagrass. Further research is necessary in corn gluten steam gasification to confirm these initial results.

7.1.4 Modeling of the gasification equilibrium.

An equilibrium Gibbs reactor model was programmed in LabView. The model can calculate equilibrium of air, flaming pyrolytic and steam gasifications and pyrolysis at different temperatures steam to biomass and equivalence ratio for four biomass types with 2D and 3D graphics. The characterization of the tar and char defined in laboratory experiments was implemented. The model was also programmed to calculate equilibrium

of the high temperature outputs at 298K with water removal from the equilibrium due to its condensation during the gas cool down for comparison of the model results with GC-TCD data. Technical difficulties with the virtual instrument provided by LabView, prevented the solver from finding solutions to low temperature equilibrium.

Considering the particulate matter as char with a CHO composition and a free enthalpy not equal to zero, allowed, the model to increase tar production to more realistically level, and decrease char production.

It is satisfactory to assume tar as one hypothetical compound for equilibrium modeling, because tar atomic composition remained constant through most gasification processes at constant temperature.

Tar and char taken as non-pure element influenced each other production in their equilibrium modeling.

All three biomass types are suitable for gasification but show better results in different processes. Switchgrass showed the best results for all gasification processes of all three biomasses tested. It is matched by corn gluten using steam gasification. Bermudagrass like corn gluten induces agglomeration of the bed when the reactor bed temperature exceeded about 800°C. The high ash content of corn gluten might have a catalytic effect on the gasification reaction. Bermudagrass showed better results than corn gluten except in steam gasification.

7.2 FUTURE RESEARCH

At the process level, particulate matter combustion could generate enough heat to replace the electrical heaters. An additional inner cyclone was installed before the expansion to protect the hot gas recycling loop turbine and to collect PM for combustion inside the gasifier. It was combined to a finned pipe located below the cyclone as an inner PM combustor. The intent of this gasifier-combustor concentric design is to allow the separation of the flue gas and syngas, and generate heat inside the bed and the freeboard of the gasifier. Future test will reveal if the heat from the PM combustion and the heat recycled from the gas outlet as steam would allow the system to be energetically self-sustainable. Also this design allows possible future use of the pilot plant as a recirculated fluidized bed gasifier if the finned pipe is not fed with air but simply used as a sand recycle open the gasifier bed. At the sampling level, improvement can be achieved by increasing the accuracy of the isokinetic conditions and sampling flow measurement. At the modeling level, characterization of the char is definitely important to further the study of this modeling hypothesis.

REFERENCES

Aznar, M. P., Caballero, M. A., Gil, J., Martin, J. A., & Corella, J. (1998). *Industrial Engineering Chemical Research, 37*.

Aznar, M. P., Corella, J., Delgado, J., & Lahoz, J. (1993). *Industrial Engineering Chemical Research, 32*, 1.

Aznar, M. P., Corella, J., Martin, J. A., Caballero, M. A., Olivares, A., & Frances, E. (1996). *Proceedings of conference on developments in thermochemical biomass conversion*, Banff, Canada.

Baker, E. G., Mudge, L. K., & Wilcox, W. A. (1996). *Proceedings from conference on developments in thermochemical biomass conversion*, Banff, Canada.

Bettagli, N., Desideri, U., & Fiaschi, D. (1995). A biomass combustion gasification model: Validation and sensitivity analysis. *Journal of Energy Resources Technology, 117*, 329-336.

Bredwell, M. D. W., R. M. (1995). Formation and coalescence of microbubbles. *Applied Biochemistry and Biotechnology, 51*, 501-509.

Bredwell, M. D. W., R. M. (1998). Mass transfer properties of microbubbles. *Biotechnology Progress, 14*, 31-38.

Ciesielczy, E. G., A. (1994). Non-isothermal fluidized-bed reactor model for char gasification, taking into account bubble growth. *Fuel, 73*(1), 105-112.

Corella, J., Herguido, J., Gonzalez-Saiz, J. (1989). Steam gasification of biomass in fluidized bed effects of the type of feedstock. In G. L. Ferrero, Maniatis, K., Buekens, A., & Bridgwater, A. V. (Ed.), *Pyrolysis and gasifications*, London: Elsevier Applied Science, 618-623.

Cooper, C., Alley, F.C. (1986). Air pollution control a design approach, Waveland press Inc., 500-509.

Datar, R. P., Shenkman, R. M., Cateni, B. G., Huhnke, R. L., & Lewis, R. S. (2004). Fermentation of biomass-generated producer gas to ethanol. *Biotechnology and Bioengineering, 86*, 587-594.

Delgado, J., Aznar, M. P., & Corella, J. (1997). Biomass gasification with steam in fluidized bed: Effectiveness of CaO, MgO, and CaO-MgO for hot raw gas cleaning. *Industrial Engineering Chemical Research, 36*, 1535-1543.

Ekstrom, C., Lindman, N., & Pettersson, R. (1996). *Proceedings of conference on developments in thermochemical biomass conversion*, Banff, Canada.

Gaddy, J.L. (1992). Clostridium Ljungdahlii, An anaerobic ethanol and acetate producing microorganism. *US patent 5,173,429*.

Garcia, L., Salvador, M. L., Arauzo, J., Arauzo, J., & Bilbao, R. (1998). *Industrial Engineering Chemical Research, 37*, 3812.

Garcia, L., Salvador, M. L., Arauzo, J., Bilbao, R., & Arauzo, J. (1996). *Proceedings of conference on developments in thermochemical biomass conversion*, Banff, Canada.

Gebhard, S. C., Wang, D., Overend, R. P., & Paisley, M. A. (1994). *Biomass and Bioenergy, 7*, 307.

Gil, J., Aznar, M., Caballero, M., Frances, E., & Corella, J. (1997). Biomass gasification in fluidized bed at pilot scale with steam-oxygen mixtures: Product distribution for very different operating conditions. *Energy and Fuels*, *11*(6), 1109-1118.

Hallen, R. T., Sealock, L. T., Cuello, R., & Bridgwater, A. V. (1988). Research in thermochemical biomass conversion. In J. L. Kuester (Ed.), London: Elsevier Applied Science, 157.

HSC5 Chemistry (2002) software from Outokumpu HSC Chemistry® for Windows. Chemical Reaction and Equilibrium Software with Extensive Thermochemical Database

Kinoshita, C. M., Wang, Y., & Zhou, J. (1995). *Industrial Engineering Chemical Research*, *34*, 2949.

Klass, D. L. (1998). *Biomass for renewable energy, fuels, and chemicals*. San Diego: Academic Press.

Klasson, K. T., Ackerson, M. D., Clausen, E. C., & Gaddy, J. L. (1992). Bioconversion of synthesis gas into liquid or gaseous fuels. *Enzyme and Microbial Technology, 14*, 602-608.

National Instrument, (1999). LabView V5.1 Graphic programming software.

Marias, F., Puiggali, J. R., & Flamant, G. (2001). Modeling for simulation of fluidized-bed incineration process. *Environmental and Energy Engineering, 47*(6), 1438-1460.

Milioli, F. E., & Foster, P. J. (1995). Entrainment and elutriation modelling in bubbling fluidized beds. *Powder Technology, 83*(3), 233-244.

Minowa, T., Ogi, T., & Yokoyama, S. (1996). *Fuel, 7*, 1342.

Mudge, L. K., Baker, E. G., Mitchell, D. H., & Brown, M. D. (1985). Catalytic steam gasification of biomass for methanol and methane production. *Journal of Solar Energy Engineering, 107*, 88-92.

Mudge, L. K., Baker, E. G., Mitchell, D. H., & Brown, M. D. (1992). *Canadian Journal of Chemical Engineering, 70*.

Myren, C., Homell, C., Yu, Q., Brage, C., & Bjombom, E. (1996). *Proceedings of conference on developments in thermochemical biomass conversion*, Banff, Canada.

Narvaez, I., Orio, A., Aznar, M., & Corella, J. (1996). Biomass gasification with air in an atmospheric bubbling fluidized bed: Effect of six operational variables on the quality of the produced raw gas. *Industrial Engineering Chemical Research, 35*, 2110-2120.

Natarajan, E., Nordin, A., & Rao, A. N. (1998). Overview of combustion and gasification of rice husk in fluidized bed reactors. *Biomass and Bioenergy, 14*(5), 533-546.

Orio, A., Corella, J., & Narvaez, I. (1996). *Proceedings of conference on developments in thermochemical biomass conversion*, Banff, Canada.

Reed, T. B. (Ed.). (1981). *Biomass gasification principles and technology* Park Ridge: Noyes Data Corporation.

Sadaka, S. S., Ghaly, A. E., & Sabbah, M. A. (2002a). Two phase biomass air-stream gasification model for fluidized bed reactors: Part 1-Model development. *Biomass and Energy, 22*, 439-462.

Sadaka, S. S., Ghaly, A. E., & Sabbah, M. A. (2002b). Two phase biomass air-stream gasification model for fluidized bed reactors: Part 2-Model sensitivity. *Biomass and Energy, 22*, 463-477.

Sadaka, S. S., Ghaly, A. E., & Sabbah, M. A. (2002c). Two phase biomass air-stream gasification model for fluidized bed reactors: Part 3-Model validation. *Biomass and Energy, 22*, 479-487.

Smith J. M, Van Ness H. C., (1996) Introduction to chemical engineering thermodynamics, fifth edition. New York : McGraw-Hill.

Vassilatos, V., Taralas, G., Sjostrom, K., & Bjombom, E. (1992). *Canadian Journal of Chemical Engineering, 70*.

Wang, D., Czemik, S., Chomet, E. (1998). *Energy Fuel, 12*.

Wang, Y. K., C. M. (1992). Experimental analysis of biomass gasification with steam and oxygen. *Solar Energy, 49*(3), 153-158.

Werther, J. (1980). Modeling and scale-up of industrial fluidized bed reactors. *Chemical Engineering Science, 35*, 372-379.

Worden, R. M., Bredwell, M. D., & Grethlein, A. J. (1997). Engineering issues in synthesis-gas fermentations, *ACS Symposium Series Fuels and Chemicals from Biomass*, 320-335.

8 APPENDICES

8.1 GAS CHROMATOGRAPH CALIBRATION GRAPHS

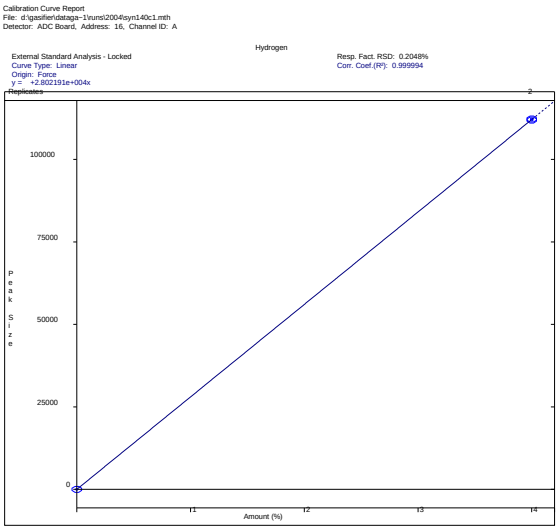

Hydrogen gas

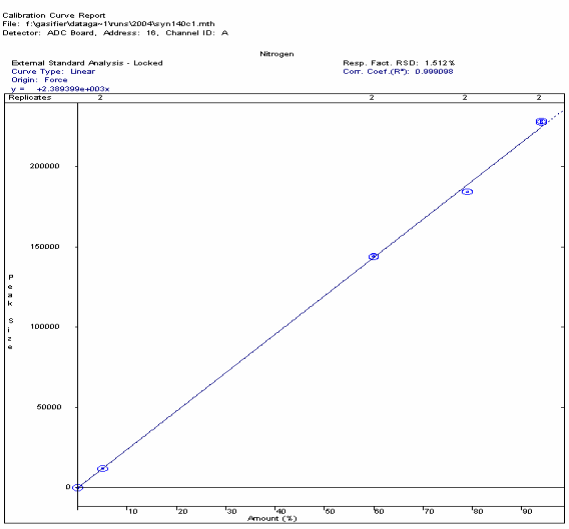

Nitrogen gas

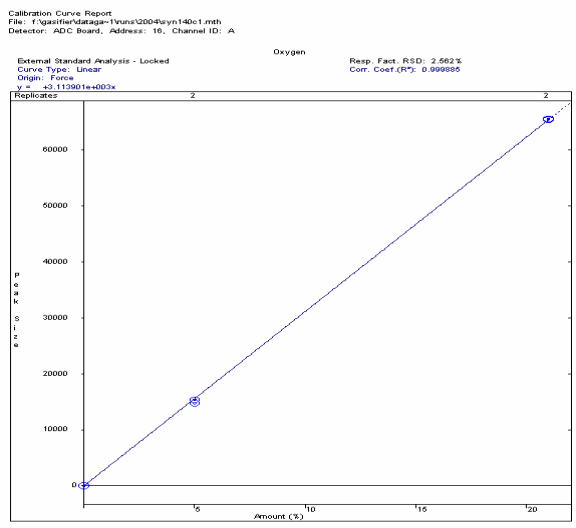

Oxygen

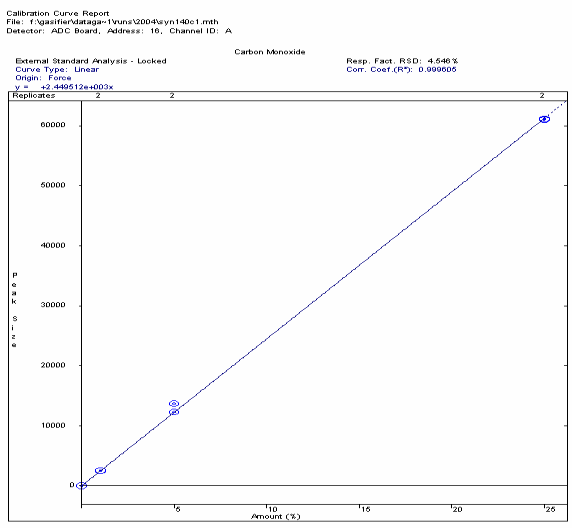

Carbon monoxide

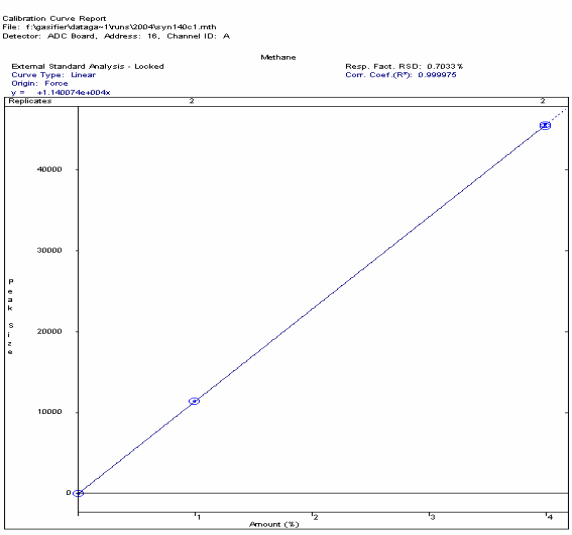

Methane

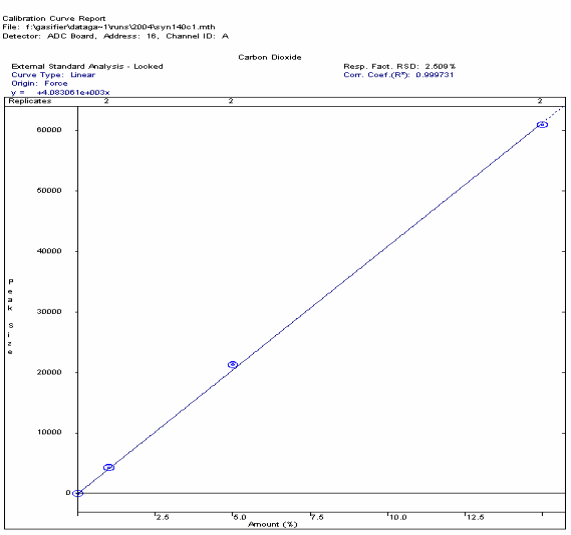

Carbon dioxide

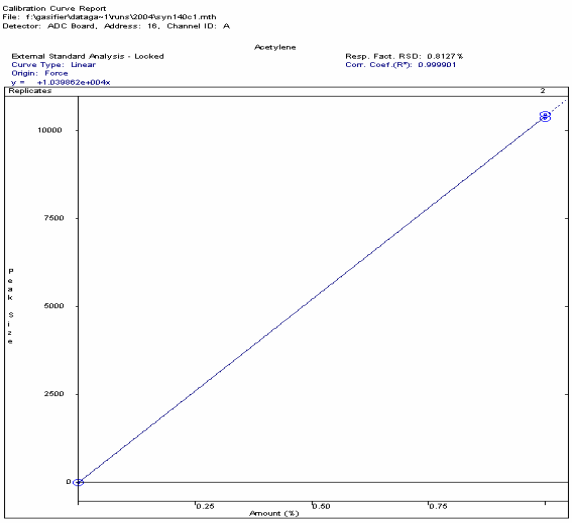

Acethylene

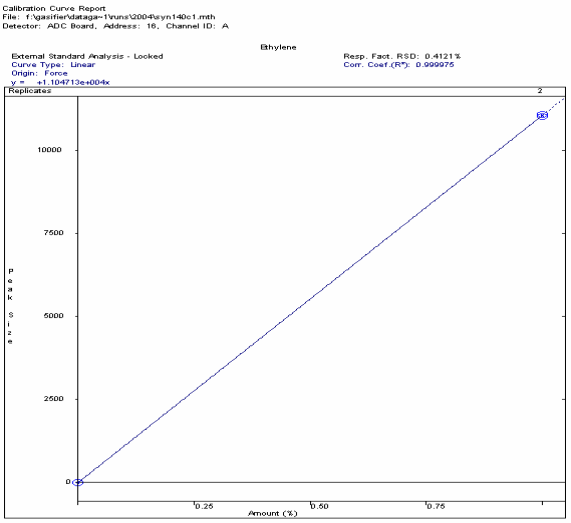

Ethylene

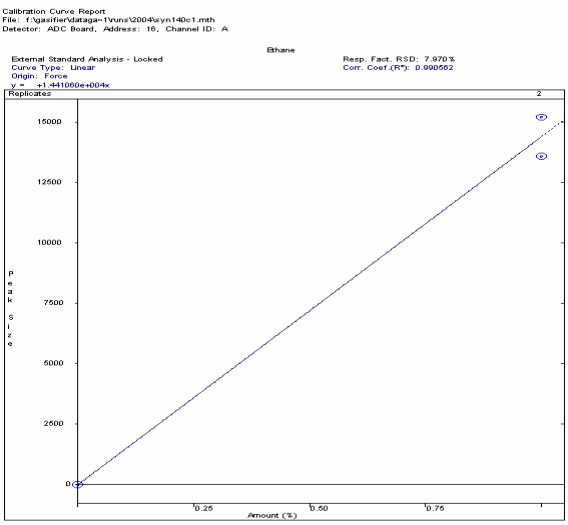

Ethane

8.2 PROCEDURES FOR FLUIDIZED BED GASIFIER PILOT PLANT AND TAR SAMPLING SYSTEM

8.2.1 Procedure for Automatic Start.

1. First check for biomass in the hopper.
2. Plug in the plenum heaters in the extension cord below the gasifier and plug the extension cord at the south east corner of the annex Lab near the entrance.
3. Flip the main switch of the baffle heaters on at the north wall.
4. Connect the electrical devices such as the mass flow meter (Check), load cell (Check), power supply to the two electrical air valve plugged in (Check)
5. Open the main air valve (Set pressure @ 75 psi for auto mode with solenoid valve or 50 psi for normal use with actuated valve).
6. Check that the bi-pass valve (needle valve black handle) is closed and that the yellow valve is open of the gasifier.
7. Set air lock needle valve to 1.5 scfm to be read directly on mass flow meter.

NOTE: Plug in the sampling system the night before running for the temperature of the second ice bath to reduce to at-least -20^0 Celsius. During that night switch off temperature control of first ice chest (according to gas flow).

8.2.2 Starting the Gasifier Program

When a user starts the program, he can indicate a file name under which he wants to save the data on the system (Text.dat by default). At this point the programs is running.

1. In the program the user go to the 'Auto Start Section' on the program panel and indicates the delay before start in hours and minutes (from the time at which the auto start button is activated).
2. After this step the user indicates the rate at which the temperature baffle heaters setpoint is going to rise (degrees/ min) to warm up the Gasifier bed.

3. Next check the air flow rate by activating air booster valve on the program panel. (flow rate should be between 10 and 12 scfm. Regulate flow with pressure regulator on the main line from step 5 paragraph 8.2.1, it should be around 75psi. Switch off air booster after check).
4. Switch 'Auto Start' on, switch baffle heaters on with the desired set point (air heater and plenum heater are not part of the auto start).

8.2.3 Procedure After the Gasifier is in Temperature

1. Start the cyclone airlocks (No. 1 & 2), heaters over the cyclones (the heaters should be set at 400^0 F).
2. Start piston vibrators (timer) if desired.
3. Start injection auger.
4. Start the feeding airlock and hopper mixer.
5. Start steam generator and check for water inflow at 0.2 gal/min on rotameter when solenoid valve opens. Enter this value on panel for boiler water inflow.
6. On the program panel set air valve to desired percentage (0.425 at 50 psi is usual setting).
7. Next switch off the 'Auto start' as soon as the air flow rate starts to increase.
8. If steam is used start plenum heater and steam measurement system.
9. Then open the steam valve on the steam generator; wait for the stable steam flow rate.
10. Switch on the biomass with desired frequency and wait for the time set in biomass array minutes for accurate biomass flow.
11. Set stoichiometric ratio according to the biomass experimented and desired Equivalence Ratio (ER) in air mode. Switch air mode to automatic when all parameters are in range.
12. Switch off heaters if desired.
13. Open tracer valve at graduation 70 on rotameter which is 23.5 liters/min and switch on tracer mass flow meter (zero calibration may be required).

8.2.4 Procedure for the Gravimetric Tar Analysis

1. Start the Coolant.
2. Start the rotary evaporator water bath (RO or DI water), and set it to 55^0C.
3. Place the round bottom flask (250ml) in the oven for 5min at 110°C.
4. Cool down the round bottom flask in the desiccators.
5. Weigh the round bottom flask on the precision scale and write down the weight (up to 10^{-4} g accuracy).
6. Take a clean beaker (100ml). Pour some of the tar solution obtained from the gasification run into the beaker.
7. Pour solution from the beaker into the burette (50ml).
8. Measure 50 ml of solution with the burette into the round bottom flask. Repeat the operation a second time to obtain a total of 100 ml.
9. Place the round bottom flask with the solution on the rotary evaporator. Lower the rotary evaporator so that the round bottom flask is half way into the water bath and start rotation at 100 rpm.
10. Open the upper vacuum knob on the rotary evaporator condenser and close the lower knob in such way that the injection tube is not on the path of the condensing solvent.
11. Start the vacuum pump; trim the vacuum valve so that vacuum is between 40 to 50 KPa, in order to initially have 4 droplets per second according to the guidelines.
12. Check for presence of water in round bottom flask. If there is water then inject Nitrogen so that vacuum pressures do not go lower than 35 KPa of vacuum. Continue until traces of water disappear. If there is no trace of water in the flask, time 15 min until end of the experiment.
13. Stop vacuum pump and break vacuum in the rotary evaporator.
14. Raise rotary evaporator until the flask out of the water, dry flask outer surface with paper towel and remove flask from rotary evaporator. Place flask in the desiccators to cool down according to guidelines
15. Weigh flask and note down the value.

8.2.5 Procedures for the tar-sampling system

8.2.5.1 Cleaning the probe which is full of ashes

1. First the compress air plug has to be attached to the port, which is behind the U-Tube Manometer.
2. The two round black knob valves of the U-Tube manometer are closed and the three way valve (A black knob which is above the compressed air port is turned to the right).
3. Compressed air is passed through the probe static pressure ports by opening the Red valve on the compressed air line ($1/8^{th}$ of a turn only) and by changing direction on three-way valve several times.
4. Return the three-way valve back to initial position; turned to the right with the air still open. There are 4 valves, which have to be opened to clean the probe.
5. First open the Yellow valve and with a wire brush clean the passage until it is ash free. After that open the green valve and clean the passage. Now keeping

the Green Valve open close the yellow valve in order to flush out some residual ashes. Repeat the same procedure by opening the Red and the Black valves.

6. Now close all the valves except the compressed air valve with three way valve turned to the right (open towards inner probe static pressure port). The reason for a leakage of compressed air is to keep ashes from accumulating into the probe prior to an experiment.

- ***Note: The two circular knob valves over the U-Tube Manometer must be closed while cleaning and the three-way valve turned to the right. The three-way valve and compressed air valve will be closed at the beginning of a sampling experiment.***

8.2.5.2 Cleaning the Filter Casing, the Connecting Tube & the Impingers

1. Make sure that the filter casing and the connecting tube are free of ashes and tar. To ensure this, the entire passage has to be rinsed with acetone 2 to 3 times after every run or untill there is clean acetone coming out of the lower end of the tube.
2. Check the first impinger in the first ice chest for any kind of impurity. If there are any impurities then clean the first impinger and rinse it with acetone.

8.2.5.3 Steps to be followed during the run: Preparing the system for a run:

1. Take a clean ceramic filter. Keep it in the oven at 110°C for 5 minutes (to remove moisture.
2. Place the filter to cool down into the desiccator in order.
3. Weigh the filter on a precision weighing scale and note the weight (accuracy up to 0.1 mg)
4. Next bring the filter and place if into the filter casing along with the Vitton seal (‘O’ Ring).

Note: The seal should be about 3 to 4 mm below the top circumference of the filter. Make sure that al 4 valves on the probe exhaust are closed before fixing the filter casing.

5. After placing the filter with the 'O' Ring into the casing the entire arrangement is properly fixed to the exhaust port. Make sure that the screw squeezes the 'O' Ring between the exhaust port and the filter casing. Switch on the heathers placed on the filter casing and the connecting tube by flipping the switch to the ON position. (Make sure that the thermocouples on both and the electric plugs are connected to the control units.). Allow the temperature of the casing and the connecting tube to reach up to 490 to 500 Degree F.

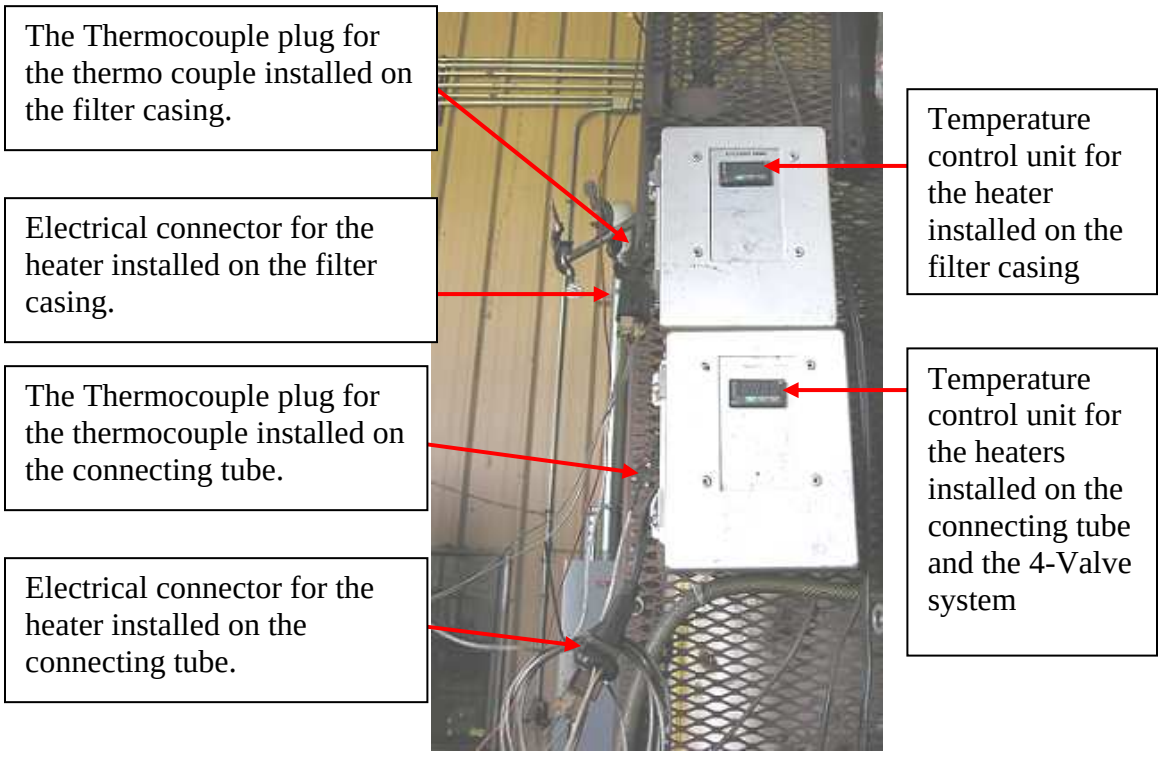

6. Connect the glass elbow adapter at the end of the connecting tube by using the black plastic nut, which has a vitton 'O' Ring housed into it. Make sure that the 'O' Ring and the black plastic connecting nut are over the connecting tube,

Note: The stainless connecting tube should be 10 to 15 mm inside the glass elbow adapter and then black plastic nut is tightened the elbow adapter.

7. Now connect the larger end of the glass elbow to the inlet of the first impinger and clamp it using the metal clamps.

IMPINGER

METALIC CLAMP

GLASS ELBOW ADAPTER

8. Place all the impingers into the two ice chests. There are 4 impingers in the first ice chest and 2 in the second ice chest. Before making any connections make sure that the impingers are properly submerged into the coolant and are properly located between the two plexi – glass round plate holders.

Note: The inlet of the impinger is right at the top and the outlet is a 'U' tube on the side. Check the 'O' Rings for damage on the inlet and the outlet joints and replace them if necessary.

9. After all the checks are done, add the following amounts of acetone into the impingers: first Impinger 200ml, last Impinger 0ml and 150 ml in all the other impingers.

IMPINGER

10. Once the entire setup is ready, make the connections as followed. Connect the elbow adapter which is on the connecting tube over the inlet of the first impinger. Then connect the outlet of the first impinger to the inlet of the second with the glass U-connectors (the connections are repeated in the counter-clock wise direction in which the impingers are placed along the periphery of the first ice chest.)

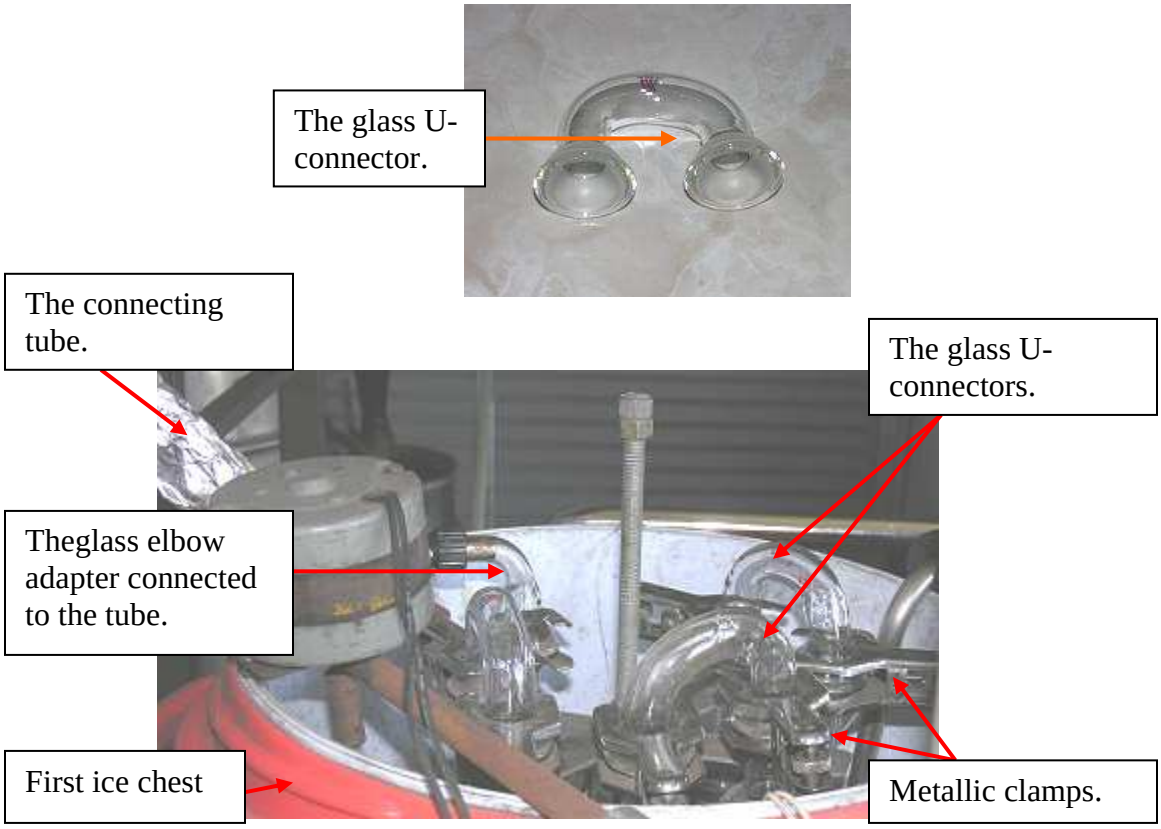

11. The outlet of the last impinger should be connected to the inlet of the column containing activated carbon. The outlet of the column goes to the inlet of a vacuum pump.
12. After all these connections are done, check that the K-thermocouple and the flow sensor (black plug) are connected to their receiving ports. One measures the outlet temperature of the gas and other measures the flow of the gas.
13. Test system for leakage according to guidelines.
14. Before running the system, check that the temperature in the second ice chest is -20^0 C and that the first one is around 5^0 Celsius.

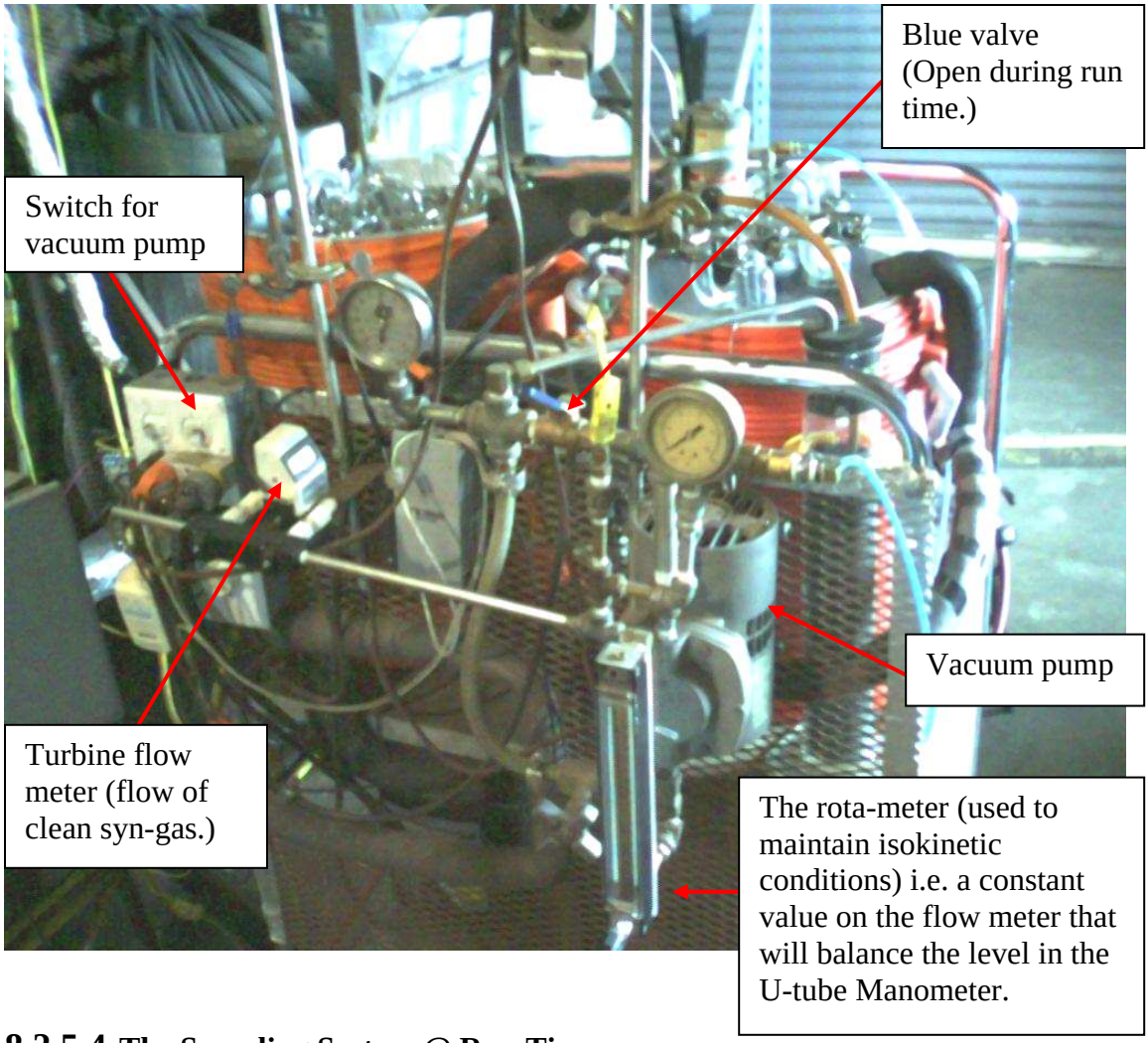

8.2.5.4 The Sampling System @ Run Time.

1. Flip the switch of the vacuum pump to the 'ON' position. Immediately open the green valve above the exhaust port. Then close the red valve, which is on the compressed air tube, and close the black valve above the compressed air valve. The two circular black valves placed on the either sides of the U-tube manometer are open. (Make sure that the two blue valves above the Vacuum Pump are in the following position; extreme right valve closed and the valve at the left open.).

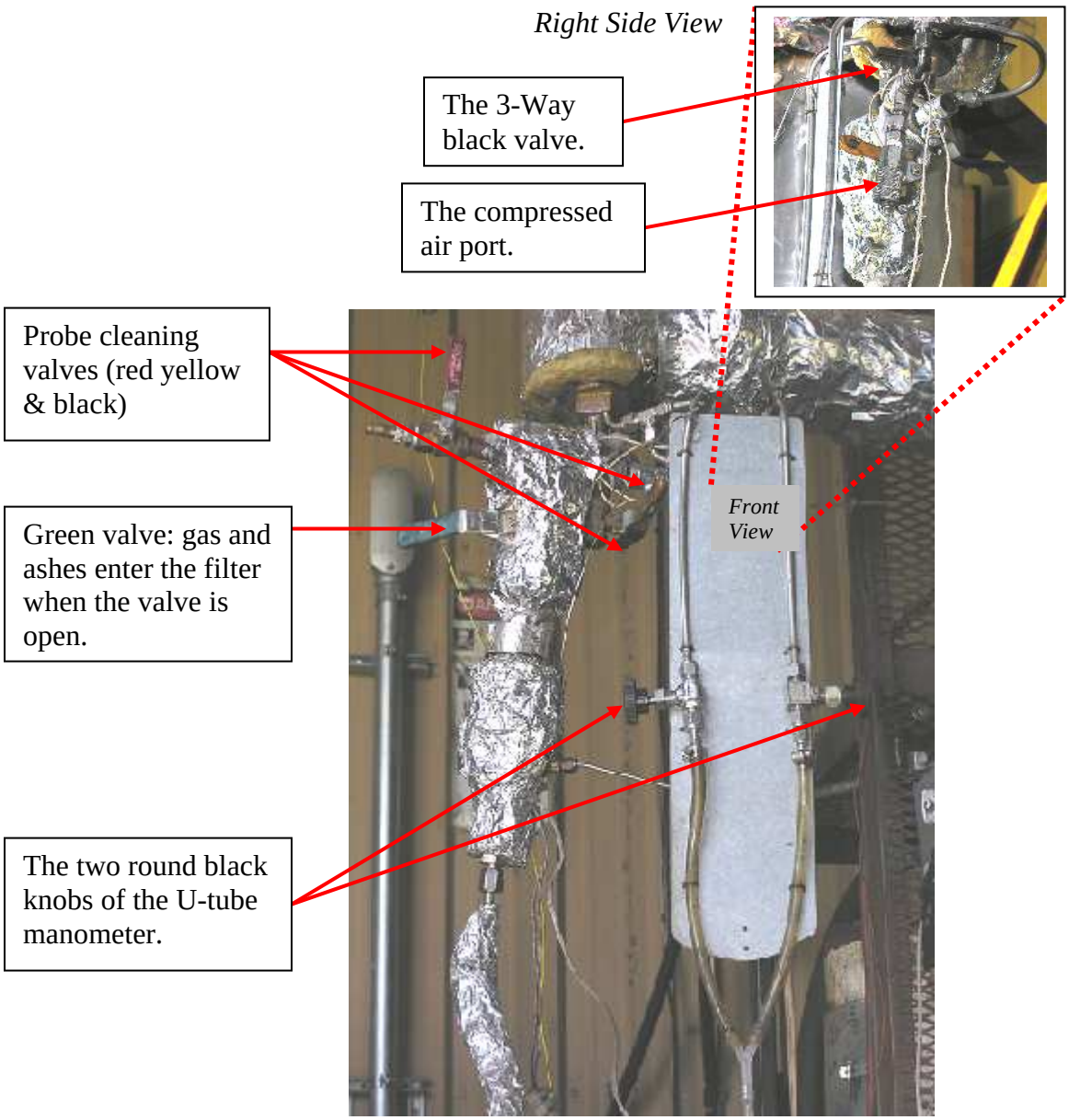

2. Check if there level of water in the manometer is leveled. To equalize them use the Rota meter and adjust the value of the gas flow on the flow Meter.
3. Once the system is at isokinetic conditions, allow it to run until a gas volume of 150 l has been sampled through the system. Simultaneously maintain the isokinetic conditions by constantly checking the manometer and by using the black valve on the Rota meter.

8.2.5.5 Procedures to be followed After the Run is Completed.

Once the run is completed, the system is turned off as followed:

Turn off the vacuum pump by flipping the switch to off position. Then close the Green valve above the filter housing once the vacuum pressure is zero. Close the two Black knobs attached to the U-tube manometer. Then turn off the heaters on the filter housing and the connecting tube by switching off the power to the temperature control boxes.

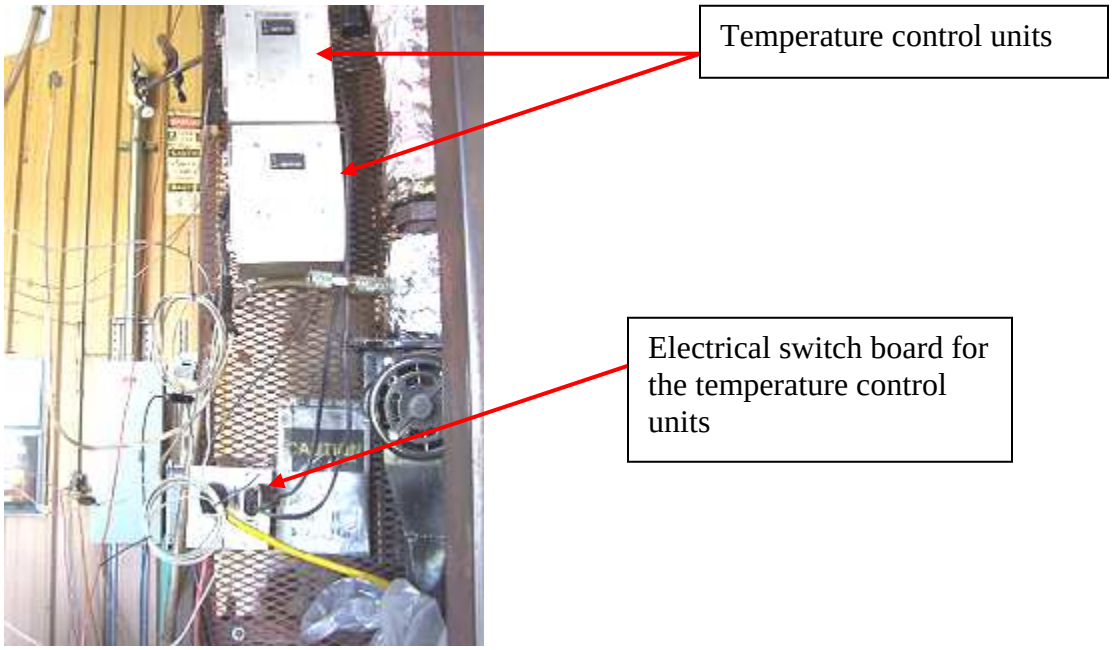

1. Once the system is turned off, let it cool down.
2. Remove the glass elbow adapter and place it in a beaker with clean acetone allow all the tar to get dissolved into the acetone.
3. Allow the filter housing and the connecting tube to cool down. Mean while reverse the position of the two blue valves. (The valves are shown in the picture below.)
4. Remove the metal clamp fitted at the outlet of the last impinger and disconnect the plastic hose. Fill the last impinger with clean acetone.

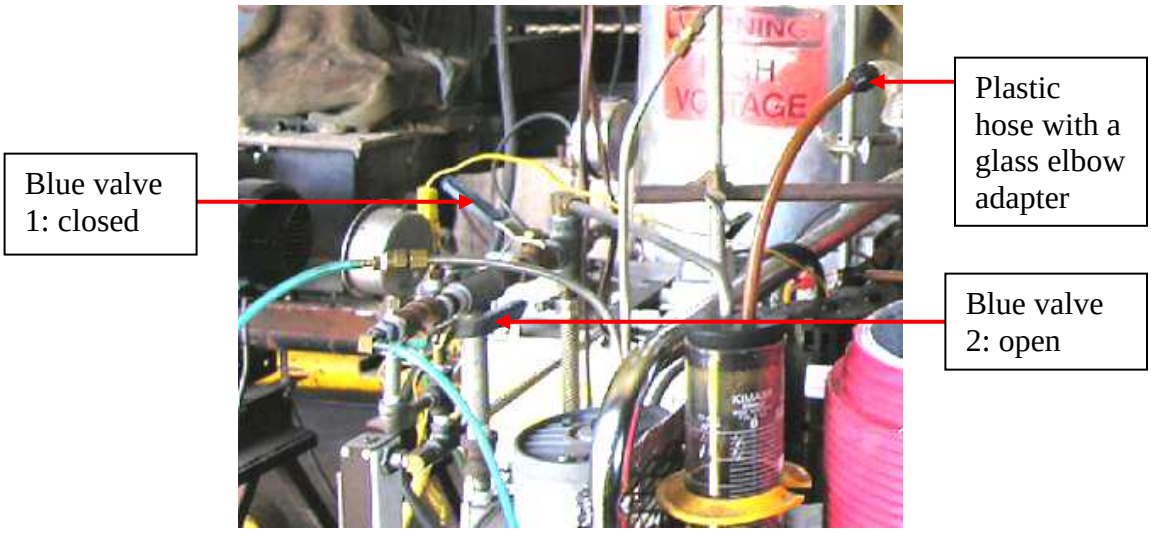

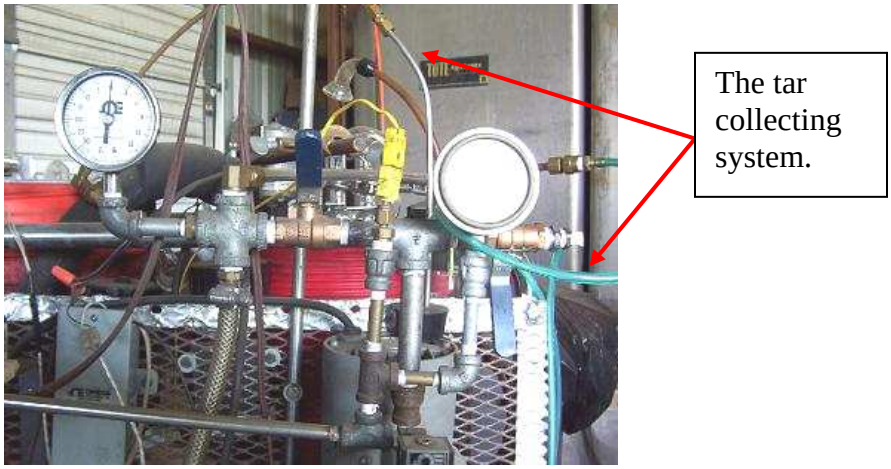

5. Connect the longer end of the tar collecting system (which is attached with the acetone resistance hose and a glass elbow adapter) to the inlet port of the first impinger. Attach the metal clamp in order to ensure that there is no leak.
6. Now insert the tar collecting system with the rubber stopper into a 4000ml Erlenmeyer flask. The rubber stopper should be pressed down hard to make sure that it is air tight.
7. Start the vacuum pump and adjust the flow to 6 to 8 l/min. Then the system flushes counter current to the gas sampling flow and all the tar and acetone mixture from all the impingers flow into the conical flask.

8. Refill the last impinger (with the vacuum pump switched off) with clean acetone and flush the system. Repeat this process until you get clean acetone out of the impingers.

Note: Check the first impinger if there is ammonia (a white precipitate at the bottom of the impinger or stuck to the walls) then drain the acetone and add a measured volume of DI water (Deionized Water) and dissolve the ammonia.

9. Refill all the impingers with fresh clean acetone with the specified quantity mentioned in section 4.3 step 9.
10. If recycled acetone is used make sure to keep a blank sample for data analysis later.

8.3 GUIDELINES FOR TAR MEASUREMENT

Guideline for Sampling and Analysis of Tar and Particles in Biomass Producer Gases

Version 3.3

J.P.A. Neeft, H.A.M. Knoef, U. Zielke, K. Sjöström,
P. Hasler, P.A. Simell, M.A. Dorrington, L. Thomas,
N. Abatzoglou, S. Deutch, C.Greil,
G.J. Buffinga, C. Brage, M. Suomalainen

Prepared for

European Commission (DGXII)
Netherlands Agency for Energy and the Environment (NOVEM)
Swiss Federal Office of Education and Science
Danish Energy Agency (Energistyrelsen)
US Department of Energy (DoE)
National Resources Canada

Table of content

1. Abstract

This Guideline provides a set of procedures for the measurement of organic contaminants and particles in producer gases from biomass gasifiers. The procedures are designed to cover different gasifier types (updraft or downdraft fixed bed or fluidised bed gasifiers), operating conditions (0 - 900°C and 0.6 - 60 bars) and concentration ranges (1 mg/m_n^3 to 300 g/m_n^3).

The Guideline describes a modular sampling train, and a set of procedures, which include: planning and preparation of the sampling, sampling and post-sampling, analysis, calculations, error analysis and reporting.

The **modular sampling train** consists of 4 modules. Module 1 is a preconditioning module for isokinetic sampling and gas cooling. Module 2 is a particle collection module including a heated filter. Module 3 is a tar collection module with a gas quench (optionally by circulating a liquid), impinger bottles and a backup adsorber. Module 4 is a volume-sampling module consisting of a pump, a rotameter, a gas flow meter and pressure and temperature indicators. The equipment and materials that are required for procuring this modular sampling train are given in the Guideline.

The **sampling** procedures consist of a description for isokinetic sampling, a leakage test prior to sampling, the actual sampling and its duration, how the equipment is cleaned after the sampling, and how the samples are prepared and stored.

Analysis of the samples is performed via three procedures. Prior to these procedures, the sample is prepared by Soxhlet extraction of the tars on the particle filter and by collection of all tars in one bulk solution. The first procedure describes the weighing of the particle filter to obtain the concentration of particles in the biomass producer gas. The bulk tar solution is used for two purposes: for determination of gravimetric tar and for analysis of individual compounds. The second procedure describes how to determine the gravimetric tar mass from the bulk solution. The third procedure describes how the solution can be analysed by GC-MS or GC-FID to obtain the concentrations of individual tar compounds.

2. Aim of this Guideline

This Guideline is aimed to give a set of procedures for the measurement of organic contaminants and particles in producer gases from biomass gasifiers. Biomass gasifiers can be updraft fixed bed gasifiers, downdraft fixed bed gasifiers and fluidised bed gasifiers, operating under atmospheric or pressurised conditions. The Guideline is aimed to measure organic contaminants and particles in the concentration range typically from 1 mg/m_n^3 to 300 g/m_n^3 at all relevant conditions (0 - 900°C and 0.6 - 60 bar).

As organic contaminants ("tars") from pyrolysis or gasification of coal are similar in nature compared to (high temperature) biomass gasification tars, also coal tars can be measured with this Guideline.

The procedures and methods described in this report differ from most of the methods used for sampling organic compounds present in the gaseous emissions from various industrial processes such as flue gases or automobile exhaust gases. The differences are related to the fact that the concentration level of the organic species present in the producer gases exceed the concentrations found in flue gases generally by more than 3 orders of magnitude. Hence the methods described within this Guideline are not intended to be applicable for sampling organic components in trace concentrations (ppm or sub-ppm range).

The Guideline, previously entitled 'Protocol', has now been changed to 'Guideline' thus providing a 'temporary status'. A standardisation trajectory at CEN has been initiated, with the aim to convert the Guideline to a Standard.

The Guideline describes sampling and analysis of organic contaminants in product gases from gasification of biomass. Biomass in this Guideline is defined as uncontaminated organic materials of non-fossil origin. The Guideline can also be applied for non-biomass materials (that is: for sampling and analysis of organic contaminants from gasification of *contaminated* organic materials of non-fossil origin, such as waste wood, sludge and manure). However, this can only be undertaken for analysis of the same compounds that are found from uncontaminated organic materials. In other words: The Guideline is not specifically designed to measure organics formed from gasification of the contaminated organic materials or from interactions between these contaminants and gasification products of the biomass. Examples of such organic contaminants are halogenated compounds, monomers of degradation of plastic materials, and compounds containing nitrogen and sulphur apart from the most common ones also found in biomass producer gases listed in Appendix 13.2.

3. Definitions

b.p.:	Boiling point
Biomass:	Uncontaminated organic materials of non-fossil origin such as wood, straw or short rotation forestry fuels
BTX:	Benzene, Toluene and Xylenes
GC-FID	Gas Chromatography – Flame Ionisation Detector
GC-MS	Gas Chromatography – Mass Spectrometer
Gravimetric tar:	Evaporation/distillation residue from particle free sampling solution(s) determined by gravimetric analysis (see Chapter 8.1.4)
IC engine:	Internal Combustion Engine
Organic compounds:	Generic term for individual organic compounds listed in Appendix 13.3
Producer gas:	Gas produced from thermal biomass conversion reactor (gasifier). May include also pyrolysis gas
Particles:	Solid residue from particle filter after solvent extraction or solid residue from filtration of sampling solution(s) (Chapter 8.1.4)
Main gas stream:	Producer gas stream in gas pipes of gasification reactor
Normal conditions:	273.15 K, 101325 Pa = 1.01325 bar, dry (according to DIN 1343)
Slip gas stream:	Representative (small) part of the main gas stream
Tar:	Generic (unspecific) term for entity of all organic compounds present in the producer gas excluding gaseous hydrocarbons (C1 through C6). Benzene is not included in tar.
VOC:	Volatile organic compounds. Generic term for organic compounds (e.g. with b.p. < 250°C) which exhibit a considerable vapour pressure at room temperature. VOC represent the lower boiling fraction of gaseous hydrocarbons (C1 through C6) and tar.
XAD:	Not an abbreviation of a substance. XAD is a registered trademark of Rohm & Hass (It). XAD is a resin of polystyrene (XAD-2 and XAD-4) or polyacrylic (XAD-7 and XAD-8).
PTFE:	Polytetrafluoroethene

4. Units and indices

Notation and units (in agreement with ISO 9096):

Sign	Parameter	Unit
a	Linear coefficient	-
a	Effective nozzle area	m^2
A	Surface area	m^2
C	Mass fraction of carbon	-
c	Concentration in producer gas	kg/m_n^3
cc	Carbon content (non-condensable gases = CO, CO_2, CH_4, C_2H_2, C_2H_4 etc.)	kg C / m_n^3 or kg C / kg biomass[1]
d	(Inner) diameter	m
Δ	Error	
f	Water vapour concentration	kg/m^3
H	Mass fraction of hydrogen	-
$\dot{m}$	Mass flow (of fuel, ash, producer gas)	kg / h
M	Mass	kg
N	Number	-
p	Absolute pressure	Pa or bar
P_0	Pressure at normal conditions: 101325 Pa = 1.01325 bar (according to DIN 1343)	Pa or bar
p_{am}	Ambient pressure	Pa or bar
Δp	Differential pressure	Pa or bar
q_m	Mass flow rate	kg/h on dry basis
q_V	Volumetric flow rate	m_n^3/h
RF	Response Factor	
ρ	Density	kg/m^3
σ	Standard deviation	
t	Sampling time (total)	h
cc	Carbon content (non-condensable gases = CO, CO_2, CH_4, C_2H_2, C_2H_4 etc.)	kg C / m_n^3 or kg C / kg biomass[1]
T	Temperature (absolute)	K
T_0	Temperature at normalconditions: 273.15 (according to DIN 1343)	K
Θ	Temperature	°C
v	Velocity	m/s
V	Volume	m_n^3
$\dot{V}$	Gas volume flow rate	m_n^3/ hr
v	Velocity of producer gas in duct	m/s
Y_{gas}	Gas yield	m_n^3/kg biomass[1]
<>	Average	

[1]: Biomass on dry and as-free (daf) basis

Used subscripts:

Sign	Subscript means
A	Individual compound
a	Actual conditions in sampling plane
act	Actual, measured at the gas meter
agent	Gasification agent
ash	Solid residue from gasification process
drygas	Dry producer gas (not including H_2O)
c	Compound
D	Main gas duct
F	Particle filter
fuel	Solid biomass
g	Any gas measuring devise
gas	Producer gas
gasif. agent	Gasification agent/agents
H_2Ogas	Water in the producer gas
i	Individual value
is	Internal standard
N	Sample nozzle
n	Normal conditions (DIN 1343, in English often called standard conditions)
p	Quantity of particles
<p>	Average pressure
particles	Particles in producer gas
p,0	Dry clean particle filter
p,1	Dry loaded particle filter obtained after sampling and Soxhlet extraction
Pt	Pitot tube
s	Compound
sol	Quantity in the tar solution sample
solid	Solid residues from gasification (bottom ashes, fly ash)
tar	Organic compounds in producer gas
T	Quantity of "Gravimetric tar"
w	Water vapour
0	Start of the sampling procedure
1	Stop of the sampling procedure

Sign	Superscript means
‘	Moisture included

5. Measuring principle

5.1. Overview

The required level of information about the gasification products often depends on the end use of the gas. In some applications a very rough estimate of the gas heating value is sufficient for successful operation while very detailed chemical characterisation of the effluents may be needed in another application.

The measurement principle is described in this chapter. The principle is based on the discontinuous sampling of a gas stream containing particles and organic compounds (tar) under isokinetic conditions. The instructions of isokinetic sampling of flue gases are given in the standards ISO 9096 or VDI 2066.

The aim of the principle has been to keep it as simple as possible. This is because the measuring conditions can vary from 'comfortable' laboratory rooms to an executive plant gasifier where there is no customised room for measurements or measurement apparatus. Also the weather conditions can be challenging, for instance in northern Europe measurements might have to be performed at temperatures below 0°C.

The tar and particle sampling system consists of a heated probe, a heated particle filter, a condenser and a series of impinger bottles containing a solvent for tar absorption. The bottles collecting tar are placed in a cold bath so that gradual cooling of the sampled gas from about 20°C to the final temperature - 20°C takes place. The gas is sampled for a specified period through the sampling line and filter. The flow rate is maintained with the aid of either process pressure or a pump. The sampling train set-up with solvent impingers is designed for flow rates up to 0.6 m_n^3/h.

The sampling lines including the filter are heated to prevent tar condensation. However, to avoid thermal decomposition of organic compounds, these temperatures must be properly selected. In updraft gasification the temperature of the sampling line and the particle filter should be 100-125°C, whereas in downdraft and fluidised-bed gasification 300 – 350°C has been found as suitable temperatures

The tar collection occurs both by condensation and absorption utilising impingers containing isopropanol, which was found to be the most suitable solvent. The volume, temperature, pressure, and gas flow rate through the equipment are measured after the impinger bottles. The gases from by-pass lines and sample gas are vented safely to atmosphere.

Immediately after sampling the content of the impinger bottlesis decanted into a storage bottle. All surfaces (including metal surfaces) contacting the gas, at temperatures lower than the process temperature, are washed with the solvent. The washes are combined with the actual sample. This is easy to arrange in atmospheric processes, but very difficult in pressurised systems. The storage bottle is stored tightly closed at cool, < 5°C, temperature for later analysis.

In general, sampling of tar and particles is performed simultaneously except for pressurised and/or large-scale gasifiers (>20 MWth) where a sampling strategy based on separate sampling of tar and particles is applied. In pressurised processes, isokinetic operating conditions would require much higher sampling flow rates than 0.6 m_n^3/h when using the minimal nozzle diameter of 4 mm. Hence tar sampling is performed non-isokinetically for pressurised gases. Non-isokinetic tar sampling is also practical in large-scale atmospheric gasifiers where the pipe diameter is large.

Isokinetic sampling is also not necessary when only tar is sampled and when the gas temperature under study at the sampling site exceeds 350°C. Such temperatures generally safely avoid tar condensation in the form of aerosols and/or droplets and also minimises adsorption of organic species on particles.

For non-isokinetic sampling the alignment of the probe in relation to the gas flow is not so stringent, also more freedom is available for the design of the probe nozzle to reduce blockages. This is important especially in pressurised gasification since the probe cannot be removed from the gas line during operation.

5.2. Basic concept of the sampling train

The modular sampling train consists of 4 main modules and respective submodules. The main modules are gas preconditioning, particle collection, tar collection and volume measurement.

In the preconditioning module (Module 1) the process gas is cooled or heated, depending on the process temperature, to a constant temperature of 300-350°C using a heated probe. For updraft gasifiers a temperature of 100-125°C should be chosen. With pressurised gasification the pressure is reduced to atmospheric pressure. The module includes an airtight (sealed) lock.

In the particle collection module (Module 2) a heated filter, maintained at the same temperature as the probe, collects the solids from the gas.

The tar collection module (Module 3) consists of three submodules. In the first submodule the gas is cooled and moisture and some of the tar is collected in a condenser at a temperature of approximately 20°C. The use of a liquid quench, which facilitates cleaning of sampling lines after the sampling, is optional. In the second submodule tar and VOCs are absorbed into the solvent at -20°C in a series of impinger bottles. In the third and optional submodule a backup VOC adsorber collects residual VOC's which may have penetrated the impinger train. The backup VOC adsorber is not necessary when enough impinger bottles, appropriate solvents and collection temperatures are used.

The volume-sampling module (Module 4) consists of three submodules. The purpose of these submodules is to: (a) maintain the sample flow by a pump (not needed in pressurised gasification); (b) adjust and control of flow rate; (c) measure the sample volume; and (d) vent the gas.

The concept of the modular sampling train is shown in Figure 5-1. Table 5-1 summarises the function of each module.

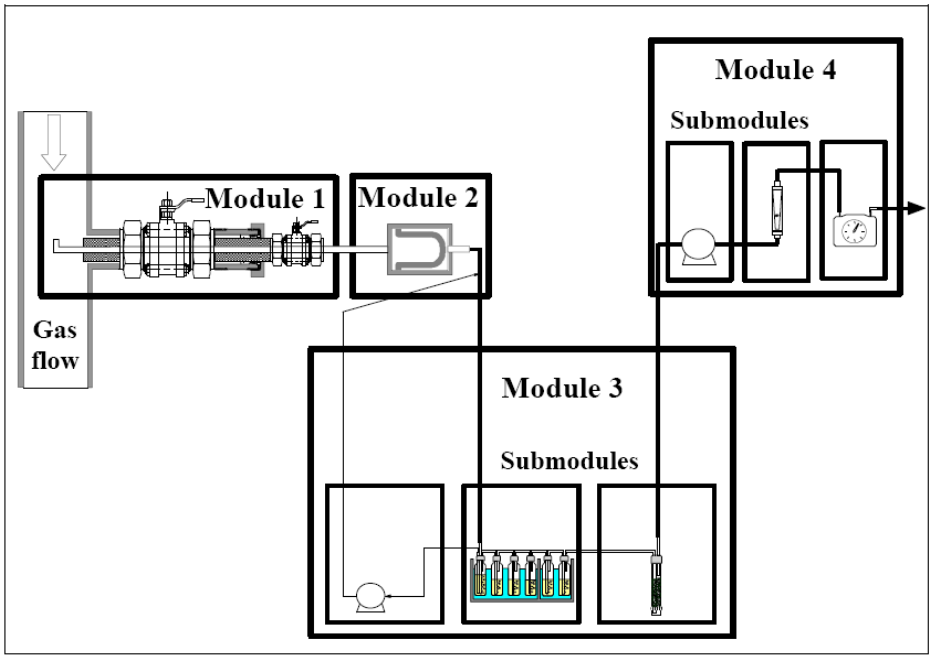

Figure 5-1: Concept of the modular sampling train. The liquid quench is optional.

	Function	Equipment
Module 1 (Gas preconditioning)	Gas cooling, pressure letdown	Nozzle, valves, sampling lines
Module 2 (Particle collection)	Separation and collection of solids	Heated filter (high temperature)
Module 3 (Tar collection)		
SubModule 3.1	Moisture and partial tar condensation	Condenser at 20°C
SubModule 3.2	Tar and VOC collection	Impingers with solvent at T < -20°C
SubModule 3.3	Backup VOC sampler	Adsorber tower (act. carbon, XAD, others) at T_{amb} or lower
Module 4 (Volume sampling)		
SubModule 4.1	Gas suction	Pump
SubModule 4.2	Gas volume integration	Gas meter, needle valve (adjustment and control of flow rate), pressure and temperature indicators
SubModule 4.3	Vent/exhaust gas handling	Outdoor ventilation

Table 5-1: General description of modules and submodules with purpose and equipment used

5.3. Description of sampling module 1 (gas preconditioning)

5.3.1. General

The sampling line consist of a sampling probe (the part that enters gasification conditions), a sampling port (through which the probe is mounted) and additional heated tubes and valves. The line should be short, small in volume and as simple as possible. Additional joints, valves, filters, etc., should be avoided to minimise the risk of leaks. When designing the sampling line, cleaning of the line, sufficient cleaning of sample gas and prevention of condensation should be considered.

5.3.2. Isokinetic or non-isokinetic sampling?

For high-temperature (> 350°C) sampling, where the tar is completely in gas phase, non-isokinetic sampling is sufficient for measuring tar. In non-isokinetic sampling the alignment of the probe in relation to the gas flow as well as the shape of the probe nozzle can be designed more freely to prevent the nozzle from blocking. This is important especially during pressurised operation since the probe cannot be removed from the gas line. Both straight-ended nozzles and those angled at 45° can be used.

Isokinetic sampling requires a special probe. The design of such a probe is described in Paragraph 6.3.

5.3.3. Gas preconditioning for atmospheric gasifiers

The sampling line for an atmospheric process is shown in Figure 5-2.

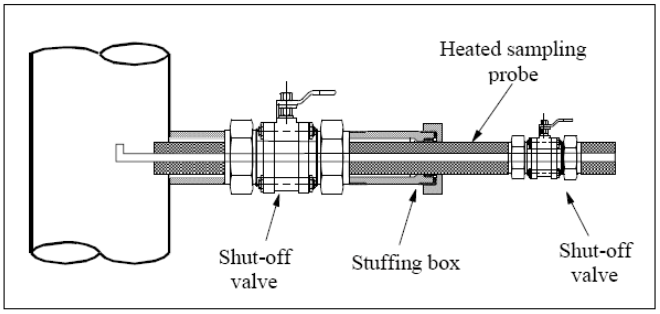

Figure 5-2: Sampling line for gases containing solid and gaseous impurities at atmospheric pressure.

The sampling line is designed in such a way that the probe can be removed through the shut-off valve (ball valve) during operation of the gasifier. The design of the stuffing box is shown in more detail in Paragraph 6.4. A second shut-off valve (ball valve) is mounted between the probe and the particle filter for shutting off the sampling line at any time (also in case of leaks). The valve should be resistant to process temperature (high temperature shut-off valve). Electrical heating of the sampling line prevents condensation of water vapour and condensable gases (clogging of the sampling line). The insulating material should completely cover the sampling line and particle filter to sustain the minimum necessary temperature level and to avoid the formation of cold spots (possible tar condensation) in the line or in the filter.

When tar only is measured, the particle removal from the sample gas can be carried out also at the process temperature with a ceramic filter positioned at the tip of the probe (SiC is a suitable material, since it has very little or no catalytic effects on tar decomposition).

The pressure and temperature of gas is measured at the sampling point.

5.3.4. Gas preconditioning for pressurised gasifiers

For pressurised gases a sampling strategy with separate sampling of tar and particles is required. The gas preconditioning is composed of an inline ceramic filter for the particle collection followed by a pressure relief device (Figure 5-3). The whole sampling line is heated and tar is sampled at ambient pressure.

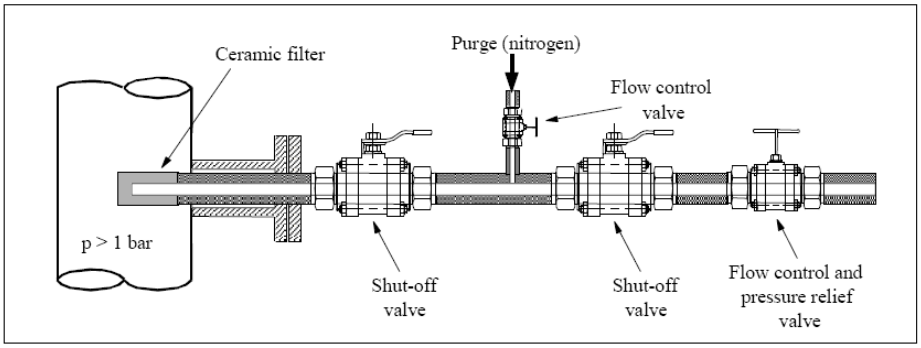

Figure 5-3: An example of a sampling line for a pressurised process for tar measurement only

A shut-off valve is positioned first in the sampling line enabling shut off at any time (also in case of leaks). The shut-off valves must endure the gas temperature (maximum 400°C) at the process pressure. The material of the valves must be carefully selected for each process.

Pressure relief is carried out in stages with three manual control valves. It can also be performed with one valve only (flow control), but a steadier pressure relief and higher reliability in service (leaks due to contamination of valves) are achieved by installing several valves. Pressure relief and clogging in the sampling line are monitored by pressure measurements.

The flow of sample gas is regulated by the last control valve in the line, from which the gas is led through a PTFE hose or through a glass pipe into the condenser. This line should be kept to a minimum length.

Condensation of water vapour and condensable gases before the condenser is prevented by electrically heating the sampling line to 300-350°C. This will prevent blocking of the sampling line. Blocking problems can also be minimised by using two parallel sampling lines equipped with facilities for purging and solvent washing. The type and number of particle separators in the sampling line is chosen on the basis of solids contents in the sample gas. Quartz and fibreglass filters can be used as hot filters. When measuring tar only, ceramic filters can be employed.

As it is not possible to remove the probe from the sample port under pressurised conditions, the sampling probe and the filters can be cleaned by nitrogen purge. Nitrogen flush lines are positioned to ensure that the most important valves and gas lines are cleaned in both directions.

The nitrogen flush of the probe tip has to be continuous except during the sampling.

5.4. Description of sampling module 2 (particle filter)

Particles are collected in an external heated filter system. Quartz filters (absolute filters) must be used as filter material. Retention capacity of the filters should be at least 99,998 % of the particles of size 0,3 µm (DOP standard[1]).

Plate filters are used for particle concentrations below 20 mg/m_n^3 (VDI 2066, part 7). The recommended minimum diameter for the plate filter is 90 mm.

For particle concentrations above 20 mg/m_n^3, filter thimbles are used. Dimensions of filter thimbles are selected for subsequent Soxhlet extraction procedures. The recommended dimensions for the filter thimble are a diameter of 30 mm and a length of 77 or 100 mm. As a general indication, a filter surface area of 100 cm^2 allows the collection of several grams of particles without significant increase in pressure drop over the filter. This is valid for sample flows of 0.6 m^3_n/h and for producer gases containing high temperature tar.

The filter holder must be gas tight. An example of a possible way to mount the filter is shown in Figure 5-4.

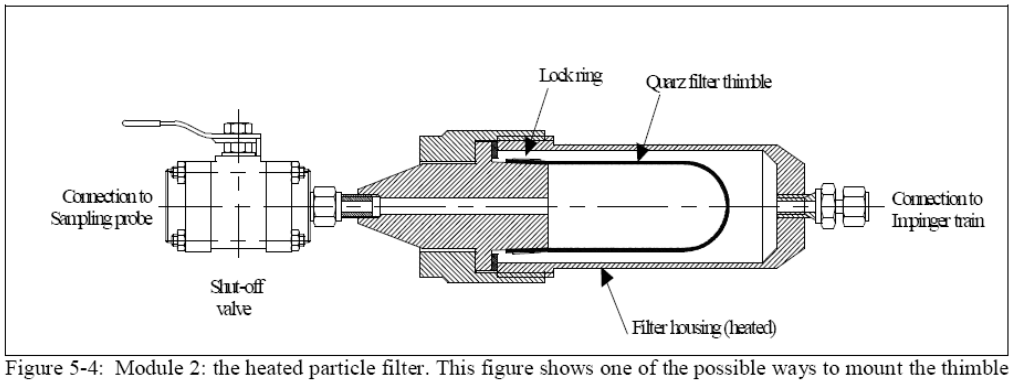

Figure 5-4: Module 2: the heated particle filter. This figure shows one of the possible ways to mount the thimble filter in the housing.

The material of the filter holder should not affect the composition of tar compounds and must endure 50°C higher temperature than the operating temperature is (e.g. AISI 310, AISI 316). A thermocouple is placed inside the filter holder to measure the gas temperature at the filter.

The temperature of the filter is critical and has to be sufficiently high in order to prevent filter plugging caused by the tar build-up, but low enough to prevent further reactions of tar on the filter surface. Operating temperatures are given in Paragraph 5.8.

In case of non-isokinetic tar sampling applications, the particle removal from the sample gas can be undertaken with a ceramic filter at the process temperature, which is positioned at the tip of the probe. SiC is a suitable material for this filter, since SiC has very little or no catalytic effects on tar decomposition. Reverse flow, high-pressure nitrogen purge should be available to clean the SiC filter from particles.

---

[1]: The test method was developed in USA during World War II. DOP is Bis(2-ethylhexyl) Phthalate and is (like other Phthalates) an undesirable compound according to National and EU environmental rules. The most common test aerosols nowadays are Latex particles or DEHS Di (2-ethylhexyl) Sebacate or DOS Dioctyl Sebacate. The term 'DOP test' is used in everyday language, but DOP is not used any more.

The temperature of the stainless steel filter holder (AISI 310, AISI 316) and the SiC filters should be < 700°C to prevent any catalytic change in the concentrations of tar compounds.

5.5. Description of sampling module 3 (tar collection)

The module 3 is schematically shown in Figure 5-5.

The connection between the hot metal tubing and the impinger bottle should be designed accurately to assure the tightness of the joint. The joint can be practised for instance in the following way. The end of the metal tubing is formed identical to the male glass ball ground joint so that it fits the female ground joint of the impinger bottle. The radius of the metal ground joint should be the same or slightly smaller than the similar glass joint. The smaller radius makes the cracking of the glass female joint due to different thermal expansion less likely, but then special attention is needed to the sealing of the joint.

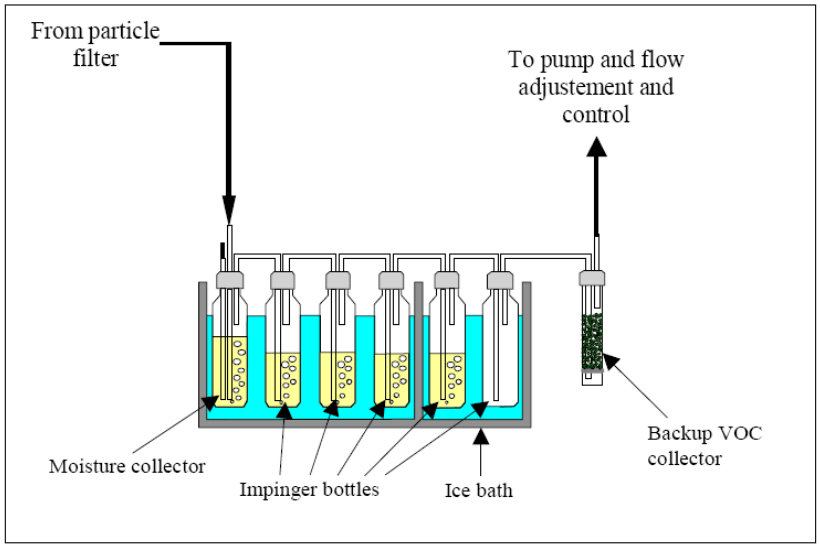

Figure 5-5: Module 3 of the sampling train: impinger bottles and VOC collector

5.5.1. Moisture collector

In the moisture collector, water and tar are condensed from the process gas by absorption in isopropanol at 20°C. The heat released by gas cooling and condensation is removed either in an external water bath or by an additional heat exchanger before the condenser. The heat exchanger may be necessary for high moisture producer gases (e.g. from steam gasification) and designed to meet the demands of the gasifier (see also Chapter 7).

The condenser is a standard impinger bottle (reference arrangement) or can optionally be equipped with an internal liquid quench system which is especially suitable for producer gases containing higher tar levels. The end of the metal tubing connected to the impinger bottle is formed identical to the male glass joint so that it fits the female ground joint of the impinger bottle. When using a liquid quench, isopropanol is the circulating liquid. The working principle of the liquid quench is described in Appendix 13.4.

5.5.2. Liquid tar impingers

After the moisture collector the gas is passed through a series of impingers (at least 3, preferentially 5) each containing approximately 50 ml of solvent. Direct condensation of the liquid effluent without diluting media, e.g., with cold trapping, can result in further reactions of the trapped compounds.

Optionally measures can be taken to disperse the gas flow and thus enhance both mass and heat transfer. One possible measure is the use of glass beads, which can be used in all impingers or in some only. The impinger bottle is half-filled with glass beads. Another possibility is the use of glass frits, either as large as the diameter of the impinger bottle or mounted as filter to the bottom of the impinger bottle gas inlet tube. Fine-meshed frits give better results than coarse-meshed frits, it is recommended to install at least one G3 frit in the impinger train.

Standard glass impingers (100 ml or 250 ml volume) with an inner tube diameter of 4 mm are used. Alternatively, it is also possible to use a modified impinger design as shown in Appendix 13.5.

Temperatures of the impinger bottles are 20°C for the moisture collector and the first three impinger bottles, and -15 or -20°C for the last two impinger bottles. Cooling liquid can be either made of a mixture of salt/ice/water, or a mixture of dry ice with isopropanol or by a mechanical cooling device. The bath should be insulated.

5.5.3. Backup VOC sampler

The optional backup VOC sampler collects the residual solvent or VOC's which may have penetrated the impinger train. The backup VOC adsorber is unnecessary when using several impingers in series, appropriate solvents and collection temperatures. It is primarily used as a pump and volume metering protection device. The backup VOC sampler contains an adsorbent such as activated carbon, XAD or Tenax. The temperature of the adsorbent should be kept low (< 50 °C) to prevent decrease in sampling capacity. With XAD or Tenax, the compounds, which have penetrated the tar impingers, can be recovered and analysed.

5.5.4. Alternative sampling train

During preparation of the Guideline, the partners have gathered experience of the use of the described sampling train. This configuration is the standard configuration. One of the project partners has gained experience with an alternative configuration which is described in Appendix 13.6.

5.6. Description of sampling Module 4 (volume metering)

Figure 5-6 displays the Module 4 equipment: a pump, a flow indicator, pressure and temperature measurement and a volume flow meter.

5.6.1. Sample gas suction device

The gas suction pump (vacuum pump) must be oil free, airtight and pulsation must be minimal. Membrane pumps are recommended because of easy clean up and maintenance. The gas pump must be able to displace at least 1 m^3_n/h at an absolute pressure of 0.5 bar. A flow control valve is recommended to adjust the sample flow rate.

There is no need for a pump when sampling pressurised gasification systems at pressures much larger than 1 bar. However, for slightly overpressurised gasification systems (up to 1,5 bar) a pump might still be needed.

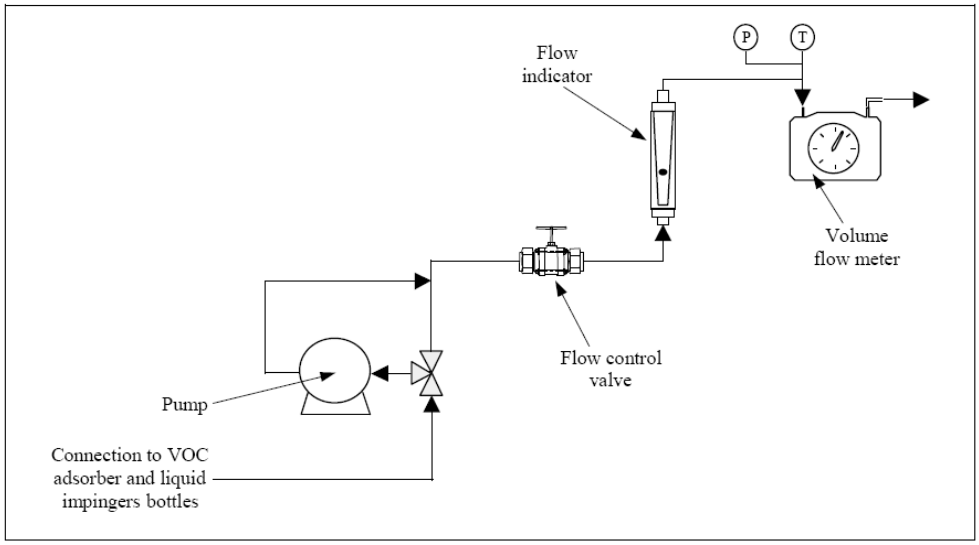

Figure 5-6: Pump and flow measuring equipment in Module 4.

5.6.2. Sample gas meter

To determine the volume of sampled gas, a calibrated dry gas meter with thermocouple is used. The pressure drop over the volume-measuring device should not exceed few hundred Pa.

The gas flow during the removal of flushing gases and essential sampling is monitored with a rotameter. Preferentially, a rotameter is located between the pump and the volume-measuring device, which is used to adjust and compensate the sample flow. A temperature indicator and a barometer is used to correct for temperature and ambient pressure to normal conditions.

The exhaust gases from by-pass lines and sample gas are vented safely to atmosphere.

5.7. Equipment and materials

For sampling line temperatures below 200°C, PTFE or glass tubing is used. For higher temperatures up to 700°C, stainless steel tube (AISI 316 or AISI 310) is a suitable material.

When the temperature exceeds 700°C the accumulation of the catalytically active matter (for example limestone or dolomite) to the tip and bends of the probe may prove problematic.

The equipment and materials required for the construction of sampling system are presented in Table 5-2. All materials and equipment used in sampling should be compatible with national safety regulations. In case the sampling environment is classified as potential explosion area (e.g. standard EN 60079-10) electrical equipment used in sampling should fulfil the required national safety regulation for potentially explosive atmospheres (e.g. standard EN-50014).

Table 5-2: Materials and equipment for sampling system.

Probe :	Acid-proof stainless steel, AISI 316 or Fire-proof stainless steel, AISI 310
Condenser:	Acid-proof steel, AISI 316, glass
	Ice bath
	Compression cooler
Filter:	Quartz fibre filter, size 30 x 77mm
	Max. temperature 950°C
	Retention capacity 99.998% (0.3 μm), DOP-stand.
Filtration:	Filter holder: Acid-proof steel, AISI 316
Ceramic filter:	Silicon carbide, 50 x 30 x 135 mm
	Silicon carbide, o.d. 12.7 mm, i.d. 20.5 mm, length 100 - 300 mm
Liquid quench	Peristaltic pump (3 l/h; 3 m riser level) with Tygon tube, PTFE and stainless steel tubing
Backup VOC adsorber	e.g. activated carbon, XAD or Tenax
Pumps (e.g.):	Membrane pump
Rotameters (e.g.):	Standard rotameter for gas flow rates 1 - 20 l/min
Gas meter:	Dry gas meter

Impinger bottles:	Material is standard laboratory glass (100 ml or 250 ml)
Glass beads:	o.d. 6 mm
Solvent:	Isopropanol, minimum purity 99 % The solvent should not include GC detectable amounts of relevant tar compounds (blank determination by GC essential).
Cold bath:	Acid-proof steel, AISI 316
	Salt, Ice
Sample bottles:	500 ml storage bottle with PTFE coated screw plug (GL45) and pouring ring
Gaskets in the filter holder etc.	PTFE or graphite or copper or Viton

5.8. Design operating conditions for the sampling train

The design sample gas flow rate of the solvent impingement sampling train is 0.1 – 0.6 m^3_n/h whereas the minimum absolute pressure in the sampling duct is 0.6 bar.

The volume of the gas sampled depends on the tar content of the gas. The recommended minimal sampling volume is 0.1 m_n^3 for all producer gas types. The total content of tar in the solution should be at least 100 mg/kg for gravimetric analysis and about 10 mg/kg (10 ppm) of solution for each compound analysed by GC. However, the GC detection limit is significantly lower for single components (0.25 ppm).

The sample probe temperature in updraft gasifiers is maintained between 100 and 125°C and in downdraft and fluidised-bed gasification at 300-350°C.

The temperature of the particle filter varies with the gasifier type. When sampling high temperature tar from downdraft and fluidised bed gasifiers, the preferable filter temperature is 300-350°C or higher in order to avoid condensation of tar on carbon rich particles. When sampling low temperature tar from updraft gasifiers the filter temperature is 100°C to avoid polymerisation of the tar.

At filter temperatures above 250°C, Viton gaskets or plate rings made of copper can be used for the filter housings sealing. At temperatures below 250°C, PTFE can be used.

5.9. Site specific sampling train set-ups

The application of a sampling procedure is dependent on the gasifier type. Most of the gasifiers fall in four categories, which are: 1) fixed-bed updraft, 2) fixed-bed down-draft, 3) fluidised-bed and 4) entrained-flow. In the Appendix 13.1 (Figure 13-1), the basic principles of these gasifier types and typical operating behaviour are shown.

Tar concentrations and its composition and particle concentration depends on the gasifier type and design, on the operating condition, feedstock etc. The tar concentration in countercurrent (updraft) gasifiers is usually high (typically 100 – 200 g/m^3_n) compared to other gasification applications (tar content usually under 20 g/m^3_n). Fluidised bed gasifiers typically produce the highest particle concentration.

Table 5-3 provides an overview of various site specific sampling train arrangements. The term 'Raw Gas' in the figure means gas collected direct from the gasifier without any gas cleaning. The term 'Clean Gas' in the figure means gas cleaned either catalytically, by scrubbing or physical methods (ceramic or bag filters etc).

Gasifier type / Sampling site		Fixed bed cocurrent		Fixed bed countercurrent		FB / CFB atmospheric		FB / CFB pressurised	
		RawG	CleanG	RawG	CleanG	RawG	CleanG	RawG	CleanG
Module 1	(Gas conditioning)	X	X	X	X	X	X	X	X
Module 2	(Particle collection)	X	X	(X)	X	X	X	X	X
SubModule 3.1	(Moisture/tar condensation)	X	(X)	X	X	X	(X)	X	(X)
SubModule 3.2	(Tar/VOC collection)	X	X	X	X	X	X	X	X
SubModule 3.3	(Backup/guard filter)	X	(X)	X	X	X	(X)	X	(X)
SubModule 4.1	(Gas suction)	X	X	X	X	X	X	-	-
SubModule 4.2	(Volume integration)	X	X	X	X	X	X	X	X
SubModule 4.3	(Offgas handling)	X	X	X	X	X	X	X	X

Table 5-3: Overview of sampling train arrangements depending on gasifier type.

Remarks: X = Reference arrangement; (X) = site specific; - = not needed; RawG = Raw gas after gasification reactor (before gas cleaning); CleanG = Clean gas after gas cleaning.

The complete reference set-up of the isokinetic sampling train for tar and particles from biomass producer gases at ambient pressure is shown in Figure 5-7.

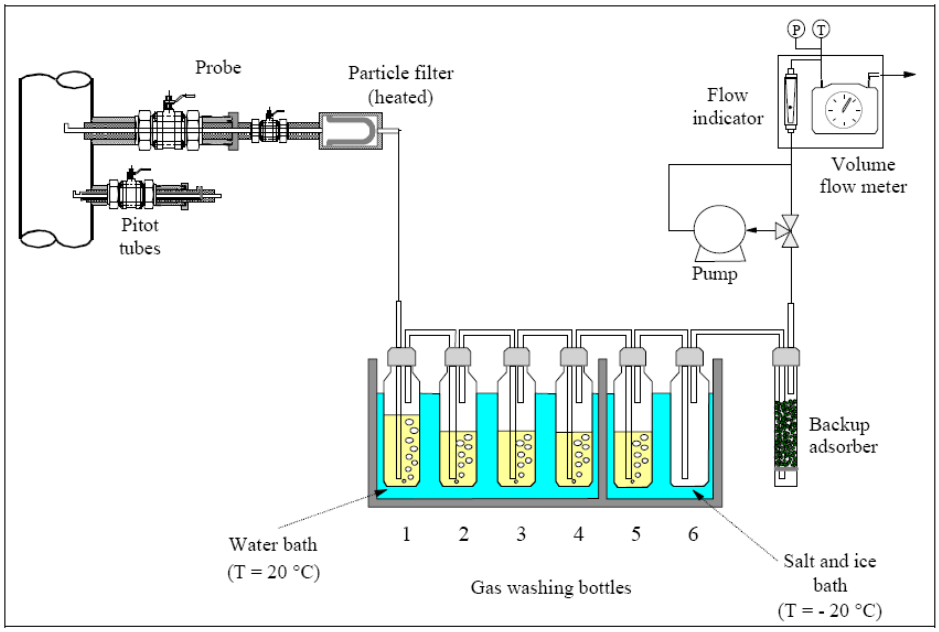

Figure 5-7: Atmospheric and isokinetic sampling train for tar and particles with removable probe and pitot tubes for flow measurement

Remarks: The set-up is based on the use of isopropanol as a tar collecting solvent; alternatively to the pitot tube, an O-type probe can be used for isokinetic measurement

5.10. Type of solvent used

The condensate and the organic compounds present in the producer gas are collected in a solvent. Direct condensation of the liquid effluent without a solvent as a diluting media can result in further reactions of the trapped compounds. The reactivity is suppressed by the solvent. Direct condensation of the effluent also causes that tar aerosols (which are formed when the producer gases cools down, i.e. in the moisture collector) will likely pass the condenser. The absorbing liquid captures these aerosols and the design of sampling train and the choice of the solvent has been optimised to perform this function.

The modular sampling train set-up displayed in Figure 5-1 to Figure 5-7 can be used for both water miscible and non-water miscible (non-polar) solvents.

The boiling point (evaporation rate) and the water solubility are the main parameters, which influence the sampling train set-up:

- With water miscible solvents exhibiting a medium volatility (like isopropanol), a liquid quench with the solvent can be used as an option for gases with high tar levels.
- With water miscible solvents exhibiting a high volatility (like acetone), the first impinger (kept at 0°C) after the condenser can not be filled with solvent. Also the liquid quench option with the solvent cannot be used. Instead conventional cooling (with heat exchangers) or a liquid quench with water can be used.
- With non-polar solvents (like iso-octane) a liquid quench with the solvent cannot be used (at least two-phase liquids or even formation of emulsions occurs). Instead conventional cooling (with heat exchangers) or a liquid quench with water can be used. Besides, attention should be paid to possible formation of ice on the tip of (small) impinger tubes.

In this Guideline isopropanol has been selected to be the most appropriate solvent. The R&D that was performed to come to this selection is described elsewhere (Neeft, Knoef, Zielke, Sjöström, Hasler, Simell, Dorrington, Abatzoglou, Deutch, Greil, Buffinga, Brage, Suomalainen, 2001).

6. Planning and preparation of sampling

6.1. Requirements for the plant operating conditions

Measurements should be performed during stable and known operating conditions of the gasifier. The characteristic operating conditions (such as heat rate, gas production rate, fuel type) during the sampling are summarised together with the plant specification in the sampling logs (Chapter 13.7.4).

6.2. Requirements for the main gas stream

The flow in the main gas duct must be undisturbed for ideal isokinetic sampling. The measuring port(s) should not be positioned in bends or near ventilators, valves etc. As a general rule, the length of the main gas duct before the sampling port should be at least 5 times its hydraulic diameter D and at least 3 times its hydraulic diameter after the sampling port (ISO9096 or VDI2066, part 1). The number of sampling points at one port depends of the diameter of the gas pipe. The instruction to calculate the number of sampling points is given in ISO 9096 or in VDI 2066 (part 1).

Preferentially the main duct is in a vertical position for the mounting of the sampling port. The gas velocities in the main gas duct should be higher than 5 m/s.

6.3. Requirements for the sampling line

The sampling line should be kept as short as possible. To prevent plugging problems, the inside diameter of the sampling line should be at least 3 mm. The sample nozzle diameter can be calculated with the equations given in Paragraph 7.1. The minimal nozzle diameter is 4 mm according to ISO 9096 and 5 mm according to VDI 2066, part 2. In this Guideline, the nozzle diameter should at least be 4 mm. Design parameters for nozzle shapes used to isokinetic measurements can be found in ISO 9096 or VDI 2066.

The sample probe is positioned in the same direction as the flow or positioned at a 90° angle to it. The sampling line is heat-traced at a constant temperature over the filter. The probe is maintained at the process temperature, but above tar condensing temperature, so as to prevent any condensation in the probe. Since high temperature gas cools very quickly, tubes made of stainless steel are appropriate. For gas temperatures below 200°C, PTFE or glass tubing can be used. For gas temperatures above 600°C, special material such as Inconel is preferred. The temperature of stainless steel sampling probe (AISI 310, AISI 316) should be limited to below 700°C preventing changes to the concentrations of tar compounds.

To avoid particle deposition in the sampling tubes, the gas velocity in the tubes must be higher than 25 m/s. The temperature of the tube must be 300 - 350°C to prevent the particles adhering to tar condensed on the tube walls.

Gas contact times with hot parts of the sampling line should be minimised.

In atmospheric sampling the sampling probe is cleaned after each sampling either by flushing with nitrogen pulses or by dismantling and cleaning it manually. As it is not possible to dismantle the probe between samplings in pressurised conditions, the probe and the filters are cleaned by nitrogen purge.

6.3.1. Measurement of actual gas velocity

Isokinetic measurement requires the knowledge of the actual gas velocity at the sample point or the use of an O-type probe (see Figure 6-2).

Gas velocities in producer gas streams at near ambient pressure are preferentially measured with (calibrated) pitot tubes. The instructions for using pitot tubes are given in ISO 9096, an example of the layout is given in Figure 6-1. Pitot tubes must be heated to process temperature, back-flushing facilities being advantageous.

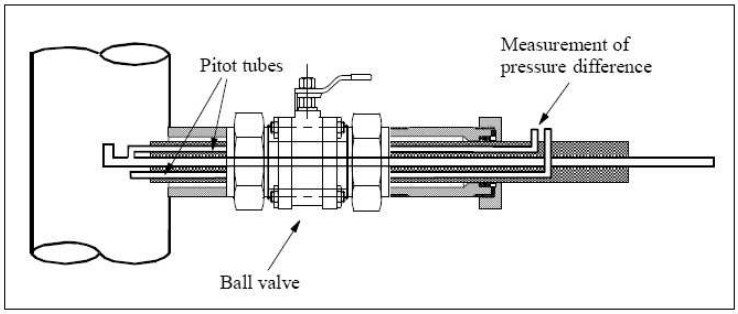

Figure 6-1: Pitot tubes for measurement of the producer gas flow.

In pressurised gasification applications removable pitot tubes cannot be used and hence gas velocities at the probe tip can not be measured. Alternatively, an O-type probe has been found to work well for pressurised producer gases (Figure 6-2). The O-type probe is also suitable for atmospheric applications.

If there is no velocity meter available calculation is performed according to Paragraph 7.1.

6.3.2. O-type probe for isokinetic sampling

Isokinetic sampling can be performed using an O-type probe configuration (Figure 6-2) both for sampling atmospheric pressure gas and pressurised gases. For sampling from pressurised systems an O-type probe configuration is the preferred choice. This type of probe has been found to operate relatively well under pressure.

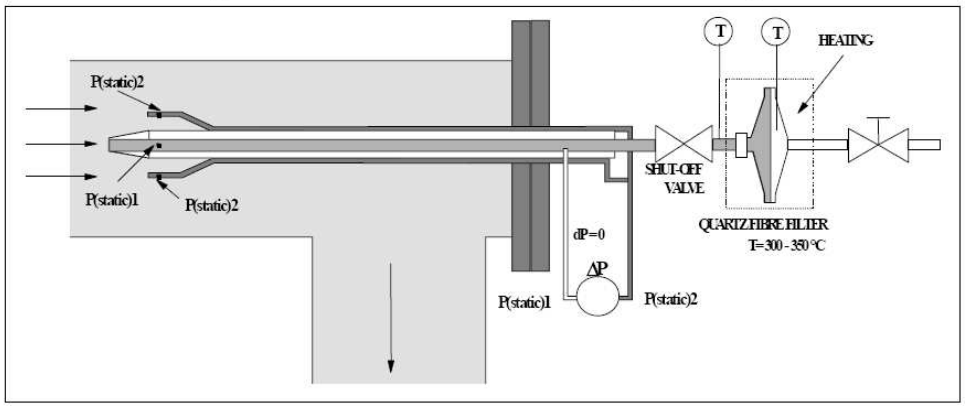

Figure 6-2 The configuration of the O-type probe

Isokinetic sampling is required for particles and low-temperature tar sampling points (temperatures under 350°C), where a proportion of the tar can be present as aerosols in the gas. In the case of isokinetic measurements the number of measuring points is defined by the diameter of the gas pipe. Details are found in ISO 9096 or VDI 2066. For non-isokinetic sampling one measurement point is sufficient.

6.4. Requirements for the sampling port

Sufficient space must be available to ensure easy access to sampling ports and placement of sampling equipment, typically an area of 4 m^2. There should be good air-conditioning in the sampling site and exhaust gases must be safely vented to atmosphere. Work in the vicinity of pressurised systems should be avoided or kept to a minimum.

In pressurised gasification processes, the O-type probe (Figure 6-2) or other sampling probe(s) must be mounted before the start-up of the plant. The nitrogen flush through the probe tip has to be continuous except during the sampling.

In atmospheric processes, probe mounting during operation is possible. The mounting must be carried out safely both for producer gases with positive or negative pressure since combustible and poisonous sample gas exhibits a potential risk of explosion, fire and poisoning.

The joint of the atmospheric sampling probe is illustrated in Figure 6-3. The sampling port includes a main shut-off valve (a 2" ball valve) which must be assembled before plant startup. The sampling probe with the gas tight joint (stuffing box) can be mounted during gasifier operation. The stuffing box structure enables mounting the probe, warming the probe after mounting and displacing the probe without the danger of a gas leak.

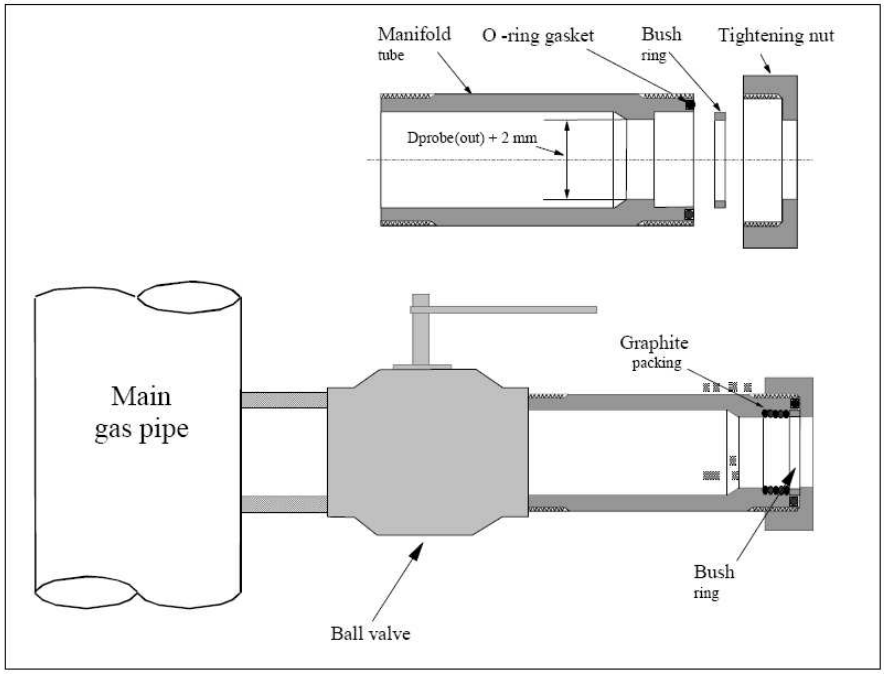

Figure 6-3: Sampling port with lock consisting of ball valve and stuffing box (the sampling probe is not shown)

6.5. Preparation of the sampling

6.5.1. Gas velocity meter

The pitot tube is the only measurement principle described within this Guideline which allows a measurement of the absolute gas velocity in the main gas stream. However, its use is limited to gases near atmospheric pressure. Accurate gas velocity measurement asks for calibrated pitot tubes. The pitot tubes are preferentially heated to process temperature. Possible plugging can be tested e.g. by gently blowing nitrogen through the tube. The preparation and calibration instructions of pitot tubes are found in ISO 9096.

6.5.2. Particle filter

Filter thimbles or plates must be preconditioned according to Paragraph 8.1.2. A fast, easy and gas-tight clamp system should be used at both ends of the filter holder.

The filter holder including the filter is heated to its set value.

6.5.3. Moisture collector

Prior to sampling the moisture collector cooling system is checked. The preparation procedure depends on the chosen collector system. However, sufficient time should be allowed to ensure that the cooling system reaches the required temperature.

In case where a liquid quench system is used, the recirculating system is filled with the chosen liquid. After that, the liquid pump is switched off.

6.5.4. Tar impingers

The solvent used for tar absorption and the (optional) glass beads used for improving heat and mass transfer are added in gas impinger bottles. In each impinger, approximately 50 ml of solvent is added. The drop-collecting bottle is placed after the impingers. The entire impinger train (incl. drop separator) is placed in the salt/ice bath. For a sampling temperature of –20°C, this cooling procedure requires approximately 30 minutes.

The cooling liquid can either be a mixture of ice/salt/water or of isopropanol/dry ice or by cryostatic cooling of isopropanol. When using an ice/salt/water cooling mixture, make sure that the mixture is wet.

6.5.5. Cleaning of equipment before site measurements

Before using the equipment in connection with a site measurement, all glass equipment (sampling probe, impinger bottles, fritts, transport bottles etc.) have to be cleaned according to an internal laboratory instruction. Oil or tar contaminated glass equipment have to be put to soak in an alkaline bath (pH 11-12) for 24 hours. After this the glass parts have to be washed in a laboratory dishwasher with the following program:

1. Primary rinse with soften water
2. Wash at 85 °C for 45 minutes.
3. Rinse 4 times with demineralizated water.

After this, the glass parts are heated in an oven to 500°C for 2 hours in order to remove possible organic residue on the glass.

After cooling, the glass parts are sealed with plastic wrap (parafilm).

PTFE hosing has to be rinsed with DCM and acetone under save laboratory conditions until the tubes appear clean. From time to time, the cleaning procedure is checked by analysis of rinsing liquid. After washing, the tubes are sealed with plastic wrap (parafilm).

6.5.6. Choice of correct nozzle size

The diameter of the sampling nozzle is normally determined by the requirement that the isokinetic sample flow in the beginning of a measurement should equal to about 70% of the sampling trains pump capacity. In this Guideline the sample flow rate is limited to 0.1-0.6 m^3_n/h. The calculation of the correct nozzle size appears from Paragraph 7.1.

6.5.7. Backup VOC adsorber

The backup VOC sampler is positioned as specified and prepared according the type of adsorbens selected.

6.5.8. Gas suction and volume metering

The calibrated gas volume meter and the pump are connected to the sampling line and to the vent gas line. The temperature and the atmospheric pressure are measured.

7. Sampling procedures

7.1. Isokinetic sampling

Isokinetic sampling means that the velocity entering the sample probe (nozzle) must equal the free stream velocity of the gas being sampled:

$$v'_a = v'_N \qquad \text{(Eq. 7-1)}$$

When the sample gas velocity v'_N is higher than the gas velocity in the duct v'_a, the sampling is designated as over isokinetic. Since over isokinetic sampling implies lower sampling errors in particle concentrations and exact isokinetic sampling is not always possible in practice, the sampling should to be conducted within the following limits

$$0.95 < \frac{v'_N}{v'_a} < 1.15 \qquad \text{(Eq. 7-2)}$$

Within this Guideline, two isokinetic sampling principles and one quasi isokinetic principle based on a mass balance are described. The principles are:

a) Measurement of dynamic pressure with a pitot tube followed by determination of actual gas velocity and isokinetic flow rates
b) Measurement of static pressure difference with an O-type probe and adjustment of isokinetic sampling conditions
c) Estimation of the producer gas generation rate by applying a mass balance

7.1.1. Adjustment of isokinetic sampling based on pitot tube measurement

Pitot tubes measure the pressure difference between the total pressure and the static pressure = the dynamic pressure in the sampling line. When using a standard pitot tube, the gas velocity v'_a at a sampling point is expressed as

$$v'_a = \sqrt{\frac{2 \cdot \Delta p_{Pt}}{\rho'_a}} = \frac{q'_{Va}}{A \cdot 3600} \qquad \text{(Eq. 7-3)}$$

In connection with this Guideline the dried gas sample flow rate q_{Vg} is measured by a gas volume meter. The velocity in the nozzle opening amounts to

$$v'_N = \frac{q'_{VN}}{a \cdot 3600} = \frac{q_{Vg}}{a \cdot 3600} \cdot \frac{p_{am} + p_g}{p_{am} + p_a} \cdot \frac{273.15 + \Theta_a}{273.15 + \Theta_g} \cdot \left(1 + \frac{f_n}{0.804}\right) \qquad \text{(Eq. 7-4)}$$

From equations 7-1, 7-3 and 7-4 it follows that the volumetric gas flow rate through the gas meter becomes

$$q_{Vg} = \sqrt{\Delta p_{Pt}} \cdot 3600\, a \cdot \sqrt{\frac{2}{\rho'_a}} \cdot \frac{p_{am} + p_a}{p_{am} + p_g} \cdot \frac{273.15 + \Theta_g}{273.15 + \Theta_a} \cdot \frac{1}{(1 + \frac{f_n}{0.804})} \qquad \text{(Eq. 7-5)}$$

7.1.2. Adjustment of isokinetic sampling conditions using O-type probe

Isokinetic sampling is best performed using an O-type probe, which incorporates separated hollow chambers surrounding the nozzle. The hollow chambers (measurement chambers) are provided with a number of holes internally and externally which connect the chambers with the interior and the exterior of the nozzle through which the main stream of gases pass. The static pressure in the chambers is monitored via pipe connections to the pressure gauge. Figure 7-2 shows an O-type nozzle of this design, however, it has the disadvantage that special fabrication is required. A simpler O-type probe is illustrated in Figure 7-1.

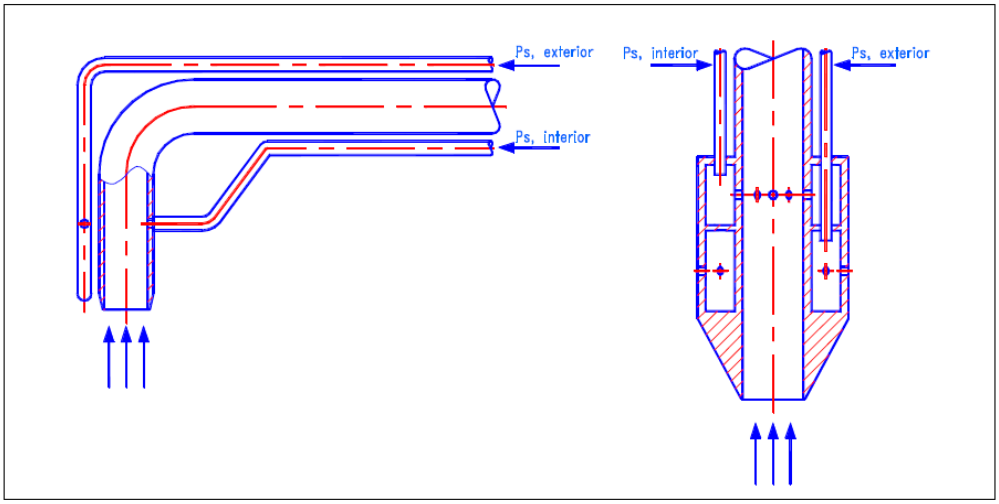

Figure 7-1 Simple O-type probe

Figure 7-2 O-type probe

Isokinetic sampling conditions are achieved by equalising the interior and exterior static pressure signal. When the difference between the two signals is zero, the gas velocity in the nozzle is deemed to be the same as outside the nozzle. Continuous equalisation is established by means of the bypass valve on the vacuum pump.

A series of tests have been carried out in order to determine the magnitude of errors resulting from deviations from the zero pressure. The tests show that in low velocity streams significant sampling errors may result from small deviations from zero pressure. For example, in a duct with a gas velocity of 5 m/s, a 40% sampling error may result from a 12 Pa deviation from zero. For a gas velocity of 15 m/s, the same deviation from zero would result in only a 3% sampling error. In sites where steady flow conditions frequently do not exist and in low velocity streams the use of O-type probe is not reliable and it is useful only as a rough means of adjustment to approximate isokinetic conditions.

7.1.3. Estimation of isokinetic sampling based on calculation from the gasifier load

Where pitot tubes or O-type probes can not be used or are not available, the producer gas flow rate and the isokinetic sampling rate can be calculated from a mass balance. The method presented here determines the producer gas flow rate from the gas yield and the gasifier load and can be applied to all types of gasifiers.

The calculation method presented here is based on a total carbon balance and can be applied when the following requirements are satisfied:

a) Gasifier operation is stable;
b) Main gas composition (CO, CO_2, CH_4) are known;
c) Fuel feeding rate (in kg/h), fuel moisture and carbon content are known;
d) Solid or liquid carbonaceous effluent streams (bottom ashes, particles, tar) and their carbon content are known.

The general calculation of the producer gas flow rate based on an elemental carbon balance can be written as

$$q_{m,fuel}\,cc_{fuel} + \sum q_{V,agent}\,cc_{agent} = q_{V,gas}\cdot\left(cc_{gas} + c_{tar}\,cc_{tar} + c_{particles}\,cc_{particles}\right) + q_{m,ash}\,cc_{ash} \quad \text{(Eq. 7-6)}$$

with
$q_{m,fuel}$ = Fuel feeding rate [kg dry biomass / h]
cc_{fuel} = Carbon content of fuel [kg C / kg dry biomass] (= 0.47 for woody biomass)
$q_{V,agent}$ = Gasification agent feeding rate [m^3_n/h]
cc_{agent} = Carbon content of gasification agent [kg C / m^3_n]
$q_{V,gas}$ = Producer gas generation rate [m^3_n/h]
cc_{gas} = Carbon content of non-condensable gases (CO, CO_2, CH_4) in producer gas [kg C / m^3_n]

c_{tar} = Tar concentration in producer gas [kg/m^3_n]

cc_{tar} = Carbon content of tar [kg C / kg tar]

$c_{particles}$ = Particle concentration in producer gas [kg/m^3_n]

$cc_{particles}$ = Carbon content of particles [kg C / kg dry biomass]

$q_{m,ash}$ = Bottom ash rate [kg dry ash / h]

cc_{ash} = Carbon content of bottom ash [kg C / kg dry ash]

Generally, the gasification agent does not contain carbonaceous gas components, hence $cc_{agent} = 0$. Dividing equation by the fuel feeding rate and rearrangement gives the specific producer gas yield

$$Y_{gas} = \frac{q_{V,gas}}{q_{m,fuel}} = \frac{cc_{fuel} - c_{ash,fuel}\ cc_{ash}}{cc_{gas} + c_{tar}\ cc_{tar} + c_{particles}\ cc_{particles}} \qquad \text{(Eq. 7-7)}$$

with Y_{gas} = Producer gas yield [m^3_n/kg dry biomass]

$c_{ash,fuel}$ = Ash content of fuel [kg / kg dry biomass]

The method determines the dry producer gas yield on dry basis and does not require any information on the moisture content of the producer gas. Multiplication of the gas yield by the fuel feeding rate (dry basis) provides the actual producer gas flow rate (dry basis; 0°C, 101300 Pa). As the sampled gas volume is also measured as dry gas, the target isokinetic sampling flow can be controlled during sampling by monitoring and adjusting the gas meter.

Analogous to the pitot tube velocity measurement, the calculation of the effective isokinetic sampling conditions from equation (Eq. 7-7) can also be performed after the sampling.

The producer gas yield is a characteristic feature of the chosen gasification reactor under the given operating conditions (load, fuel moisture, fuel type etc.). Examples of producer gas yields are given Table 7-1.

		Countercurrent fixed bed gasifier	Cocurrent fixed bed gasifier	CFB gasifier
Fuel moisture	wt% (daf)	50	16	15
Ash content	wt% (daf)	1	1	1
C in bottom ash	wt%	1	50	10
H_2	%	18.0	14.2	14.8
CO_2	%	7.0	12.9	15.0
CO	%	32.0	18.0	15.4
CH_4	%	5.0	1.9	4.2
Particle	mg/m^3_n	200	1,000	20,000
C in particles	wt%	80	80	80
Tar	mg/m^3_n	100,000	1,000	20,000
C in tar	wt%	60	90	90
Gas yield according to (Eq. 7-7) Y_{gas}	m^3_n/kg (daf)	1.84	2.73	2.23
Fraction of C in particles, bottom ash and tar	% of total C in gas	11.3	1.0	15.5

Table 7-1 Calculated producer gas yields from various gasifiers using wood as fuel

Remarks: A survey of typical gas composition, tar and particle concentration from various gasifier reactor types is given in Appendix 13.1. Carbon content of the fuel is 49 wt% (typical for leavy wood); carbon content in particles, bottom ash and tar are estimated from typical experimental data.

For a typical cocurrent gasifier, the fraction of carbon found in the bottom ash, particles and tar typically amounts to 1% of the total carbon in the gas. Hence, the carbon in the carbonaceous effluent streams has no significance for the producer gas yield calculation for such type of gasifiers. For countercurrent and fluidised bed gasifiers, the amount of carbon in particles and tar ranges from 10% to 15% of the total carbon in the gas. In these cases, some (pre) information of the tar and particle levels is required to determine gas yields accurately.

Another method for estimation of the producer gas flow rate which can be used e.g. for cocurrent gasifiers coupled to IC engines is based on the determination of the displaced gas volumes within the engine cylinders [BTG, 2000 and Ramackers, 1985]. This method requires the cylinder volume, the engine speed and air supply and the oxygen content in the exhaust gas.

7.1.4. Calculation of nozzle diameter

The nozzle diameter is chosen in order to adjust the velocity in the nozzle to the surrounding duct velocity. Furthermore, the correct choice of nozzle contributes to obtain a suitable duration of sampling and a suitable sample flow rate. The suitable sample flow rate through impinger bottles is often a barrier for proper isokinetic sampling. Several CEN standards recommend a flow rate between 8 and 33 l/min for Midget and Greenburg-Smith impingers and a flow rate between 1 and 3 l/min for impinger bottles with frits. A specially designed VTT impinger is suitable in the range of 2 to 10 l/min.

With a maximum flow rate of 10 l/min and a minimum nozzle diameter of 5 mm it is possible to make isokinetic samplings up to a maximum gas velocity of 8.5 m/s on the condition that there are constant gas conditions through the sampling train. As producer gas normally contains some humidity and has a higher temperature than the gas in the sampling train, the velocity will be higher than 8.5 m/s in practice.

A general expression for calculation of nozzle diameter based on known gas velocity (measurement with pitot tube including moisture content) appears from the following equations:

$$v'_N \cdot a \cdot 3600 \;=\; q'_{VN} \;=\; q_{Vg}\,(1+\frac{f_n}{0.804})\cdot\frac{p_{am}+p_g}{p_{am}+p_a}\cdot\frac{273.15+\Theta_a}{273.15+\Theta_g} \qquad \text{(Eq. 7-8)}$$

the nozzle face area a

$$a \;=\; A\cdot\frac{q_{Vg}}{q'_{Va}}\,(1+\frac{f_n}{0.804})\cdot\frac{p_{am}+p_g}{p_{am}+p_a}\cdot\frac{273.15+\Theta_a}{273.15+\Theta_g} \qquad \text{(Eq. 7-9)}$$

where $0.1 \le q_{Vg} \le 0.6$ m^3_n/h and the nozzle diameter d_N is calculated as follows

$$d_N \;=\; \sqrt{\frac{4\cdot a}{\pi}} \qquad \text{(Eq. 7-10)}$$

A general expression for calculation of nozzle diameter based on the assumption of a gas yield shown in Table 7-1 appears from the following equation:

With a gas yield value from Table 7-1, which fits the present object, it is possible to calculate the wet producer gas flow q'_{Va} and the gas velocity v'_a

$$q'_{Va} \;=\; Y_{gas}\cdot\dot{m}_{fuel}\cdot\frac{101300\cdot(273.15+\Theta_a)}{273.15\cdot(p_{am}+p_a)}\cdot(1+\frac{f_n}{0.804}) \qquad \text{(Eq. 7-11)}$$

$$v'_a = \frac{q'_{Va}}{A \cdot 3600} \quad \text{(Eq. 7-12)}$$

The appropriate nozzle area is expressed by

$$a = A \cdot \frac{q'_{Vg}}{q'_{Va}} = A \cdot \frac{q_{Vg} \cdot (1 + \frac{f_n}{0.804})}{q'_{Va}} = A \cdot \frac{q_{Vg} \cdot 273.15 \cdot (p_{am} + p_a)}{Y_{gas} \cdot \dot{m}_{fuel} \cdot 101300 \cdot (273.15 + \Theta_a)} \quad \text{(Eq. 7-13)}$$

According to ISO 9096 the minimum nozzle size should be 4 mm.

7.2. Sampling train leak test

Leaking of the sampling train can be tested either by pressurising or underpressurising the entire sampling train starting from the particle filter inlet to the gas meter inlet. The test should be done at a pressure, which is 0.2 bar above or below the maximum sampling over or under pressure.

Pressurising of the train is carried out gently feeding gas from a cylinder into the particle filter inlet and the rest of the sampling train. The exit of the gas pump is locked by a ball valve. The pressure in the sampling line is monitored/observed by a pressure indicator (should stay constant). Possible leaks can also be detected as gas bubbles in the impingers or by leak indicators. Stopping the gas supply from the cylinder and carefully opening the shutoff valves after the pump terminates the leakage test. The pressure release procedure must be undertaken with utmost care and generally lasts for at least one minute.

The vacuum leakage test is done by using the gas metering pump. A shut-off valve is placed in a closed position at the inlet of the particle filter. The gas pump is turned on and the pressure is gently reduced to its desired value. Possible leaks are detected as gas bubbles in the impingers or by monitoring the gas meter reading. Termination of the leakage test is performed by carefully opening of the ball valve at the particle filter inlet while the pump is still displacing. When gas bubbles penetrate the condenser and the impingers, the gas flow rate is reduced by gently opening the bypass valve over the pump. The pressure release procedure must be performed with utmost care and generally lasts for at least one minute.

If the gas mixture to be studied does not contain oxygen, leaks can be detected also during sampling by an oxygen analyser connected to the sampling line.

7.3. Execution of sampling

It is preferred that the gas composition, the gas temperature and the static pressure in the gas line are measured and recorded continuously.

The leak test of the sampling train (see Paragraph 7.2) must be made before the probe and the particle filter are mounted.

The sampling apparatus for atmospheric gasifiers is designed such that the probe can be inserted and removed from the sampling port during gasifier operation without any gas leaks or entry of air into the gas line. The probe is inserted via the sampling port to the closed shut-off valve. The procedure is as follows:

1. Ensure that the sampling port is free from tar and particle deposits between the ball valve and the gas line. Ensure that the ball valve can be operated easily and that the stuffing box can be tightened.
2. Ensure that the impinger train is connected correctly and that the stop valve in the sample line is closed. Mark the distance from the sampling point to the stuffing box on the sampling probe. Insert the probe into the lock and tighten the stuffing box slightly. Heat the sampling probe to its set value and cool the impinger bath to its set value.
3. Impurities must not enter the nozzle opening during insertion and withdrawing of the probe. Do not touch any walls with the nozzle opening.
4. Open the ball valve and move the heated probe forward into sampling position (normally one point in the centre of the gas line is sufficient in gas lines with a diameter smaller than (or equal to) 350 mm). In gas lines with a larger diameter, the number of sampling points have to be determined according to ISO 9096. The nozzle axis is held at a right angle to the gas flow direction. Tighten the stuffing box.
5. Mount the particle filter and heat to its set value.

6. Wait for the correct sampling temperature.
7. Read the gas volume meter. Record the starting time. Turn the probe tube until the nozzle faces directly upstream, start the vacuum pump, start the timing device and open the stop valve. Then adjust the control valve to give the required flow reading as calculated according to nozzle size, gas velocity, etc.
8. Monitor the rotameter, which is used as a indicator of the gas flow and the static pressure measurement at the gas volume meter. Adjust the control valve as necessary throughout the sampling period to maintain isokinetic sampling. Record the temperature and static pressure at the gas volume meter at regular intervals. During sampling check the temperature of the impinger cooling bath and the temperature of the filter housing.
9. Occasionally agitate the condenser cooling liquid and the impingers to ensure even temperature distribution in the cooling media.
10. When an adequate quantity of tar and particles has been collected or if the pressure drop in the sampling train prevents isokinetic sampling, the sampling has to be terminated (see Paragraph 7.4).
11. Close the stop valve in the sample line, stop the timing device, stop the vacuum pump and turn the probe tube through 90 °. Dismantle the particle filter. Withdraw the probe until the ball valve can be closed and then remove the probe with great care in order to avoid contact with any deposits within the gas line or the sampling port.
12. Record the time for stopping and the gas volume meter; as soon as possible remove the filter cartridge from the filter housing and store it in solvent in a tightly closed bottle, to avoid polymerisation of tar during cooling. Then clean the sample line (see paragraph 7.5) and prepare the samples for subsequent analysis (see paragraph 7.6).
13. When the probe is not removed (e.g. press. gasifiers), the probe is flushed with N_2.

When it is necessary to repeat the measurements of the tar and particle concentration, then repeat procedures 1 to 13. Prepare the next sampling (including leakage test) as soon as possible and be sure that comparable plant conditions are available. Normally, between 2 and 6 measurements should be sufficient for determination of tar and particle content in producer gas. If the gasification process is not quite stable, it could be necessary to carry out even more measurements.

7.4. Duration of sampling

The actual quantity that is collected depends on the concentration, sampling time and pump capacity. For low concentrations, increased sampling time and pump capacity will be needed in order to collect an adequate quantity. Otherwise, improvement of the weighing procedure is necessary to obtain an acceptable weighing error.

With gravimetric measurements of tar and particle concentrations it is assumed that the weighing inaccuracy is better than 5%. To achieve this, an adequate quantity of tar and particle matter has to be collected. With an error of 0.2 mg per weighing, and considering the fact that the collected amount is calculated from the difference of two weightings (5% ≡ 0.3 mg), an adequate quantity of gravimetric tar in the sample for the analysis amounts to about 6 mg.

For GC based individual compound analysis, the adequate compound quantity amounts to about 5 to 10 mg/litre solution. The sampling duration can be calculated on the basis that 300 ml solvent is used for sampling and equipment cleaning and 300 ml of solvent is used for the Soxhlet extraction procedure from the particle filter. In case where the optional liquid quench system is used, an additional amount of approx. 300 ml of solution will be generated.

In connection with high concentration measurements the minimum sampling time for collection of an adequate quantity of matter can be < 30 minutes. In this case it is recommended to sample more matter than the minimum matter required. If the particle filter clog up within 30 minutes, it is recommended to stop the measurement and start a new measurement with smaller nozzle and lower sample flow rate, but still in accordance with isokinetic sampling.

In connection with low concentration measurements it is recommended to use the largest nozzle possible and the highest allowed sampling flow rate, also in accordance with isokinetic sampling.

With high moist gas, a large amount of condensate will be generated thus requiring adequate volumes of condensers. Generally, also the moisture content of the gas is determined thus a certain amount of condensate is required to accurately determine the gas moisture.

7.5. Equipment cleaning after sampling

After termination of sampling, the unheated parts of the sampling train must be rinsed in order to collect tar deposits from the train. Disconnect the flexible tubing from the probe tube. With a wash bottle inject solvent into the hose and shake until the hose appears clean. Use no more solvent than necessary. Transfer the rinsing solvents to a storage bottle.

7.6. On-site preparation and storage of samples for analysis

The sampling solution is stored in a sealed, dark bottle, which is marked with a clear identification label and kept at a temperature < 5 °C until analysis. In some cases (e.g. countercurrent raw gases) it may be necessary to store the liquids in nitrogen atmosphere and in dark bottles. The analysis is preferably performed as soon as possible and should be completed within a month after sampling. Instead of a dark bottle, also a glass bottle can be used that is kept in the dark.

The particle filter must be handled with great care. When removing the filter from the housing it is imperative that no particles are added to or dropped from the filter. It is also imperative that no filter material is lost during handling.

The filter cartridge is stored in solvent in a jar with sealed screw cap. At least the same solvent must be used for the filter storage as for the Soxhlet extraction, preferably the same solvent as for sampling and/or for analysis). The storage jar is marked with a clear identification label and it is kept at a temperature < 5 °C until analysis.

The plate or membrane filters are stored in a sealed Petri dish with a suitable diameter.

8. Analysis of samples

Biomass tar is a complex material consisting of hundreds of compounds, varying widely in polarity and molecular mass. The main products from the thermal processing of biomass are carbon monoxide, carbon dioxide, hydrogen and methane. However, small amounts of organic 'contaminants' are formed as undesirable by-products and it is a common perception that these toxic by-products will have detrimental effects both on down-stream treatment plant and power generation packs, and if emitted to atmosphere, the local environment. Reliable sampling and analysis of these products from biomass gasification is essential for the successful process development and economical operation of commercial gasifiers.

During the tar formation period in the gasifier the free radical content is high rendering the tar mixture unstable and reactive. When the tar is isolated and allowed to cool down polymerisation/oxidation reactions occur resulting in a high molecular weight material with complex structures. The analysis of the tar should be performed as soon as possible after sampling but within one month, minimising any polymerisation/oxidation reactions.

Positive identification of the condensed material as biomass tar is performed using GC-MS, which is used to identify the compounds present in the tar. The presence of tar is indicated typically by the presence of the US-EPA suite of PAH compounds, phenols and BTX. Quantitative determination of each compound can then be performed either by GC-MS or GC-FID analysis using internal standards. It may be necessary for the process operator to quantify certain compounds present in the tar and to use these as markers in order to improve the gasification process.

Not all of the tar constituents are amenable to GC analysis, because of the presence of high molecular weight material. GC analysis will usually determine more than 80% of the tar, the remainder being high molecular weight material of >350 g/mol. Only for updraft gasifier tars, this fraction can be considerably lower.

The main compounds of interest to operators, particularly of gas turbines, are the PAH compounds in the range naphthalene to indeno (1,2,3 cd) pyrene, phenols, methylphenols and dimethylphenols.

Figure 8.1 shows schematic for post sampling procedures

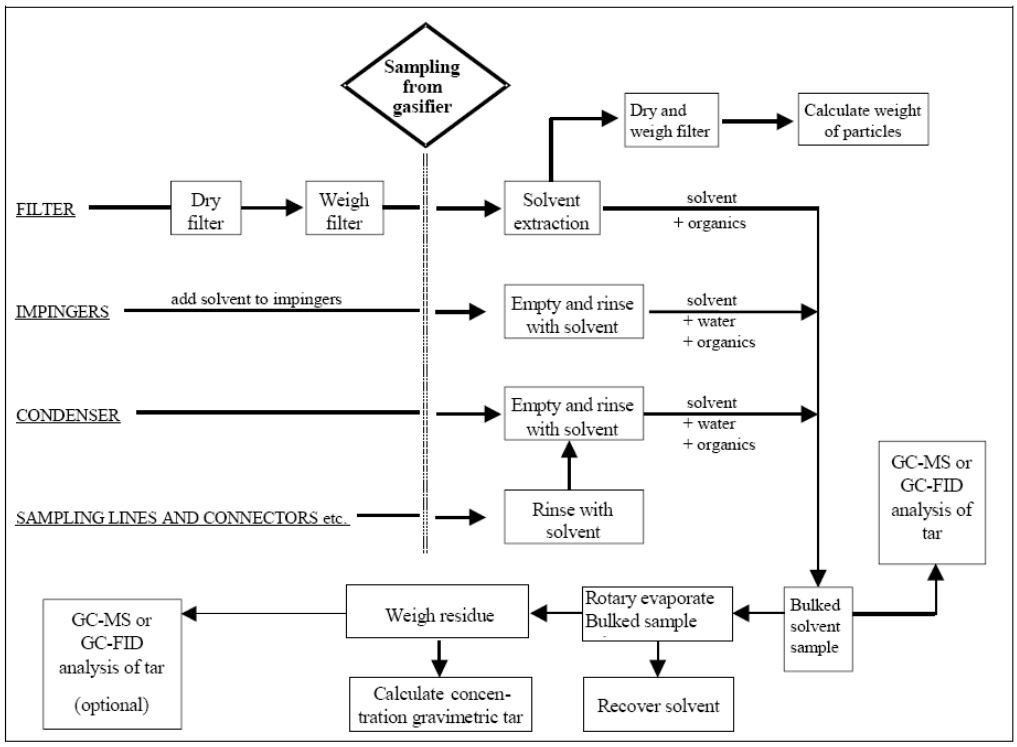

Figure 8.1 Schematic Showing Post Sampling Procedures

8.1. Gravimetric analysis

This procedure is based on conventional and well-proven methods for the gravimetric determination of both solid particles and organic species. Equipment utilised in this Guideline is available in most analytical laboratories.

8.1.1. Equipment for gravimetric analysis

Main items:
Soxhlet apparatus, standard rotary evaporator with pressure indicator, desiccator.
Calibrated analytical balance, accuracy 0.1mg.

8.1.2. Preparation of particle filter

Note: plate filters are recommended for particle concentrations of less than 20 mg/m_n^3 and thimble filters for concentrations greater than 20 mg/m_n^3. See section 5.4. When a plate filter is used, the determination of particle concentrations is less accurate or might prove impossible.

i. Dry the quartz thimble or plate filter in an oven at 110°C at atmospheric pressure overnight (according to ISO 9096).

ii. Allow to acclimatise in a desiccator at room temperature. Weigh the filter using an analytical balance with an accuracy of ± 0.1 mg.

iii. After sampling and extraction, the same weighing procedure is followed to determine the particle content.

iv. Calculate the mass of particulate material collected as described in Chapter 9.

8.1.3. Soxhlet extraction procedure

i. Open the filter housing and transfer the thimble or plate filter to the Soxhlet apparatus. Keep it in the vertical position to avoid loss of particles. To avoid polymerisation of tar this procedure should be undertaken immediately after finishing the sampling, when the filter is still hot. Carefully add the appropriate amount (250-500 ml) of isopropanol to the Soxhlet apparatus. Extract the filter until the isopropanol is clear, but at least overnight.

i. Remove the filter from the Soxhlet and keep in the vertical position.

ii. Dry the extracted filter thimble at 110°C at atmospheric pressure overnight.

iii. The amount of particulate matter is determined by weighing the dry/washed filter cartridge. The same drying method described for the clean filter must be used. The weight of particles is determined by difference. The concentration of particles in the producer gas can be calculated in mg per normal cubic metre (mg/m_n^3) using the volume of gas sampled, the temperature and pressure readings, as described Chapter 9.

iv. For quality control purposes an unused 'blank' filter can be run in parallel to the used filter. This will ensure that there are no error contributing factors from the Soxhlet procedure.

8.1.4. Determination of gravimetric tar mass

Isopropanol from the filter extraction procedure (Section 8.1.3) is bulked with the isopropanol solution collected from the impingers and condenser. The mass of gravimetric tar is determined by means of solvent distillation and evaporation. The recommended procedure for evaporation of the isopropanol tar solution is as follows:

i. Using a standard rotary evaporator with a pressure indicator. Adjust the flow rate of water to reach a vacuum of 100 mbar with an empty flask.

ii. Use a 200 or 250 ml flask and acclimatise it for at least 5 minutes at a specific site in the lab. Then, weigh it with an accuracy of 1 mg or preferably 0.1 mg. Pour about 100 ml of the tar solution in the flask. Weigh the flask again to determine the weight of the solution.

iii. Connect the flask to the rotary evaporator and start the evaporation with the water bath at 55°C. The pressure will be higher than 100 mbar at the start and will gradually fall to 100 mbar. Drops should fall from the cold finger at a rate of 1-2 drops per second. Once almost all solvent is evaporated, the rate of drops falling will decrease. With a stopwatch observe the time between two drops falling. Continue until there are at least four (4) seconds between two consecutive drops falling.

iv. After the latter of these two drops, continue the evaporation for a further fifteen (15) more minutes. If at this point traces of water are observed, add 20 ml of ethanol and restart at step (ii.). If no traces of water are observed, continue the evaporation for another thirty (30) more minutes while the sample is flushed with nitrogen. Adjust the nitrogen flow so that the vacuum pressure does not exceed 350 mbar.

v. Remove the vacuum by letting in air and shutting off the nitrogen purge. Then stop the rotation of the flask, remove the flask from the heated water bath and dry it. Give the flask and tar at least 5 minutes to acclimatise at the same location as in step (i.). Then, weigh the flask accurately and calculate the amount of gravimetric tar as described in Section 9.

vi. To determine the GC-detectable components in the gravimetric tars (which is optional) re-dissolve the tars as described in Section 8.2.5 and perform a GC analysis.

8.2. Gas chromatographic analysis

The gas chromatographic analysis techniques described in this section are based on standard analytical methods used for the detection of aromatic hydrocarbons. Quantitative analysis by GC-FID and GC-MS is described in this section, although qualitative GC analysis can be useful for 'finger-printing' compounds in the sample. Addition of an internal standard is useful to estimate semi-quantitatively the composition of the tar. If an internal standard is not used then no estimation of the proportion of components can be undertaken. Chromatographic data obtained by GC-FID will not be as detailed as that obtained by GC-MS.

8.2.1. Gas chromatographic equipment and columns

Main items:

Gas Chromatograph-Mass Spectrometer (GC-MS)
Gas Chromatograph – Flame Ionisation Detector (GC-FID)
Column – non-polar capillary GC column (5% diphenyl-95% polysiloxane)
Analytical balance (accuracy 0.1mg)*
Volumetric flask*
Syringe*
Pipette*

* calibrated to relevant National Standards

8.2.2. Operating conditions of gas chromatographs

The chromatographic equipment and operating parameters employed will ultimately depend on the physical and chemical characteristics of the solvent used to dissolve the tar sample. Operating parameters described are generalised and may need to be modified to accommodate the requirements of the selected analyser used (GC-MS or GC-FID) and the type of column fitted.

Typical equipment required for GC-MS and GC-FID analysis of tar solutions:

GC column	for example DPDM-siloxane (5%diphenyl + 95% dimethyl) copolymer phase typically: 30 to 60 m length, 0.25 mm id., film thickness 0.25 μm (The column is conditioned using the following temperature programme: 30°C up to 300°C at a rate of 3°C min^{-1} with a final hold temperature of 1 hour)
High resolution gas chromatograph	
Bench top mass spectrometer with mass range of 20-400 g/mol.	
Integration software package (usually included with MS)	
Carrier gas:	Helium

Linear velocity of carrier gas:	typically 31.6 cm/s (or to suit system selected)
Pressure:	typically 80 kPa
Flow rate of carrier gas:	1-2 cm^3/min
Split ratio:	typically 75:1 (ratio depends on sensitivity of instrumentation and sample concentration)
Injection volume:	typically 1 to 5µl
Oven programming:	Initial isothermal at 50°C for 5 minutes
	Temperature programme at heating rate of 8°C min^{-1} up to 250°C
	Total run time 30 minutes
Injector temperature:	250°C

8.2.3. Quantitative GC-MS analysis

8.2.3.1. Preparation of Internal Standard (ISTD)

Internal standard solutions are prepared from pure standard materials and are prepared in dichloromethane, although isopropanol is often preferred on health and safety considerations. If the standard is a suspected carcinogen, primary dilutions of this material must be undertaken in a fume cupboard. For GC-MS analysis the recommended internal standard suite of compounds is phenanthrene-d_{10}., benzene-d_8, phenol-d_6, or benzopyrene-d_{12}.

i. A small amount of solvent is placed at the bottom of a ground glass stoppered volumetric flask. The solvent is the same as the solvent used in the sampling procedure, which is isopropanol.

ii. Each compound is weighed in its own decanter in the following way (getting solid compounds into a volumetric flask is difficult without loosing some part of solids for instance on the surface of the flask neck):
- A small decanter is tared on the analytical balance;
- A compound is weighed in the flask;
- Solvent is poured into the decanter and the compound is dissolved;
- Dissolved compound is poured into the volumetric flask;
- The decanter is rinsed and the rinsing solvent is also poured to the flask;

The lightest model substances, being readily volatile, should be treated quickly.

iii. Dilute to volume, stopper the flask, and then mix by inverting the flask several times. Calculate the concentration in micrograms per microlitre from the net gain in weight.

iv. Transfer the ISTD solution into an amber teflon-sealed screw-cap bottle and store in a refrigerator. All standards must be replaced after six months or if comparison with check standards indicates a problem.

8.2.3.2. Preparation of calibration standards

Calibration standards are made up from pure compounds listed in Section 13.2 using the same procedure described for preparation of the ISTD (Section 8.2.3.1). The presence of tar is indicated typically by the presence of the US-EPA suite of PAH compounds, phenols and BTEX. The calibration standard should be made up using these compounds in order to quantify the level of each compounds present.

Organic compounds that are not included in the calibration standards list, or are not available can be reported semi-quantitatively by assuming a response factor of unity or taking an average response factor for type of compound.

Prepare calibration standards at between two and five concentration levels for each compound of interest. A calibration file can now be set up using both the calibration and internal standard solutions. The operating parameters and conditions for quantitative GC-MS analysis are the same as those described for qualitative GC-MS analysis.

8.2.4. Quantitative GC-FID analysis

A GC-FID quantitative analysis is also possible as an alternative using a similar procedure to that described for quantitative GC-MS analysis. It should be noted however, that the identification of compounds is not absolute because compounds are identified by retention time only, which can lead to compounds with similar retention times being wrongly identified.

8.2.4.1. Preparation of Internal Standards (ISTD)

As described in Section 8.2.3.1 for GC-MS analysis, but use n-dodecane made up accurately to about 100-500 ng/µl as the internal standard.

8.2.4.2. Preparation of calibration standards

As described in Section 8.2.3.2 for GC-MS analysis.

8.2.5. GC–MS and GC-FID analysis procedures

8.2.5.1. Preparation of sample for GC-MS and GC-FID analysis

i Take 10 ml of the bulk sample solution (see Figure 8-1) and add 0.01 mg of ISTD solution. Depending on the concentration of tar, the sample can be diluted to ensure that the concentration of organic components fall within the detection limits of the instrument.

ii Shake contents of volumetric flask. Transfer the sample into an amber teflon-sealed screw-cap bottle and store in a refrigerator until ready to use.

iii All volumes and weights will vary depending on the levels of each compound present, and the type of biomass initially used.

Optionally, GC-FID or GC-MS analysis can also be performed with the tar residue from Section 8.1.4. Then, prepare the sample as follows:

i Accurately weigh about 0.1 g of the tar residue into a 10 ml ground glass stoppered volumetric flask. Depending on the concentration of tar, the sample can be diluted to ensure that the concentration of organic components fall within the detection limits of the instrument.

ii Add 0.01 g of ISTD solution, make up to the mark with dichoromethane and shake contents of volumetric flask. Transfer the sample into an amber teflon-sealed screw-cap bottle and store in a refrigerator until ready to use.

iii All volumes and weights will vary depending on the levels of each compound present, and the type of biomass initially used.

8.2.5.2. Analysis by GC-MS or GC-FID

i Prior to analysis allow the sample to reach room temperature. Inject between 1 µl and 5 µl of the sample from Section 8.2.5.1 onto the GC column using a calibrated syringe. The volume injected will depend on tar concentration, and will be known from experience with analysis of each type of biomass tar.

ii The operation of the GC-MS and GC-FID systems will be dependent on the type of system used, the manufacturer's instructions, the data processing system used, the column used etc.

8.2.5.3. Identification of compounds

This is based upon retention times in combination with mass spectra.

i **Identification by retention time.** The width of the retention time window entered in the software program and used to make identifications should be based upon measurement of actual retention time variation of standards. Three times the standard deviation of a retention time for a compound can be used to calculate a suggested window size; however, the experience of the analyst should weigh heavily in the interpretation of chromatograms.

ii **Identification by mass spectrometry.** Set up the calibration software to search for the specified components based on their retention time and their mass spectrum. Identification of the compounds present in the total ion chromatogram is performed by comparison of the unknown spectra with the mass spectral library.

8.2.6 Calculation of GC results

The results are calculated as described in Chapter 9, in conjunction with the following equations.

The system software can be set up and used to automatically quantify the compounds analysed. Response factors can also be calculated manually using the following equation:

$$RF_c = \frac{A_c / A_{is}}{M_c / M_{is}}$$

where RF_c = Response factor for compound
A_c = Area of compound
A_{is} = Area of internal standard
M_c = Mass of compound
M_{is} = Mass of internal standard

The mass of each compound can be calculated using one of several methods:

i Automatically using the system software if an appropriate calibration file has been set up
ii Using a spreadsheet with response factors and manual input of peak areas
iii Manual calculations using response factors and peak areas:

$$M_c = \frac{A_c M_{is}}{A_{is} RF_c}$$

9. Calculation of results

9.1. Error calculation

9.1.1. Classification of errors

This chapter deals with error calculation and accuracy of measurement. In this context it is useful to make a few general remarks on the classification of errors.

Generally, errors can be divided in two categories: *systematic errors* and *accidental errors*.

Systematic errors are caused, for example, by wrong calibrations of measurement instruments, by poor measurements, by impurities in used chemicals or by unknown causes. The latter becomes clear only if results are compared with those of other researchers or other laboratories using different measuring devices and preferably other methods.

Accidental errors are unpredictable. They find their cause in physical noise, fluctuations by other causes and reading errors. Repeating of measurements will show a normal distribution around a certain average. From this the estimated error in the average can be determined.

In case of only a single experiment, the error has to be estimated. As an example, with a ruler length can be read with accuracy of ± 0.2 mm. The accuracy of good commercial measuring devices is normally - sometimes as an individual calibration report - indicated by the supplier. In general the maximum deviation is indicated, which may have a systematic character and is bigger than the mean accidental error.

Errors can be presented as an *absolute error* or *relative error*. *Absolute errors* have the same dimension as the measured quantity, a length for example can be presented as 21.3 ± 0.2 mm. *Relative errors* are given as a fraction of the measured quantity, or as a percentage. A relative error is a dimensionless number. For example 21.3 mm ± 1%.

9.1.2. Propagation of errors in the final result

Normally we are interested in the final result, being a function of one or more measured quantities. Here the issue is to find out how errors in the measured quantities carry over in the final result. As an example, the equilibrium constant K of a reaction is measured as K= 305 ± 5.What will the error be in the standard free enthalpy of reaction (at T=300 K): G= RTlnK=14.268 kJ/mol ?

The answer to this question can be found by differentiation:

If the error in x is equal to Δ x, then the error Δ f in f(x) is equal to $\Delta f = \left|\frac{df}{dx}\right| \Delta x$.

In this example the error in G is equal to -RTΔK/K=41 J/mol; The final result is thus written as G=14.27 ± 0.04 kJ/mol.

Note that normally, errors, indicated without any further note are always meant as the mean error or standard deviation σ. Due to the existence of different types of errors, the general abbreviation for 'error' used in this section is chosen to be Δ.

Where an error is built up of errors of more independent measured quantities, the different contributions should be summed. However, normal summing of errors is wrong: errors of different independent sources can be + or – en will partially compensate each other. Therefore, the right way of summing is to the square root of the sum of the quadratic individual errors:

If f=x+y, then $(\Delta f)^2 = (\Delta x)^2 + (\Delta y)^2$. In other words: independent errors sum quadratic. In general the error propagation law for f, a function of x,y,z,…. is[i]:

$$\Delta_f^2 = \left(\frac{\partial f}{\partial x}\right)^2 \Delta x^2 + \left(\frac{\partial f}{\partial y}\right)^2 \Delta y^2 + \left(\frac{\partial f}{\partial z}\right)^2 \Delta z^2 + \ldots\ldots \qquad \text{(Eq. 9-1)}$$

9.2. Sampled gas volume

The sampled producer gas volume V at normal conditions is the difference of the readings from the calibrated gas meter during the sampling procedure, corrected for the actual p and T of the sampled gas at the dry gas meter. As the gas

temperature and pressure can increase or decrease during the sampling period, the exact calculation of the displaced gas volume would require continuous gas meter, temperature and pressure reading followed by fractional volume integration. Within this Guideline, a simplified equation is used which contains the difference in the gas meter reading between the start and finish of the sampling period, the mean gas meter temperature <T> and mean pressure <p> over the sampling period:

$$V = \left(V_{stop} - V_{start}\right) \cdot \frac{< p >}{P_0} \cdot \frac{T_0}{< T >} \quad [m_n^3] \pm \Delta V \qquad \text{(Eq. 9-2)}$$

, with P_0=101300 Pa and T_0=273.15 K and ΔV being the 'error' in V.

The best estimate of the average of N values of p or N values of T is given by:

$$< p >= \frac{1}{N}\sum_{i=1}^{N} p_i \quad \text{and} \quad < T >= \frac{1}{N}\sum_{i=1}^{N} T_i \quad \text{(available routine in most spreadsheet programs)}$$

9.2.1. Error propagation

The 'error' ΔV in V (see Eq.9.2), depends on the errors in V_{stop} and V_{start} and the standard deviations of <T> and <p> ,$\sigma_{<T>}$ and $\sigma_{<P>}$.

The best estimate of the standard deviation σ of an averaged value is the square root of the variance. Therefore:

$$\sigma_{<p>} = \sqrt{\sigma_{<p>}^{\,2}} = \sqrt{\frac{N}{N-1} < (\Delta p)^2 >} = \sqrt{\frac{N}{N-1}(< p^2 > - < p >^2)} \quad \text{(available in most spreadsheet programs)}$$

, and

$$\sigma_{<T>} = \sqrt{\sigma_{<T>}^{\,2}} = \sqrt{\frac{N}{N-1} < (\Delta T)^2 >} = \sqrt{\frac{N}{N-1}(< T^2 > - < T >^2)} \quad \text{(available in most spreadsheet programs)}$$

Although measuring accuracy depends on the type of equipment, the following values are typical:

$\mathbf{\Delta V_{start}}$	$\leq 2.10^{-4}$ [m^3]
$\mathbf{\Delta V_{stop}}$	$\leq 2.10^{-4}$ [m^3]
$\mathbf{\sigma T}$	$\leq$ 5 K [°C]
$\mathbf{\sigma p}$	$\leq$ 1000 [Pa]

For calculation of the error ΔV in V, the general error propagation law (See Eq. 9.1) is applied:

$$\Delta V = \sqrt{\frac{< p >^2}{< T >^2}\frac{T_0^{\,2}}{P_0^{\,2}}\left(\Delta V_{stop}^{\,2} + \Delta V_{start}^{\,2} + \frac{\left(V_{stop} - V_{start}\right)^2}{< p >^2}\sigma_{<p>}^{\,2} + \frac{\left(V_{start} - V_{stop}\right)^2}{< T >^2}\sigma_{<T>}^{\,2}\right)} \qquad \text{(Eq. 9-3)}$$

Example 1 (sampled gas volume):

Suppose that <p> = 121300±1000 Pa <T>=297.2±5 K, V_{start} = 213.1230 ± 0.0005 m_n^3 and V_{stop} = 213.1780 ± 0.0005 m_n^3, then according to Eq. 9.2 V becomes (213.1780-213.1230)*(121300/101300)*(273.15/297.2) = 0.0061 m_n^3. The error in V is calculated by Eq. 9-3:

$$\Delta V = \sqrt{\frac{121300^2}{297.2^2}\frac{273.15^2}{101300^2}\left(0.0005^2 + 0.0005^2 + \frac{(213.1780 - 213.1230)^2}{121300^2}1000^2 + \frac{(213.1230 - 213.1780)^2}{297.2^2}5^2\right)} = 0.001$$

The sampled volume should be presented as V=0.061 ± 0.001 m_n^3. The relative error is 2.1%.

9.3. Gravimetric analysis

9.3.1. Determination of gravimetric tar content

It is assumed that enough solvent is used during extraction of the filter and rinsing of the impingers.

After distillation/evaporation of the bulk tar sample by rotary evaporation, the gravimetric mass of tar, M_T, is calculated by mass-subtraction of the tar containing 'constant' weight flask and the empty acclimatised flask:

$$M_T = M_{T1} - M_{T0} \text{ [kg]} \qquad \text{(Eq. 9-4)}$$

With: $M_{T0} \pm \Delta M_{T0}$ Mass of the empty flask.[kg]
$M_{T1} \pm \Delta M_{T1}$ Mass of tar containing flask after rotary evaporation. [kg]

When M_T is known, the concentration of gravimetric tar in producer gas can be calculated according to:

$$c_T = \frac{M_T}{V} \text{ [g/ m}_n^3\text{]} \pm \Delta c_T \qquad \text{(Eq. 9-5)}$$

9.3.2. Determination of particle content

The amount of particles is calculated from the difference in mass between the dry clean filter and the dry particle containing filter, obtained after sampling, storage in a solvent, extraction in a Soxhlet extractor and drying:

$$c_p = \frac{M_p}{V} = \frac{(M_{p1} - M_{p0})}{V} \text{ [kg/ m}_n^3\text{]} \pm \sigma c_P \qquad \text{(Eq. 9-6)}$$

With: $M_{P0} \pm \Delta M_{P0}$ Mass of the dry clean filter (mg)
$M_{P1} \pm \Delta M_{P1}$ Mass of the dry filter after usage and extraction (mg)

9.3.3. Error propagation

Application of the general error propagation law on Eq. 9-5 results:

$$\Delta c_T = \sqrt{\left(\frac{1}{V}\right)^2 \left(\Delta M_T{}^2\right) + \left[\frac{(M_{T1} - M_{T0})}{V^2}\right]^2 \Delta V^2} \qquad \text{(Eq. 9-7)}$$

The error in M_T is:

$$\Delta M_T = \sqrt{\left(\Delta M_{T1}{}^2 + \Delta M_{T0}{}^2\right)} \qquad \text{(Eq. 9-8)}$$

$\Delta M_{T,1 \text{ and }} \Delta M_{T,0}$ represent the inaccuracy introduced by weighing of the flask. Reproducibility tests of the acclimatising method prescribed in section 8.1.4, show a weighing error of 2 mg the weighing of a flask, which is more than the analytical balance accuracy of 0.1 mg. However, R&D research by BTG and ECN has also shown that the maximum error ΔM_T is about 5 % of M_T for tar concentrations in isopropanol of about 1 g/l. Note that this error is not simply introduced by the limited precision of the weighing balance but also by other inaccuracies due to extraction, rotary evaporation and hydrogen bonding of the solvent.

Summarised:

ΔM_T $\sqrt{\left((2 \cdot 10^{-6})^2 + (2 \cdot 10^{-6})^2\right)} \leq \mathbf{\Delta M_T} \leq 0.05 \cdot M_T$ [kg]

ΔV See section 9.2.

Similar to equation 9-7 the error introduced in the particle concentration is calculated by:

$$\Delta c_p = \sqrt{\left(\frac{1}{V}\right)^2 \left(\Delta M_p{}^2\right) + \left[\frac{(M_{p1} - M_{p0})}{V^2}\right]^2 \Delta V^2} \qquad \text{(Eq. 9-9)}$$

According to section 7.1.2 particle sampling error is influenced by the deviation from isokinetic conditions, which in practice are never exactly reached and also depend on the gas flow in the duct. In case the sampling is conducted under the conditions of Eq. 7-2 the typical relative error in Mp will be about 5%.

Summarised:

ΔM_p $0.14 \cdot 10^{-6} \leq \mathbf{\Delta M_p} \leq 0.05 \cdot M_p$ [kg]
ΔV See section 9.2.

Parallel measurements will provide more information on accuracy with respect to isokinetics and mass loss during post-sampling.

Example 2 (gravimetric tar):

If $M_{T1} = 126.3821 \cdot 10^{-3} \pm 2 \cdot 10^{-6}$ kg, and $M_{T0} = 126.1705 \cdot 10^{-3} \pm 2 \cdot 10^{-6}$ kg, and V=0.061 ± 0.001 m_n^3 (as in example 1), then according to Eq. 9.5 c_T is equal to $((126.3821 \cdot 10^{-3} - 126.1705 \cdot 10^{-3})/0.061) = 3.496 \cdot 10^{-3}$ kg/m_n^3. Using an error of 5% in M_T, the error in c_T is calculated by Eq. 9-7as follows:

$$\Delta c_T = \sqrt{\left(\frac{1}{0.061}\right)^2 \left((0.05 \cdot 0.2116 \cdot 10^{-3})^2\right) + \left[\frac{(0.2116 \cdot 10^{-3})}{0.061^2}\right]^2 0.001^2} = 0.1893 \cdot 10^{-3} \quad [\text{kg/ m}_n^3]$$

In this example the concentration of gravimetric tar in the gas phase is c_P=3.5 ± 0.2 g/m_n^3 and the relative error is 5.4 %.

Example 3 (particle content):

Suppose that $Mp_1 = 5.1631 \cdot 10^{-3} \pm 0.1 \cdot 10^{-6}$ kg, and $Mp_0 = 5.0020 \cdot 10^{-3} \pm 0.1$kg and V=0.061 ± 0.001 m_n^3 (as in example 1), then according to Eq. 9.8 C_P is equal to $(5.1631 \cdot 10^{-3} - 5.0020 \cdot 10^{-3})/0.061 = 2.6615 \cdot 10^{-3}$ kg/m_n^3. Using an error of 3% in M_p, the error in C_P is calculated by Eq. 9-8:

$$\Delta C_P = \sqrt{\left(\frac{1}{0.061}\right)^2 \left((0.03 \cdot 0.1611 \cdot 10^{-3})^2\right) + \left[\frac{(0.1611 \cdot 10^{-3})}{0.061^2}\right]^2 0.001^2} = 0.09719 \cdot 10^{-3} \quad [\text{kg/ m}_n^3]$$

In this example the concentration of gravimetric tar in the gas phase is C_P=2.7 ± 0.1 g/m_n^3 and the relative error is 3.6 %.

9.4. Gas chromatographic analysis

9.4.1. Determination of individual compound concentrations

Individual tar compounds are identified by the mass selective detector (MSD) of the gas chromatograph (GC) and the use of model compounds. The gas content of tar components is calculated as follows (see also section 8.2.6):

$$c_A = \frac{M_A \cdot c_T}{M_S} = \frac{A_S \cdot M_{is} \cdot c_T}{A_{is} \cdot RF \cdot M_S} \pm \Delta C_A \, [\text{g/m}_n^3] \quad \text{(Eq. 9-10)}$$

With:

$c_A \pm \Delta c_A$	Concentration of compound A in the gas phase [g/ m_n^3]
$M_A \pm \Delta M_A$	Mass of component [kg],
$M_S \pm \Delta M_S$	Solved mass of gravimetric tar (usual 0.1 g)
$M_{is} \pm \Delta$Mis	Mass of internal standard [kg]
$A_s \pm \Delta A_s$	Area of compound
$A_{is} \pm \Delta A_{is}$	Area of internal standard
$c_T \pm \Delta c_T$	Gravimetric tar concentration [g/ m_n^3]
V ± ΔV	Sampled gas volume (m_n^3)

9.4.2. Error propagation

The error made in the determination of component concentrations can calculated by following formula, based on the general error propagation law.

$$\Delta c_A = \sqrt{\left(\frac{M_{iS} \cdot c_T}{A_{is} \cdot RF \cdot M_S}\right)^2 \Delta A_S^{\,2} + \left(\frac{A_S \cdot c_T}{A_{is} \cdot RF \cdot M_S}\right)^2 \Delta M_{is}^{\,2} + \left(\frac{A_S \cdot M_{is}}{A_{is} \cdot RF \cdot M_S}\right)^2 \Delta c_T^{\,2}}$$

$$\sqrt{\ldots\ldots\ldots\left(\frac{A_S \cdot M_{iS} \cdot c_T}{A_{is}^{\,2} \cdot RF \cdot M_S}\right)^2 \Delta A_{iS}^{\,2} + \left(\frac{A_S \cdot M_{is} \cdot c_T}{A_{is} \cdot RF^2 \cdot M_S}\right)^2 \Delta RF^2 + \left(\frac{A_S \cdot M_{is} \cdot c_T}{A_{is} \cdot RF \cdot M_S^{\,2}}\right)^2 \Delta M_S^{\,2}} \quad \text{(Eq. 9-11)}$$

10. Reports and documentation

10.1. General

Analysis data and results obtained in the laboratory during sampling and at the completion of experimental work are typically recorded and stored in a standardised computer format suitable for easy dissemination. Similarly analysis quality control data should be stored in a suitable master database. Such data typically contain information on gasifier parameters, analysis instrument type and analytical conditions, calibration data including precision, accuracy, percent RSD, matrix spike recovery etc. Reported analysis values should have been rounded off to its maximum allowed number of significant figures, i.e. the smallest number in any factor.

10.2. Analytical report

Final results of all analyses (particles and tar) are provided in a standard computer file format and forwarded to the requester with cover memorandum. The reports are prepared on the basis of raw data from sampling logs and analysis result files. Examples of sampling logs are given below in paragraph 10.4. The raw log data can be customised to suit a particular report or usage.

Four different numbers are reported in the Guideline, which are:

1. The concentration of gravimetric tar in g/m_n^3 (see Paragraph 8.1);
2. The concentration of the individual tar compounds as measured by GC (in a list as given in Appendix 13.2, compounds ranging from benzene to coronene, see Paragraph 8.2);
3. The sum of concentrations of GC-detected, identified compounds (sum of compounds reported in 2.);
4. The sum of concentrations of GC-detected, non-identified compounds in the range of benzene to coronene, given that this concentration can be determined. For the analysis of tars from some gasifier types and/or conditions (e.g. updraft gasifiers, fluidised bed gasifiers operated at 750°C or lower) the number of identified compounds might be that high that the baseline cannot be properly determined. As this will result in an erroneous amount of GC detected, non-identified compounds, this number will then not be reported.

Remarks using suitable designations (see Appendix 13.7) should be provided with reported data to alert the user to some specific condition that may have affected the data.

Essential information to be contained in a report may be the following:

- The name of the laboratory (or factory), where the sample was received from
- The date of sampling and analysis
- Analyst and/or examiner name
- The type of reactor, fuel type, fuel moisture, test number and operation parameters including actual power output (kW), actual fuel feeding rate (kg wet/h), dry raw gas flow rate (m_n^3/h), gasifier start
- Sampling place, i.e. in which part of the reactor the sample was taken
- Sampling technique and essential parameters including tar trapping solvent, ambient temperature and pressure, duct diameter, diameter of sampling nozzle and particle filter temperature
- Sample treatment, solvent, dilution factors etc.
- Sample storage
- Analytical technique and parameter settings
- Target analytes values, usually reported in mg/m_n^3 or g/m_n^3
- Analytical precision and accuracy

10.3. Designation

Examples of designations (EPA, 1997) for an analysis data sheet are:

- "U" – The analyte was analysed for but not detected. The value preceding the "U" is the "minimum quantitation limit (MQL)". Minimum Quantitation Limit (MQL) – Every sample has a concentration level below which the variance of the results for a particular analyte exceeds the acceptable quality control criteria. This level is the MQL

and is based on the value preceding the "U". The MQL is based on the lowest quantitative data point of the instrument calibration curve. The MQL is derived using this data point and other factors such as: sample size, dilution required, and sample interference. Analytes varies from analyte to analyte within a sample. Analytes are often detected at levels below the MQL and are reported as estimated values (J). Generally, analytes identified below the MQL will only be reported if the concentration is greater than one tenth of the MQL.

- "J" – The identification of the analyte is acceptable, but the quantitative value is an estimate. The value preceding the "J " is the "estimated value".
- "N" – There is presumptive evidence that the analyte is present but it has not been confirmed. The analyte is "tentatively identified". Tentative Identification: There is an indication that the analyte reported is present. The quality control requirements necessary for confirmation were not met.
- "C" – The analyte is determined to be present. The presence of the analyte was "confirmed by GC / MS".
- "A" – The analyte was analysed in replicate. The value preceding the "A" is an "average value" of the replicates.
- "K" – The analyte is determined to be present. The actual value is known to be "less than" the value preceding the "K". Less Than Values – The analyte is present, but the amount of the analyte is determined to be below an acceptable level for quantitation. The concentration can not be calculated, but is determined to be less than the value given.
- "L" – The analyte is determined to be present. The actual value is known to be "greater than" the value preceding the "L". Greater Than Values – The analyte is present, but the amount of the analyte is determined to be above an acceptable level for quantitation.
- "R" – Data is "rejected" and should not be used. Rejected data – some or all of the quality control data for the analyte were outside criteria. The presence or absence of the analyte can not be determined from the data. Resampling and reanalysis are necessary to confirm or deny the presence of the analyte.

10.4. Sampling log

It is essential to keep records of the principal operating parameters of each gasification run. Examples of typical sampling logs are given in Appendix 13.7.

11. Safety aspects

This section is intended to briefly list potential dangers associated with tar analysis and recommended precautions to avoid exposure to hazardous chemicals and accidents. For a more comprehensive description of chemical safety issues, the reader should consult the reference sources at the end of the section.

11.1. Introduction

No chemical work is completely risk free but the likelihood of accidents during tar analytical work will be greatly reduced if adequate safety precautions are followed. Health and safety legislation in most countries place duties on employers to ensure health and safety by providing employees with adequate information and training in the inherent hazards of chemical work. Safety issues are usually addressed jointly by supervisors, employees, the local safety representatives and the employer.

11.2. Hazards

Since tar analytical work typically involves handling of relatively small quantities of material the likelihood of acute overexposure to chemical vapour and serious injuries during normal work are less likely. However, acute toxicity hazards may arise during sampling from leaking reactor or sampling system or during sample preparation from spillage and splashes. One should also bear in mind that many sub-operations including operating vacuum devices and handling compressed gases are potentially hazardous and require attention to safety requirements.

Chemical hazards

The use of chemicals is always potentially associated with health-, fire and explosion hazards. The health risks associated with accidental exposure to the chemicals being handled depend mainly on their physio-chemical properties, the exposure concentration and exposure time. Toxic body responses can be reversible or irreversible and response time may be immediate or delayed several days depending on the rates of absorption, biotransformation, distribution and excretion as well as other factors. Nearly all chemicals found in tar matrices are more or less toxic and for that reason, great care should be exercised in handling samples, solvents and reagents and lengthy exposure above safety limits must be avoided.

The most probable routes to exposure may be through inhalation of nonpolar organic solvent vapours since they are the most volatile chemicals. In contrast to water-soluble chemicals and large molecules nonpolar solvents diffuse readily through the blood-brain barrier. About 90% of all occupational poisoning are caused by inhalation of nonpolar solvents and in particular aromatics and halogenated solvents, which are the most toxic. Solvents can effect the nervous system, the respiratory system, eyes, internal organs including reproductive systems and damage the skin by de-fatting, irritation, sensitisation or dermatitis. Dichloromethane, an often-used tar solvent is a probable human carcinogen and should be handled with great caution and if possible replaced by another safer solvent. For this Guideline, 2-Propanol (isopropanol) has been selected as a less toxic alternative to dichloromethane. Skin absorption is the second route of concern. The rate of skin penetration for solid chemicals is significantly increased if they are dissolved in an organic solvent.

Tar samples can contain many groups of organic compounds (see Appendix 13.2) depending on the condition for their formation. The long-term health implications of exposures to such substances are essentially unknown but available literature data that refer to coal-tars present evidence for carcinogenicity to humans. Biomass tars obtained at high temperatures (~900 °C) typically contain several of the carcinogenic polycyclic aromatic hydrocarbons (PAH) found in coal-tars. Benzene and some of the polyaromatics found in biomass tars have been reported to be carcinogenic for all routes of exposure although skin absorption is the most likely route for PAHs due to their low volatility. Such substances are indirect acting carcinogens and their acute toxicity is generally low. Benzofuran found in low temperature tar is possibly carcinogenic.

Examples of other substances considered most likely to pose a potential risk to human health may be toluene, phenol and its derivatives. The acute toxicity of individual substances may be roughly assessed by comparison with available data (see references). Accordingly, low level exposure to toluene has its primary effect on the CNS and is more acutely toxic than benzene. Phenols are relatively lipophilic and are readily absorbed via the lungs, the digestive organ and skin. Phenol is corrosive to skin, which increase the rate of penetration also for other compounds. It is also toxic to the kidneys and can cause skin allergy, especially following chronic exposure. Phenol is considered as a co-carcinogen by many experts.

In view of the low volatility and pungent odour of many compounds excessive exposure to vapours does not seem likely unless fumes are generated by heating or leakage from gasifier or sampling system. Therefore, the most toxic effects of low volatility substances are expected from dermal exposure. Phenol derivatives, i.e. cresols, xylenols and guaiacyl type phenols are less toxic and corrosive than the mother compound.

Vacuum hazards

Solvents are typically removed under a moderate vacuum of about 1000 Pa in a rotary evaporator. Similarly samples are often dried under vacuum in a desiccator.

When working with such devices be aware of implosion hazards that may result in flying glass and airborne chemicals. Always check for signs of damage (stars or cracks) before use. For greater protection , use a desiccator shield during and after evacuation and wear safety spectacles.

Compressed gas hazards

Compressed gases present potential mechanical and chemical hazards and cylinders and regulators must therefore be handled carefully. Cylinders must always be secured by chains or strong straps to prevent tipping and regulators must always be accessible. Flammable gases must be stored in a well-ventilated area and kept away from open flame and spark sources. Piping system must regularly be checked for leaks. Always use safety glasses when connecting and disconnecting gas regulators and lines.

Sampling hazards

Product gases typically contain high levels of carbon monoxide and benzene, both of which are highly toxic and inhalation of fumes that may result from leaking gasifiers and sampling system pose an obvious health hazard to the workers. With adequate general laboratory ventilation short-term and long-term exposure levels will not be exceeded.

Acute toxicity hazards can also arise from leaks and solvent splashes from impingers caused by a rapid change in gas pressure.

A Plexiglas shield around the sampling system provides a suitable safety. Furthermore the use of a personal carbon monoxide detector is recommended.

11.3. Safety precautions

One key to prevent accidents is to use the safest possible practices in laboratory. All chemical work should therefore be performed only by individuals with proper training and experience to deal with the expected risks and hazards during laboratory operations.

All work spaces must be equipped with first aid kits, safety showers, eyewash fountains, fire extinguishers and fire blankets and a laboratory safety manual and Material Safety Data Sheets (MSDS) should be available. Plans for medical and chemical accident response must have been established and emergency telephone numbers must be readily available. Organic solvents shall be stored in specialised flammable and well ventilated storage areas and chemicals should have well-ventilated storage places. The laboratory should be equipped with clean-up equipment for chemical spills including appropriate absorbents (vermiculite[2], clay, dry sand, or towelling) for collecting and disposal containers.

Waste chemicals must be collected in suitable containers and stored in a properly ventilated place until disposed of according to safe disposal procedures that is commonly handled by a chemical hygiene officer.

The following basic personal safety rules should be followed when laboratory work is being conducted:

- Make sure that the ventilation system is switched on and is working before starting chemical work.
- Protective helmet should be worn at the sampling site.
- The sampling system should be checked for leaks before sampling.
- Wear eye protection (safety spectacles with sideshields, goggles, faceshield), protective gloves[3] and chemical- and fire-resistant laboratory coat as needed for the work at hand.
- Handle chemicals, solvent and samples in an efficient chemical fume cupboard.
- Carry out sampling in a well-ventilated area.
- Do not eat, drink or smoke in the laboratory or sampling area.
- Do not wear open shoes.

For more about this topic, the following Internet link may be useful: Chemical guide and permeation tables for laboratory gloves are available at http://www.pp.okstate.edu/ehs/hazmat/gloves.htm

11.4. Accidents

In the event of splashes on the skin, immediately rinse with water for 15 – 30 minutes and final cleaning with soap. In the event of large splashes on the body, remove contaminated clothing and promptly use the safety shower. Lipophilic substances can be rinsed of with polyethylene glycol. Splashes of chemicals in the eye are promptly flushed of with copious amounts of water for 15-30 min using the eyewash and then seek medical advice.

Spills of chemicals should be cleaned up as they occur using a suitable absorbent, dry sand or towelling to collect and then disposed of residues according to safe disposal procedures.

Avoid breathing vapours of spilled chemicals and do not touch the spill without protective gloves.

11.5. Safety and health information resources

A broad coverage of chemical hazard topics is freely available on Internet resources. Here are some useful links:

- National Institute for Occupational Safety and Health (NIOSH) provides International Chemical Safety Cards (ICSCs) database including index with chemical names and synonyms. http://www.cdc.gov/niosh/ipcs/ipcssyn.html

[2]: Hydrated magnesium-aluminium-iron silicate that can absorb large quantities of liquids.

[3]: There is no single glove material that is resistant to all chemicals and they should be chosen for each specific job. For compatibility and breakthrough characteristics of different glove material, an excellent information is ***Guidelines for the Selection of Chemical Protective Clothing*** published by the American Conference of Governmental Industrial Hygienists (ACGIH) or information provided by glove manufacturers.

- The National Library of Medicine's Toxnet: http://toxnet.nlm.nih.gov/
- The United States Environmental Protection Agency (EPA) provides the Integrated Risk Information System (IRIS) database: http://www.epa.gov/ngispgm3/iris/index.html
- Minimal Risk Levels (MRLs) for hazardous substances can be found at Agency for Toxic Substances and Disease Registry (ATSDR): http://www.atsdr.cdc.gov/mrls.html
- Chemical guide and permeation tables for laboratory gloves are available at http://www.pp.okstate.edu/ehs/hazmat/gloves.htm

Additional information about chemical characteristics and hazards can also be found in the following sources:

- Material Safety Data Sheets (MSDS) or International Chemical Safety Cards (ICSCs)
- Merck Index
- The Kirk-Othmer Encyclopaedia of Chemical Technology
- Sax's Dangerous Properties of Industrial Materials
- Bretheric´s Handbook of Reactive Chemical Hazards
- Patty's Industrial Hygiene and Toxicology
- Dictionary of Substances and their effects

12. References

BTG, 2000: *Calculation method to determine flow rate of producer gas (not published).*

DIN1343. Deutsche Norm: *Referenzzustand, Normzustand, Normvolumen. Begriffe und Werte (Reference conditions, normal conditions, normal volume: concepts and values)*, January 1990

EPA, 1997: "Analytical Support Branch: Operation and Quality Control Manual", Environmental Protection Agency, Science and Ecosystem Support Division, Region 4, 980 College station road, Athens, GA 30605, U.S.A., December 1, 1997

ISO 9096: *Stationary source emissions – Determination of concentration and mass flow rate of particulate material in gas-carrying ducts – Manual gravimetric method.*

Milne, T.A.; Abatzoglou, N.; Evans, R.J.: Biomass Gasifier Tars: Their Nature, Formation and Conversion, NREL/TP-570-25357, November 1998

Neeft, Knoef, Zielke, Sjöström, Hasler, Simell, Dorrington, Abatzoglou, Deutch, Greil, Buffinga, Brage, Suomalainen: *R&D supporting the development of a Guideline for sampling and analysis of tars and particles from biomass producer gases*, 2001

Ramackers, M.W.A. and Heynis G.H.P.; *Engines and adaptation of engines for producer gas*, presented at the second International Producergas Course and Conference in Bandung, Indonesia, 1985

VDI 2066, part 1: *Measurement of particulate matter – Measurement of particulate matter in flowing gases. Gravimetric determination of dust load. Fundamentals*, VDI, October 1975

VDI 2066, part 2: *Measurement of particulate matter – Manual dust measurement in flowing gases. Gravimetric determination of dust load. Tubular filter devices (4 m^3/h, 12 m^3/h*, VDI, August 1993

VDI 2066, part 7: *Measurement of particulate matter – Manual dust measurement in flowing gases. Gravimetric determination of dust load. Plane filter devices*, VDI, August 1993

13. Appendices

13.1. General design and operating conditions of gasifiers

Gasification is a thermochemical process which converts solid carbonaceous fuels into gas by mixing the fuel with an appropriate gasification agent. Most of the gasifiers fall into four categories (see Figure 13-1) based on the design, feedstock and on the gasification agent. These four types are:

1) Fixed-bed updraft (or countercurrent)
2) Fixed-bed down-draft (or cocurrent)
3) Fluidised-bed and
4) Entrained-flow.

Within the gasification reactor, the processes of fuel drying, pyrolysis reduction and oxidation occur. The oxidative gasification agent converts char and tar from the pyrolysis process into gas. As the gas generation is an endothermic process, some of the gasification agent is required to supply the chemical energy by combusting a fraction of the fuel. The combustion process generally is internal.

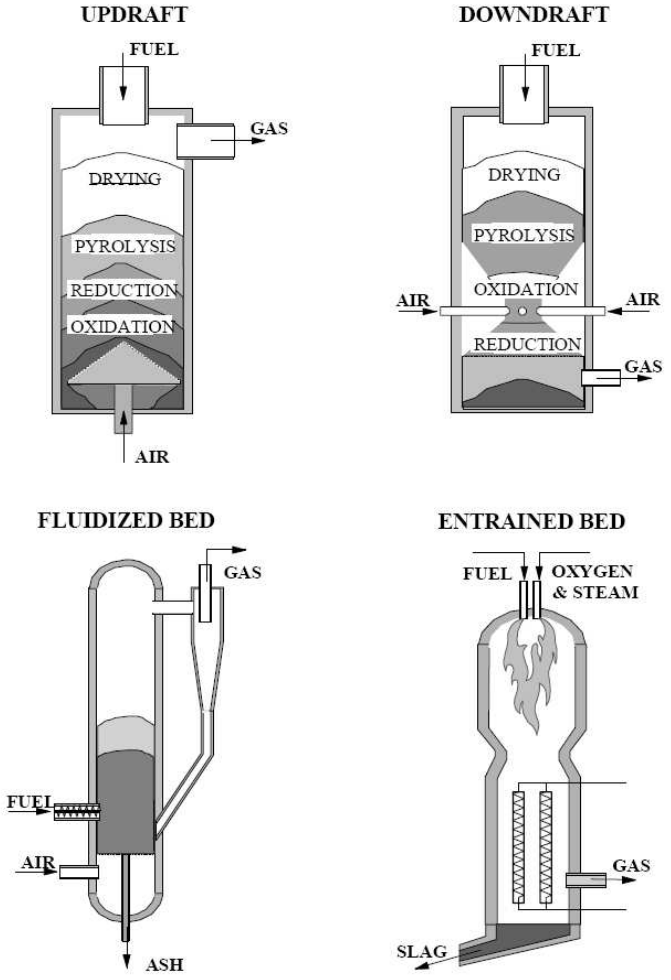

Figure 13-1: Schematic drawing of four basic gasifier types

In updraft gasifiers, the fuel generally moves from downwards and the gasification agent moves from the bottom upwards (updraft). As the gas leaves the reactor near the pyrolysis zone, the gas generated in updraft gasifiers exhibit a high level of organic components (tar). The solid carbon in the fuel is completely converted into gas and tar. Updraft gasifiers can be used for wet fuels and are relatively insensitive to the fuel size.

In cocurrent gasifiers, the fuel and gasification agent flow cocurrently, hence the gas leaves the reactor near the hottest zone and the tar levels are much lower than in updraft gasifiers. The cold gas efficiency (conversion of fuel carbon into non-condensable gases) of cocurrent gasifiers is generally higher than in updraft gasifiers. Generally, cocurrent gasifiers can only be used with dried fuel (typically 15 wt%) and the size of the fuel are in narrow limits.

With increasing expansion of the fuel bed, the reactor behaviour transforms from a fixed bed to a (stationary) fluidised bed (FB) reactor and further to a circulating fluidised bed (CFB) reactor. The highest heat and mass transfer rates are observed in CFB reactors. A further increase leads then to entrained flow reactor types. FB and CFB gasifiers are characterised by high gas throughputs and require dried fuel with sizes typically <2 cm. CFB type gasifiers can be designed both for near atmospheric pressure and for pressurised applications.

Entrained flow gasifiers operate at elevated pressure and are found in coal gasification. The flow of fuel and gasification agent is cocurrent. In contrast with the other principles, the temperatures in the reactors are above the melting point of the ashes, which therefore leave the gasifier as molten slag.

In the Table 13-1, typical operating conditions and gas composition are displayed for some of the gasifier principles. No data were found for entrained flow gasifiers fuelled with biomass.

		Countercurrent	**Cocurrent**	**CFB**
Typical heat output	kW_{th}	1'000 – 10'000	100 – 1'000	>10'000
Fuel moisture	wt% (daf)	50	16	15
Typical gas composition				
Carbon dioxide (CO_2)	%	10.0	12.9	15.0
Carbon monoxide (CO)	%	20.0	18.0	15.4
Hydrogen (H_2)	%	14.0	14.2	14.8
Methane (CH_4)	%	2.5	1.9	4.2
Nitrogen (N_2, by diff.)	%	53.5	53.0	39.6
Typical contaminant levels				
Particles	g/m^3_n	0.1 – 0.5	0.1 – 1	20 - 60
Tar (generic definition)	g/m^3_n	50 – 150	0.5 – 2	7 – 10

Table 13-1: Typical operating conditions and gas compositions of various wood fuelled gasifiers at atmospheric pressure. Data source (tar and particles): Milne et al 1998

13.2. Available list of organic condensable ("tar") compounds to be analysed

In this table, compounds that are commonly measured are printed in standard style. Compounds that can be expected but are analysed less frequently or occur in lower concentrations are printed in *italics*.

Downdraft / Fluidised bed gasification	Pyrolysis and Updraft gasification
Phenols Phenol *Cresols (o, m or p)* *Xylenols* *(Methyl)Naphthols* **Furans** *Benzofuran* *Methylbenzofurans* *Dimethylbenzofurans* *Dibenzofuran* **Aromatic compounds** Benzene Toluene Xylenes (o, m and p) *Ethynylbenzene* *Styrene* Indene (1H-Indene) Methylindene **PAHs** (* indicate EPA list of 16 PAHs) Naphthalene* (1- or 2-) Methylnaphthalene Diphenyl Acenaphthylene* Acenaphtene* Fluorene* (9H-Fluorene) Phenanthrene* Anthracene* Fluoranthene* Pyrene* Benzo(a,b,c) fluorene *Benzo(a)anthracene** Chrysene* *Benzo(b*, j or k*)fluoranthene* *Benzo(a* or e)pyrene* *Dibenzo(a,h)anthracene** *Perylene* *Indeno(1,2,3-cd)pyrene** *Benzo(g,h,i)perylene** *Dibenzopyrenes* *Anthanthrene* *Coronene* **Nitrogen containing aromatics** Pyridine Methylpyridines, Picolines (Iso)Quinonoline	**Acids** Formic acid, Propionic acid, Butyric acid Acetic acid **Sugars** Levoglucosan *Alpha-D-Glucose, Beta-D-Fructose, Cellobiosan* **Alcohols and phenols** *Methanol, Ethanol* Phenols, Cresols (o, m or p), Xylenols **Aldehydes and ketones** *Formaldehyde, Acetaldehyde* *Acetone* *2-Cyclopenten-1-one, (Methyl)- 2-Cyclopenten-1-one* **Guaiacols** Guaiacol, Creosol (= 4-methyl-guaiacol) Ethylguaiacol, Eugenol, Isoeugenol **Furans** Dimethylfuran, Furfural (2-furaldehyde) Methyl Furfural, Furfuryl alcohol *(Methyl- or dimethyl-)benzofurans and dibenzofurans* **Mixed oxygenates** Hydroxyacetaldehyde, Acetol, Vanillin Propanal-2-one, Glyoxal *2-hydroxy-3-methyl-2-cyclopentene-1-one* *(di-, tri-)Methoxybenzenes, Trimethoxyphenols* **Aromatic compounds** Benzene, Toluene, Xylenes (o, m and p) Ethynylbenzene Styrene Indene (1H-Indene), Methylindene **PAHs** (* indicate EPA list of 16 PAHs) Naphthalene* (1- or 2-) Methylnaphthalene *Diphenyl* Acenaphthylene* *Acenaphtene** Fluorene* (9H-Fluorene) *Phenanthrene*, Anthracene*, Fluoranthene*, Pyrene** **Nitrogen containing aromatics** (Methyl)pyridines, Picolines, *(Iso)Quinoline*

13.3. List of individual organic compounds found in biomass producer gases

Group / **common name**	**Other / (more) trivial name**	**Chemical Abstract Service (CAS) Registry Number**	**Boiling point (°C) (Handbook of Chemistry and Physics, vol. 77)**
Acids			
Formic acid	Methanoic acid	64-18-6	101
Acetic acid	Ethanoic acid	64-19-7	117.9
Propionic acid	Propanoic acid	79-09-4	141.1
Butyric acid	Butanoic acid	107-92-6	163.7
Sugars			
Levoglucosan	1,6-amhydro-beta-D-Glucopyranose		
Alpha-D-Glucose	Alpha-D-Glucopyranose	604-68-2	Sub1
Beta-D-Fructose	Beta-Levulose	53188-23-1	
Cellobiosan			
Alcohols			
Methanol	Methyl alcohol	67-56-1	64.6
Ethanol	Ethyl alcohol	64-17-5	78.2
Aldehydes and ketones			
Formaldehyde	Methanal	50-00-0	-19.1
Acetaldehyde	Ethanal	75-07-0	20.1
Acetone	2-Propanone	67-64-1	56.0
2-Cyclopenten-1-one	Cyclopenten-3-one	930-30-3	136
(Methyl)- 2-Cyclopenten-1-one	(2- 3- 5-) methyl-2-cyclopenten-1-one	1120-73-6, 2758-18-1, 14963-40-7	157, 157.5, 140
Phenols			
Phenol	Hydroxybenzene	108-95-2	181.8
Cresols (o, m or p)	(2-, 3- or 4-)methyl-phenol	95-48-7, 108-39-4, 106-44-5	191.0, 202.2, 201.9
Xylenols	(2,3- 2,4- 2,5- 2,6- 3,4- or 3,5-) dimethylphenol	526-75-0, 105-67-9, 95-87-4, 576-26-1, 95-65-8, 108-68-9	216.9, 210.9, 211.1, 201.0, 227, 221.7
Butylphenols	(2-, 3- or 4-)butyl-phenol	3180-09-4, 4074-43-5, 1638-22-8	235, 248, 248
Methylbutylphenols	2-butyl-4-methyl-phenol	6891-45-8	228
Naphthols	(1- 2-) Naphthol or -Naphthalenol	90-15-3, 135-19-3	288, 285
Methylnaphthols	4-methyl-1-naphthol, 1-methyl-2-naphthol	10240-08-1, 1076-26-2	166, 160

Guaiacols			
Guaiacol	2-methoxy-phenol	90-05-1	205
Creosol = 4-methyl-guaiacol	2-methoxy-4-methyl-phenol	93-51-6	221
Ethylguaiacol	2-methoxy-4-ethyl-phenol	2785-89-9	236.5
Eugenol	2-methoxy-4-(2-propenyl)-phenol	97-53-0	253.2
Isoeugenol	2-methoxy-4-(1-propenyl)-phenol	97-54-1	266
Furans			
Dimethylfuran	(2,4- 2,5-)dimethylfuran	3710-43-8, 625-86-5	94, 93.5
Furfural (2-furaldehyde)	2-Furancarboxaldehyde	98-01-1	161.7
Methyl Furfural	5-Methyl-2-furancarboxaldehyde	620-02-0	187
Furfuryl alcohol	2-Furanmethanol	98-00-0	171
Benzofuran	Coumarone	271-89-6	174
Methylbenzofurans	(2- 3- 5- 7-) methylbenzofuran	4265-25-2, 21535-97-7, 18441-43-5, 17059-52-8	197.5, 197, 198, 190.5
Dimethylbenzofurans	(2,5- 2,6- 2,7- 3,5- 3,6- 4,6- 4,7- 5,6- 5,7- 6,7-) dimethylbenzofuran	29040-46-8, 24410-51-3, 59020-74-5, 10410-35-2, 24410-50-2, 116668-34-9, 28715-26-6, 24410-52-4, 64965-91-9, 35355-36-3	220, 217.5, 216, 220.5, 222, 219, 216, 221, 222, 218
Dibenzofuran	2,2'-biphenylene oxide	132-64-9	287
Methyldibenzofurans			
Mixed oxygenates			
Glyoxal	Ethandial	107-22-2	50.4
Hydroxyacetaldehyde	(Hydroxyethanal, glycolaldehyde)	141-46-6	
Propanal-2-one	(methyl glyoxal, 2-oxopropanal, pyruvaldehyde)	78-98-8	72
Acetol	1-hydroxy-2-propanone	116-09-6	145.5
2-hydroxy-3-methyl-2-cyclopentene-1-one			
Methoxybenzene	Anisol	100-66-3	153.7
Dimethoxybenzenes	(1,2- 1,3- 1,4-) dimethoxybenzene	91-16-7, 151-10-0, 150-78-7	206, 217.5, 212.6
Trimethoxybenzenes	(1,2,3- 1,3,5-) trimethoxybenzene	634-36-6, 621-23-8	235, 255.5
Trimethoxyphenols			
Vanillin	4-hydroxy-3-methoxybenzaldehyde	121-33-5	285
Aromatic compounds			
Benzene		71-43-2	80.0
Toluene	Methylbenzene	108-88-3	110.6
Xylenes (o, m and p)	(1,2- 1,3- and 1,4-)dimethylbenzene	95-47-6, 108-38-3, 106-42-3	144.5, 139.1, 138.3
Ethynylbenzene		536-74-3	143

Styrene	Ethenylbenzene	100-42-5	145
4-Methylstyrene	1-ethenyl-4-methyl-benzene	622-97-9	172.8
Indene (1H-Indene)	Indonaphthene	95-13-6	182
Methylindene	(1- 2- 3- 4- 6- 7-)methyl-1H-indene	767-59-9, 2177-47-1, 767-60-2, 7344-34-5, 20232-11-5, 7372-92-1	199, 206, 198, 209, 207, 209
PAHs (* indicate EPA list of 16 PAHs)			
Naphthalene*		91-20-3	217.9
(1- or 2-) Methylnaphthalene		90-12-0, 91-57-6	244.7, 241.1
Diphenyl	1,1-Biphenyl	92-52-4	256.1
Acenaphthylene*	Acenaphthalene	208-96-8	280; 150[2]
Acenaphtene*	1,2-dihydro-Acenaphthylene	83-32-9	279
Fluorene* (9H-Fluorene)	2,2'-Methylenebiphenyl	86-73-7	295
Phenanthrene*		85-01-8	340
Anthracene*		120-12-7	339.9
Fluoranthene*	1,2-(1,8-Naphthylene)benzene	206-44-0	384
Pyrene*	Benzo(def)phenanthrene	129-00-0	404
Benzo(a,b,c) fluorene	11H-Benzo(a)fluorene, ?, ?	238-84-6, ?, ?	405
Benzo(a)anthracene*	1,2-Benzanthracene	56-55-3	-
Chrysene*	1,2-Benzophenanthrene	218-01-9	448
Benzo(b*, j or k*) fluoranthene	B.(b)fl.=Benz(e)acephenanthrylene B.(j)fl.=Dibenzo(a,jk)fluorene B.(k)fl.=2,3,1',8'-Binaphthalene	205-99-2, 205-82-3, 207-08-9	-, -, 480
Benzo(a* or e)pyrene	(2,3- 1,2-)Benzopyrene	50-32-8, 85-02-9	-, 352
Dibenzo(a,h)anthracene*	1,2,5,6-dibenzanthracene	53-70-3	-
Perylene	Dibenzo(de,kl)anthracene	198-55-0	-
Indeno(1,2,3-cd)pyrene*			
Benzo(g,h,i)perylene*	1,12-Benzperylene	191-24-2	-
Dibenzopyrenes			
Anthanthrene			
Coronene		191-07-1	525
Nitrogen containing aromatics			
Pyridine	Azine	110-86-1	115.2
Methylpyridines, Picolines	(2- 3- 4-)Methylpyridine (2- 3- 4-)Picoline	109-06-08, 108-99-6, 108-89-4	129.3, 144.1, 145.3
Quinoline	1-Azanaphthalene	91-22-5	237.1
Isoquinoline	Benzopyridine	119-65-3	243.2

[1]: sublimates

13.4. Liquid Quench

The working principle of liquid quench with circulating fluid is shown in Figure 13-2. Liquid injection into the sample gas stream must occur immediately after the particle filter outlet. A liquid flow rate in the order 10 - 50 ml/min (depending on the sample gas flow rate) is sufficient to cool the gas from 250 to 50°C.

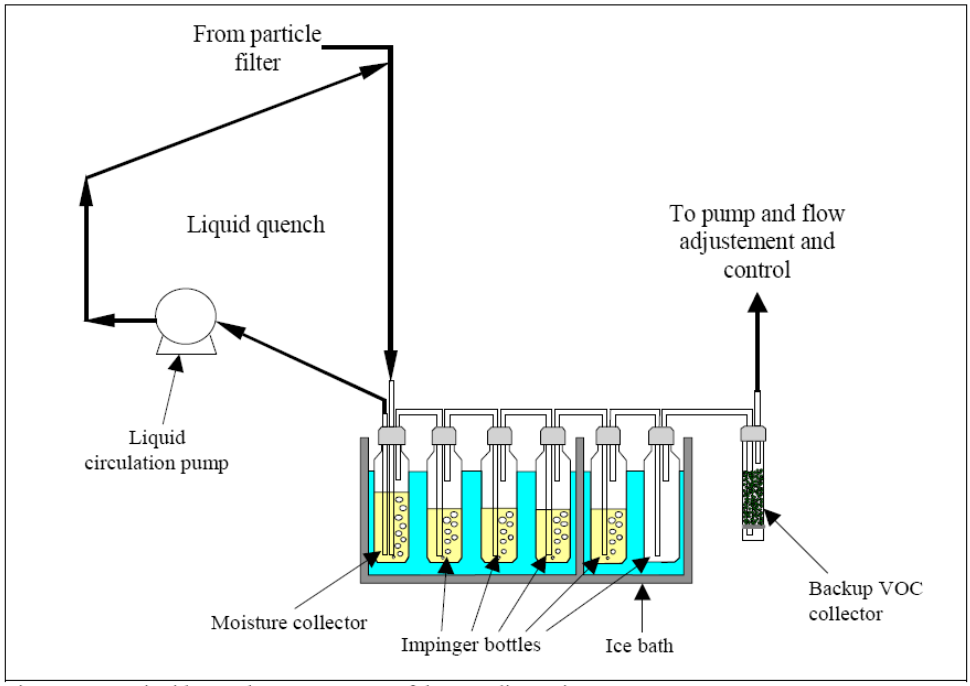

Figure 13-2: Liquid quench system as part of the sampling train arrangement

13.5. Modified (VTT) design of impinger bottles

The mass and heat transfer in impinger bottles can be improved by improving the design of impinger bottles. An improved design by VTT is shown in Figure 13-3. Glass bends using ball ground joints (Figure 13-3) ensure correct connection of the impinger bottles. To ensure impinger bottle connections (conical and ball ground joints) are gas tight, only PTFE gaskets, PTFE tapes or solvent are accepted as the sealing media.

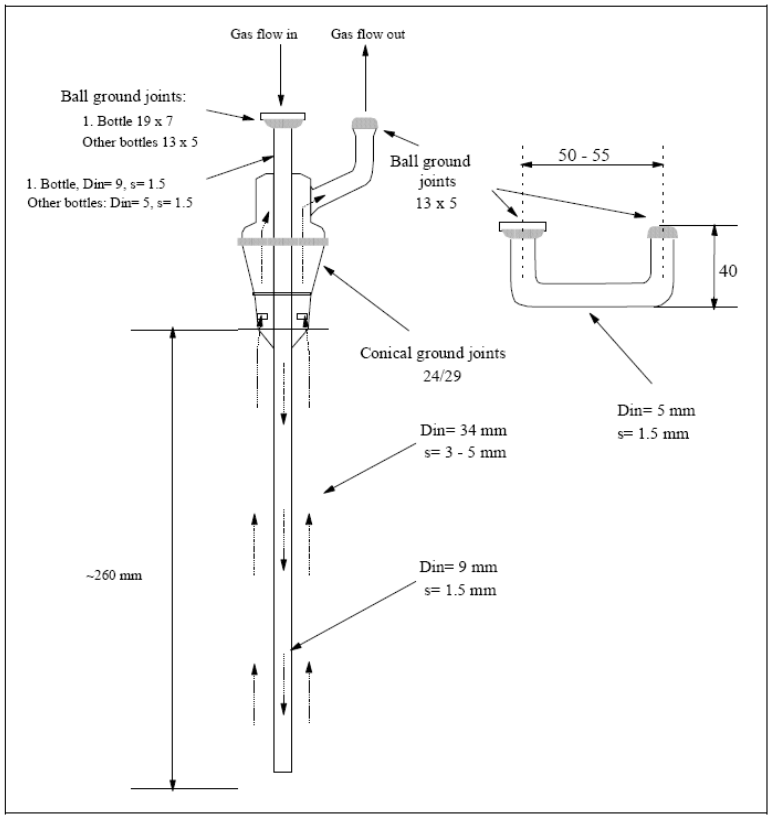

Figure 13-3: The impinger bottle and the glass bend used by VTT.

13.6. Alternative sampling train: the Petersen column

During preparation of the Guideline, the partners have gathered experience of the use of the described sampling train. The Danish participant, Danish Technological Institute (DTI), suggests that an alternative for module 3 proves more convenient when used in the field, compared to the standard configuration. It is DTI's opinion that the use of a liquid quench and 6 washing bottles containing solvent in a cooling bath which also contains solvent means that the sampling staff to a great extent has to handle the solvent and is exposed to the solvent. Furthermore, there is a risk of aerosol penetration through module 3. Therefore, DTI developed an alternative sampling train, which possibly eliminates the disadvantages of module 3.

The new sampling train is called the "Petersen column" after the inventor Finn Petersen. The "Petersen column" consists of two washing stages filled with isopropanol. Stage 1 is a traditional washing stage with impinger. The bottom of stage 2 consists of a G3 glass frit with two functions: a) it retains tar droplets (aerosol) and b) it generates a large number of very small gas bubbles in washing stage 2 which results in an improved washing efficiency. The two washing stages are filled with the washing medium (solvent, isopropanol) through two nozzles. During normal pressure (atmospheric pressure), the solvent is kept back in stage 2 by the glass frit, as the liquid runs very slowly through the frit. If there is a little vacuum in washing stage 2, no liquid runs through the frit.

When sampling has ended, the tube which is connected to the vacuum pump is moved to the connecting stub at the drain cock at the bottom of the "Petersen column". By creating a little vacuum in washing stage 1, the solvent is sucked from washing stage 2 through the frit. That results in washing stage 2 being emptied at the same time as the frit is cleaned by the solvent. Solvent from both washing stages is collected in a storage bottle which is kept sealed against the cone of the drain cock.

The "Petersen column" is jacket cooled. The cooling fluid and cooling temperature can be selected as required e.g. in relation to the gas temperature. The column is constructed in such a way so it is easy to replace the glass frit if it is polluted by particles that cannot immediately be rinsed out with solvent.

Tests have shown that the "Petersen column" has a high sampling efficiency. During measurements in heavily polluted countercurrent gas, less than 1% of the chromatographable tar is found in a backup system after the column and 85% of this penetration causes benzene. Furthermore, the "Petersen column" is easy to handle and the staff is hardly exposed to solvent steam from the washing and cooling medium. Figure 13-4 shows the "Petersen column".

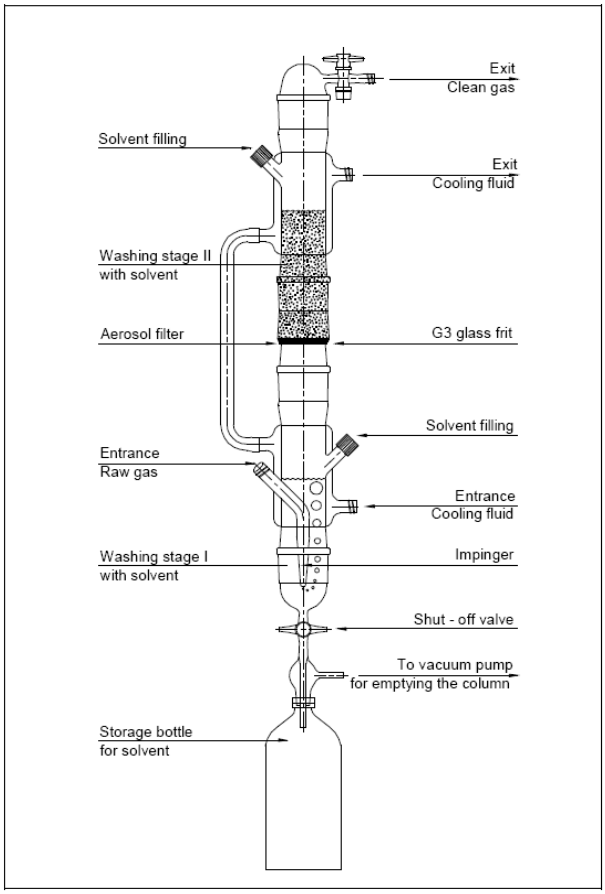

Figure 13-4 The "Petersen column"

13.7. Example test and analysis logs for sampling and result documentation

13.7.1. Parameter log for sampling of P&T

Sampling of P&T from Biomass Producer Gases						
					Examiner:	X
Gasifier Type/Site:		X			Date:	X
Test No.:		X				
Gasifier parameter						
Actual power output:			kW	(max. ..... kW)		
(based on fuel fuel input)						
Raw gas flow rate (dry):			[Nm^3/h]	(if calc., spec. gas rate:	2,6	Nm^3/kg **wet**
Gasifier start *:				stationary since *:		
Fuel type *:		Pine wood chips (approx. 20 x 20 x 10 mm; 5 wt% sawdust), dried				
Fuel moisture *:			[%, dry basis]			
Actual fuel feeding rate *:			[kg wet/h]			
Sampling parameters						
Sampling site (hot/cold end):		Raw gas after gasifier				
Tar trapping solvent:		Isopropanol				
Ambient temperature:			[°C]			
Ambient pressure:		1000	[mbar]			
Duct diameter:			cm			
Diameter of sampling nozzle:			mm			
Particle filter temperature:		250	[°C]	Filter tube no.:		
		init. weight	**final weight**			
Solvent stock bottle:						
Solvent storing bottle:				[g]		
Summary protocol						
Solvent from P&T sampling:			[g]			
Approx. mass of condensate:		n.d.	[g]			
Solvent from Soxhlet extraction:			[g]			
Total particle mass in filter tubes:			[mg]			
Normalised sampled gas flow rate:			[Nm^3/h]			
Remarks:		-Values given by the gasifier operators are marked with *.				
		- In the condenser, only Isopropanol is used.				
		- All the liquid is stored in one bottle (under nitrogen blanket and in a refrigerator).				

13.7.2. Parameter log for gas meter reading

Sampling of P&T from Biomass Producer Gases						
Gasifier Type/Site:		X				
Sampling site (hot/cold end):		Raw gas after gasifier			Date:	X
Test No.:		X				
Rated sampling gas flow rate (dry):			Nm^3/h (calculated set point;			
10% over isokinetic)						
P+T sampling start:			P+T sampling end:			
			Temperature in gas meter	Pressure In gas meter		
Gas meter protocol			[°C]	bar		
Time	Gas temperature	Reading			Δp pump	Sampling
	in duct	gas meter				Flow rate
[hh:mm]	[°C]	[m^3]			[mbar]	[Nm^3/h]

Remarks:	- Condensation train: liquid quench, 1 condenser (0°C; Isopropanol), no saturator.					
	- Tar absorption train: 3 wash bowls with Isopropanol (type Dreschel, -24°C), drop separator					
	- Before the pump an activated carbon filter is used as pump, protection (lignite coke; Dreschel impinger)					
	- After a few minutes, aerosol formation occurs (as mist) in the sampling train.					
	Mist colour is white. Some mist is found before the coke adsorber.					
Averaged sample flow rate:			Nm^3/h			
Total amount of gas sampled:			Nm^3			
Total sampling duration:			hours			
Mean gas meter temperature:			°C			

13.7.3. Log for particulate measurement

Sampling of P&T from Biomass Producer Gases						
Gasifier Type/Site:		X			Date:	X
Sampling site (hot/cold end):		Raw gas after gasifier			Test No.:	X
Particle filter pre-treatment						
Type of particle filter used:		Munktell			Filter tube no.:	0
Preconditioning temperature:				°C		
Preconditioning duration:				hours		
Initial tube weight after preconditioning:				g		
Tar extraction from particle filter with Isopropanol						
Soxhlet extraction		Start:			hh:mm	
		End:			hh:mm	
		Duration:			hours	
	tara weight	**gross weight**		**net weight**		
Storing bottle					[g]	
Remarks:	The Soxhlet extraction is made immediately after the sampling.					
	The Soxhlet extraction is made with fresh solvent at ambient pressure.					
	No acetone rinsing is made.					
	The solvent in the Soxhlet thimble housing is colourless after hours of extraction.					
Particle filter post-treatment						
Post-conditioning temperature:				°C		
Post-conditioning duration:				hours		
Final tube weight after post-conditioning:				g		
Remarks:						

13.7.4. General logbook of test performer

This chapter contains the information mentioned in the logbook of the test performer. It describes all the relevant aspects regarding the sampling site, the sampling and analysis procedures should be given.

The following information should be given in a number of log-parts:

- Installation description (type of gasifier, gas cleaning, capacity, year of construction .....)
- Fuel characterisation (origin, moisture, size (distribution) .....)
- Description of sampling site and (gasifier) operation conditions
- Sampling train set-up (arrangement of type of modules used)
- Sampling (duration, temperatures, pressure, flow rate ....)
- Sample(s) post treatment
- Type of analysis used (incl. calibration methods)
- Tables with results

8.4 TAR COMPOUNDS ANALYZED ON GC-MS

GC-MS tar compounds	MW g/mol	Formula	Hf kJ/mol
Isobutyronitrile*	69.1	C4H7N	22.8
1,4-Cyclohexadiene*	80.1	C6H8	104.75
3-Butenenitrile*	67.1	C4H5N	157.7
2-Propanone, 1-hydroxy- *	74.0	C3H6O2	-410
(BTEX); Benzene	78.1	C6H6	82.9
3-Penten-2-one, (E)- *	84.1	C5H8O	-240.2
(PAH); N-Nitrosodimethylamine	74.0	C2H6N2O	-1650
1H-1,2,4-Triazole*	69.1	C2H3N3	192.7
(PAH); Pyridine	79.1	C5H5N	140.4
Pyrrole *	67.1	C4H5N	108.3
Furan, 2,5-dihydro-*	70.0	C4H6O	-109.7
(BTEX);Toluene	92.1	C7H8	50.2
1H-Pyrazole*	68.1	C3H4N2	179.4
2-Amino-4-methylbut-2-enenitrile*	70.1	C5H10	-77.1
3-Penten-2-one, 4-methyl- *	98.1	C6H10O	-195.56
2-Pentanone, 4-hydroxy-*	102.0	C5H10O2	439.82
Furfural *	96.1	C5H4O2	-151.04
2-Pentanone, 4-hydroxy-4-methyl- *	116.0	C5H10O2	439.82
(Mix 4); Benzene, Chloro-	112.6	C6H5Cl	54.42
(BTEX); Ethylbenzene	106.2	C8H10	29.8
(Mix 4); m-Xylene	106.2	C8H10	17.2
(BTEX); p-xylene	106.2	C8H10	18
Phenylethyne *	102.1	C8H6	306.6
(Mix 4); Styrene	104.2	C8H8	148.3
(BTEX); o-xylene	106.2	C8H10	19.1
(Mix 4); Benzene, isopropyl-	120.2	C9H12	3.9
Furan *	68.1	C4H4O	-34.7
1,3,5-Triazine *	81.1	C3H3N3	229.3
1,3-Cyclopentadiene, 5-(1-methylethyli*	106.2	C8H10	144
Benzene, 1-ethynyl-4-methyl*	116.0	C9H8	-1.8
(Mix 4); Benzene, n-propyl-	120.2	C9H12	3.9
1H-Pyrrole, 2-ethyl-3,4,5-trimethyl-*	137.2	C9H15N	n/a
Benzene, 1-ethyl-3-methyl- *	120.2	C9H12	-1.8
Benzene, (1-methylethyl)-*	120.2	C9H12	3.9
(Mix 4); Benzene, 1,3,5-trimethyl-	120.2	C9H12	385.3
(PAH); Aniline	93.1	C6H7N	86.86
(PAH); Phenol	94.1	C6H6O	-96.4
Benzene, (1-methylethyl)-**	120.2	C9H12	3.9
alpha.-Methylstyrene*	118.2	C9H10	118.3
(PAH); Bis(2-chloroethyl) ether	143.0	C4H8Cl2O	-153.3
Benzonitrile *	161.2	C10H11NO	137.4
(PAH); Phenol, 2-chloro-	128.6	C6H5ClO	-153.3
Benzene, 1,2,4 trimethyl -*	120.2	C9H12	-13.8
Pyridine, 2,4,6-trimethyl- *	121.0	C8H11N	103.9
Benzene, 1-ethenyl-3-methyl- *	134.0	C9H10O	-63.1

Benzofuran*	118.1	C8H6O		-34.89
2,2,5,5-Tetramethyl-4-ethyl-3-imidazol*	169.0	C9H17N2O	n/a	
(PAH); Benzene, 1,3-dichloro-	147.0	C6H4Cl2		25.5
(PAH); Benzene, 1,4-dichloro-	147.0	C6H4Cl2		22.2
(Mix 4); Benzene, tert-butyl-	134.2	C10H14		-22.7
Benzene, 1-ethenyl-2-methyl- *	116.2	C9H7		119.7
Benzene, 1-ethenyl-4-methyl-*	116.2	C9H8		-94.4
(PAH); Benzyl Alcohol	108.1	C7H8O		-100.4
Pyridine, 2,5-dimethyl- *	107.0	C7H9N		56.1
(PAH); Benzene, 1,2-dichloro-	147.0	C6H4Cl2		29.7
Piperidine, 3-isopropyl- *	85.1	C5H11N		-48.9
Indene *	116.2	C9H8		163.4
(PAH); Phenol, 2-methyl-	108.1	C7H8O		-128.6
(PAH); Bis(2-chloroisopropyl) ether	170.0	C6H12Cl2O	n/a	
Acetic acid, phenyl ester*	136.2	C8H8O2		-279.7
N,N-bis(1-methylethyl-2-Propen-1-amine*	141.0	C9H19N		-161.5
(PAH); 4-Methylphenol & 3-Methylphenol	108.1	C7H8O		-125.3
(PAH); N-nitroso-di-n-propylamine	130.0	C6H14N2O		-82.7
Phenol, 4-methyl-*	108.1	C7H8O		-125.3
(PAH); Ethane, hexachloro-	236.7	C2Cl6		-138.9
(PAH); Benzene, nitro-	123.1	C6H5NO2		67.6
(IS); 1,4-Dichlorobenzene-D4	150.0	C6Cl2D4	n/a	
Benzene, 4-ethenyl-1,2-dimethyl-	132.0	C10H12		-263.6
Benzofuran, 2-methyl- *	132.0	C9H8O		13.6
Benzofuran, 7-methyl- **	132.0	C9H8O		13.6
Benzofuran, 2-methyl- **	279.0	C9H8O		13.6
Benzene, 1,3-diethenyl- *	130.0	C10H10		248.2
4-Piperidinone, 2,2,6,6-tetramethyl(M)*	155.0	C9H17NO		-334.3
1H-Indene, 2,3-dihydro-4-methyl-*	132.2	C10H12		28
(PAH); Isophorone	138.2	C9H14O		-251
(PAH); Phenol, 2-nitro-	139.0	C6H5NO3		-204.6
Benzyl nitrile *	117.0	C8H7N	n/a	
(PAH); Phenol, 2,4-dimethyl-	122.2	C8H10O		-162.9
Phenol, 2,5-dimethyl-*	122.2	C8H10O		-161.7
Phenol, 3,5-dimethyl-*	122.2	C8H10O		-161.6
1H-Indene, 1-methyl- *	130.2	C10H10		122
Benzene, 1-butynyl-*	130.2	C10H10		248.6
Phenol, 2-ethyl- *	122.2	C8H10O		-145.2
Benzene, (1-methyl-2-cyclopropen-1-yl)*	130.2	C10H10		297
1H-Indene, 3-methyl-*	130.2	C10H10		122
Naphtalene*	128.2	C10H8		150.6
(PAH); Methane, bis(2-chloroethoxy)-	172.0	C5H10Cl2O2	n/a	
4-Piperidinone, 2,2,6,6-tetramethyl-(R)	155.0	C9H17NO		-334.3
(PAH); Phenol, 2,4-dichloro-	162.0	C6H4Cl2O		-226.4
Phenol, 4-ethyl- *	122.2	C8H10O		-144.05
Naphthalene, 1,2-dihydro-*	130.0	C10H10	n/a	
(PAH); Benzene, 1,2,4-trichloro-	181.4	C6H3Cl3		-0.2
(IS); Naphthalene-D8	128.0	C10D8	n/a	
(PAH); Naphthalene	128.2	C10H8		150.6
Benzene, (ethenyloxy)-*	120.0	C8H8O		-52

1-Hexadecene *	224.4	C16H32		-248.6
(PAH); p-Chloroaniline	127.0	C6H6NCl	n/a	
(PAH); 1,3-Butadiene, hexachloro-	260.8	C4Cl6		-29.2
Benzofuran, 2,3-dihydro- *	120.0	C8H8O		-47.3
1H-Indazole, 3,6-dimethyl-*	146.0	C9H10N2		199
Benzofuran, 2-ethenyl-*	144.0	C10H8O		-29.9
Methenamine *	140.2	C6H12N4		199
Quinoline *	129.2	C9H7N		200.52
Benzenamine, N,N-dimethyl-4-[[(1-methy*	121.0	C8H11N		103.9
1H-Indene, 2,3-dimethyl-*	144.0	C11H12		261
Benzofuran, 2,3-dihydro-*	120.2	C8H8O		-46.5
(PAH); Phenol, 4-chloro-3-methyl-	142.0	C7H7ClO	n/a	
p-Isobutylbenzaldehyde*	162.0	C11H14O		-209.2
Naphthalene, 1-methyl-*	142.2	C11H10		116.9
Indole *	117.0	C8H7N		100.2
(PAH); Naphthalene, 2-methyl-	142.2	C11H10		116.11
(PAH); Naphthalene, 1-methyl-	142.2	C11H10		116.86
Benzofuran, 7-methyl-*	132.0	C9H8O		13.6
(PAH); 1,3-Cyclopentadiene, hexach	272.8	C5Cl6		-102
1H-Indenol *	132.0	C9H8O	n/a	
(PAH); Phenol, 2,4,6-trichloro-	196.0	C6H3Cl3O	n/a	
(PAH); Phenol, 2,4,5-trichloro-	196.0	C6H3Cl3O	n/a	
1H-Indole, 4-methyl-*	131.0	C9H9N		146.2
(PAH); Naphthalene, 2-chloro-	162.0	C10H7Cl		55.2
Biphenyl *	154.2	C12H10		182.4
3-Tetradecene(Z) *	196.0	C14H28		-271.3
Naphthalene, 1-ethyl*	156.0	C12H12		111.8
(PAH); o-Nitroaniline	138.1	C6H6N2O2		63.8
Naphthalene, 1,4-dimethyl-*	156.2	C12H12		76.1
Naphthalene, 2,3-dimethyl-*	156.2	C12H12		76.1
Naphthalene, 2-ethenyl-*	154.0	C12H10		160
Naphthalene, 1,6-dimethyl-*	156.2	C12H12		76.1
Naphthalene, 2,6-dimethyl-*	156.2	C12H12		76.1
Naphthalene, 1,6-dimethyl-**	156.2	C12H12		76.1
(PAH); Benzene, 1,4-dinitro-	168.1	C6H4N2O4		50.8
Naphthalene, 2-ethenyl-**	154.0	C12H10		160
(PAH); Acenaphthylene	152.0	C12H8		193
(PAH); Dimethyl phthalate	194.2	C10H10O4		-663
(PAH); 2,6-Dinitrotoluene	162.0	C3H6N4O4	n/a	
(PAH); Benzene, 1,2-dinitro-	168.1	C6H4N2O4		27.8
Naphthalene, 1,4-dimethyl-**	156.2	C12H12		76.1
(PAH); 3-Nitroaniline	138.1	C6H6N2O2		58.5
(IS); Acenaphthene-D10	152.0	C12H8	n/a	
(PAH); Acenaphthene	154.2	C12H10		155
1,1'-Biphenyl, 3-methyl-*	168.0	C13H12		166.4
(PAH); Phenol, 2,4-dinitro-	184.0	C6H4N2O5	n/a	
1-Naphthalenol*	144.2	C10H8O		-29.9
2-Naphthalenol*	144.2	C10H8O		-29.9
Phenol, 3,5-bis(1,1-dimethylethyl)- *	206.0	C14H22O		-410
(PAH); Dibenzofuran	168.2	C12H8O		83.4

(PAH); Phenol, 4-nitro-	139.0	C6H5NO3		-207.1
(PAH); 2,4-Dinitrotoluene	234.0	C10H6N2O5		-172
(PAH); Phenol, 2,3,4,6-tetrachloro-	230.0	C6H2Cl4O	n/a	
Naphthalene, 2-(1-methylethenyl)-*	168.0	C13H12		154.3
(PAH); Phenol, 2,3,5,6-tetrachloro-	230.0	C6H2Cl4O	n/a	
1(2H)-Acenaphthylenone*	168.0	C12H8O		52.1
(PAH); Fluorene	166.2	C13H10		171
(PAH); Benzene, 1-chloro-4-phenoxy-	204.0	C12H9ClO	n/a	
Fluorene-9-methanol*	196.0	C14H12O	n/a	
(PAH); Diethyl Phthalate	222.2	C12H14O4		-688.3
Fluorene*	166.2	C13H10		171
Dibenzofuran*	168.2	C12H8O		47.3
2-Naphthalenol, acetate*	186.0	C12H10O2	n/a	
Fluorene**	166.2	C13H10		171
(PAH); p-Nitroaniline	138.1	C6H6N2O2		59.5
(PAH); Phenol, 2-methyl-4,6-dinitro-	198.0	C7H6N2O5		-279
Fluorene***	166.2	C13H10		171
(PAH); Diphenylamine	198.0	C12H10N2O		227
Dibenzofuran, 4-methyl-*	182.0	C13H10O		52.9
(PAH); Azobenzene	182.0	C12H10N2		374
Fluorene****	166.2	C13H10		171
Fluorene*****	166.2	C13H10		171
(PAH); Benzene, 1-bromo-4-phenoxy-	248.0	C12H9BrO	n/a	
(PAH); Benzene, hexachloro-	284.8	C6Cl6		-33.9
9H-Fluorene, 1-methyl-*	180.0	C14H12		149.1
Phenol, 2-(1-phenylethyl)-*	198.0	C14H14O		93.6
9H-Fluorene, 9-methyl-*	180.3	C14H12		148
9H-Fluorene, 2-methyl-*	180.3	C14H12		149.1
(PAH); Phenol, pentachloro-	264.0	C6HCl5O		-292.5
(PAH); Phenanthrene	178.2	C14H10		207.5
(IS); Anthracene-D10	188.0	C14D10	n/a	
(PAH); Anthracene	178.2	C14H10		227.7
(PAH); Carbazole	167.2	C12H9N		209.6
Anthracene, 2-methyl-*	192.3	C15H12		196.9
Anthracene, 9-methyl-*	192.3	C15H12		196.9
Phenanthrene, 4-methyl-*	192.3	C15H12		195.8
4H-Cyclopenta[def]phenanthrene*	190.0	C15H10		227
(PAH); Dibutyl phthalate	278.3	C16H22O4		-750.9
Phenanthrene, 1-methyl-*	192.3	C15H12		196.9
4H-Cyclopenta[def]phenanthrene**	190.0	C15H10		227
Naphthalene, 2-phenyl-*	204.0	C16H12		466.1
(PAH); Fluoranthene	202.3	C16H10		289
(PAH); Pyrene	202.3	C16H10		225.7
Fluoranthene*	202.3	C16H10		292
11H-Benzo[c]fluorene*	216.0	C17H12		294.2
Pyrene, 1-methyl-*	216.0	C17H12		294.2
Pyrene, 1-methyl-**	216.0	C17H12		294.2
Benzanthrene*	228.0	C18H12		277
(PAH); Benzyl butyl phthalate	312.0	C19H20O4	n/a	
(PAH); bis(2-ethylhexyl) adipate	370.0	C22H42O4	n/a	

Phenol, 2,4-bis(1-phenylethyl)-*	302.0	C22H22O	n/a
Phenol, 2,4-bis(1-phenylethyl)-**	302.0	C22H22O	n/a
Phenol, 2,4-bis(1-phenylethyl)-***	302.0	C22H22O	n/a
(PAH); Benz[a]anthracene	228.0	C18H12	275.73
(IS); Chrysene-D12	240.0	C18D12	n/a
(PAH); Chrysene	228.3	C18H12	269.8
(PAH); Bis(2-ethylhexyl) phthalate	390.6	C24H38O4	-967
(PAH); Di-n-octyl phthalate	390.6	C24H38O4	-966.72
(PAH); Benzo[b] fluoranthene	252.0	C20H12	348.025
(PAH); Benzo[k] fluoranthene	252.0	C20H12	348.025
(PAH); Benzo[a] pyrene	252.0	C20H12	307.4505
(IS); Perylene-D12	264.0	C20D12	n/a
(PAH); Indeno[1,2,3-cd]pyrene	276.0	C22H12	371.03
(PAH); Dibenz[a,h]anthracene	278.0	C22H14	317.908
(PAH); Benzo[ghi]perylene	276.0	C22H12	316.234

Table 8.1: List of tar compounds analyzed with GC-MS method

TOPLEVEL PARAMETERS

Method Information For: C:\MSDCHEM\1\METHODS\TAR_PROJECT\TAR7JRGI.M

Method Sections To Run:

( ) Save Copy of Method With Data
( ) MSTOP Pre-Run Cmd/Macro =
( ) Instrument Control Pre-Run Cmd/Macro =
( ) Data Analysis Pre-Run Cmd/Macro =
(X) Data Acquisition
(X) Data Analysis
( ) MSTOP Post-Run Cmd/Macro =
( ) Instrument Control Post-Run Cmd/Macro =
( ) Data Analysis Post-Run Cmd/Macro =

Method Comments:
This is the default method

END OF TOPLEVEL PARAMETERS

INSTRUMENT CONTROL PARAMETERS

==========
6890 GC METHOD
==========

OVEN
Initial temp: 60 'C (On) Maximum temp: 340 'C
Initial time: 1.25 min Equilibration time: 0.00 min
Ramps:

#	Rate	Final temp	Final time
1	20.00	320	4.00
2	0.0(Off)		

Post temp: 60 'C
Post time: 0.00 min
Run time: 18.25 min

FRONT INLET (SPLIT/SPLITLESS)
Mode: Split
Initial temp: 300 'C (On)
Pressure: 2.14 psi (Off)
Split ratio: 10:1
Split flow: 11.9 mL/min
Total flow: 19.9 mL/min
Gas saver: Off
Gas type: Hydrogen

BACK INLET (SPLIT/SPLITLESS)
Mode: Split
Initial temp: 300 'C (On)
Pressure: 9.49 psi (On)
Split ratio: 10:1
Split flow: 12.0 mL/min
Total flow: 19.9 mL/min
Gas saver: Off
Gas type: Hydrogen

COLUMN 1
Capillary Column
Model Number: Agilent 122-5536

COLUMN 2
Capillary Column
Model Number: Agilent 128-5522

Method: TAR7JRGI.M Thu Apr 26 08:36:11 2007 Page: 1

DB-5ms, 0.25mm * 30m * 0.5um
Max temperature: 350 'C
Nominal length: 29.8 m
Nominal diameter: 250.00 um
Nominal film thickness: 0.50 um
Mode: constant flow
Initial flow: 1.2 mL/min
Nominal init pressure: 2.14 psi
Average velocity: 60 cm/sec
Inlet: Front Inlet
Outlet: MSD
Outlet pressure: vacuum

DB-5ms, 0.2mm * 25m * 0.33um
Max temperature: 350 'C
Nominal length: 25.0 m
Nominal diameter: 200.00 um
Nominal film thickness: 0.33 um
Mode: constant flow
Initial flow: 1.2 mL/min
Nominal init pressure: 9.49 psi
Average velocity: 65 cm/sec
Inlet: Back Inlet
Outlet: MSD
Outlet pressure: vacuum

FRONT DETECTOR (TCD)
Temperature: 250 'C (Off)
Reference flow: 20.0 mL/min (Off)
Mode: Constant makeup flow
Makeup flow: 7.0 mL/min (Off)
Makeup Gas Type: Hydrogen
Filament: Off
Negative polarity: Off

BACK DETECTOR (NO DET)

SIGNAL 1
Data rate: 20 Hz
Type: test plot
Save Data: Off
Zero: 0.0 (Off)
Range: 0
Fast Peaks: Off
Attenuation: 0

SIGNAL 2
Data rate: 20 Hz
Type: test plot
Save Data: Off
Zero: 0.0 (Off)
Range: 0
Fast Peaks: Off
Attenuation: 0

COLUMN COMP 1
(No Detectors Installed)

COLUMN COMP 2
(No Detectors Installed)

THERMAL AUX 2
Use: MSD Transfer Line Heater
Description: MSD Transfer Line
Initial temp: 300 'C (On)
Initial time: 18.25 min

#	Rate	Final temp	Final time
1	0.0(Off)		

POST RUN
Post Time: 0.00 min

TIME TABLE

Time	Specifier	Parameter & Setpoint

7673 Injector

Front Injector:
No parameters specified

Back Injector:

Sample Washes	2
Sample Pumps	4
Injection Volume	1.0 microliters
Syringe Size	10.0 microliters

PostInj Solvent A Washes 0
PostInj Solvent B Washes 2
Viscosity Delay 0 seconds
Plunger Speed Fast
PreInjection Dwell 0.00 minutes
PostInjection Dwell 0.00 minutes

Column 1 Inventory Number : RGI006
Column 2 Inventory Number : RGI005

MS ACQUISITION PARAMETERS

General Information
------- -----------

Tune File : atune.u
Acquistion Mode : Scan

MS Information
-- -----------

Solvent Delay : 1.00 min

EM Absolute : False
EM Offset : 400
Resulting EM Voltage : 2211.8

[Scan Parameters]

Low Mass : 15.0
High Mass : 150.0
Threshold : 50
Sample # : 3 A/D Samples 8
Plot 2 low mass : 15.0
Plot 2 high mass : 20.0

Start Time : 2.20
Low Mass : 35.0
High Mass : 325.0
Threshold : 50
Sample # : 2 A/D Samples 4
Plot 2 low mass : 35.0
Plot 2 high mass : 200.0

[MSZones]

MS Quad : 150 C maximum 200 C
MS Source : 230 C maximum 250 C
Timed Events
----- ------

[Timed MS Detector Entries]

Time (min) State (MS on/off)
1.00 On

END OF MS ACQUISITION PARAMETERS

Method: TAR7JRGI.M Thu Apr 26 08:36:11 2007 Page: 3

END OF INSTRUMENT CONTROL PARAMETERS

DATA ANALYSIS PARAMETERS

Method Name: C:\MSDCHEM\1\METHODS\TAR_PROJECT\TAR7JRGI.M

Percent Report Settings

Sort By: Signal

Output Destination
Screen: No
Printer: Yes
File: No

Integration Events: Meth Default

Generate Report During Run Method: No

Signal Correlation Window: 0.020

Quantitative Report Settings

Report Type: Summary

Output Destination
Screen: Yes
Printer: No
File: No

Generate Report During Run Method: No

PAH's and BTEX Calibration
Calibration Last Updated: Wed Sep 27 09:08:08 2006

Reference Window: 2.00 Minutes
Non-Reference Window: 1.00 Minutes
Correlation Window: 0.10 minutes
Default Multiplier: 1.00
Default Sample Concentration: 0.00

Compound Information

---
1) (BTEX); Benzene ( )
Ret. Time 1.30 min., Extract & Integrate from 1.20 to 1.40 min.

Lvl	ID	Conc (ug/ml)	Response
1		1.000	159019
2		10.000	515185
3		20.000	842376
4		50.000	2297581
5		100.000	4652321
6		1.000	-1
7		10.000	-1
8		20.000	-1
9		50.000	-1
10		100.000	-1
11		1.000	-1
12		10.000	-1
13		20.000	-1
14		50.000	-1
15		100.000	-1

Curve Fit: Linear
---

2) 2-Propanone, 1-hydroxy- * ( )
Ret. Time 1.28 min., Extract & Integrate from 1.18 to 1.38 min.

Lvl	ID	Conc (ug/ml)	Response
1		1.000	159019
2		10.000	515185
3		20.000	842376
4		50.000	2297581
5		100.000	4652321
6		1.000	-1
7		10.000	-1
8		20.000	-1
9		50.000	-1
10		100.000	-1
11		1.000	-1
12		10.000	-1
13		20.000	-1
14		50.000	-1
15		100.000	-1

Curve Fit: Linear
---

3) 3-Penten-2-one, (E)- * ( )
Ret. Time 1.71 min., Extract & Integrate from 1.61 to 1.81 min.

Lvl	ID	Conc (ug/ml)	Response
1		1.000	-1
2		10.000	-1
3		20.000	-1
4		50.000	-1

5	100.000	-1
6	1.000	-1
7	10.000	-1
8	20.000	-1
9	50.000	-1
10	100.000	-1
11	1.000	-1
12	10.000	73271
13	20.000	132702
14	50.000	206521
15	100.000	596525

Curve Fit: Linear

---

4) (PAH); N-Nitrosodimethylamine ( )

Ret. Time 1.73 min., Extract & Integrate from 1.63 to 1.83 min.

Lvl	ID	Conc (ug/ml)	Response
1		1.000	-1
2		10.000	-1
3		20.000	-1
4		50.000	-1
5		100.000	-1
6		1.000	-1
7		10.000	-1
8		20.000	-1
9		50.000	-1
10		100.000	-1
11		1.000	-1
12		10.000	73271
13		20.000	132702
14		50.000	206521
15		100.000	596525

Curve Fit: Linear

---

5) (PAH); Pyridine ( )

Ret. Time 1.78 min., Extract & Integrate from 1.68 to 1.88 min.

Lvl	ID	Conc (ug/ml)	Response
1		1.000	-1
2		10.000	-1
3		20.000	-1
4		50.000	-1
5		100.000	-1
6		1.000	-1
7		10.000	-1
8		20.000	-1
9		50.000	-1
10		100.000	-1
11		1.000	-1
12		10.000	165880
13		20.000	312381
14		50.000	436534
15		100.000	1359433

Curve Fit: Linear

---

6) (BTEX);Toluene ( )
Ret. Time 1.95 min., Extract & Integrate from 1.85 to 2.05 min.

Lvl	ID	Conc (ug/ml)	Response
1		1.000	197562
2		10.000	536347
3		20.000	877703
4		50.000	2319364
5		100.000	4690515
6		1.000	-1
7		10.000	-1
8		20.000	-1
9		50.000	-1
10		100.000	-1
11		1.000	-1
12		10.000	-1
13		20.000	-1
14		50.000	-1
15		100.000	-1

Curve Fit: Linear

---

7) 2-Amino-4-methyl-oxazole * Cyclopentane ( )
Ret. Time 3.32 min., Extract & Integrate from 3.22 to 3.42 min.

Lvl	ID	Conc (ug/ml)	Response
1		1.000	-1
2		10.000	-1
3		20.000	-1
4		50.000	-1
5		100.000	-1
6		1.000	47714
7		10.000	380523
8		20.000	708891
9		50.000	2615182
10		100.000	3923110
11		1.000	-1
12		10.000	-1
13		20.000	-1
14		50.000	-1
15		100.000	-1

Curve Fit: Linear

---

8) 3-Penten-2-one, 4-methyl- * ( )
Ret. Time 2.17 min., Extract & Integrate from 2.07 to 2.27 min.

Lvl	ID	Conc (ug/ml)	Response
1		1.000	197562
2		10.000	536347
3		20.000	877703
4		50.000	2319364

5	100.000	4690515
6	1.000	-1
7	10.000	-1
8	20.000	-1
9	50.000	-1
10	100.000	-1
11	1.000	-1
12	10.000	-1
13	20.000	-1
14	50.000	-1
15	100.000	-1

Curve Fit: Linear

---

9) Furfural * ( )

Ret. Time 2.49 min., Extract & Integrate from 2.39 to 2.59 min.

Lvl	ID	Conc (ug/ml)	Response
1		1.000	-1
2		10.000	-1
3		20.000	-1
4		50.000	-1
5		100.000	-1
6		1.000	22913
7		10.000	210246
8		20.000	389986
9		50.000	1447900
10		100.000	2141423
11		1.000	-1
12		10.000	-1
13		20.000	-1
14		50.000	-1
15		100.000	-1

Curve Fit: Linear

---

10) 2-Pentanone, 4-hydroxy-4-methyl- * ( )

Ret. Time 2.57 min., Extract & Integrate from 2.47 to 2.67 min.

Lvl	ID	Conc (ug/ml)	Response
1		1.000	-1
2		10.000	-1
3		20.000	-1
4		50.000	-1
5		100.000	-1
6		1.000	-1
7		10.000	-1
8		20.000	-1
9		50.000	-1
10		100.000	-1
11		1.000	-1
12		10.000	-1
13		20.000	-1
14		50.000	-1
15		100.000	-1

Curve Fit: Linear

---

11) (Mix 4); Benzene, Chloro- ( )
Ret. Time 2.63 min., Extract & Integrate from 2.53 to 2.73 min.

Lvl	ID	Conc (ug/ml)	Response
1		1.000	-1
2		10.000	-1
3		20.000	-1
4		50.000	-1
5		100.000	-1
6		1.000	22913
7		10.000	210246
8		20.000	389986
9		50.000	1447900
10		100.000	2141423
11		1.000	-1
12		10.000	-1
13		20.000	-1
14		50.000	-1
15		100.000	-1

Curve Fit: Linear

---

12) (BTEX); Ethylbenzene ( )
Ret. Time 2.75 min., Extract & Integrate from 2.65 to 2.85 min.

Lvl	ID	Conc (ug/ml)	Response
1		1.000	65229
2		10.000	447530
3		20.000	790513
4		50.000	2391292
5		100.000	5025587
6		1.000	-1
7		10.000	-1
8		20.000	-1
9		50.000	-1
10		100.000	-1
11		1.000	-1
12		10.000	-1
13		20.000	-1
14		50.000	-1
15		100.000	-1

Curve Fit: Linear

---

13) (Mix 4); Xylene, m- ( )
Ret. Time 2.83 min., Extract & Integrate from 2.73 to 2.93 min.

Lvl	ID	Conc (ug/ml)	Response
1		1.000	-1
2		10.000	-1
3		20.000	-1
4		50.000	-1

5	100.000	-1
6	1.000	51729
7	10.000	304813
8	20.000	591357
9	50.000	2096395
10	100.000	3173239
11	1.000	-1
12	10.000	-1
13	20.000	-1
14	50.000	-1
15	100.000	-1

Curve Fit: Linear

---

14) (BTEX); p-xylene ( )

Ret. Time 2.84 min., Extract & Integrate from 2.74 to 2.94 min.

Lvl	ID	Conc (ug/ml)	Response
1		1.000	54326
2		10.000	347298
3		20.000	638753
4		50.000	2060219
5		100.000	4563077
6		1.000	-1
7		10.000	-1
8		20.000	-1
9		50.000	-1
10		100.000	-1
11		1.000	-1
12		10.000	-1
13		20.000	-1
14		50.000	-1
15		100.000	-1

Curve Fit: Linear

---

15) Phenylethyne * ( )

Ret. Time 2.88 min., Extract & Integrate from 2.77 to 2.98 min.

Lvl	ID	Conc (ug/ml)	Response
1		1.000	54326
2		10.000	347298
3		20.000	638753
4		50.000	2060219
5		100.000	4563077
6		1.000	-1
7		10.000	-1
8		20.000	-1
9		50.000	-1
10		100.000	-1
11		1.000	-1
12		10.000	-1
13		20.000	-1
14		50.000	-1
15		100.000	-1

Curve Fit: Linear

---

16) (Mix 4); Styrene ( )
Ret. Time 3.03 min., Extract & Integrate from 2.93 to 3.13 min.

Lvl	ID	Conc (ug/ml)	Response
1		1.000	-1
2		10.000	-1
3		20.000	-1
4		50.000	-1
5		100.000	-1
6		1.000	19660
7		10.000	208523
8		20.000	413087
9		50.000	1555086
10		100.000	2360085
11		1.000	-1
12		10.000	-1
13		20.000	-1
14		50.000	-1
15		100.000	-1

Curve Fit: Linear

---

17) (BTEX); o-xylene ( )
Ret. Time 3.04 min., Extract & Integrate from 2.94 to 3.14 min.

Lvl	ID	Conc (ug/ml)	Response
1		1.000	62799
2		10.000	386580
3		20.000	671103
4		50.000	1986486
5		100.000	4101020
6		1.000	-1
7		10.000	-1
8		20.000	-1
9		50.000	-1
10		100.000	-1
11		1.000	-1
12		10.000	-1
13		20.000	-1
14		50.000	-1
15		100.000	-1

Curve Fit: Linear

---

18) (Mix 4); Benzene, isopropyl- ( )
Ret. Time 3.32 min., Extract & Integrate from 3.22 to 3.42 min.

Lvl	ID	Conc (ug/ml)	Response
1		1.000	-1
2		10.000	-1
3		20.000	-1
4		50.000	-1

5	100.000	-1
6	1.000	47714
7	10.000	380523
8	20.000	708891
9	50.000	2615182
10	100.000	3923110
11	1.000	-1
12	10.000	-1
13	20.000	-1
14	50.000	-1
15	100.000	-1

Curve Fit: Linear

---

19) Furan * ( )

Ret. Time 3.33 min., Extract & Integrate from 3.23 to 3.43 min.

Lvl	ID	Conc (ug/ml)	Response
1		1.000	-1
2		10.000	-1
3		20.000	-1
4		50.000	-1
5		100.000	-1
6		1.000	47714
7		10.000	380523
8		20.000	708891
9		50.000	2615182
10		100.000	3923110
11		1.000	-1
12		10.000	-1
13		20.000	-1
14		50.000	-1
15		100.000	-1

Curve Fit: Linear

---

20) 1,3-Cyclopentadiene, 5-(1-methylethylid ( )

Ret. Time 3.46 min., Extract & Integrate from 3.36 to 3.56 min.

Lvl	ID	Conc (ug/ml)	Response
1		1.000	-1
2		10.000	-1
3		20.000	-1
4		50.000	-1
5		100.000	-1
6		1.000	77814
7		10.000	438031
8		20.000	848479
9		50.000	3140930
10		100.000	4830774
11		1.000	-1
12		10.000	-1
13		20.000	-1
14		50.000	-1
15		100.000	-1

Curve Fit: Linear

---

21) (Mix 4); Benzene, n-propyl- ( )
Ret. Time 3.59 min., Extract & Integrate from 3.50 to 3.69 min.

Lvl	ID	Conc (ug/ml)	Response
1		1.000	-1
2		10.000	-1
3		20.000	-1
4		50.000	-1
5		100.000	-1
6		1.000	77814
7		10.000	438031
8		20.000	848479
9		50.000	3140930
10		100.000	4830774
11		1.000	-1
12		10.000	-1
13		20.000	-1
14		50.000	-1
15		100.000	-1

Curve Fit: Linear

---

22) Benzene, 1-ethyl-3-methyl- * ( )
Ret. Time 3.65 min., Extract & Integrate from 3.55 to 3.75 min.

Lvl	ID	Conc (ug/ml)	Response
1		1.000	-1
2		10.000	-1
3		20.000	-1
4		50.000	-1
5		100.000	-1
6		1.000	41918
7		10.000	323826
8		20.000	621412
9		50.000	2310772
10		100.000	3522022
11		1.000	-1
12		10.000	-1
13		20.000	-1
14		50.000	-1
15		100.000	-1

Curve Fit: Linear

---

23) (Mix 4); Benzene, 1,3,5-trimethyl- ( )
Ret. Time 3.73 min., Extract & Integrate from 3.63 to 3.83 min.

Lvl	ID	Conc (ug/ml)	Response
1		1.000	-1
2		10.000	-1
3		20.000	-1
4		50.000	-1

5	100.000	-1
6	1.000	41918
7	10.000	323826
8	20.000	621412
9	50.000	2310772
10	100.000	3522022
11	1.000	-1
12	10.000	-1
13	20.000	-1
14	50.000	-1
15	100.000	-1

Curve Fit: Linear

---

24) (PAH); Aniline ( )

Ret. Time 3.79 min., Extract & Integrate from 3.69 to 3.89 min.

Lvl	ID	Conc (ug/ml)	Response
1		1.000	-1
2		10.000	-1
3		20.000	-1
4		50.000	-1
5		100.000	-1
6		1.000	-1
7		10.000	-1
8		20.000	-1
9		50.000	-1
10		100.000	-1
11		1.000	-1
12		10.000	142706
13		20.000	322262
14		50.000	650592
15		100.000	1348903

Curve Fit: Linear

---

25) (PAH); Phenol ( )

Ret. Time 3.74 min., Extract & Integrate from 3.64 to 3.84 min.

Lvl	ID	Conc (ug/ml)	Response
1		1.000	-1
2		10.000	-1
3		20.000	-1
4		50.000	-1
5		100.000	-1
6		1.000	-1
7		10.000	-1
8		20.000	-1
9		50.000	-1
10		100.000	-1
11		1.000	-1
12		10.000	74623
13		20.000	238673
14		50.000	445861
15		100.000	1346346

Curve Fit: Linear

---

26) Benzene, (1-methylethenyl)-* (styrene-a ( )
Ret. Time 3.84 min., Extract & Integrate from 3.74 to 3.94 min.

Lvl	ID	Conc (ug/ml)	Response
1		1.000	-1
2		10.000	-1
3		20.000	-1
4		50.000	-1
5		100.000	-1
6		1.000	-1
7		10.000	-1
8		20.000	-1
9		50.000	-1
10		100.000	-1
11		1.000	-1
12		10.000	109497
13		20.000	256869
14		50.000	427152
15		100.000	1140874

Curve Fit: Linear

---

27) (PAH); Bis(2-chloroethyl) ether ( )
Ret. Time 3.85 min., Extract & Integrate from 3.76 to 3.95 min.

Lvl	ID	Conc (ug/ml)	Response
1		1.000	-1
2		10.000	-1
3		20.000	-1
4		50.000	-1
5		100.000	-1
6		1.000	-1
7		10.000	-1
8		20.000	-1
9		50.000	-1
10		100.000	-1
11		1.000	-1
12		10.000	109497
13		20.000	256869
14		50.000	427152
15		100.000	1140874

Curve Fit: Linear

---

28) (PAH); Phenol, 2-chloro- ( )
Ret. Time 3.91 min., Extract & Integrate from 3.81 to 4.01 min.

Lvl	ID	Conc (ug/ml)	Response
1		1.000	-1
2		10.000	-1
3		20.000	-1
4		50.000	-1

5	100.000	-1
6	1.000	-1
7	10.000	-1
8	20.000	-1
9	50.000	-1
10	100.000	-1
11	1.000	-1
12	10.000	95259
13	20.000	244646
14	50.000	413763
15	100.000	1138567

Curve Fit: Linear

---

29) Benzene, 1,2,4 trimethyl -* ( )

Ret. Time 3.75 min., Extract & Integrate from 3.65 to 3.85 min.

Lvl	ID	Conc (ug/ml)	Response
1		1.000	-1
2		10.000	-1
3		20.000	-1
4		50.000	-1
5		100.000	-1
6		1.000	-1
7		10.000	-1
8		20.000	-1
9		50.000	-1
10		100.000	-1
11		1.000	-1
12		10.000	74623
13		20.000	238673
14		50.000	445861
15		100.000	1346346

Curve Fit: Linear

---

30) (PAH); Benzene, 1,3-dichloro- ( )

Ret. Time 4.08 min., Extract & Integrate from 3.99 to 4.18 min.

Lvl	ID	Conc (ug/ml)	Response
1		1.000	-1
2		10.000	-1
3		20.000	-1
4		50.000	-1
5		100.000	-1
6		1.000	-1
7		10.000	-1
8		20.000	-1
9		50.000	-1
10		100.000	-1
11		1.000	16145
12		10.000	195360
13		20.000	418091
14		50.000	625578
15		100.000	1597310

Curve Fit: Linear

---

31) (PAH); Benzene, 1,4-dichloro- ( )
Ret. Time 4.16 min., Extract & Integrate from 4.07 to 4.26 min.

Lvl	ID	Conc (ug/ml)	Response
1		1.000	-1
2		10.000	-1
3		20.000	-1
4		50.000	-1
5		100.000	-1
6		1.000	-1
7		10.000	-1
8		20.000	-1
9		50.000	-1
10		100.000	-1
11		1.000	21109
12		10.000	191288
13		20.000	427045
14		50.000	649308
15		100.000	1677925

Curve Fit: Linear

---

32) (Mix 4); Benzene, tert-butyl- ( )
Ret. Time 4.01 min., Extract & Integrate from 3.91 to 4.11 min.

Lvl	ID	Conc (ug/ml)	Response
1		1.000	-1
2		10.000	-1
3		20.000	-1
4		50.000	-1
5		100.000	-1
6		1.000	32888
7		10.000	287577
8		20.000	536503
9		50.000	1977587
10		100.000	3062272
11		1.000	-1
12		10.000	-1
13		20.000	-1
14		50.000	-1
15		100.000	-1

Curve Fit: Linear

---

33) Benzofuran * ( )
Ret. Time 4.07 min., Extract & Integrate from 3.97 to 4.17 min.

Lvl	ID	Conc (ug/ml)	Response
1		1.000	-1
2		10.000	-1
3		20.000	-1
4		50.000	-1

5	100.000	-1
6	1.000	32888
7	10.000	287577
8	20.000	536503
9	50.000	1977587
10	100.000	3062272
11	1.000	-1
12	10.000	-1
13	20.000	-1
14	50.000	-1
15	100.000	-1

Curve Fit: Linear

---

34) Benzene, 1-ethynyl-2-methyl- * ( )

Ret. Time 4.04 min., Extract & Integrate from 3.94 to 4.14 min.

Lvl	ID	Conc (ug/ml)	Response
1		1.000	-1
2		10.000	-1
3		20.000	-1
4		50.000	-1
5		100.000	-1
6		1.000	32888
7		10.000	287577
8		20.000	536503
9		50.000	1977587
10		100.000	3062272
11		1.000	-1
12		10.000	-1
13		20.000	-1
14		50.000	-1
15		100.000	-1

Curve Fit: Linear

---

35) (PAH); Benzyl Alcohol ( )

Ret. Time 4.29 min., Extract & Integrate from 4.19 to 4.39 min.

Lvl	ID	Conc (ug/ml)	Response
1		1.000	-1
2		10.000	-1
3		20.000	-1
4		50.000	-1
5		100.000	-1
6		1.000	-1
7		10.000	-1
8		20.000	-1
9		50.000	-1
10		100.000	-1
11		1.000	-1
12		10.000	56194
13		20.000	146911
14		50.000	222616
15		100.000	791566

Curve Fit: Linear

---

36) (PAH); Benzene, 1,2-dichloro- ( )
Ret. Time 4.33 min., Extract & Integrate from 4.23 to 4.43 min.

Lvl	ID	Conc (ug/ml)	Response
1		1.000	-1
2		10.000	-1
3		20.000	-1
4		50.000	-1
5		100.000	-1
6		1.000	-1
7		10.000	-1
8		20.000	-1
9		50.000	-1
10		100.000	-1
11		1.000	16622
12		10.000	184502
13		20.000	387686
14		50.000	592998
15		100.000	1528039

Curve Fit: Linear

---

37) Piperidine, 3-isopropyl- * ( )
Ret. Time 4.73 min., Extract & Integrate from 4.63 to 4.83 min.

Lvl	ID	Conc (ug/ml)	Response
1		1.000	-1
2		10.000	-1
3		20.000	-1
4		50.000	-1
5		100.000	-1
6		1.000	-1
7		10.000	-1
8		20.000	-1
9		50.000	-1
10		100.000	-1
11		1.000	4500
12		10.000	40747
13		20.000	92400
14		50.000	137251
15		100.000	375413

Curve Fit: Linear

---

38) Indene * ( )
Ret. Time 4.43 min., Extract & Integrate from 4.33 to 4.53 min.

Lvl	ID	Conc (ug/ml)	Response
1		1.000	-1
2		10.000	-1
3		20.000	-1
4		50.000	-1

5	100.000	-1
6	1.000	-1
7	10.000	-1
8	20.000	-1
9	50.000	-1
10	100.000	-1
11	1.000	-1
12	10.000	88137
13	20.000	170509
14	50.000	239242
15	100.000	737362

Curve Fit: Linear

---

39) (PAH); Phenol, 2-methyl- ( )
Ret. Time 4.41 min., Extract & Integrate from 4.31 to 4.51 min.

Lvl	ID	Conc (ug/ml)	Response
1		1.000	-1
2		10.000	-1
3		20.000	-1
4		50.000	-1
5		100.000	-1
6		1.000	-1
7		10.000	-1
8		20.000	-1
9		50.000	-1
10		100.000	-1
11		1.000	-1
12		10.000	99259
13		20.000	239101
14		50.000	403062
15		100.000	1154860

Curve Fit: Linear

---

40) (PAH); Bis(2-chloroisopropyl) ether ( )
Ret. Time 4.45 min., Extract & Integrate from 4.35 to 4.55 min.

Lvl	ID	Conc (ug/ml)	Response
1		1.000	-1
2		10.000	-1
3		20.000	-1
4		50.000	-1
5		100.000	-1
6		1.000	-1
7		10.000	-1
8		20.000	-1
9		50.000	-1
10		100.000	-1
11		1.000	13711
12		10.000	193534
13		20.000	433283
14		50.000	652788
15		100.000	1715038

Curve Fit: Linear

---

41) N,N-bis(1-methylethyl-2-Propen-1-amine* ( )
Ret. Time 4.63 min., Extract & Integrate from 4.53 to 4.73 min.

Lvl	ID	Conc (ug/ml)	Response
1		1.000	-1
2		10.000	-1
3		20.000	-1
4		50.000	-1
5		100.000	-1
6		1.000	-1
7		10.000	-1
8		20.000	-1
9		50.000	-1
10		100.000	-1
11		1.000	4500
12		10.000	40747
13		20.000	92400
14		50.000	137251
15		100.000	375413

Curve Fit: Linear

---

42) (PAH); 4-Methylphenol & 3-Methylphenol ( )
Ret. Time 4.58 min., Extract & Integrate from 4.49 to 4.68 min.

Lvl	ID	Conc (ug/ml)	Response
1		1.000	-1
2		10.000	-1
3		20.000	-1
4		50.000	-1
5		100.000	-1
6		1.000	-1
7		10.000	-1
8		20.000	-1
9		50.000	-1
10		100.000	-1
11		1.000	-1
12		10.000	74023
13		20.000	206344
14		50.000	346326
15		100.000	1068937

Curve Fit: Linear

---

43) (PAH); N-nitroso-di-n-propylamine ( )
Ret. Time 4.59 min., Extract & Integrate from 4.49 to 4.69 min.

Lvl	ID	Conc (ug/ml)	Response
1		1.000	-1
2		10.000	-1
3		20.000	-1
4		50.000	-1

5	100.000	-1
6	1.000	-1
7	10.000	-1
8	20.000	-1
9	50.000	-1
10	100.000	-1
11	1.000	-1
12	10.000	60526
13	20.000	156103
14	50.000	251825
15	100.000	750074

Curve Fit: Linear

---

44) (PAH); Ethane, hexachloro- ( )
Ret. Time 4.71 min., Extract & Integrate from 4.61 to 4.81 min.

Lvl	ID	Conc (ug/ml)	Response
1		1.000	-1
2		10.000	-1
3		20.000	-1
4		50.000	-1
5		100.000	-1
6		1.000	-1
7		10.000	-1
8		20.000	-1
9		50.000	-1
10		100.000	-1
11		1.000	4500
12		10.000	40747
13		20.000	92400
14		50.000	137251
15		100.000	375413

Curve Fit: Linear

---

45) (PAH); Benzene, nitro- ( )
Ret. Time 4.79 min., Extract & Integrate from 4.69 to 4.89 min.

Lvl	ID	Conc (ug/ml)	Response
1		1.000	-1
2		10.000	-1
3		20.000	-1
4		50.000	-1
5		100.000	-1
6		1.000	-1
7		10.000	-1
8		20.000	-1
9		50.000	-1
10		100.000	-1
11		1.000	-1
12		10.000	88137
13		20.000	170509
14		50.000	239242
15		100.000	737362

Curve Fit: Linear
---

46) (IS); 1,4-Dichlorobenzene-D4 (ISTD)
Ret. Time 4.14 min., Extract & Integrate from 4.04 to 4.24 min.

Lvl	ID	Conc (ug/ml)	Response
1		20.000	407643
2		20.000	437127
3		20.000	418570
4		20.000	388321
5		20.000	389012
6		20.000	390017
7		20.000	371183
8		20.000	384448
9		20.000	378557
10		20.000	402869
11		20.000	382250
12		20.000	472235
13		20.000	508514
14		20.000	613916
15		20.000	499974

ISTD conc: 20.000 ug/ml
Curve Fit: Linear
---

47) Benzofuran, 2-methyl- * ( )
Ret. Time 4.86 min., Extract & Integrate from 4.76 to 4.96 min.

Lvl	ID	Conc (ug/ml)	Response
1		1.000	-1
2		10.000	-1
3		20.000	-1
4		50.000	-1
5		100.000	-1
6		1.000	-1
7		10.000	-1
8		20.000	-1
9		50.000	-1
10		100.000	-1
11		1.000	-1
12		10.000	-1
13		20.000	-1
14		50.000	-1
15		100.000	-1

Curve Fit: Linear
---

48) Benzofuran, 7-methyl- * ( )
Ret. Time 5.01 min., Extract & Integrate from 4.91 to 5.11 min.

Lvl	ID	Conc (ug/ml)	Response
1		1.000	-1
2		10.000	-1
3		20.000	-1
4		50.000	-1

5	100.000	-1
6	1.000	-1
7	10.000	-1
8	20.000	-1
9	50.000	-1
10	100.000	-1
11	1.000	-1
12	10.000	132309
13	20.000	333161
14	50.000	569290
15	100.000	1832607

Curve Fit: Linear

---

49) 1-phenyl-, o-(4-coumarinyl)ox-Ethanone* ( )
Ret. Time 4.99 min., Extract & Integrate from 4.89 to 5.09 min.

Lvl ID	Conc (ug/ml)	Response
1	1.000	-1
2	10.000	-1
3	20.000	-1
4	50.000	-1
5	100.000	-1
6	1.000	-1
7	10.000	-1
8	20.000	-1
9	50.000	-1
10	100.000	-1
11	1.000	-1
12	10.000	132309
13	20.000	333161
14	50.000	569290
15	100.000	1832607

Curve Fit: Linear

---

50) 4-Piperidinone, 2,2,6,6-tetramethyl- * ( )
Ret. Time 5.10 min., Extract & Integrate from 5.00 to 5.20 min.

Lvl ID	Conc (ug/ml)	Response
1	1.000	-1
2	10.000	-1
3	20.000	-1
4	50.000	-1
5	100.000	-1
6	1.000	-1
7	10.000	-1
8	20.000	-1
9	50.000	-1
10	100.000	-1
11	1.000	-1
12	10.000	132309
13	20.000	333161
14	50.000	569290
15	100.000	1832607

Curve Fit: Linear

---

51) (PAH); Isophorone ( )
Ret. Time 5.06 min., Extract & Integrate from 4.97 to 5.16 min.

Lvl	ID	Conc (ug/ml)	Response
1		1.000	-1
2		10.000	-1
3		20.000	-1
4		50.000	-1
5		100.000	-1
6		1.000	-1
7		10.000	-1
8		20.000	-1
9		50.000	-1
10		100.000	-1
11		1.000	-1
12		10.000	132309
13		20.000	333161
14		50.000	569290
15		100.000	1832607

Curve Fit: Linear

---

52) (PAH); Phenol, 2-nitro- ( )
Ret. Time 5.15 min., Extract & Integrate from 5.06 to 5.25 min.

Lvl	ID	Conc (ug/ml)	Response
1		1.000	-1
2		10.000	-1
3		20.000	-1
4		50.000	-1
5		100.000	-1
6		1.000	-1
7		10.000	-1
8		20.000	-1
9		50.000	-1
10		100.000	-1
11		1.000	-1
12		10.000	23070
13		20.000	57563
14		50.000	109736
15		100.000	349526

Curve Fit: Linear

---

53) 1H-Indene, 3-methyl-* ( )
Ret. Time 5.42 min., Extract & Integrate from 5.33 to 5.52 min.

Lvl	ID	Conc (ug/ml)	Response
1		1.000	-1
2		10.000	-1
3		20.000	-1
4		50.000	-1

Curve Fit: Linear

---

51) (PAH); Isophorone ( )
Ret. Time 5.06 min., Extract & Integrate from 4.97 to 5.16 min.

Lvl	ID	Conc (ug/ml)	Response
1		1.000	-1
2		10.000	-1
3		20.000	-1
4		50.000	-1
5		100.000	-1
6		1.000	-1
7		10.000	-1
8		20.000	-1
9		50.000	-1
10		100.000	-1
11		1.000	-1
12		10.000	132309
13		20.000	333161
14		50.000	569290
15		100.000	1832607

Curve Fit: Linear

---

52) (PAH); Phenol, 2-nitro- ( )
Ret. Time 5.15 min., Extract & Integrate from 5.06 to 5.25 min.

Lvl	ID	Conc (ug/ml)	Response
1		1.000	-1
2		10.000	-1
3		20.000	-1
4		50.000	-1
5		100.000	-1
6		1.000	-1
7		10.000	-1
8		20.000	-1
9		50.000	-1
10		100.000	-1
11		1.000	-1
12		10.000	23070
13		20.000	57563
14		50.000	109736
15		100.000	349526

Curve Fit: Linear

---

53) 1H-Indene, 3-methyl-* ( )
Ret. Time 5.42 min., Extract & Integrate from 5.33 to 5.52 min.

Lvl	ID	Conc (ug/ml)	Response
1		1.000	-1
2		10.000	-1
3		20.000	-1
4		50.000	-1

5	100.000	-1
6	1.000	-1
7	10.000	-1
8	20.000	-1
9	50.000	-1
10	100.000	-1
11	1.000	-1
12	10.000	93461
13	20.000	263738
14	50.000	11721
15	100.000	1274659

Curve Fit: Linear

---

54) (PAH); Phenol, 2,4-dimethyl- ( )
Ret. Time 5.20 min., Extract & Integrate from 5.10 to 5.30 min.

Lvl	ID	Conc (ug/ml)	Response
1		1.000	-1
2		10.000	-1
3		20.000	-1
4		50.000	-1
5		100.000	-1
6		1.000	-1
7		10.000	-1
8		20.000	-1
9		50.000	-1
10		100.000	-1
11		1.000	-1
12		10.000	88309
13		20.000	230681
14		50.000	387799
15		100.000	1241163

Curve Fit: Linear

---

55) 2-Methylindene * ( )
Ret. Time 5.39 min., Extract & Integrate from 5.29 to 5.49 min.

Lvl	ID	Conc (ug/ml)	Response
1		1.000	-1
2		10.000	-1
3		20.000	-1
4		50.000	-1
5		100.000	-1
6		1.000	-1
7		10.000	-1
8		20.000	-1
9		50.000	-1
10		100.000	-1
11		1.000	-1
12		10.000	93461
13		20.000	263738
14		50.000	11721
15		100.000	1274659

Curve Fit: Linear

---

56) (PAH); Methane, bis(2-chloroethoxy)- ( )
Ret. Time 5.42 min., Extract & Integrate from 5.32 to 5.52 min.

Lvl	ID	Conc (ug/ml)	Response
1		1.000	-1
2		10.000	-1
3		20.000	-1
4		50.000	-1
5		100.000	-1
6		1.000	-1
7		10.000	-1
8		20.000	-1
9		50.000	-1
10		100.000	-1
11		1.000	-1
12		10.000	93461
13		20.000	263738
14		50.000	11721
15		100.000	1274659

Curve Fit: Linear

---

57) 4-Piperidinone, 2,2,6,6-tetramethyl * ( )
Ret. Time 5.49 min., Extract & Integrate from 5.39 to 5.59 min.

Lvl	ID	Conc (ug/ml)	Response
1		1.000	-1
2		10.000	-1
3		20.000	-1
4		50.000	-1
5		100.000	-1
6		1.000	-1
7		10.000	-1
8		20.000	-1
9		50.000	-1
10		100.000	-1
11		1.000	-1
12		10.000	45203
13		20.000	103708
14		50.000	231682
15		100.000	887046

Curve Fit: Linear

---

58) (PAH); Phenol, 2,4-dichloro- ( )
Ret. Time 5.43 min., Extract & Integrate from 5.33 to 5.53 min.

Lvl	ID	Conc (ug/ml)	Response
1		1.000	-1
2		10.000	-1
3		20.000	-1
4		50.000	-1

5	100.000	-1
6	1.000	-1
7	10.000	-1
8	20.000	-1
9	50.000	-1
10	100.000	-1
11	1.000	-1
12	10.000	45203
13	20.000	103708
14	50.000	231682
15	100.000	887046

Curve Fit: Linear

---

59) Phenol, 4-ethyl- * ( )

Ret. Time 5.44 min., Extract & Integrate from 5.34 to 5.54 min.

Lvl	ID	Conc (ug/ml)	Response
1		1.000	-1
2		10.000	-1
3		20.000	-1
4		50.000	-1
5		100.000	-1
6		1.000	-1
7		10.000	-1
8		20.000	-1
9		50.000	-1
10		100.000	-1
11		1.000	-1
12		10.000	45203
13		20.000	103708
14		50.000	231682
15		100.000	887046

Curve Fit: Linear

---

60) (PAH); Benzene, 1,2,4-trichloro- ( )

Ret. Time 5.54 min., Extract & Integrate from 5.44 to 5.64 min.

Lvl	ID	Conc (ug/ml)	Response
1		1.000	-1
2		10.000	-1
3		20.000	-1
4		50.000	-1
5		100.000	-1
6		1.000	-1
7		10.000	-1
8		20.000	-1
9		50.000	-1
10		100.000	-1
11		1.000	11582
12		10.000	164077
13		20.000	339589
14		50.000	529732
15		100.000	1353270

Curve Fit: Linear

---

61) (IS); Naphtalene-D8 (ISTD)
Ret. Time 5.60 min., Extract & Integrate from 5.50 to 5.70 min.

Lvl	ID	Conc (ug/ml)	Response
1		20.000	875811
2		20.000	979636
3		20.000	871453
4		20.000	818892
5		20.000	807142
6		20.000	815803
7		20.000	816361
8		20.000	811707
9		20.000	804882
10		20.000	839869
11		20.000	875316
12		20.000	1082119
13		20.000	1129778
14		20.000	1307821
15		20.000	1239200

ISTD conc: 20.000 ug/ml
Curve Fit: Linear

---

62) (PAH); Naphthalene ( )
Ret. Time 5.63 min., Extract & Integrate from 5.53 to 5.73 min.

Lvl	ID	Conc (ug/ml)	Response
1		1.000	-1
2		10.000	-1
3		20.000	-1
4		50.000	-1
5		100.000	-1
6		1.000	-1
7		10.000	-1
8		20.000	-1
9		50.000	-1
10		100.000	-1
11		1.000	40229
12		10.000	526799
13		20.000	1130433
14		50.000	1732822
15		100.000	4593390

Curve Fit: Linear

---

63) 1-Hexadecene * ( )
Ret. Time 5.79 min., Extract & Integrate from 5.69 to 5.89 min.

Lvl	ID	Conc (ug/ml)	Response
1		1.000	-1
2		10.000	-1
3		20.000	-1
4		50.000	-1

5	100.000	-1
6	1.000	-1
7	10.000	-1
8	20.000	-1
9	50.000	-1
10	100.000	-1
11	1.000	8129
12	10.000	87330
13	20.000	190407
14	50.000	299629
15	100.000	795782

Curve Fit: Linear

---

64) (PAH); p-Chloroaniline ( )
Ret. Time 5.70 min., Extract & Integrate from 5.60 to 5.80 min.

Lvl	ID	Conc (ug/ml)	Response
1		1.000	-1
2		10.000	-1
3		20.000	-1
4		50.000	-1
5		100.000	-1
6		1.000	-1
7		10.000	-1
8		20.000	-1
9		50.000	-1
10		100.000	-1
11		1.000	-1
12		10.000	64384
13		20.000	203647
14		50.000	423186
15		100.000	1110562

Curve Fit: Linear

---

65) (PAH); 1,3-Butadiene, hexachloro- ( )
Ret. Time 5.78 min., Extract & Integrate from 5.68 to 5.88 min.

Lvl	ID	Conc (ug/ml)	Response
1		1.000	-1
2		10.000	-1
3		20.000	-1
4		50.000	-1
5		100.000	-1
6		1.000	-1
7		10.000	-1
8		20.000	-1
9		50.000	-1
10		100.000	-1
11		1.000	8129
12		10.000	87330
13		20.000	190407
14		50.000	299629
15		100.000	795782

Curve Fit: Linear

---

66) Benzofuran, 2,3-dihydro- * ( )
Ret. Time 5.74 min., Extract & Integrate from 5.64 to 5.84 min.

Lvl	ID	Conc (ug/ml)	Response
1		1.000	-1
2		10.000	-1
3		20.000	-1
4		50.000	-1
5		100.000	-1
6		1.000	-1
7		10.000	-1
8		20.000	-1
9		50.000	-1
10		100.000	-1
11		1.000	8129
12		10.000	87330
13		20.000	190407
14		50.000	299629
15		100.000	795782

Curve Fit: Linear

---

67) (PAH); Phenol, 4-chloro-3-methyl- ( )
Ret. Time 6.28 min., Extract & Integrate from 6.18 to 6.38 min.

Lvl	ID	Conc (ug/ml)	Response
1		1.000	-1
2		10.000	-1
3		20.000	-1
4		50.000	-1
5		100.000	-1
6		1.000	-1
7		10.000	-1
8		20.000	-1
9		50.000	-1
10		100.000	-1
11		1.000	-1
12		10.000	39316
13		20.000	141546
14		50.000	264277
15		100.000	920657

Curve Fit: Linear

---

68) (PAH); Naphthalene, 2-methyl- ( )
Ret. Time 6.47 min., Extract & Integrate from 6.37 to 6.56 min.

Lvl	ID	Conc (ug/ml)	Response
1		1.000	-1
2		10.000	-1
3		20.000	-1
4		50.000	-1

Curve Fit: Linear

---

66) Benzofuran, 2,3-dihydro- * ( )
Ret. Time 5.74 min., Extract & Integrate from 5.64 to 5.84 min.

Lvl ID	Conc (ug/ml)	Response
1	1.000	-1
2	10.000	-1
3	20.000	-1
4	50.000	-1
5	100.000	-1
6	1.000	-1
7	10.000	-1
8	20.000	-1
9	50.000	-1
10	100.000	-1
11	1.000	8129
12	10.000	87330
13	20.000	190407
14	50.000	299629
15	100.000	795782

Curve Fit: Linear

---

67) (PAH); Phenol, 4-chloro-3-methyl- ( )
Ret. Time 6.28 min., Extract & Integrate from 6.18 to 6.38 min.

Lvl ID	Conc (ug/ml)	Response
1	1.000	-1
2	10.000	-1
3	20.000	-1
4	50.000	-1
5	100.000	-1
6	1.000	-1
7	10.000	-1
8	20.000	-1
9	50.000	-1
10	100.000	-1
11	1.000	-1
12	10.000	39316
13	20.000	141546
14	50.000	264277
15	100.000	920657

Curve Fit: Linear

---

68) (PAH); Naphthalene, 2-methyl- ( )
Ret. Time 6.47 min., Extract & Integrate from 6.37 to 6.56 min.

Lvl ID	Conc (ug/ml)	Response
1	1.000	-1
2	10.000	-1
3	20.000	-1
4	50.000	-1

Curve Fit: Linear

---

71) (PAH); Phenol, 2,4,6-trichloro- ( )
Ret. Time 6.81 min., Extract & Integrate from 6.71 to 6.91 min.

Lvl ID	Conc (ug/ml)	Response
1	1.000	-1
2	10.000	-1
3	20.000	-1
4	50.000	-1
5	100.000	-1
6	1.000	-1
7	10.000	-1
8	20.000	-1
9	50.000	-1
10	100.000	-1
11	1.000	-1
12	10.000	37333
13	20.000	124195
14	50.000	222422
15	100.000	709552

Curve Fit: Linear

---

72) (PAH); Phenol, 2,4,5-trichloro- ( )
Ret. Time 6.84 min., Extract & Integrate from 6.74 to 6.94 min.

Lvl ID	Conc (ug/ml)	Response
1	1.000	-1
2	10.000	-1
3	20.000	-1
4	50.000	-1
5	100.000	-1
6	1.000	-1
7	10.000	-1
8	20.000	-1
9	50.000	-1
10	100.000	-1
11	1.000	-1
12	10.000	37333
13	20.000	180048
14	50.000	294114
15	100.000	809153

Curve Fit: Linear

---

73) (PAH); Naphthalene, 2-chloro- ( )
Ret. Time 7.05 min., Extract & Integrate from 6.95 to 7.15 min.

Lvl ID	Conc (ug/ml)	Response
1	1.000	-1
2	10.000	-1
3	20.000	-1
4	50.000	-1

5	100.000	-1
6	1.000	-1
7	10.000	-1
8	20.000	-1
9	50.000	-1
10	100.000	-1
11	1.000	-1
12	10.000	276628
13	20.000	627837
14	50.000	1009020
15	100.000	2788747

Curve Fit: Linear

---

74) Biphenyl * ( )

Ret. Time 7.04 min., Extract & Integrate from 6.94 to 7.13 min.

Lvl	ID	Conc (ug/ml)	Response
1		1.000	-1
2		10.000	-1
3		20.000	-1
4		50.000	-1
5		100.000	-1
6		1.000	-1
7		10.000	-1
8		20.000	-1
9		50.000	-1
10		100.000	-1
11		1.000	-1
12		10.000	276628
13		20.000	627837
14		50.000	1009020
15		100.000	2788747

Curve Fit: Linear

---

75) 3-Tetradecene(Z) * ( )

Ret. Time 7.10 min., Extract & Integrate from 7.00 to 7.20 min.

Lvl	ID	Conc (ug/ml)	Response
1		1.000	-1
2		10.000	-1
3		20.000	-1
4		50.000	-1
5		100.000	-1
6		1.000	-1
7		10.000	-1
8		20.000	-1
9		50.000	-1
10		100.000	-1
11		1.000	-1
12		10.000	276628
13		20.000	627837
14		50.000	1009020
15		100.000	2788747

Curve Fit: Linear

---

76) (PAH); o-Nitroaniline ( )
Ret. Time 7.18 min., Extract & Integrate from 7.09 to 7.28 min.

Lvl	ID	Conc (ug/ml)	Response
1		1.000	-1
2		10.000	-1
3		20.000	-1
4		50.000	-1
5		100.000	-1
6		1.000	-1
7		10.000	-1
8		20.000	-1
9		50.000	-1
10		100.000	-1
11		1.000	-1
12		10.000	16784
13		20.000	61490
14		50.000	98677
15		100.000	355742

Curve Fit: Linear

---

77) (PAH); Benzene, 1,4-dinitro- ( )
Ret. Time 7.36 min., Extract & Integrate from 7.26 to 7.46 min.

Lvl	ID	Conc (ug/ml)	Response
1		1.000	-1
2		10.000	-1
3		20.000	-1
4		50.000	-1
5		100.000	-1
6		1.000	-1
7		10.000	-1
8		20.000	-1
9		50.000	-1
10		100.000	-1
11		1.000	-1
12		10.000	10792
13		20.000	33380
14		50.000	53921
15		100.000	202517

Curve Fit: Linear

---

78) (PAH); Acenaphthylene ( )
Ret. Time 7.56 min., Extract & Integrate from 7.46 to 7.66 min.

Lvl	ID	Conc (ug/ml)	Response
1		1.000	-1
2		10.000	-1
3		20.000	-1
4		50.000	-1

5	100.000	-1
6	1.000	-1
7	10.000	-1
8	20.000	-1
9	50.000	-1
10	100.000	-1
11	1.000	29240
12	10.000	341061
13	20.000	818980
14	50.000	1337600
15	100.000	4016667

Curve Fit: Linear

---

79) (PAH); Dimethyl phthalate ( )
Ret. Time 7.43 min., Extract & Integrate from 7.33 to 7.53 min.

Lvl	ID	Conc (ug/ml)	Response
1		1.000	-1
2		10.000	-1
3		20.000	-1
4		50.000	-1
5		100.000	-1
6		1.000	-1
7		10.000	-1
8		20.000	-1
9		50.000	-1
10		100.000	-1
11		1.000	-1
12		10.000	166963
13		20.000	460563
14		50.000	778947
15		100.000	2577135

Curve Fit: Linear

---

80) (PAH); 2,6-Dinitrotoluene ( )
Ret. Time 7.49 min., Extract & Integrate from 7.39 to 7.59 min.

Lvl	ID	Conc (ug/ml)	Response
1		1.000	-1
2		10.000	-1
3		20.000	-1
4		50.000	-1
5		100.000	-1
6		1.000	-1
7		10.000	-1
8		20.000	-1
9		50.000	-1
10		100.000	-1
11		1.000	-1
12		10.000	22776
13		20.000	63834
14		50.000	105141
15		100.000	345147

Curve Fit: Linear

---

81) (PAH); Benzene, 1,2-dinitro- ( )
Ret. Time 7.45 min., Extract & Integrate from 7.35 to 7.55 min.

Lvl	ID	Conc (ug/ml)	Response
1		1.000	-1
2		10.000	-1
3		20.000	-1
4		50.000	-1
5		100.000	-1
6		1.000	-1
7		10.000	-1
8		20.000	-1
9		50.000	-1
10		100.000	-1
11		1.000	-1
12		10.000	21613
13		20.000	32634
14		50.000	55616
15		100.000	191198

Curve Fit: Linear

---

82) (PAH); 3-Nitroaniline ( )
Ret. Time 7.69 min., Extract & Integrate from 7.59 to 7.79 min.

Lvl	ID	Conc (ug/ml)	Response
1		1.000	-1
2		10.000	-1
3		20.000	-1
4		50.000	-1
5		100.000	-1
6		1.000	-1
7		10.000	-1
8		20.000	-1
9		50.000	-1
10		100.000	-1
11		1.000	-1
12		10.000	42936
13		20.000	53557
14		50.000	177136
15		100.000	415927

Curve Fit: Linear

---

83) (IS); Acenaphtene-D10 (ISTD)
Ret. Time 7.73 min., Extract & Integrate from 7.63 to 7.83 min.

Lvl	ID	Conc (ug/ml)	Response
1		20.000	470899
2		20.000	503351
3		20.000	489974
4		20.000	475700

5	20.000	437595
6	20.000	470050
7	20.000	435800
8	20.000	450811
9	20.000	435596
10	20.000	433319
11	20.000	456821
12	20.000	537270
13	20.000	590546
14	20.000	689699
15	20.000	661907

ISTD conc: 20.000 ug/ml
Curve Fit: Linear

---

84) (PAH); Acenaphthene ( )
Ret. Time 7.77 min., Extract & Integrate from 7.70 to 7.85 min.

Lvl	ID	Conc (ug/ml)	Response
1		1.000	-1
2		10.000	-1
3		20.000	-1
4		50.000	-1
5		100.000	-1
6		1.000	-1
7		10.000	-1
8		20.000	-1
9		50.000	-1
10		100.000	-1
11		1.000	31692
12		10.000	326414
13		20.000	714616
14		50.000	1118463
15		100.000	3054269

Curve Fit: Linear

---

85) (PAH); Phenol, 2,4-dinitro- ( )
Ret. Time 7.82 min., Extract & Integrate from 7.72 to 7.92 min.

Lvl	ID	Conc (ug/ml)	Response
1		1.000	-1
2		10.000	-1
3		20.000	-1
4		50.000	-1
5		100.000	-1
6		1.000	-1
7		10.000	-1
8		20.000	-1
9		50.000	-1
10		100.000	-1
11		1.000	-1
12		10.000	-1
13		20.000	-1
14		50.000	-1
15		100.000	121904

Curve Fit: Linear

---

86) Phenol, 3,5-bis(1,1-dimethylethyl)- * ( )
Ret. Time 8.02 min., Extract & Integrate from 7.92 to 8.11 min.

Lvl	ID	Conc (ug/ml)	Response
1		1.000	-1
2		10.000	-1
3		20.000	-1
4		50.000	-1
5		100.000	-1
6		1.000	-1
7		10.000	-1
8		20.000	-1
9		50.000	-1
10		100.000	-1
11		1.000	-1
12		10.000	-1
13		20.000	-1
14		50.000	-1
15		100.000	-1

Curve Fit: Linear

---

87) (PAH); Dibenzofuran ( )
Ret. Time 7.98 min., Extract & Integrate from 7.88 to 8.08 min.

Lvl	ID	Conc (ug/ml)	Response
1		1.000	-1
2		10.000	-1
3		20.000	-1
4		50.000	-1
5		100.000	-1
6		1.000	-1
7		10.000	-1
8		20.000	-1
9		50.000	-1
10		100.000	-1
11		1.000	14007
12		10.000	447915
13		20.000	1035207
14		50.000	1649256
15		100.000	4686175

Curve Fit: Linear

---

88) benzene, 1-(1-hydroxyethyl)-4-Isobutyl* ( )
Ret. Time 8.02 min., Extract & Integrate from 7.92 to 8.12 min.

Lvl	ID	Conc (ug/ml)	Response
1		1.000	-1
2		10.000	-1
3		20.000	-1
4		50.000	-1

5	100.000	-1
6	1.000	-1
7	10.000	-1
8	20.000	-1
9	50.000	-1
10	100.000	-1
11	1.000	-1
12	10.000	-1
13	20.000	-1
14	50.000	-1
15	100.000	-1

Curve Fit: Linear

---

89) (PAH); Phenol, 4-nitro- ( )
Ret. Time 7.90 min., Extract & Integrate from 7.80 to 8.00 min.

Lvl	ID	Conc (ug/ml)	Response
1		1.000	-1
2		10.000	-1
3		20.000	-1
4		50.000	-1
5		100.000	-1
6		1.000	-1
7		10.000	-1
8		20.000	-1
9		50.000	-1
10		100.000	-1
11		1.000	-1
12		10.000	157269
13		20.000	369614
14		50.000	590087
15		100.000	158650

Curve Fit: Linear

---

90) (PAH); 2,4-Dinitrotoluene ( )
Ret. Time 7.98 min., Extract & Integrate from 7.88 to 8.08 min.

Lvl	ID	Conc (ug/ml)	Response
1		1.000	-1
2		10.000	-1
3		20.000	-1
4		50.000	-1
5		100.000	-1
6		1.000	-1
7		10.000	-1
8		20.000	-1
9		50.000	-1
10		100.000	-1
11		1.000	-1
12		10.000	23688
13		20.000	71951
14		50.000	113560
15		100.000	431879

Curve Fit: Linear

---

91) (PAH); Phenol, 2,3,4,6-tetrachloro- ( )
Ret. Time 8.08 min., Extract & Integrate from 7.99 to 8.18 min.

Lvl	ID	Conc (ug/ml)	Response
1		1.000	-1
2		10.000	-1
3		20.000	-1
4		50.000	-1
5		100.000	-1
6		1.000	-1
7		10.000	-1
8		20.000	-1
9		50.000	-1
10		100.000	-1
11		1.000	-1
12		10.000	36575
13		20.000	136935
14		50.000	209233
15		100.000	754243

Curve Fit: Linear

---

92) (PAH); Phenol, 2,3,5,6-tetrachloro- ( )
Ret. Time 8.14 min., Extract & Integrate from 8.04 to 8.24 min.

Lvl	ID	Conc (ug/ml)	Response
1		1.000	-1
2		10.000	-1
3		20.000	-1
4		50.000	-1
5		100.000	-1
6		1.000	-1
7		10.000	-1
8		20.000	-1
9		50.000	-1
10		100.000	-1
11		1.000	-1
12		10.000	71007
13		20.000	163750
14		50.000	253498
15		100.000	806966

Curve Fit: Linear

---

93) (PAH); Fluorene ( )
Ret. Time 8.41 min., Extract & Integrate from 8.31 to 8.51 min.

Lvl	ID	Conc (ug/ml)	Response
1		1.000	-1
2		10.000	-1
3		20.000	-1
4		50.000	-1

5	100.000	-1
6	1.000	-1
7	10.000	-1
8	20.000	-1
9	50.000	-1
10	100.000	-1
11	1.000	30360
12	10.000	401718
13	20.000	904804
14	50.000	1409076
15	100.000	3921739

Curve Fit: Linear

---

94) (PAH); Benzene, 1-chloro-4-phenoxy- ( )
Ret. Time 8.42 min., Extract & Integrate from 8.32 to 8.52 min.

Lvl	ID	Conc (ug/ml)	Response
1		1.000	-1
2		10.000	-1
3		20.000	-1
4		50.000	-1
5		100.000	-1
6		1.000	-1
7		10.000	-1
8		20.000	-1
9		50.000	-1
10		100.000	-1
11		1.000	-1
12		10.000	161531
13		20.000	389598
14		50.000	625270
15		100.000	1818219

Curve Fit: Linear

---

95) (PAH); Diethyl Phthalate ( )
Ret. Time 8.30 min., Extract & Integrate from 8.20 to 8.40 min.

Lvl	ID	Conc (ug/ml)	Response
1		1.000	-1
2		10.000	-1
3		20.000	-1
4		50.000	-1
5		100.000	-1
6		1.000	-1
7		10.000	-1
8		20.000	-1
9		50.000	-1
10		100.000	-1
11		1.000	-1
12		10.000	144187
13		20.000	391513
14		50.000	677892
15		100.000	2298025

Curve Fit: Linear

---

96) (PAH); p-Nitroaniline ( )
Ret. Time 8.44 min., Extract & Integrate from 8.34 to 8.54 min.

Lvl	ID	Conc (ug/ml)	Response
1		1.000	-1
2		10.000	-1
3		20.000	-1
4		50.000	-1
5		100.000	-1
6		1.000	-1
7		10.000	-1
8		20.000	-1
9		50.000	-1
10		100.000	-1
11		1.000	-1
12		10.000	-1
13		20.000	39554
14		50.000	35700
15		100.000	226316

Curve Fit: Linear

---

97) (PAH); Phenol, 2-methyl-4,6-dinitro- ( )
Ret. Time 8.47 min., Extract & Integrate from 8.37 to 8.57 min.

Lvl	ID	Conc (ug/ml)	Response
1		1.000	-1
2		10.000	-1
3		20.000	-1
4		50.000	-1
5		100.000	-1
6		1.000	-1
7		10.000	-1
8		20.000	-1
9		50.000	-1
10		100.000	-1
11		1.000	-1
12		10.000	-1
13		20.000	26402
14		50.000	-1
15		100.000	235199

Curve Fit: Linear

---

98) (PAH); Diphenylamine ( )
Ret. Time 8.56 min., Extract & Integrate from 8.47 to 8.66 min.

Lvl	ID	Conc (ug/ml)	Response
1		1.000	-1
2		10.000	-1
3		20.000	-1
4		50.000	-1

5	100.000	-1
6	1.000	-1
7	10.000	-1
8	20.000	-1
9	50.000	-1
10	100.000	-1
11	1.000	-1
12	10.000	244892
13	20.000	613264
14	50.000	1034299
15	100.000	3181972

Curve Fit: Linear

---

99) (PAH); Azobenzene ( )

Ret. Time 8.61 min., Extract & Integrate from 8.51 to 8.71 min.

Lvl	ID	Conc (ug/ml)	Response
1		1.000	-1
2		10.000	-1
3		20.000	-1
4		50.000	-1
5		100.000	-1
6		1.000	-1
7		10.000	-1
8		20.000	-1
9		50.000	-1
10		100.000	-1
11		1.000	-1
12		10.000	190105
13		20.000	443276
14		50.000	677803
15		100.000	2361867

Curve Fit: Linear

---

100) (PAH); Benzene, 1-bromo-4-phenoxy- ( )

Ret. Time 9.02 min., Extract & Integrate from 8.92 to 9.12 min.

Lvl	ID	Conc (ug/ml)	Response
1		1.000	-1
2		10.000	-1
3		20.000	-1
4		50.000	-1
5		100.000	-1
6		1.000	-1
7		10.000	-1
8		20.000	-1
9		50.000	-1
10		100.000	-1
11		1.000	-1
12		10.000	85056
13		20.000	217256
14		50.000	339925
15		100.000	1034479

Curve Fit: Linear

---

101) (PAH); Benzene, hexachloro- ( )
Ret. Time 9.07 min., Extract & Integrate from 8.97 to 9.17 min.

Lvl ID	Conc (ug/ml)	Response
1	1.000	-1
2	10.000	-1
3	20.000	-1
4	50.000	-1
5	100.000	-1
6	1.000	-1
7	10.000	-1
8	20.000	-1
9	50.000	-1
10	100.000	-1
11	1.000	5548
12	10.000	46444
13	20.000	93128
14	50.000	139634
15	100.000	379968

Curve Fit: Linear

---

102) (PAH); Phenol, pentachloro- ( )
Ret. Time 9.32 min., Extract & Integrate from 9.22 to 9.42 min.

Lvl ID	Conc (ug/ml)	Response
1	1.000	-1
2	10.000	-1
3	20.000	-1
4	50.000	-1
5	100.000	-1
6	1.000	-1
7	10.000	-1
8	20.000	-1
9	50.000	-1
10	100.000	-1
11	1.000	-1
12	10.000	4285
13	20.000	30339
14	50.000	36090
15	100.000	176855

Curve Fit: Linear

---

103) (PAH); Phenanthrene ( )
Ret. Time 9.59 min., Extract & Integrate from 9.49 to 9.69 min.

Lvl ID	Conc (ug/ml)	Response
1	1.000	-1
2	10.000	-1
3	20.000	-1
4	50.000	-1

5	100.000	-1
6	1.000	-1
7	10.000	-1
8	20.000	-1
9	50.000	-1
10	100.000	-1
11	1.000	46397
12	10.000	572265
13	20.000	1302609
14	50.000	2058069
15	100.000	5703703

Curve Fit: Linear

---

104) (IS); Anthracene-D10 (ISTD)
Ret. Time 9.57 min., Extract & Integrate from 9.47 to 9.67 min.

Lvl	ID	Conc (ug/ml)	Response
1		20.000	893284
2		20.000	938410
3		20.000	900294
4		20.000	869824
5		20.000	861352
6		20.000	818018
7		20.000	814159
8		20.000	811680
9		20.000	769985
10		20.000	838867
11		20.000	822027
12		20.000	986397
13		20.000	1061623
14		20.000	1242948
15		20.000	1180369

ISTD conc: 20.000 ug/ml
Curve Fit: Linear

---

105) (PAH); Anthracene ( )
Ret. Time 9.65 min., Extract & Integrate from 9.55 to 9.75 min.

Lvl	ID	Conc (ug/ml)	Response
1		1.000	-1
2		10.000	-1
3		20.000	-1
4		50.000	-1
5		100.000	-1
6		1.000	-1
7		10.000	-1
8		20.000	-1
9		50.000	-1
10		100.000	-1
11		1.000	43837
12		10.000	390166
13		20.000	893102
14		50.000	1498504
15		100.000	4630362

Curve Fit: Linear

---

106) (PAH); Carbazole ( )
Ret. Time 9.85 min., Extract & Integrate from 9.75 to 9.95 min.

Lvl	ID	Conc (ug/ml)	Response
1		1.000	-1
2		10.000	-1
3		20.000	-1
4		50.000	-1
5		100.000	-1
6		1.000	-1
7		10.000	-1
8		20.000	-1
9		50.000	-1
10		100.000	-1
11		1.000	-1
12		10.000	297372
13		20.000	795905
14		50.000	1313837
15		100.000	4227199

Curve Fit: Linear

---

107) (PAH); Dibutyl phthalate ( )
Ret. Time 10.32 min., Extract & Integrate from 10.22 to 10.42 min.

Lvl	ID	Conc (ug/ml)	Response
1		1.000	-1
2		10.000	-1
3		20.000	-1
4		50.000	-1
5		100.000	-1
6		1.000	-1
7		10.000	-1
8		20.000	-1
9		50.000	-1
10		100.000	-1
11		1.000	-1
12		10.000	171700
13		20.000	444710
14		50.000	757252
15		100.000	2707506

Curve Fit: Linear

---

108) (PAH); Fluoranthene ( )
Ret. Time 11.05 min., Extract & Integrate from 10.95 to 11.15 min.

Lvl	ID	Conc (ug/ml)	Response
1		1.000	-1
2		10.000	-1
3		20.000	-1
4		50.000	-1

5	100.000	-1
6	1.000	-1
7	10.000	-1
8	20.000	-1
9	50.000	-1
10	100.000	-1
11	1.000	39107
12	10.000	435120
13	20.000	1024148
14	50.000	1644765
15	100.000	4965996

Curve Fit: Linear

---

109) (PAH); Pyrene ( )
Ret. Time 11.33 min., Extract & Integrate from 11.23 to 11.43 min.

Lvl	ID	Conc (ug/ml)	Response
1		1.000	-1
2		10.000	-1
3		20.000	-1
4		50.000	-1
5		100.000	-1
6		1.000	-1
7		10.000	-1
8		20.000	-1
9		50.000	-1
10		100.000	-1
11		1.000	48896
12		10.000	497021
13		20.000	1158625
14		50.000	1831514
15		100.000	5626422

Curve Fit: Linear

---

110) (PAH); Benzyl butyl phthalate ( )
Ret. Time 12.17 min., Extract & Integrate from 12.07 to 12.27 min.

Lvl	ID	Conc (ug/ml)	Response
1		1.000	-1
2		10.000	-1
3		20.000	-1
4		50.000	-1
5		100.000	-1
6		1.000	-1
7		10.000	-1
8		20.000	-1
9		50.000	-1
10		100.000	-1
11		1.000	-1
12		10.000	62209
13		20.000	151419
14		50.000	247876
15		100.000	846483

Curve Fit: Linear

---

111) (PAH); bis(2-ethylhexyl) adipate ( )
Ret. Time 12.29 min., Extract & Integrate from 12.19 to 12.39 min.

Lvl	ID	Conc (ug/ml)	Response
1		1.000	-1
2		10.000	-1
3		20.000	-1
4		50.000	-1
5		100.000	-1
6		1.000	-1
7		10.000	-1
8		20.000	-1
9		50.000	-1
10		100.000	-1
11		1.000	-1
12		10.000	54221
13		20.000	133539
14		50.000	207418
15		100.000	731999

Curve Fit: Linear

---

112) (PAH); Benz[a]anthracene ( )
Ret. Time 12.81 min., Extract & Integrate from 12.71 to 12.91 min.

Lvl	ID	Conc (ug/ml)	Response
1		1.000	-1
2		10.000	-1
3		20.000	-1
4		50.000	-1
5		100.000	-1
6		1.000	-1
7		10.000	-1
8		20.000	-1
9		50.000	-1
10		100.000	-1
11		1.000	20030
12		10.000	295056
13		20.000	740917
14		50.000	1245988
15		100.000	4312993

Curve Fit: Linear

---

113) (IS); Chrysene-D12 (ISTD)
Ret. Time 12.84 min., Extract & Integrate from 12.74 to 12.93 min.

Lvl	ID	Conc (ug/ml)	Response
1		20.000	800373
2		20.000	767909
3		20.000	744064
4		20.000	753383

5	20.000	675393
6	20.000	787627
7	20.000	689737
8	20.000	627482
9	20.000	568153
10	20.000	709193
11	20.000	631490
12	20.000	840364
13	20.000	957481
14	20.000	1183246
15	20.000	1282816

ISTD conc: 20.000 ug/ml
Curve Fit: Linear

---

114) (PAH); Crysene ( )
Ret. Time 12.86 min., Extract & Integrate from 12.76 to 12.96 min.

Lvl	ID	Conc (ug/ml)	Response
1		1.000	-1
2		10.000	-1
3		20.000	-1
4		50.000	-1
5		100.000	-1
6		1.000	-1
7		10.000	-1
8		20.000	-1
9		50.000	-1
10		100.000	-1
11		1.000	58681
12		10.000	576441
13		20.000	1261998
14		50.000	1921325
15		100.000	5904174

Curve Fit: Linear

---

115) (PAH); Bis(2-ethylhexyl) phthalate ( )
Ret. Time 12.89 min., Extract & Integrate from 12.80 to 12.99 min.

Lvl	ID	Conc (ug/ml)	Response
1		1.000	-1
2		10.000	-1
3		20.000	-1
4		50.000	-1
5		100.000	-1
6		1.000	-1
7		10.000	-1
8		20.000	-1
9		50.000	-1
10		100.000	-1
11		1.000	12581
12		10.000	98109
13		20.000	213338
14		50.000	346609
15		100.000	1160926

Curve Fit: Linear

---

116) (PAH); Di-n-octyl phthalate ( )
Ret. Time 13.66 min., Extract & Integrate from 13.56 to 13.76 min.

Lvl	ID	Conc (ug/ml)	Response
1		1.000	-1
2		10.000	-1
3		20.000	-1
4		50.000	-1
5		100.000	-1
6		1.000	-1
7		10.000	-1
8		20.000	-1
9		50.000	-1
10		100.000	-1
11		1.000	10581
12		10.000	147445
13		20.000	338672
14		50.000	553040
15		100.000	1816478

Curve Fit: Linear

---

117) (PAH); Benzo[b] fluoranthene ( )
Ret. Time 14.06 min., Extract & Integrate from 13.96 to 14.16 min.

Lvl	ID	Conc (ug/ml)	Response
1		1.000	-1
2		10.000	-1
3		20.000	-1
4		50.000	-1
5		100.000	-1
6		1.000	-1
7		10.000	-1
8		20.000	-1
9		50.000	-1
10		100.000	-1
11		1.000	18442
12		10.000	366833
13		20.000	885444
14		50.000	1512910
15		100.000	5058565

Curve Fit: Linear

---

118) (PAH); Benzo[k] fluoranthene ( )
Ret. Time 14.09 min., Extract & Integrate from 13.99 to 14.19 min.

Lvl	ID	Conc (ug/ml)	Response
1		1.000	-1
2		10.000	-1
3		20.000	-1
4		50.000	-1

5	100.000	-1
6	1.000	-1
7	10.000	-1
8	20.000	-1
9	50.000	-1
10	100.000	-1
11	1.000	37370
12	10.000	355922
13	20.000	874236
14	50.000	1397375
15	100.000	5190650

Curve Fit: Linear

---

119) (PAH); Benzo[a] pyrene ( )
Ret. Time 14.41 min., Extract & Integrate from 14.31 to 14.51 min.

Lvl	ID	Conc (ug/ml)	Response
1		1.000	-1
2		10.000	-1
3		20.000	-1
4		50.000	-1
5		100.000	-1
6		1.000	-1
7		10.000	-1
8		20.000	-1
9		50.000	-1
10		100.000	-1
11		1.000	-1
12		10.000	261244
13		20.000	649494
14		50.000	1083317
15		100.000	3931766

Curve Fit: Linear

---

120) (IS); Perylene-D12 (ISTD)
Ret. Time 14.48 min., Extract & Integrate from 14.38 to 14.58 min.

Lvl	ID	Conc (ug/ml)	Response
1		20.000	475119
2		20.000	487375
3		20.000	498127
4		20.000	498456
5		20.000	416869
6		20.000	477167
7		20.000	453969
8		20.000	447832
9		20.000	416661
10		20.000	438163
11		20.000	343785
12		20.000	499327
13		20.000	547333
14		20.000	676911
15		20.000	742815

ISTD conc: 20.000 ug/ml
Curve Fit: Linear
---

121) (PAH); Indeno[1,2,3-cd]pyrene ( )
Ret. Time 15.82 min., Extract & Integrate from 15.72 to 15.92 min.

Lvl	ID	Conc (ug/ml)	Response
1		1.000	-1
2		10.000	-1
3		20.000	-1
4		50.000	-1
5		100.000	-1
6		1.000	-1
7		10.000	-1
8		20.000	-1
9		50.000	-1
10		100.000	-1
11		1.000	-1
12		10.000	313748
13		20.000	734421
14		50.000	870030
15		100.000	3139707

Curve Fit: Linear
---

122) (PAH); Dibenz[a,h]anthracene ( )
Ret. Time 15.85 min., Extract & Integrate from 15.75 to 15.95 min.

Lvl	ID	Conc (ug/ml)	Response
1		1.000	-1
2		10.000	-1
3		20.000	-1
4		50.000	-1
5		100.000	-1
6		1.000	-1
7		10.000	-1
8		20.000	-1
9		50.000	-1
10		100.000	-1
11		1.000	-1
12		10.000	278800
13		20.000	656164
14		50.000	1020424
15		100.000	4030323

Curve Fit: Linear
---

123) (PAH); Benzo[ghi]perylene ( )
Ret. Time 16.22 min., Extract & Integrate from 16.12 to 16.32 min.

Lvl	ID	Conc (ug/ml)	Response
1		1.000	-1
2		10.000	-1
3		20.000	-1
4		50.000	-1

5	100.000	-1
6	1.000	-1
7	10.000	-1
8	20.000	-1
9	50.000	-1
10	100.000	-1
11	1.000	-1
12	10.000	389700
13	20.000	802105
14	50.000	1276426
15	100.000	4233801

Curve Fit: Linear

END OF DATA ANALYSIS PARAMETERS

Thu Apr 26 08:36:11 2007

8.5 DATA ANALYSIS

This chapter relates of the calculations of mass and energy balances determined from the results obtained from a gasification run.

An Excel file provides the user the opportunity to analyze runs made on the fluidized bed gasifier (FBG) pilot plant in order to obtain mass and energy balances and take into account other important analytical data from the GC-TCD gas analyzer and the GC-MS tar compounds analyzer.

The file contains multiple spreadsheets linked to each other for calculations, which tabs are in order from left to right. This order is important because it is recognized by the macros programmed for calculation and organization of the data. They are:

- Sheet 1: “Graphs” contains all the charts that can be generated via macro; Graph spreadsheet data source is “All”.
- Sheet 2: “All” contains all results from all the file experiments.
- Sheet 3: “Biomass” contains each biomass and char characteristics
- Sheet 4: “Constants” contains all chemical and thermodynamics contants for all calculations.
- Sheet 5: “Inputs” contains all inputs external to the fluidized bed gasifier Labview data set
- Sheet 6: “Gas GC” contains all gas compositions from the GC-TCD
- Sheet 7: “Tar GCMS” contains all tar compounds compositions from the GC-MS

- Sheet 8: “Water” contains all water samples results from the GC-MS
- Sheet 9-last: All runs calculations named by process and biomass types:
    - “SA(#)” switchgrass air gasification
    - “SP(#)” switchgrass pyrolysis and heat supplemented air gasification
    - “SS(#)” switchgrass steam gasification.
    - “BA(#)”bermudagrass air gasification
    - “BP(#)” bermudagrass pyrolysis and heat supplemented air gasification
    - “BS(#)” bermudagrass steam gasification.
    - “CGA(#)” corn gluten air gasification
    - “CGP(#)” corn gluten pyrolysis and heat supplemented air gasification
    - “CGS(#)” corn gluten steam gasification.

8.5.1 SHEET 1: “GRAPHS”

These graphes are generated by three macros:

- Sub Graph() creates seven graphes for 3 processes.
- Sub Align_Graph() subroutine of Sub Graph() aligns graphes on the spreadsheet in an orderly display, user may call it or not call it from Sub Graph() as desired.
- Sub Align_titles() positions titles for charts and axis and sets fonts and color.

The user may modify these macros manually through the visual basic editor.

8.5.2 SHEET 2: "ALL"

All results from the entire file of runs calculations are linked for display in this spreadsheet.

Date	
Run	#
ER	ratio
S/B	ratio
Time	h
Tbed (Celsius)	Celsius
Biomass used	kg
Measured Gas flow (scfm) stp BS usa	scfm
Airflow	scfm
Sampling flow	l/min
Total sampling	liters
Airlock leak	scfm
RAirflow	scfm
Biomassflow	kg/h
SR	ratio
MC	%wb
Baffle	% power
Air Ht	% power
Steam flow	kg/h
H2	% mol
N2	% mol
CO	% mol
CH4	% mol
CO2	% mol
C2H2	% mol
C2H4	% mol
C2H6	% mol
HHVg	kJ/kg
HHVg	kJ/Nm3
dry gas density	kg/Nm3
wet gas density	kg/Nm3
Gas mol wt	g/mol
C to gas	%
C to CO	%

C to PM	%
C to tar	%
Tar grav.	g/Nm3
Tar GCMS	g/Nm3
Tar appGCMS	g/Nm3
PM flow	g/Nm3
H2O conc	g/Nm3
Tar compound #1	g/Nm3
Tar compound #2	g/Nm3
Tar compound #3	g/Nm3
Tar compound #4	g/Nm3
Tar compound #5	g/Nm3
Tar compound #6	g/Nm3
Tar compound #7	g/Nm3
Tar compound #8	g/Nm3
Tar compound #9	g/Nm3
Tar compound #10	g/Nm3
Tar compound #11	g/Nm3
C	#
H	#
N	#
O	#
Tar average MW	g/mol
Hf tar	kJ/kg
DHr	kJ/kg CHO
H2O	mg/ml
Mass Bal	kg/h
Airleak	scfm
C bal	mol/h
H Bal	mol/h
O Bal	mol/h
C bal err	%
H bal err	%
O bal err	%
waste heat	kW
Tar compound #1	Name

Tar compound #2	Name
Tar compound #3	Name
Tar compound #4	Name
Tar compound #5	Name
Tar compound #6	Name
Tar compound #7	Name
Tar compound #8	Name
Tar compound #9	Name
Tar compound #10	Name
Tar compound #11	Name
CHObiomass	mol/h
C	mol/h
H	mol/h
O	mol/h
N	mol/h
H2Omoist.	mol/h
H2Osteam	mol/h
O2	mol/h
N2	mol/h
H2	mol/h
N2	mol/h
CO	mol/h
CH4	mol/h
CO2	mol/h
C2H2	mol/h
C2H4	mol/h
C2H6	mol/h
H2Og	mol/h
Csolids	mol/h
Hsolids	mol/h
Osolids	mol/h
Nsolids	mol/h
C7HNOtar	mol/h
Ctar	mol/h

Htar	mol/h
Otar	mol/h
Ntar	mol/h
CHObiomass	kg/h
C	kg/h
H	kg/h
O	kg/h
N	kg/h
Ash	kg/h
H2Omoist.	kg/h
H2Osteam	kg/h
O2	kg/h
N2	kg/h
H2	kg/h
N2	kg/h
CO	kg/h
CH4	kg/h
CO2	kg/h
C2H2	kg/h

C2H4	kg/h
C2H6	kg/h
H2O	kg/h
Csolids	kg/h
Hsolids	kg/h
Osolids	kg/h
Nsolids	kg/h
Ashsolids	kg/h
CHONtar	kg/h
Ctar	kg/h
Htar	kg/h
Otar	kg/h
CHOy	# mole
C	# mole
H	# mole
O	# mole
N	# mole
H2O	# mole

O2	# mole
N2	# mole
H2	# mole
N2	# mole
CO	# mole
CH4	# mole
CO2	# mole
C2H2	# mole
C2H4	# mole
C2H6	# mole
H2O	# mole
Csolids	# mole
Hsolids	# mole
Osolids	# mole
Nsolids	# mole
C7HOtar	# mole

Table 8.2 Analysis results

8.5.3 SHEET 3: "BIOMASS"

This sheet relates of the experimental characteristics of each biomass type and respective chars. It also contains the calculations defining a hypothetical molecule of biomass, such as stoichiometric ratios and enthalpies of formation.

The requested inputs in this spreadsheet are:

- High heating value-(HHV) of moisture ash free biomass (MAF), (Btu/lb)
- Elemental analysis of the biomass:
  - %wt dry basis (db) composition
  - Moisture content, %

%wt wb composition for each atom:

$$\%\ i^{wt\,wb} = \%\ i^{wt\,db} \times \frac{100 - \%\ H_2O^{wt\,wb}_{biomass}}{100} \qquad (8.1)$$

Considering the stoichiometric combustion of biomass:

$$1\ CH_xO_y + (1+x/4-y/2)\ O_2 \rightarrow 1\ CO_2 + x/2\ H_2O \qquad (8.2)$$

Stoichiometric Ratio (SR):

$$SR = \frac{mass\ of\ oxygen\ for\ combustion}{mass\ of\ dry\ biomass} = \frac{M_{O_2} \times \left(1 + \frac{x}{4} - \frac{y}{2}\right)}{\left(M_C + x \times M_H + y \times M_O\right) \times \left(\frac{100}{\%\ CHO^{wt\,db}_{biomass}}\right)} \qquad (8.3)$$

Carbon ratio formula for biomass is CH_xO_y with:

$$Atomic\#_H = x = \frac{\frac{H\%}{M_H}}{\frac{C\%}{M_C}} \quad Atomic\#_O = y = \frac{\frac{O\%}{M_O}}{\frac{C\%}{M_C}} \qquad (8.4)$$

The enthalpy of formation of the hypothetical molecule of biomass or char is calculated from the measured HHV and elemental analysis of a biomass or char sample. Considering the stoichiometric combustion of this hypothetical molecule of biomass:

$$CHxOy + (1 + \frac{x}{4} - \frac{y}{2})O_2 \xrightarrow{HHV} CO_2 + \frac{x}{2}H_2O \qquad (8.5)$$

and

$$HHV = \sum \text{products} - \sum \text{reactants} \qquad (8.6)$$

since $\Delta H_{f\,O_2} = 0$

$$\Delta H_{CH_xO_y} = \Delta H_{f\,CO_2} + \Delta H_{f\,H_2O} - HHV \qquad (8.7)$$

since $\Delta H_{f\,CO_2} = -393510\ J/mol$ and $\Delta H_{f\,H_2O} = -285830\ J/mol$

$$\Delta H_{f\,CH_xO_y} = -393510\ J/mol - 285830\ J/mol \times \frac{x}{2} - HHV \qquad (8.8)$$

8.5.4 SHEET 4: "CONSTANTS"

This spreadsheet contains all the thermodynamic constants common to most calculations in the entire file:

Constant's name	Value	Unit
R	8.21E-02	l.atm/K /mol
K factor for Mass-track He conversion	1.454	
Helium density stp	0.1786	g/l
Conversion CF to liters	28.31685	l/cf
Mol % O2 in Air	20.95%	
Mol % N2 in Air	78.08%	
Mass % O2 in Air	23.46%	
Mass % N2 in Air	76.52%	
Normalized Mol % O2 in Air (N2 O2)	21.16%	
Normalized Mol % N2 in Air (N2 O2)	78.84%	
Molecular weight of dry air	28.9644	g/mol
Molecular ratio N2/O2	3.727	
Conversion Btu/lbs to kJ/kg	2.3244	
Hf He	0.00	kJ/mol
Hf H2	0.00	kJ/mol
Hf N2	0.00	kJ/mol
Hf O2	0.00	kJ/mol

Constant's name	Value	unit
Hf CO	-110.53	kJ/mol
Hf CH4	-74.81	kJ/mol
Hf CO2	-393.51	kJ/mol
Hf C2H2	226.73	kJ/mol
Hf C2H4	52.26	kJ/mol
Hf C2H6	-84.68	kJ/mol
Hf water	-285.83	kJ/mol
Latent heat of evaporation of water	2270.00	kJ/kg
Sensitive heat of water	4.19	kJ/kg.K
Sensitive heat of dry air	1.01	kJ/kg.K
H2	14.27	kJ/kg/K
N2	1.00	kJ/kg/K
O2	0.92	kJ/kg/K
CO	1.04	kJ/kg/K
CH4	2.23	kJ/kg/K
CO2	0.85	kJ/kg/K
C2H2	1.47	kJ/kg/K
C2H4	1.54	kJ/kg/K
C2H6	1.77	kJ/kg/K

Table 8.3 Thermodynamic constants

	Air standard condition					
	SI	BS	BS in USA		Mass flow meter	
T (K) / (F)	273.15	80	288.7056	60	294.2611	70
Pa (atm) / (psi)	1	14.4		14.696	1	14.696
Vol mol (l/mol)	22.414					
Humidity (%)	0	60				
Air density (kg/m3)or(g/l)	1.293					

Table 8.4 Air standard conditions in British systems, American BS, and SI system

Heating Values of	kJ/kg		kJ/Nm3	
Pure Gases	HHV	LHV	HHV	LHV
H2	141854.33	119527.00	12766.85	10757.64
N2	0	0	0	0
O2	0	0	0	0
CO	10092.09	10092.09	12616.16	12616.16
CH4	55604.86	50004.19	39891.17	35872.75
CO2	0	0	0	0
C2H2	49945.58	48195.90	58518.21	56467.14
C2H4	50313.94	47174.55	63206.36	59439.10
C2H6	51904.56	47509.42	69903.73	64043.53

Table 8.5 Heating values of pure gases

8.5.5 SHEET 5: "INPUTS"

The Inputs are:

- Date
- Run number
- Material type (switchgrass, bermudagrass, corn gluten)
- Steam flow rate (kg/h)
- Initial particulate matter filter weight (g)
- Filter and particulate matter weight after cooling (g)
- Filter and particulate matter weight after Soxhlet extraction (g)
- Total solvent volume (Acetone) used (impingers, rinsing, and Soxhlet) (ml)
- Solvent (acetone) volume used in the rotary evaporator (ml); tar gravimetric method.

- Rotary evaporator flask weight (g)
- Gas total measured sample volume (l)
- Solvent sample water content (mg/ml) from GC-MS
- Tar method used for mass balance:“gc” (for gas chromatograph method) or “grav” (for gravimetric method)
- power to plenum heater (0 = no, 1 = yes)
- % power baffle heaters (0-100%)
- % power air heater (0-100%)
- Number of baffle heaters in use (1-3)

8.5.6 SHEET 6: “GAS GC”

Results of GC analysis of gases results are stored in this spreadsheet. It allows storage up to four gas sampling composition results of the 10 gases calibrated in the method of the Varian 3800P GC-TCD. In order of elution, the gases are: He, (tracer), H_2, N_2, O_2, CO, CO_2, CH_4, C_2H_2, C_2H_4, C_2H_6.

As all the rest of the file first spreadsheets for data inputs, each line of the “Gas GC” spreadsheet represents one run. Thus the four gas samples raw compositions results are lined up over 40 columns in the precise order of their elution, listed above. The 4 first columns are used for run referencing: Date, Run #, ER, S/B.

The mention of a raw composition is important. It does not matter whether or not the compositions are normalized, or with oxygen from incorrect sampling. The calculations are such that all samples will be normalized without their tracer or the oxygen coming from incorrect sampling. This calculation also takes into account the amount of nitrogen associated with the presence of oxygen from the air.

This line of data is linked to a run sheet starting from sheet #9; excel counts sheets from left to right starting at #1. This detail is important in using the visual basic (VB) macro used for general modifications of cell addressing and calculation formulas.

8.5.7 SHEET 7: "TAR GCMS"

As for the GC spreadsheet, all GC-MS results are loaded in a single line per run. The list of the 210 compounds is listed in Table 2.1. Again, the four first columns are used for run referencing: Date, Run #, ER, S/B.

The compositions in this spreadsheet must be in μg/ml of solvent (in our case, acetone) used in the tar sampling system with any dilution calculations already taken into account.

8.5.8 SHEET 8: “WATER”

This spreadsheet is a temporary storage location for the water inputs with no link to the rest of the file. Water concentration from the solvent are actually entered in column D in the input spreadsheet.

8.5.9 SHEET 9 TO LAST: “ALL RUNS”

This spreadsheet template is color coded:

- Gold for the biomass feed
- Sky blue for air and gases
- Turquoise for steam
- Light gray for particulate matter
- Dark gray for tar
- Green for the helium tracer
- Purple text for energy balance results in kW
- Orange text for energy balance results in kJ/mol
- Brown for mass balance
- Black for mole balance

Depending on the user choice performed in the Input spreadsheet, the mass balance is calculated relative to the amount of inert gas either N_2 or He. In the case of N_2,

an important parameter is to evaluate the airlock leakage. Because there is considerable variation in the airlock leakage, its calibration may vary. As the result, it is recommended that helium be used as a tracer even in air gasification; It is easier and more precise for all process types.

For each run, all data are calculated in this sheet type. The set of data from the GAS11.vi recorded run file of the fluidized bed gasifier (FBG) unit is copied for each spreadsheet starting on rows 70 to 1000 in the same column order.

All averages, minimums and maximums necessary from the data recording of a FBG run for calculations are made on row 69. This row is also copied in black on the right side of the “Input” spreadsheet so that all inputs can be viewed at once.

All calculations for biomass, air, steam, gas, tar, water, particulate matter, mass balance and energy balance are made individually for each run. A nitrogen balance was initially performed since this inert gas is the most abundant element in air gasification. But a helium tracer was later introduced as a more accurate method to perform mass balance and energy balance calculations. A second basis for mass balance is also the oxygen balance.

Each sheet currently recognizes three biomass names: switchgrass, bermudagrass, corn gluten.

Each sheet works with two gasifying agents (air and steam) simultaneously

In these spreadsheets, all data in **red** are inputs from the "Biomass","Input","Gas GC", and "Tar GCMS" spreadsheets. All other numbers are either constants or calculation results. Row #1-#3 are dedicated to those inputs see Table 4.5.

R\C	C#1	C#2	C#3	C#4	C#5	C#6	C#7
R#1	Date	Run#	Material	steam (kg/h)	Filter (g)	PMt + filter wet (g)	PM + filter washed & dry (g)
R#2	5/27/2004	1	Switchgrass	0.00	2.74	12.73	12.74
R#3	Tracer (He or N2)	N2	He flow (lpm)	22.50			

R\C	C#6	C#7	C#8	C#9	C#10	C#11	C#12
R#1	Acetone (ml)	Evap.Vol. (ml)	Tar Flask (g)	Tar Flask dry (g)	H2O mg/ml acetone	Feed C (%db)	H (%db)
R#2	1500.00	1500.00	3.99	16.88	102.91	49.67	5.27
R#3	Tar method (gc/grav)			Gc	55.95	Goalseek	102.91

R\C	C#13	C#14	C#15	C#16	C#17	C#18
R#1	O (%db)	N (%db)	S (%db)	Ash (%db)	Moist (%wb)	HHV maf kJ/kg
R#2	40.31	0.57	0.07	4.11	8.73	8401.00

	C#19	C#20	C21	C#22	C#23	C#24	C#25
R1	PM						PM maf
	C (%db)	H (%db)	O (%db)	N (%db)	S (%db)	Ash (%db)	HHV kJ/kg
R#2	50.08	0.68	1.97	1.00	0.15	46.12	13635

Table 8.6 Run sheet input area rows#1-3 column#1-27 example (all four tables are aligned left to right)

The cells between rows #4-15 over the first 17 columns, Table 4.6, are reserved for gas normalization, oxygen sampling leak removal and gas HHV calculation. The red lined pattern in the helium row indicates that the tracer in NOT part of the percentage calculation.

R\C	C#1	C#2	C#3	C#4	C#5	C#6	C#7
R#4	Gas	Aver norm	StdDev	Sample1	Sample2	Sample3	Sample4
R#5	He	0.00	0.00	0.0000	0.0000	0.0000	0.0000
R#6	H2	4.87	1.14	3.5380	4.7978	0.0000	0.0000
R#7	N2	57.67	5.21	57.7913	56.1439	0.0000	0.0000
R#8	O2	0.00	0.00	1.1550	2.8290	0.00	0.0000
R#9	CO	15.75	3.94	11.3053	15.6704	0.0000	0.0000
R#10	CH4	3.78	1.35	2.4667	3.9997	0.0000	0.0000
R#11	CO2	15.26	0.22	13.4444	12.7631	0.0000	0.0000
R#12	C2H2	0.23	0.21	0.3306	0.0685	0.0000	0.0000
R#13	C2H4	1.95	0.53	2.0282	1.3302	0.0000	0.0000
R#14	C2H6	0.49	0.25	0.5778	0.2599	0.0000	0.0000
R#15	totals	100.00		92.64	97.86	0.00	0.00

R\C	C#8	C#9	C#10	C#11
R#4	kJ/kg		kJ/Nm3	
R#5	HHV	LHV	HHV	LHV
R#6	141854.3	119527	12766.85	10757.64
R#7	0	0	0	0
R#8	0	0	0	0
R#9	10092.09	10092.09	12616.16	12616.16
R#10	55604.86	50004.19	39891.17	35872.75
R#11	0	0	0	0
R#12	49945.58	48195.9	58518.21	56467.14
R#13	50313.94	47174.55	63206.36	59439.1
R#14	51904.56	47509.42	69903.73	64043.53
R#15	4524.64819	4245.46452	5823.69989	5467.35079

R\C	C#12	C#13	C#14	C#15	C#16	C#17
R#4	Normalized	Normalized	Normalized	Normalized	g/mol	% wt dg
R#5	0.00	0.00	#DIV/0!	#DIV/0!		
R#6	4.06	5.68	#DIV/0!	#DIV/0!	2	0.34
R#7	61.36	53.98	#DIV/0!	#DIV/0!	28	56.21
R#8	0.00	0.00	0.00	0.00	32	0.00
R#9	12.97	18.54	#DIV/0!	#DIV/0!	28	15.36
R#10	2.83	4.73	#DIV/0!	#DIV/0!	16	2.11
R#11	15.42	15.10	#DIV/0!	#DIV/0!	44	23.37
R#12	0.38	0.08	#DIV/0!	#DIV/0!	26	0.21
R#13	2.33	1.57	#DIV/0!	#DIV/0!	28	1.90
R#14	0.66	0.31	#DIV/0!	#DIV/0!	30	0.51
R#15	100.00	100.00	#DIV/0!	#DIV/0!	28.73	100.00

Table 8.7 Gas composition and HHV calculations rows #4-15 columns #1-17 (all three tables are aligned left to right)

The area between row #16-30 and column #4-18 in Table 4.7 is dedicated to tar approximation calculation over the 11 most important compounds in this run.(molecular weight (MW) and atomic composition)

R\C	C#4	C#5	C#6	C#7	C#8	C#9
R#16	**Tar**	g/mol	C	H	N	O
R#17	(BTEX); Benzene	78.114	6	6	0	0
R#18	(BTEX);Toluene	92.141	7	8	0	0
R#19	(PAH); Phenol	94.113	6	6	0	1
R#20	(PAH); Naphthalene	128.174	10	8	0	0
R#21	Indene *	116.163	9	8	0	0
R#22	Benzene, 1-ethenyl-3-methyl- *	134	9	10	0	1
R#23	(PAH); 4-Methylphenol & 3-Methylphenol	108.14	7	8	0	1
R#24	(PAH); N-nitroso-di-n-propylamine	130	6	14	2	1
R#25	(Mix 4); Styrene	104.152	8	8	0	0
R#26	(PAH); Pyridine	79.102	5	5	1	0
R#27	Benzofuran*	118.13	8	6	0	1
R#28	**MW**	14.00	**1**	**1.07**	**0.02**	**0.04**
R#29	**MW**	**107.72**	**7.70**	**8.11**	**0.13**	**0.34**
R#30	Error	0.01%				

R\C	C#10	C#11	C#12	C#13
R#16	g/Nm3	% mass total	% mass 11 first compounds	% mol
R#17	2.73	19.65	30.19	36.70
R#18	1.31	9.41	14.46	14.90
R#19	1.05	7.57	11.64	11.74
R#20	0.67	4.81	7.39	5.47
R#21	0.63	4.52	6.95	5.68
R#22	0.61	4.37	6.72	4.76
R#23	0.60	4.33	6.65	5.84
R#24	0.55	3.93	6.03	4.41
R#25	0.46	3.31	5.08	4.63
R#26	0.44	3.19	4.90	5.88
R#27	0.38	2.73	4.20	3.37
R#28	9.05	**65.06**	100.00	100.00

R\C	C#14	C#15	C#16	C#17	C#18
R#16	mol/Nm3 C	mol/Nm3 H	mol/Nm3 N	mol/Nm3 O	mol/Nm3
R#17	0.21	0.21	0.00	0.00	3.50E-02
R#18	0.10	0.11	0.00	0.00	1.42E-02
R#19	0.07	0.07	0.00	0.01	1.12E-02
R#20	0.05	0.04	0.00	0.00	5.22E-03

R#21	0.05	0.04	0.00	0.00	5.42E-03
R#22	0.04	0.05	0.00	0.00	4.54E-03
R#23	0.04	0.04	0.00	0.01	5.57E-03
R#24	0.03	0.06	0.01	0.00	4.20E-03
R#25	0.04	0.04	0.00	0.00	4.42E-03
R#26	0.03	0.03	0.01	0.00	5.61E-03
R#27	0.03	0.02	0.00	0.00	3.22E-03
R#28	6.46E-01	6.88E-01	1.40E-02	2.55E-02	9.54E-02

Table 8.8 Calculations for tar approximation to 11 compounds rows#16-30 columns#4-18 (all three table are aligned left to right)

The area between row #16-30 and column #1-3 in Table 4.8 calculates and display ER, S/B ratio, input and output flows of the fluidized bed gasifier pilot plant.

Important: *This is also where the total volume of the gas sampled is calculated with correction for air from vacuum leakage in the sampled gas.*

R\C	C#1	C#2	C#3
R#16	Biomass mass flow (kg/h)	11.79	
R#17	**Real Air (kg/h) / (scfm)**	13.55	6.52
R#18	**Air leak (kg/h) / (scfm)**	6.09	2.93
R#19	**Steam (kg/h) / (cfm)**	0.00	0.00
R#20	**ER**	**0.22**	
R#21	**S/Biomass**	**0.10**	
R#22	Dry Gas density (kg/m3) / Wet	**1.28**	0.92
R#23	Measured gas flow (kg/h) stp / (scfm)	32.41	15.73
R#24	Std Gas sample volume (l)	627.43	
R#25	Leak corrected Std Gas sample volume (l)	543.67	
R#26	**Dry Gas flow (kg/h) / (Nm3/h)**	18.19	**14.19**
R#27	**PM flow (kg/h) / (g/Nm3dg)**	0.26	**18.39**
R#28	**Gravimetric tar (kg/h) / (g/Nm3dg)**	0.34	**23.71**
R#29	**GCMS TAR (kg/h) / (g/Nm3dg)**	0.20	**13.92**
R#30	**H2O (kg/h) / (g/Nm3dg)**	4.03	283.93

Table 8.9 ER, S/B ratios, input and output flow rates rows#16-30 columns#1-3

Finally, all detailed tar calculations over the method 210 compounds are made in the area between rows #1-22 columns #28-239 see in Table 4.9. The second row of this zone is reserved for receiving data from the 210 concentrations from the “Tar GCMS” spreadsheet #7. Column 29 contains all totals and averages for tar.

R\C	C#28	C#29	C#30	C#31	C#32	C#33	C#34	C#35	C#36……
R#1	GC-MS sample	Total Tar	Isobutyronitrile*	1,4-Cyclohexadiene*	3-Butenenitrile*	2-Propanone, 1-hydroxy- *	(BTEX); Benzene	3-Penten-2-one, (E)- *	(PAH); N-Nitrosodimethylamine
R#2	ug/ml	8337.09	0	0	0	0	990.84	5.54	0
R#3	exclusion	12.00				y		y	
R#4	g/Nm3	13.92	0.00	0.00	0.00	0.00	2.73	0.00	0.00
R#5	% mass	100.00	0.00	0.00	0.00	0.00	19.65	0.00	0.00
R#6	g/mol	107.72	69.11	80.13	67.09	74	78.114	84.118	74
R#7	C multiplier / Formulas	7.70	C4H7N	C6H8	C4H5N	C3H6O2	C6H6	C5H8O	C2H6N2O
R#8	C	1	4	6	4	3	6	5	2
R#9	H	1.053	7	8	5	6	6	8	6
R#10	N	0.017	1		1				2
R#11	O	0.044				2		1	1
R#12	Cl	0.000							
R#13	mol/Nm3	0.13	0.00	0.00	0.00	0.00	0.03	0.00	0.00
R#14	% mol	100.00	0.00	0.00	0.00	0.00	27.09	0.00	0.00
R#15	mol/Nm3 C	0.99	0.00	0.00	0.00	0.00	0.21	0.00	0.00
R#16	mol/Nm3 H	1.05	0.00	0.00	0.00	0.00	0.21	0.00	0.00
R#17	mol/Nm3 N	0.02	0.00	0.00	0.00	0.00	0.00	0.00	0.00
R#18	mol/Nm3 O	0.04	0.00	0.00	0.00	0.00	0.00	0.00	0.00
R#19	mol/Nm3 Cl	0.00	0.00	0.00	0.00	0.00	0.00	0.00	0.00
R#20	Hf kJ/mol	31.36	22.8	104.75	157.7	-410	82.9	-240.2	-1650
R#21	Hf kJ/kg	291.11	0.00	0.00	0.00	0.00	208.49	0.00	0.00
R#22	Hf kJ/mol	31.36	0.00	0.00	0.00	0.00	22.46	0.00	0.00

Table 8.10 Tar calculations example rows#1-22 columns#28-239

The following is the last area of the run sheet in Table 4.10. It contains all the detailed calculations of the mole, mass and energy balances. All totals are calculated in the left two first columns.

R\C	C#1	C#2	C#3	C#4	C#5	C#6	C#7	C#8	C#9	C#10	C#11	C#12	C#13	C#14	C#15	C#16	C#17	C#18	C#19	C#20
R#39	**Input**		**Biomass**	12		1		16		14		32		**Moisture**		18	**Air**	32		28
R#40	Hf kJ/mol	-162.9	-126.23	12		1		16		14		32		-36.70	1	16	0	16	0	14
R#41	**Balance C/mol Cin**	**0.000**	**1**	**C**	**1.27**	**H**	**0.61**	**O**	**0.01**	**N**	**0.00**	**S**	**Ash**	**0.13**	**H**	**O**	**0.220**	**O**	**0.83**	**N**
R#42	Hf kJ/h	-72542.08	-56203.52	**1**		**1.00**		**1.00**		**1**		**1**		-16338.56	**2**	**1**	0	**2**	0	**2**
R#43	mol/h			445.25		566.90		271.01		4.38		0.24				57.16		97.98		365.16
R#44	kg/h	**25.15**	10.25	5.34		0.57		4.34		0.06		0.01	0.44			1.03		3.14		10.22
R#45	% wt wb of biomass feed	100.00		45.33		4.81		36.79		0.52		0.06	3.75			8.73				
R#46	**Gas Output**		**Tracer**		**Fuel Gas**	2		28			28			16			44			26
R#47	Hf kJ/mol	-256.3			0.0	1	0	14	-24.76	12	16	-4.02	12	1	-85.40	12	16	0.74	12	1
R#48	**mol Cgas/mol Cin**	0.571			**0.07**	**H**	**0.82**	**N**	**0.22**	**C**	**O**	**0.05**	**C**	**H**	**0.22**	**C**	**O**	**0.00**	**C**	**H**
R#49	Hf kJ/h	-114113.50			0.00	**2**	0.00	**2**	-11025.81	**1**	**1**	-1790.97	**1**	**4**	-38025.04	**1**	**2**	330.36	**2**	**2**
R#50	mol/h	857.04				30.82		365.16			99.75			23.94			96.63			1.46
R#51	kg/h	22.22				0.06		10.22			2.79			0.38			4.25			0.04
R#52	% Vol of gas	100.00				4.87		57.67			15.75			3.78			15.26			0.23
R#53	**Particulate Matter Output**		**Char**	12		1		16	**Nitrogen**	14	**Sulphur**	32	**Ash**							
R#54	Hf kJ/mol	-16.5	-16.46	12		1		16		14		32								
R#55	**mol Cpm/mol Cin**	0.398	**1**	**C**	**0.16**	**H**	**0.03**	**O**	**0.02**	**N**	**0.00**	**S**		**Ash**						
R#56	Hf kJ/h	-2285.79	-2285.79	**1**		**1**		**1**		**1**		**1**								
R#57	mol/h			177.07		28.85		5.22		3.03		0.20								
R#58	kg/h	2.73		2.12		0.03		0.08		0.04		0.01		0.44						
R#59	% wt db of solids	100.00		77.86		1.06		3.06		1.55		0.233		16.20						
R#60	**Tar output (gc/grav)**		**Tar**					107.72												
R#61	Hf kJ/mol	0.1	0.1291	12	1	14		16												
R#62	**mol Ctar/mol Cin**	0.032	**0.00**	**C**	**H**	**N**		**O**												
R#63	Hf kJ/h	57.49	57.49	**7.70**	**8.11**	**0.129**		**0.341**												
R#64	mol/h							1.83												
R#65	kg/h	0.20						0.20												
R#66	**Total output kg/h**	**25.15**																		

R\C	C#21	C#22	C#23	C#24	C#25	C#26	C#27	C#28	C#29
R#39	**Steam**		18	**Tracer**					
R#40	0.00	1	16						
R#41	**0.00**	**H**	**O**						
R#42	0.00	**2**	**1**						
R#43			0.00						
R#44			0.00						
R#45									
R#46			28			30	**Water**		18
R#47	1.45	12	1	-0.58	12	1	-143.71	1	16
R#48	**0.03**	**C**	**H**	**0.01**	**C**	**H**	**0.50**	**H**	**O**
R#49	645.29	**2**	**4**	-260.11	**2**	**6**	-63987.23	**2**	**1**
R#50			12.35			3.07			223.86
R#51			0.35			0.09			4.03
R#52			1.95			0.49			35.36

Table 8.11 Detailed calculations of mass mole and energy balances

The carbon balance is then closed in Table 4.11 by assuming that all remaining carbon, besides tar and gas, are part of the chars. Results of balances are displayed between rows#31-38 columns#1-19

R\C	C#1	C#2	C#3	C#4	C#5	C#6	C#7	C#8	C#9	C#10	C#11	C#12	C#13	C#14	C#15	C#16	C#17	C#18	C#19
R#31	Reactants	1 C	1.00	H	1.27	O	0.61	N	0.010	0.13	H2O	0.220	O2+3.76 N2	0.00	H2O				
R#32	Products: Gas	0.07	H2	0.82	N2	0.22	CO	0.05	CH4	0.22	CO2	0.00	C2H2	0.03	C2H4	0.01	C2H6	0.50	H2O
R#33	Solids	1.00	C	0.03	O	0.16	H	0.017	N	0.00	S								
R#34	Tar	0.00	C	7.70	H	8.11	O	0.34	N	0.13									
R#35																			
R#36	C Bal. (mol/h)	0.000	H Bal. (mol/h)	38.359	O Bal. (mol/h)	-1.396	Wet gas out mol/h	857.04	Dry gas out mol/h	633.18									
	error %mol in	0.000%		-5.631%		0.266%													
R#37	C Bal. (kg/h)	0.000	H Bal. (kg/h)	0.038	O Bal. (kg/h)	-0.022	Total Mass Balance kg/h	0.000											
R#38	ΔHr (kJ/kg CHO)	-4263.73	ΔHr (kJ/mol c)	-109.70	Energy for reaction (kW)	-12.1	Elect. Heaters (kW)	0.0	Loss (kW)	12.1	Gas cool down (kW)	9.11	Wasted heat (kW)	3.0					

Table 8.12 Summary equation of the reaction with mass and energy balance rows#31-38 columns#1-19

8.6 LABVIEW GRAPHIC PROGRAMMING

8.6.1 Gas11.vi, pilot plant program

8.6.1.1 Main program

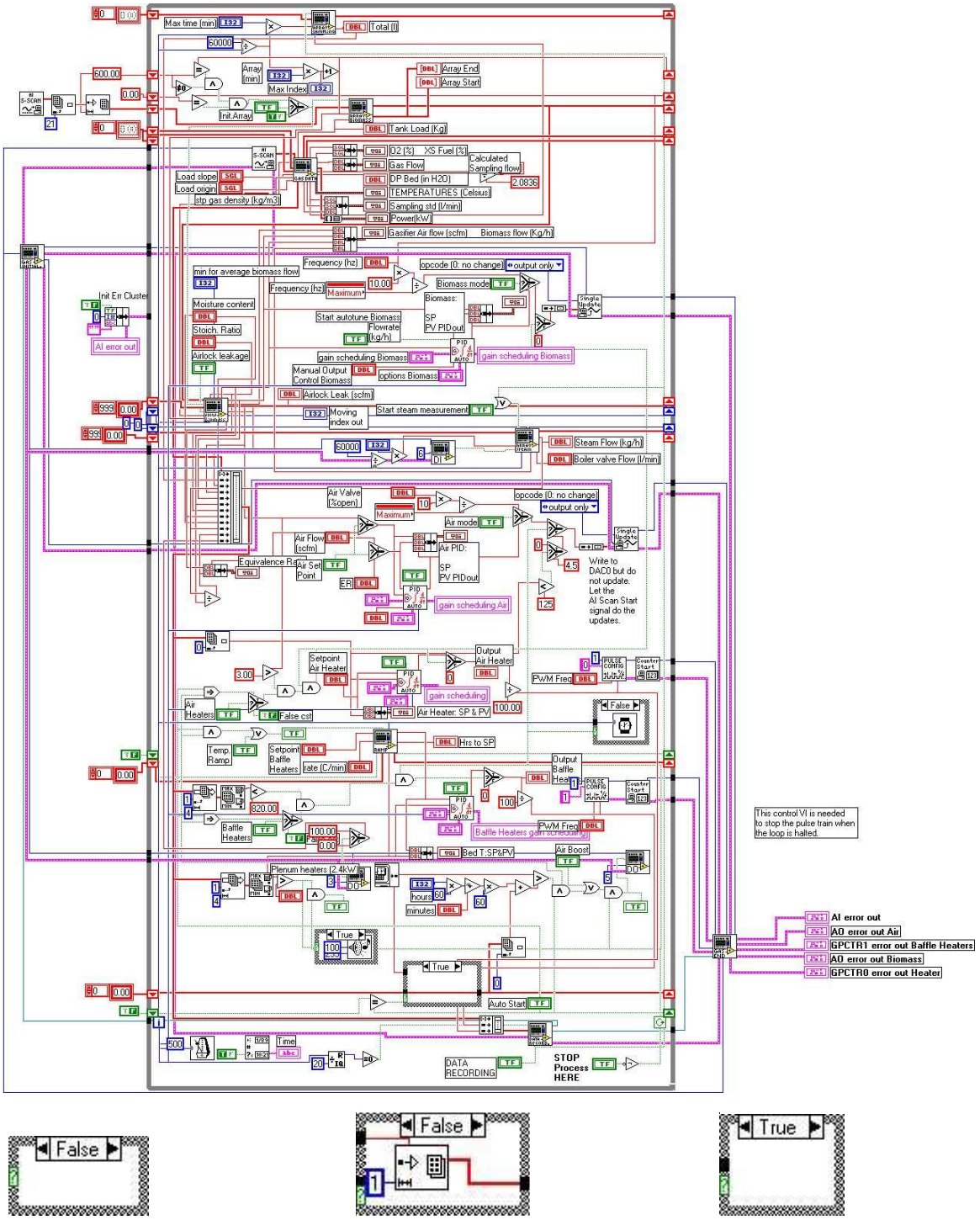

8.6.1.2 Gas 11 init.vi

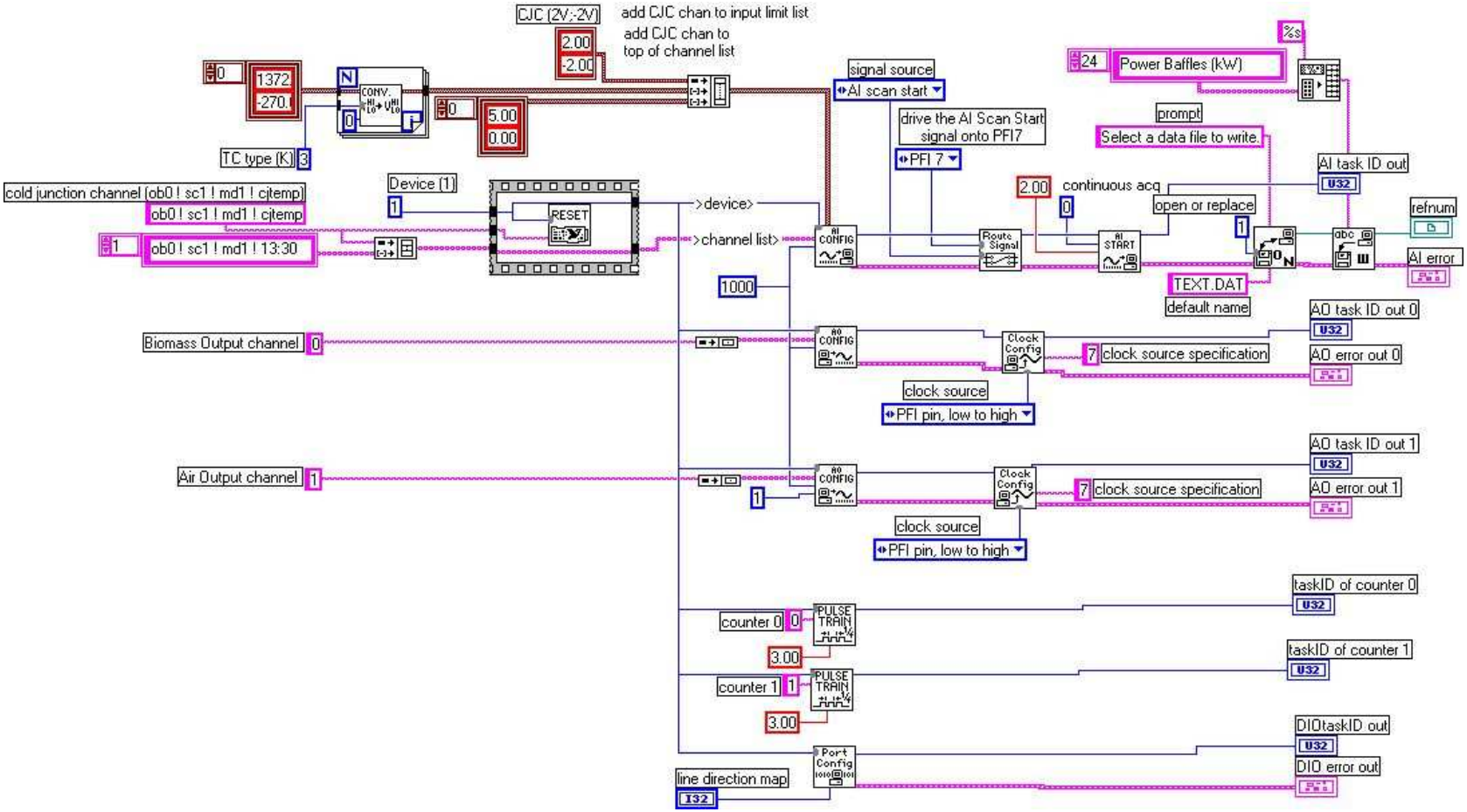

8.6.1.3 Gas 10 sampling flow array.vi

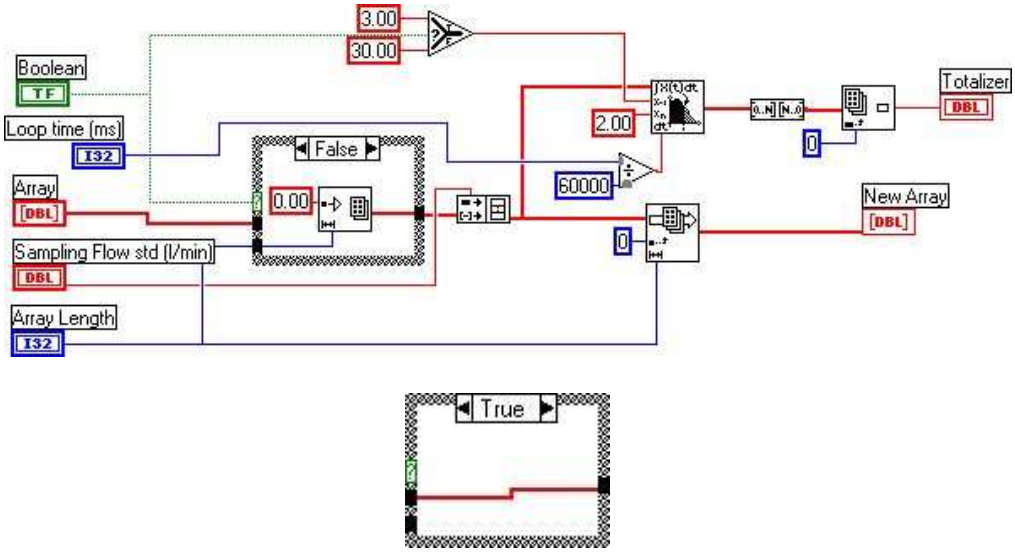

8.6.1.4 Gas 10 biomass array.vi

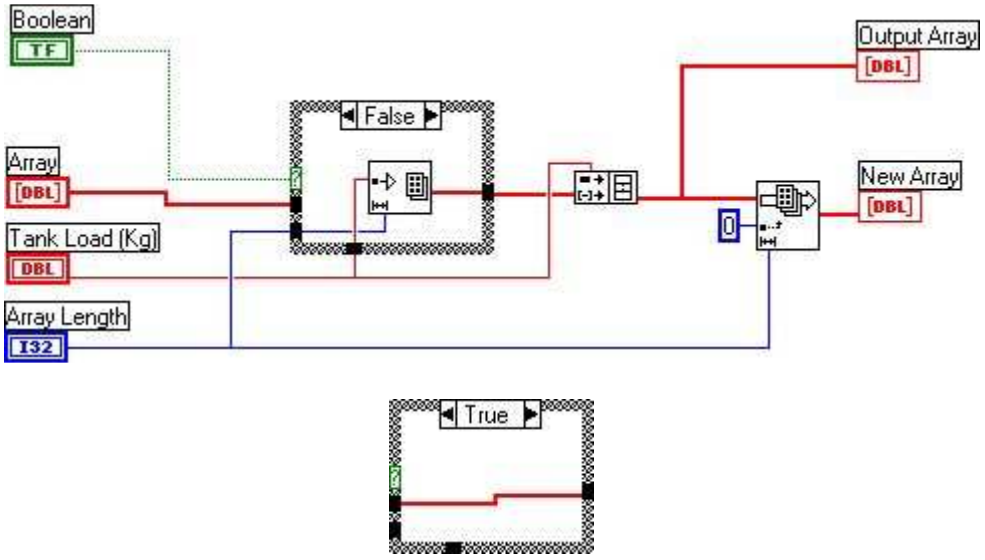

8.6.1.5 Gas 11 Data.vi

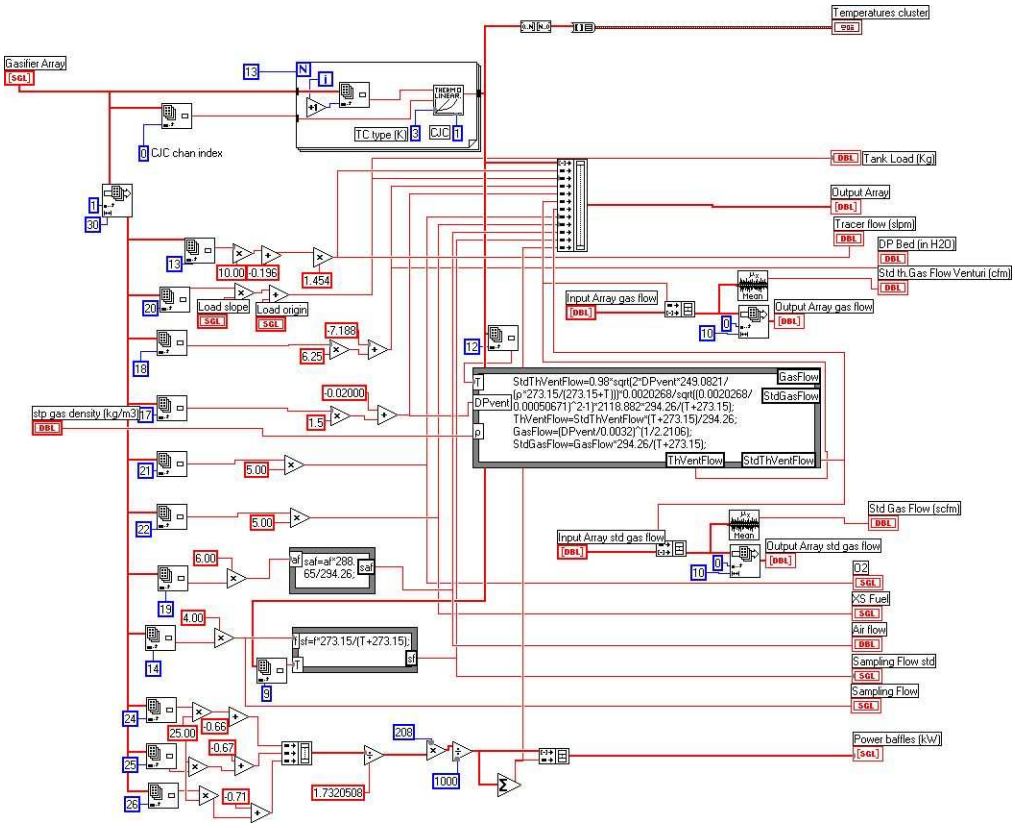

8.6.1.6 PID with autotuning.vi

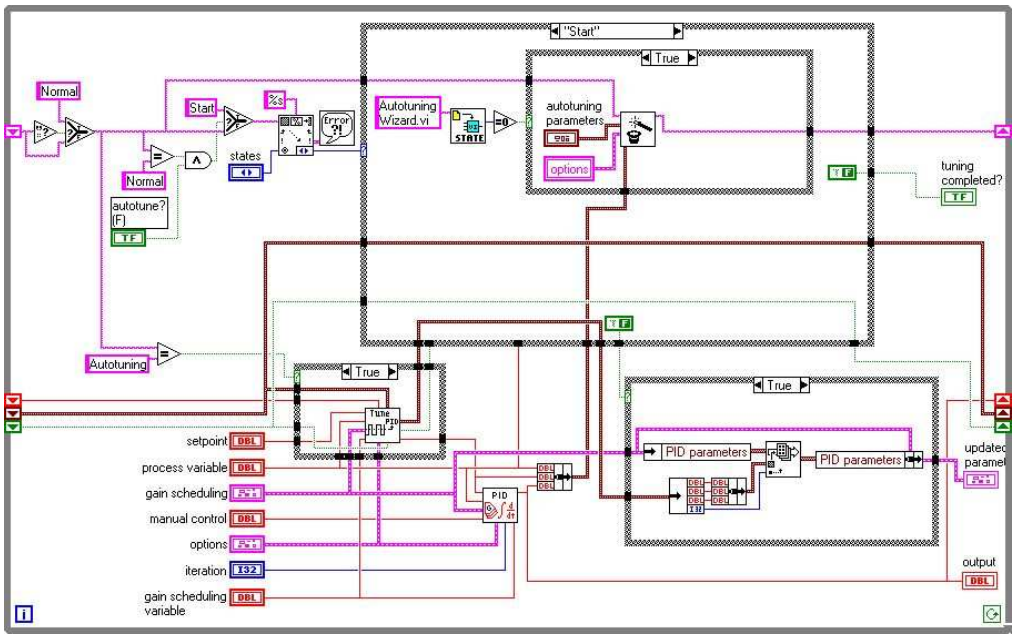

8.6.1.7 Gas 10 Flow biomass.vi

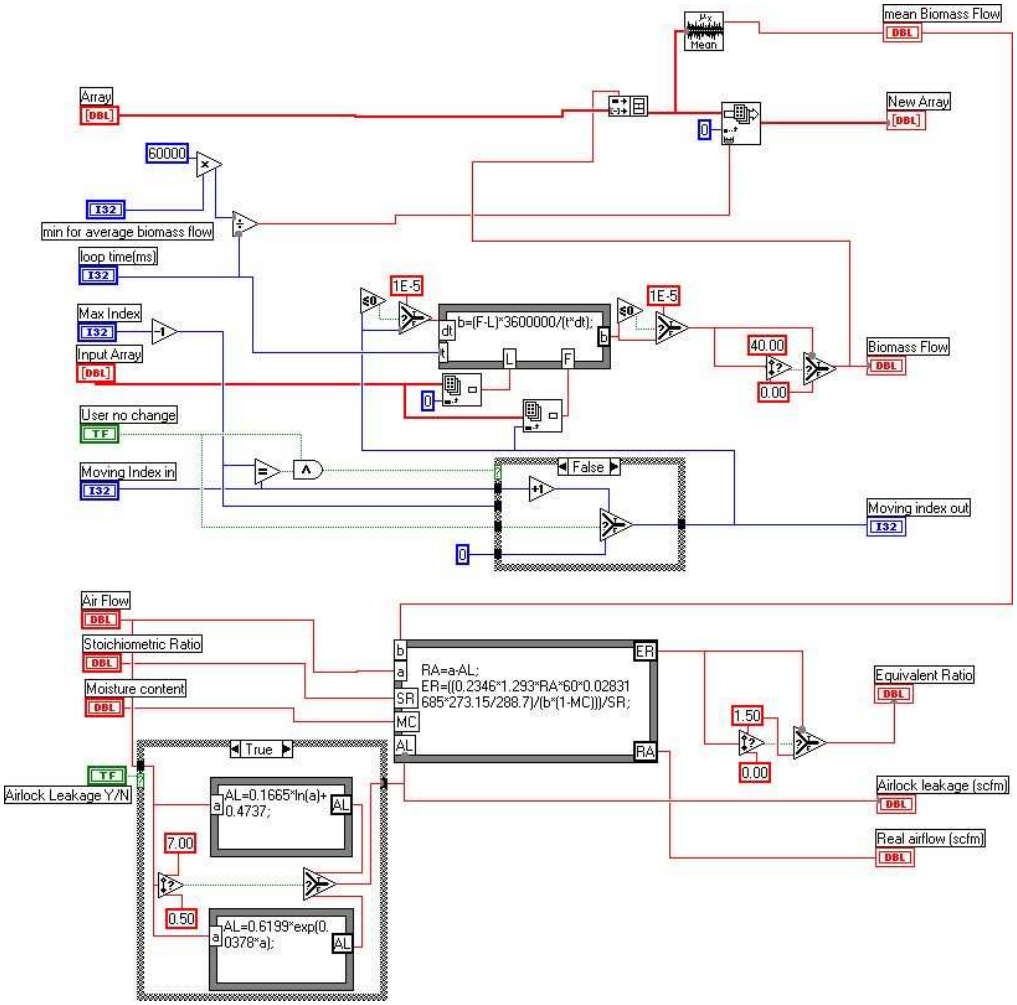

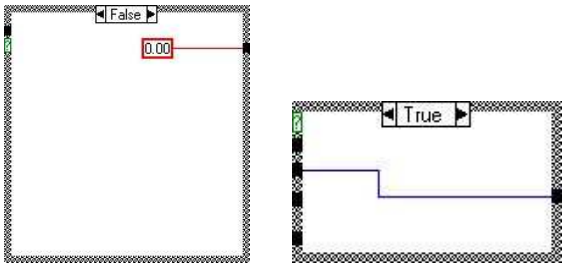

8.6.1.8 Gas 10 steam flow array.vi

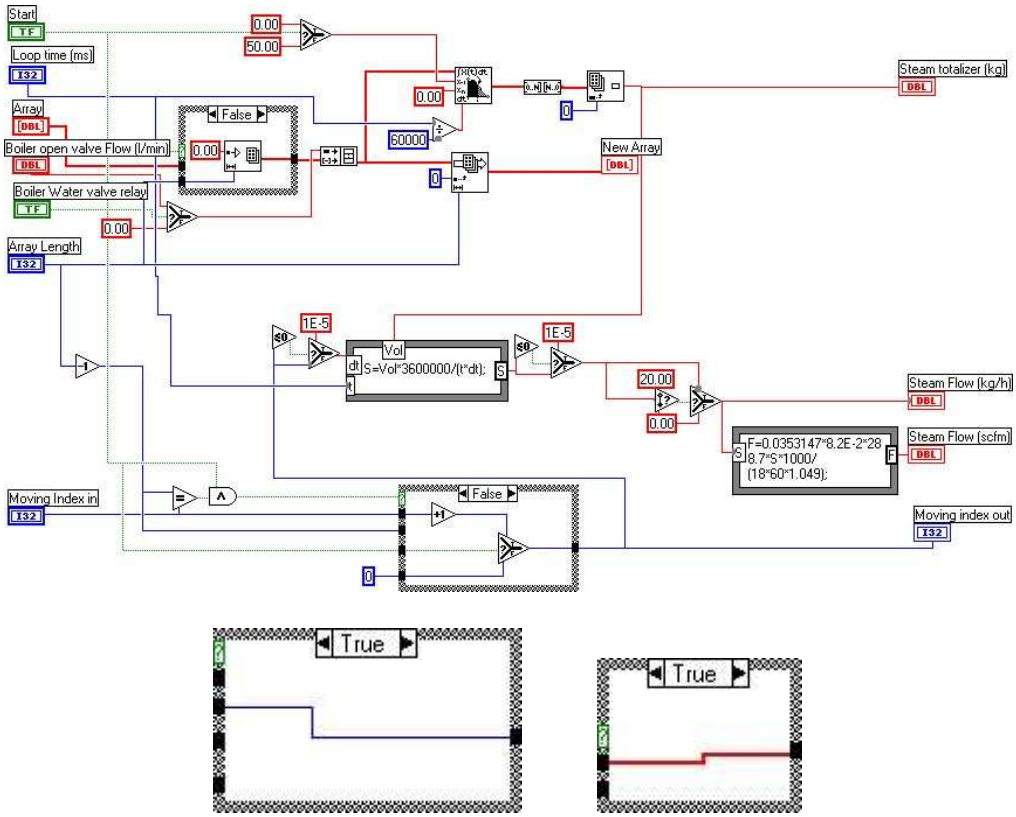

8.6.1.9 Gas 11 DI.vi

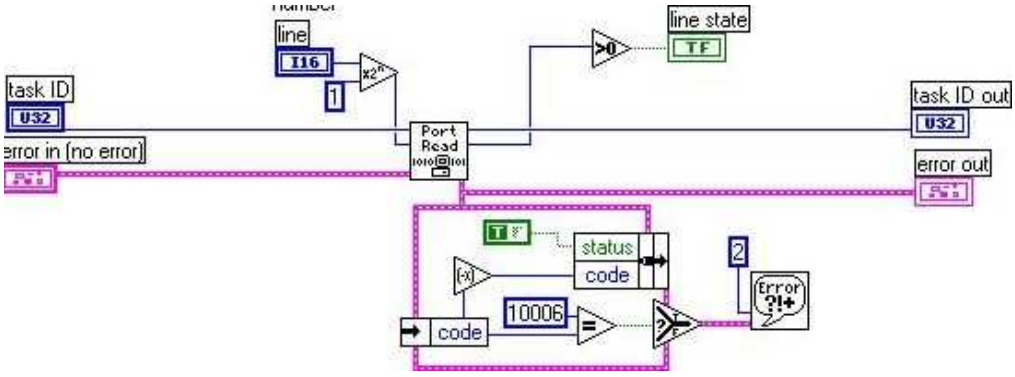

8.6.1.10 Gas 10 Ramp.vi

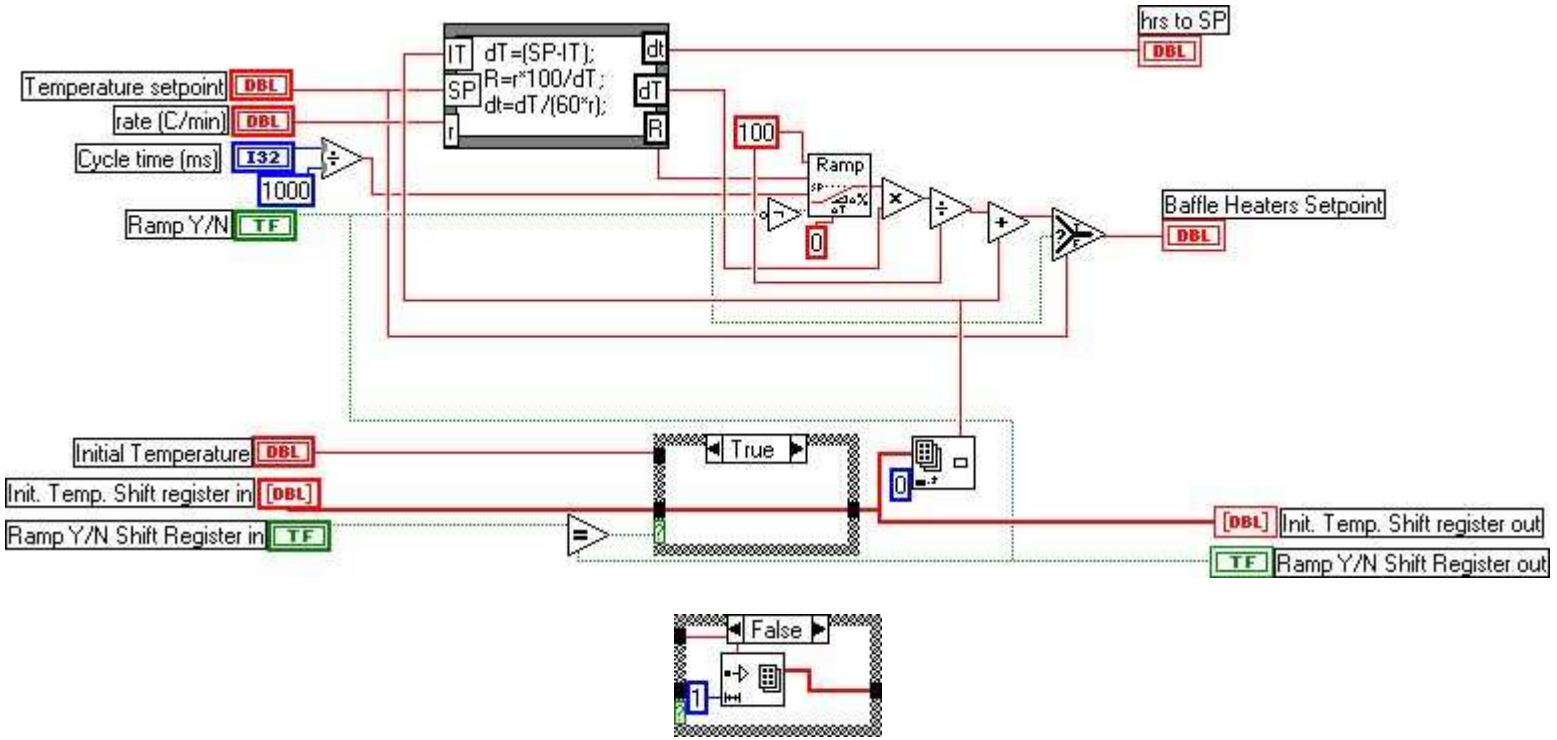

8.6.1.11 Gas 11 DO.vi

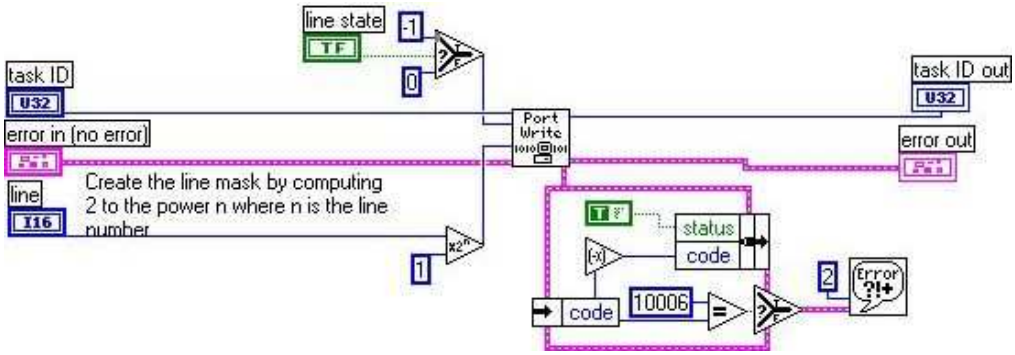

8.6.1.12 Gas 10 Data recording.vi

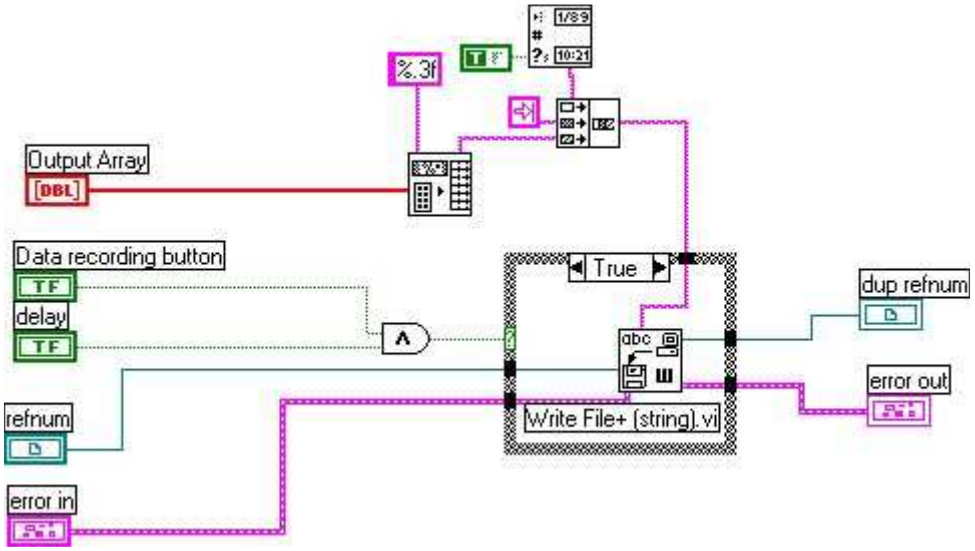

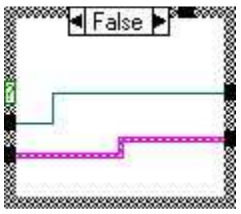

8.6.1.13 Gas 10 end.vi

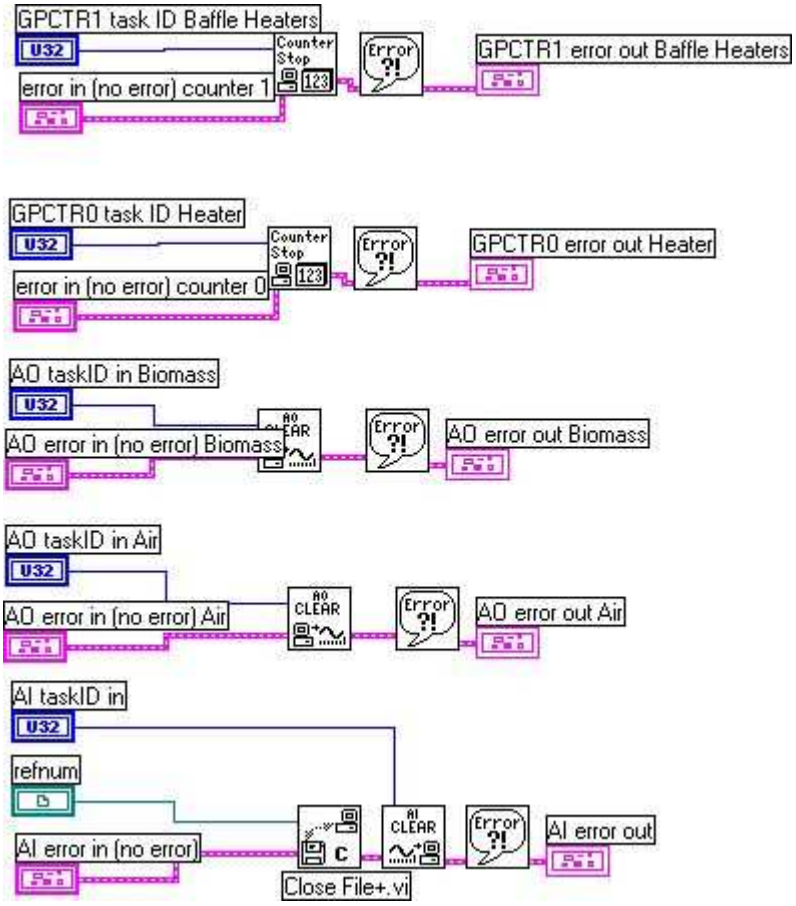

8.6.2 Gibbs reactor modeling program

8.6.2.1 Main program

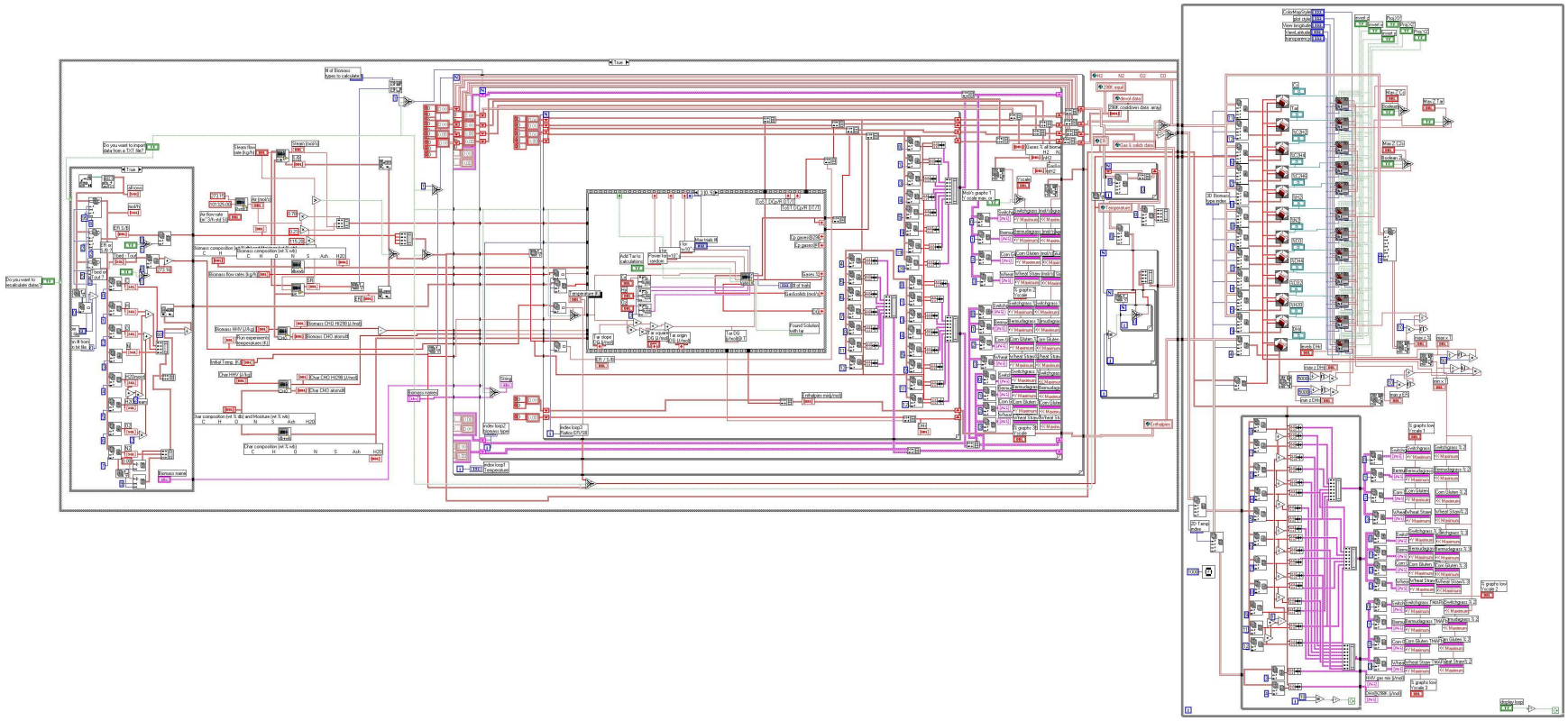

Other cases from previous page case structures in main program:

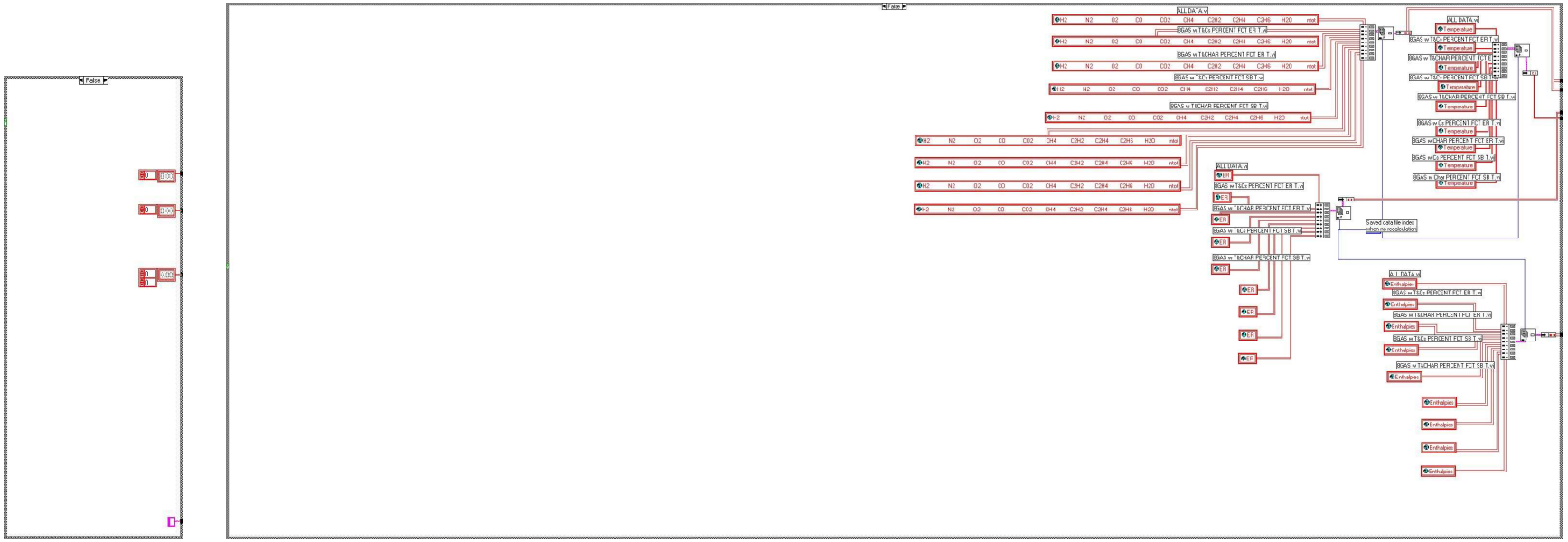

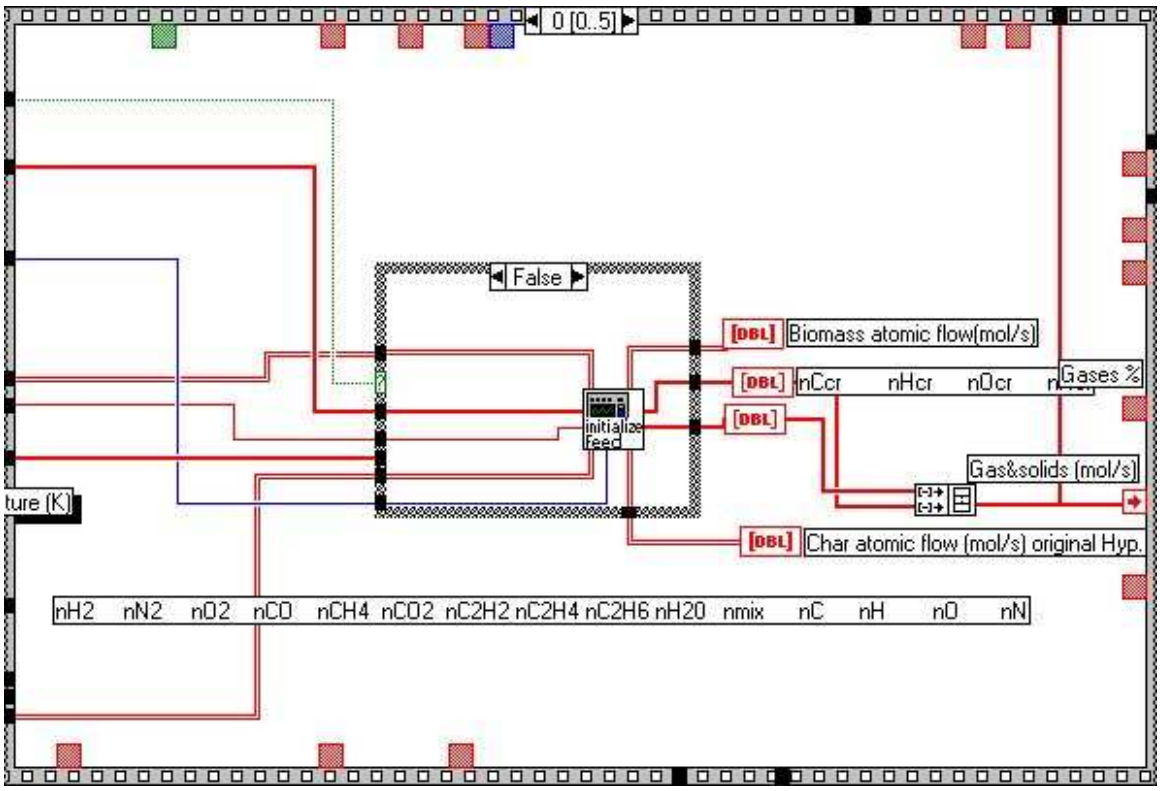

Other case from above case structures in sequence 0:

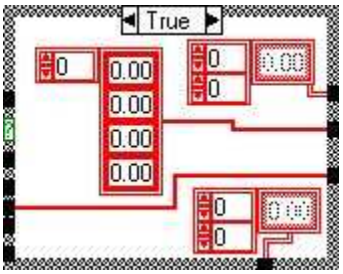

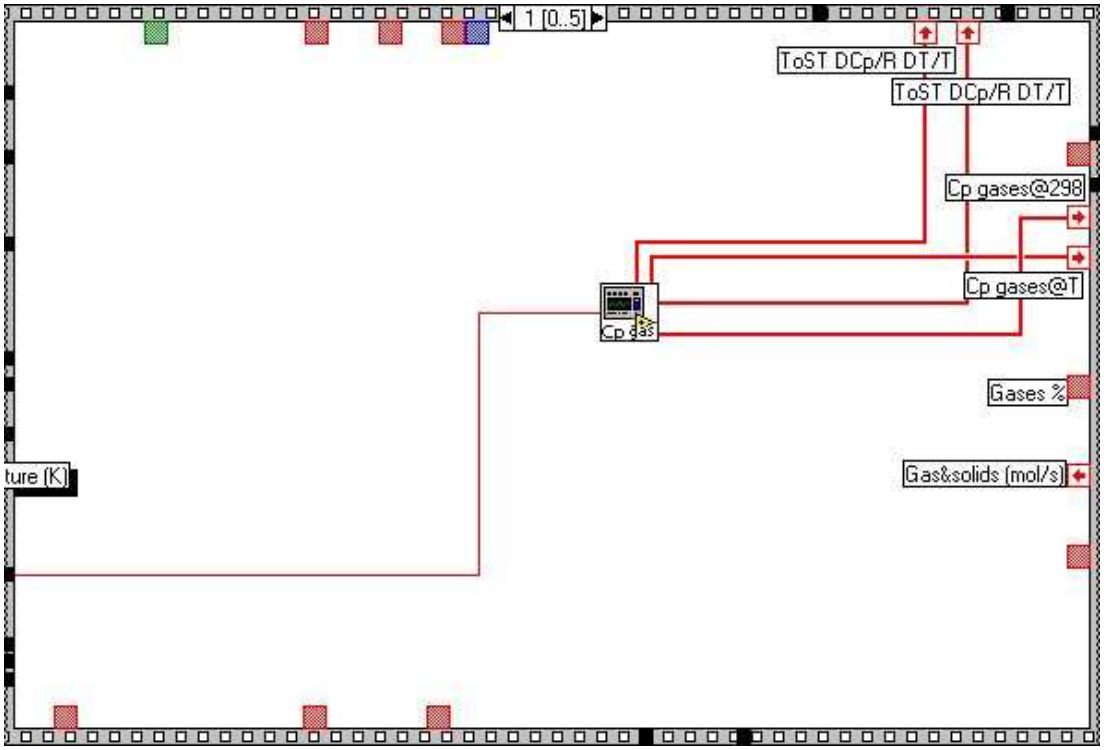
1 [0..5]
ToST DCp/R DT/T
ToST DCp/R DT/T
Cp gases@298
Cp gases@T
Cp gas
Gases %
ture (K)
Gas&solids (mol/s)

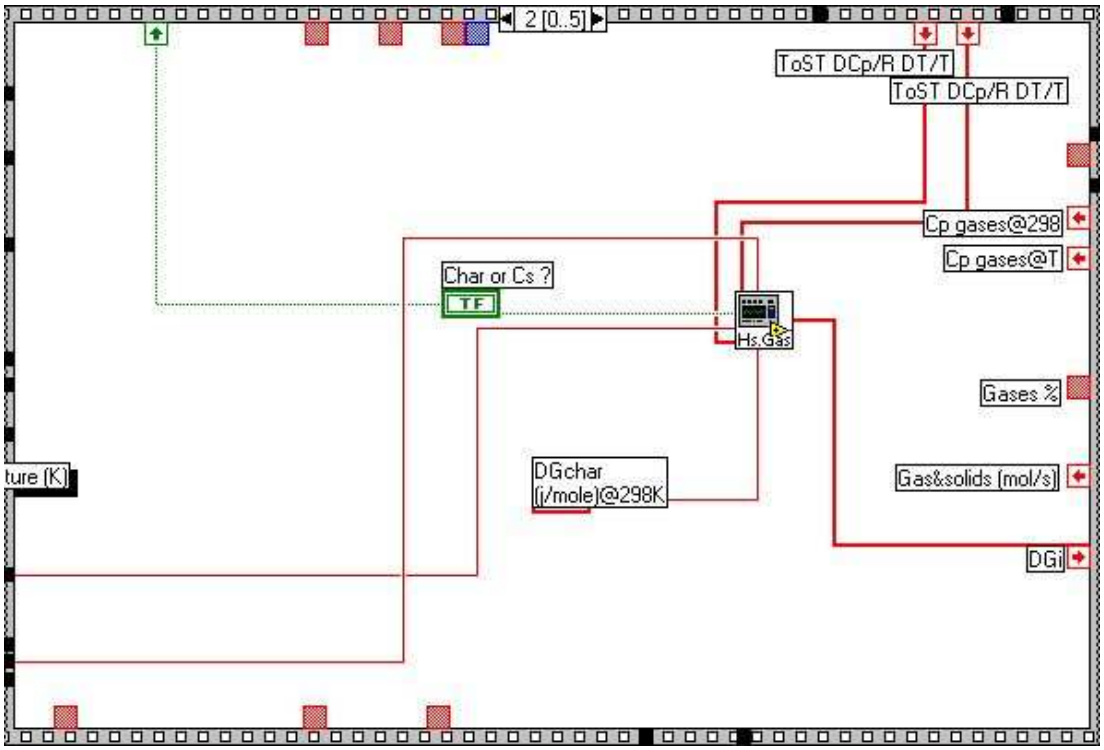
2 [0..5]
ToST DCp/R DT/T
ToST DCp/R DT/T
Cp gases@298
Cp gases@T
Char or Cs ?
TF
Hs,Gas
Gases %
ture (K)
DGchar
(j/mole)@298K
Gas&solids (mol/s)
DGi

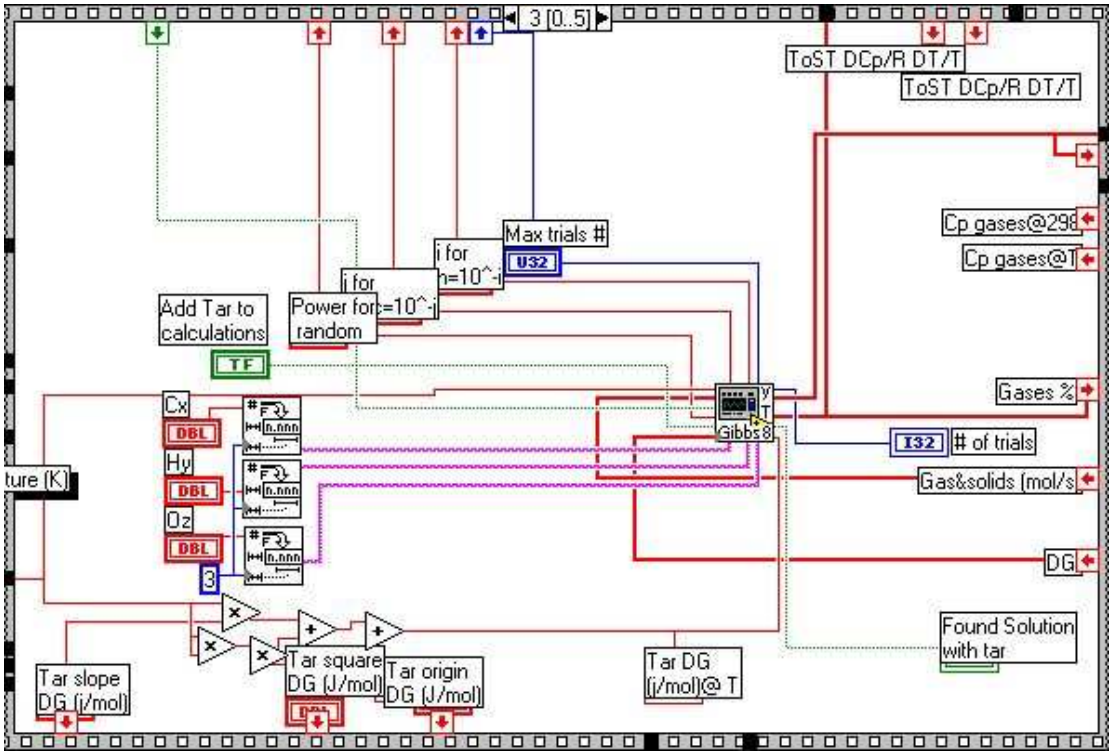
3 [0..5]
ToST DCp/R DT/T
ToST DCp/R DT/T
Max trials #
U32
i for
Power for
random
Add Tar to
calculations
TF
Cx
DBL
Hy
DBL
Oz
DBL
3
Gibbs
Cp gases@298
Cp gases@T
Gases %
I32
# of trials
Gas&solids (mol/s
DG
Found Solution
with tar
ture (K)
Tar slope
DG (j/mol)
Tar square
DG (J/mol)
Tar origin
DG (J/mol)
Tar DG
(j/mol)@ T

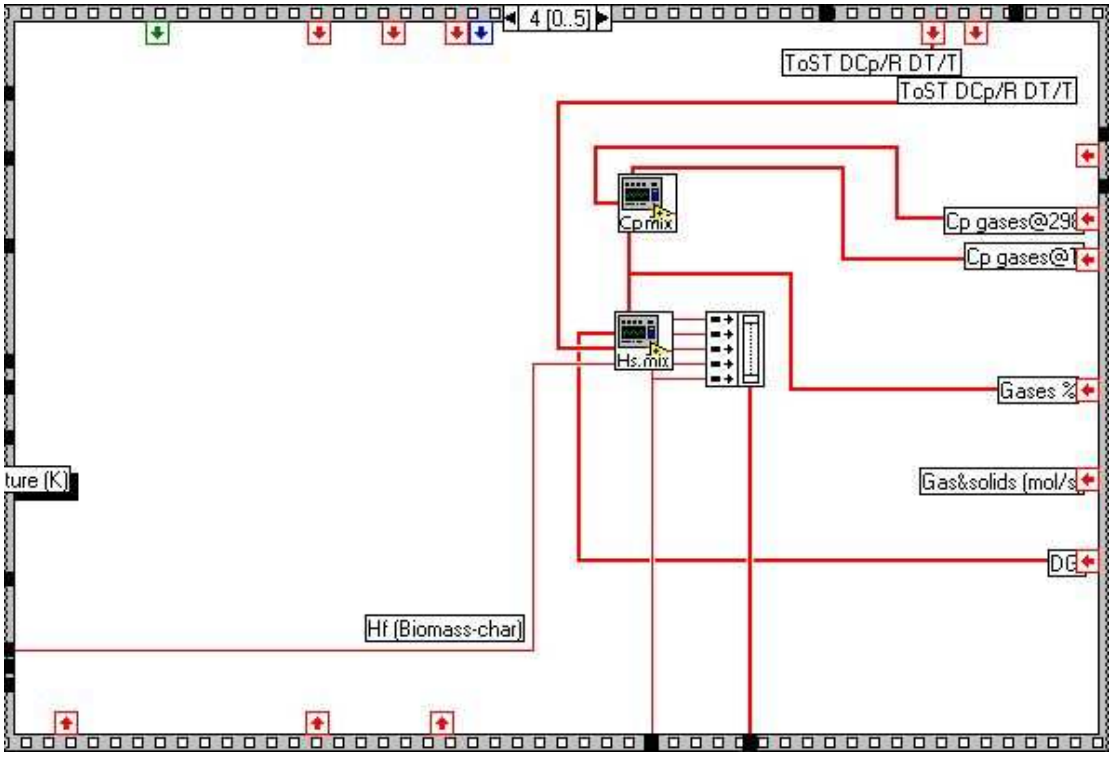
4 [0..5]
ToST DCp/R DT/T
ToST DCp/R DT/T
Cp mix
Hs. mix
Cp gases@298
Cp gases@T
Gases %
Gas&solids (mol/s
DG
ture (K)
Hf (Biomass-char)

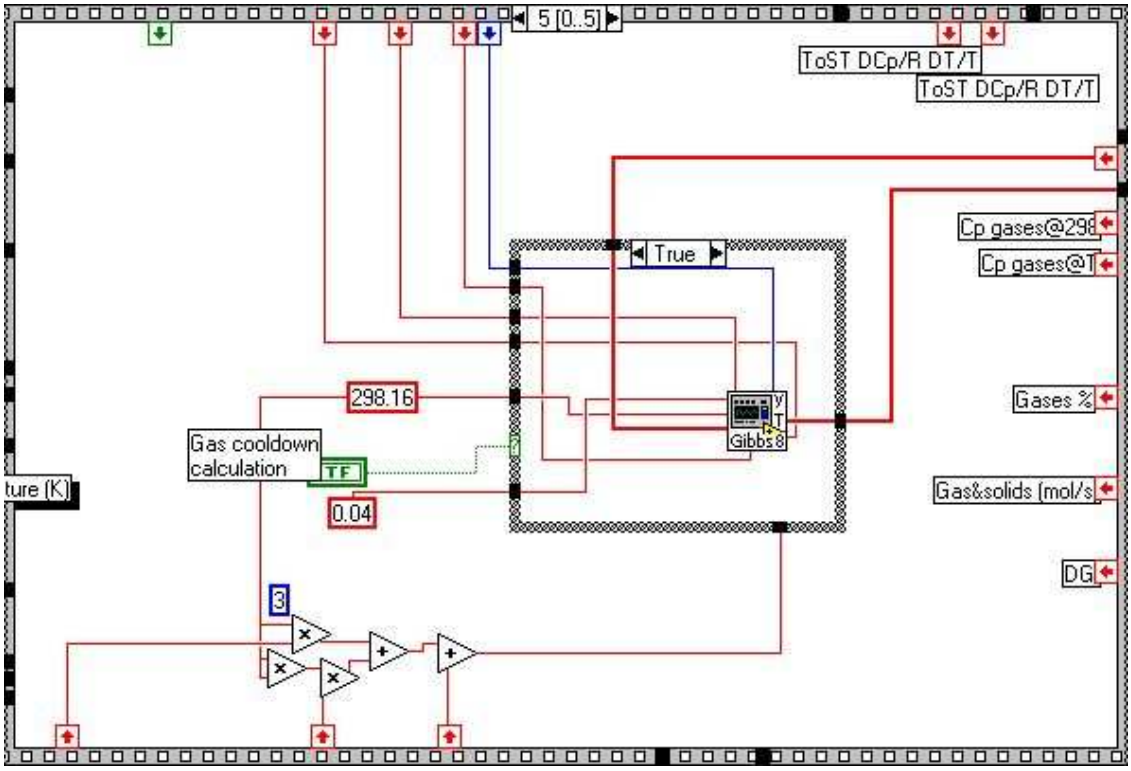

Other case from above case structures in sequence 5:

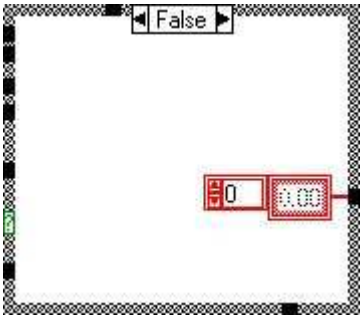

8.6.2.2 PV=nRT.vi: calculates mole number from ideal gas law

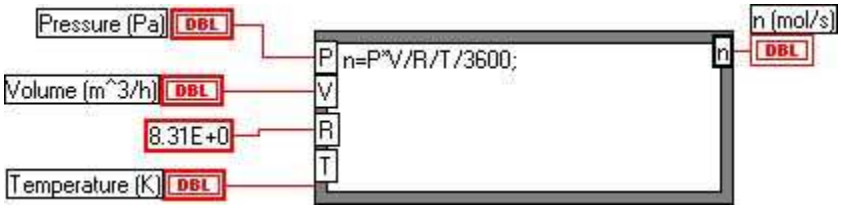

8.6.2.3 Dry to wet.vi: % composition basis conversion

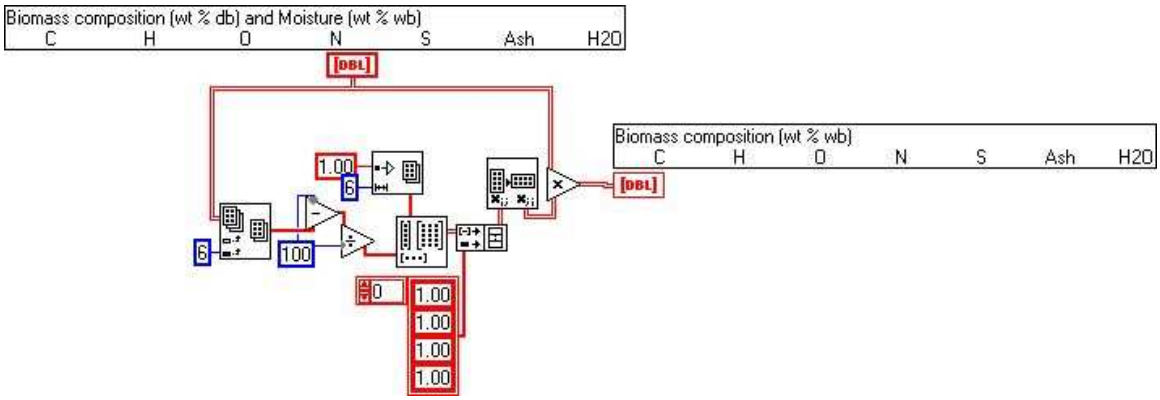

8.6.2.4 ER.vi: calculation of ER ratio

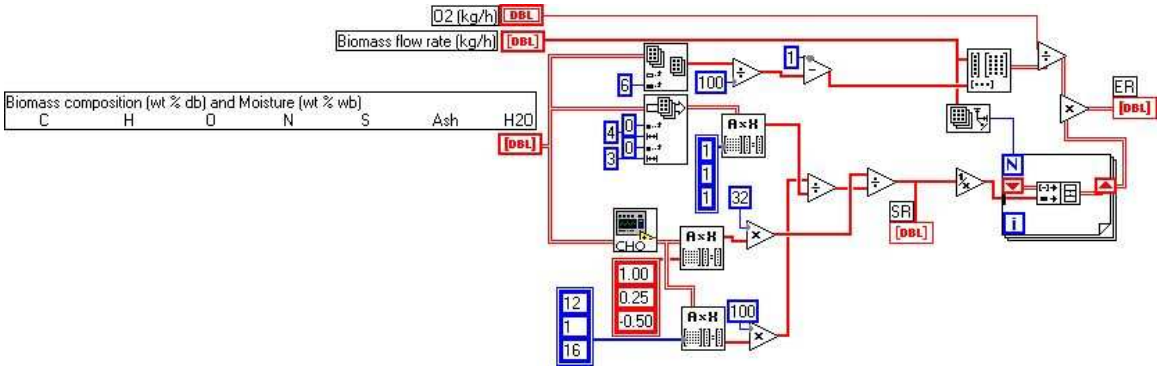

8.6.2.5 SB.vi: calculation of S/B ratio

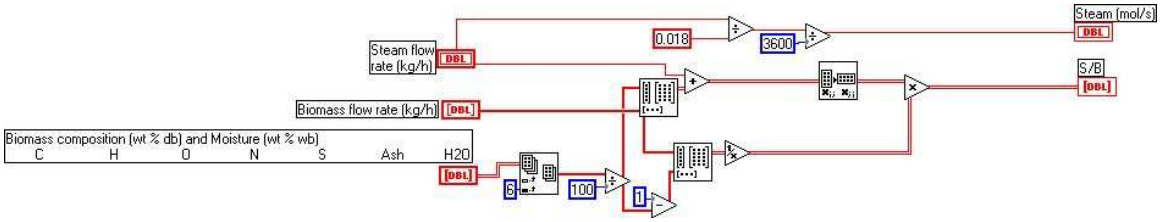

8.6.2.6 CHO.vi: conversion to atomic composition

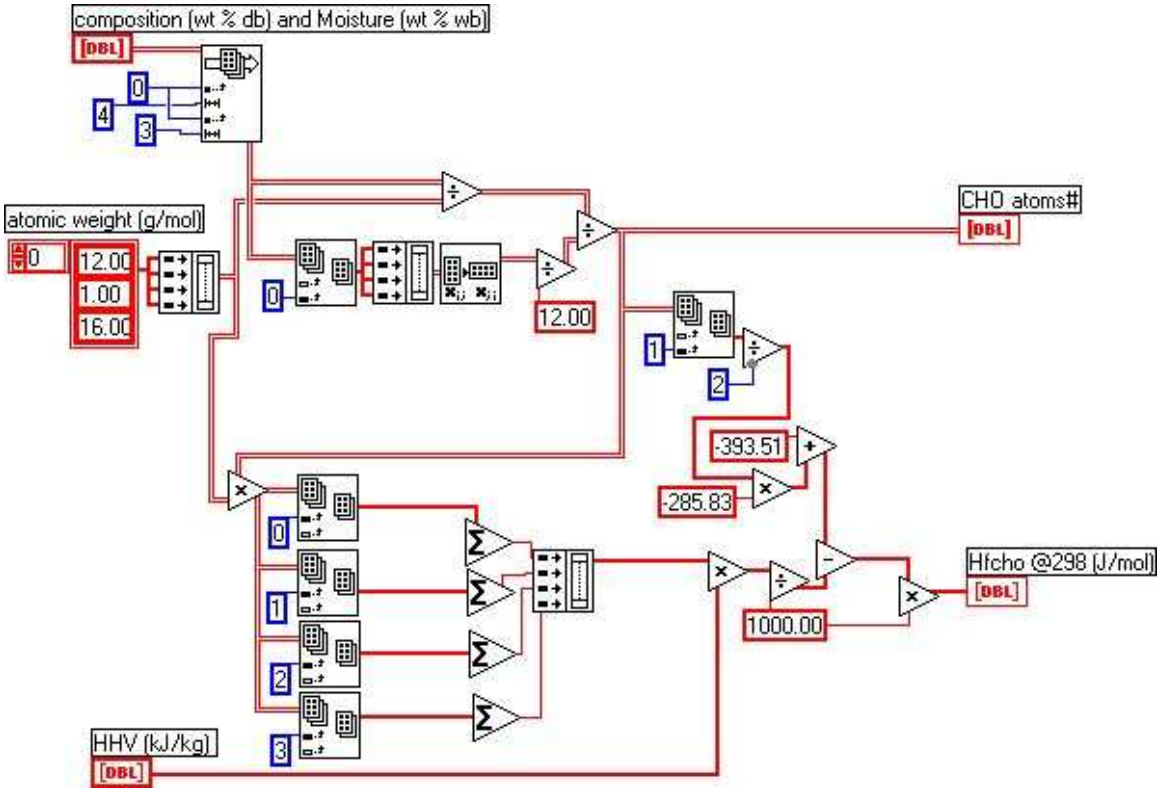

8.6.2.7 Initialize feed.vi: conversion of mass flow rates to biomass and char atomic flow rates

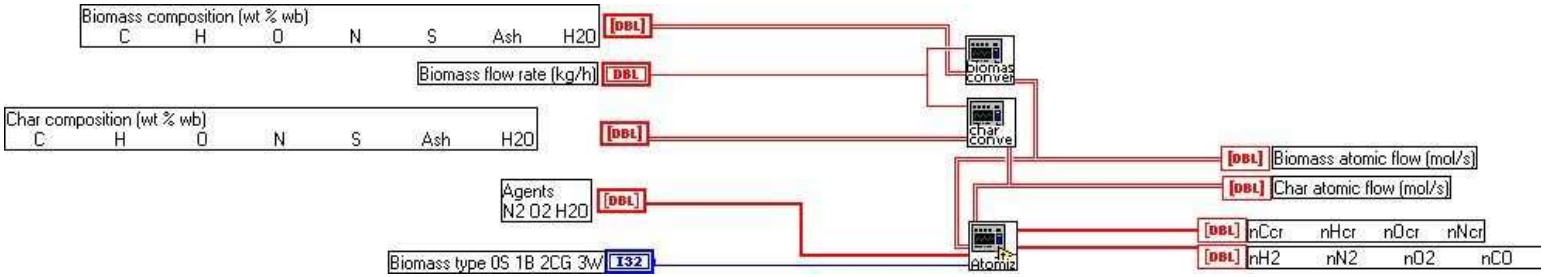

8.6.2.8 Atomization.vi:Agent biomass and char atomic flow rates

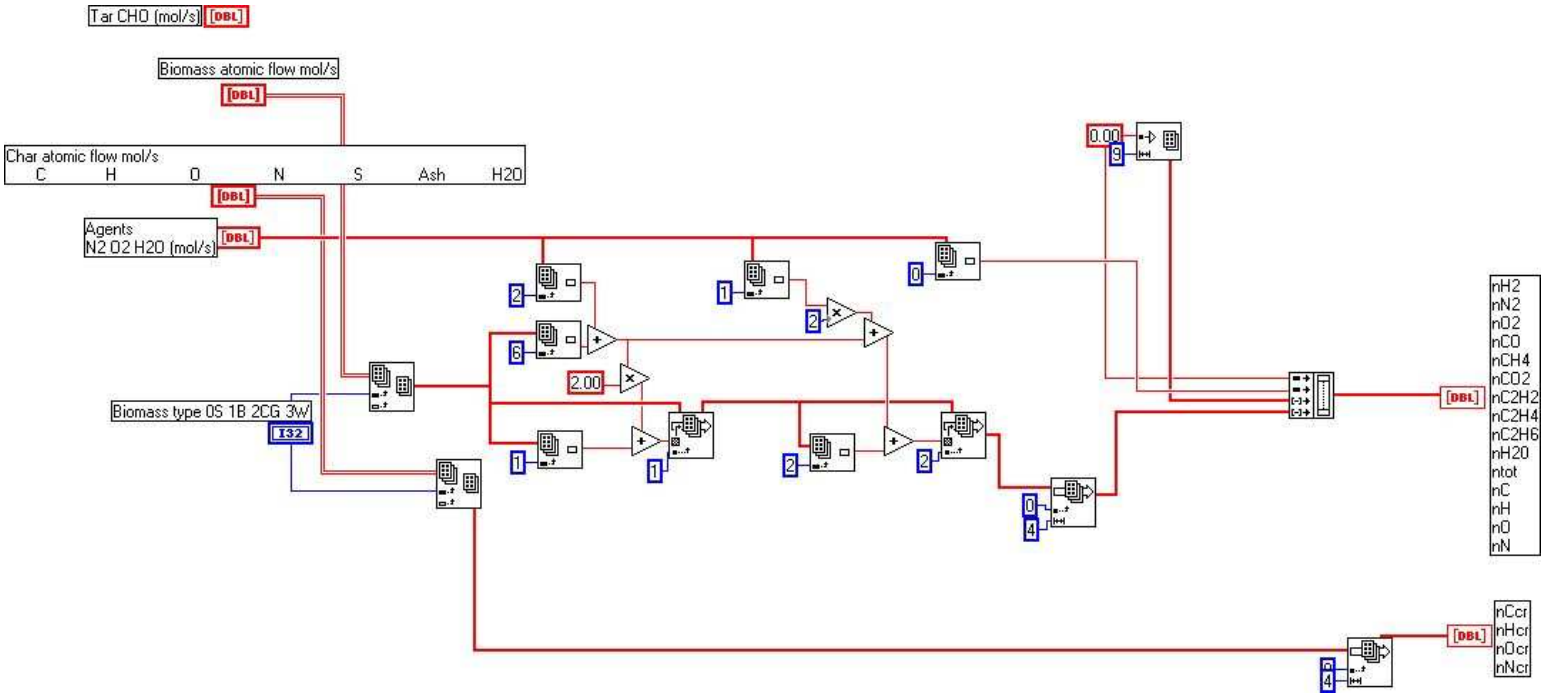

8.6.2.9 Biomass composition conversion.vi

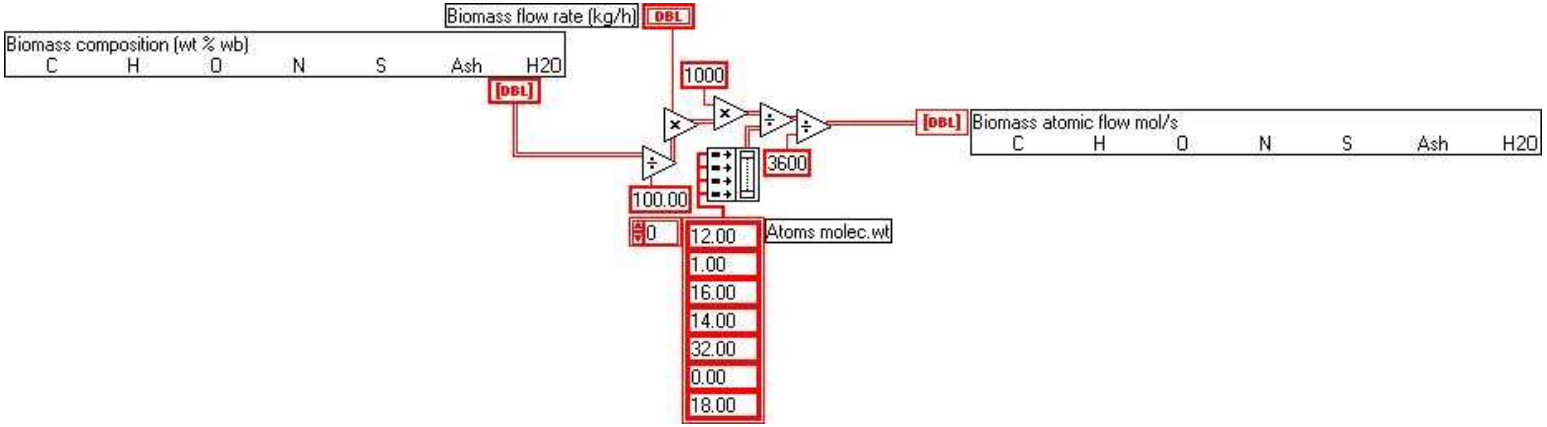

8.6.2.10 Char composition conversion.vi

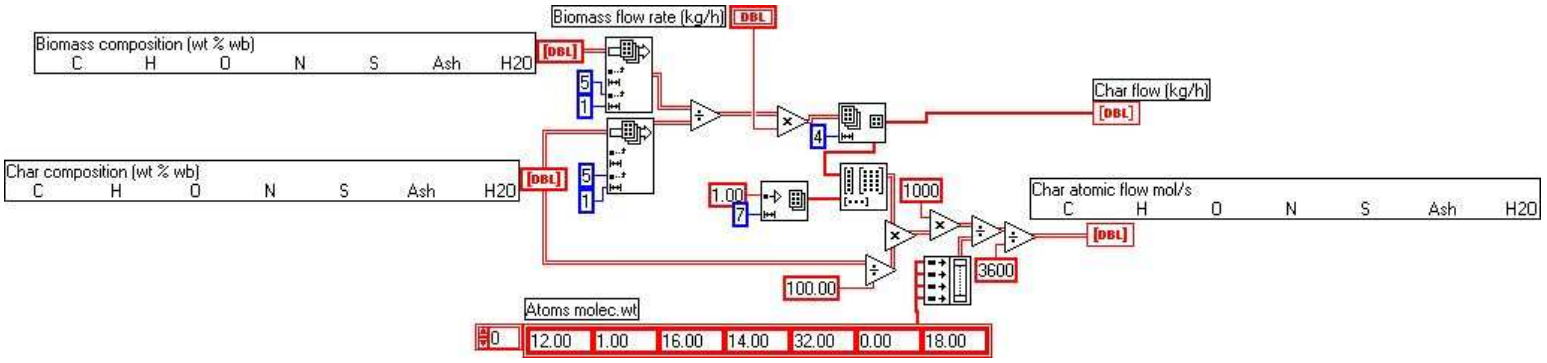

8.6.2.11 Cp Equil gases.vi: gases heat capacities calculations

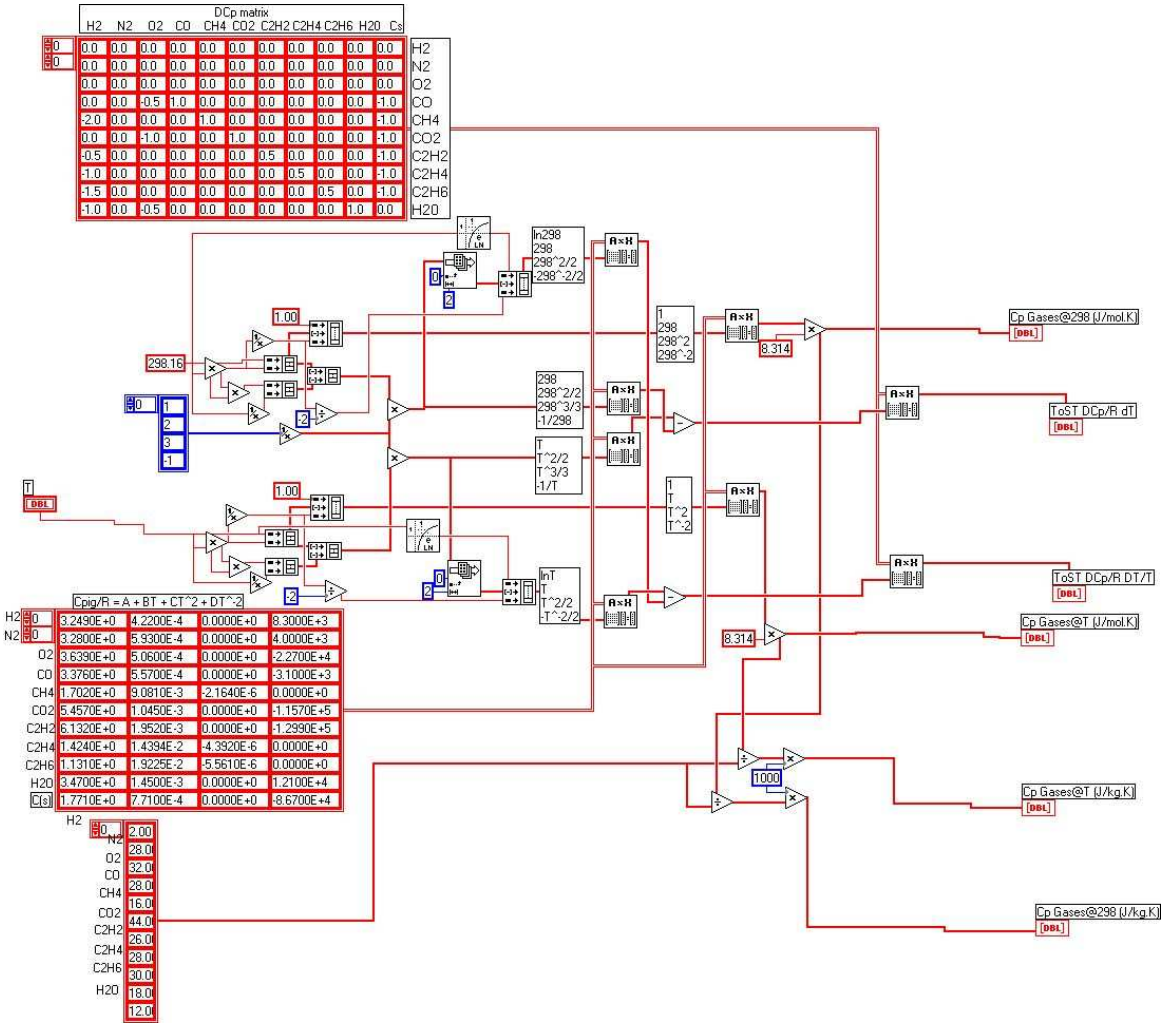

8.6.2.12 Equil enthalpy w char.vi: enthalpies of formation and free enthalpy calculation

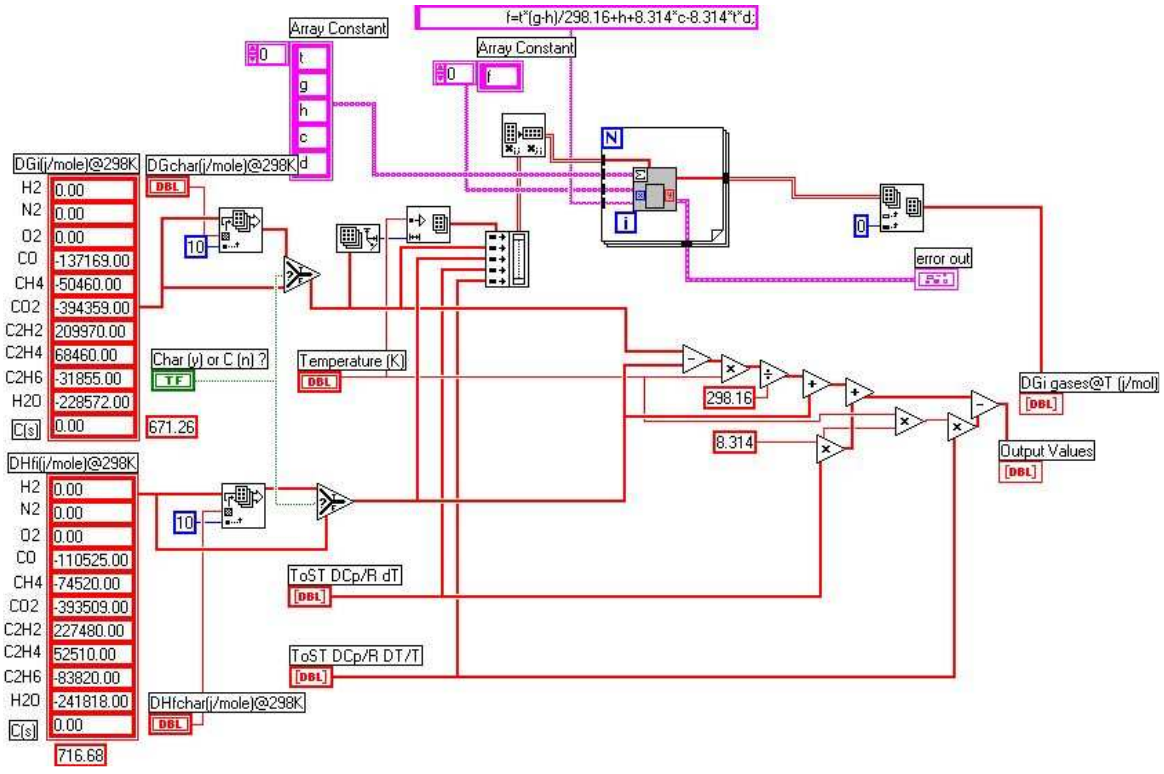

8.6.2.13 Equil Yield All n Tar n C.vi: non linear equations system solver

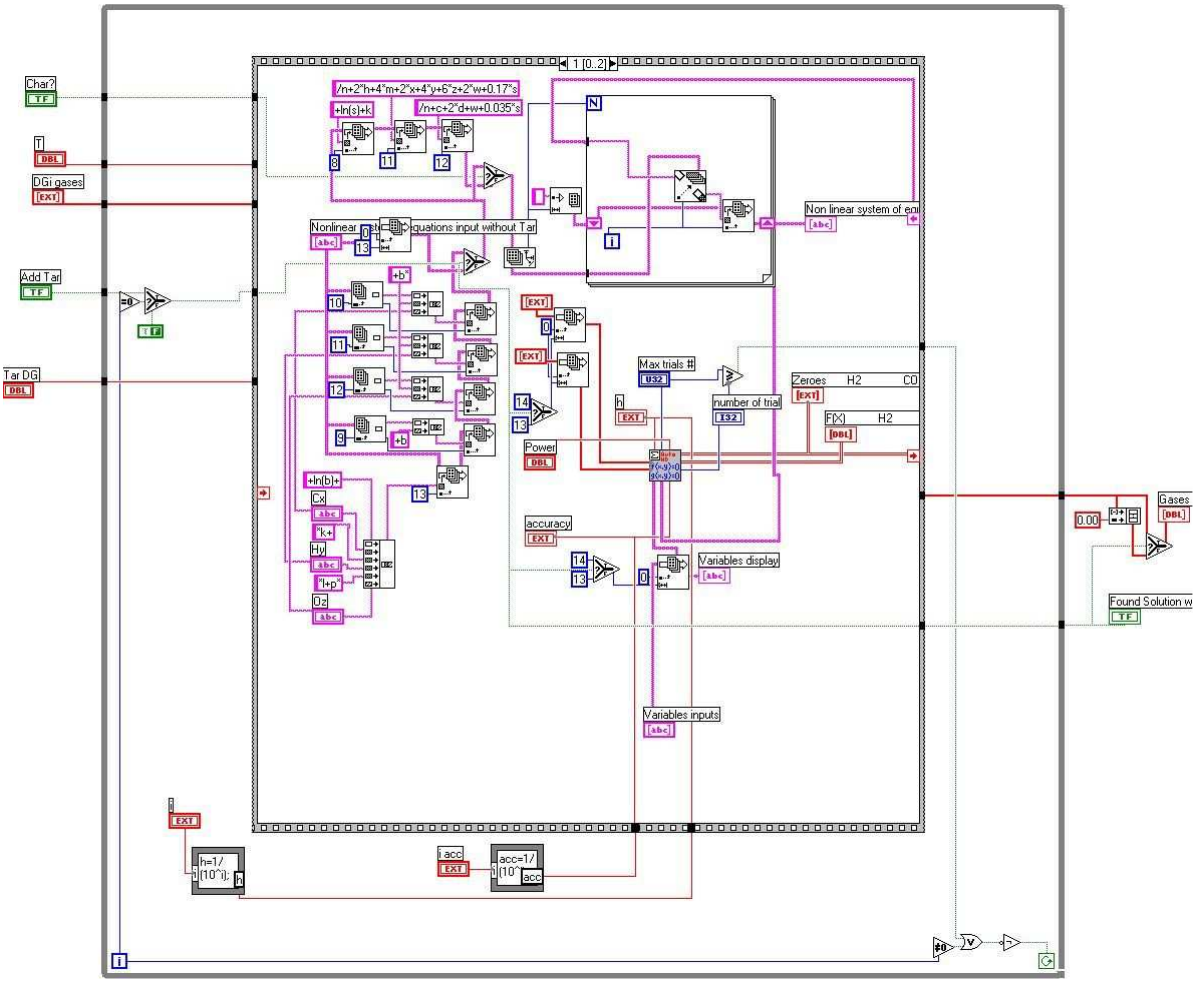

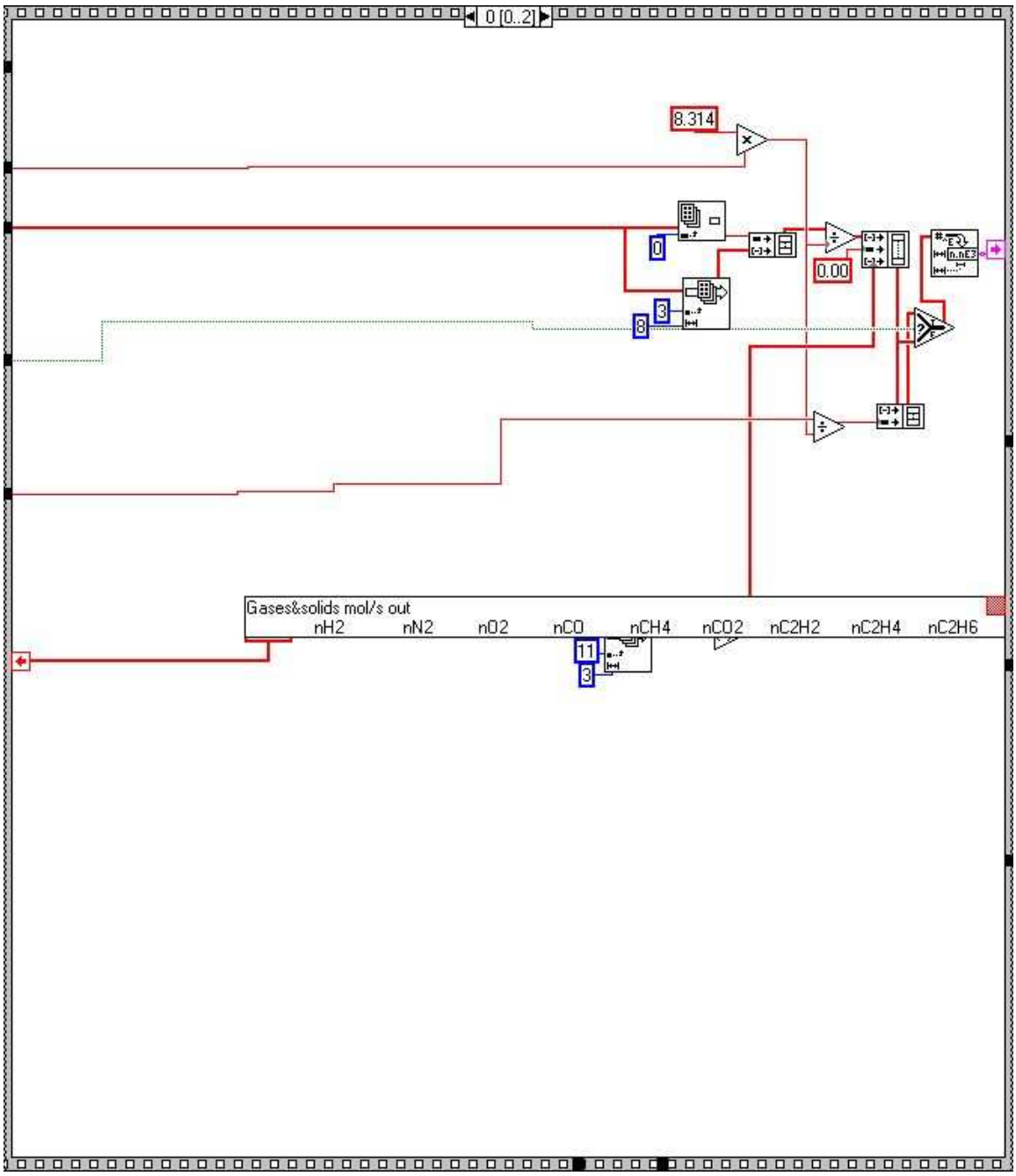
0 [0..2]
8.314
0
0.00
3
8
Gases&solids mol/s out
nH2
nN2
nO2
nCO
nCH4
nCO2
nC2H2
nC2H4
nC2H6
11
3

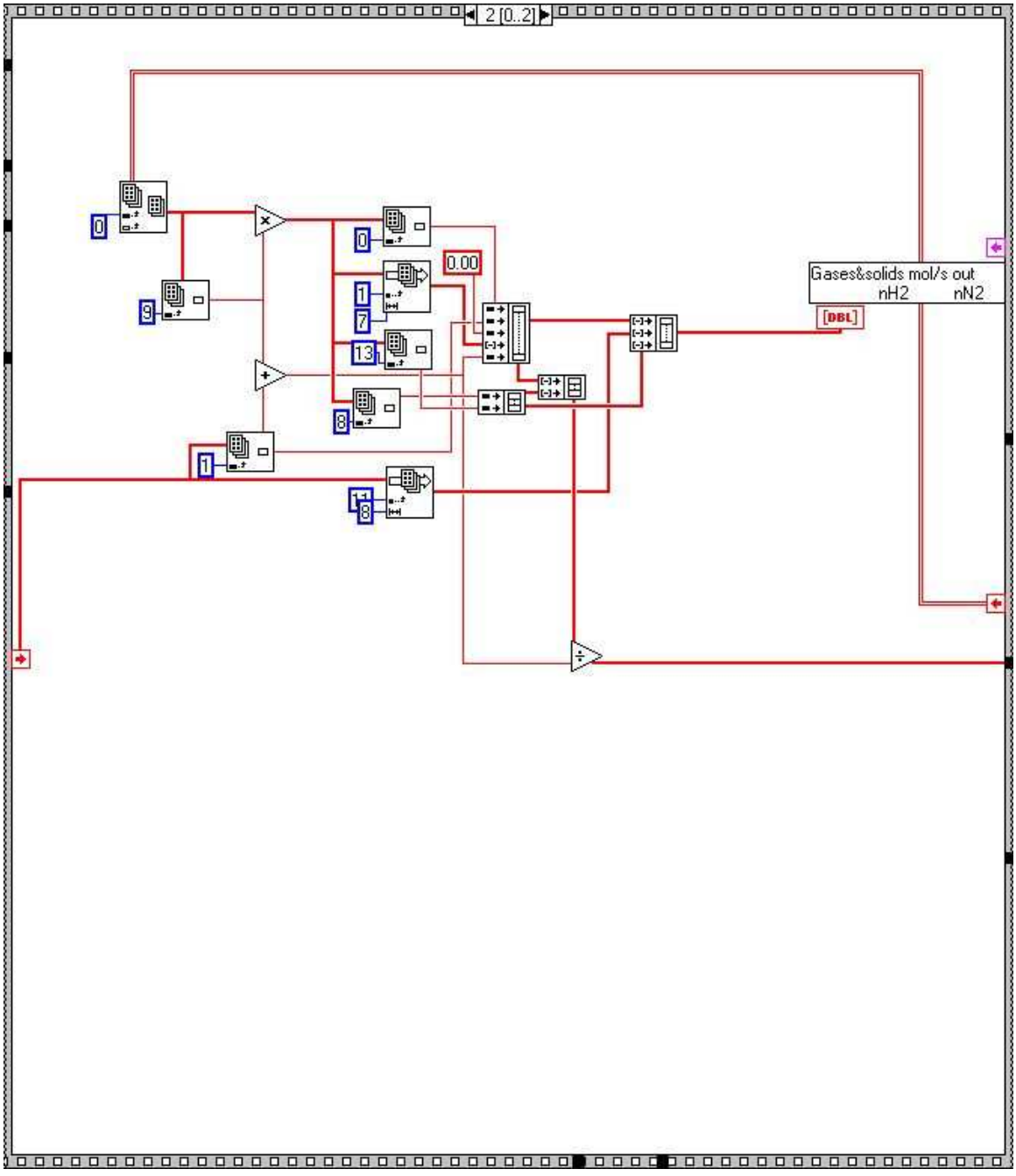
2 [0..2]
0
9
0
1
7
13
8
1
13
8
0.00
Gases&solids mol/s out
nH2
nN2
DBL

8.6.2.14 Cp Equil mix.vi: gas mix heat capacity calculation

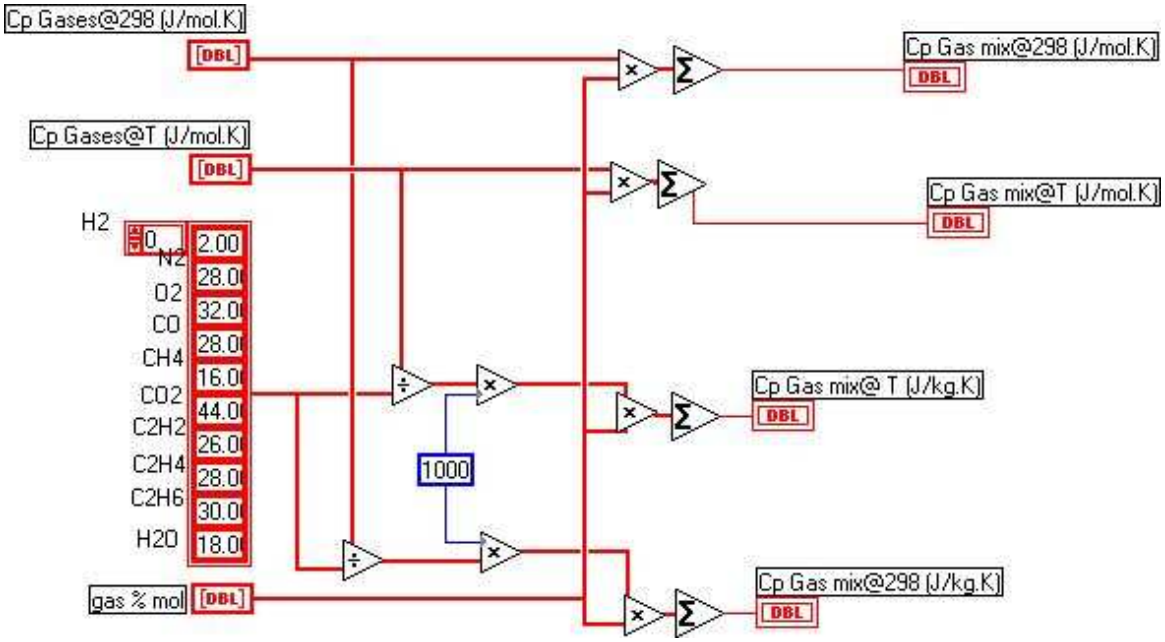

8.6.2.15 Equil Enthalpies mix.vi: gas mix enthalpies calculation

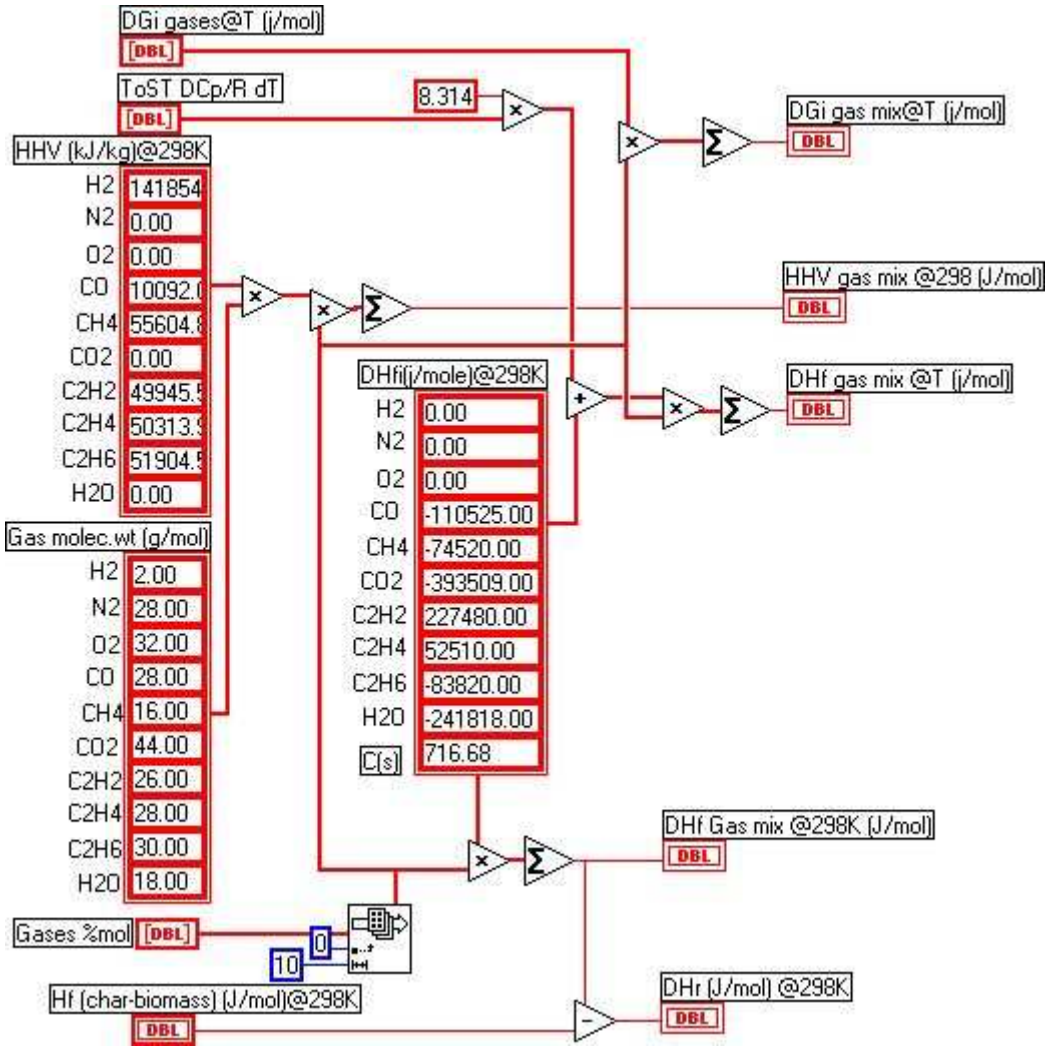

8.6.2.16 Equil Yield All n Tar n C cooldown.vi: non linear equations system solver

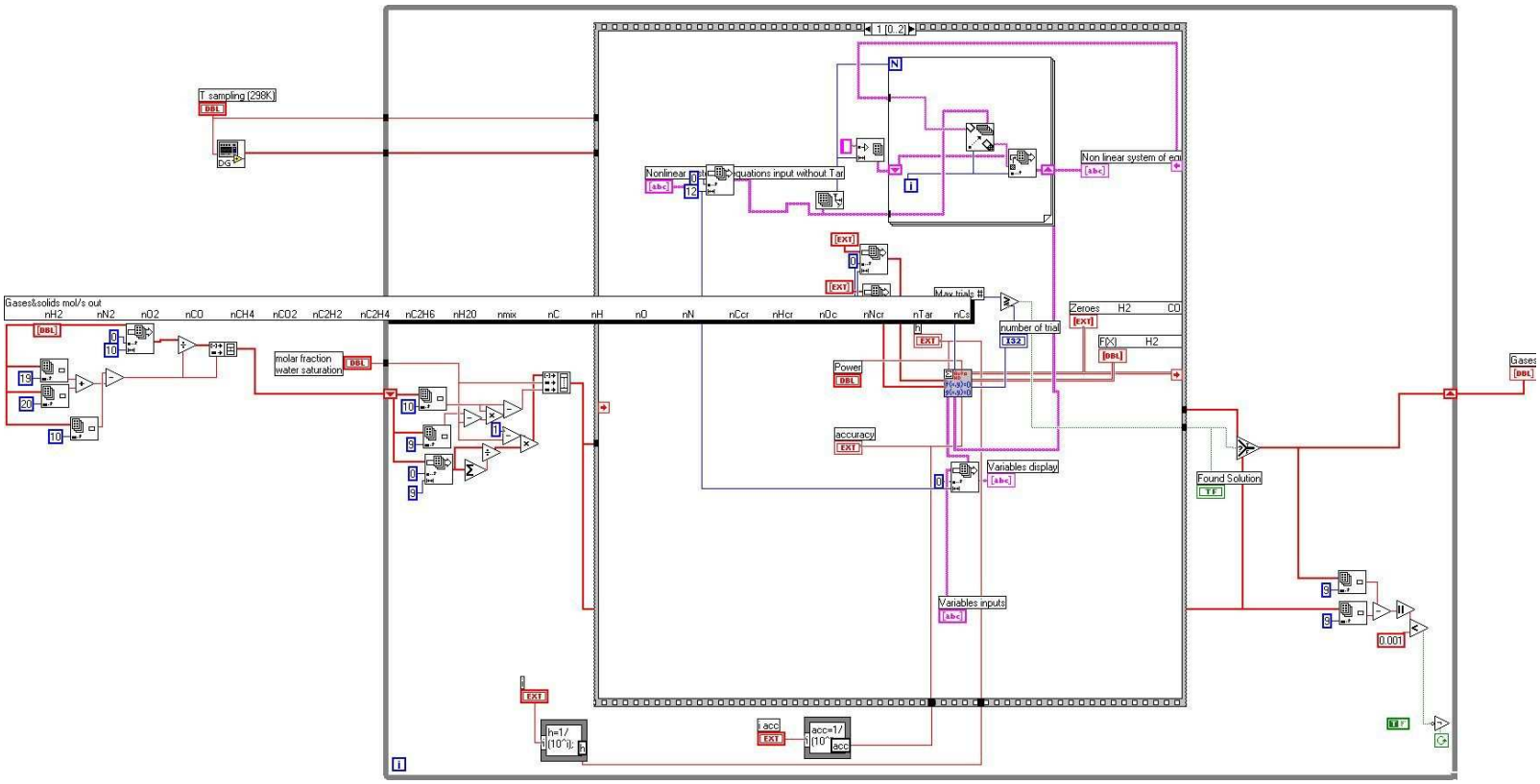

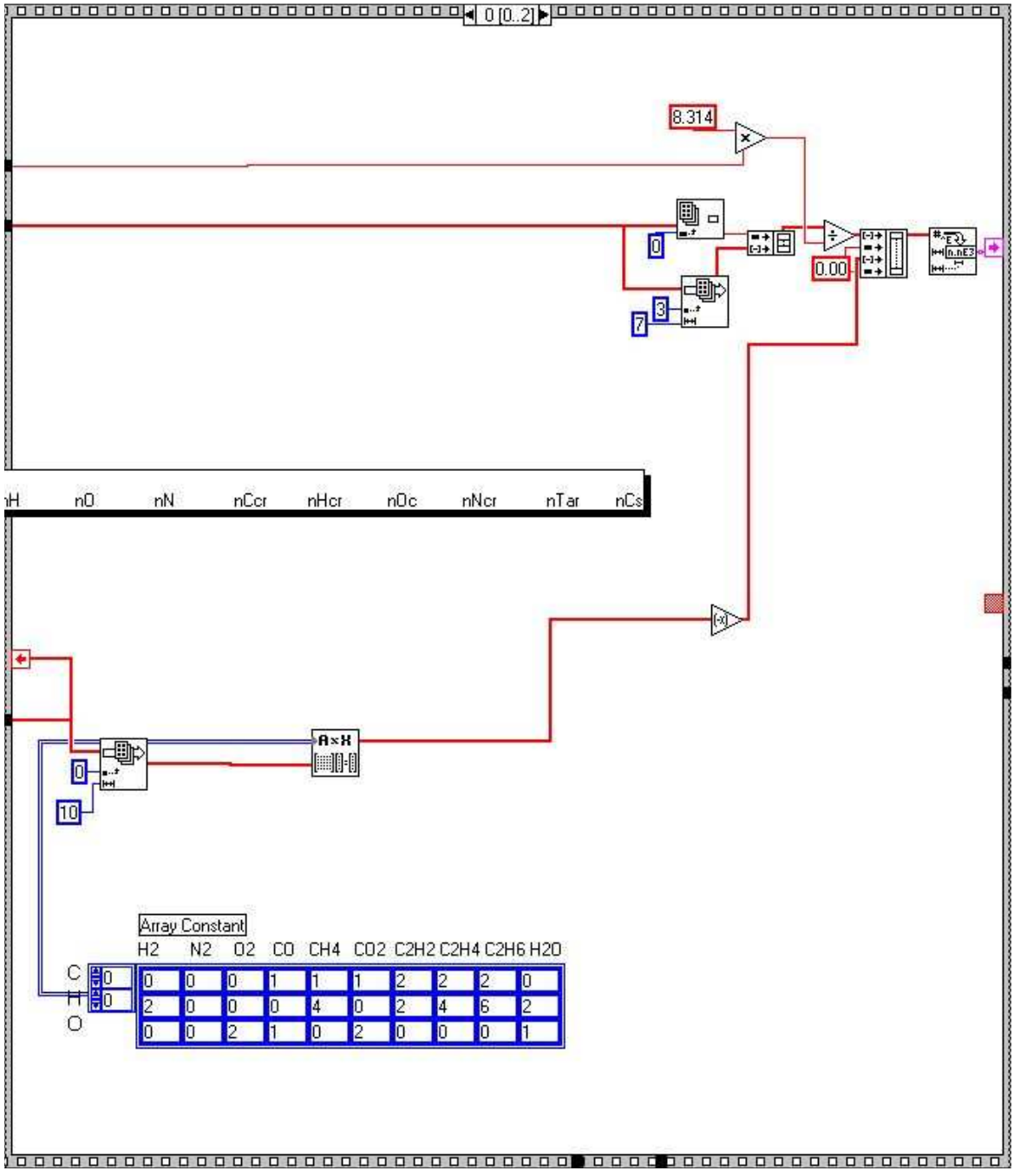
0 [0..2]
8.314
0
0.00
3
7
nH
nO
nN
nCcr
nHcr
nOc
nNcr
nTar
nCs
A×H
0
10
Array Constant
H2 N2 O2 CO CH4 CO2 C2H2 C2H4 C2H6 H2O
C
H
O
0 0 0 1 1 1 2 2 2 0
2 0 0 0 4 0 2 4 6 2
0 0 2 1 0 2 0 0 0 1

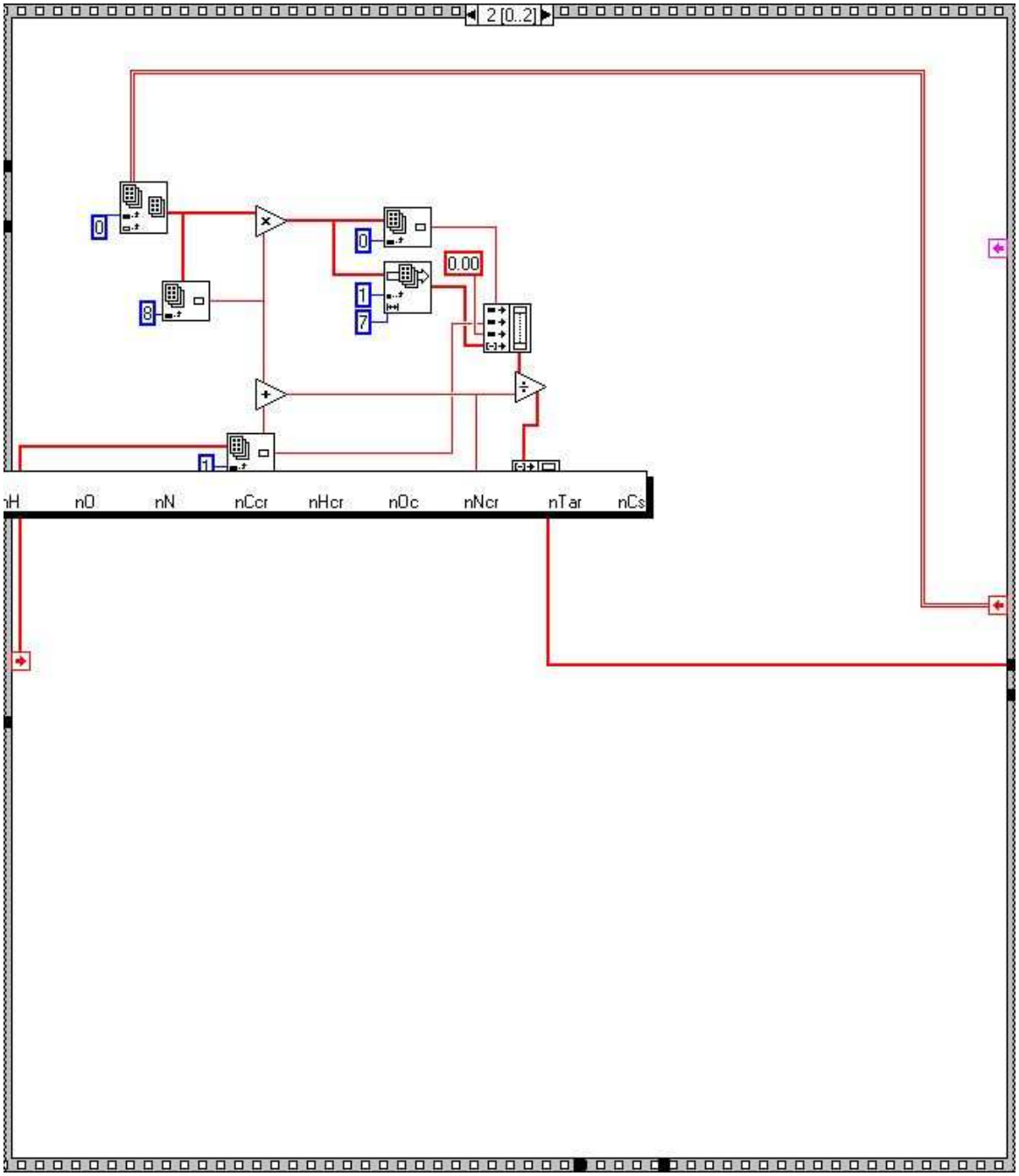
2 [0..2]
0
8
0
1
7
0.00
nH
nO
nN
nCcr
nHcr
nOc
nNcr
nTar
nCs

8.6.2.17 gas 3D graph Basic Properties.vi: 3 dimensional graphs setup

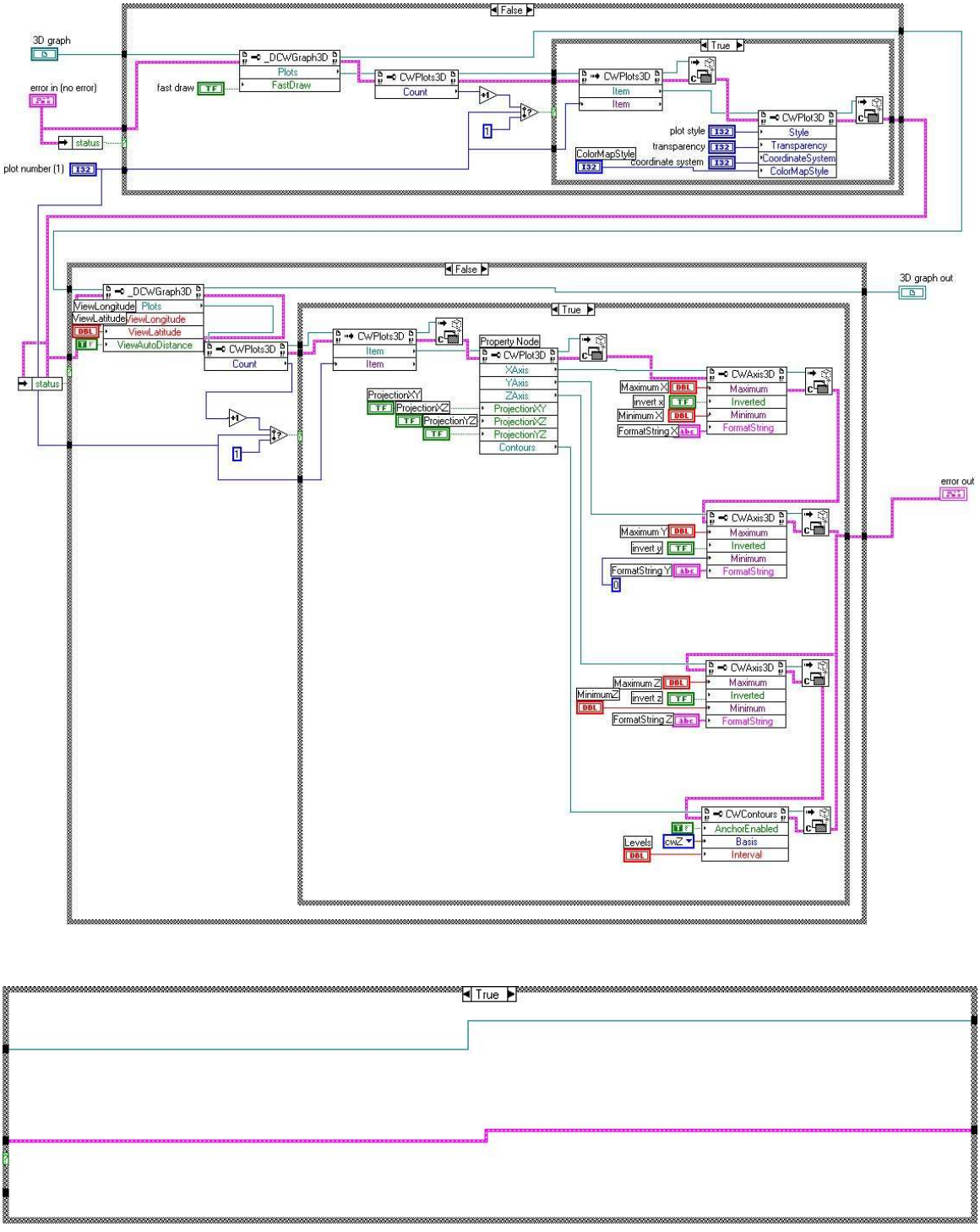

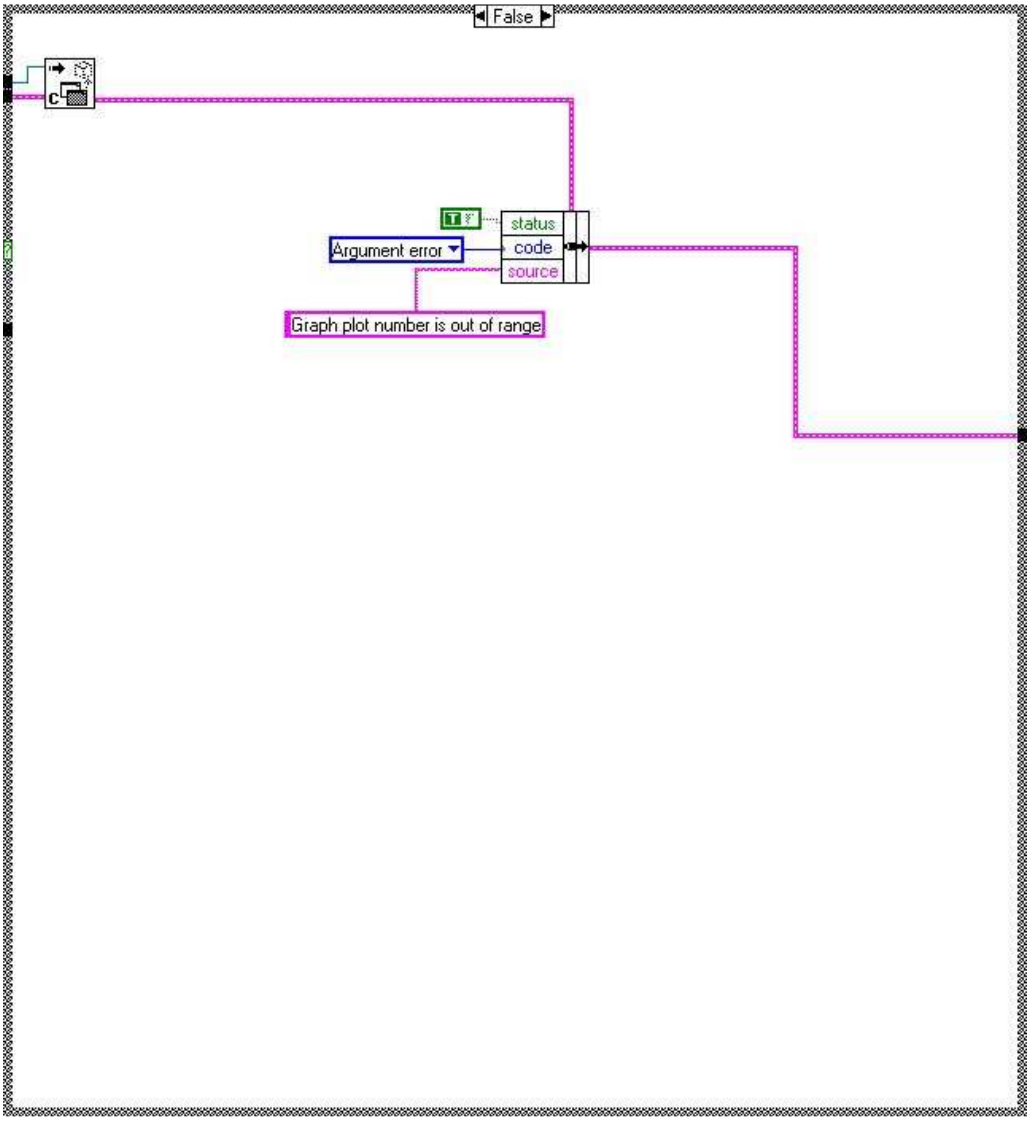
False
status
code
source
Argument error
Graph plot number is out of range

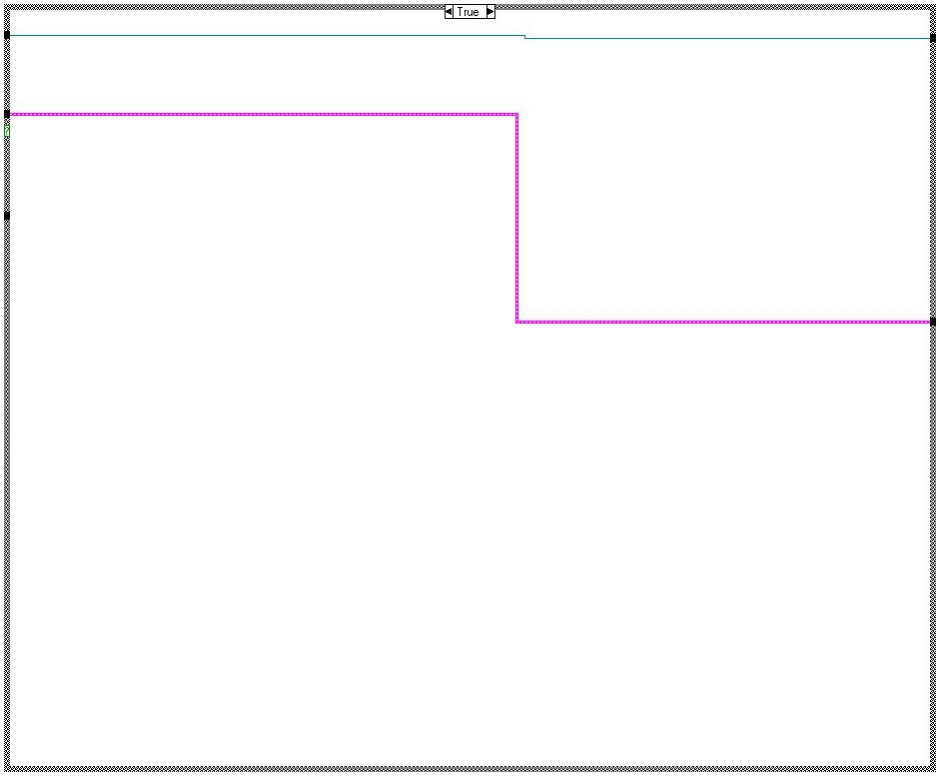
True

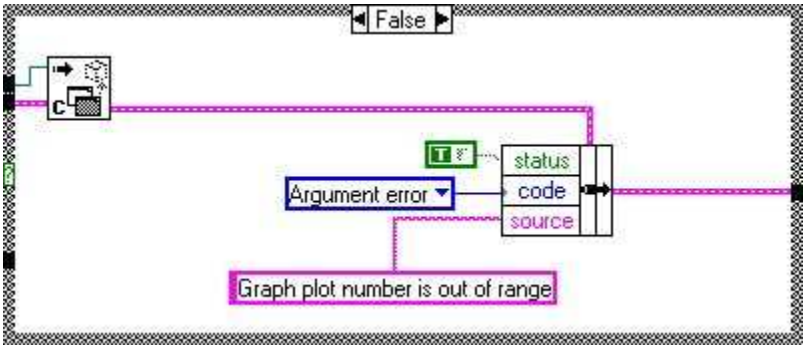
False
status
code
source
Argument error
Graph plot number is out of range

8.6.2.18 3D Surface.vi: 3 dimensional graphs

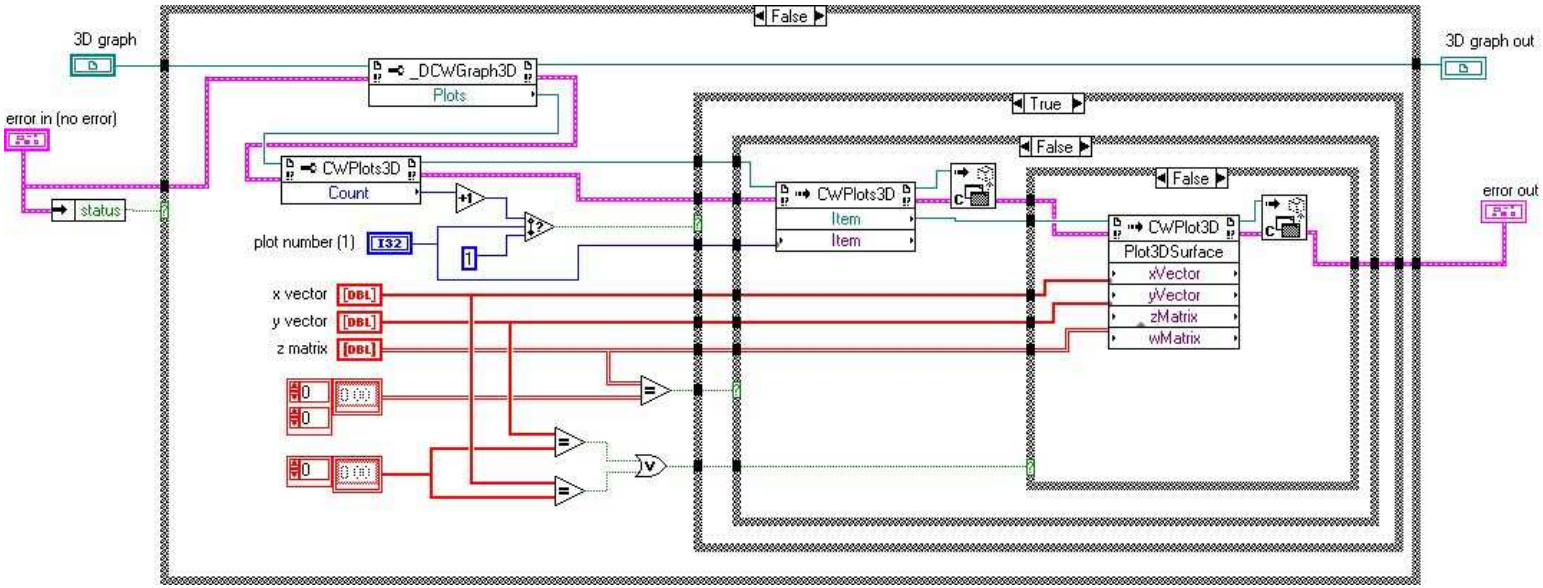

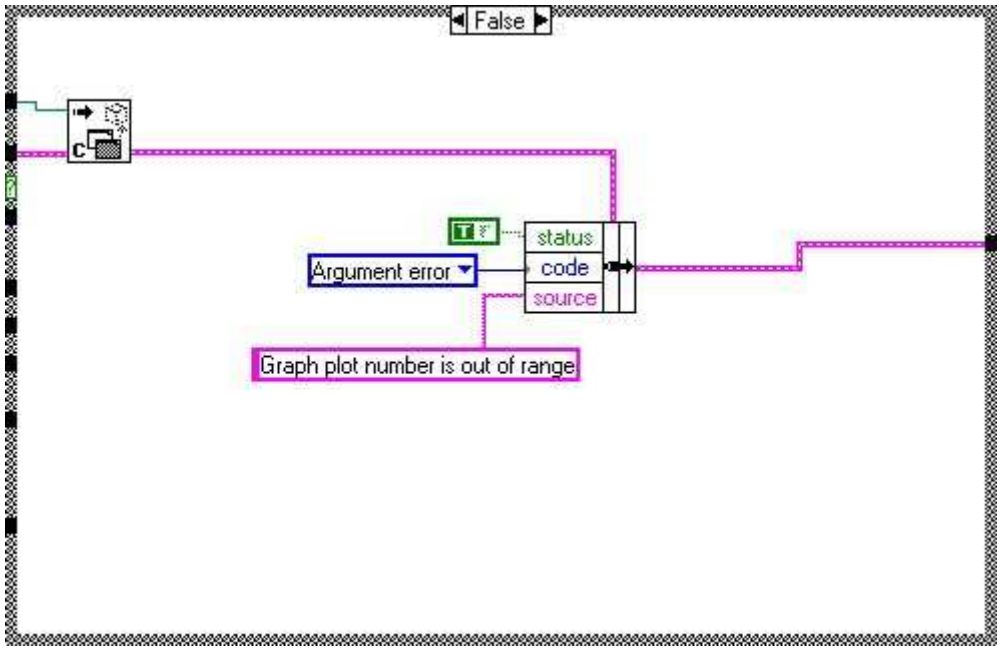
False
status
code
source
Argument error
Graph plot number is out of range

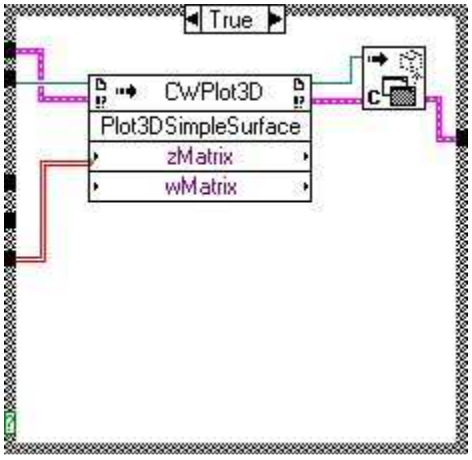
True
CWPlot3D
Plot3DSimpleSurface
zMatrix
wMatrix

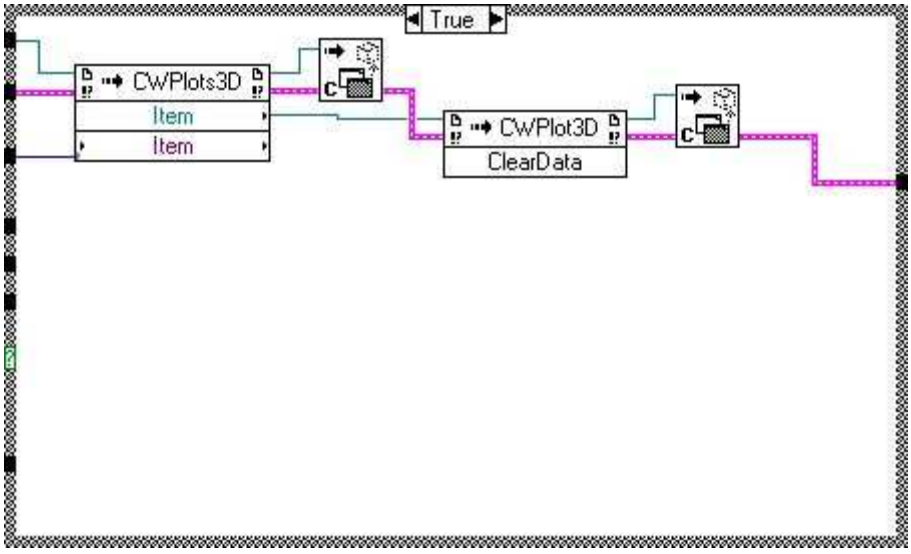
True
CWPlots3D
Item
Item
CWPlot3D
ClearData

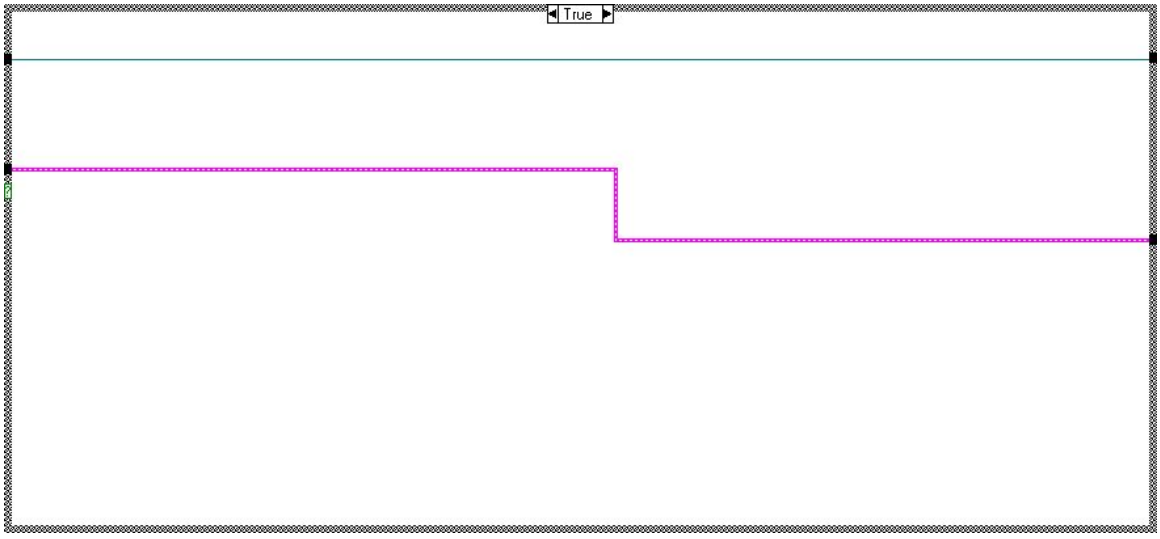
True

VITA

Bruno Ghislain Cateni

Candidate for the Degree of

Doctor of Philosophy

Thesis: EFFECT OF FEED COMPOSITION AND GASIFICATION PARAMETERS ON PRODUCT GAS FROM A PILOT SCALE FLUIDIZED BED GASIFIER

Major Field: Biosystems and Agricultural Engineering

Biographical:

Personal Data: Born in Marseilles, France, on September 28, 1970. Son of Robert Cateni and Colette Cateni born Borjela

Education: Graduated from Ausone High School, Trier, Germany in 1989; received an associate DEUG A SSM degree (Structure of Matter Sciences) from the University of Toulon and Var, La Gardes, France in 1994; received a Bachelor of Science degree in food process engineering from Ecole Nationale Supérieure des Industries Agro-alimentaires (ENSIA), Massy, France in 1996; received a Master of Science degree in industrial food process engineering from Ecole Nationale Supérieure des Industries Agro-alimentaires (ENSIA), Massy, France in 1997; Completed the requirements for Doctor of philosophy degree with a major in Biosystems Engineering in 2007.

Experience: Employed by the Audubon Sugar Institute, Louisiana State University, Baton Rouge, Louisiana as a research intern in fall 1995; employed by Ecole Nationale Supérieure des Industries Agro-alimentaires (ENSIA), Massy, France and UGINOR SACILOR, Paris, France as a research intern in spring and summer 1997; employed by Cooperative Winery**,** Pierrefeu du Var, France as a laboratory and process technician in fall 1998; employed by Oklahoma State University Biosystems and Agricultural Engineering Department, Stillwater, Oklahoma as a research engineer in 1998 to present.

Professional Memberships: American Society of Agricultural Engineers, Alpha Epsilon, Phi Beta Delta

Name: Bruno Ghislain Cateni Date of Degree: July, 2007

Institution: Oklahoma State University Location: Stillwater, Oklahoma

Title of Study: EFFECT OF FEED COMPOSITION AND GASIFICATION PARAMETERS ON PRODUCT GAS FROM A PILOT SCALE FLUIDIZED BED GASIFIER

Pages in Study: Candidate for the Degree of Doctor of Philosophy

Major Field: Biosystems Engineering

Scope and Method of Study: Biomass gasification is an integral part of a holistic project where low-value feedstocks are converted into ethanol via a gasification-fermentation process. Because microbial catalysts are used in the fermentation process, it is vital to know the product gas characteristics. In addition to carbon monoxide, hydrogen, and carbon dioxide utilized in the bioconversion process, potentially toxic tar compounds are present and must also be evaluated. In this study, a 10-inch diameter, fluidized bed gasifier was operated in three gasification modes: air, flaming pyrolitic and steam. Switchgrass, bermudagrass, and corn gluten have been gasified at equivalence ratios from 0.0 to 0.35 and steam-to-biomass ratios of 0.4 to 1.25. At each operating condition, synthesis gas and tar compositions were measured. A Gibbs reactor equilibrium model of gas, tar and char compounds was developed for each gasification mode.

Findings and Conclusions: As expected, steam gasification generated significantly higher levels of carbon monoxide and hydrogen compared to the air gasification modes. At steam-to-biomass ratio of 1.0, product gas measured over 30 mol% carbon monoxide and 35 mol% hydrogen. Results also showed quantitative and qualitative variations in tars, consisting of over 210 compounds, depending on the feedstock and reactor operating conditions. Of all three biomasses, switchgrass exhibited the highest gas compositions and lowest tar concentrations. High ash content in bermudagrass and corn gluten induced bed agglomeration at reactor temperatures above about 800°C. Steam gasification of corn gluten showed gas results equivalent to those of switchgrass. Tar atomic composition was constant at $C_{7.55}H_{8.62}O_{0.37}N_{0.20}$ over the range of 700 to 800°C reactor bed temperatures. Gibbs reactor equilibrium modeling showed tar levels were mostly influenced by unreacted carbon.

ADVISER'S APPROVAL: Dr. Raymond L. Huhnke